# EMERGING INFECTIOUS DISEASES®

CDC Centers for Disease Control and Prevention

Emerging Viruses

July 2020


**Pierre Joseph Redouté (1759–1840). *Iris Germanica* (1812).** Watercolor on vellum. 21 in × 13 3/4 in/53.3 cm × 35 cm.
Public domain image from Biodiversity Heritage Library. Holding institution: Missouri Botanical Garden, Peter H. Raven Library, Saint Louis, Missouri, USA.

# EMERGING INFECTIOUS DISEASES®





*Emerging Infectious Diseases* is published monthly by the Centers for Disease Control and Prevention, 1600 Clifton Rd NE, Mailstop H16-2, Atlanta, GA 30329-4027, USA. Telephone 404-639-1960; email, eideditor@cdc.gov

# EMERGING INFECTIOUS DISEASES®

**Emerging Viruses** **July 2020**


## On the Cover

**Pierre Joseph Redouté (1759–1840). *Iris Germanica* (1812).** Watercolor on vellum. 21 in x 13¾ in/53.3 cm x 35 cm. Public domain image from Biodiversity Heritage Library. Holding institution Missouri Botanical Garden, Peter H. Raven Library, St. Louis, Missouri, USA.

**About the Cover p. 1639**

## Synopses



## Research

## Policy Review



## Dispatches



EMERGING INFECTIOUS DISEASES®
July 2020

## Another Dimension



## Research Letters



EMERGING INFECTIOUS DISEASES®
July 2020



## Comment Letter



## Books and Media



## About the Cover



### Etymologia



## Online Report

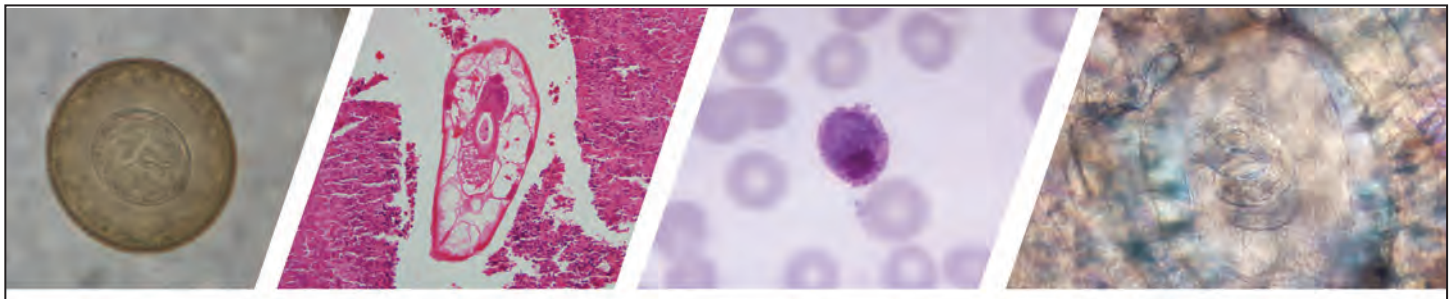

# DPDx

# Diagnostic Assistance and Training in Laboratory Identification of Parasites

A free service of CDC available to laboratorians, pathologists, and other health professionals in the United States and abroad

- Diagnosis from photographs of worms, histological sections, fecal, blood, and other specimen types
- Expert diagnostic review
- Formal diagnostic laboratory report
- Submission of samples via secure file share

Visit the DPDx website for information on laboratory diagnosis, geographic distribution, clinical features, parasite life cycles, and training via Monthly Case Studies of parasitic diseases.

www.cdc.gov/dpdx
dpdx@cdc.gov

U.S. Department of Health and Human Services
Centers for Disease Control and Prevention

CS272346-DE

# Case Manifestations and Public Health Response for Outbreak of Meningococcal W Disease, Central Australia, 2017

Eva L. Sudbury, Siobhan O'Sullivan, David Lister, Deepa Varghese, Keshan Satharasinghe

*Neisseria meningitidis* serogroup W has emerged as an increasingly common cause of invasive meningococcal disease worldwide; the average case-fatality rate is 10%. In 2017, an unprecedented outbreak of serogroup W infection occurred among the Indigenous pediatric population of Central Australia; there were 24 cases over a 5-month period. Among these cases were atypical manifestations, including meningococcal pneumonia, septic arthritis, and conjunctivitis. The outbreak juxtaposed a well-resourced healthcare system against unique challenges related to covering vast distances, a socially disadvantaged population, and a disease process that was rapid and unpredictable. A coordinated clinical and public health response included investigation of and empiric treatment for 649 febrile children, provision of prophylactic antimicrobial drugs for 465 close contacts, and implementation of a quadrivalent meningococcal ACWY conjugate vaccine immunization program. The response contained the outbreak within 6 months; no deaths and only 1 case of major illness were recorded.

Invasive meningococcal disease (IMD) remains a major cause of death and permanent disability worldwide (*1*). IMD is caused by *Neisseria meningitidis*, a gram-negative diplococcus bacterium, which frequently colonizes the human nasopharynx and might spread from person-to-person by respiratory droplets or direct contact with respiratory secretions. However, only a small proportion of persons will show development of invasive infection, typically with serogroups A, B, C, W or Y (*2*). IMD is most common in the dry winter and spring, in overcrowded households, and in persons who have preceding upper respiratory tract infections, splenectomy, and in the presence of terminal complement deficiencies (*3*,*4*).

Author affiliation: Alice Springs Hospital, Alice Springs, Northern Territory, Australia

DOI: https://doi.org/10.3201/eid2607.181491

Untreated, IMD can rapidly progress to death or major disability because of sepsis and the sequelae of meningitis. Early disease identification and treatment with parenteral antimicrobial drugs are vital in reducing illness and death. Initial signs and symptoms of the disease can be nonspecific and difficult to distinguish from those of less severe illnesses (*5*). In addition to the typical manifestations of sepsis or meningitis, atypical manifestations are well described and include septic arthritis, pneumonia, pericarditis, gastroenteritis, and epiglottitis (*5*–*9*). Conjunctivitis is also recognized, although is not usually associated with systemic illness (*10*,*11*).

Since early outbreaks were described during the Hajj pilgrimages of 2000 and 2001 (*12*,*13*), IMD caused by *N. meningitidis* serogroup W (MenW) has been increasingly responsible for epidemics globally (*1*,*14*–*16*). MenW has also emerged as a cause for endemic disease in South Africa, the United Kingdom, and Chile (*17*–*19*).

In Australia, IMD has historically been caused by endemic cases of serogroup B and C infection (*3*,*6*). Since 2013, there has been an increase in the incidence and proportion of IMD caused by MenW; in 2016, it was the predominant meningococcal serogroup in Australia (*3*,*6*). During 2003–2015, the case-fatality rate for infection with MenW in Australia was 10.7%, which was more than twice the case-fatality rate for all IMD serogroups combined (*6*). Until 2017, the Northern Territory was the only state in Australia that had not experienced an increase in IMD caused by MenW (*20*).

A conjugate meningococcal C vaccine has been funded and provided by the Australian National Immunisation Program since 2003 for all children at the age of 12 months, which reflects the previous predominance of IMD caused by this serogroup (*6*,*21*). A meningococcal B vaccine, and several quadrivalent

meningococcal A, C, W, Y (MenACWY) conjugate vaccines, are registered for use in Australia but were not part of the funded program during 2017 (*6*,*21*).

During July–December 2017, an outbreak of IMD caused by MenW occurred in Central Australia. We report case manifestations and the clinical and public health response.

## Methods

### Ethics and Setting

This study was approved by the Central Australian Human Research Ethics Committee (CA-18-3032). Alice Springs Hospital is the regional referral center for Central Australia and has a catchment area that covers ≈1.6 million km$^2$ (Figure 1). This area encompasses the city of Alice Springs, Northern Territory, and the surrounding remote communities and has a total population of ≈60,000 persons, many of whom are Indigenous Australians, identifying as Aboriginal or Torres Strait Islander (ATSI). The hospital has a 40-bed pediatric ward with ≈1,800 pediatric admissions/year. The closest tertiary pediatric service with a pediatric intensive care unit (ICU) is ≈1,600 km away, in Adelaide, South Australia.

Of the 58 communities within the catchment area, 20 are within South Australia and Western Australia state jurisdictions. Pediatric patients from these communities are treated at Alice Springs Hospital because of cultural links and the relative proximity of the pediatric unit in comparison to those within state borders. The communities are located 80–1,000 km from the hospital. Most remote communities are serviced by a local medical clinic staffed by remote area nurses or general practitioners. The clinics are equipped with common antimicrobial drugs, including ceftriaxone, and are able to administer these drugs by intravenous cannulation or intramuscular injection. The clinic staff do not routinely perform more complex investigative procedures such as lumbar punctures and difficult venipuncture.

### Case Definitions and Laboratory Methods

After the outbreak period, we conducted a retrospective review of MenW cases treated by the Alice Springs Hospital pediatric service during July–December 2017. We used a standardized questionnaire to gather information from medical records at the hospital and, where necessary, at the community clinics. We defined cases as detection of *N. meningitidis* by culture or PCR from a usually sterile site (blood, cerebrospinal fluid [CSF], or synovial fluid) or from purulent eye discharge, with serogrouping demonstrating serogroup W.

Culture samples were initially incubated in the Bact/Alert 3D Microbial Detection System (bioMérieux, https://www.biomerieux.com). Positive blood cultures were then inoculated onto chocolate agar and further incubated in an atmosphere of 5% $CO_2$ at 35°C. Colonies were identified *N. meningitidis* by using API NH (bioMérieux). Susceptibility testing was performed by using Etest (bioMérieux) and the Australian Meningococcal Surveillance Programme interpretive criteria (*20*) and serogroup determined by using Pastorex Meningitis test kits (Bio-Rad, https://www.bio-rad.com) and Remel Meningococcus Agglutinating Sera (ThermoFisher Scientific, https://www.thermofisher.com). Meningococcal PCR was used for the *sod*C, *por*A, and *ctr*A genes by using reported methods (*22*,*23*). Cultured isolates were subsequently characterized by using multilocus sequence typing (*24*).

### Clinical and Public Health Response

In September 2017, after 9 case-patients with MenW (4.1 cases/100,000 persons in the ATSI population <15 years of age) had been admitted to the pediatric ward at Alice Springs Hospital, the Centre for Disease Control (CDC) in the Northern Territory declared an outbreak (*25*). A clinical and public health response was coordinated by CDC and Alice Springs Hospital.

The team developed a clinical case definition to denote any child <16 years of age who had a fever (temperature ≥38°C) as a suspected case-patient with IMD. A management protocol, referred to as the fever protocol, was instituted in which all patients from the Alice Springs Hospital catchment area who fit the case definition were investigated by using a blood culture and meningococcal PCR, and treated empirically with intravenous or intramuscular ceftriaxone (100 mg/kg/d) until their results were available. Additional investigations (e.g., lumbar puncture) were performed as clinically indicated. All primary and secondary health services in the Alice Springs Hospital catchment area across the Northern Territory, South Australia, and Western Australia followed this protocol. Patients from remote communities were retrieved by the Royal Flying Doctor Service (RFDS) and admitted to Alice Springs Hospital for observation until their results were available. For patients from urban Alice Springs, access to transport and social circumstances were considered in determining admission to the pediatric ward or discharge


**Figure 1.** Alice Springs Hospital catchment area, Central Australia. Red dot indicates Alice Springs township; orange dots indicate Northern Territory communities; purple dots indicate Western Australia communities; gray dots indicate South Australia communities.

home with outpatient review within 24 hours by a dedicated, daily, pediatric fever clinic. Cases were classified on the basis of clinical signs and symptoms at presentation and investigation results (Table 1) and based on case definitions used in previous outbreaks (*7*,*10*,*11*,*26*–*29*).

Concurrent to the clinical response, CDC launched a widespread public health response that included providing prophylactic antimicrobial drugs (ceftriaxone or ciprofloxacin) to close contacts and implementing of an MenACWY immunization campaign. A total of 530 close contacts (*30*) were identified, of whom 465 (87.7%) received prophylactic antimicrobial drugs.

The immunization campaign began in early October 2017. Initially, the vaccine was provided for all persons 1–19 years of age who were living in remote communities in the Central Australia, Barkly, and Katherine West regions. In urban Alice Springs, Tennant Creek, and Katherine, the vaccine was initially provided to ATSI persons (1–19 years of age), but on

**Table 1.** Diagnostic categories of patients with meningococcal serogroup W infection, Central Australia, 2017*

| Diagnostic category (reference) | Clinical signs/symptoms | Site of MenW isolation by culture or PCR | Additional investigations |
|---|---|---|---|
| Meningococcemia (*28*,*29*) | Fever (temperature ≥38°C) without a focus | Blood | None |
| Meningitis | Fever; any signs of meningism (e.g., headache, neck stiffness, photophobia) | CSF | None |
| Bacteremic pneumonia (*7*,*26*,*27*) | Fever; cough | Blood | Radiologic consolidation by chest radiograph |
| Septic arthritis (*7*) | Fever; joint pain and swelling | Synovial fluid | None |
| Conjunctivitis (*10*,*11*) | Conjunctival inflammation with purulent discharge | Eye discharge | None |

*CSF, cerebrospinal fluid; MenW, serogroup W of *Neisseria meningitidis*.

November 1, 2017, this campaign was expanded to also include non-Indigenous persons. On December 1, 2017, the MenACWY vaccine replaced the meningococcal C vaccine in the Northern Territory vaccination schedule for all babies 12 months of age. As March 21, 2018, the MenACWY vaccine had been administered to 81% of the estimated eligible ATSI population and to 49% of the estimated eligible non-Indigenous population living in the outbreak area (*31*).

As the immunization campaign was implemented, the protocol for managing febrile patients was adjusted to reflect immunization status. Management of immunized patients was based on their clinical signs and symptoms, rather than on the presumption of IMD. The outbreak was declared over on March 23, 2018, 3 months after the last case was identified.

## Results

### Outbreak Description

During the 5 months starting in July 2017, a total of 24 patients with MenW were admitted to the Alice Springs Hospital pediatric ward. We found an attack rate of 10.9 cases/100,000 persons for the ATSI population <15 years of age (Figure 2). In comparison, in Australia during 2011–2015, there were 0–2 cases/year in the ATSI population (0–0.9 cases/100,000 persons/year) and 9 cases during 2016 (4.1 cases/100,000 persons) (*20*,*25*,*32*).

During the 9-month outbreak period, ≈649 patients were managed under the fever protocol. In addition to the 24 cases of MenW, 1 case was caused by meningococcal serogroup Y and 1 by nongroupable meningococci. One additional case-patient had MenW during March 2017 (isolated meningococcemia) but the isolate was a different sequence type (ST) and was not classified as part of the outbreak. Two additional cases of MenW occurred in adult patients during this time but were not managed according to the pediatric fever protocol.

The 24 cases of MenW during the outbreak comprised 23 cases of IMD and 1 case of MenW conjunctivitis. Only 1 patient had had possible contact with an index case-patient; this contact was 4 days before development of MenW infection. For all other patients, there was no identified contact with an index case-patient.

We compiled demographic and clinical details for the 24 outbreak patients (Table 2). The patients came from 18 of the 58 communities in the Alice Springs Hospital catchment area (Figure 1). All cases were among ATSI children. Fifteen (63%) patients were transferred to Alice Springs Hospital from remote communities by the RFDS. There were more male (71%) patients than female (29%) patients. Patients ranged in age from 3 months to 14 years; 54% were ≤4 years of age.

The MenACWY immunization campaign started in early October 2017. After mid-October, 6 additional cases of IMD were reported; the final case-patient came to the hospital on December 23, 2017 (Figure 2). All cases of MenW occurred in unimmunized patients. One patient with suspected MenW infection had received the MenACWY vaccine 12 days before being identified. For this case-patient, the blood PCR result was equivocal; the patient was given intravenous antimicrobial drugs for 5 days, but results for this patient are not included in this report.

Seventeen (71%) cases were confirmed by culture (blood, synovial fluid, or eye swab specimen) and 7 by PCR (blood or CSF). Of the cases that were culture positive, susceptibility to penicillin was intermediate (MIC 0.064 to <0.5 μg/mL) for 15 cases (88%) and resistant (MIC ≥0.5 to 1 μg/mL) for 2 cases (12%). No isolates were penicillin susceptible, and all were susceptible to ceftriaxone. Multilocus sequence typing of isolates indicated that all belonged to clonal complex 11 (MenW:cc11), ST 1287 (*33*).

All but 1 case-patient (96%) had samples that were tested by PCR. For 7 case-patients, this testing was necessary to obtain a diagnosis because ceftriaxone had been administered before blood or CSF collection. For the remaining 16 case-patients, PCR testing was used to obtain a more rapid diagnosis because PCR results were available in a shorter time

frame than culture results, thereby enabling prompt allocation of appropriate resources.

All case-patients with invasive disease had a fever (temperature ≥38°C) (Table 2). The time interval between first arrival at a clinic and commencement of appropriate antimicrobial drug treatment (ceftriaxone) varied between 36 minutes and almost 55 hours (median 4.7 hours) (Table 2). For the patient who received ceftriaxone 55 hours after first arrival, the patient received daily examinations at the local clinic for respiratory symptoms. The first documented fever was on day 3 of illness, at which point ceftriaxone was administered and the patient was transferred to Alice Springs Hospital by RFDS. The patient was given a diagnosis of isolated meningococcemia, given ceftriaxone for 5 days, and showed a full recovery.

Seven patients received penicillin (amoxicillin or benzathine penicillin) before ceftriaxone. Of those patients, 5 had positive cultures, 4 had intermediate penicillin sensitivity, and 1 had penicillin resistance. For 6 case-patients, penicillin was administered before specimen collection (≈8–24 hours before for each case-patient). The mean time from initial clinic arrival to first dose of ceftriaxone was significantly longer for these patients compared with patients who received ceftriaxone as first-line treatment (26.1 hours vs. 6.0 hours; p = 0.0011). The mean length of stay was also significantly longer for patients who initially received penicillin compared with patients who received ceftriaxone as first-line therapy (25.6 days vs. 6.4 days, p = 0.06). These patients include 1 patient who required transfer to a tertiary center because of meningococcemia, purpura fulminans, and a below-knee amputation and who had a prolonged hospital admission (128 days). The time interval from initial clinic arrival to the first dose of ceftriaxone for this patient was 16.8 hours. Benzathine penicillin had been administered previously, and the isolate from this case-patient showed intermediate susceptibility to penicillin.

There were no deaths during the outbreak. Four (17%) patients (2 with meningitis, 1 with isolated meningococcemia, and 1 with purpura fulminans) were initially admitted to the ICU; the remainder were admitted directly to the pediatric ward. When we excluded the patient who had major illness and required transfer to a tertiary center, we found that the median length of stay for the remaining 23 patients was 5 days (range 4–15 days) (Table 2).

The most common diagnosis was isolated meningococcemia (50%), followed by meningitis (25%), bacteremic pneumonia (17%), septic arthritis (4%), and conjunctivitis (4%) (Table 2). Typical manifestations occurred across all age groups, whereas atypical

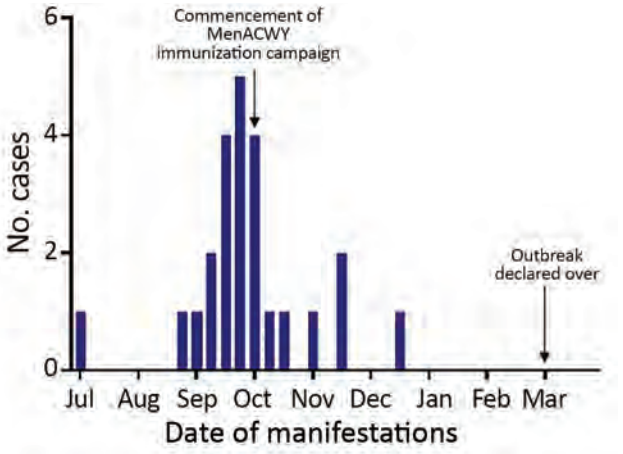


**Figure 2.** Timeline for outbreak of meningococcal W disease, showing case manifestations, by month, Central Australia, 2017. MenACWY, quadrivalent meningococcal A, C, W, Y conjugate vaccine.

manifestations occurred only in younger patients (<7 years of age). Of the 12 patients with isolated meningococcemia, 7 (58%) were suspected by the admitting clinician of having alternative dignoses: pneumonitis/bronchiolitis (2), gastroenteritis (2), meningitis (1), acute rheumatic fever (1), and viral illness (1). Three patients had a purpuric rash (purpura fulminans developed in 1 of these patients). There was no significant difference in age (mean 9.3 years vs. 3.8 years; p = 0.08) or the time interval to receiving ceftriaxone (mean 11.5 hours vs. 11.5 hours; p = 0.30) between patients with isolated meningococcemia who had a purpuric rash compared with patients who did not have this rash.

Six (25%) patients had meningitis, all confirmed by PCR for CSF. One patient who had meningitis also had meningococcemia (positive blood culture and PCR). Four patients with meningitis (80%) had persistent bradycardia during their admission.

Four (17%) patients had MenW bacteremic pneumonia. Eight (33%) patients had arthritis or arthralgia as an initial symptom, but only 1 patient was given a diagnosis of MenW septic arthritis. One patient had severe, bilateral MenW conjunctivitis that was confirmed by culture and PCR. Although conjunctivitis was not invasive disease, this patient was admitted for administration of parenteral antimicrobial drugs and required a public health response. Despite appropriate antimicrobial treatment, 4 patients had a prolonged admission at Alice Springs Hospital (12–15 days) because of persistent fevers, persistent arthralgias, or both.

Anaphylaxis developed in 1 patient managed under the fever protocol after administration of

ceftriaxone. This patient was given treatment in the emergency department at Alice Springs Hospital and admitted to the ICU overnight for observation. The patient had had no history of allergy or anaphylaxis to any antimicrobial drug. This episode was the only adverse event that occurred as a result of the fever protocol.

**Table 2.** Characteristics of 24 case-patients who had meningococcal serogroup W infection, Central Australia, 2017*

| Characteristic | Value |
|---|---|
| Age, y | |
| Median (25%–75% percentile) | 5.2 (1.7–7.2) |
| Range | 0.3–14.7 |
| Sex | |
| M | 17 (71) |
| F | 7 (29) |
| Australian Aboriginal | 24 (100) |
| No. communities affected (n = 58) | 18 (31) |
| Location of communities | |
| Northern Territory | 14 (78) |
| South Australia | 3 (17) |
| Western Australia | 1 (5) |
| Air retrieval to Alice Springs Hospital | 15 (63) |
| Signs/symptoms | |
| Fever | 23 (96) |
| Tachycardia | 18 (75) |
| Vomiting | 10 (42) |
| Cough/respiratory distress | 7 (29) |
| Arthritis/arthralgia | 8 (33) |
| Meningism | 7 (29) |
| Hypotension | 6 (25) |
| Purpuric rash | 3 (13) |
| Diarrhea | 2 (8) |
| Petechial rash | 1 (4) |
| Conjunctivitis | 1 (4) |
| Diagnosis | |
| Isolated meningococcemia | 12 (50) |
| Meningitis | 6 (24) |
| Bacteremic pneumonia | 4 (16) |
| Septic arthritis | 1 (4) |
| Conjunctivitis | 1 (4) |
| Admission location | |
| Pediatric ward | 20 (83) |
| Intensive care unit | 4 (17) |
| Length of admission, d | |
| Median (25%–75% percentile) | 5.5 (5–8.5) |
| Range | 4–128 |
| Duration of antimicrobial drug use, d | |
| Median (25%–75% percentile) | 6 (5–8) |
| Range | 4–14 |
| Time from visit to health service to first dose of ceftriaxone, h | |
| Median (25%–75% percentile) | 4.7 (1.6–15.6) |
| Range | 0.6–54.9 |
| Complications | |
| Persistent bradycardia | 4 (17) |
| Persistent arthralgia | 4 (17) |
| Persistent fevers | 3 (13) |
| Coagulopathy | 1 (4) |
| Acute kidney injury | 1 (4) |
| Below-knee amputation | 1 (4) |
| Culture positive | 17 (71) |
| Penicillin sensitivity | |
| Intermediate | 15 (88) |
| Resistant | 2 (12) |
| PCR positive | 23 (96) |

*Values are no. (%) unless otherwise indicated.

## Discussion

The outbreak of MenW among the ATSI population in Central Australia was unique because it juxtaposed a well-resourced healthcare system against challenges related to covering vast distances, a socially disadvantaged population, and a disease process that was rapid and unpredictable. The clinical and public health responses resulted in no deaths and only 1 case-patient who had major illness, in contrast to previously documented case-fatality rates elsewhere of 10% (*2*,*6*,*34*,*35*).

The ATSI population of Australia has a higher rate of IMD than the non-Indigenous population (*36*,*37*). During 2016, Indigenous persons in Australia comprised 3.3% of the total population of this country but accounted for >10% of IMD reports (*38*). The ATSI population has a high disease burden for numerous infectious conditions, including lower respiratory tract infections, group A *Streptococcus* skin sores, and scabies (*39*,*40*). The underlying determinants relate to socioeconomic factors and include higher rates of overcrowded housing, educational disadvantage, poorer nutrition, higher unemployment rates, and reduced access to specialist medical care (*41*). These factors overlap with known risk factors for IMD (*42*–*44*).

Early signs of IMD make it difficult to distinguish from other causes of febrile illness. Therefore, the broad case definition used in the fever protocol was considered necessary, given the remote location of the affected communities. The spread of a relatively small number of pediatric patients across a wide and remote area, with access to well-equipped local medical services, an air retrieval service (RFDS), and a secondary pediatric referral service, made the fever protocol response possible.

A total of 25% of case-patients had atypical manifestations of IMD (bacteremic pneumonia, septic arthritis, conjunctivitis), and all those cases were in younger children (<7 years of age). In previous MenW outbreaks overseas, rates of atypical manifestations have varied from 4% to 25% (*29*,*45*,*46*). Gastrointestinal symptoms (vomiting, diarrhea, or both) were present in 11 (44%) patients during this outbreak, although only 2 (8%) patients were initially believed to have gastroenteritis at initial clinic visit. Gastrointestinal symptoms have been associated with a high case-fatality rate in 2 previous studies, although these studies involved a hypervirulent ST11 strain of MenW (*8*,*46*).

For the 17 case-patients from whom MenW was isolated by culture, reduced susceptibility to penicillin reflected previously documented antimicrobial drug susceptibility patterns for MenW in Australia

(*22*,*47*). ST1287 isolates have previously been described in sporadic cases in Western Australia and were associated with penicillin resistance (*48*). Of the 7 patients in this outbreak who initially received penicillin, 1 patient had a major illness (purpura fulminans) and a complication (below-knee amputation). The other 6 patients did not have a complicated clinical course. Treatment with penicillin is still effective against penicillin-intermediate strains if given at high doses (*48*), and it is possible that the clinical course for these patients was somewhat attenuated compared with if they had received no initial treatment before being given ceftriaxone.

Prolonged hospital admission was required for 5 case-patients (4 patients at Alice Springs Hospital and 1 patient at a tertiary referral center). The cause of the prolonged duration of symptoms for the 4 patients at Alice Springs Hospital was not clear, but all patients had their illnesses resolve before discharge from the hospital. No characteristics clearly differentiated these patients from the rest of the cohort. The 4 patients had meningitis, septic arthritis, bacteremic pneumonia, and meningococcemia. Two of these patients had a comparatively longer time interval between first presentation to a clinic and receiving their first dose of ceftriaxone (20.8 hours for the patient with meningitis and 39.2 hours for the patient with septic arthritis). However, the intervals were much shorter for the other 2 patients (1.2 hours for the patient with bacteremic pneumonia and 14.3 hours for the patient with meningococcemia). For the second 2 patients, there was an interval of only 2.2 hours between their first documented fever and their first dose of ceftriaxone. These case-patients were clinically challenging, which resulted in longer admissions, additional investigations (e.g., echocardiogram, lumbar puncture, joint aspirate) and longer courses of antimicrobial drug therapy. A possible cause was immune complex disease, known to occur in the subacute phase of meningococcal disease. This disease can cause symptoms of arthritis, vasculitis, pleuritis, body temperature increase, and increased levels of inflammatory markers 4–10 days after systemic disease (*49*).

The public health response coordinated by CDC required complex planning because of geographic and logistical challenges. This response was further limited by movement of persons between communities, which is inherent to the ATSI population of Central Australia. This limitation complicated the task of locating contacts for provision of prophylactic antimicrobial drugs, as well as the subsequent MenACWY vaccination campaign.

The number of pediatric meningococcal case-patients admitted to Alice Springs Hospital decreased after the vaccination campaign was initiated (Figure 2). The fever protocol considered persons to be protected 4 weeks after vaccination (*50*), at which time their management was based on clinical manifestations, rather than on the presumption of IMD.

The response incurred costs and might not be practical for other settings. The response also greatly increased the workload of the local medical clinics, the RFDS, and the Alice Springs Hospital emergency department and pediatric department. There was an economic impact of increased staffing; additional investigations, including meningococcal PCR and blood cultures; and increased provision of antimicrobial drugs. However, this impact must be balanced against the cost of the probable increased rate of complications and transfers to a tertiary center, which might have occurred if treatment had been delayed. The empiric administration of ceftriaxone to all patients who had fever during the early phase of the outbreak also carries the potential for promoting antimicrobial drug resistance.

Replicating the response to this outbreak in more densely populated areas would be challenging, and a different approach might be appropriate in situations in which direct access to secondary and tertiary health services is available. However, the response to this outbreak was extremely effective in this particular setting and resulted in a low illness rate and a zero fatality rate for a disease that is typically devastating.

#### Acknowledgments

We thank Kevin Freeman for providing tireless laboratory work during the outbreak and assistance in the preparation of this manuscript and Belinda Greenwood-Smith for providing information on the CDC response to the outbreak.

### About the Author

Dr. Sudbury is a doctoral candidate at the University of Melbourne, Parkville, Victoria, Australia. Her primary research interest is pediatric tuberculosis.

#### References

1. Borrow R, Alarcón P, Carlos J, Caugant DA, Christensen H, Debbag R, et al.; Global Meningococcal Initiative. The Global Meningococcal Initiative: global epidemiology, the impact of vaccines on meningococcal disease and the importance of herd protection. Expert Rev Vaccines. 2017;16:313–28. https://doi.org/10.1080/14760584.2017.1258308
2. Manchanda V, Gupta S, Bhalla P. Meningococcal disease: history, epidemiology, pathogenesis, clinical manifestations,

diagnosis, antimicrobial susceptibility and prevention. Indian J Med Microbiol. 2006;24:7–19. https://doi.org/10.4103/0255-0857.19888
3. Veitch MG, Owen RL. Rise in invasive serogroup W meningococcal disease in Australia 2013–2015. Commun Dis Intell Q Rep. 2016;40:E451–3.
4. Lewis LA, Ram S. Meningococcal disease and the complement system. Virulence. 2014;5:98–126. https://doi.org/ 10.4161/viru.26515
5. Thompson MJ, Ninis N, Perera R, Mayon-White R, Phillips C, Bailey L, et al. Clinical recognition of meningococcal disease in children and adolescents. Lancet. 2006;367:397–403. https://doi.org/10.1016/S0140-6736(06)67932-4
6. Martin NV, Ong KS, Howden BP, Lahra MM, Lambert SB, Beard FH, et al.; Communicable Diseases Network Australia MenW Working Group. Rise in invasive serogroup W meningococcal disease in Australia 2013–2015. Commun Dis Intell Q Rep. 2016;40:E454–9.
7. Vienne P, Ducos-Galand M, Guiyoule A, Pires R, Giorgini D, Taha M-K, et al. The role of particular strains of *Neisseria meningitidis* in meningococcal arthritis, pericarditis, and pneumonia. Clin Infect Dis. 2003;37:1639–42. https://doi.org/10.1086/379719
8. Campbell H, Parikh SR, Borrow R, Kaczmarski E, Ramsay ME, Ladhani SN. Presentation with gastrointestinal symptoms and high case fatality associated with group W meningococcal disease (MenW) in teenagers, England, July 2015 to January 2016. Euro Surveill. 2016;21:1–4. https://doi.org/10.2807/1560-7917.ES.2016.21.12.30175
9. Schaad UB. Arthritis in disease due to *Neisseria meningitidis*. Rev Infect Dis. 1980;2:880–8. https://doi.org/10.1093/clinids/2.6.880
10. Barquet N, Gasser I, Domingo P, Moraga FA, Macaya A, Elcuaz R. Primary meningococcal conjunctivitis: report of 21 patients and review. Rev Infect Dis. 1990;12:838–47. https://doi.org/10.1093/clinids/12.5.838
11. Orden B, Martínez R, Millán R, Belloso M, Pérez N. Primary meningococcal conjunctivitis. Clin Microbiol Infect. 2003;9:1245–7. https://doi.org/10.1111/j.1469-0691.2003.00799.x
12. Lingappa JR, Al-Rabeah AM, Hajjeh R, Mustafa T, Fatani A, Al-Bassam T, et al. Serogroup W-135 meningococcal disease during the Hajj, 2000. Emerg Infect Dis. 2003;9:665–71. https://doi.org/10.3201/eid0906.020565
13. Yezli S, Assiri AM, Alhakeem RF, Turkistani AM, Alotaibi B. Meningococcal disease during the Hajj and Umrah mass gatherings. Int J Infect Dis. 2016;47:60–4. https://doi.org/10.1016/j.ijid.2016.04.007
14. Ladhani SN, Ramsay M, Borrow R, Riordan A, Watson JM, Pollard AJ. Enter B and W: two new meningococcal vaccine programmes launched. Arch Dis Child. 2016;101:91–5. https://doi.org/10.1136/archdischild-2015-308928
15. Smith-Palmer A, Oates K, Webster D, Taylor S, Scott KJ, Smith G, et al.; IMT and investigation team in Sweden. Outbreak of *Neisseria meningitidis* capsular group W among scouts returning from the World Scout Jamboree, Japan, 2015. Euro Surveill. 2016;21:1–7. https://doi.org/10.2807/1560-7917.ES.2016.21.45.30392
16. Nathan N, Rose AMC, Legros D, Tiendrebeogo SRM, Bachy C, Bjørløw E, et al. Meningitis serogroup W135 outbreak, Burkina Faso, 2002. Emerg Infect Dis. 2007;13:920–3. https://doi.org/10.3201/eid1306.060940
17. von Gottberg A, du Plessis M, Cohen C, Prentice E, Schrag S, de Gouveia L, et al.; Group for Enteric, Respiratory and Meningeal Disease Surveillance in South Africa. Emergence of endemic serogroup W135 meningococcal disease associated with a high mortality rate in South Africa. Clin Infect Dis. 2008;46:377–86. https://doi.org/10.1086/525260
18. Abad R, López EL, Debbag R, Vázquez JA. Serogroup W meningococcal disease: global spread and current affect on the Southern Cone in Latin America. Epidemiol Infect. 2014;142:2461–70. https://doi.org/10.1017/S0950268814001149
19. Campbell H, Saliba V, Borrow R, Ramsay M, Ladhani SN. Targeted vaccination of teenagers following continued rapid endemic expansion of a single meningococcal group W clone (sequence type 11 clonal complex), United Kingdom 2015. Euro Surveill. 2015;20:21188. https://doi.org/10.2807/1560-7917.ES2015.20.28.21188
20. Australian Government Department of Health. Invasive meningococcal disease national surveillance report, December 2017 [cited 2018 Jun 27]. http://www.health.gov.au/internet/main/publishing.nsf/Content/5FEABC4B495BDEC1CA25807D001327FA/$File/1Jan-31-Dec2017-Consol-Invasive-Men-W.pdf
21. National Centre for Immunisation Research and Surveillance. History of vaccination in Australia, December 2017 [cited 2018 Jun 18]. http://www.ncirs.org.au/sites/default/files/2018-12/Meningococcal-history-Dec-2018.pdf
22. Dolan Thomas J, Hatcher CP, Satterfield DA, Theodore MJ, Bach MC, Linscott KB, et al. sodC-based real-time PCR for detection of Neisseria meningitidis. PLoS One. 2011;6:e19361. https://doi.org/10.1371/journal.pone.0019361
23. Jordens JZ, Heckels JE. A novel porA-based real-time PCR for detection of meningococcal carriage. J Med Microbiol. 2005;54:463–6. https://doi.org/10.1099/jmm.0.45847-0
24. Jolley KA, Brehony C, Maiden MC. Molecular typing of meningococci: recommendations for target choice and nomenclature. FEMS Microbiol Rev. 2007;31:89–96. https://doi.org/10.1111/j.1574-6976.2006.00057.x
25. Australian Bureau of Statistics. 2016 Census: Aboriginal and/or Torres Strait Islander peoples QuickStats [cited 2019 Aug 16]. https://quickstats.censusdata.abs.gov.au/census_services/getproduct/census/2016/quickstat/IQS036
26. Vossen M, Mitteregger D, Steininger C. Meningococcal pneumonia. Vaccine. 2016;34:4364–70. https://doi.org/10.1016/j.vaccine.2016.07.013
27. Romero-Gomez MP, Rentero Z, Paño JR, Mingorance J. Bacteraemic pneumonia caused by *Neisseria meningitidis* serogroup Y. Respir Med Case Rep. 2012;5:23–4. https://doi.org/10.1016/j.rmedc.2011.11.005
28. Centre for Disease Control. Meningococcal disease: signs and symptoms [cited 2019 Aug 22]. https://www.cdc.gov/meningococcal/about/symptoms.html
29. Gaschignard J, Levy C, Deghmane AE, Dubos F, Muszlak M, Cohen R, et al. Invasive serogroup w meningococcal disease in children: a national survey from 2001 to 2008 in France. Pediatr Infect Dis J. 2013;32:798–800. https://doi.org/10.1097/INF.0b013e31828e9e91
30. Communicable Diseases Network Australia. Invasive meningococcal disease CDNA national guidelines for public health units, 2017 [cited 2019 Aug 22]. https://www1.health.gov.au/internet/main/publishing.nsf/Content/0A31EEC4953B7E6FCA257DA3000D19DD/$File/IMD-SoNG.pdf
31. The Northern Territory Department of Health. Brief for the meningococcal outbreak task force. Darwin: The Department; 2018.
32. Australian Government Department of Health. Meningococcal disease (invasive) public dataset. National Notifiable Diseases Surveillance System [cited 2019 Aug 13]. http://www9.health.gov.au/cda/source/pub_menin.cfm

33. PubMLST. Neisseria profile/sequence definitions database [cited 2019 Aug 15]. https://pubmlst.org/bigsdb?db=pubmlst_neisseria_seqdef
34. Rosenstein NE, Perkins BA, Stephens DS, Lefkowitz L, Cartter ML, Danila R, et al. The changing epidemiology of meningococcal disease in the United States, 1992–1996. J Infect Dis. 1999;180:1894–901. https://doi.org/10.1086/315158
35. Rosenstein NE, Perkins BA, Stephens DS, Popovic T, Hughes JM. Meningococcal disease. N Engl J Med. 2001; 344:1378–88. https://doi.org/10.1056/NEJM200105033441807
36. Harley D, Hanna JN, Hills SL, Bates JR, Smith HV. Epidemiology of invasive meningococcal disease in north Queensland, 1995 to 1999. Commun Dis Intell Q Rep. 2002; 26:44–50.
37. Massey P, Durrheim D. Aboriginal and Torres Strait Islander peoples at higher risk of invasive meningococcal disease in NSW. N S W Public Health Bull. 2008;19:100–3. https://doi.org/10.1071/NB07047
38. Australian Government. Australian Institute of Health and Welfare. Vaccine preventable disease among Aboriginal and Torres Strait Islander people [cited 2019 Aug 22]. https://www.aihw.gov.au/getmedia/2fca3ed6-d242-4454-a00f-e298dd120ccb/aihw-phe-236_ATSI.pdf.aspx
39. Cuningham W, McVernon J, Lydeamore MJ, Andrews RM, Carapetis J, Kearns T, et al. High burden of infectious disease and antibiotic use in early life in Australian Aboriginal communities. Aust N Z J Public Health. 2019;43:149–55. https://doi.org/10.1111/1753-6405.12876
40. Hendrickx D, Bowen AC, Marsh JA, Carapetis JR, Walker R. Ascertaining infectious disease burden through primary care clinic attendance among young Aboriginal children living in four remote communities in Western Australia. PLoS One. 2018;13:e0203684. https://doi.org/10.1371/journal.pone.0203684
41. Parnaby MG, Carapetis JR. Rheumatic fever in indigenous Australian children. J Paediatr Child Health. 2010;46:527–33. https://doi.org/10.1111/j.1440-1754.2010.01841.x
42. Bilukha OO, Rosenstein N; National Center for Infectious Diseases, Centers for Disease Control and Prevention (CDC). Prevention and control of meningococcal disease. Recommendations of the Advisory Committee on Immunization Practices (ACIP). MMWR Recomm Rep. 2005;54:1–21.
43. Umaru ET, Ludin AN, Majid MR, Sabri S, Moses C, Enegbuma W, et al. Risk factors responsible for the spread of meningococcal meningitis. International Journal of Educational Research. 2013;1:1–30.
44. Olea A, Matute I, González C, Delgado I, Poffald L, Pedroni E, et al. Case–control study of risk factors for meningococcal disease in Chile. Emerg Infect Dis. 2017;23:1070–8. https://doi.org/10.3201/eid2307.160129
45. Ladhani SN, Beebeejaun K, Lucidarme J, Campbell H, Gray S, Kaczmarski E, et al. Increase in endemic *Neisseria meningitidis* capsular group W sequence type 11 complex associated with severe invasive disease in England and Wales. Clin Infect Dis. 2015;60:578–85. https://doi.org/ 10.1093/cid/ciu881
46. Moreno G, López D, Vergara N, Gallegos D, Advis MF, Loayza S. Clinical characterization of cases with meningococcal disease by W135 group in Chile, 2012 [in Spanish]. Rev Chilena Infectol. 2013;30:350–60.
47. Lahra MM, Enriquez R. Australian meningococcal surveillance programme annual report, 2016. Commun Dis Intell Q Rep. 2017;41:E369–82.
48. Mowlaboccus S, Jolley KA, Bray JE, Pang S, Lee YT, Bew JD, et al. Clonal expansion of new penicillin-resistant clade of Neisseria meningitidis serogroup W clonal complex 11, Australia. Emerg Infect Dis. 2017;23:1364–7. https://doi.org/10.3201/eid2308.170259
49. Goedvolk CA, von Rosenstiel IA, Bos AP. Immune complex associated complications in the subacute phase of meningococcal disease: incidence and literature review. Arch Dis Child. 2003;88:927–30. https://doi.org/10.1136/adc.88.10.927
50. Sanofi-Aventis Pte Ltd. Menactra: meningococcal (groups A,C,Y and W-135) polysaccharide diptheria toxoid conjugate vaccine Australian product information, 2011 [cited 2020 Mar 31]. https://www.menactra.com

Address for correspondence: Eva L. Sudbury, Department of Paediatrics, The University of Melbourne, The Royal Children's Hospital Melbourne, Flemington Rd, Parkville, VIC 3052, Australia; email: eva.sudbury@student.unimelb.edu.au

# Transmission of Chikungunya Virus in an Urban Slum, Brazil

Rosângela O. Anjos, Vánio André Mugabe, Patrícia S.S. Moreira, Caroline X. Carvalho, Moyra M. Portilho, Ricardo Khouri, Gielson A. Sacramento, Nivison R.R. Nery Jr., Mitermayer G. Reis, Uriel D. Kitron, Albert I. Ko, Federico Costa, Guilherme S. Ribeiro

After a chikungunya outbreak in Salvador, Brazil, we performed a cross-sectional, community-based study of 1,776 inhabitants to determine chikungunya virus (CHIKV) seroprevalence, identify factors associated with exposure, and estimate the symptomatic infection rate. From November 2016 through February 2017, we collected sociodemographic and clinical data by interview and tested serum samples for CHIKV IgG. CHIKV seroprevalence was 11.8% (95% CI 9.8%–13.7%), and 15.3% of seropositive persons reported an episode of fever and arthralgia. Infections were independently and positively associated with residences served by unpaved streets, a presumptive clinical diagnosis of chikungunya, and recall of an episode of fever with arthralgia in 2015–2016. Our findings indicate that the chikungunya outbreak in Salvador may not have conferred sufficient herd immunity to preclude epidemics in the near future. The unusually low frequency of symptomatic disease points to a need for further longitudinal studies to better investigate these findings.

In the 21st century, chikungunya virus (CHIKV) has emerged as a mosquitoborne disease of global relevance, causing large epidemics because of its widespread dissemination in tropical and subtropical areas (*1*). Infected persons usually develop an acute febrile illness associated with joint pains, myalgia, headache, and other signs and symptoms that can lead to misdiagnosis with other arboviral illnesses, such as dengue virus (DENV) and Zika virus (ZIKV) infections. Noteworthy with chikungunya, the arthralgia is often severely debilitating and may last for months to years (*1*,*2*).

After the introduction of CHIKV into the Caribbean region in 2013, the virus spread rapidly, causing large outbreaks (*3*,*4*). In certain Caribbean islands, such as Puerto Rico and the US Virgin Islands, the rate at which CHIKV infection was symptomatic was estimated at >70% (*5*,*6*). However, it remains unclear whether the attack rates in outbreaks in large population centers in the Americas created sufficiently high levels of herd immunity to preclude subsequent epidemics. Furthermore, 2 CHIKV strains were introduced and are cocirculating in the Americas; it is unclear whether the proportions of symptomatic infections differ on the basis of strain type, population, or region.

In Brazil, CHIKV was first detected in September 2014, almost simultaneously in the cities of Oiapoque, in the northern state of Amapá, where the Asian genotype was implicated (*7*), and in Feira de Santana, in the northeast state of Bahia, where the East/Central/South African (ECSA) genotype was detected (*7*,*8*). The virus spread rapidly throughout the country, reaching all states by 2015 (*9*), and peaked in 2016, when ≈280,000 probable cases were recorded (*10*). The northeast region was the most affected by CHIKV (*9*,*10*,*11*); this same area was also the most affected by ZIKV in 2015–2016 (*12*,*13*).

In Salvador (population 2.9 million [*14*]), the capital of Bahia state, which is located ≈100 km from Feira de Santana, we retrospectively identified that CHIKV had been circulating since September 2014 (*15*), but outbreaks first occurred between June and November 2015 (*12*,*15*). In this study, we used the prevalence of CHIKV IgG as an indicator of all (i.e., symptomatic and asymptomatic) previous infection in a slum

Author affiliations: Fundação Oswaldo Cruz, Salvador, Brazil (R.O. Anjos, P.S.S. Moreira, C.X. Carvalho, M.M. Portilho, R. Khouri, G.A. Sacramento, N.R.R. Nery Jr., M.G. Reis, U.D. Kitron, A.I. Ko, F. Costa, G.S. Ribeiro); Universidade Licungo, Quelimane, Mozambique (V.A. Mugabe); Universidade Federal da Bahia, Salvador (V.A. Mugabe, R. Khouri, N.R.R. Nery Jr., M.G. Reis, F. Costa, G.S. Ribeiro); Yale University, New Haven, Connecticut, USA (M.G. Reis, A.I. Ko, F. Costa); Emory University, Atlanta, Georgia, USA (U.D. Kitron); University of Liverpool, Liverpool, UK (F. Costa); Lancaster University, Lancaster, UK (F. Costa)

DOI: https://doi.org/10.3201/eid2607.190846

community of Salvador and assessed the proportion of cases in which these infections were symptomatic. In addition, we investigated factors potentially associated with prior CHIKV infection.

## Methods

### Study Site and Participant Selection

We performed a cross-sectional study in Pau da Lima, a poor community in Salvador characterized by high population density and substandard sanitation infrastructure (*16*,*17*). Since 2003, this community has been the site for several studies aiming to determine the epidemiology and the transmission dynamics of leptospirosis (*17*–*19*), dengue, and other arboviral diseases (*15*,*16*,*20*,*21*), as well as the burden of chronic noncommunicable diseases on the community and its residents (*22*,*23*). Detailed information about the sociodemographics of the Pau da Lima community, environment, and urban infrastructure has been previously described in these studies.

We surveyed the residents of 3 contiguous valleys in Pau da Lima from November 2016 through February 2017. During the enrollment process, we visited all households in the study site and invited all residents ≥5 years of age who slept ≥3 nights per week in the house to participate.

### Data Collection

We used a standardized questionnaire during household visits to obtain data on participant demographic and socioeconomic conditions. Data collected were age, sex, self-reported skin color, education level, occupation or work, household per capita income, material of housing walls (wood or other material that is not brickwork, plastered or not plastered), quality of streets accessing house (paved or unpaved), and number of residents per household (Appendix, https://wwwnc.cdc.gov/EID/article/26/7/19-0846-App1.pdf). We also collected self-reported data on prior presumptive clinical diagnosis of DENV, ZIKV, and CHIKV infection and on history of fever, arthralgia, myalgia, rash, and pruritus, at any time after January 2015. This information covered health effects from the period immediately before and after the peak of CHIKV transmission in Salvador, which occurred during June–November 2015 (*12*,*15*). We recorded the duration of arthralgia among participants who reported this symptom. We conducted the interviews on computer tablets and used Research Electronic Data Capture software (REDCap; https://projectredcap.org/software/) to store the data (*24*).

### Serologic Evaluation

During the household visits, we collected 10 mL of blood from each participant and transported the samples on the same day, stored at 2°C–8°C, to our laboratory at the Instituto Gonçalo Moniz, Fundação Oswaldo Cruz, in Salvador. We centrifuged the samples to obtain serum, which we aliquoted and stored at -20°C until evaluation. We tested serum samples by using the IgG ELISA technique (Euroimmun, https://www.euroimmun.com) to detect specific CHIKV IgG.

For samples showing positive results for IgG, we then tested with a CHIKV IgM ELISA (InBios, https://inbios.com); we used the presence of IgM as a proxy for a more recent CHIKV infection than if there were no IgM. We interpreted both the CHIKV IgG and IgM ELISA results according to manufacturer instructions: CHIKV IgG absorbance/calibrator levels were negative at <0.8, indeterminate at ≥0.8 to <1.1, and positive at ≥1.1; CHIKV IgM absorbance/calibrator levels were negative at <0.9, indeterminate at ≥0.9 to <1.1, and positive at ≥1.1. We retested samples indicating indeterminant results on the initial test and considered the results obtained final.

To confirm the accuracy of results from the IgG ELISA, we performed a blind plaque-reduction neutralization test (PRNT) of a stratified random sample of 60 serum samples (30 positive and 30 negative from the CHIKV IgG ELISA) for CHIKV to determine ≥90% reductions in plaque counts ($PRNT_{90}$), as described elsewhere (*25*). To investigate whether cryoglobulinemia could have reduced the sensitivity of the IgG ELISA, we retested 100 samples, randomly selected from those that had been IgG negative, using a prewarmed (2 h at 37°C) and centrifuge protocol (*26*).

### Data Analysis

We used absolute and relative frequencies or medians and interquartile ranges (IQR) to characterize the sociodemographics and also reported presumptive diagnoses and history of symptoms of study participants. We used $\chi^2$ or Wilcoxon rank-sum tests to compare the sex and age distribution for those who did agree to be enrolled in the study with the distribution for those who did not. We used a 2-tailed p value of <0.05 to define statistically significant differences.

We calculated the prevalence of CHIKV IgG overall and according to participants' characteristics and categorized continuous variables so we could estimate CHIKV seroprevalence by groups. We stratified age into ranges of 5–14 years, 15–39 years, and ≥40 years to account for the disproportionately young average age of the sample; we characterized education level as illiterate for participants who had

never studied and literate for participants who had studied ≥1 year. We determined those living in poverty using the World Bank's criteria for poverty in upper-middle-income countries of ≤$5.50/day (US dollars) per capita household income (*27*). We obtained 95% CIs for the prevalence measures, adjusting them for the design effect of sampling households as clusters.

We used bivariate and multivariate Poisson regression models with robust variance and adjustment for design effect to verify associations between previous CHIKV infection and the sociodemographic and clinical characteristics of participants. We calculated prevalence ratios with 95% CIs and included all variables that had bivariate analyses with a p value <0.20 in the multivariate analyses. We then used a backward selection method to build 2 final multivariate models, retaining variables with a p value <0.05. The first model included only sociodemographic variables to investigate their role in CHIKV infection, whereas the second model included only clinical characteristics to address their capacity to predict a positive serologic result.

Among the participants with a positive CHIKV IgG ELISA, we estimated the frequencies of symptomatic CHIKV infection by calculating the proportion of those who reported fever simultaneously accompanied by arthralgia after January 2015, likely recent CHIKV infection by calculating the proportion of those with a positive IgM test result, and presumptive clinical suspicion of chikungunya by calculating the proportion of those who reported having received that diagnosis. Wilcoxon rank-sum test was used to compare the median duration of arthralgia between those reporting arthralgia accompanied by fever and those reporting only arthralgia. Poisson regression models with robust variance, adjusted for design effect, were used to compare sociodemographic and clinical characteristics between participants with symptomatic CHIKV infections and those with asymptomatic infections and between participants with likely recent and those with likely nonrecent CHIKV infections. We set a two-tailed p value <0.05 to define statistically significant differences. We performed data analysis using Stata version 14 software (StataCorp, https://www.stata.com) (*28*).

### Ethics Considerations

This study was approved by the Research Ethics Committee of Gonçalo Moniz Institute, Oswaldo Cruz Foundation (CAAE n° 55904616.4.0000.0040). Before any study procedure, all participants ≥18 years of age signed an informed consent form; those <18 years of age who were able to read signed an informed assent, with their parents providing a signed consent.

## Results

### Participants Characteristics

Among the 2,651 eligible residents in the study site, 1,776 (67.0%) agreed to participate in this study. Those who consented were younger than those who refused (median age 26 years [IQR 16–40] vs. 35 years [IQR 21–46]; p <0.01). Of those who consented, a greater proportion were female (57.0%) than those who did not consent (52.0%; p<0.01). Most participants had a nonwhite (black or mixed) skin color (93.8%), lived in a household with a per capita income ≤$5.50/day (US dollars) (80.8%), and had not completed elementary school education (59.0%) or were illiterate (4.3%).

### Prevalence of Previous CHIKV Infection and Associated Factors

Among the 1,772 (99.8%) participants from whom we collected and tested a blood sample, 209 (11.8%, 95% CI 9.8%–13.7%) had had a previous CHIKV infection, as determined by the detection of CHIKV IgG. Of the 30 random IgG ELISA positive samples tested by CHIKV $PRNT_{90}$, 27 (90%) were positive; of the 30 random IgG-negative samples, all were also negative in $PRNT_{90}$ (agreement 95%; kappa 90%). Of the 100 IgG-negative samples that we retested to evaluate whether cryoglobulinemia had reduced ELISA sensitivity, 2 (2%) returned positive results, but these results had low absorbance/calibrator levels (1.11 and 1.15) compared with those observed for the 209 positive samples (median 3.53, IQR 3.11–3.82).

In bivariate analyses, prevalence of previous CHIKV infection did not differ by sex, skin color, poverty level, or number of residents per household (Table 1). However, we found a statistically significant association with other indicators of socioeconomic status, residing on unpaved streets and living in houses whose walls were unplastered or were made of wood or other materials; in addition, we found a nonsignificant trend of greater prevalence among participants who were older, illiterate, or reported not working (Table 1). Furthermore, the prevalence of previous CHIKV infection was statistically greater for participants who had received a presumptive clinical diagnosis of an infection by any of 3 cocirculating arboviruses—CHIKV, DENV, or ZIKV—and for those who reported having symptoms compatible with an arboviral infection—fever with arthralgia, myalgia, rash, or pruritus—after January 2015, when CHIKV emerged in Salvador (Table 1).

The only sociodemographic characteristic associated with previous CHIKV infection in the multiple variable analyses was residence on an unpaved street (prevalence ratio [PR] 1.52, 95% CI 1.07–2.15) (Table 2). In addition, independent clinical predictors for previous CHIKV infection included recall of a presumptive medical diagnosis of chikungunya (PR 2.83, 95% CI 1.97–4.05) and report of an episode of fever

**Table 1.** Prevalence of previous chikungunya virus infection, determined by detection of IgG, by demographic and clinical characteristics, Salvador, Brazil, November 2016–February 2017

| Characteristic | No. participants | No. positive (prevalence, %) | p value |
|---|---|---|---|
| Sociodemographic | | | |
| Sex | | | |
| M | 761 | 93 (12.2) | 0.60 |
| F | 1,011 | 116 (11.5) | |
| Age, y | | | |
| 5–14 | 396 | 41 (8.1) | 0.35 |
| 15–39 | 921 | 104 (11.9) | |
| ≥40 | 455 | 63 (14.9) | |
| Skin color | | | |
| Nonwhite | 1,662 | 199 (12.0) | 0.39 |
| White | 110 | 10 (9.1) | |
| Household per capita income in US$/day* | | | |
| ≤5.50 | 1,429 | 171 (12.0) | 0.69 |
| >5.50 | 340 | 37 (10.9) | |
| Education | | | |
| Illiterate | 76 | 14 (18.4) | 0.06 |
| Literate | 1,696 | 195 (11.5) | |
| Occupation/work | | | |
| Yes | 604 | 60 (9.9) | 0.08 |
| No | 1,164 | 148 (12.7) | |
| Residence located in an unpaved street | | | |
| Yes | 1,003 | 139 (13.9) | 0.02 |
| No | 767 | 70 (9.1) | |
| Type of residence construction | | | |
| Plastered wall | 1,447 | 154 (10.6) | 0.04 |
| Unplastered wall | 211 | 33 (15.6) | |
| Wood or other material | 106 | 21 (19.8) | |
| Residents per household | | | |
| 1 | 145 | 13 (9.0) | 0.31 |
| 2–3 | 676 | 89 (13.2) | |
| 4–5 | 608 | 60 (9.0) | |
| ≥6 | 340 | 5 (13.5) | |
| Clinical: reported symptoms† | | | |
| Fever and arthralgia | | | |
| None | 1,212 | 111 (9.2) | <0.01 |
| Only fever | 322 | 38 (11.8) | |
| Only arthralgia | 89 | 20 (22.5) | |
| Both, not simultaneous | 40 | 7 (17.5) | |
| Both, simultaneous | 96 | 32 (33.3) | |
| Myalgia | | | |
| Yes | 222 | 42 (18.9) | <0.01 |
| No | 1,548 | 167 (10.8) | |
| Rash | | | |
| Yes | 216 | 50 (23.2) | <0.01 |
| No | 1,554 | 158 (10.2) | |
| Pruritus | | | |
| Yes | 206 | 46 (22.3) | <0.01 |
| No | 1,563 | 163 (10.4) | |
| Presumptive clinical diagnosis | | | |
| Chikungunya | | | |
| Yes | 48 | 24 (50.0) | <0.01 |
| No | 1,724 | 185 (10.7) | |
| Dengue | | | |
| Yes | 111 | 21 (18.9) | 0.02 |
| No | 1,661 | 188 (11.3) | |
| Zika | | | |
| Yes | 147 | 38 (25.9) | <0.01 |
| No | 1,625 | 171 (10.5) | |

*Data not shown for 3 participants.
†Reported symptoms with onset after January 2015.

**Table 2.** Crude and adjusted prevalence ratios for persons with previous chikungunya virus infection, by demographic and clinical characteristics, Salvador, Brazil, November 2016–February 2017

| Characteristic | Crude prevalence ratio (95% CI)* | Adjusted prevalence ratio (95% CI)† |
|---|---|---|
| Sociodemographic | | Model 1 |
| Illiteracy | 1.60 (0.99–2.60) | |
| Not working | 1.28 (0.97–1.68) | |
| Residence located in an unpaved street | 1.52 (1.07–2.15) | 1.52 (1.07–2.15) |
| Type of residence construction | | |
| Plastered wall | Referent | |
| Unplastered wall | 1.47 (0.92–2.35) | |
| Wood/Other material | 1.86 (1.06–3.28) | |
| Clinical: reported symptoms‡ | | Model 2 |
| Fever and arthralgia | | |
| None | Referent | Referent |
| Only fever | 1.29 (0.89–1.86) | 0.96 (0.62–1.49) |
| Only arthralgia | 2.45 (1.60–3.75) | 1.55 (0.95–2.53) |
| Both, not simultaneous | 1.91 (0.97–3.77) | 1.22 (0.56–2.67) |
| Both, simultaneous | 3.64 (2.51–5.28) | 2.26 (1.43–3.57) |
| Myalgia | 1.75 (1.23–2.50) | |
| Rash | 2.28 (1.68–3.08) | |
| Pruritus | 2.14 (1.51–3.03) | |
| Presumptive clinical diagnosis | | |
| Chikungunya | 4.66 (3.35–6.48) | 2.83 (1.97–4.05) |
| Dengue | 1.67 (1.09–2.56) | |
| Zika | 2.45 (1.78–3.39) | |

*Crude prevalence ratios shown for variables with bivariate p values <0.20, selected for inclusion in the initial multiple variable model.
†Two different multiple variable models were applied using backward selection. The first model included only sociodemographic variables to investigate potential exposures associated with CHIKV infection; the second model included only clinical characteristics to investigate predictors of seropositivity.
‡Reported symptoms with onset after January 2015.

with arthralgia (PR 2.26, 95% CI 1.43–3.57) after January 2015, but not for separate episodes of fever or arthralgia (Table 2).

### Frequency of Symptomatic Infections among Participants with CHIKV IgG

Of the 209 participants with detected CHIKV IgG, 32 (15.3%) recalled an episode of fever and arthralgia after January 2015. The median duration of arthralgia for these 32 positive participants was 5 (IQR 3–9) days; the longest duration was 60 days for 1 person. Participants with symptomatic infection tended to be older (p = 0.07); more frequently reported other clinical manifestations compatible with CHIKV infection, such as myalgia, rash, and pruritus (p<0.01 for each symptom); and more commonly received a presumptive clinical diagnosis of chikungunya or Zika (p<0.01 for both) but not of dengue (p = 0.62) (Table 3).

### Frequency of Presumptive Clinical Diagnosis of Chikungunya

Among the 209 participants with a previous CHIKV infection, 24 (11.5%) reported receiving a clinical presumptive diagnosis of chikungunya. Although low, this frequency was 7.5 (95% CI 4.3–12.9) times greater than the 1.5% (24/1,563) frequency among the participants who were negative for CHIKV IgG (p<0.01). Noteworthy for the 32 CHIKV-infected participants who had symptomatic disease, 20 (62.5%) reported a presumptive clinical diagnosis of chikungunya (Table 3). On the other hand, of the 48 participants who reported having received a clinical presumptive diagnosis of chikungunya, 24 had CHIKV IgG detected, indicating a positive predictive value of 50% for the presumptive diagnosis.

### Frequency of CHIKV IgM

Among the 209 participants who were positive for CHIKV IgG, 49 (23.4%) also had CHIKV IgM, possibly indicating a recent infection. We found no associations between sociodemographic or clinical characteristics and the presence of CHIKV IgM (data not shown).

## Discussion

Despite retrospective evidence of a chikungunya outbreak in Salvador during June–November 2015 (*12*,*15*), we found that ≈2 years later (November 2016–February 2017), <12% of the subjects enrolled in this large cross-sectional neighborhood survey had been infected by CHIKV. This seroprevalence is much lower than that found in 3 additional CHIKV serologic surveys performed in Brazil at that time. During November–December 2015, in Feira de Santana, ≈100 km from Salvador, the prevalence of prior CHIKV infection was estimated at 57.1%; in the urban area of Riachão do Jacuípe, 185 km from Salvador, prevalence was estimated at 45.7% (*29*). In the rural area of Riachão do Jacuípe, the prevalence of prior CHIKV

infection was 20.0% in April 2016 (*30*). It is unlikely that a gradual decrease in the IgG levels over time influenced these differences, because we surveyed the participants relatively soon after the outbreak. Thus, the wide range of prevalence levels in adjacent cities most possibly indicates that the intensity of CHIKV transmission, after its first introduction, may vary greatly even among relatively close locations.

Serum surveys performed in Haiti during December 2014 and February 2015, about 1 year after detection of the index case in the country, also found large variations in the seroprevalence (mean of 78.4% for the urban sites and 44.9% for the rural sites) (*31*). These differences may be related to *Aedes* spp. infestation levels and diversity, variations in local geographic and climate conditions, the predominant CHIKV strain circulating, and even by interactions when the vector species may be coinfected with CHIKV and other circulating arboviruses, such as ZIKV and DENV. Furthermore, a very localized and self-restricted CHIKV outbreak has been recently described in Salvador (*32*), which suggests that local environmental characteristics and patterns of human activity and movement in specific regions may be responsible for the emergence of CHIKV and the extent of its spread.

**Table 3.** Comparison of sociodemographic and clinical characteristic of participants with symptomatic versus asymptomatic chikungunya virus infection Salvador, Brazil, November 2016 to February 2017*

| Characteristic | Disease status of infected participants, no. %† | | p value |
|---|---|---|---|
| | Symptomatic, n = 32 | Asymptomatic, n = 177 | |
| Sociodemographic | | | |
| Sex | | | |
| M | 12 (37.5) | 81 (45.8) | 0.39 |
| F | 20 (62.5) | 96 (54.2) | |
| Age, y | | | |
| 5–14 | 2 (6.3) | 40 (22.6) | 0.07 |
| 15–39 | 22 (68.8) | 82 (46.3) | |
| ≥40 | 8 (24.9) | 55 (31.1) | |
| Education‡ | | | |
| Illiterate | 1 (3.1) | 13 (7.4) | 0.42 |
| Literate | 31 (96.9) | 163 (92.6) | |
| Skin color | | | |
| White | 0 | 10 (5.7) | NA |
| Nonwhite | 32 (100) | 167 (94.3) | |
| Household per capita income, US$/day‡ | | | |
| ≤5.50 | 27 (84.4) | 144 (81.8) | 0.73 |
| >5.50 | 5 (15.6) | 32 (18.2) | |
| Clinical: reported symptoms | | | |
| Fever and arthralgia | | | |
| None | 0 | 111 (62.7) | <0.01 |
| Only fever | 0 | 39 (22.0) | |
| Only arthralgia | 0 | 20 (11.3) | |
| Both, not simultaneous | 0 | 7 (4.0) | |
| Both, simultaneous | 32 (100) | 0 | |
| Myalgia | | | |
| Yes | 18 (56.3) | 24 (13.6) | <0.01 |
| No | 14 (43.7) | 153 (86.4) | |
| Rash | | | |
| Yes | 22 (68.7) | 28 (15.9) | <0.01 |
| No | 10 (31.3) | 148 (84.1) | |
| Pruritus | | | |
| Yes | 21 (65.6) | 25 (14.1) | <0.01 |
| No | 11 (34.4) | 152 (85.9) | |
| Presumptive clinical diagnosis | | | |
| Chikungunya | | | |
| Yes | 20 (62.5) | 12 (6.8) | <0.01 |
| No | 12 (37.5) | 165 (93.2) | |
| Dengue | | | |
| Yes | 4 (12.5) | 17 (9.6) | 0.62 |
| No | 28 (87.5) | 160 (90.4) | |
| Zika | | | |
| Yes | 18 (56.3) | 20 (11.3) | <0.01 |
| No | 14 (43.7) | 157 (88.7%) | |

*NA, not available
†CHIKV disease status was defined as symptomatic on the basis of self-reported fever accompanied by arthralgia after January 2015.
‡Data not available for 1 participant with an asymptomatic CHIKV infection.

In bivariate analyses, we found that structural deficiencies in the housing and on the streets where the houses were located were associated with previous CHIKV infection, pointing to a social gradient that poses an increased risk for virus exposure among the most vulnerable residents. Urban areas served by unpaved streets and where the walls of houses are not plastered, or made of wood or of other material other than brick, often also lack basic sanitation services, such as regular garbage collection and potable water. These conditions, in turn, influence improper disposal of trash and accumulation of water in containers, both well-known breeding grounds for *Aedes* mosquitoes.

In addition, low education levels in such settings may limit residents' ability to access, understand, and act on information about measures to prevent mosquitoborne diseases (*33*,*34*). Individual- and ecologic-level studies in rural Kenya (*35*), Nicaragua (*36*), and Colombia (*37*) have also showed that socioeconomic vulnerability and living near sites where water accumulates are associated with increased chikungunya incidence.

The widely accepted understanding of CHIKV infection has been that the majority (>70%) of infected persons develop a symptomatic form of the disease (*1*). We, conversely, found a frequency of symptomatic infection, defined by having arthralgia accompanied by fever, of only 15.3%. Other studies have also found low proportions of symptomatic CHIKV infection. In Brazil, serologic surveys estimated the proportion of symptomatic CHIKV infection to be 32.7% in Feira de Santana and 41.2% in Riachão do Jacuípe (*29*). Prospective cohort studies, a more robust study design for determining the natural history of disease, have also found low proportions of symptomatic infections. For example, during a cohort follow-up in the Philippines, the subclinical incidence of CHIKV infection was 10.0 per 100 person-years, while the incidence of symptomatic CHIKV infection was 2.2 per 100 person-years, indicating that <20% of those infected exhibited symptoms (*38*). However, because of the small geographic range of the studies, these findings should be considered limited.

Differences in symptomatic infection rates may be related to the lineage of CHIKV that is circulating (*39*,*40*), the diversity in human immunological responses driven by specific genetic characteristics (*41*), or even by the CHIKV exposure dose delivered by mosquitoes (*42*). In our study, we found that both women and persons ≥15 years of age were more likely to have symptomatic CHIKV infections than others, but the power of our analyses was limited by the small number of CHIKV infections that we detected. However, our results are in accordance with other studies that suggest that women are at increased risk for symptomatic disease and that risk for symptomatic disease increases with age (*29*). Further cohort studies are needed to determine the factors that may influence whether the infection becomes symptomatic. We also found that chronic arthralgia after CHIKV infection was uncommon; the maximum reported duration for the articular pain was 60 days, observed in just 1 (0.5%) of the 209 CHIKV-infected persons.

On the basis of these findings, we hypothesize that asymptomatic and milder clinical manifestations with less severe arthralgia and low rates of the disease becoming chronic may occur under certain circumstances of CHIKV infection. If further investigation supports this hypothesis, this finding might partially explain the low proportion of participants testing positive for CHIKV who received a correct presumptive diagnosis.

We did find that report of a presumptive clinical diagnosis of chikungunya disease was strongly associated with having CHIKV IgG (positive predictive value of 50%). Thus, during and after outbreaks, persons exhibiting CHIKV-associated symptoms and suspected disease should be clinically tested because of the likelihood of having confirmed chikungunya disease.

Our study findings have limitations. First, we surveyed just 1 neighborhood of Salvador and, thus, could not capture potential variations in prior exposure to CHIKV within the city. However, because the community where we conducted the study has poor sanitation infrastructure, which is associated with a higher density of *Aedes aegypti* mosquitoes, and high population density, associated with greater risk of arboviral transmission, it is unlikely that the CHIKV seroprevalence of the city population overall was much higher than the one we measured in the Pau da Lima community.

Second, we used a commercial CHIKV IgG ELISA to detect previous CHIKV infections. Prior studies have reported high accuracy levels for this test (sensitivity 88%–100%, specificity 82%–95% (*43*,*44*). In our ELISA retesting of 100 IgG negative samples, we found that cryoglobulinemia likely did not influence our seroprevalence; moreover, we found an excellent agreement between the IgG ELISA and the $PRNT_{90}$. However, because cryoglobulinemia had been described for CHIKV (*45*), further surveys should consider this possible effect.

Third, although transmission of other alphaviruses, such as Mayaro and o'nyong-nyong, has not been reported in northeastern Brazil, because we

did not perform $PRNT_{90}$ for other alphaviruses, we cannot completely rule out the possibility of cross-reactions. In addition, it has been shown that IgG seroconversion might not occur or may occur at later stages after CHIKV infection, possibly due to a strong and longlasting CHIKV IgM immune response (*46*). It is possible that this diagnostic limitation hampered detection of some cases of CHIKV infection, especially those occurring shortly before the survey was conducted.

Fourth, the proportion of symptomatic infections may have been underestimated because of the 2-year gap between the chikungunya outbreak in Salvador and when the study was conducted and because we did not consider those reporting only fever or only arthralgia to have symptomatic disease. Thus, the observed symptomatic rate from our study should be considered a minimum level. Last, the cross-sectional design made it difficult to determine the temporal relation between exposures to risk and occurrence of CHIKV infection.

In summary, our findings suggest that although CHIKV and ZIKV both spread through Salvador in the same year, 2015 (*12*,*15*,*47*), transmission of CHIKV seems to have been much less intense, reaching ≈12% of the population, compared to estimates of 63%–73% for ZIKV (*22*,*48*). Viral competition within hosts and vectors may be a key element in explaining this dynamic. Further comparative studies on immunopathogenesis and vectorial competence are needed to clarify why these 2 arboviruses, transmitted by the same mosquito vectors, presented such different patterns of transmission spread, given that the population was completely naive for both of them.

Our findings also show that other parts of Brazil and the Americas may be largely susceptible to CHIKV transmission. It is thus necessary to maintain surveillance to promptly detect further epidemics and to invest in developing and evaluating target interventions, such as vaccines and novel approaches for vector control, that will help protect the population from CHIKV and other arboviral infections.

#### Acknowledgments

We thank the study participants and the community leaders from the Pau da Lima Urban Health Council who provided support for the investigation and the team members from Fundação Oswaldo Cruz (especially Perla Santana, Renan Rosa, Paula Sousa Barbosa, Leile Camila Jacob Nascimento, and Isabele de Pádua Carvalho), who participated in the data collection, laboratory experiments, or provided assistance with data management and administrative matters.

This study was supported by the Brazilian National Council for Scientific and Technological Development (grants 400830/2013-2, 440891/2016-7, and 421522/2016-0 to G.S.R., grant 439967/2016-3 to R.K., and scholarships to M.G.R., U.K., and G.S.R.); the Coordination for the Improvement of Higher Education Personnel, Brazilian Ministry of Education (grant 88887.130746/2016-00 to G.S.R.); the Research Support Foundation for the State of Bahía (grant FAPESB PET0022/2016 to G.S.R.); the US National Institutes of Health (grants NIAID 5 R01 AI121207, FIC 5 R01 TW009504, FIC 5 R25 TW009338, and NIAID 5 U01 AI088752 to A.I.K.); the Wellcome Trust (102330/Z/13/Z to F.C.); the Yale School of Public Health; the Oswaldo Cruz Foundation; the Federal University of Bahia; and the Department of Science and Technology, Secretariat of Science, Technology and Strategic Inputs, Brazilian Ministry of Health.

### About the Author

Ms. Anjos is a nurse with a master of science degree and is a PhD candidate at the Fundação Oswaldo Cruz, Salvador, Brazil. Her primary research interests are epidemiology of arboviruses and infectious diseases of global relevance.

#### References

1. Weaver SC, Lecuit M. Chikungunya virus and the global spread of a mosquito-borne disease. N Engl J Med. 2015;372:1231–9. https://doi.org/10.1056/NEJMra1406035
2. Thiberville SD, Moyen N, Dupuis-Maguiraga L, Nougairede A, Gould EA, Roques P, et al. Chikungunya fever: epidemiology, clinical syndrome, pathogenesis and therapy. Antiviral Res. 2013;99:345–70. https://doi.org/10.1016/j.antiviral.2013.06.009
3. Fischer M, Staples JE, Arboviral Diseases Branch, National Center for Emerging and Zoonotic Infectious Diseases, CDC. Chikungunya virus spreads in the Americas—Caribbean and South America, 2013–2014. MMWR Morb Mortal Wkly Rep. 2014;63:500–1.
4. Gallian P, Leparc-Goffart I, Richard P, Maire F, Flusin O, Djoudi R, et al. Epidemiology of chikungunya virus outbreaks in Guadeloupe and Martinique, 2014: an observational study in volunteer blood donors. PLoS Negl Trop Dis. 2017;11:e0005254. https://doi.org/10.1371/journal.pntd.0005254
5. Sharp TM, Roth NM, Torres J, Ryff KR, Rodríguez NMP, Mercado C, et al. Chikungunya cases identified through passive surveillance and household investigations—Puerto Rico, May 5–August 12, 2014. MMWR Morb Mortal Wkly Rep. 2014;63:1121–8.
6. Hennessey MJ, Ellis EM, Delorey MJ, Panella AJ, Kosoy OI, Kirking HL, et al. Seroprevalence and symptomatic attack rate of chikungunya virus infection, United States Virgin Islands, 2014–2015. Am J Trop Med Hyg. 2018;99:1321–6. https://doi.org/10.4269/ajtmh.18-0437
7. Nunes MRT, Faria NR, de Vasconcelos JM, Golding N, Kraemer MU, de Oliveira LF, et al. Emergence and potential for spread of chikungunya virus in Brazil. BMC Med. 2015;13:102. https://doi.org/10.1186/s12916-015-0348-x

8. Teixeira MG, Andrade AMS, Costa MC, Castro JN, Oliveira FLS, Goes CSB, et al. East/Central/South African genotype chikungunya virus, Brazil, 2014. Emerg Infect Dis. 2015;21:906–7. https://doi.org/10.3201/eid2105.141727
9. Secretaria de Vigilância em Saúde/Ministério da Saúde. Monitoring of cases of dengue, chikungunya fever and fever by the Zika virus until epidemiological week 49, 2016 [in Portuguese]. Vol. 47, Boletim Epidemiológico. 2016 [cited 2018 Dec 23]. https://www.saude.gov.br/images/pdf/2016/dezembro/20/2016-033---Dengue-SE49-publicacao.pdf
10. Secretaria de Vigilância em Saúde/Ministério da Saúde. Monitoring of cases of dengue, chikungunya fever and fever by the Zika virus until epidemiological week 35, 2017 [In Portuguese]. Vol. 48, Boletim Epidemiológico. 2017 [cited 2018 Dec 23]. https://www.saude.gov.br/images/pdf/2017/setembro/15/2017-028-Monitoramento-dos-casos-de-dengue--febre-de-chikungunya-e-febre-pelo-virus-Zika-ate-a-Semana-Epidemiologica-35.pdf
11. Secretaria de Vigilância em Saúde/Ministério da Saúde. Monitoring of cases of dengue, chikungunya fever and fever by the Zika virus until epidemiological week 43, 2018 [in Portuguese]. Vol. 49, Boletim Epidemiológico. 2018 [cited 2018 Dec 23]. http://portalarquivos2.saude.gov.br/images/pdf/2018/novembro/13/2018-056.pdf
12. Cardoso CW, Kikuti M, Prates APPB, Paploski IAD, Tauro LB, Silva MMO, et al. Unrecognized emergence of chikungunya virus during a Zika virus outbreak in Salvador, Brazil. PLoS Negl Trop Dis. 2017;11:e0005334. https://doi.org/10.1371/journal.pntd.0005334
13. de Oliveira WK, Carmo EH, Henriques CM, Coelho G, Vazquez E, Cortez-Escalante J, et al. Zika virus infection and associated neurologic disorders in Brazil. N Engl J Med. 2017;376:1591–3. https://doi.org/10.1056/NEJMc1608612
14. Instituto Brasileiro de Geografia e Estatística. Brazil/Bahia/Salvador. 2018 [cited 2019 Jun 5]. https://cidades.ibge.gov.br/brasil/ba/salvador/panorama
15. Silva MMO, Tauro LB, Kikuti M, Anjos RO, Santos VC, Gonçalves TSF, et al. Concomitant transmission of dengue, chikungunya and Zika viruses in Brazil: clinical and epidemiological findings from surveillance for acute febrile illness. Clin Infect Dis. 2019;69:1353–9. https://doi.org/10.1093/cid/ciy1083
16. Kikuti M, Cunha GM, Paploski IAD, Kasper AM, Silva MM, Tavares AS, et al. Spatial distribution of dengue in a Brazilian urban slum setting: role of socioeconomic gradient in disease risk. PLoS Negl Trop Dis. 2015;9:e0003937. https://doi.org/10.1371/journal.pntd.0003937
17. Reis RB, Ribeiro GS, Felzemburgh RDM, Santana FS, Mohr S, Melendez AXTO, et al. Impact of environment and social gradient on *Leptospira* infection in urban slums. PLoS Negl Trop Dis. 2008;2:e228. https://doi.org/10.1371/journal.pntd.0000228
18. Felzemburgh RDM, Ribeiro GS, Costa F, Reis RB, Hagan JE, Melendez AXTO, et al. Prospective study of leptospirosis transmission in an urban slum community: role of poor environment in repeated exposures to the *Leptospira* agent. PLoS Negl Trop Dis. 2014;8:e2927. https://doi.org/10.1371/journal.pntd.0002927
19. Hagan JE, Moraga P, Costa F, Capian N, Ribeiro GS, Wunder EA Jr, et al. Spatiotemporal determinants of urban leptospirosis transmission: four-year prospective cohort study of slum residents in Brazil. PLoS Negl Trop Dis. 2016;10:e0004275. https://doi.org/10.1371/journal.pntd.0004275
20. Rodriguez-Barraquer I, Costa F, Nascimento EJM, Nery N, Castanha PMS, Sacramento GA, et al. Impact of preexisting dengue immunity on Zika virus emergence in a dengue endemic region. Science. 2019;363:607–10. https://doi.org/10.1126/science.aav6618
21. Silva MM, Rodrigues MS, Paploski IA, Kikuti M, Kasper AM, Cruz JS, et al. Accuracy of dengue reporting by national surveillance system, Brazil. Emerg Infect Dis. 2016;22:336–9. https://doi.org/10.3201/eid2202.150495
22. Unger A, Felzemburgh RDM, Snyder RE, Ribeiro GS, Mohr S, Costa VBA, et al.; Pau da Lima Urban Health Team. Hypertension in a Brazilian urban slum population. J Urban Health. 2015;92:446–59. https://doi.org/10.1007/s11524-015-9956-1
23. Snyder RE, Rajan JV, Costa F, Lima HCAV, Calcagno JI, Couto RD, et al. Differences in the prevalence of non-communicable disease between slum dwellers and the general population in a large urban area in Brazil. Trop Med Infect Dis. 2017;2:47. https://doi.org/10.3390/tropicalmed2030047
24. Harvey LA. REDCap: web-based software for all types of data storage and collection. Spinal Cord. 2018;56:625. https://doi.org/10.1038/s41393-018-0169-9
25. Baer A, Kehn-Hall K. Viral concentration determination through plaque assays: using traditional and novel overlay systems. J Vis Exp. 2014; (93):e52065. https://doi.org/10.3791/52065
26. Kolopp-Sarda MN, Miossec P. Cryoglobulins: an update on detection, mechanisms and clinical contribution. Autoimmun Rev. 2018;17:457–64. https://doi.org/10.1016/j.autrev.2017.11.035
27. World Bank. Piecing together the poverty puzzle. 2018 [cited 2018 Dec 21]. https://openknowledge.worldbank.org/bitstream/handle/10986/30418/9781464813306.pdf
28. StataCorp. Stata Statistical Software: release 14. College Station (TX): StataCorp LP. 2015 [cited 2018 Sep 30]. https://www.stata.com
29. Dias JP, Costa MCN, Campos GS, Paixao ES, Natividade MS, Barreto FR, et al. Seroprevalence of chikungunya virus after its emergence in Brazil. Emerg Infect Dis. 2018;24:617–24. https://doi.org/10.3201/eid2404.171370
30. Cunha RV, Trinta KS, Montalbano CA, Sucupira MVF, de Lima MM, Marques E, et al. Seroprevalence of chikungunya virus in a rural community in Brazil. PLoS Negl Trop Dis. 2017;11:e0005319. https://doi.org/10.1371/journal.pntd.0005319
31. Rogier EW, Moss DM, Mace KE, Chang M, Jean SE, Bullard SM, et al. Use of bead-based serologic assay to evaluate chikungunya virus epidemic, Haiti. Emerg Infect Dis. 2018;24:995–1001. https://doi.org/10.3201/eid2406.171447
32. Tauro LB, Cardoso CW, Souza RL, Nascimento LC, Santos DRD, Campos GS, et al. A localized outbreak of chikungunya virus in Salvador, Bahia, Brazil. Mem Inst Oswaldo Cruz. 2019;114:e180597. https://doi.org/10.1590/0074-02760180597
33. Higuera-Mendieta DR, Cortés-Corrales S, Quintero J, González-Uribe C. KAP surveys and dengue control in Colombia: disentangling the effect of sociodemographic factors using multiple correspondence analysis. PLoS Negl Trop Dis. 2016;10:e0005016. https://doi.org/10.1371/journal.pntd.0005016
34. Whiteman A, Mejia A, Hernandez I, Loaiza JR. Socioeconomic and demographic predictors of resident knowledge, attitude, and practice regarding arthropod-borne viruses in Panama. BMC Public Health. 2018;18:1261. https://doi.org/10.1186/s12889-018-6172-4
35. Grossi-Soyster EN, Cook EAJ, de Glanville WA, Thomas LF, Krystosik AR, Lee J, et al. Serological and spatial analysis of

alphavirus and flavivirus prevalence and risk factors in a rural community in western Kenya. PLoS Negl Trop Dis. 2017;11:e0005998. https://doi.org/10.1371/journal.pntd.0005998s
36. Kuan G, Ramirez S, Gresh L, Ojeda S, Melendez M, Sanchez N, et al. Seroprevalence of anti-chikungunya virus antibodies in children and adults in Managua, Nicaragua, after the first chikungunya epidemic, 2014–2015. PLoS Negl Trop Dis. 2016;10:e0004773. https://doi.org/10.1371/journal.pntd.0004773
37. Krystosik AR, Curtis A, Buritica P, Ajayakumar J, Squires R, Dávalos D, et al. Community context and sub-neighborhood scale detail to explain dengue, chikungunya and Zika patterns in Cali, Colombia. PLoS One. 2017;12:e0181208. https://doi.org/10.1371/journal.pone.0181208
38. Yoon I-K, Alera MT, Lago CB, Tac-An IA, Villa D, Fernandez S, et al. High rate of subclinical chikungunya virus infection and association of neutralizing antibody with protection in a prospective cohort in the Philippines. PLoS Negl Trop Dis. 2015;9:e0003764. https://doi.org/10.1371/journal.pntd.0003764
39. Teo T-H, Her Z, Tan JJL, Lum F-M, Lee WWL, Chan Y-H, et al. Caribbean and La Réunion chikungunya virus isolates differ in their capacity to induce proinflammatory Th1 and NK cell responses and acute joint pathology. J Virol. 2015;89:7955–69. https://doi.org/10.1128/JVI.00909-15
40. Langsjoen RM, Haller SL, Roy CJ, Vinet-Oliphant H, Bergren NA, Erasmus JH, et al. Chikungunya virus strains show lineage-specific variations in virulence and cross-protective ability in murine and nonhuman primate models. MBio. 2018;9:e02449–17. https://doi.org/10.1128/mBio.02449-17
41. Chaaithanya IK, Muruganandam N, Anwesh M, Rajesh R, Ghosal SR, Kartick C, et al. HLA class II allele polymorphism in an outbreak of chikungunya fever in Middle Andaman, India. Immunology. 2013;140:202–10. https://doi.org/10.1111/imm.12128
42. Gordon A, Gresh L, Ojeda S, Chowell G, Gonzalez K, Sanchez N, et al. Differences in transmission and disease severity between 2 successive waves of chikungunya. Clin Infect Dis. 2018;67:1760–7. https://doi.org/10.1093/cid/ciy356
43. Prat CM, Flusin O, Panella A, Tenebray B, Lanciotti R, Leparc-Goffart I. Evaluation of commercially available serologic diagnostic tests for chikungunya virus. Emerg Infect Dis. 2014;20:2129–32. https://doi.org/10.3201/eid2012.141269
44. De Salazar PM, Valadere AM, Goodman CH, Johnson BW. Evaluation of three commercially-available chikungunya virus immunoglobulin G immunoassays. Rev Panam Salud Publica. 2017;41:e62. https://doi.org/10.26633/RPSP.2017.62
45. Oliver M, Grandadam M, Marimoutou C, Rogier C, Botelho-Nevers E, Tolou H, et al. Persisting mixed cryoglobulinemia in chikungunya infection. PLoS Negl Trop Dis. 2009;3:e374. https://doi.org/10.1371/journal.pntd.0000374
46. Bozza FA, Moreira-Soto A, Rockstroh A, Fischer C, Nascimento AD, Calheiros AS, et al. Differential shedding and antibody kinetics of Zika and chikungunya viruses, Brazil. Emerg Infect Dis. 2019;25:311–5. https://doi.org/10.3201/eid2502.180166
47. Cardoso CW, Paploski IAD, Kikuti M, Rodrigues MS, Silva MMO, Campos GS, et al. Outbreak of exanthematous illness associated with Zika, chikungunya, and dengue viruses, Salvador, Brazil. Emerg Infect Dis. 2015;21:2274–6. https://doi.org/10.3201/eid2112.151167
48. Netto EM, Moreira-Soto A, Pedroso C, Höser C, Funk S, Kucharski AJ, et al. High Zika virus seroprevalence in Salvador, Northeastern Brazil limits the potential for further outbreaks. MBio. 2017;8:e01390–407. https://doi.org/10.1128/mBio.01390-17

Address for correspondence: Guilherme Sousa Ribeiro. Instituto Gonçalo Moniz, Fundação Oswaldo Cruz, Rua Waldemar Falcão, 121, Candeal, 40296-710 Salvador, BA, Brazil; email: guilherme.ribeiro@bahia.fiocruz.br

# Public Health Role of Academic Medical Center in Community Outbreak of Hepatitis A, San Diego County, California, USA, 2016–2018

Minji Kang, Sarah F. Horman, Randy A. Taplitz, Brian Clay, Marlene Millen, Amy Sitapati, Frank E. Myers, Eric C. McDonald, Shira R. Abeles, Danelle R. Wallace, Sarah Stous, Francesca J. Torriani

During 2016–2018, San Diego County, California, USA, experienced one of the largest hepatitis A outbreaks in the United States in 2 decades. In close partnership with local healthcare systems, San Diego County Public Health led a public health response to the outbreak that focused on a 3-pronged strategy to vaccinate, sanitize, and educate. Healthcare systems administered nearly half of the vaccinations delivered in San Diego County. At University of California San Diego Health, the use of informatics tools assisted with the identification of at-risk populations and with vaccine delivery across outpatient and inpatient settings. In addition, acute care facilities helped prevent further disease transmission by delaying the discharge of patients with hepatitis A who were experiencing homelessness. We assessed the public health roles that acute care hospitals can play during a large community outbreak and the critical nature of ongoing collaboration between hospitals and public health systems in controlling such outbreaks.

Hepatitis A virus (HAV) is transmitted through the fecal–oral route either by person-to-person contact or by ingestion of contaminated food or water (*1*). With the availability of the hepatitis A vaccine in 1995 and the routine vaccination of children in high-incidence states (including California) since 1999 and nationally since 2006, the incidence of HAV infection has declined dramatically in the United States (*2*,*3*). Hepatitis A vaccine is highly effective; it has a seroconversion rate of ≈100% (*4*). Nevertheless, despite the substantial decline in HAV infection, sporadic cases and outbreaks continue to occur.

During 2016–2018, San Diego County, California, experienced one of the largest hepatitis A outbreaks in the United States in 2 decades (*5*). This outbreak was characterized by hepatitis A spread through person-to-person contact among persons experiencing unstable housing situations with or without illicit drug use (*5*). Since 2017, similar outbreaks have been reported in 25 states; some of the index cases in those outbreaks were linked to San Diego. As of November 1, 2019, a total of 27,634 cases, 16,679 hospitalizations, and 275 deaths have been recorded in the United States (*6*).

The public health response to the outbreak in San Diego focused on a 3-pronged strategy to vaccinate, sanitize, and educate (*7*). Local health systems, including University of California San Diego Health (UCSDH), closely and proactively collaborated with San Diego County Public Health (SDCPH) to participate in the outbreak control initiatives. We report the public health contribution of the academic medical center through the implementation of hospital-level prevention and outbreak management activities.

## Methods

### Study Setting

Our study was a retrospective review of hepatitis A diagnoses and vaccinations administered by SDCPH and UCSDH. SDCPH first declared a hepatitis A outbreak on March 8, 2017, and traced the first case to November 22, 2016 (Figure 1). The outbreak control vaccination initiatives began on March 10,

Author affiliations: University of California, San Diego, California, USA (M. Kang, S.F. Horman, R.A. Taplitz, B. Clay, M. Millen, A. Sitapati, F.E. Myers, S.R. Abeles, F.J. Torriani); County of San Diego Health and Human Services Agency, San Diego (E.C. McDonald, D.R. Wallace, S. Stous)

DOI: https://doi.org/10.3201/eid2607.191352


**Figure 1.** Timeline of hepatitis A outbreak, San Diego County, California, USA, 2017–2018. BPA, best practice advisory; ED, emergency department.

2017. SDCPH declared a public health emergency on September 1, 2017, and California health officials declared a state of emergency on October 13, 2017 (Figure 1). A declining number of cases resulted in lifting of the public health emergency on January 23, 2018. SDCPH declared the outbreak over on October 18, 2018 (*7*) (Figure 1).

UCSDH comprises 2 geographically distinct campuses within the same healthcare system. The Hillcrest campus of UCSDH is a 386-bed hospital in the urban center of the city of San Diego and is located at the epicenter of the acute hepatitis A outbreak. The Institutional Review Board at University of California San Diego reviewed this study and deemed it to be exempt from approval as a category 4 study.

### Implementation of Hospital-Level Outbreak-Control Initiatives

Hospital-level prevention and outbreak management focused on a similar strategy. The strategy comprised 3 components: vaccinate, sanitize, and educate.

#### Vaccination

Vaccination initiatives began with self-identified homeless patients seeking care at the UC San Diego Medical Center Hillcrest emergency department (ED) upon outbreak recognition in March 2017. To optimize vaccination administration, a best practice advisory (BPA), a customized alert in the electronic health records (EHR) (EpicSystems, https://www.epic.com), was constructed to flag the charts of self-identified homeless patients starting August 1, 2017. This BPA prompted providers to order the hepatitis A vaccine as described in Castillo et al. (*8*). From June 2017 through full implementation of the intervention in homeless persons in October 2017, these efforts were expanded with a second BPA, designed to identify patients with ≥1 of the following risk factors: homelessness, illicit drug use, alcohol abuse, cirrhosis, hepatitis B infection, and hepatitis C infection. This second BPA was constructed to increase preexposure vaccination efforts during inpatient hospitalizations at both campuses or when patients entered the care system in the ambulatory clinics or urgent care centers at UCSDH. Patients were not tested for HAV immunity before vaccination, but with each vaccination ordered, we reviewed the countywide vaccination registry for prior vaccinations. In addition, we contacted a subgroup of high-risk patients using the online patient portal for prioritized vaccination.

In May 2017, acute hepatitis A developed in a healthcare worker at UCSDH. The healthcare worker had provided care to several patients hospitalized with acute HAV infection and did not report any risk factors for hepatitis A other than occupational exposure. According to SDCPH, 7 additional healthcare workers acquired acute hepatitis A occupationally throughout San Diego County. Thus, healthcare personnel were deemed to be at risk, and SDCPH supported the recommendation by the UCSDH healthcare epidemiologist to offer vaccines at no charge to healthcare workers. Priority was given to healthcare providers with direct patient contact, along with environmental service workers and food handlers employed by the hospital, given the possibility of HAV transmission through ingestion of contaminated food or water. Hepatitis A vaccine and seasonal influenza vaccine were offered together as peer-to-peer vaccines during hospitalwide influenza vaccination drives, and hepatitis A vaccine was not denied to any healthcare workers requesting vaccination.

#### Sanitation

Enhanced contact precautions were implemented in patients with acute HAV infection during the outbreak period. These precautions were instituted in

the setting of difficult-to-control diarrhea in patients with HAV infection, which most likely contributed to the documented transmission to healthcare workers who had direct contact with patients. Enhanced cleaning and disinfection were applied to rooms of patients with hepatitis A. Given some data suggesting that quaternary ammonium compounds provide insufficient virucidal disinfection (*9*), rooms occupied by patients with hepatitis A were cleaned daily with chlorine bleach products using the same disinfection procedures used for rooms occupied by patients with *Clostridioides difficile* infection. Potluck meals on hospital units were temporarily discontinued to further reduce the possibility that healthcare workers would acquire hepatitis A at work. In addition, because the outbreak centered on poor sanitary conditions, personal hygiene kits provided by SDCPH, which included hand sanitizers, soaps, cleansing wipes, bottled water, informational flyers, and waste bags, were widely distributed to at-risk patients in EDs and inpatient hospitalizations. Because the population at risk lacked regular access to sanitary living conditions, SDCPH coordinated with hospital staff on discharge planning. Patients who were potentially contagious and homeless remained hospitalized until they were able to be discharged to a temporary shelter with private restrooms. Starting October 2017, SDCPH contracted with a hotel for housing of infectious patients. All hotel staff who interacted with patients were vaccinated, and rooms were disinfected using a standard protocol.

#### Education

Several articles and communications on hepatitis A were published and disseminated in UCSDH patient-oriented email newsletters to educate the general public. Nurses distributed information about hepatitis A, along with personal hygiene kits, to at-risk patients. Healthcare personnel were informed of the ongoing HAV outbreak and employee vaccination clinics through regularly scheduled UCSDH communications emails.

#### Data Collection

We defined a hepatitis A case as illness that met the clinical case definition (an acute illness with a discrete onset of any signs or symptoms consistent with acute viral hepatitis and either jaundice or elevated serum alanine aminotransferase or aspartate aminotransferase) with laboratory criteria for diagnosis (positive IgM) or an epidemiologic link to a person with laboratory-confirmed hepatitis A (*10*). We obtained the number of hepatitis A cases in San Diego County during November 1, 2016–October 31, 2018, from SDCPH. We obtained the number of hepatitis A cases diagnosed at UCSDH from the infection prevention/clinical epidemiology unit and Epic Icon (EpicSystems), a data-mining software used in infection surveillance. We further stratified hepatitis A cases diagnosed at UCSDH on the basis of whether patients required inpatient hospitalization. We derived length of stay using Epic Icon.

We obtained the number of hepatitis A vaccines administered in San Diego County March 1, 2017–October 31, 2018, through the vaccination initiative from SDCPH. To collect the number of vaccinations administered at UCSDH, we used Epic Slicer Dicer (EpicSystems), a self-service analytics tool within the Epic EHR. We further stratified vaccinations administered at UCSDH according to the locations in which vaccinations were delivered (inpatient hospitalization, urgent care, ambulatory clinic, ED, or occupational health) and the patients' risk factors (homelessness, illicit drug use, alcohol abuse, hepatitis B virus infection, hepatitis C virus infection, HIV infection, cirrhosis) within the EHR-based registries. The risk factors were not mutually exclusive, and we stratified data to identify patients with ≥1 risk factors.

## Results

#### Hepatitis A Cases

During November 1, 2016–October 31, 2018, a total of 592 confirmed or probable outbreak-associated cases of HAV infection occurred in San Diego County. Although the initial cases of hepatitis A could be traced back to November 2016, the outbreak was recognized in March 2017, and cases peaked in August 2017 (Figure 2). During the 2-year period, acute hepatitis A was diagnosed in 144 patients at UCSDH. Cases began in March 2017 and peaked in July 2017 (Figures 2, 3). Among these 144 patients, 119 (83%) were hospitalized (Figure 3). In comparison, before the outbreak period (November 1, 2012–October 31, 2016), acute hepatitis A was diagnosed in 9 patients at UCSDH, of whom 5 (56%) were hospitalized.

The mean length of stay for the 119 patients admitted to UCSDH was 6.0 days (median 3.0 days, range 1–57 days) (Figure 3). Mean length of stay for all patients admitted to UC San Diego Medical Center was 5.38 days during November 1, 2016–October 31, 2018. Starting October 2017, SDCPH contracted with a hotel for housing of infectious patients. During November 1, 2016–September 31, 2017, before the availability of housing, mean length of stay for the 102 patients hospitalized was 6.4 days (range 1–57 days)

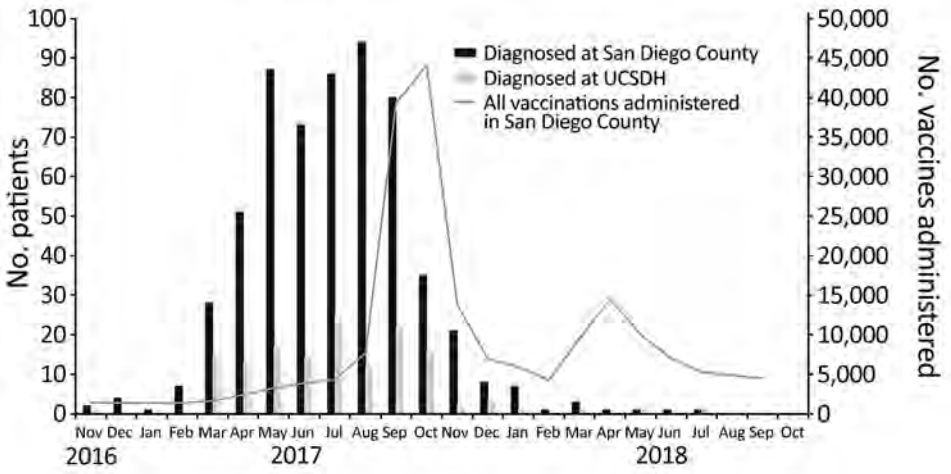


**Figure 2.** Monthly trend of hepatitis A cases in San Diego and UCSDH and all vaccinations administered in San Diego County, California, USA, 2016–2018. UCSDH, University of California San Diego Health.

(Figure 3). In comparison, during October 1, 2017–October 31, 2018, after housing became available, 17 patients were hospitalized; mean length of stay was 3.8 days (range 1–17 days) (Figure 3).

### Vaccine Administration

During March 1, 2017–October 31, 2018, a total of 207,862 hepatitis A vaccines were administered in San Diego County (Table 1). Vaccination efforts in San Diego County began in March 2017, sharply increased in August 2017, and peaked in October 2017. A second peak occurred around April 2018, when the second dose, which is typically given 6–12 months after the primary vaccination, was due (Figure 2). Among the 207,862 vaccines delivered in San Diego, San Diego County administered 57,052 (27%) vaccines: 23,620 (11%) by mass vaccination events, 5,820 (3%) by foot teams, and 848 (<1%) by mobile vans (Table 1). The remaining 150,810 (73%) vaccines were administered by noncounty providers; 99,931 (48%) were administered by healthcare systems, which included EDs, outpatient clinics, inpatient hospitals, and urgent care centers. Occupational health units throughout San Diego County administered 7,831 (4%) vaccines (Table 1).

At UCSDH, 10,324 vaccines were administered during March 1, 2017–October 31, 2018; 9,288 hepatitis A vaccine (Havrix; GlaxoSmithKline, https://www.gsksource.com) doses and 1,036 recombinant hepatitis A and B vaccine (Twinrix; GlaxoSmithKline) doses were administered (Table 2; Appendix Figure, https://wwwnc.cdc.gov/EID/article/26/7/19-1352-App1.pdf). Similar to vaccination efforts in the county, vaccinations at UCSDH increased sharply in August 2017 and peaked in October 2017 and then peaked again in April 2018 (Figures 4, 5). In comparison, during March 1, 2016–February 28, 2017, before the outbreak-control vaccination initiatives, a mean (± SD) of 118.7 (± 17.5) hepatitis A vaccines (Havrix) and 55.8 (± 11.8) recombinant hepatitis A and B vaccines (Twinrix) were administered each month. Most vaccines were delivered in ambulatory care clinics (7,700 [75%]), followed by urgent care centers (1,208 [12%]) and occupational health (961 [9%]) (Table 2;

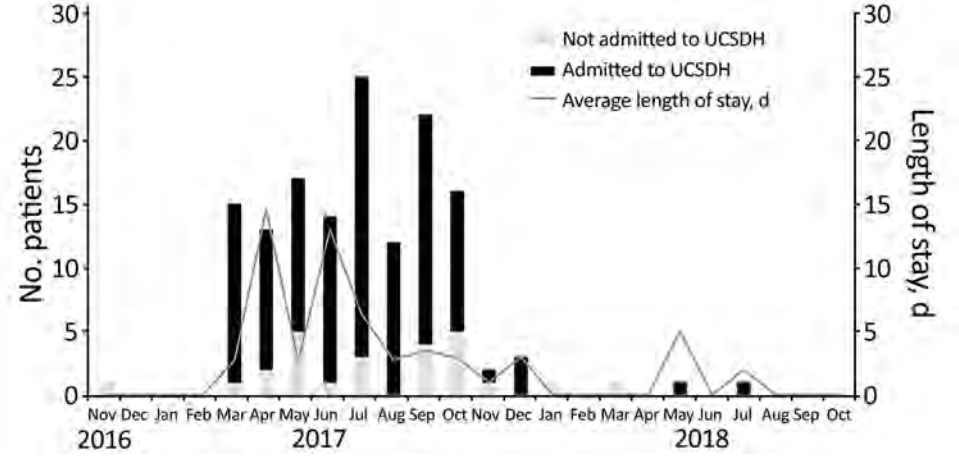


**Figure 3.** Monthly trend of persons with hepatitis A admitted to UCSDH and mean length of stay, San Diego, California, USA, 2016–2018. UCSDH, University of California San Diego Health.

**Table 1.** Adult hepatitis A virus vaccinations registered in the vaccination registry, San Diego, California, USA, March 1, 2017–October 31, 2018

| Vaccination reason or provider | No. (%) |
|---|---|
| County | |
| Postexposure prophylaxis | 1,026 (0.5) |
| Jail | 9,862 (4.7) |
| Psychiatric hospital | 522 (0.3) |
| Public health center | 13,584 (6.5) |
| Public health clinic | 1,770 (0.9) |
| Field event | |
| Mobile van | 848 (0.4) |
| Foot team | 5,820 (2.8) |
| Point of dispensing/mass vaccination | 23,620 (11.4) |
| Noncounty | |
| Federally qualified health center | 30,877 (14.9) |
| Healthcare system | 99,931 (48.1) |
| Pharmacy | 12,171 (5.9) |
| Occupational health entity | 7,831 (3.8) |
| Total | 207,862 (100) |

Figure 4). Illicit drug use was the most common risk factor (2,477 [24%]) of patients who were vaccinated at UCSDH, followed by homelessness (1,385 [13%]) and alcohol abuse (970 [9%]) (Table 2; Figure 5). For patients experiencing homelessness, vaccinations peaked in August 2017; for patients with risk factors of illicit drug use, alcohol abuse, HIV, and cirrhosis, vaccination peaked in October 2017 (Figure 5). Vaccination rates remained unchanged throughout the vaccination initiative for patients with chronic infections from hepatitis B, hepatitis C, or both (Figure 5).

A total of 882 (85.1%) of 1,036 Twinrix doses were administered in ambulatory primary and specialty care clinics. Another 117 (11%) were provided in the urgent care setting. The Twinrix vaccination series was administered to established patients who also met criteria for hepatitis B vaccination, such as patients with HIV infection, hepatitis C infection, end-stage liver disease, or active illicit drug use, and who were expected to return to complete the series. A second peak of Twinrix administration occurred 6 months later in these same clinics. In contrast, Twinrix was administered twice at the UCSD Free Clinic, which focused on care of the uninsured community.

## Discussion

This study highlights the public health contribution of an acute care hospital to prevention and outbreak management activities during a hepatitis A outbreak. Unlike many other counties in California, San Diego does not have a county hospital; therefore, local acute care hospitals are actively involved in the care of vulnerable and uninsured populations. This outbreak and subsequent similar ones across the United States have been characterized by direct human-to-human spread and poor sanitary conditions disproportionately affecting the homeless population and to some extent illicit drug users (*7*,*11*–*13*). In response, the Advisory Committee on Immunization Practices recently added homelessness as an indication for hepatitis A vaccination (*14*,*15*).

Because this outbreak affected persons with limited access to routine medical care, outbreak management and prevention efforts were particularly challenging. Nevertheless, close coordination between public health and the city, behavioral health, acute care hospitals at the epicenter of the epidemic, and pharmacies helped contain the outbreak. Healthcare systems provided nearly half of the vaccinations administered in San Diego County. Although 75% of vaccinations administered at UCSDH were delivered at ambulatory clinics, and similar efforts occurred in other outpatient clinics in San Diego (*16*), proactive vaccination administration in EDs and urgent care settings or during inpatient hospitalizations with real-time access to analytics and clinical informatics

**Table 2.** Characteristics of adults receiving hepatitis A virus vaccine administered at University of California San Diego Health, March 1, 2017–October 31, 2018*

| | No. vaccines administered | | |
|---|---|---|---|
| Characteristic | Hepatitis A, n = 9,288 | Hepatitis A and hepatitis B, recombinant, n = 1,036 | Total (%), N = 10,324 |
| Location administered | | | |
| Inpatient admission | 135 | 4 | 139 (1) |
| Urgent care | 1,091 | 117 | 1,208 (12) |
| Ambulatory clinic | 6,818 | 882 | 7,700 (75) |
| Occupational health | 865 | 96 | 961 (9) |
| ED BPA triggered | 1,369 | 5 | 1,374 (13) |
| Risk factors | | | |
| Homelessness | 1,357 | 28 | 1,385 (13) |
| Illicit drug use | 2,247 | 230 | 2,477 (24) |
| Alcohol abuse | 873 | 97 | 970 (9) |
| Hepatitis C infection | 55 | 49 | 104 (1) |
| Hepatitis B infection | 0 | 0 | 0 (0) |
| HIV infection | 444 | 141 | 585 (6) |
| Cirrhosis | 411 | 127 | 538 (5) |

*ED, emergency department; BPA, best practice advisory.

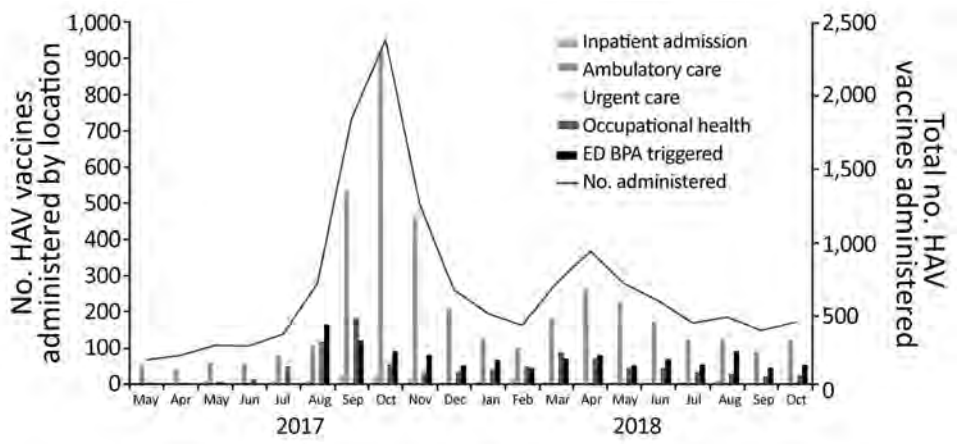


**Figure 4.** Location and monthly trend of HAV vaccinations administered at University of California San Diego Health, San Diego, California, USA, 2017–2018. BPA, best practice advisory; ED, emergency department; HAV, hepatitis A virus.

support were crucial given that highest-risk population most likely had limited access to routine outpatient care (*8*,*17*).

Data are sparse on the use of acute care inpatient facilities as a setting for an aggressive outbreak-control vaccination program. However, programs to receive catch-up vaccinations among hospitalized children, as well as routine vaccinations against pneumococcus and influenza during inpatient hospitalizations, have been shown to be effective (*16*–*18*). Similarly, ED-based vaccination programs for pneumococcus and influenza have proven successful (*19*–*21*). Because EDs and urgent care may be the sole contact of a disenfranchised population with the medical system, data on EDs partnering with public health departments to administer outbreak-control vaccinations have increased (*8*,*17*,*22*).

As healthcare systems become an important site for vaccination administration, optimizing EHR support tools is crucial in increasing vaccination rates. Previous efforts focused on EDs only, but for this response, UCSDH implemented EHR-based alerts across the continuum of care to achieve higher vaccination rates (*8*). Although the direct effects of the alerts cannot be measured, vaccination of the homeless population peaked in August 2017 when the ED-focused alert was first implemented, whereas vaccination of other at-risk populations peaked in October 2017, when the second BPA alert with the wider range of risk factors was implemented across all care settings. Prior studies have shown that both computerized reminders and standing orders are effective in increasing influenza and pneumococcal vaccination rates (*23*,*24*).

In addition, although HAV infection is not typically viewed as a healthcare-associated infection, 8 unvaccinated healthcare personnel acquired hepatitis A in the healthcare setting during this outbreak. The Centers for Disease Control and Prevention does not recommend routine hepatitis A vaccination of healthcare workers because healthcare-associated HAV infection is considered infrequent. Instead, because hepatitis A is transmitted through the fecal–oral route, the Centers for Disease Control and Prevention recommends routine infection control precautions with proper hand hygiene to prevent transmission to hospital staffs (*25*). However, continued and prolonged exposure to patients with acute hepatitis A

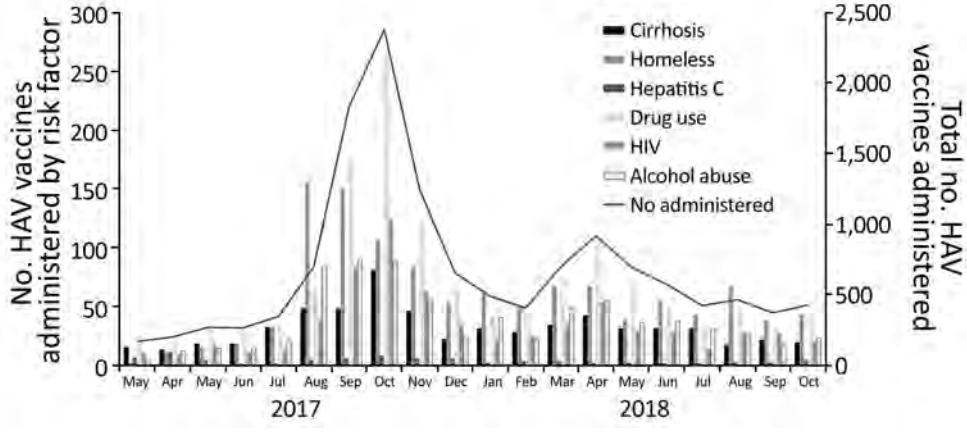


**Figure 5.** Risk factors and monthly trend of HAV vaccinations administered at University of California San Diego Health, San Diego, California, USA. HAV, hepatitis A virus.

infection can result in disease in unvaccinated healthcare workers; therefore, vaccination of healthcare personnel can be considered in outbreak settings.

Finally, compared with prior outbreaks, in this outbreak, disproportionate numbers of patients with acute hepatitis A required inpatient hospitalization. Prior studies have reported that hospitalization rates for all reported hepatitis A cases were 33%–43% during 2005–2011 (*6*,*26*–*29*). Before the outbreak, during November 1, 2012–October 31, 2016, five (56%) of 9 patients in whom acute hepatitis A was diagnosed required inpatient hospitalization. During the outbreak we report, 83% of all hepatitis A patients at UCSDH were admitted, and their mean length of stay was of 6.0 days. Given that this outbreak centered on homelessness and poor sanitation, hospitalization of patients with hepatitis A most likely prevented continued human-to-human transmission through prolonged viral shedding in the homeless community. Starting in October 2017, SDCPH contracted with a hotel to arrange housing for potentially infectious patients and coordinated with hospital staff on discharge planning. Designation of protected facilities increased housing capacity and decreased the length of hospitalization for acutely infected homeless patients.

Limitations to this study include its single-center and retrospective study designs. Although other local acute care centers participated in the outbreak control initiatives, we do not have information about the number of vaccinations administered and hepatitis A cases diagnosed at other facilities. In addition, the retrospective nature of the study precludes a precise assessment of the direct effect of BPAs on the number of hepatitis A vaccines administered and the effect on vaccinations by risk factors and on the scope of the sanitation efforts within the UCSDH system. Finally, the effect of inpatient hospitalizations on limiting human-to-human transmission in the homeless community cannot be definitively demonstrated. Communitywide initiatives, in addition to hospital-level efforts, might have influenced the actions of UCSDH providers.

Although the hepatitis A outbreak in San Diego and California was ultimately contained, ongoing epidemiologically linked larger outbreaks are occurring in other states (*6*,*12*,*13*). Because acute care hospitals play an increasing role in outbreak-control programs, close coordination between public health and acute care hospitals, as well as optimization of informatic tools to improve the identification of at-risk population, can contribute substantially to control of communitywide outbreaks.

## About the Author

Dr. Kang is an infectious diseases fellow at the University of California San Diego. Her primary research interests are healthcare epidemiology and antimicrobial stewardship.

## References

1. Bennett JE, Dolin R, Blaser MJ. Mandell, Douglas, and Bennett's principles and practice of infectious diseases. 8th ed. Amsterdam: Saunders; 2015.
2. Wasley A, Samandari T, Bell BP. Incidence of hepatitis A in the United States in the era of vaccination. JAMA. 2005;294:194–201. https://doi.org/10.1001/jama.294.2.194
3. Murphy TV, Denniston MM, Hill HA, McDonald M, Klevens MR, Elam-Evans LD, et al. Progress toward eliminating hepatitis A disease in the United States. MMWR Suppl. 2016;65:29–41. https://doi.org/10.15585/mmwr.su6501a6
4. André FE, D'Hondt E, Delem A, Safary A. Clinical assessment of the safety and efficacy of an inactivated hepatitis A vaccine: rationale and summary of findings. Vaccine. 1992;10(Suppl 1):S160–8. https://doi.org/10.1016/0264-410X(92)90576-6
5. California Department of Public Health. Hepatitis A [cited 2019 Apr 16]. https://www.cdph.ca.gov/Programs/CID/DCDC/pages/immunization/hepatitis-a.aspx
6. Centers for Disease Control and Prevention. Widespread outbreaks of hepatitis A across the United States [cited 2019 Nov 11]. https://www.cdc.gov/hepatitis/outbreaks/2017March-HepatitisA.htm
7. County of San Diego. Hepatitis A outbreak after action report [cited 2019 Apr 16]. https://www.sandiegocounty.gov/content/dam/sdc/cosd/SanDiegoHepatitisAOutbreak-2017-18-AfterActionReport.pdf
8. Castillo EM, Chan TC, Tolia VM, Trumm NA, Powell RA, Brennan JJ, et al. Effect of a computerized alert on emergency department hepatitis A vaccination in homeless patients during a large regional outbreak. J Emerg Med. 2018;55:764–8. https://doi.org/10.1016/j.jemermed.2018.09.004
9. Mbithi JN, Springthorpe VS, Sattar SA. Chemical disinfection of hepatitis A virus on environmental surfaces. Appl Environ Microbiol. 1990;56:3601–4. https://doi.org/10.1128/AEM.56.11.3601-3604.1990
10. Centers for Disease Control and Prevention. National Notifiable Diseases Surveillance System (NNDSS). Hepatitis A, acute 2012 case definition [cited 2019 Nov 1]. https://wwwn.cdc.gov/nndss/conditions/hepatitis-a-acute/case-definition/2012/
11. Kushel M. Hepatitis A outbreak in California—addressing the root cause. N Engl J Med. 2018;378:211–3. https://doi.org/10.1056/NEJMp1714134
12. Foster M, Ramachandran S, Myatt K, Donovan D, Bohm S, Fiedler J, et al. Hepatitis A virus outbreaks associated with drug use and homelessness—California, Kentucky, Michigan, and Utah, 2017. MMWR Morb Mortal Wkly Rep. 2018;67:1208–10. https://doi.org/10.15585/mmwr.mm6743a3
13. Foster MA, Hofmeister MG, Kupronis BA, Lin Y, Xia GL, Yin S, et al. Increase in hepatitis A virus infections—United States, 2013–2018. MMWR Morb Mortal Wkly Rep. 2019;68:413–5. https://doi.org/10.15585/mmwr.mm6818a2
14. Doshani M, Weng M, Moore KL, Romero JR, Nelson NP. Recommendations of the Advisory Committee on Immunization Practices for use of hepatitis A vaccine for persons experiencing homelessness. MMWR Morb Mortal Wkly Rep. 2019;68:153–6. https://doi.org/10.15585/mmwr.mm6806a6

15. Peak CM, Stous SS, Healy JM, Hofmeister MG, Lin Y, Ramachandran S, et al. Homelessness and Hepatitis A — San Diego County, 2016–2018. Clin Infect Dis. 2019;ciz788. https://doi.org/10.1093/cid/ciz788
16. Duncan L. A community clinic's response to a hepatitis A outbreak. Am J Infect Control. 2018;46:1057–9. https://doi.org/10.1016/j.ajic.2018.02.007
17. James TL, Aschkenasy M, Eliseo LJ, Olshaker J, Mehta SD. Response to hepatitis A epidemic: emergency department collaboration with public health commission. J Emerg Med. 2009;36:412–6. https://doi.org/10.1016/j.jemermed.2007.10.001
18. Rimple D, Weiss SJ, Brett M, Ernst AA. An emergency department-based vaccination program: overcoming the barriers for adults at high risk for vaccine-preventable diseases. Acad Emerg Med. 2006;13:922–30.
19. Pahud B, Clark S, Herigon JC, Sherman A, Lynch DA, Hoffman A, et al. A pilot program to improve vaccination status for hospitalized children. Hosp Pediatr. 2015;5:35–41. https://doi.org/10.1542/hpeds.2014-0027
20. Robke JT, Woods M. A decade of experience with an inpatient pneumococcal vaccination program. Am J Health Syst Pharm. 2010;67:148–52. https://doi.org/10.2146/ajhp080638
21. Middleton DB, Fox DE, Nowalk MP, Skledar SJ, Sokos DR, Zimmerman RK, et al. Overcoming barriers to establishing an inpatient vaccination program for pneumococcus using standing orders. Infect Control Hosp Epidemiol. 2005;26:874–81. https://doi.org/10.1086/502511
22. Lindegren ML, Atkinson WL, Farizo KM, Stehr-Green PA. Measles vaccination in pediatric emergency departments during a measles outbreak. JAMA. 1993;270:2185–9. https://doi.org/10.1001/jama.1993.03510180055033
23. Dexter PR, Perkins SM, Maharry KS, Jones K, McDonald CJ. Inpatient computer-based standing orders vs physician reminders to increase influenza and pneumococcal vaccination rates: a randomized trial. JAMA. 2004;292:2366–71. https://doi.org/10.1001/jama.292.19.2366
24. Dexter PR, Perkins S, Overhage JM, Maharry K, Kohler RB, McDonald CJ. A computerized reminder system to increase the use of preventive care for hospitalized patients. N Engl J Med. 2001;345:965–70. https://doi.org/10.1056/NEJMsa010181
25. Centers for Disease Control and Prevention. Hepatitis A [cited 2019 Jul 26]. https://www.cdc.gov/hepatitis/HAV/HAVfaq.htm#general
26. Daniels D, Grytdal S, Wasley A; Centers for Disease Control and Prevention (CDC). Surveillance for acute viral hepatitis—United States, 2007. MMWR Surveill Summ. 2009;58:1–27.
27. Wasley A, Miller JT, Finelli L; Centers for Disease Control and Prevention (CDC). Surveillance for acute viral hepatitis—United States, 2005. MMWR Surveill Summ. 2007;56:1–24.
28. Wasley A, Grytdal S, Gallagher K; Centers for Disease Control and Prevention (CDC). Surveillance for acute viral hepatitis—United States, 2006. MMWR Surveill Summ. 2008;57:1–24.
29. Collier MG, Tong X, Xu F. Hepatitis A hospitalizations in the United States, 2002-2011. Hepatology. 2015;61:481–5. https://doi.org/10.1002/hep.27537

Address for correspondence: Francesca J. Torriani, UC San Diego Infection Prevention and Clinical Epidemiology Unit, 200 West Arbor Dr, MC8951, San Diego, CA 92103-8951, USA; email: ftorriani@ucsd.edu

# Macrolide-Resistant *Mycoplasma pneumoniae* Infections in Pediatric Community-Acquired Pneumonia

Yu-Chin Chen,[1] Wei-Yun Hsu,[1] Tu-Hsuan Chang[1]

A high prevalence rate of macrolide-resistant *Mycoplasma pneumoniae* (MRMP) has been reported in Asia. We performed a systematic review and meta-analysis to investigate the effect of macrolide resistance on the manifestations and clinical judgment during *M. pneumoniae* infections. We found no difference in clinical severity between MRMP and macrolide-sensitive *Mycoplasma pneumoniae* (MSMP) infections. However, in the pooled data, patients infected with MRMP had a longer febrile period (1.71 days), length of hospital stay (1.61 day), antibiotic drug courses (2.93 days), and defervescence time after macrolide treatment (2.04 days) compared with patients infected with MSMP. The risk of fever lasting for >48 hours after macrolide treatment was also significantly increased (OR 21.24), and an increased proportion of patients was changed to second-line treatment (OR 4.42). Our findings indicate diagnostic and therapeutic challenges after the emergence of MRMP. More precise diagnostic tools and clearly defined treatment should be appraised in the future.

*Mycoplasma pneumoniae* is a common causative pathogen in community-acquired pneumonia (CAP) during childhood. In the post–pneumococcal conjugate vaccine (PCV) 13 era, the epidemiology of pediatric pneumonia has changed. In some countries where PCV13 is already included in national immunization program, *M. pneumoniae* has become the leading pathogen in pediatric CAP (*1*,*2*).

The clinical manifestations of *M. pneumoniae* infection are usually mild and self-limited. However, life-threatening pneumonia or even acute respiratory distress syndrome requiring extracorporeal membrane oxygen has been reported (*3*). Furthermore, some extrapulmonary symptoms, such as mucositis, hepatitis, encephalitis, hemolysis, or erythema multiforme, have linked *M. pneumoniae* infection to the formation of autoimmunity or immune complexes. The association between *M. pneumoniae* and refractory asthma has also been mentioned (*4*).

Macrolides are the first-line therapy for *M. pneumoniae*. Because of high oral bioavailability and once-daily formulation, macrolides have been widely used in outpatient settings. During the past 10 years, however, macrolide-resistant *Mycoplasma pneumoniae* (MRMP) has emerged worldwide. The most prevalent area is Asia, where prevalence rates are 13.6%–100% (*5*). In Japan and China, resistance rates are >90% in some epidemic years (*5*,*6*).

The treatment of MRMP has become challenging. Although 1 report showed more complications in managing MRMP infections (*7*), the association between severe disease and resistance remains inconsistent and unclear. We conducted a systematic review and meta-analysis to examine the effect of macrolide resistance on the manifestations, outcomes, and clinical judgment of *M. pneumoniae* infection.

## Methods

### Search Strategy

We conducted a systematic literature search in PubMed, Embase, and the Cochrane Library database using the keywords *Mycoplasma pneumoniae*, macrolide, antibiotic resistance, and drug resistance. There was no language restriction in our search. We reviewed eligible full texts and the reference lists of the relevant studies. The last update of the study was on December 1, 2019.

Two independent reviewers (Y.-C.C. and T.-H.C.) screened all titles and abstracts for eligibility. Studies were eligible for inclusion if the study population was restricted to children (<18 years of age) with community-acquired pneumonia; macrolide

Author affiliations: Chi-Mei Medical Center, Chiali, Tainan, Taiwan (Y.-C. Chen); Chi-Mei Medical Center, Tainan, Taiwan (W.-Y. Hsu, T.-H. Chang)

DOI: https://doi.org/10.3201/eid2607.200017

[1]All authors contributed equally to this article.

resistance was detected by PCR including the 2 common point mutations, positions 2063 and 2064; and a direct comparator was used in the same cohorts (macrolide-sensitive *M. pneumoniae* [MSMP] group). We excluded review articles, editorial comments, case reports, and posters but included correspondence or letters that fulfilled these criteria.

### Data Extraction and Quality Assessment

After full-text screening for eligibility and review, the 3 authors extracted data independently of one another. We resolved disagreements by consensus or review by another reviewer. We extracted the following variables from each study, if available: author, journal, year of publication, study design, study country, time period, detected point mutations, clinical symptoms, total febrile days, length of hospital stay, defervescence days after macrolide, antibiotic history, laboratory results, and chest radiographic findings. We also extracted pediatric data from studies with both children and adults, if available. We assessed the quality of nonrandomized studies included in the meta-analysis using the Newcastle-Ottawa Scale and excluded articles with poor quality (score 0–3).

### Data Analysis

We used Review Manager software version 5.3 (Cochrane Collaboration, https://training.cochrane.org) and Comprehensive Meta-Analysis version 3 (Biostat, https://www.meta-analysis.com) for the analysis and conducted meta-analysis when ≥3 studies with available data reported the same outcome. We calculated heterogeneity ($I^2$) to examine statistical heterogeneity across the included studies. We considered $I^2$ >50% and $p<0.05$ to indicate substantial heterogeneity. We used random effects models to calculate odds ratios for binary outcomes and mean differences for continuous outcomes. We used Egger precision weighted linear regression tests and funnel plots to test potential publication bias. If publication bias was present, we used

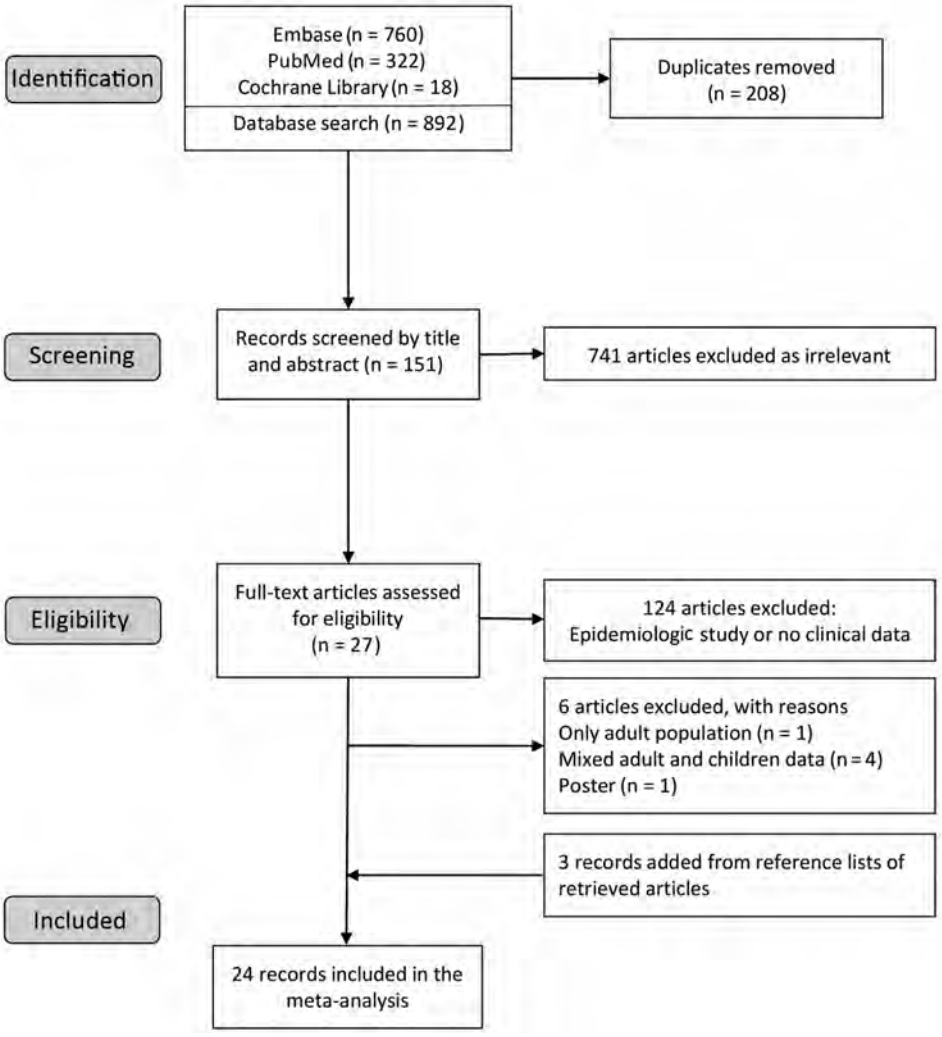


**Figure 1.** Flow diagram of selection process for meta-analysis of macrolide-resistant *Mycoplasma pneumoniae* infections in pediatric community-acquired pneumonia.

**Table.** Characteristics of the eligible studies of macrolide resistance and *Mycoplasma pneumoniae* infections.

| Author | Study period | Country | Mutations detected | Disease entity | Case no. | Resistance |
|---|---|---|---|---|---|---|
| Chen (*8*) | 2014–2016 | China | A2063G, A2064G | CAP, inpatient | 136 | 60% |
| Ma (*9*) | 2010–2011 | China | A2063G, A1290G | CAP, inpatient | 57 | 63% |
| Xin (*10*) | 2004–2005 | China | A2063G, A2064G | CAP, inpatient | 64 | 59% |
| Yuan (*11*) | 2016 | China | A2063G, A2064G, C2617G | CAP, inpatient | 120 | 82% |
| Zhou (*7*) | 2009–2010 | China | A2063G, A2063T, A2064G | CAP, inpatient | 235 | 88% |
| Cheong (*12*) | 2011–2013 | HK | A2063G | CAP, inpatient | 93 | 27% |
| Lung (*13*) | 2010–2013 | HK | A2063G | CAP, inpatient | 48 | 71% |
| Cardinale (*14*) | 2010 | Italy | A2063G, A2064G | CAP, inpatient | 46 | 17% |
| Akashi (*15*) | 2016–2017 | Japan | A2063G, A2064G | CAP, mixed | 222 | 65% |
| Ishiguro (*16*) | 2013–2015 | Japan | A2063G | CAP, mixed | 109 | 54% |
| Kawai (*17*) | 2005–2010 | Japan | A2063G, A2064G | CAP, mixed | 29 | 72% |
| Kawai (*18*) | 2005–2012 | Japan | A2063G, A2064G | CAP, mixed | 188 | 80% |
| Matsubara (*19*) | 2002–2006 | Japan | A2063G, A2064G | CAP, NS | 69 | 32% |
| Miyashita (*20*) | 2008–2011 | Japan | A2063G, A2064G | CAP, NS | 71 | 59% |
| Okada (*21*) | 2011 | Japan | A2063G, A2064G | CAP, mixed | 202 | 87% |
| Kim JH (*22*) | 2011–2015 | Korea | A2063G | CAP, inpatient | 250 | 74% |
| Kim YJ (*23*) | 2010–2015 | Korea | A2063G | CAP, inpatient | 107 | 10% |
| Lee (*24*) | 2015 | Korea | A2063G | CAP, mixed | 94 | 13% |
| Seo (*25*) | 2011 | Korea | A2063G | CAP, inpatient | 95 | 52% |
| Yoo (*26*) | 2011 | Korea | A2063G | CAP, mixed | 91 | 30% |
| Yoon (*27*) | 2010–2015 | Korea | A2063G | CAP, inpatient | 116 | 71% |
| Wu HM (*28*) | 2011 | Taiwan | A2063G | CAP, inpatient | 73 | 12% |
| Wu PS (*29*) | 2010–2011 | Taiwan | A2063G | CAP, inpatient | 60 | 23% |
| Yang (*30*) | 2010–2017 | Taiwan | A2063G, A2063T, A2064G | CAP, mixed | 471 | 24% |

*CAP, community acquired pneumonia; HK, Hong Kong; NS, not specified.

the trim-and-fill method and calculated Rosenthal's fail-safe *N* to evaluate the effect.

## Results

### Study Characteristics

We identified 1,100 articles in the initial search (Figure 1). After removing duplicates, we screened 892 articles by titles and abstracts. We excluded obviously irrelevant articles and retrieved the remaining 151 for full text assessment. We then excluded epidemiologic or in vitro studies without clinical data. We included 27 full-text studies in the qualitative synthesis. We identified 3 records through manual search of the reference lists of retrieved articles. Finally, we included 24 full-text articles in the meta-analysis. The studies

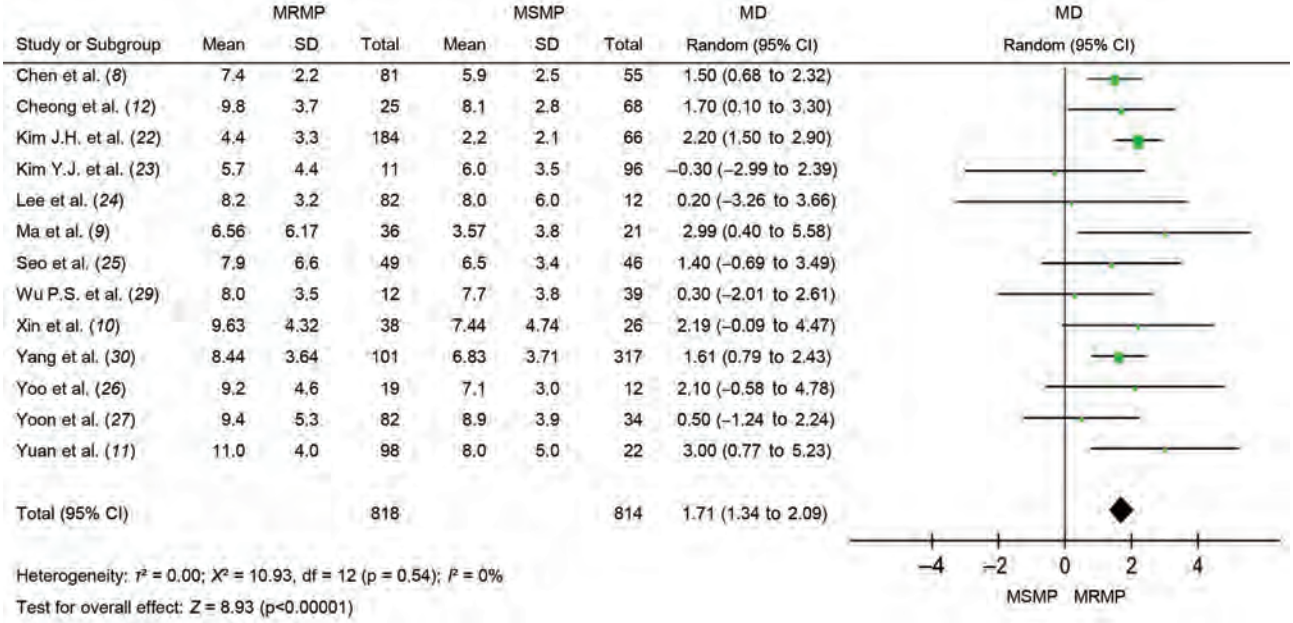


**Figure 2.** Forest plots of difference in total febrile days between MRMP and MSMP in meta-analysis of MRMP infections in pediatric community-acquired pneumonia. MD, mean difference; MRMP, macrolide-resistant *Mycoplasma pneumoniae*; MSMP, macrolide-sensitive *Mycoplasma pneumoniae*.

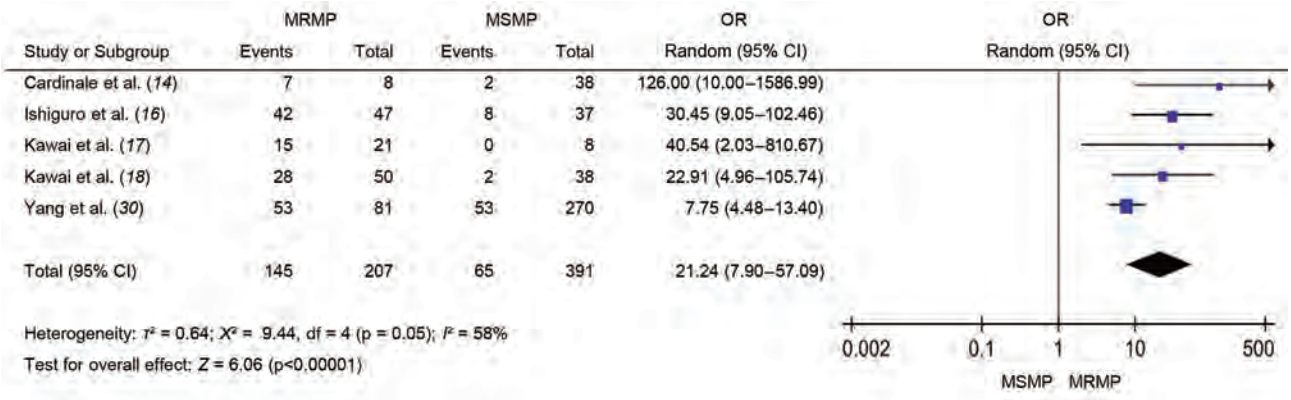


**Figure 3.** Forest plots comparing the pooled odds ratio of fever lasting for 48 hours after macrolide treatment between MRMP and MSMP in meta-analysis of MRMP infections in pediatric community-acquired pneumonia. MRMP, macrolide-resistant *Mycoplasma pneumoniae*; MSMP, macrolide-sensitive *Mycoplasma pneumoniae*; OR, odds ratio.

were conducted in the Asia-Pacific region, except for 1 in Italy. The range of resistance rates was 10%–88%. The A2063G transition mutation was detected in all studies (Table).

### Effect on Clinical Features and Outcomes

The duration of fever was longer in patients with MRMP than in patients with MSMP (mean difference [MD] 1.71, 95% CI 1.34–2.09; p<0.001) (Figure 2). The result was stable and consistent within studies ($I^2$ = 0%; p = 0.54). MRMP infections were also associated with prolonged hospitalization compared with MSMP infections (MD 1.61, 95% CI 1.08–2.13; p<0.001) (Appendix Figure 1, https://wwwnc.cdc.gov/EID/article/26/7/20-0017-App1.pdf). We found no significant heterogeneity in the studies included ($I^2$ = 28%; p = 0.18).

We examined the effect of macrolide resistance on work of breath and extrapulmonary symptoms. We found a slight trend toward MRMP patients with more extensive disease (Appendix Figure 2). Nevertheless, we found no difference in clinical features, such as dyspnea (OR 1.71, 95% CI 0.69–4.24; p = 0.24) or extrapulmonary manifestations (OR 1.31, 95% CI 0.85–2.02; p = 0.22), in patients with MRMP infections.

### Laboratory Results

We assessed inflammatory markers commonly examined during *M. pneumoniae* infection (Appendix Figure 3). Eleven studies provided data on leukocyte count; we found no significant difference between MRMP and MSMP patients (MD 0.09, 95% CI -0.31 to 0.50; p = 0.65). Nine studies assessed C-reactive protein (mg/L) during infection; again, we found no significant differences between MRMP and MSMP patients (MD -2.79, 95% CI -8.33 to 2.76; p = 0.32).

### Chest Radiographic Findings

We assessed the difference in chest radiographic findings in MRMP and MSMP patients (Appendix Figure 4). Neither consolidation ratio (OR 1.06, 95% CI 0.88–1.27; p = 0.52) nor pleural effusion (OR 1.19, 95% CI 0.70–2.03; p = 0.51) was influenced by macrolide resistance.

### Effect on Macrolide Efficacy and Antibiotic Prescription

In children with MRMP infection, fever may persist for >48 hours despite macrolide use. Figure 3 illustrates significantly increased odds of poor response to macrolide in patients with MRMP infections (OR 21.24, 95% CI 7.90–57.09; p<0.001).

Because efficacy of macrolides was reduced in patients with MRMP infections, we further investigated the exact effect of macrolide resistance on defervescence. The pooled results show significantly longer febrile duration (days) after ineffective treatment (MD 2.04, 95% CI 1.40–2.69; p<0.001). However, we observed an overall low-to-moderate heterogeneity within studies ($I^2$ = 49%; p = 0.07). Considering different treatment policies (timing to initiate second-line antibiotic or corticosteroid) for *M. pneumoniae* among regions, we performed a subgroup analysis according to country (Figure 4).

During macrolide treatment, some patients with *M. pneumoniae* infection would be switched to other classes of antibiotic drugs, such as the most commonly used fluoroquinolones and tetracyclines, that have different mechanisms of action (Figure 5). Increased proportions of patients were changed to second-line treatment when infected with MRMP (OR 4.42, 95% CI 2.32–8.41; p<0.001). Subgroup analysis divided by countries reveals that the heterogeneities were still high in Japan and Hong Kong.

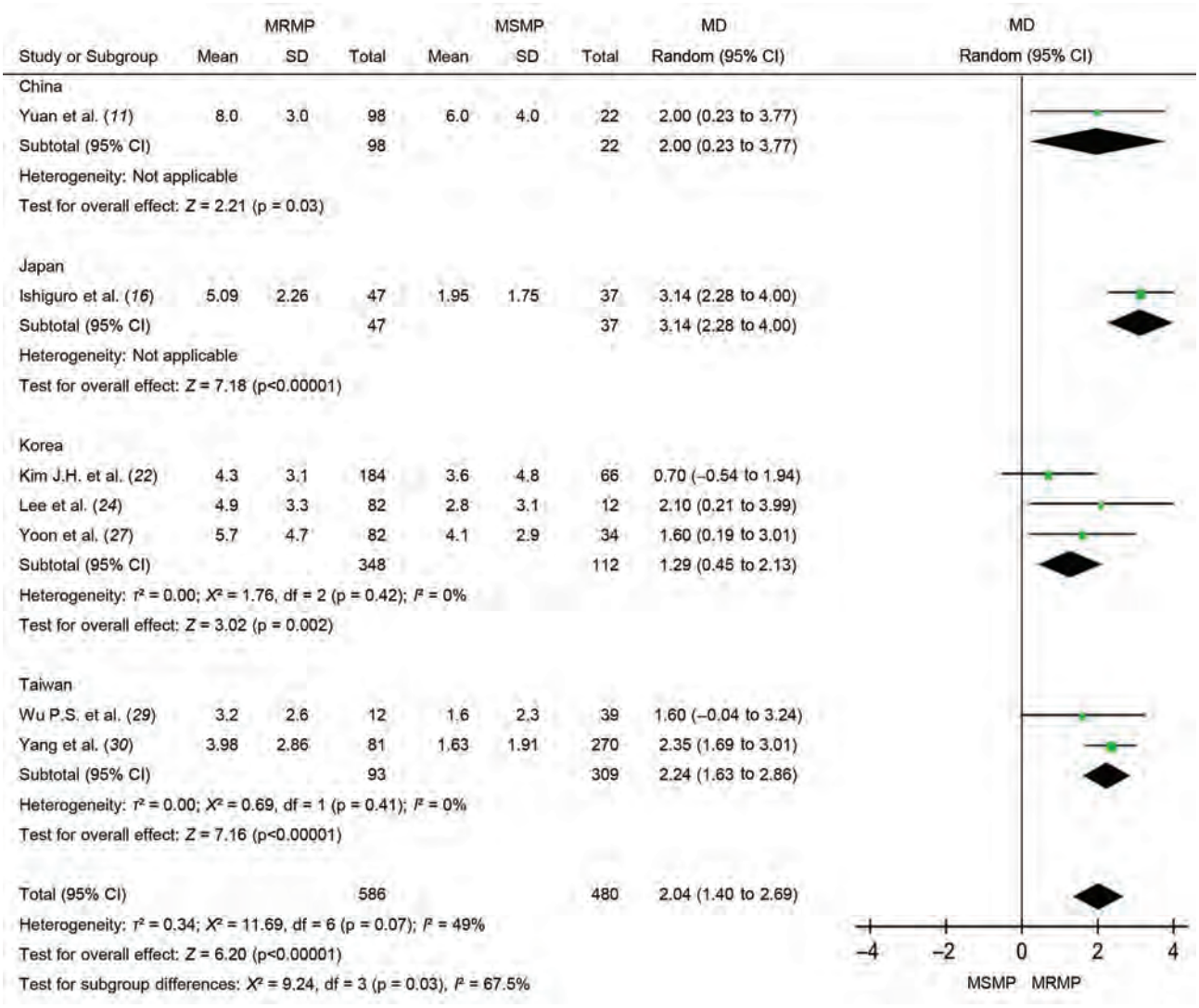


**Figure 4.** Forest plots depicting the defervescence time (days) after macrolide treatment in meta-analysis of MRMP infections in pediatric community-acquired pneumonia. Subgroup analysis was performed according to country. MD, mean difference; MRMP, macrolide-resistant *Mycoplasma pneumoniae*; MSMP, macrolide-sensitive *Mycoplasma pneumoniae*.

The total duration of antibiotic drug treatment was longer when used to treat MRMP infections than when used to treat MSMP infections (MD 2.93, 95% CI 1.97–3.89; p<0.001) (Figure 6). There was no substantial heterogeneity ($I^2$ = 0%; p = 0.48).

## Discussion

This systematic review and meta-analysis summarized currently available studies to compare the difference between MRMP and MSMP infections. The resistance rates varied within the studies, even in the same country (*5*). The overall resistance rate in large cohort studies in South Korea and Taiwan (*30*,*31*) increased over time; in contrast, the rate has gradually decreased in Japan since 2012 (*32*,*33*).

We applied multiple molecular methods to explain the spread of MRMP in Asia. Some reports using multilocus variable-number tandem-repeat analysis as the molecular typing method showed that the spread of *M. pneumoniae* seemed to be polyclonal (*34*,*35*). However, 2 recently published reports in South Korea and Japan that used multilocus sequence typing as the diagnostic method revealed that the wide spread of MRMP was associated with clonal expansion of the resistant ST3 clone (*31*,*36*). Whole-genome sequencing might be a better and more comprehensive tool for solving inconsistency and investigating *M. pneumoniae* evolutionary trends in the future.

The clinical manifestations, chest radiographic findings, and laboratory data were not altered

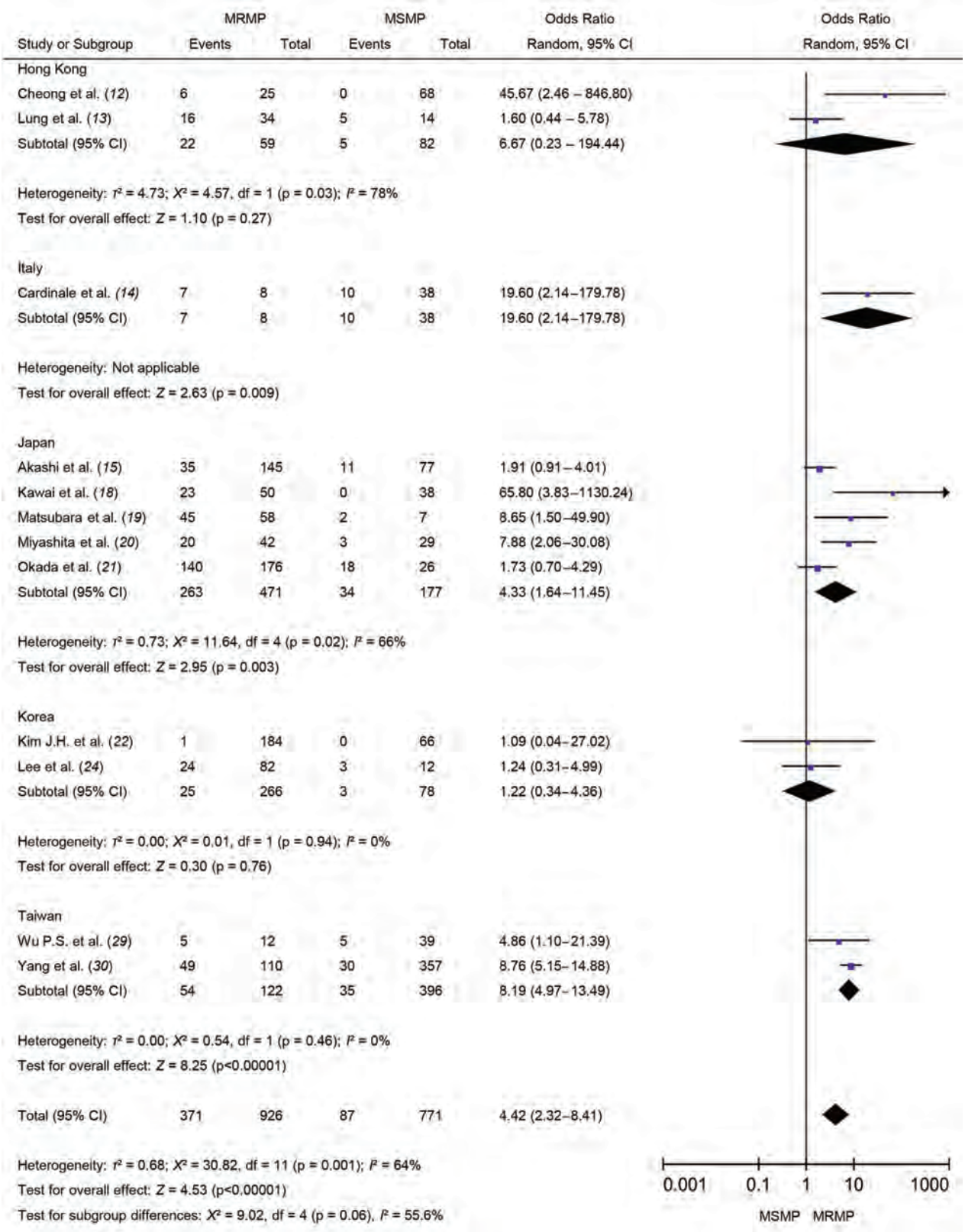


**Figure 5.** Forest plots comparing MRMP and MSMP by the pooled odds ratio of changing antibiotics in meta-analysis of MRMP infections in pediatric community-acquired pneumonia. MRMP, macrolide-resistant *Mycoplasma pneumoniae*; MSMP, macrolide-sensitive *Mycoplasma pneumoniae*; OR, odds ratio.

by macrolide resistance. Although some studies showed more severe radiological findings (*30*) and more complications (*7*) after MRMP infections, there appeared to be no significant difference in the pooled data. *M. pneumoniae* presents a unique virulence factor in humans, an ADP-ribosyl transferase known as the community-acquired respiratory distress syndrome toxin (CARDS toxin). Lluch-Senar et al. (*37*) performed sequence analysis of the P1 adhesin gene and stated that type 2 strain produced more CARDS toxin. However, Zhao et al. (*38*) and Eshaghi et al. (*39*) failed to demonstrate this difference between MRMP and MSMP. Currently, no evidence supports the causal relationship between macrolide resistance and disease severity.

The efficacy of macrolide is significantly decreased during MRMP treatment compared to MSMP treatment. The most common point mutation in the domain V 23S rRNA is A2063G, which will cause great MIC increase to all macrolide drugs. Other than A2063G, some studies also reported A2064G mutation, which could result in decreased macrolide affinity and elevation of MIC (*21*). Based on these results, we expected to see much longer fever duration from ineffective treatment. However, the pooled data revealed only an interval difference of 1.71 days between fever durations in MRMP and MSMP infections. We further examined the exact days of patients being afebrile after macrolide treatment and the clinical judgment on antibiotic drug use. The study results showed significant heterogeneity.

We then performed subgroup analysis by country. The results reflected different treatment policies among countries, even among institutions. Treatment selection for MRMP might modify the effect of macrolide resistance on clinical course. For instance, a report in South Korea (*22*) demonstrated less effect of resistance on macrolide efficacy. The possible reason is that steroids were given to 18.5% of patients with MRMP in this cohort, but not to MSMP patients (3%; p = 0.002). The initiation of corticosteroid treatment is early in South Korea (*40*) but reserved for refractory cases in Japan (*41*). Another study in China (*7*) noted that all patients in the report received only macrolides, given that the antimicrobial drug options are limited for preschool-age children. Therefore, more extrapulmonary complications (encephalitis, myocarditis, or hepatitis) occurred.

To treat or not to treat *M. pneumoniae* is still a dilemma to be resolved. MRMP treatment has raised another problem. Our meta-analysis identified 2 knowledge gaps. The first is the diagnostic gap. Macrolide resistance detection in most institutions relied on in-house PCR. Weighing the costs and benefits, it usually takes time to provide formal reports. Physicians usually base their suspicions of MRMP infections on clinical judgment of patients' response to treatment. In Japan and Taiwan, if fever persists for 48–72 hours after macrolide treatment, second-line antimicrobial drugs, such as fluoroquinolone or tetracycline, would be considered (*42*,*43*). Delayed defervescence of 2 days after macrolide (Figure 4) could be explained by this clinical practice. Timeliness of diagnostic tests after disease onset can be a factor in confirming macrolide resistance. Real-time or point-of-care testing should be used to make the diagnosis more precisely and quickly.

The second challenge is the therapeutic gap. In Japan, the therapeutic efficacy of tosufloxacin and minocycline has been demonstrated in several studies (*16*,*18*,*21*). However, because of side effects and the development of new resistant strains, empirical treatment for MRMP, especially in endemic areas, is the subject of an ongoing debate. In addition, delayed effective antimicrobial treatment for *M. pneumoniae* has been found to be related to immune reaction, which may lead to prolonged or extrapulmonary disease (*30*). Macrolide resistance is one of the significant risk factors for delayed effective treatment. This finding partially explains why patients with MRMP

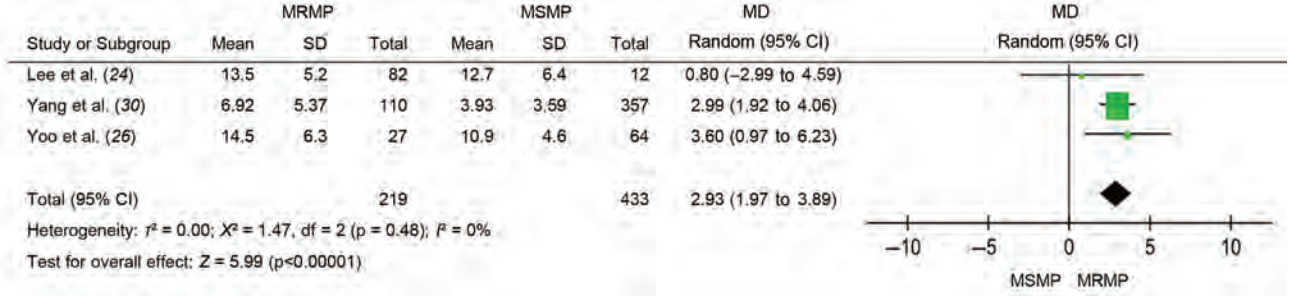


**Figure 6.** The duration difference (days) of antibiotic use between MRMP and MSMP infections in meta-analysis of MRMP infections in pediatric community-acquired pneumonia. MD, mean difference; MRMP, macrolide-resistant *Mycoplasma pneumoniae*; MSMP, macrolide-sensitive *Mycoplasma pneumoniae*.

infections showed a trend of more extrapulmonary manifestations or consolidation in 2 studies (*7*,*30*). Some randomized controlled trials indicated a positive effect on early corticosteroid treatment whether or not there was macrolide resistance (*44*,*45*). However, a retrospective study of a large database in Japan did not support this viewpoint (*46*). A well-designed randomized trial or meta-analysis should be considered to clarify the role of corticosteroids. In conclusion, the management of *M. pneumoniae* infection might need to be reappraised.

In addition to prolonged clinical courses, our study indicates the effect of macrolide resistance on antibiotic drug consumption and imprecision. Increased macrolide usage in primary healthcare settings, as well as unnecessary and inappropriate prescriptions to treat acute respiratory tract infections, are common in countries in Asia (*47*–*49*). Continuous selective pressure of routinely used antibiotic drugs and high population density can possibly explain the emergence of MRMP. The extent of *M. pneumoniae* simultaneously increased with rising resistance, further resulting in increased consumption of antibiotic drugs. Antibiotic stewardship should be promoted to reduce macrolide resistance.

Our meta-analysis has limitations. First, not all reported mutations (such as C2617G) were described or checked in the included studies. Because positions 2063 and 2064 accounted for most of the mutations and have been reported in all articles included in this analysis, this influence could be minimized. Second, co-infection was not excluded in all studies. The co-infection rate with *M. pneumoniae* is low in some studies (*1*,*12*,*30*). Nevertheless, how to discriminate between carriage and infection is still a key issue. A combination of PCR and serologic tests, such as measurement of *M. pneumoniae*–specific IgM-secreting cells, would be a better way to determine the role of macrolide resistance in the future (50). Third, the natural course of MRMP infection is modified because in institutions where physicians are alert to MRMP, second-line therapy or corticosteroids will be administered promptly. Although this bias existed in the initial selection process, it reflected the current clinical practice in MRMP-prevalent areas and the dilemma in management of MRMP.

In summary, our analysis found that MRMP infections are associated with longer febrile duration than MSMP infections. Decreased macrolide efficacy and increased ineffective antimicrobial drug use have also been found. The effect of macrolide resistance on disease severity is inconclusive, and there are still diagnostic and therapeutic gaps in the management of MRMP. Reappraisal of precise diagnostic tools and clearly defined treatment are needed.

## About the Author

Dr. Chen is a pediatrician in Chi-Mei Medical Center, Chiali, Tainan, Taiwan. Her research interests include microbiology, neonatology, and vaccinology.

## References

1. Jain S, Williams DJ, Arnold SR, Ampofo K, Bramley AM, Reed C, et al.; CDC EPIC Study Team. Community-acquired pneumonia requiring hospitalization among U.S. children. N Engl J Med. 2015;372:835–45. https://doi.org/10.1056/NEJMoa1405870
2. Shin EJ, Kim Y, Jeong J-Y, Jung YM, Lee M-H, Chung EH. The changes of prevalence and etiology of pediatric pneumonia from National Emergency Department Information System in Korea, between 2007 and 2014. Korean J Pediatr. 2018;61:291–300. https://doi.org/10.3345/kjp.2017.06100
3. Hsieh YC, Tsao KC, Huang CG, Tong S, Winchell JM, Huang YC, et al. Life-threatening pneumonia caused by macrolide-resistant *Mycoplasma pneumoniae*. Pediatr Infect Dis J. 2012;31:208–9. https://doi.org/10.1097/INF.0b013e318234597c
4. Wood PR, Hill VL, Burks ML, Peters JI, Singh H, Kannan TR, et al. Mycoplasma pneumoniae in children with acute and refractory asthma. Ann Allergy Asthma Immunol. 2013;110:328–34.e1. http://doi.org/10.1016/j.anai.2013.01.022
5. Pereyre S, Goret J, Bébéar C. *Mycoplasma pneumoniae*: current knowledge on macrolide resistance and treatment. Front Microbiol. 2016;7:974. https://doi.org/10.3389/fmicb.2016.00974
6. Meyer Sauteur PM, Unger WW, Nadal D, Berger C, Vink C, van Rossum AM. Infection with and carriage of *Mycoplasma pneumoniae* in children. Front Microbiol. 2016;7:329. https://doi.org/10.3389/fmicb.2016.00329
7. Zhou Y, Zhang Y, Sheng Y, Zhang L, Shen Z, Chen Z. More complications occur in macrolide-resistant than in macrolide-sensitive *Mycoplasma pneumoniae* pneumonia. Antimicrob Agents Chemother. 2014;58:1034–8. https://doi.org/10.1128/AAC.01806-13
8. Chen Y, Tian WM, Chen Q, Zhao HY, Huang P, Lin ZQ, et al. Clinical features and treatment of macrolide-resistant *Mycoplasma pneumoniae* pneumonia in children [in Chinese]. Zhongguo Dang Dai Er Ke Za Zhi. 2018;20:629–34.
9. Ma Z, Zheng Y, Deng J, Ma X, Liu H. Characterization of macrolide resistance of *Mycoplasma pneumoniae* in children in Shenzhen, China. Pediatr Pulmonol. 2014;49:695–700. https://doi.org/10.1002/ppul.22851
10. Xin D-L, Wang S, Han X, Ma S-J, Chen X-G. Clinical characteristics of children with macrolide-resistant *Mycoplasma pneumoniae* pneumonia [in Chinese]. J Appl Clin Pediatr. 2010;16:1213–5.
11. Yuan C, Min FM, Ling YJ, Li G, Ye HZ, Pan JH, et al. Clinical characteristics and antibiotic resistance of *Mycoplasma pneumoniae* pneumonia in hospitalized Chinese children. Comb Chem High Throughput Screen. 2018;21:749–54. https://doi.org/10.2174/1386207322666190111112946
12. Cheong KN, Chiu SS, Chan BW, To KK, Chan EL, Ho PL. Severe macrolide-resistant *Mycoplasma pneumoniae*

pneumonia associated with macrolide failure. J Microbiol Immunol Infect. 2016;49:127–30. https://doi.org/10.1016/j.jmii.2014.11.003
13. Lung DC, Yip EK, Lam DS, Que TL. Rapid defervescence after doxycycline treatment of macrolide-resistant *Mycoplasma pneumoniae*-associated community-acquired pneumonia in children. Pediatr Infect Dis J. 2013;32:1396–9. https://doi.org/10.1097/INF.0b013e3182a25c71
14. Cardinale F, Chironna M, Chinellato I, Principi N, Esposito S. Clinical relevance of *Mycoplasma pneumoniae* macrolide resistance in children. J Clin Microbiol. 2013;51:723–4. https://doi.org/10.1128/JCM.02840-12
15. Akashi Y, Hayashi D, Suzuki H, Shiigai M, Kanemoto K, Notake S, et al. Clinical features and seasonal variations in the prevalence of macrolide-resistant *Mycoplasma pneumoniae*. J Gen Fam Med. 2018;19:191–7. https://doi.org/10.1002/jgf2.201
16. Ishiguro N, Koseki N, Kaiho M, Ariga T, Kikuta H, Togashi T, et al.; Hokkaido Pediatric Respiratory Infection Study Group. Therapeutic efficacy of azithromycin, clarithromycin, minocycline and tosufloxacin against macrolide-resistant and macrolide-sensitive *Mycoplasma pneumoniae* pneumonia in pediatric patients. PLoS One. 2017;12:e0173635. https://doi.org/10.1371/journal.pone.0173635
17. Kawai Y, Miyashita N, Yamaguchi T, Saitoh A, Kondoh E, Fujimoto H, et al. Clinical efficacy of macrolide antibiotics against genetically determined macrolide-resistant *Mycoplasma pneumoniae* pneumonia in paediatric patients. Respirology. 2012;17:354–62. https://doi.org/10.1111/j.1440-1843.2011.02102.x
18. Kawai Y, Miyashita N, Kubo M, Akaike H, Kato A, Nishizawa Y, et al. Therapeutic efficacy of macrolides, minocycline, and tosufloxacin against macrolide-resistant *Mycoplasma pneumoniae* pneumonia in pediatric patients. Antimicrob Agents Chemother. 2013;57:2252–8. https://doi.org/10.1128/AAC.00048-13
19. Matsubara K, Okada T, Matsushima T, Komiyama O, Iwata S, Morozumi M, et al. A comparative clinical study of macrolide-sensitive and macrolide-resistant *Mycoplasma pneumoniae* infections in pediatric patients. J Infect Chemother. 2009;15:380–3. https://doi.org/10.1007/s10156-009-0715-7
20. Miyashita N, Kawai Y, Akaike H, Ouchi K, Hayashi T, Kurihara T, et al.; Atypical Pathogen Study Group. Macrolide-resistant *Mycoplasma pneumoniae* in adolescents with community-acquired pneumonia. BMC Infect Dis. 2012;12:126. https://doi.org/10.1186/1471-2334-12-126
21. Okada T, Morozumi M, Tajima T, Hasegawa M, Sakata H, Ohnari S, et al. Rapid effectiveness of minocycline or doxycycline against macrolide-resistant *Mycoplasma pneumoniae* infection in a 2011 outbreak among Japanese children. Clin Infect Dis. 2012;55:1642–9. https://doi.org/10.1093/cid/cis784
22. Kim JH, Kim JY, Yoo CH, Seo WH, Yoo Y, Song DJ, et al. Macrolide resistance and its impacts on *M. pneumoniae* pneumonia in children: comparison of two recent epidemics in Korea. Allergy Asthma Immunol Res. 2017;9:340–6. https://doi.org/10.4168/aair.2017.9.4.340
23. Kim YJ, Shin KS, Lee KH, Kim YR, Choi JH. Clinical characteristics of macrolide-resistant *Mycoplasma pneumoniae* from children in Jeju. J Korean Med Sci. 2017;32:1642–6. https://doi.org/10.3346/jkms.2017.32.10.1642
24. Lee E, Cho HJ, Hong SJ, Lee J, Sung H, Yu J. Prevalence and clinical manifestations of macrolide resistant *Mycoplasma pneumoniae* pneumonia in Korean children. Korean J Pediatr. 2017;60:151–7. https://doi.org/10.3345/kjp.2017.60.5.151
25. Seo YH, Kim JS, Seo SC, Seo WH, Yoo Y, Song DJ, et al. Predictive value of C-reactive protein in response to macrolides in children with macrolide-resistant *Mycoplasma pneumoniae* pneumonia. Korean J Pediatr. 2014;57:186–92. https://doi.org/10.3345/kjp.2014.57.4.186
26. Yoo SJ, Kim HB, Choi SH, Lee SO, Kim SH, Hong SB, et al. Differences in the frequency of 23S rRNA gene mutations in *Mycoplasma pneumoniae* between children and adults with community-acquired pneumonia: clinical impact of mutations conferring macrolide resistance. Antimicrob Agents Chemother. 2012;56:6393–6. https://doi.org/10.1128/AAC.01421-12
27. Yoon IA, Hong KB, Lee HJ, Yun KW, Park JY, Choi YH, et al. Radiologic findings as a determinant and no effect of macrolide resistance on clinical course of *Mycoplasma pneumoniae* pneumonia. BMC Infect Dis. 2017;17:402. https://doi.org/10.1186/s12879-017-2500-z
28. Wu HM, Wong KS, Huang YC, Lai SH, Tsao KC, Lin YJ, et al. Macrolide-resistant *Mycoplasma pneumoniae* in children in Taiwan. J Infect Chemother. 2013;19:782–6. https://doi.org/10.1007/s10156-012-0523-3
29. Wu PS, Chang LY, Lin HC, Chi H, Hsieh YC, Huang YC, et al. Epidemiology and clinical manifestations of children with macrolide-resistant *Mycoplasma pneumoniae* pneumonia in Taiwan. Pediatr Pulmonol. 2013;48:904–11. https://doi.org/10.1002/ppul.22706
30. Yang TI, Chang TH, Lu CY, Chen JM, Lee PI, Huang LM, et al. *Mycoplasma pneumoniae* in pediatric patients: do macrolide-resistance and/or delayed treatment matter? J Microbiol Immunol Infect. 2019;52:329–35. https://doi.org/10.1016/j.jmii.2018.09.009
31. Lee JK, Lee JH, Lee H, Ahn YM, Eun BW, Cho EY, et al. Clonal expansion of macrolide-resistant sequence type 3 *Mycoplasma pneumoniae*, South Korea. Emerg Infect Dis. 2018;24:1465–71. https://doi.org/10.3201/eid2408.180081
32. Tanaka T, Oishi T, Miyata I, Wakabayashi S, Kono M, Ono S, et al. Macrolide-resistant *Mycoplasma pneumoniae* infection, Japan, 2008–2015. Emerg Infect Dis. 2017;23:1703–6. https://doi.org/10.3201/eid2310.170106
33. Katsukawa C, Kenri T, Shibayama K, Takahashi K. Genetic characterization of *Mycoplasma pneumoniae* isolated in Osaka between 2011 and 2017: decreased detection rate of macrolide-resistance and increase of p1 gene type 2 lineage strains. PLoS One. 2019;14:e0209938. https://doi.org/10.1371/journal.pone.0209938
34. Suzuki Y, Seto J, Shimotai Y, Itagaki T, Katsushima Y, Katsushima F, et al. Polyclonal spread of multiple genotypes of *Mycoplasma pneumoniae* in semi-closed settings in Yamagata, Japan. J Med Microbiol. 2019;68:785–90. https://doi.org/10.1099/jmm.0.000969
35. Pereyre S, Charron A, Hidalgo-Grass C, Touati A, Moses AE, Nir-Paz R, et al. The spread of *Mycoplasma pneumoniae* is polyclonal in both an endemic setting in France and in an epidemic setting in Israel. PLoS One. 2012;7:e38585. https://doi.org/10.1371/journal.pone.0038585
36. Ando M, Morozumi M, Adachi Y, Ubukata K, Iwata S. Multilocus sequence typing of *Mycoplasma pneumoniae*, Japan, 2002–2016. Emerg Infect Dis. 2018;24:1895–901. https://doi.org/10.3201/eid2410.171194
37. Lluch-Senar M, Cozzuto L, Cano J, Delgado J, Llórens-Rico V, Pereyre S, et al. Comparative "-omics" in *Mycoplasma pneumoniae* clinical isolates reveals key virulence factors. PLoS One. 2015;10:e0137354. https://doi.org/10.1371/journal.pone.0137354
38. Zhao F, Liu G, Wu J, Cao B, Tao X, He L, et al. Surveillance of macrolide-resistant *Mycoplasma pneumoniae* in Beijing,

China, from 2008 to 2012. Antimicrob Agents Chemother. 2013;57:1521–3. https://doi.org/10.1128/AAC.02060-12
39. Eshaghi A, Memari N, Tang P, Olsha R, Farrell DJ, Low DE, et al. Macrolide-resistant *Mycoplasma pneumoniae* in humans, Ontario, Canada, 2010–2011. Emerg Infect Dis. 2013;19:1525. https://doi.org/10.3201/eid1909.121466
40. Yang EA, Kang HM, Rhim JW, Kang JH, Lee KY. Early corticosteroid therapy for *Mycoplasma pneumoniae* pneumonia irrespective of used antibiotics in children. J Clin Med. 2019;8:726. https://doi.org/10.3390/jcm8050726
41. Izumikawa K. Clinical features of severe or fatal *Mycoplasma pneumoniae* pneumonia. Front Microbiol. 2016;7:800. https://doi.org/10.3389/fmicb.2016.00800
42. Yamazaki T, Kenri T. Epidemiology of *Mycoplasma pneumoniae* infections in Japan and therapeutic strategies for macrolide-resistant *M. pneumoniae*. Front Microbiol. 2016;7:693. https://doi.org/10.3389/fmicb.2016.00693
43. Chou CC, Shen CF, Chen SJ, Chen HM, Wang YC, Chang WS, et al.; Infectious Diseases Society of Taiwan; Taiwan Society of Pulmonary and Critical Care Medicine; Medical Foundation in Memory of Dr. Deh-Lin Cheng; Foundation of Professor Wei-Chuan Hsieh for Infectious Diseases Research and Education; CY Lee's Research Foundation for Pediatric Infectious Diseases and Vaccines; 4th Guidelines Recommendations for Evidence-based Antimicrobial agents use in Taiwan (GREAT) working group. Recommendations and guidelines for the treatment of pneumonia in Taiwan. J Microbiol Immunol Infect. 2019;52:172–99. https://doi.org/10.1016/j.jmii.2018.11.004
44. Huang L, Gao X, Chen M. Early treatment with corticosteroids in patients with *Mycoplasma pneumoniae* pneumonia: a randomized clinical trial. J Trop Pediatr. 2014;60:338–42. https://doi.org/10.1093/tropej/fmu022
45. Yang E-A, Kang H-M, Rhim J-W, Kang J-H, Lee K-Y. Early corticosteroid therapy for *Mycoplasma pneumoniae* pneumonia irrespective of used antibiotics in children. J Clin Med. 2019;8:726. https://doi.org/10.3390/jcm8050726
46. Okubo Y, Michihata N, Morisaki N, Uda K, Miyairi I, Ogawa Y, et al. Recent trends in practice patterns and impact of corticosteroid use on pediatric *Mycoplasma pneumoniae*-related respiratory infections. Respir Investig. 2018;56:158–65. https://doi.org/10.1016/j.resinv.2017.11.005
47. Teratani Y, Hagiya H, Koyama T, Adachi M, Ohshima A, Zamami Y, et al. Pattern of antibiotic prescriptions for outpatients with acute respiratory tract infections in Japan, 2013–15: a retrospective observational study. Fam Pract. 2019;36:402–9. http://doi.org10.1093/fampra/cmy094
48. Uda K, Kinoshita N, Morisaki N, Kasai M, Horikoshi Y, Miyairi I. Targets for optimizing oral antibiotic prescriptions for pediatric outpatients in Japan. Jpn J Infect Dis. 2019;72:149–59. https://doi.org/10.7883/yoken.JJID.2018.374
49. Park J, Han E, Lee SO, Kim D-S. Antibiotic use in South Korea from 2007 to 2014: a health insurance database-generated time series analysis. PLoS One. 2017;12:e0177435. https://doi.org/10.1371/journal.pone.0177435
50. Meyer Sauteur PM, Trück J, van Rossum AMC, Berger C. Circulating antibody-secreting cell response during *Mycoplasma pneumoniae* childhood pneumonia. J Infect Dis. 2020;jiaa062. https://doi.org/10.1093/infdis/jiaa062

Address for correspondence: Tu-Hsuan Chang, Department of Pediatrics, Chi-Mei Medical Center No. 901, Zhonghua Rd., Yongkang Dist, Tainan City 710, Taiwan; email: a755115@yahoo.com.tw

# Efficient Surveillance of *Plasmodium knowlesi* Genetic Subpopulations, Malaysian Borneo, 2000–2018

Paul C.S Divis,[1] Ting H. Hu,[1] Khamisah A. Kadir, Dayang S.A. Mohammad, King C. Hii, Cyrus Daneshvar, David J. Conway, Balbir Singh

Population genetic analysis revealed that *Plasmodium knowlesi* infections in Malaysian Borneo are caused by 2 divergent parasites associated with long-tailed (cluster 1) and pig-tailed (cluster 2) macaques. Because the transmission ecology is likely to differ for each macaque species, we developed a simple genotyping PCR to efficiently distinguish between and survey the 2 parasite subpopulations. This assay confirmed differences in the relative proportions in areas of Kapit division of Sarawak state, consistent with multilocus microsatellite analyses. Analyses of 1,204 human infections at Kapit Hospital showed that cluster 1 caused approximately two thirds of cases with no significant temporal changes from 2000 to 2018. We observed an apparent increase in overall numbers in the most recent 2 years studied, driven mainly by increased cluster 1 parasite infections. Continued monitoring of the frequency of different parasite subpopulations and correlation with environmental alterations are necessary to determine whether the epidemiology will change substantially.

The monkey parasite *Plasmodium knowlesi* was discovered to be a common cause of malaria in humans in 2004, initially from investigations in the Kapit division of Sarawak state, Malaysian Borneo (*1*). Humans acquire infection primarily from wild long-tailed (*Macaca fascicularis*) and pig-tailed (*M. nemestrina*) macaque reservoirs (*2*); *Anopheles* mosquitoes of the leucosphyrus group are vectors (*3*,*4*). *P. knowlesi* malaria has been described across Southeast Asia, but most clinical cases are still reported in Malaysian Borneo (*3*,*5*–*8*). In 2017 and 2018, a total of 7,745 cases were reported in Malaysia, 86.8% of which were detected in Malaysian Borneo (B. Singh, unpub. data) (*9*). *P. knowlesi* infections can be asymptomatic (*10*,*11*), and clinical cases exhibit a wide spectrum of disease ranging from mild symptoms to death (*3*).

Population genetic surveys of *P. knowlesi* infections in humans across Malaysia have revealed 2 divergent subpopulations of the parasite in Malaysian Borneo that are associated with the 2 macaque species locally, suggesting 2 independent zoonoses (*12*,*13*). The cluster 1 type has been associated with long-tailed macaques and the cluster 2 type with pig-tailed macaques (*12*). The existence of 2 sympatric subpopulations also has been confirmed by whole-genome sequencing (WGS) of *P. knowlesi* from patients in Malaysian Borneo (*13*,*14*). In peninsular Malaysia on the Asia mainland, all cases have been caused by another subpopulation, cluster 3, that has not been detected in Malaysian Borneo (*13*,*15*). Limited WGS (*14*,*15*) and microsatellite (*13*) genotyping of *P. knowlesi* isolates derived from human and only long-tailed macaque hosts from peninsular Malaysia showed allopatric divergence for this subpopulation cluster from those of Malaysian Borneo because of geographic separation by the South China Sea.

Increasing numbers of *P. knowlesi* malaria cases detected might be due to increased zoonotic exposure along with a reduction of endemic malaria parasite species (*16*). With the recent identification of different zoonotic *P. knowlesi* genetic subpopulations, determining whether these populations vary in frequency over space and time is important. Interactions with

Author affiliations: Universiti Malaysia Sarawak, Kota Samarahan, Malaysia (P.C.S. Divis, T.H. Hu, K.K. Kadir, D.S.A Mohammad, C. Daneshvar, D.J Conway, B. Singh); London School of Hygiene and Tropical Medicine, London, UK (P.C.S. Divis, D.J. Conway); Kapit Hospital, Kapit, Malaysia (K.C. Hii); University Hospitals Plymouth National Health Service Trust, Plymouth, UK (C. Daneshvar)

DOI: https://doi.org/10.3201/eid2607.190924

[1]These authors contributed equally to this article.

vectors and reservoir hosts will affect distributions of these parasite subpopulations, and human contacts with these vectors and reservoir hosts would determine zoonotic incidence. Because the previously used microsatellite genotyping and WGS are time consuming and expensive, we developed a simple PCR to discriminate between the 2 *P. knowlesi* subpopulations in Malaysian Borneo.

## Materials and Methods

### Identification of Cluster-Specific Markers

We identified high-quality bi-allelic single-nucleotide polymorphisms (SNPs) from whole-genome sequence data of *P. knowlesi* isolates from cluster 1 (n = 38) and cluster 2 (n = 10) subpopulations (*15*). We identified 9,293 SNPs with complete fixation of alternative alleles between the 2 subpopulations. Oligonucleotides for allele-specific PCRs were designed on the basis of genome regions with a high density of fixed SNPs and having multiple SNPs <5 nt apart, especially at the 3′ ends of the designed primers. For each subpopulation, we chose 5 pairs of forward and reverse PCR primers to evaluate for genotyping assays (Appendix Table 1, https://wwwnc.cdc.gov/EID/article/26/7/19-0924-App1.pdf).

### Cluster-Specific Genotyping PCR

PCRs to discriminate subpopulation clusters were optimized in 11-μL reaction volume containing 1X Green GoTaq Flexi buffer (Promega, https://www.promega.com), 5 mmol/L MgCl2, 0.275 U GoTaq DNA polymerase, 0.2 mmol/L dNTP (Bioline, https://www.bioline.com), 1–2-μL DNA template, and 0.25 μmol/L each forward and reverse primers. We tested 2 thermal cycling methods to determine the optimum annealing temperature. The first conventional method was 94°C for 2 min, followed by 35 cycles of initial denaturation of 94°C for 30 s, gradient annealing from 50°C to 66°C for 1 min, extension at 72°C for 30 s, and final elongation at 72°C for 2 min. For the second method, we used the touchdown PCR to increase the specificity and sensitivity in amplification (*17*) with the following 2 phases. We initiated the first phase with denaturation at 94°C for 2 min, followed by 10 cycles of touchdown program of 94°C for 30 s, annealing of 10°C above the primer melting temperature for 45 s and 72°C for 30 s, with a decreased on 1°C of the annealing temperature every cycle. Then, we performed an additional 25 cycles as follows: 94°C for 30 s, annealing of 5°C below the primer annealing primer melting temperature for 45 s, 72°C for 30 s, and final elongation at 72°C for 5 min. We analyzed PCR products by electrophoresis on agarose gel stained with ethidium bromide and visualized them under ultraviolet transillumination.

### DNA and Blood Samples from Malaria Infections

To validate allele-specific PCRs, we obtained DNA samples of *P. knowlesi* infections in Malaysian Borneo from previous studies (*12*,*13*,*15*). Samples from humans were from Betong (n = 29), Kanowit (n = 34), Miri (n = 46), Sarikei (n = 23), Kapit (n = 52), Kudat (n = 46), Ranau (n = 62), and Tenom (n = 48); we also used samples from long-tailed macaques (n = 10) and pig-tailed macaques (n = 5) from Kapit (*2*). We determined subpopulation assignments (cluster 1 or cluster 2) of each infection by analyzing multilocus microsatellite data (*12*) or whole-genome sequence data (*15*). *Plasmodium* DNA controls of humans (*P. falciparum*, *P. vivax*, *P. malariae*, and *P. ovale*) and macaques (*P. knowlesi*, *P. inui*, *P. cynomolgi*, *P. fieldi*, and *P. coatneyi*) were also used for specificity tests of the PCRs.

To determine the frequency of the 2 *P. knowlesi* subpopulations over time, we investigated samples derived from Kapit division, Sarawak state, Malaysian Borneo, where high incidence of cases has been reported (*7*). New samples were collected as dried blood spots on filter papers (3MM Whatman, https://www.sigmaaldrich.com) from *P. knowlesi* clinical cases in Kapit Hospital during September 2016–May 2018 (440 cases). DNA was extracted and *P. knowlesi* confirmed by species-specific nested PCRs (*2*) at the Malaria Research Centre, Universiti Malaysia Sarawak (UNIMAS, Kota Samarahan, Malaysia). We also analyzed 764 DNA samples from persons with *P. knowlesi* infection at Kapit Hospital collected previously: March 2000–December 2002, 110 samples (*1*); March 2006–February 2008, 176 samples (*18*); and June 2013–mid-September 2016, 478 samples (*13*).

### Data Analysis and Ethics Approval

We tabulated genotyping data in Excel and conducted statistical analysis using R (https://www.r-project.org). We also explored temporal patterns for overall *P. knowlesi* subpopulation cases over the previous 5 years using the R package seasonal decomposition of time series (STL) by LOESS (locally estimated scatterplot smoothing) (*19*). We generated STL decomposition using periodic as smoothing parameter for the seasonal component ($n_s$) with no robustness iterations. LOESS is the seasonal-trend decomposition method used in estimating trend from the time series data. The Medical Ethics Committees of UNIMAS (NC-21.02/03-02 Jld 2 [*19*]) and the Medical Research

and Ethics Committee, Malaysian Ministry of Health (NMRR-16-943-31224), approved this study.

## Results

### Development of Simple PCR to Discriminate *P. knowlesi* Cluster 1 and 2 Subpopulations

We tested 10 PCRs on the basis of fixed SNP differences for performance in discriminating the 2 sympatric *P. knowlesi* subpopulations. Of these, 1 assay each for cluster 1 (primer pair C1A) and cluster 2 (primer pair C2J) showed complete specificity when tested on 5 cluster 1 and 9 cluster 2 DNA samples (Figure 1; Appendix Table 2) that were previously confirmed by microsatellites cluster assignments (*13*). These primers were also *P. knowlesi*–specific and did not show amplification on DNA of other simian malaria parasites (*P. coatneyi*, *P. cynomolgi*, *P. fieldi*, and *P. inui*) or human malaria parasites (*P. falciparum*, *P. vivax*, *P. malariae*, and *P. ovale*), or host DNA from humans or either macaque host species (Appendix Figure 1).

We further tested these primer sets for sensitivity using pure DNA of cluster 1 samples with starting parasitemias of 13,793 parasites/μL blood and cluster 2 samples with starting parasitemias of 8,017 parasites/μL blood. We prepared 5-fold serial dilutions to serve as template in separate PCRs. Tests of sensitivity showed limit of detection at ≈4 parasites/μL blood for primer pair C1A and ≈13 parasites/μL blood for primer pair C2J (Appendix Figure 2).

### Proportions of *P. knowlesi* Subpopulations in Different Areas

Analysis of DNA samples of 1,492 *P. knowlesi* malaria cases in different regions of Malaysian Borneo showed cluster 1 as the predominant subpopulation (70%), followed by cluster 2 (28%) (Figure 2; Appendix Table 3). Only 2% of infections were positive for both primer sets, and these infections had mixed genotypes as identified by previous microsatellite analysis (*12*,*13*). Cluster 1 infections were more common at most individual locations sampled throughout Malaysian Borneo, except for Miri and Kanowit, where cluster 2 infections were more common.

We also tested the primer sets on 15 natural infections of wild macaques (10 long-tailed and 5 pig-tailed) from Kapit. *P. knowlesi* infections from all macaques showed concordant macaque host association (cluster 1 in long-tailed macaques and cluster 2 in pig-tailed macaques), except for 1 long-tailed macaque that was infected by both cluster 1 and cluster 2 parasites (Appendix Table 3).

### Temporal Analysis of *P. knowlesi* Subpopulation Types in a High-Incidence Area

In Kapit, where a high incidence of cases has been reported since the zoonosis was discovered to be common (*1*,*7*,*18*), we analyzed DNA samples from 1,204 human *P. knowlesi* infections collected in 3 study periods during 2000–2018. Of those infections, 69% belonged to the cluster 1 subpopulation (Figure 3, panel A; Appendix Table 4). Most (28%) of the remaining *P. knowlesi* infections belonged to the cluster 2 subpopulation, and only 2% had parasites of both types. During 3 study periods of 2000–2002 (n = 110 cases), 2006–2008 (n = 176 cases), and 2013–2018 (n = 918 cases), the proportion of cluster 1 and cluster 2 subpopulations showed similar patterns of distribution with cluster 1 subpopulation as the predominant ones (Pearson p = 0.74). We also observed similar patterns across 12 months of these study periods (Figure 3, panel B), indicating a lack of strong seasonal variation between cluster 1 and cluster 2 infections in Kapit (p = 0.56 by Fisher exact test).

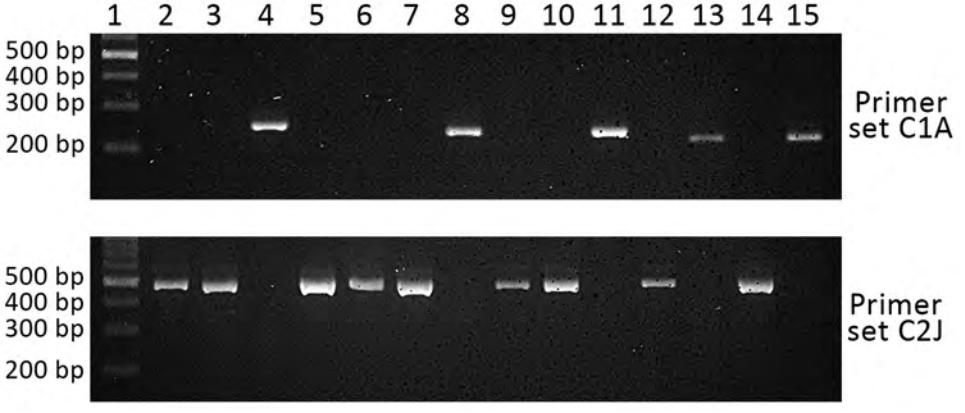


**Figure 1.** Specificity of PCR primer sets C1A and C2J for discriminating *Plasmodium knowlesi* infections of cluster 1 and cluster 2 subpopulations, Kapit division, Sarawak state, Malaysian Borneo. Lane 1, DNA ladder; lane 2, KT025; lane 3, KT027; lane 4, KT029; lane 5, KT031; lane 6, KT042; lane 7, KT055; lane 8, KT057; lane 9, KT114; lane 10, BTG025; lane 11, BTG026; lane 12, BTG033; lane 13, BTG035; lane 14, BTG044; lane 15, BTG062. Primer sequences and amplification conditions are shown in Appendix Table 1 (https://wwwnc.cdc.gov/EID/article/26/7/19-0924-App1.pdf).

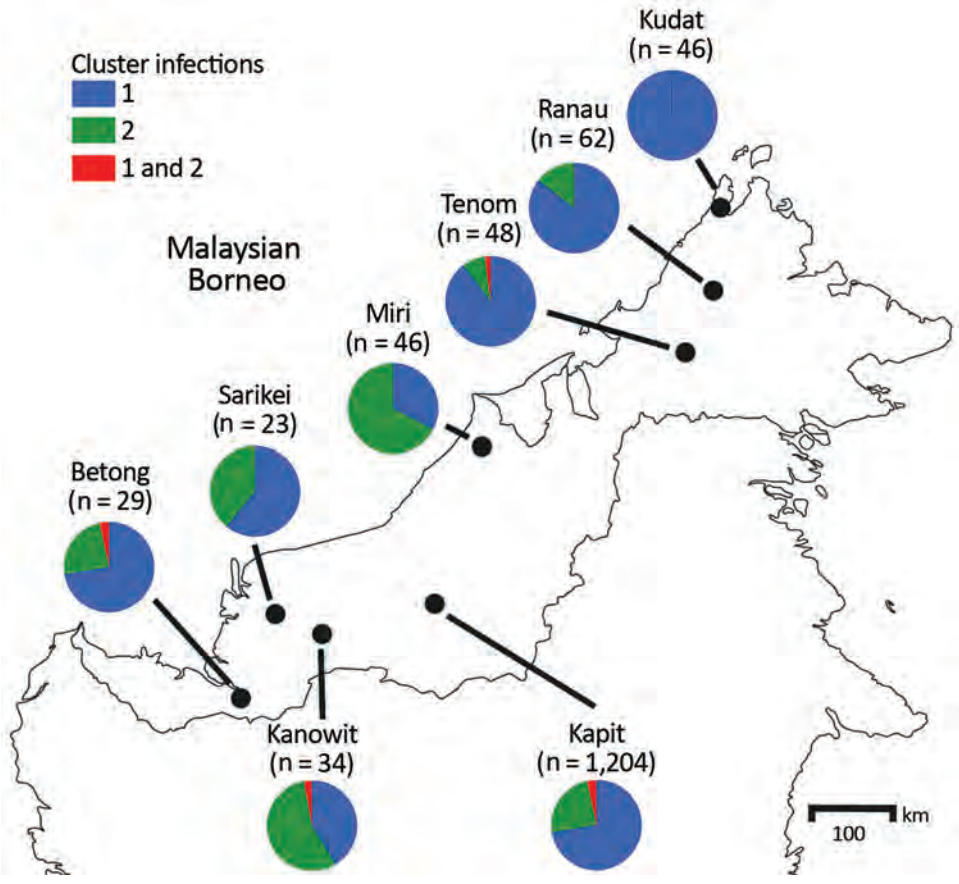


**Figure 2.** Proportions of cluster 1 and cluster 2 *Plasmodium knowlesi* infections as defined with the cluster-specific PCRs, Malaysian Borneo. A total of 1,492 *P. knowlesi* infections from humans were genotyped using the cluster-specific PCR primers. The exact numbers for each location are shown in Appendix Table 3 (https://wwwnc.cdc.gov/EID/article/26/7/19-0924-App1.pdf).

We conducted a more intensive analysis on infections sampled during the most recent 5-year study period (June 2013–May 2018); we made a particular effort to recruit most of the case-patients seeking care at Kapit Hospital during this time. Of the 918 infections genotyped from this period, 637 were cluster 1 infections, 258 were cluster 2 infections, and 23 were mixed cluster infections. The proportion of cluster 1 infections always ranged from 63% to 78% (Pearson p = 0.007) and was highest in the most recent year. The total number of *P. knowlesi* cases was also highest in the most recent year (Figure 4, panel A). Using an STL decomposition method of analysis based on numbers plotted on a monthly basis (Figure 4, panel B), we noted a trend of increasing numbers of cases overall, as well as of the cluster 1 subpopulation

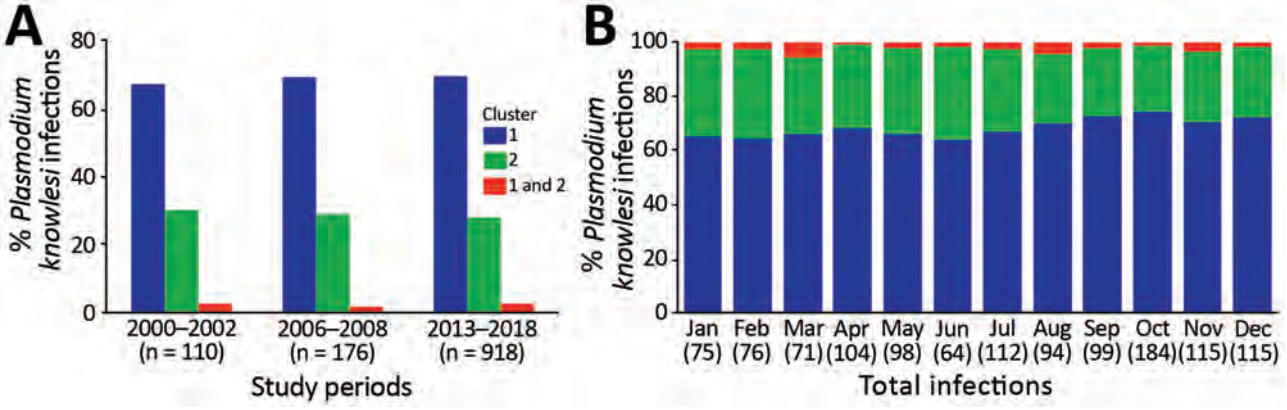


**Figure 3.** Proportions of *Plasmodium knowlesi* subpopulations in humans of the Kapit division, Sarawak state, Malaysian Borneo, 2000–2018. A total of 1,204 *P. knowlesi* infections were genotyped, and distribution patterns of subpopulation clusters were analyzed for 3 different study periods (A) and by months (B). Numbers in parentheses indicate numbers of cases. Blue indicates cluster 1; green, cluster 2; red, clusters 1 and 2.

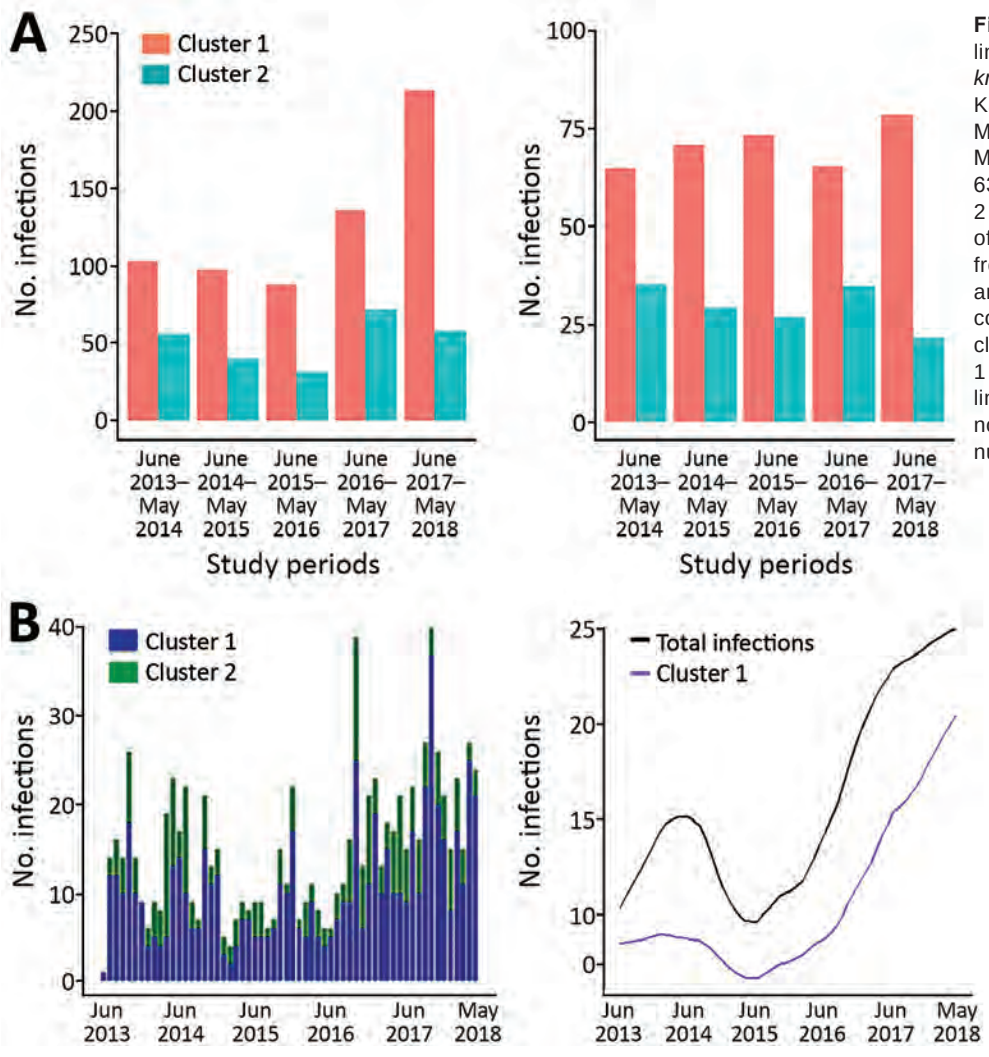


**Figure 4.** Frequency and trend line patterns of *Plasmodium knowlesi* subpopulations in Kapit division, Sarawak state, Malaysian Borneo, June 2013–May 2018. A) Distribution of 637 cluster 1 and 258 cluster 2 infections during each year of the 5-year period. B) The frequency pattern of infections and estimation of trend for the combination of cluster 1 and cluster 2 infections, and cluster 1 infection alone. The trend line of cluster 2 infections is not shown because of a low number of cases.

separately, from June 2016 onward. We found no significant trend for cluster 2 cases separately.

## Discussion

On the basis of fixed SNP differences between the 2 *P. knowlesi* genetic subpopulations in Malaysian Borneo, identified by whole-genome sequence data analysis (*14*,*15*), we successfully developed an allele-specific PCR for discriminating these in large-scale studies. This method enables identification of cluster 1 and cluster 2 subpopulations from field isolates throughout the sympatric distribution, without the need to perform population genetic analysis of multilocus data on all samples. A different *P. knowlesi* subpopulation termed cluster 3 has been described to account for all cases in Peninsular Malaysia (*13*,*15*), but we did not study that subpopulation because it has not been detected in Malaysian Borneo.

The use of these allele-specific PCRs is limited to *P. knowlesi* infections in Malaysian Borneo because they were designed on the basis of the genome sequences of the cluster 1 and cluster 2 parasites found there. These assays could potentially be applied to analyze *P. knowlesi* infections in Kalimantan, Indonesian Borneo, which shares international borders with Malaysian Borneo. The allopatric divergence of cluster 3 subpopulations in Peninsular Malaysia (*13*) indicates the need for development of a separate allele-specific PCR for those parasites, which would require analysis of whole-genome data from substantially more *P. knowlesi* isolates from Peninsular Malaysia.

The validation of this allele-specific PCR shows remarkable sensitivity with single-round (nonnested) amplification, even at a parasitemia of ≈4 parasites/μL blood. Although all samples tested from patients at Kapit Hospital could be genotyped, this PCR

would have limitations on subpatent *P. knowlesi* infections when parasites are undetectable under the microscope (*10*,*11*,*20*).

No clear evidence of direct human–mosquito–human transmission of *P. knowlesi* has yet been determined, although such transmission might be occurring. Most hospitalized *P. knowlesi* malaria patients have been adult farmers or logging camp workers, who regularly spend time in forests or forest fringes, or travelers entering forests (*3*), suggesting that macaque–vector–human transmission is the primary route of infection (*21*). Although the distribution of long-tailed and pig-tailed macaques overlaps throughout Southeast Asia, these macaque species show different habitat preferences (*22*). The preference of long-tailed macaques for cropland, wetland, and urban areas brings them in close proximity to humans, but whether transmission occurs outside of the forests is not known. The widespread distribution of long-tailed macaques corresponds with the cluster 1 parasite subpopulation accounting for most *P. knowlesi* infections in Kapit. The lower frequency of the cluster 2 subpopulation in humans is as expected, given that those parasites are associated with pig-tailed macaques, which occur in more remote forested areas (*22*).

Like many other vectorborne parasitic diseases, malaria is sensitive to environmental changes such as deforestation (*23*); the association between incidences of *P. knowlesi* infections and environmental changes in Sabah, Malaysian Borneo, supports this fact (*16*,*24*), because overall numbers of cases have increased in the past few years (*8*). We have shown that most of the cases in Sabah are of the cluster 1 genetic subpopulation of *P. knowlesi*, and that numbers of this parasite subpopulation have increased in Kapit in the most recent 2 years of the study period. Whether changes in the landscape in Sarawak or other factors have contributed to the increasing numbers of *P. knowlesi* cases needs to be studied. Determining whether any significant differences exist between the clinical outcomes after infection with the different subpopulations also is important. Such determination requires collecting detailed clinical and laboratory data on *P. knowlesi* patients infected with the 2 different subpopulation clusters and performing careful association study analysis to deliver robust inference for the benefits of both clinicians and public health experts.

*P. knowlesi* infections require separate efforts from those being targeting elimination of human malaria (*P. falciparum* and *P. vivax*), particularly in Malaysia, where zoonotic malaria is dominant (*25*). Although *P. knowlesi* is not part of the national elimination program (*26*), monitoring this parasitic infection is crucial because of its increasing incidence. Zoonotic malaria requires new strategies in prevention and control, including monitoring of the different parasite genetic subpopulations.


## Acknowledgments

We thank colleagues at the Malaria Research Centre of UNIMAS and the London School of Hygiene and Tropical Medicine, as well as medical laboratory technologists in Kapit Hospital, Sarawak, for laboratory assistance. We also thank the Director General of Health in Malaysia for permission to publish this article.

This study is supported by postgraduate scholarship from the Sarawak Scholarship Foundation and Ministry of Higher Education in Malaysia, and research grants from UNIMAS (grants nos. F05/SPTDG/1447/16/4, F05/DPP/1505/2016, and F05/SpGS/1551/2017).



## About the Author

Dr. Divis is a senior lecturer at the Faculty of Medicine and Health Sciences and a research fellow at the Malaria Research Centre in UNIMAS, Malaysia. His research interests include molecular epidemiology, population genetics, and genomics of *P. knowlesi*.


## References


1. Singh B, Kim Sung L, Matusop A, Radhakrishnan A, Shamsul SS, Cox-Singh J, et al. A large focus of naturally acquired *Plasmodium knowlesi* infections in human beings. Lancet. 2004;363:1017–24. https://doi.org/10.1016/S0140-6736(04)15836-4
2. Lee KS, Divis PC, Zakaria SK, Matusop A, Julin RA, Conway DJ, et al. *Plasmodium knowlesi*: reservoir hosts and tracking the emergence in humans and macaques. PLoS Pathog. 2011;7:e1002015. https://doi.org/10.1371/journal.ppat.1002015
3. Singh B, Daneshvar C. Human infections and detection of *Plasmodium knowlesi*. Clin Microbiol Rev. 2013;26:165–84. https://doi.org/10.1128/CMR.00079-12
4. Vythilingam I, Lim YA, Venugopalan B, Ngui R, Leong CS, Wong ML, et al. *Plasmodium knowlesi* malaria an emerging public health problem in Hulu Selangor, Selangor, Malaysia (2009–2013): epidemiologic and entomologic analysis. Parasit Vectors. 2014;7:436. https://doi.org/10.1186/1756-3305-7-436
5. William T, Rahman HA, Jelip J, Ibrahim MY, Menon J, Grigg MJ, et al. Increasing incidence of *Plasmodium knowlesi* malaria following control of *P. falciparum* and *P. vivax* malaria in Sabah, Malaysia. PLoS Negl Trop Dis. 2013;7:e2026. https://doi.org/10.1371/journal.pntd.0002026
6. Yusof R, Lau YL, Mahmud R, Fong MY, Jelip J, Ngian HU, et al. High proportion of knowlesi malaria in recent malaria cases in Malaysia. Malar J. 2014;13:168. https://doi.org/10.1186/1475-2875-13-168
7. Ooi CH, Bujang MA, Tg Abu Bakar Sidik TMI, Ngui R, Lim YA. Over two decades of *Plasmodium knowlesi* infections

in Sarawak: trend and forecast. Acta Trop. 2017;176:83–90. https://doi.org/10.1016/j.actatropica.2017.07.027
8. Cooper DJ, Rajahram GS, William T, Jelip J, Mohammad R, Benedict J, et al. *Plasmodium knowlesi* malaria in Sabah, Malaysia, 2015–2017: ongoing increase in incidence despite near-elimination of the human-only *Plasmodium* species. Clin Infect Dis. 2020;70:361–7. https://doi.org/10.1093/cid/ciz237
9. World Health Organization. World malaria report. Geneva: The Organization; 2018.
10. Fornace KM, Nuin NA, Betson M, Grigg MJ, William T, Anstey NM, et al. Asymptomatic and submicroscopic carriage of *Plasmodium knowlesi* malaria in household and community members of clinical cases in Sabah, Malaysia. J Infect Dis. 2016;213:784–7. https://doi.org/10.1093/infdis/jiv475
11. Lubis IND, Wijaya H, Lubis M, Lubis CP, Divis PCS, Beshir KB, et al. Contribution of *Plasmodium knowlesi* to multi-species human malaria infections in North Sumatera, Indonesia. J Infect Dis. 2017;215:1148–55. https://doi.org/10.1093/infdis/jix091
12. Divis PC, Singh B, Anderios F, Hisam S, Matusop A, Kocken CH, et al. Admixture in humans of two divergent *Plasmodium knowlesi* populations associated with different macaque host species. PLoS Pathog. 2015;11:e1004888. https://doi.org/10.1371/journal.ppat.1004888
13. Divis PC, Lin LC, Rovie-Ryan JJ, Kadir KA, Anderios F, Hisam S, et al. Three divergent subpopulations of the malaria parasite *Plasmodium knowlesi*. Emerg Infect Dis. 2017;23:616–24. https://doi.org/10.3201/eid2304.161738
14. Divis PCS, Duffy CW, Kadir KA, Singh B, Conway DJ. Genome-wide mosaicism in divergence between zoonotic malaria parasite subpopulations with separate sympatric transmission cycles. Mol Ecol. 2018;27:860–70. https://doi.org/10.1111/mec.14477
15. Assefa S, Lim C, Preston MD, Duffy CW, Nair MB, Adroub SA, et al. Population genomic structure and adaptation in the zoonotic malaria parasite *Plasmodium knowlesi*. Proc Natl Acad Sci U S A. 2015;112:13027–32. https://doi.org/10.1073/pnas.1509534112
16. Fornace KM, Abidin TR, Alexander N, Brock P, Grigg MJ, Murphy A, et al. Association between landscape factors and spatial patterns of *Plasmodium knowlesi* infections in Sabah, Malaysia. Emerg Infect Dis. 2016;22:201–8. https://doi.org/10.3201/eid2202.150656
17. Korbie DJ, Mattick JS. Touchdown PCR for increased specificity and sensitivity in PCR amplification. Nat Protoc. 2008;3:1452–6. https://doi.org/10.1038/nprot.2008.133
18. Daneshvar C, Davis TM, Cox-Singh J, Rafa'ee MZ, Zakaria SK, Divis PC, et al. Clinical and parasitological response to oral chloroquine and primaquine in uncomplicated human *Plasmodium knowlesi* infections. Malar J. 2010;9:238. https://doi.org/10.1186/1475-2875-9-238
19. Cleveland RB, Cleveland WS, McRae JE, Terpenning I. STL: a seasonal-trend decomposition procedure based on LOESS. J Off Stat. 1990;6:3–73.
20. Siner A, Liew ST, Kadir KA, Mohamad DSA, Thomas FK, Zulkarnaen M, et al. Absence of *Plasmodium inui* and *Plasmodium cynomolgi*, but detection of *Plasmodium knowlesi* and *Plasmodium vivax* infections in asymptomatic humans in the Betong division of Sarawak, Malaysian Borneo. Malar J. 2017;16:417. https://doi.org/10.1186/s12936-017-2064-9
21. Imai N, White MT, Ghani AC, Drakeley CJ. Transmission and control of *Plasmodium knowlesi*: a mathematical modelling study. PLoS Negl Trop Dis. 2014;8:e2978. https//doi.org/10.1371/journal.pntd.0002978
22. Moyes CL, Shearer FM, Huang Z, Wiebe A, Gibson HS, Nijman V, et al. Predicting the geographical distributions of the macaque hosts and mosquito vectors of *Plasmodium knowlesi* malaria in forested and non-forested areas. Parasit Vectors. 2016;9:242. https://doi.org/10.1186/s13071-016-1527-0
23. Confalonieri UE, Margonari C, Quintão AF. Environmental change and the dynamics of parasitic diseases in the Amazon. Acta Trop. 2014;129:33–41. https://doi.org/10.1016/j.actatropica.2013.09.013
24. Brock PM, Fornace KM, Grigg MJ, Anstey NM, William T, Cox J, et al. Predictive analysis across spatial scales links zoonotic malaria to deforestation. Proc Biol Sci. 2019;286:20182351. https://doi.org/10.1098/rspb.2018.2351
25. Barber BE, Rajahram GS, Grigg MJ, William T, Anstey NM. World malaria report: time to acknowledge *Plasmodium knowlesi* malaria. Malar J. 2017;16:135. https://doi.org/10.1186/s12936-017-1787-y
26. World Health Organization. Eliminating malaria: case study 8. Progress towards elimination in Malaysia. San Francisco: University of California; 2015.

Address for correspondence: Paul C.S. Divis, Malaria Research Centre, Faculty of Medicine and Health Sciences, Universiti Malaysia Sarawak, 94300 Kota Samarahan, Sarawak, Malaysia; email: pcsimon@unimas.my

# Bat and Lyssavirus Exposure among Humans in Area that Celebrates Bat Festival, Nigeria, 2010 and 2013

Neil M. Vora, Modupe O.V. Osinubi, Lora Davis, Mohammed Abdurrahman, Elizabeth B. Adedire, Henry Akpan, Abimbola F. Aman-Oloniyo, Solomon W. Audu, Dianna Blau, Raymond S. Dankoli, Ajoke M. Ehimiyein, James A. Ellison, Yemi H. Gbadegesin, Lauren Greenberg, Dana Haberling, Christina Hutson, Jibrin M. Idris, Grace S.N. Kia, Maruf Lawal, Samson Y. Matthias, Philip P. Mshelbwala, Michael Niezgoda, Albert B. Ogunkoya, Abiodun O. Ogunniyi, Gloria C. Okara, Babasola O. Olugasa, Okechukwu P. Ossai, Akin Oyemakinde, Marissa K. Person, Charles E. Rupprecht, Olugbon A. Saliman, Munir Sani, Olufunmilayo A. Sanni-Adeniyi, P.S. Satheshkumar, Todd G. Smith, Mariat O. Soleye, Ryan M. Wallace, Sebastian K. Yennan, Sergio Recuenco

Using questionnaires and serologic testing, we evaluated bat and lyssavirus exposure among persons in an area of Nigeria that celebrates a bat festival. Bats from festival caves underwent serologic testing for phylogroup II lyssaviruses (Lagos bat virus, Shimoni bat virus, Mokola virus). The enrolled households consisted of 2,112 persons, among whom 213 (10%) were reported to have ever had bat contact (having touched a bat, having been bitten by a bat, or having been scratched by a bat) and 52 (2%) to have ever been bitten by a bat. Of 203 participants with bat contact, 3 (1%) had received rabies vaccination. No participant had neutralizing antibodies to phylogroup II lyssaviruses, but ≥50% of bats had neutralizing antibodies to these lyssaviruses. Even though we found no evidence of phylogroup II lyssavirus exposure among humans, persons interacting with bats in the area could benefit from practicing bat-related health precautions.

Bats are vital to many ecosystems and provide benefits to humans (*1*). However, under certain circumstances, bats may pose a risk to human health, as they host several zoonotic pathogens (*2*). Humans should therefore avoid bat contact unless appropriate precautions are taken. Among the most concerning batborne pathogens are viruses within the genus *Lyssavirus*. Previously unimmunized humans exposed to any of the >16 currently recognized and putative lyssaviruses (typically through a bite from an infected animal) will have 1 of 3 outcomes. First is a complete lack of any lyssavirus infection, characterized by the absence of both illness and lyssavirus-neutralizing antibody production. Second is a productive lyssavirus infection, characterized by a fatal encephalitis known as rabies (*3*). A human with rabies may produce lyssavirus-neutralizing antibodies in the end stages of illness as the disease progresses, although this response is typically inadequate for viral clearance (*4*). Third is an abortive lyssavirus infection (sometimes termed an exposure) characterized by the absence of frank encephalitis but with production of lyssavirus-neutralizing antibodies. Although

Author affiliations: Centers for Disease Control and Prevention, Atlanta, Georgia, USA (N.M. Vora, M.O.V. Osinubi, L. Davis, D. Blau, J.A. Ellison, L. Greenberg, D. Haberling, C. Hutson, M. Niezgoda, M.K. Person, C.E. Rupprecht, P.S. Satheshkumar, T.G. Smith, R.M. Wallace, S. Recuenco); Ahmadu Bello University, Zaria, Nigeria (M. Abdurrahman, S.W. Audu, A.M. Ehimiyein, G.S.N. Kia, M. Lawal, A.B. Ogunkoya, M. Sani); African Field Epidemiology Network, Abuja, Nigeria (E.B. Adedire, J.M. Idris, G.C. Okara); Federal Ministry of Health, Abuja (H. Akpan, A. Oyemakinde, O.A. Sanni-Adeniyi); Walden University, Abuja (A.F. Aman-Oloniyo); World Health Organization, Borno, Nigeria (R.S. Dankoli); Nigerian Institute of Science Laboratory Technology, Ibadan, Nigeria (Y.H. Gbadegesin); Ministry of Health, Kaduna State, Kaduna, Nigeria (S.Y. Matthias); University of Queensland, Brisbane, Queensland, Australia (P.P. Mshelbwala); University of Ibadan, Ibadan (A.B. Ogunkoya, B.O. Olugasa); Nigeria Centre for Disease Control, Abuja (A.O. Ogunniyi, S.K. Yennan); Ministry of Health, Enugu State, Enugu, Nigeria (O.P. Ossai); Ministry of Agriculture and Natural Resources, Ilorin, Nigeria (O.A. Saliman); Federal Ministry of Agriculture and Rural Development, Abuja (M.O. Soleye)

DOI: https://doi.org/10.3201/eid2607.191016

rarely documented, the prevalence of abortive lyssavirus infections among some Amazonian communities whose members experience frequent bites from vampire bats has challenged the paradigm that lyssavirus infections are nearly always productive and therefore fatal (*5*).

The various lyssaviruses sort into different phylogroups (*6*). Phylogroup I includes rabies virus, Duvenhage virus, and several others. Rabies can be prevented after exposure to phylogroup I lyssaviruses with prompt administration of postexposure prophylaxis (PEP) that includes wound cleansing, rabies vaccine, and, when indicated, rabies immune globulin (*3*,*7*,*8*). Phylogroup II includes Lagos bat virus, Shimoni bat virus, and Mokola virus. These viruses are phylogenetically and antigenically distant from phylogroup I members (*9*). West Caucasian bat virus and Ikoma lyssavirus are even more distant lyssaviruses (*10*,*11*). The rabies vaccines available for use in the previously described PEP regimen may not be effective against non–phylogroup I lyssaviruses (*10*–*12*). Evidence of abortive lyssavirus infections outside the Amazon is limited, but they could possibly occur wherever humans frequently interact with infected animals (*5*,*13*,*14*).

Twice a year in the Idanre area of Nigeria, a 1-day bat festival takes place in which boys and men enter into designated caves to capture bats, typically with their bare hands (*15*) (Figure 1). Captured bats are cooked and eaten, sold in markets, and used in cultural ceremonies. Pathogen spillover from bats to humans might occur during these festivities, given that some Nigerian bats harbor lyssaviruses such as Lagos bat virus and other pathogens such as *Bartonella rousetti* (*16*–*20*). Furthermore, the most frequently identified bat species roosting in the festival caves is the Egyptian fruit bat (*Rousettus aegyptiacus*), which is a reservoir for Marburg virus and Sosuga virus (*15*,*21*–*23*).

We evaluated bat and lyssavirus exposure among humans in the area around Idanre, Nigeria. Our objectives were to determine the prevalence of bat contact, to identify factors associated with bat contact, to assess knowledge about batborne infections and health precautions related to bats, to determine whether febrile illnesses occur following the bat festival, to determine whether abortive lyssavirus infections occur, and to identify whether lyssaviruses circulate among bats in the festival caves.

## Methods

### Study Design

Work with human participants was approved by the Centers for Disease Control and Prevention (CDC), Ahmadu Bello University, and the National Health Research Ethics Committee of Nigeria. All animal sampling was conducted in compliance with a protocol approved by the CDC Animal Institutional Care and Use Committee.

Persons eligible to participate were those residing in communities located near the 2 festival caves in the Idanre area (Figure 2). We recruited study participants through community surveys and through a convenience sample; some respondents participated in a follow-up survey. Before enrolling, adults (persons ≥18 years of age) and mature minors (persons 13–17 years of age who were married, had children, or provided for their own livelihood) provided consent. Persons <18 years of age who were not mature minors had to get guardian consent and provide assent if ≥7 years of age. We administered study questionnaires verbally and recorded responses electronically. After administering the study questionnaire, we collected blood specimens from participants who agreed.

We completed community surveys during September 26–28, 2010 (2010 community survey; 9–11 days after the September 17, 2010, bat festival) and March 2–March 6, 2013 (2013 community survey; 11–15 days after the February 19, 2013, bat festival) (Figure 3). We enrolled households into the survey from 9 rural villages near the festival caves and from the


**Figure 1.** Bat hunters and bats captured during a bat festival, Idanre area, Nigeria, 2013. A) Bat hunters with slingshots and bats captured during a bat festival. B) Bats captured during a bat festival. C) Bat hunter with a bat captured during a bat festival.

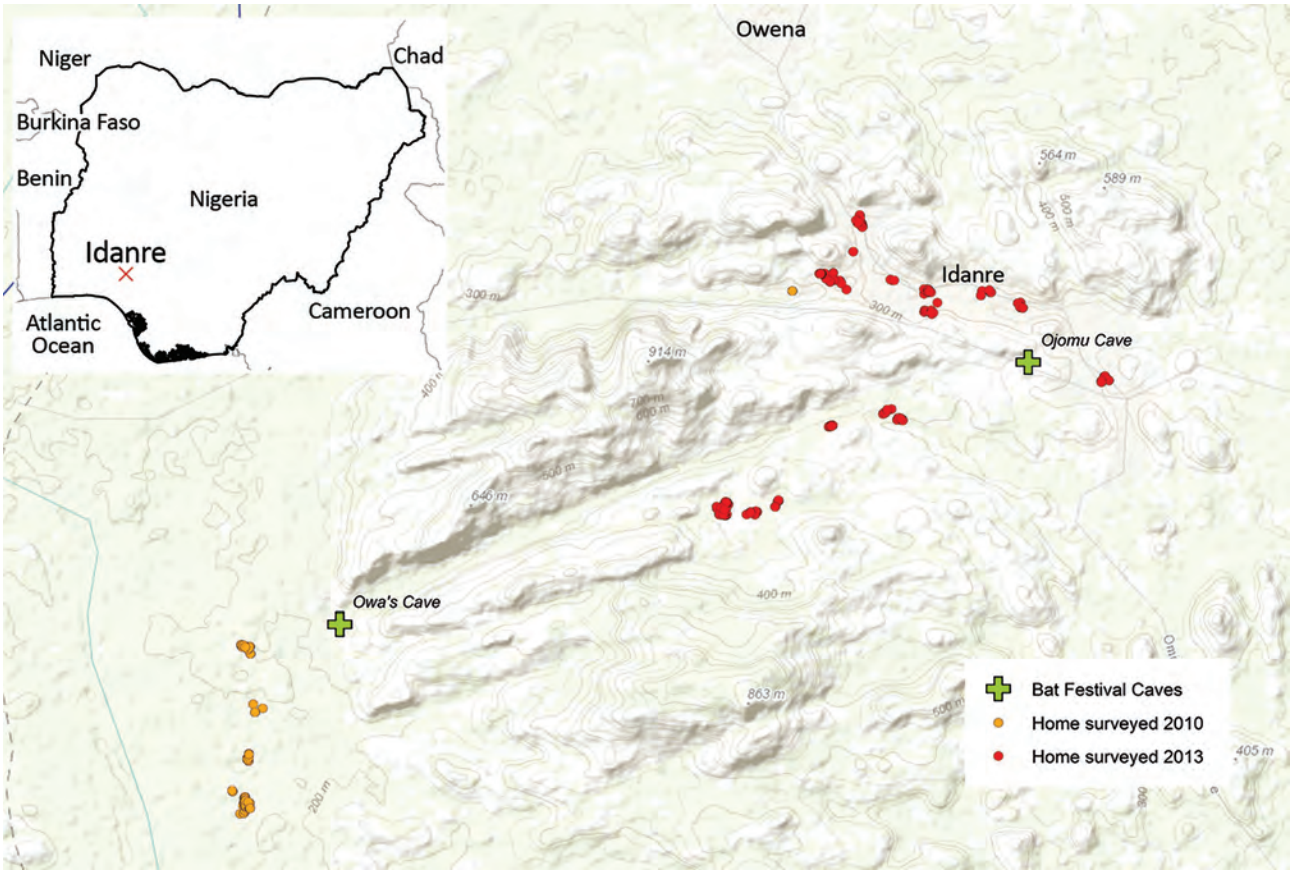


**Figure 2.** Locations of festival caves and households enrolled in 2 community surveys and a bat hunter survey of bat exposures, Idanre area, Nigeria, 2010 and 2013. Inset map shows location of Idanre area within Nigeria.

town of Idanre. Generally, all households within rural villages were offered enrollment in the study. In contrast, Idanre was divided into ≈100 zones, and households from 10 randomly selected zones were offered enrollment in the study. At the time of the household visit, an adult or mature minor had to be present. If consent was provided, this adult or mature minor was considered the main household respondent and was the first person of the household to whom the study questionnaire was administered (Appendix 1, https://wwwnc.cdc.gov/EID/article/26/7/19-1016-App1.pdf). We then administered a similar study questionnaire to additional household respondents, who were other consenting or assenting household members. However, to enroll as an additional household respondent, the household member had to be immediately available and either had previously had bat contact (defined as having touched a bat, having been bitten by a bat, or having been scratched by a bat) or had eaten a bat. This requirement was different than that for main household respondents, for whom having had bat contact or having eaten a bat were not requirements for enrollment.

We recruited additional participants outside the community surveys on March 6, 2013 (2013 bat hunter survey) using a convenience sample of bat hunters composed exclusively of persons who actively trapped bats during the bat festival (they may also have trapped bats at other times of the year) (Figure 3). These participants answered the same study questionnaire as main household respondents from the community survey (Appendix 1). Study participants in the community surveys may also have hunted bats (in that they actively trapped bats during and outside the bat festival), but data for these participants were analyzed with other community survey data and handled separately from the 2013 bat hunter survey. Persons who participated in the 2013 community survey or 2013 bat hunter survey and who agreed underwent a follow-up survey during May 14–19, 2013 (2013 follow-up survey; 85–90 days after the February 19, 2013, bat festival took place) (Appendix 1).

### Human Serologic Testing

We stored blood specimens on ice and centrifuged them within 12 hours of collection. We stored

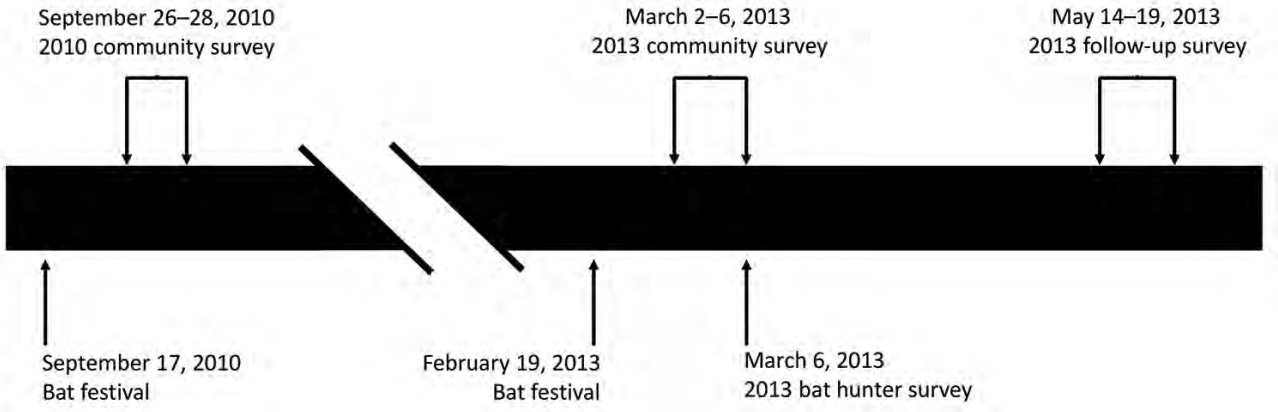


**Figure 3.** Timeline of events for 2 community surveys, a bat hunter survey, and a follow-up survey of bat exposures, Idanre area, Nigeria, 2010 and 2013.

serum specimens at -80°C except while in the field and during shipment to the United States, when they were stored on dry ice. We tested serum specimens for neutralizing antibodies against rabies virus, Duvenhage virus, Lagos bat virus, Shimoni bat virus, Mokola virus, and West Caucasian bat virus using a modification of the rapid fluorescent focus inhibition test (*5*,*24*–*26*). We considered serum samples that exhibited complete neutralization of challenge lyssavirus at a 1:5 serum dilution to have detectable neutralizing antibodies to that lyssavirus (*3*).

### Bat Capture, Species Identification, Specimen Collection, and Testing

We captured bats from the 2 festival caves (Figure 2) using nets. Taxonomic identification of bat species was based on morphology. We anesthetized bats by intramuscular injection of ketamine and then euthanized them via cardiac exsanguination. We centrifuged blood specimens within 4 hours of collection. We also collected bat brains. We stored serum and brain specimens at -80°C except while in the field and during shipment to the United States, when they were stored on dry ice.

We tested serum samples for neutralizing antibodies against Duvenhage virus, Lagos bat virus, Shimoni bat virus, Mokola virus, and Ikoma lyssavirus using a microneutralization test (*27*). We considered serum samples that exhibited >50% neutralization of challenge lyssavirus at 1:10 serum dilution to have detectable neutralizing antibodies to that lyssavirus. We tested brains for lyssavirus antigens with the direct fluorescent antibody test using a FITC-labeled monoclonal antibody kit (Fujirebio Diagnostics, https://www.fujirebio.com) (*28*) (Appendix 2, https://wwwnc.cdc.gov/EID/article/26/7/19-1016-App2.pdf).

### Data Analysis

We analyzed data using SAS software (https://www.sas.com) (details in Appendix 2). A p value <0.05 was considered statistically significant.

## Results

Through the community surveys in 2010 and 2013, we enrolled 264 households (254 unique households and 10 that participated in both years) (Table 1). Each enrolled household had a main household respondent; 87 persons from enrolled households participated as additional household respondents. Most of the 2013 respondents also participated in the 2013 follow-up survey (172/217 [79%] from the 2013 community survey and 18/21 [86%] from the 2013 bat hunter survey).

More than one quarter of enrolled households (72/264; 27%) had ≥1 household member who had ever participated in the bat festival (Table 1). Almost two thirds of enrolled households (168; 64%) had ≥1 household member who had ever had bat contact. Nearly two thirds of enrolled households (166; 63%) had ≥1 household member who had ever touched a bat. About one fifth of households had ≥1 household member who had ever been bitten (44; 17%) or scratched (56; 21%) by a bat. Nearly three quarters of households had ≥1 household member who had ever eaten a bat (188; 71%).

The enrolled households were composed of 2,112 persons, among whom 213 (10%) were reported to have ever had bat contact, 211 (10%) to have ever touched a bat, 52 (2%) to have ever been bitten by a bat, 66 (3%) to have ever been scratched by a bat, and 265 (13%) to have ever eaten a bat (Table 2). Of 254 main household respondents, 141 (56%) reported having ever had bat contact (Table 3, https://wwwnc.cdc.gov/EID/article/26/7/19-1016-T3.htm). Factors significantly associated with bat contact included

being male (OR 2.08, 95% CI 1.24–3.49), having ever participated in the bat festival (OR 20.17, 95% CI 6.09–66.82), having ever entered a bat cave or bat refuge (OR 31.45, 95% CI 7.45–132.73), having ever prepared a bat as food (OR 9.85, 95% CI 5.37–18.07), and having ever eaten a bat (OR 8.56, 95% CI 4.57–16.03).

Although more than half of participants with bat contact in the 2010 community survey, 2013 community survey, and 2013 bat hunter survey knew that animal bites are a mechanism of rabies virus transmission or that rabies is severe, they more often attributed dogs as being a rabies source (≥60%) than bats (≤3%) (Appendix 2 Table 1). About 50% of participants with bat contact in the 2010 and 2013 community surveys and 86% of participants in the 2013 bat hunter survey stated that they would do nothing if bitten or scratched by a bat. Among participants with bat contact in the 2010 community survey, 2013 community survey, and 2013 bat hunter survey, only 1%, 2%, and 5%, respectively, had ever received rabies vaccination. Furthermore, only 3%, 7%, and 5% of these participants, respectively, were aware that bats can cause diseases other than rabies.

More main household respondents with bat contact knew that animal bites are a mechanism of rabies virus transmission and that rabies is severe compared with those without bat contact (Table 3). However, knowledge about bats as a potential rabies source was low and not different among main household respondents with and without bat contact. There was no significant difference between main household respondents with and without bat contact regarding history of rabies vaccination and awareness that bats can cause diseases other than rabies. Study participants with bat contact in the 2010 community survey, 2013 community survey, and 2013 bat hunter survey infrequently reported knowledge of any illness as a result of bats or being in a bat cave (1%, 3%, and 0%, respectively) (Appendix 2 Table 1).

Among 170 main household respondents and additional household respondents in the 2013 community survey who participated in the 2013 follow-up survey, 23 (14%) had experienced a febrile illness within

**Table 1.** Characteristics of households enrolled in 2 community surveys of bat exposures, Idanre area, Nigeria, 2010 and 2013

| Characteristic | 2010 community survey, no. (%) | 2013 community survey, no. (%) | Total, no. (%) |
|---|---|---|---|
| Households visited | 90 | 183 | 273 |
| Households enrolled | 90 (100) | 174 (95) | 264 (97) |
| Total participants enrolled | 134 | 217 | 351 |
| Main household respondents* | 90 (67) | 174 (80) | 264 (75) |
| Additional household respondents* | 44 (33) | 43 (20) | 87 (25) |
| Mean participants enrolled per household (SD) | 1.5 (0.9) | 1.2 (0.6) | 1.3 (0.7) |
| Main household respondents* | 1.0 (0) | 1.0 (0) | 1.0 (0) |
| Additional household respondents* | 0.5 (0.9) | 0.2 (0.6) | 0.3 (0.7) |
| Mean persons per household (SD) | 7.6 (4.7) | 8.2 (5.7) | 8.0 (5.4) |
| Persons living within enrolled households | 688 | 1,424 | 2,112 |
| Male | 372 (54) | 734 (52) | 1,106 (52) |
| Female | 316 (46) | 690 (48) | 1,006 (48) |
| Age distribution of persons represented among enrolled households | n = 688 | n = 1,424 | n = 2,112 |
| <6 y | 115 (17) | 278 (20) | 393 (19) |
| 6–17 y | 162 (24) | 419 (29) | 581 (28) |
| ≥18 y | 411 (60) | 727 (51) | 1,138 (54) |
| Main material used to build house | n = 90 | n = 174 | n = 264 |
| Adobe/mud | 56 (62) | 82 (47) | 138 (52) |
| Cement/brick | 33 (37) | 92 (53) | 125 (47) |
| Wood | 1 (1) | 0 | 1 (0.4) |
| Openings in house that could allow bats to enter | 56 (62) | 106 (61) | 162 (61) |
| Households with animals (pets or livestock) (%) | 52 (58) | 90 (52) | 142 (54) |
| Households with ≥1 animal (pet or livestock) that had been vaccinated against rabies | 0 (0) | 7 (8) | 7 (5) |
| Households with ≥1 member who had ever participated in bat festival† | 22 (24) | 50 (29) | 72 (27) |
| Households with ≥1 member who had ever had bat contact‡ | 51 (57) | 117 (67) | 168 (64) |
| Households with ≥1 member who had ever touched a bat | 50 (56) | 116 (67) | 166 (63) |
| Households with ≥1 member who had ever been bitten by a bat | 14 (16) | 30 (17) | 44 (17) |
| Households with ≥1 member who had ever been scratched by a bat | 19 (21) | 37 (21) | 56 (21) |
| Households with ≥1 member who had ever eaten a bat | 64 (71) | 124 (71) | 188 (71) |

*Main household respondents are adults or mature minors (persons aged 13–17 y who were married, had children, or provided for their own livelihood) present at the time of household visit who provided consent to participate in the survey; the main household respondent was the first person of the household to whom the study questionnaire was administered. Additional household respondents are other consenting or assenting household members who were immediately available to answer the study questionnaire and either had previously had bat contact or had previously eaten a bat.
†This may be an underestimate, as only main and additional household respondents were asked if they had participated in the bat festival. We did not ask if other members of the household had ever participated in the bat festival.
‡Bat contact was defined as having touched a bat, having been bitten by a bat, or having been scratched by a bat.

**Table 2.** Types of bat exposure among persons living within households enrolled in 2 community surveys of bat exposures, Idanre area, Nigeria, 2010 and 2013

| Type of bat exposure | No. (%), n = 2,112 |
|---|---|
| Ever had bat contact* | 213 (10) |
| Ever touched a bat | 211 |
| Ever bitten by a bat | 52 |
| Ever scratched by a bat | 66 |
| Ever eaten a bat | 265 (13) |

*Bat contact was defined as having touched a bat, having been bitten by a bat, or having been scratched by a bat.

90 days of the February 19, 2013, bat festival (Table 4). Factors such as having had any bat contact within the past 90 days, having touched a bat within the past 90 days, having been bitten by a bat within the past 90 days, having been scratched by a bat within the past 90 days, having participated in the bat festival within the past 90 days, and having entered a bat cave or bat refuge within the past 90 days were not significantly different between those with a febrile illness and those without.

Among 18 participants from the 2013 bat hunter survey who participated in the 2013 follow-up survey, 7 (39%) had experienced a febrile illness within 90 days of the February 19, 2013, bat festival. Mean age was significantly higher among those with a febrile illness compared with those without (61 years vs. 49 years; p = 0.048). The odds of having entered a bat cave or bat refuge within the past 90 days was significantly higher among those without a febrile illness compared with those with a febrile illness (p = 0.03). There were no other significant differences between those with a febrile illness and those without when analyzing the same characteristics (Table 4).

Of all study participants who underwent serologic testing, only 2 had lyssavirus neutralizing antibodies, both against rabies virus (Appendix 2 Table 2). Both denied recent encephalitis-like illness or having ever received rabies vaccine, but 1 reported prior bat contact. One of these respondents underwent repeat serologic testing for rabies virus neutralizing antibodies during the 2013 follow-up survey, and rabies virus neutralizing antibodies were still detectable.

We sampled 211 bats: 120 bats during September 2010 (112 *Rousettus aegyptiacus*, 8 *Hipposideros gigas*) and 91 during February 2013 (all *R. aegyptiacus*); none demonstrated clinical illness at time of capture. No *R. aegyptiacus* bats had neutralizing antibodies to Duvenhage virus; ≥50% had neutralizing antibodies to Lagos bat virus, Shimoni bat virus, and Mokola virus; and 1 had neutralizing antibodies to Ikoma lyssavirus (Table 5; Appendix 2 Table 3). Lyssavirus antigens were not detected in brain specimens from any of the 211 bats.

## Discussion

The occurrence of purposeful human interactions with bats, such as hunting for food (e.g., bushmeat), has been identified in several parts of the world and can pose a risk to human health through spillover of zoonotic pathogens from bats to humans (*29*–*31*). We therefore investigated bat and lyssavirus exposures among humans in an area of Nigeria that celebrates a biannual bat festival. Overall, we found that persons who interact with bats in this area are likely at risk for phylogroup II lyssavirus exposures, and public health precautions are warranted.

Although nearly two thirds of households enrolled in our study had ≥1 household members who had ever had bat contact, only about one quarter of households reported having ≥1 household members who had ever participated in the bat festival. This finding strongly suggests that a sizable proportion of the human population in the area has had bat exposures unrelated to the bat festival. Furthermore, 10% of persons living within households enrolled in our community surveys had previously had bat contact and 2% had been bitten by a bat. We do not know whether the bat contact and bat bites among these persons are related to participation in the bat festival or to interactions with bats from the festival caves. Because entry into the festival caves is allowed only during the bat festivals, we suspect that many of these persons have had interactions with bats that are not from the festival caves. Regardless, these person-level data on the prevalence of bat contact and bat bites are likely an underestimate of the true prevalence of bat contact and bat bites in the area; persons with a history of bat interactions might not have been available or were not referred by other household members so they were not enrolled in the study, or persons who have had such bat interactions might have failed to report them when responding to the survey.

We also found strong serologic evidence that lyssaviruses circulate among bats in the festival caves. We found neutralizing antibodies to Lagos bat virus, Shimoni bat virus, and Mokola virus in ≥50% of bats, which is higher than in some prior reports (*17*,*32*–*34*). All 3 of these lyssaviruses belong to phylogroup II. We did not detect lyssavirus antigen in brains of any seropositive bat that we captured, suggesting that these bats survived past exposure to a phylogroup II lyssavirus. We cannot be sure which phylogroup II lyssavirus predominantly circulates in this bat population, given potential serologic cross reactivity and because we did not isolate any lyssavirus from bats. However, we suspect Lagos bat virus because it has

been documented in *R. aegyptiacus* bats before and because it was first isolated in a fruit bat in Nigeria, although we cannot rule out the possibility that a yet uncharacterized phylogroup II lyssavirus circulates among these bats (*18*,*35*).

Although some respondents reported a febrile illness after the 2013 bat festival, this finding was not associated with having recent bat contact or recent participation in the bat festival. We recommend caution in interpreting these findings. A variety of

**Table 4.** Characteristics associated with experiencing a febrile illness within 90 days of the bat festival in a community survey of bat exposures, Idanre area, Nigeria, 2013*

| Characteristic | Febrile illness within 90 d of bat festival, no. (%), n = 23 | No febrile illness within 90 d of bat festival, no. (%), n = 147 | p value | OR (95% CI) |
|---|---|---|---|---|
| Demographics | | | | |
| Mean age (SD) | 47 (18) | 43 (17) | 0.39 | NA |
| Age range, min–max | 18–80 | 18–89 | NA | NA |
| Median age (interquartile range) | 47 (32–65) | 38 (30–55) | NA | NA |
| Age <25 y | 2 (9) | 18 (12) | 0.63 | 0.68 (0.14–3.27) |
| Male sex | 13 (57) | 80 (54) | 0.85 | 1.09 (0.45–2.65) |
| Education | | | | |
| Some secondary or above | 11 (48) | 65 (44) | 0.73 | 1.16 (0.51–2.61) |
| Completed secondary or above | 9 (39) | 40 (27) | 0.21 | 1.72 (0.74–4.00) |
| Household characteristics | | | | |
| Persons in household | | | | |
| <5 persons | 7 (30) | 38 (26) | 0.66 | 1.25 (0.46–3.41) |
| <10 persons | 18 (78) | 97 (66) | 0.31 | 1.86 (0.56–6.15) |
| Main material used to build house | | | | |
| Adobe/mud | 14 (61) | 71 (48) | 0.29 | 1.67 (0.65–4.24) |
| Cement/brick | 9 (39) | 76 (52) | Referent | Referent |
| Wood | 0 | 0 | NP | NP |
| Openings present in house that could allow bats to enter | 14 (61) | 91 (62) | 0.93 | 0.96 (0.38–2.44) |
| Household with animals† | 12 (52) | 68 (46) | 0.62 | 1.27 (0.50–3.24) |
| Household with ≥1 animal† that has been vaccinated against rabies | 2 (17) | 6 (9) | 0.43 | 2.07 (0.34–12.64) |
| Bat contact within past 90 d‡ | | | | |
| Any bat contact | 3 (13) | 40 (27) | 0.15 | 0.40 (0.11–1.40) |
| Touched a bat with skin uncovered | 3 (13) | 40 (27) | 0.15 | 0.40 (0.11–1.40) |
| Bitten by bat | 1 (4) | 10 (7) | 0.66 | 0.62 (0.07–5.21) |
| Scratched by bat | 1 (4) | 15 (10) | 0.39 | 0.40 (0.05–3.22) |
| Other bat-related activities within past 90 d | | | | |
| Participated in bat festival | 1 (4) | 34 (23) | 0.07 | 0.15 (0.02–1.17) |
| Entered a bat cave or bat refuge | 1 (4) | 18 (12) | 0.29 | 0.33 (0.04–2.61) |
| Prepared a bat as food | 7 (30) | 57 (39) | 0.45 | 0.69 (0.26–1.82) |
| Eaten a bat | 7 (30) | 56 (38) | 0.49 | 0.71 (0.27–1.87) |
| Knowledge | | | | |
| Indicated animal bites as mechanism of rabies transmission | 13 (57) | 78 (53) | 0.74 | 1.15 (0.51–2.62) |
| Described rabies as severe | 13 (57) | 84 (57) | 0.95 | 0.98 (0.43–2.23) |
| Identified bats as a rabies source | 1 (4) | 3 (2) | 0.49 | 2.18 (0.24–20.11) |
| Identified dogs as a rabies source | 16 (70) | 84 (57) | 0.26 | 1.71 (0.67–4.36) |
| If bitten or scratched by a bat | | | | |
| Wash wound with soap and water | 0 | 5 (3) | NP | NP |
| Seek medical care | 9 (39) | 52 (35) | 0.70 | 1.17 (0.51–2.69) |
| Seek a traditional healer or pray | 2 (9) | 5 (3) | 0.24 | 2.70 (0.52–13.97) |
| Do nothing | 9 (39) | 69 (47) | 0.50 | 0.73 (0.28–1.85) |
| If bitten by a potentially rabid animal | | | | |
| Wash wound with soap and water | 0 | 1 (1) | NP | NP |
| Seek medical care | 16 (70) | 92 (63) | 0.53 | 1.37 (0.51–3.64) |
| Seek a traditional healer or pray | 3 (13) | 4 (3) | 0.03 | 5.36 (1.17–24.48) |
| Do nothing | 3 (13) | 33 (22) | 0.32 | 0.52 (0.14–1.89) |
| History of rabies vaccination | 1 (4) | 1 (1) | 0.19 | 6.64 (0.39–111.64) |
| Aware that bats can cause disease other than rabies | 3 (13) | 6 (4) | 0.08 | 3.53 (0.86–14.40) |
| Know of reports of illness as a result of bats or being in bat cave | 2 (9) | 1 (1) | 0.03 | 13.90 (1.25–154.63) |

*NA, not applicable or not calculated; NP, logistic regression could not be performed due to zero cells; OR, odds ratio.
†Pet or livestock.
‡Bat contact was defined as having touched a bat, having been bitten by a bat, or having been scratched by a bat.

**Table 5.** Summary of serologic testing results for lyssavirus antibodies among *Rousettus aegyptiacus* bats roosting in caves used in a bat festival, Idanre area, Nigeria, 2010 and 2013*

| Lyssavirus type (species) | Duvenhage virus (South Africa, 1970) | Lagos bat virus (lineage B, Nigeria, 1956) | Shimoni bat virus (Kenya, 2009) | Mokola virus (South Africa, 1998) | Ikoma lyssavirus (Tanzania, 2009) |
|---|---|---|---|---|---|
| Lyssavirus phylogroup | I | II | II | II | Undetermined |
| Year | 2013 | 2010, 2013 | 2013 | 2013 | 2013 |
| No. bats tested | 67 | 169 | 60 | 62 | 64 |
| No. (%) bats with detectable neutralizing antibodies | 0 | 89 (53) | 30 (50) | 37 (60) | 1 (2) |

*A total of 211 bats were collected: 120 bats during September 2010 (112 *Rousettus aegyptiacus*, 8 *Hipposideros gigas*) and 91 during February 2013 (all *R. aegyptiacus*). This table displays only data on serologic testing for lyssaviruses among *R. aegyptiacus* bats; serum specimens were not available for all *R. aegyptiacus* bats.

bat species, including *R. aegyptiacus*, which we identified in the festival caves, are known reservoirs for a range of potential pathogens, including filoviruses and coronaviruses (*18*,*22*,*36*,*37*). It is therefore plausible that at least some zoonotic pathogens are present in bats residing in the festival caves and that these pathogens can spill over into humans (*16*). Furthermore, the data we present on febrile illness are a snapshot from 2013, and given that excretion of virus in bats can be episodic, the risk of batborne infections may vary over time (*23*).

We did not find neutralizing antibodies to lyssaviruses in any person in the study, other than 2 persons who had neutralizing antibodies to rabies virus, perhaps reflecting prior rabies vaccination that was not recalled during the survey or abortive infection from bites of rabid dogs (*5*). Thus, we found no evidence of abortive phylogroup II lyssavirus infections among humans in this study, despite the high prevalence of neutralizing antibodies to phylogroup II lyssaviruses among bats in the festival caves and that many persons in the area frequently interact with bats. This result is perhaps not surprising. First, as previously explained, we suspect that many interactions with bats among the population are unrelated to the bat festival and unrelated to bats from the festival caves (although bat hunters who participated in the 2013 bat hunter survey, by definition, would have had interaction with bats from the festival caves). The data we present on the prevalence of neutralizing antibodies to phylogroup II lyssaviruses among bats are specific to bats from the festival caves and cannot be generalized to other bat populations in the area; the prevalence of these antibodies in other bat populations with which humans also interact might be lower than that for bats from the festival caves. Second, in the Amazon, where abortive lyssavirus infections have been documented, humans likely experience bat bites on a more continuous basis because of the predatory nature of vampire bats (*5*). In contrast, the bat festival in this part of Nigeria occurs at discrete times, leading to a lower frequency of bat bites and thus lower risk of lyssavirus exposure. Finally, the dates of the bat festivals vary each year and are determined based on traditional wisdom. Whether the bat festival timing, as determined by cultural leaders, implicitly accounts for periods of lower risk of batborne infections to festival participants warrants further investigation by an interdisciplinary team of biologists and anthropologists (*23*).

Our study has limitations. Accurate information on the distribution of communities in the area was limited, making it unclear whether persons we enrolled are representative of the area. We did not use a strict definition for febrile illness, nor could we verify the occurrence of a febrile illness; rather, we relied on retrospective, subjective reports. Our study did not have a robust method of identifying encephalitis-like illness and deaths that occurred between the initial data collection in 2013 and the 2013 follow-up survey, and we do not know what happened to participants who could not be located for the follow-up survey. Thus, we cannot draw conclusions on the ability of the predominant phylogroup II lyssavirus that circulates among bats in the festival caves to cause productive lyssavirus infections (rabies) in humans.

Emerging infectious diseases are on the rise around the world; most originate from animals (*38*). Although the source of the 2014–2016 Ebola outbreak remains unknown, it may have begun with a single spillover event involving initial bat contact (*39*), which underscores the health risks of interacting with bats without appropriate precautions. If we assume that the households we enrolled are representative of the Idanre area, then this part of Nigeria has high rates of bat contact and is at high risk for bat-related zoonoses. We therefore recommend that officials strengthen health security in the Idanre area, recognizing that an approach that bans hunting and consumption of bats is unlikely to be effective. Rather, a more productive approach will focus on harm reduction and community engagement. Specific recommendations include educating the population, particularly persons who participate in high-risk bat-related activities, about the health risks associated with bats and the ecosystem

benefits provided by bats; providing preexposure prophylaxis for rabies and possibly other batborne disease (potentially even Ebola) for persons who participate in high-risk bat-related activities; and developing surveillance and outbreak response capacity in the area for syndromes such as febrile illness, encephalitis, and hemorrhagic fevers.

### Acknowledgments

We thank Inger Damon, Amy Gilbert, Kimberly Hummel, Felix Jackson, Carl Kinkade, Jordona D. Kirby, Ivan Kuzmin, Yetunde Olagbuyi, Obe Olayinkaobe, and Caroline Olofinsao for their technical and administrative support of this research study. We also thank the Federal Ministry of Health (Abuja, Nigeria), the Ondo State Ministry of Health, the Owa of Idanre Oba Fredrick Adegunle Aroloye IV, the chiefs of the Idanre community, and the vice chancellor and management of Ahmadu Bello University for their helpful comments and assistance with logistics.

This study was supported by the Biosecurity Engagement Program of the US Department of State, Bureau of International Security and Nonproliferation, and the Office of Cooperative Threat Reduction's Global Threat Reduction Programs; One Health funding; and the Global Disease Detection Program of the Center for Global Health at CDC.

## About the Author

Dr. Vora is a physician and epidemiologist at the Center for Preparedness and Response, Centers for Disease Control and Prevention, Atlanta, Georgia, USA. His research interests include emerging infectious diseases with zoonotic origins.

### References

1. Tuttle M. The secret lives of bats: my adventures with the world's most misunderstood mammals. New York: Houghton Mifflin Harcourt; 2015.
2. Wang LF, Cowled CC, editors. Bats and viruses. A new frontier of emerging infectious diseases. Hoboken (NJ): Wiley-Blackwell; 2015.
3. Manning SE, Rupprecht CE, Fishbein D, Hanlon CA, Lumlertdacha B, Guerra M, et al. Human rabies prevention—United States, 2008: recommendations of the Advisory Committee on Immunization Practices. MMWR Recomm Rep. 2008;57(RR-3):1–28.
4. Willoughby RE Jr, Tieves KS, Hoffman GM, Ghanayem NS, Amlie-Lefond CM, Schwabe MJ, et al. Survival after treatment of rabies with induction of coma. N Engl J Med. 2005;352:2508–14. https://doi.org/10.1056/NEJMoa050382
5. Gilbert AT, Petersen BW, Recuenco S, Niezgoda M, Gomez J, Laguna-Torres VA, et al. Evidence of rabies virus exposure among humans in the Peruvian Amazon. Am J Trop Med Hyg. 2012;87:206–15. https://doi.org/10.4269/ajtmh.2012.11-0689
6. Maes P, Amarasinghe GK, Ayllon MA, Basler CF, Bavari S, Blasdell KR, et al. Taxonomy of the order Mononegavirales: second update 2018. Arch Virol. 2019;164:1233–44. https://doi.org/10.1007/s00705-018-04126-4
7. Hanlon CA, DeMattos CA, DeMattos CC, Niezgoda M, Hooper DC, Koprowski H, et al. Experimental utility of rabies virus-neutralizing human monoclonal antibodies in post-exposure prophylaxis. Vaccine. 2001;19:3834–42. https://doi.org/10.1016/S0264-410X(01)00135-9
8. Fekadu M, Shaddock JH, Sanderlin DW, Smith JS. Efficacy of rabies vaccines against Duvenhage virus isolated from European house bats (*Eptesicus serotinus*), classic rabies and rabies-related viruses. Vaccine. 1988;6:533–9. https://doi.org/10.1016/0264-410X(88)90107-7
9. Horton DL, McElhinney LM, Marston DA, Wood JL, Russell CA, Lewis N, et al. Quantifying antigenic relationships among the lyssaviruses. J Virol. 2010; 84:11841–8. https://doi.org/10.1128/JVI.01153-10
10. Ceballos NA, Moron SV, Berciano JM, Nicolas O, Aznar Lopez C, Juste J, et al. Novel lyssavirus in bat, Spain. Emerg Infect Dis. 2013;19:793–5. https://doi.org/10.3201/eid1905.121071
11. Maes P, Amarasinghe GK, Ayllon MA, Basler CF, Bavari S, Blasdell KR, et al. Taxonomy of the order Mononegavirales: second update 2018. Arch Virol. 2019;164:1233–44. https://doi.org/10.1007/s00705-018-04126-4
12. Evans JS, Wu G, Selden D, Buczkowski H, Thorne L, Fooks AR, et al. Utilisation of chimeric lyssaviruses to assess vaccine protection against highly divergent lyssaviruses. Viruses. 2018;10:130. https://doi.org/10.3390/v10030130
13. Follmann EH, Ritter DG, Beller M. Survey of fox trappers in northern Alaska for rabies antibody. Epidemiol Infect. 1994;113:137–41. https://doi.org/10.1017/S0950268800051554
14. Black D, Wiktor TJ. Survey of raccoon hunters for rabies antibody titers: pilot study. J Fla Med Assoc. 1986;73:517–20.
15. Vora NM, Osinubi M, Wallace RM, Aman-Oloniyo A, Gbadegesin YH, Sebastian YK, et al. Assessment of potential zoonotic disease exposure and illness related to an annual bat festival—Idanre, Nigeria. MMWR Morb Mortal Wkly Rep. 2014;63:334.
16. Bai Y, Osinubi MOV, Osikowicz L, McKee C, Vora NM, Rizzo MR, et al. Human exposure to novel *Bartonella* species from contact with fruit bats. Emerg Infect Dis. 2018;24:2317–23. https://doi.org/10.3201/eid2412.181204
17. Dzikwi AA, Kuzmin II, Umoh JU, Kwaga JK, Ahmad AA, Rupprecht CE. Evidence of Lagos bat virus circulation among Nigerian fruit bats. J Wildl Dis. 2010;46:267–71. https://doi.org/10.7589/0090-3558-46.1.267
18. Boulger LR, Porterfield JS. Isolation of a virus from Nigerian fruit bats. Trans R Soc Trop Med Hyg. 1958;52: 421–4. https://doi.org/10.1016/0035-9203(58)90127-5
19. Shope RE, Murphy FA, Harrison AK, Causey OR, Kemp GE, Simpson DI, et al. Two African viruses serologically and morphologically related to rabies virus. J Virol. 1970;6:690–2. https://doi.org/10.1128/JVI.6.5.690-692.1970
20. Kia GS, Kuzmin II, Umoh JU, Kwaga JK, Kazeem HM, Osinubi MO, et al. Detection of some lyssaviruses from fruigivorous and insectivorous bats in Nigeria. 2014 [cited 2019 Mar 31]. https://journals.uic.edu/ojs/index.php/ojphi/article/view/5071</eref>
21. Amman BR, Albarino CG, Bird BH, Nyakarahuka L, Sealy TK, Balinandi S, et al. A recently discovered pathogenic paramyxovirus, Sosuga virus, is present in *Rousettus aegyptiacus* fruit bats at multiple locations in Uganda.

J Wildl Dis. 2015;51:774–9. https://doi.org/10.7589/2015-02-044
22. Towner JS, Amman BR, Sealy TK, Carroll SA, Comer JA, Kemp A, et al. Isolation of genetically diverse Marburg viruses from Egyptian fruit bats. PLoS Pathog. 2009;5:e1000536. https://doi.org/10.1371/journal.ppat.1000536
23. Mortlock M, Dietrich M, Weyer J, Paweska JT, Markotter W. Co-circulation and excretion dynamics of diverse *Rubula*- and related viruses in Egyptian rousette bats from South Africa. Viruses. 2019;11:37. https://doi.org/10.3390/v11010037
24. Noah DL, Drenzek CL, Smith JS, Krebs JW, Orciari L, Shaddock J, et al. Epidemiology of human rabies in the United States, 1980 to 1996. Ann Intern Med. 1998;128:922–30. https://doi.org/10.7326/0003-4819-128-11-199806010-00012
25. Warner C, Fekadu M, Whitfield S, Shaddock J. Use of anti-glycoprotein monoclonal antibodies to characterize rabies virus in formalin-fixed tissues. J Virol Methods. 1999;77:69–74. https://doi.org/10.1016/S0166-0934(98)00136-0
26. Yager ML, Moore SM. The rapid fluorescent focus inhibition test. In: Rupprecht C, Nagarajan T, editors. Current laboratory techniques in rabies diagnosis, research and prevention. San Diego: Academic Press; 2015. p. 199–214.
27. Smith TG, Gilbert AT. Comparison of a micro-neutralization test with the rapid fluorescent focus inhibition test for measuring rabies virus neutralizing antibodies. Trop Med Infect Dis. 2017;2:24. https://doi.org/10.3390/tropicalmed2030024
28. Dean DJ, Abelseth MK, Atanasiu P. The fluorescent antibody test. In: Meslin FX, Kaplan MM, Koprowski H, editors. Laboratory techniques in rabies. 4th ed. Geneva: World Health Organization; 1996. p. 88–95.
29. Suwannarong K, Schuler S. Bat consumption in Thailand. Infect Ecol Epidemiol. 2016;6:29941. https://doi.org/10.3402/iee.v6.29941
30. Kamins AO, Rowcliffe JM, Ntiamoa-Baidu Y, Cunningham AA, Wood JL, Restif O. Characteristics and risk perceptions of Ghanaians potentially exposed to bat-borne zoonoses through bushmeat. EcoHealth. 2015;12:104–20. https://doi.org/10.1007/s10393-014-0977-0
31. Baudel H, De Nys H, Mpoudi Ngole E, Peeters M, Desclaux A. Understanding Ebola virus and other zoonotic transmission risks through human-bat contacts: exploratory study on knowledge, attitudes and practices in Southern Cameroon. Zoonoses Public Health. 2019;66:288–95. https://doi.org/10.1111/zph.12563
32. Kalemba LN, Niezgoda M, Gilbert AT, Doty JB, Wallace RM, Malekani JM, et al. Exposure to lyssaviruses in bats of the Democratic Republic of the Congo. J Wildl Dis. 2017;53:408–10. https://doi.org/10.7589/2016-06-122
33. Freuling CM, Binger T, Beer M, Adu-Sarkodie Y, Schatz J, Fischer M, et al. Lagos bat virus transmission in an *Eidolon helvum* bat colony, Ghana. Virus Res. 2015;210:42–5. https://doi.org/10.1016/j.virusres.2015.07.009
34. Wright E, Hayman DT, Vaughan A, Temperton NJ, Wood JL, Cunningham AA, et al. Virus neutralising activity of African fruit bat (*Eidolon helvum*) sera against emerging lyssaviruses. Virology. 2010;408:183–9. https://doi.org/10.1016/j.virol.2010.09.014
35. Shipley R, Wright E, Selden D, Wu G, Aegerter J, Fooks AR, et al. Bats and viruses: emergence of novel lyssaviruses and association of bats with viral zoonoses in the EU. Trop Med Infect Dis. 2019;4:E31. https://doi.org/10.3390/tropicalmed4010031
36. Sendow I, Ratnawati A, Taylor T, Adjid RM, Saepulloh M, Barr J, et al. Nipah virus in the fruit bat *Pteropus vampyrus* in Sumatera, Indonesia. PLoS One. 2013;8:e69544. https://doi.org/10.1371/journal.pone.0069544
37. Quan PL, Firth C, Street C, Henriquez JA, Petrosov A, Tashmukhamedova A, et al. Identification of a severe acute respiratory syndrome coronavirus-like virus in a leaf-nosed bat in Nigeria. MBio. 2010;1:e00208-10. https://doi.org/10.1128/mBio.00208-10
38. Jones KE, Patel NG, Levy MA, Storeygard A, Balk D, Gittleman JL, et al. Global trends in emerging infectious diseases. Nature. 2008;451:990–3. https://doi.org/10.1038/nature06536
39. Mari Saéz A, Weiss S, Nowak K, Lapeyre V, Zimmermann F, Dux A, et al. Investigating the zoonotic origin of the West African Ebola epidemic. EMBO Mol Med. 2015;7:17–23. https://doi.org/10.15252/emmm.201404792

Address for correspondence: Neil M. Vora, Centers for Disease Control and Prevention, 1600 Clifton Rd NE, Mailstop G33, Atlanta, GA 30329-4027, USA; email: nvora@cdc.gov

# Rickettsioses as Major Etiologies of Unrecognized Acute Febrile Illness, Sabah, East Malaysia

Matthew J. Grigg, Timothy William, Emily G. Clemens, Kaajal Patel, Arjun Chandna, Christopher S. Wilkes, Bridget E. Barber, Nicholas M. Anstey, J. Stephen Dumler, Tsin W. Yeo, Megan E. Reller

## Medscape EDUCATION ACTIVITY

In support of improving patient care, this activity has been planned and implemented by Medscape, LLC and Emerging Infectious Diseases. Medscape, LLC is jointly accredited by the Accreditation Council for Continuing Medical Education (ACCME), the Accreditation Council for Pharmacy Education (ACPE), and the American Nurses Credentialing Center (ANCC), to provide continuing education for the healthcare team.

Medscape, LLC designates this Journal-based CME activity for a maximum of 1.00 ***AMA PRA Category 1 Credit(s)™***. Physicians should claim only the credit commensurate with the extent of their participation in the activity.

Successful completion of this CME activity, which includes participation in the evaluation component, enables the participant to earn up to 1.0 MOC points in the American Board of Internal Medicine's (ABIM) Maintenance of Certification (MOC) program. Participants will earn MOC points equivalent to the amount of CME credits claimed for the activity. It is the CME activity provider's responsibility to submit participant completion information to ACCME for the purpose of granting ABIM MOC credit.

All other clinicians completing this activity will be issued a certificate of participation. To participate in this journal CME activity: (1) review the learning objectives and author disclosures; (2) study the education content; (3) take the post-test with a 75% minimum passing score and complete the evaluation at http://www.medscape.org/journal/eid; and (4) view/print certificate. For CME questions, see page 1642.

**Release date: June 18, 2020; Expiration date: June 18, 2021**

**Learning Objectives**

Upon completion of this activity, participants will be able to:

- Evaluate the findings of diagnostic testing for rickettsioses among patients with nonmalarial AFI in Sabah, East Malaysia, from 2013 to 2015
- Assess the clinical and laboratory findings among patients with nonmalarial AFI in Sabah, East Malaysia, who were diagnosed with rickettsioses from 2013 to 2015
- Determine the clinical and public health implications of clinical and epidemiological findings among patients with nonmalarial AFI in Sabah, East Malaysia, who were diagnosed with rickettsioses from 2013 to 2015.

**CME Editor**

**Jude Rutledge, BA,** Technical Writer/Editor, Emerging Infectious Diseases. *Disclosure: Jude Rutledge has disclosed no relevant financial relationships.*

**CME Author**

**Laurie Barclay, MD,** freelance writer and reviewer, Medscape, LLC. *Disclosure: Laurie Barclay, MD, has disclosed no relevant financial relationships.*

**Authors**

*Disclosures:* ***Matthew J. Grigg, MBBS, PhD; Timothy William, MBBS, FRCP(Edin); Emily G. Clemens, MA; Kaajal Patel, MBBS; Arjun Chandna, MD; Christopher S. Wilkes, MBBS; Bridget E. Barber, MBBS, PhD; Nicholas M. Anstey, MBBS, PhD; John Stephen Dumler, MD; Tsin Wen Yeo, MBBS, PhD;*** *and* ***Megan E. Reller, MD, PhD,*** *have disclosed no relevant financial relationships.*

Author affiliations: Infectious Diseases Society Sabah–Menzies School of Health Research, Kota Kinabalu, Malaysia (M.J. Grigg, T. William, K. Patel, A. Chanda, C.S. Wilkes, B.E. Barber, N.M. Anstey, T.W. Yeo); Menzies School of Health Research–Charles Darwin University, Darwin, Northern Territory, Australia (M.J. Grigg, K. Patel, A. Chanda, C.S. Wilkes, B.E. Barber, N.M. Anstey, T.W. Yeo); Gleneagles Hospital, Kota Kinabalu (T. William); Clinical Research Centre, Queen Elizabeth Hospital, Kota Kinabalu (T. William); QIMR Berghofer Medical Research Institute, Brisbane, Queensland, Australia (B.E. Barber); Uniformed Services University of the Health Sciences, Bethesda, Maryland, USA (J.S. Dumler); Lee Kong Chian School of Medicine, Nanyang Technological University, Singapore (T.W. Yeo); Communicable Disease Centre, Institute of Infectious Diseases and Epidemiology, Tan Tock Seng Hospital, Singapore (T.W. Yeo); Duke University, Durham, North Carolina, USA (M.E. Reller); Duke Global Health Institute, Durham (M.E. Reller)

DOI: https://doi.org/10.3201/eid2607.191722

*Orientia tsutsugamushi*, spotted fever group rickettsioses, and typhus group rickettsioses (TGR) are reemerging causes of acute febrile illness (AFI) in Southeast Asia. To further delineate extent, we enrolled patients >4 weeks of age with nonmalarial AFI in Sabah, Malaysia, during 2013–2015. We confirmed rickettsioses (past or acute, IgG titer >160) in 126/354 (36%) patients. We confirmed acute rickettsioses (paired 4-fold IgG titer rise to ≥160) in 38/145 (26%) patients: 23 *O. tsutsugamushi*, 9 spotted fever group, 4 TGR, 1 *O. tsutsugamushi*/spotted fever group, and 1 *O. tsutsugamushi*/TGR. PCR results were positive in 11/319 (3%) patients. Confirmed rickettsioses were more common in male adults; agricultural/plantation work and recent forest exposure were risk factors. Dizziness and acute hearing loss but not eschars were reported more often with acute rickettsioses. Only 2 patients were treated with doxycycline. Acute rickettsioses are common (>26%), underrecognized, and untreated etiologies of AFI in East Malaysia; empirical doxycycline treatment should be considered.

Rickettsioses and related infections, including scrub typhus, caused by *Orientia tsutsugamushi*; spotted fever group rickettsioses (SFGR), often called tick typhus; and typhus group rickettsioses (TGR), also called murine typhus, are reemerging and neglected causes of acute febrile illness (AFI) in Southeast Asia (*1*–*4*). Serologic confirmation of acute rickettsioses, however, requires demonstration of a 4-fold rise in IgG titer by indirect fluorescent antibody (IFA) because acute-phase IgG might represent prior infection and IgM might indicate recent or cross-reactive antibody (*1*). Furthermore, serologic testing in the early phase of illness is not helpful because antirickettsial antibodies are often not present within the first 2 weeks.

Rickettsioses have been reported in Malaysia historically (*2*–*4*). Malaysia state tertiary hospital data for the period 1994–1999 identified antirickettsial IgG or IgM in 6,442 (10.6%) tested samples (IgG or IgM titer >400 by the indirect immunoperoxidase test), including 4.9% *O. tsutsugamushi*, 3.1% TGR, and 2.6% SFGR (*5*). Although rickettsioses are notifiable diseases according to Malaysia Ministry of Health guidelines (*6*), routine testing is not conducted, paired acute-phase and convalescent-phase serum samples are rarely available, and only 53 infections were reported nationally during 2009–2015 (*7*). In the East Malaysia state of Sabah, 2 cases were reported over that period despite a seroprevalence of 5.5% among 11,037 patients tested in previous years at the state tertiary referral hospital (*5*) and high (>50%) seropositivity reported in febrile patients from certain rural areas (*8*). We prospectively enrolled patients and performed reference standard diagnostic testing to document and describe the epidemiology and clinical features of confirmed rickettsioses among patients with nonmalarial AFI in Sabah, East Malaysia.

## Methods

### Study Sites and Referral System

We conducted the study during December 12, 2013–July 15, 2015, in 2 adjacent district referral hospitals, Kudat and Kota Marudu, in northwest Sabah, Malaysia, on the island of Borneo. These districts cover an area of 3,204 km$^2$ and had an estimated population in 2015 of ≈169,000 (*9*). According to Malaysia Ministry of Health divisional health facility structures, each district has a single central referral hospital and subdistrict health clinics. The climate is tropical, has no defined dry season, and experiences increased rainfall during November–March. The region consists of both coastal and inland areas with elevations up to 1,000 m and extensive recent human land-use change from intact forest to oil palm plots and plantations (*10*).

### Study Population

Patients >4 weeks of age with a documented temperature of ≥38°C within 48 hours of admission to the medical or pediatric wards and a negative malarial blood film were eligible. We obtained consent from the patient or a parent or guardian if the patient was <18 years of age; we also obtained assent from persons 7–17 years of age.

### Study Procedures

Trained research nurses used standardized case record forms to collect structured epidemiologic, clinical, and laboratory data, including the admitting clinician's findings on examination, provisional diagnosis, and management. At enrollment, venous blood was obtained for routine and research-related testing after consent. Patients were requested to return for routine hospital outpatient follow-up and convalescent-phase serum sampling 14 days after enrollment.

### Laboratory Procedures

Hematologic and biochemical tests, blood cultures, and malaria smears were performed in the hospital laboratory. Anemia was classified according to World Health Organization age- and sex-based criteria (*11*). Acute kidney injury was defined per KDIGO criteria (*12*).

We conducted IFA testing at the Uniformed Services University for the Health Sciences (Bethesda, MD, USA) to confirm rickettsial infections; 2 experts read each slide, as described (*13*,*14*). We screened convalescent-phase serum samples using IFA at 1:80 dilution for IgG to *O. tsutsugamushi* (Karp strain), SFGR (*Rickettsia conorii* Malish 7 strain), and TGR (*R. typhi*); for reactive samples, we tested acute- and convalescent-phase paired serum samples together and titrated positives to 2,560. To evaluate the utility of acute-phase IgM for identifying paired IgG-confirmed acute infections, we tested a subset with paired IgG results for IgM in addition to those without convalescent-phase serum. We screened acute-phase serum samples for IgM at 1:40 and titrated positives to 1,280.

We performed multiplex real-time PCR to detect *O. tsutsugamushi* (56-kDA major outer membrane protein gene), SFGR (consensus *ompA* sequence), and TGR (*R. typhi* 17-kDa lipoprotein precursor gene) on EDTA-anticoagulated blood or buffy coat stored at -70°C as described (*15*). We tested 5 μL of DNA extracted from a 200 μL sample of EDTA-anticoagulated whole blood or buffy coat; we required 2 out of 2 or 3 replicates to confirm a positive result by PCR.

### Case Definitions

We used stringent criteria to define rickettsial infections (*16*), as reported previously (*13*,*14*). We defined confirmed rickettsioses as any IgG titer ≥160; confirmed past rickettsial infection as stable or declining IgG titer ≥160; confirmed acute rickettsial infection as a ≥4-fold rise in IgG titer by paired IFA to convalescent-phase titer of ≥160, positive PCR result, or both; confirmed probable acute rickettsial infection as a 2-fold rise in IgG titer with convalescent-phase titer ≥160 or single IgG titer ≥160 without paired serum samples; and possible rickettsioses as any IgG titer of 80 (acute infection if IgG seroconversion). We distinguished SFGR from TGR when we observed a ≥2-fold difference in SFGR versus TGR titer; if titers were equal, we categorized the infection as group indeterminate.

### Statistical Analysis

We analyzed data by using Stata (StataCorp, https://www.stata.com). We performed 2-group comparisons by using the Student *t*-test for continuous variables with normal distributions or the Wilcoxon–Mann–Whitney test for skewed distributions. For categoric variables, we used a $\chi^2$ or Fisher exact test. We calculated odds ratios (ORs) and 95% CIs by using the Mantel-Haenszel method.

### Ethics

We obtained ethics approval for this study. The study was approved by relevant institutional review boards in Malaysia (National Medical Research Ethics Committee), Australia (Menzies School of Health Research), and the United States (John Hopkins University and Duke University).

## Results

Of 557 patients who met eligibility criteria, 426 (77%) consented to enrolment and blood collection; 183 (43%) patients returned for convalescent follow-up (median 13 days; interquartile range (IQR) 12–14 days), and 157 (37%) had acute-phase serum samples, convalescent-phase serum samples, or both collected (Figure 1). Among the 243 patients who did not attend follow-up appointments, 240 had acute-phase serum samples available. A total of 354 patients had acute-phase serum samples, convalescent-phase serum samples, or both available to test for rickettsioses; of these, 145 (41%) patients had paired serum samples. Acute-phase whole blood or buffy coat was available for 319 patients. We observed no difference in median age or sex between those patients with and without paired serum samples.

### Serologic Diagnosis

Testing for IgG by IFA confirmed rickettsial infections in 126 of 354 (36%) patients, including 96 (27%) with scrub typhus (*O. tsutsugamushi* infection), 26 (7%) with SFGR, and 25 (7%) with TGR (Table 1); 6 patients had both *O. tsutsugamushi* and SFGR, 8 patients both *O. tsutsugamushi* and TGR, 1 patient both SFGR and TGR, and 3 patients *O. tsutsugamushi*, SFGR, and TGR IgG. We found confirmed past infection (stable or declining IgG titers ≥160) in 17 (12%) of 145 patients. Patients with serologic evidence of acute or past SFGR infections were older (median 60 years [IQR 45–73 years]) than patients with *O. tsutsugamushi* infection (median 38 years [IQR 24–57 years]; p = 0.003) but not patients with TGR (median 48 years [IQR 38–58 years]; p = 0.25) infections.

Among patients with paired serum samples, we confirmed 38 (26% [95% CI 20–34]) as having acute rickettsial infections based on a 4-fold rise in IgG titer, including 23 (15%) with *O. tsutsugamushi*, 9 (6%) SFGR, 4 (3%) TGR, and 2 co-infections (1 *O. tsutsugamushi*/SFGR and 1 *O. tsutsugamushi*/TGR [1% combined]). Most (22/38 [58%]) cases were associated with IgG seroconversion, including 13/25 (52%) acute *O. tsutsugamushi* infections, 9/10 (90%) acute SFGR, and 2/5 (40%) acute TGR.

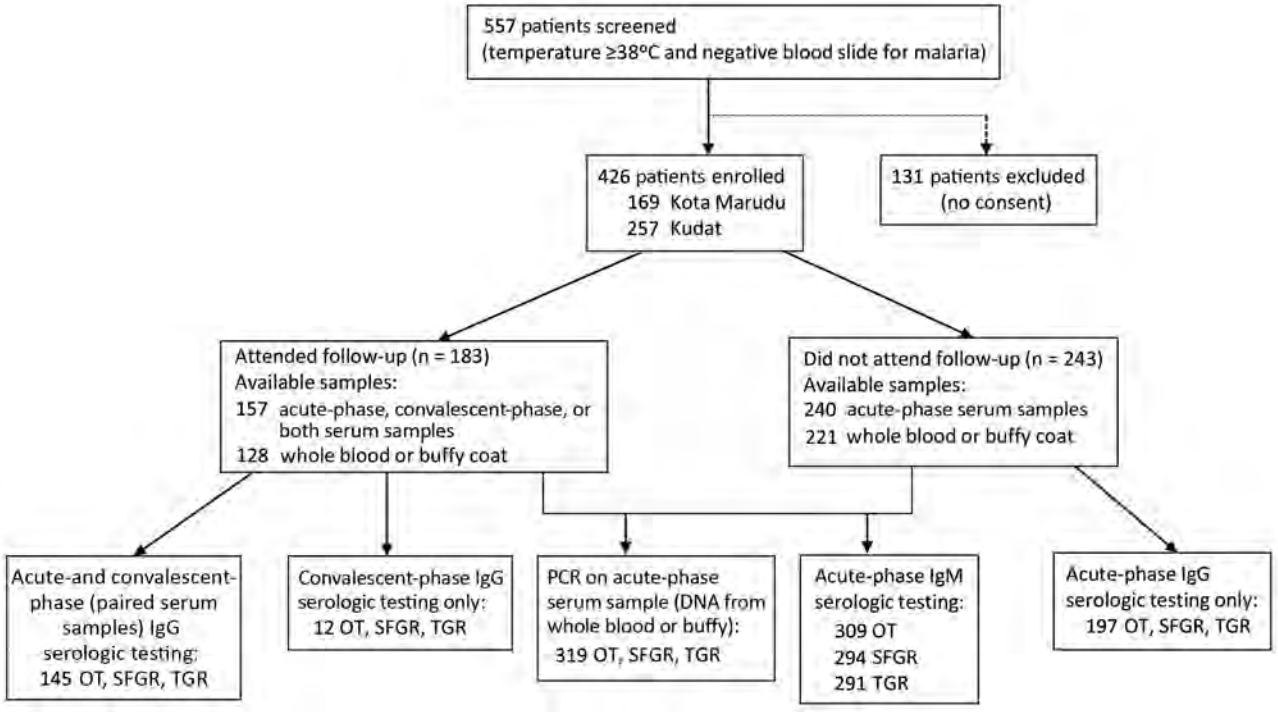


**Figure 1.** Enrollment flowchart and laboratory testing in a prospective cohort study of acute febrile illness attributable to rickettsioses, Sabah, East Malaysia, 2013–2015. OT, *Orientia tsutsugamushi*; SFGR, spotted-fever group rickettsiosis; TGR, typhus-group rickettsioses.

Probable acute rickettsial infections were detected in 77/354 (22%) persons, including 58 with *O. tsutsugamushi* , 12 with SFGR, and 16 with TGR; 70 of these lacked paired serum samples. Among those with paired serum samples, sensitivity of acute-phase IgM for acute rickettsioses was 8% (95% CI 2%–21%) and specificity was 94% (95% CI 87%–98%). We observed possible acute rickettsioses in an additional 37/354 patients (10% [95% CI 7%–14%]) (Appendix Tables 1–3, https://wwwnc.cdc.gov/EID/article/26/7/19-1722-App1.xlsx).

### Diagnosis by PCR

An additional 11 of 319 patients with acute-phase whole blood or buffy coat available had acute rickettsial infections by PCR. These infections were 1 *O. tsutsugamushi*, 8 SFGR, and 2 TGR (Table 1).

### Clinical and Laboratory Features of Acute Rickettsial Infections

Patients with confirmed acute rickettsial infections (n = 49; median age 39 years) were equally likely to be male and were of similar age (p = 0.32) to those with probable acute rickettsioses (median age 43 years); both groups were slightly older than those with no rickettsial infection (median age 29 years; p = 0.007) (Table 2). The median age of those with acute infections did not differ significantly (p = 0.69): 36 years (IQR 21–51 years) for *O. tsutsugamushi*, 49 years (IQR 12–58 years) for SFGR, and 38 years (IQR 27–56 years) for TGR. Eight children (<15 years of age) had confirmed acute rickettsial infections (5 SFGR, 2 *O. tsutsugamushi*, and 1 TGR), of whom 5 (63%) had their infections confirmed by PCR; the youngest was a 6-month-old infant. The median duration of hospitalization for those with confirmed acute rickettsial infections was 5 days (IQR 3–7 days), which was comparable to those without rickettsioses. No deaths were reported.

Clinical and laboratory features of probable acute rickettsial infections were comparable to those with confirmed infections (Table 2), except for less frequent dyspnea (17% vs. 33%; p = 0.047). Headache was more common in those with confirmed or probable acute rickettsial infection than those with no acute rickettsial infection (77% vs. 59%; p = 0.004), especially among those with SFGR or TGR (81%) compared with *O. tsutsugamushi* (76%) or neither (59%) (Appendix Tables 1–3). Dizziness was more frequent in those with confirmed and probable acute rickettsial infections (63%) than those with no rickettsial infection (48%; p = 0.029); however, vomiting was less common (32% vs. 46%; p = 0.035). Hearing loss was more common in those with acute (9%) compared with no rickettsial infection (2%; p = 0.023); this finding was most pronounced in confirmed *O. tsutsugamushi* infection (19% [95%

CI 7%–39%]; p = 0.004) but also present in SFGR (18% [95% CI 4%–43%]; p = 0.021). Thirteen (11%) patients with acute rickettsioses had a maculopapular rash, but none had an eschar.

Provisional clinical diagnoses among patients with confirmed acute rickettsioses included 7 (14%) dengue, 6 (12%) acute undifferentiated fever, 6 (12%) community-acquired pneumonia, 5 (10%) urinary tract infection, 4 (8%) leptospirosis, 4 (8%) gastroenteritis, and 23 (47%) other diagnoses. No patient with or without confirmed rickettsial infection had a provisional diagnosis of acute rickettsial infection.

Anemia occurred in 24 (51%) patients with acute rickettsioses and hematologic results available, and we noted a hemoglobin level of <80 g/L in 3 adults (Appendix Table 4). Peripheral leukocyte counts, renal function after controlling for age, and acute kidney injury, observed in 6/33 patients (18%), were similar in patients with and without acute rickettsioses.

Doxycycline was administered to 2 (4%) patients with confirmed acute rickettsioses (both *O. tsutsugamushi* infections), albeit in both cases for a provisional diagnosis of gastroenteritis. None of the 6 rickettsial case-patients with a provisional diagnosis of acute undifferentiated fever were treated with doxycycline.

### Epidemiologic Features of Patients with Confirmed Acute or Past Rickettsial Infections

Patients with acute or past rickettsial infections were older than those without (median age 43 vs. 24 years; p<0.001); however, the distribution by sex was similar (57% male among those with past rickettsial infection vs. 52% among those without rickettsial infection). Most patients (67%) reported rural residence (Appendix Table 5). Recently spending time in forest areas was more common (OR 2.1 [IQR 1.0–4.3]; p = 0.037) in patients with acute or past rickettsial infection (14%) than patients with neither (7%), including staying overnight in the forest for those with scrub typhus (11%; p = 0.047). Patients were more likely to report a primary occupation as a rubber tapper (OR 5.9 [IQR 1.9–18.5]; p = 0.002) for those with acute or past rickettsial infections (10%) than for patients without rickettsioses (2%). Of the 13 rubber tappers with seroprevalent rickettsioses, 3 (23%) had confirmed acute scrub typhus and 5 (38%) past scrub typhus. Farmers were also more likely (OR 2.8 [IQR 1.0–7.3]; p = 0.041) to have (8%) than not to have (3%) seroprevalent rickettsial infections. Patients who were unemployed had an increased risk of rickettsioses (OR 1.9 [IQR 1.0-3.5]; p = 0.042), of whom 4/24 had a recent travel history. No other occupations were associated with an increased risk of seroprevalent rickettsioses.

**Table 1.** Serologic and molecular detection of confirmed rickettsioses in a prospective cohort study of acute febrile illness attributable to rickettsioses, Sabah, East Malaysia, 2013–2015*

| Confirmed rickettsial infections | OT | SFGR | TGR | Total |
|---|---|---|---|---|
| Confirmed age indeterminate (acute or past); acute-phase or convalescent-phase IgG titer ≥160,† n = 354 | 96 (27 [23–32]) | 26 (7 [5–11]) | 25 (7 [5–10]) | 126 (36 [31–41]) |
| Confirmed past infection; acute-phase IgG titer ≥160 with stable or decreasing paired titer,‡ n = 145 | 13 (9 [5–14]) | 4 (3 [1–7]) | 4 (3 [1–7]) | 17 (12 [7–18]) |
| Confirmed rickettsial infection, acute | | | | |
| All acute confirmed,§ n = 378 | 26 (7 [5–10]) | 18 (5 [3–7]) | 7 (2 [1–4]) | 49 (13 [10–17]) |
| ≥4-fold rise in IgG titer,§ n = 145 | 25 (17 [12–24]) | 10 (7 [4–12]) | 5 (3 [1–8]) | 38 (26 [20–34]) |
| With seroconversion¶ | 13 (9 [5–14]) | 9 (6 [3–11]) | 2 (1 [<1–5]) | 22 (14 [9–20]) |
| PCR positive,# n = 319 | 1 (<1 [0–2]) | 8 (2 [1–5]) | 2 (1 [0–2]) | 11 (3 [2–6]) |
| Copy number/mL, mean | 5,164 | 482 | 3477 | |
| Confirmed rickettsial infection, probable acute | | | | |
| All probable acute, n = 354 | 58 (16 [13–21]) | 12 (3 [2–6]) | 16 (5 [3–7]) | 77 (22 [18–26]) |
| Paired serum samples | | | | |
| 2-fold IgG titer rise to ≥160,** n = 145 | 6 (4 [2–9]) | 1 (1 [<1–4]) | 2 (1 [<1–5]) | 7 (5 [2–10]) |
| Single serum samples | | | | |
| Acute-phase IgG ≥160,†† n = 197 | 45 (23 [18–29]) | 8 (4 [2–8]) | 12 (6 [4–10]) | 60 (30 [24–37]) |
| Convalescent-phase IgG ≥160,‡‡ n = 12 | 7 (58 [32–81]) | 3 (25 [9–53]) | 2 (17 [5–45]) | 10 (83 [55–95]) |

*Values are no. (% [95% CI]) unless otherwise indicated. Total does not equal sum of individual infections because some of the individual infections are co-infections. OT, *Orientia tsutsugamushi*; SFGR, spotted-fever group rickettsiosis; TGR, typhus-group rickettsioses.
†Includes 18 patients with serologic evidence of OT/SFGR (6); OT/TGR (8); SFGR/TGR (1); OT/SFGR/TGR (3).
‡Includes 3 patients with serologic evidence of OT/TGR (2) and OT/SFGR/TGR (1).
§Includes 2 co-infections: 1 patient positive for OT and SFGR (both with acute-phase IgG titer of 40 and convalescent-phase titer of 320) and 1 patient for OT and TGR (both with acute-phase IgG titer of 40 and convalescent-phase titer 160).
¶Includes 1 patient each with serologic evidence of OT/TGR and OT/SFGR.
#No PCR-positive patients were confirmed also by paired IgG serology; 8 patients had acute-phase serum samples, and 1 TGR PCR-positive patient had IgM 2,560.
**Includes 2 patients with 2-fold IgG titer rises to OT and TGR
††Includes 3 patients positive for OT and TGR and 2 patients positive for OT and SFGR
‡‡Includes 1 patient each with serologic evidence of SF/TG and OT/TG.

## Discussion

Although rickettsial infections were first documented in Malaysia in 1925 (*17*), few cases are currently confirmed and reported nationally (*18*). Paired serum samples are infrequently obtained, and IFA requires expertise; both these factors limit diagnostic efforts. By confirming acute infection based on a 4-fold rise in IgG titer, PCR positivity, or both, we documented and characterized rickettsioses as an important cause of nonmalarial AFI in Malaysia (Figure 2). We found definitive serologic evidence of acute or past rickettsioses in 36% of patients and confirmed acute infections in 26% of patients. Scrub typhus (*O. tsutsugamushi* infection) was the most common rickettsiosis, especially among rural residents.

Acute-phase IgM demonstrated insufficient sensitivity for identifying acute rickettsioses. Moreover, acute-phase IgG, which cannot distinguish acute from past rickettsioses, is an imperfect measure of seroprevalence because antibodies decline over time even in patients who are not treated (*19*). PCR also detected few acute infections compared with paired serologic tests. Rickettsial infections were unsuspected clinically, and nearly all were untreated. Therefore, increased clinical awareness, improved diagnostic tools, and empirical use of doxycycline are essential to reduce illness and death attributable to rickettsioses.

Confirmation of acute rickettsioses as a major cause of AFI in Sabah, Malaysia, is to be expected because rickettsioses have been identified elsewhere

**Table 2.** Clinical features of patients with acute rickettsioses versus no rickettsioses in a prospective cohort study of acute febrile illness attributable to rickettsioses, Sabah, East Malaysia, 2013–2015*

| Characteristic | Confirmed acute rickettsial infection | Probable acute rickettsial infection | p value for confirmed vs. probable acute infection | No rickettsial infection | p value for confirmed or probable acute vs. no infection | p value for confirmed acute vs. no infection |
|---|---|---|---|---|---|---|
| No. patients | 49 | 77 | NA | 102 | NA | NA |
| Demographics | | | | | | |
| Age, median, y (IQR) | 39 (2–56) | 43 (28–62) | 0.32 | 29 (8–55) | **0.007** | 0.15 |
| Child <15 y of age | 8 (16) | 3 (4) | **0.023** | 29 (28) | **<0.001** | 0.22 |
| Sex | | | | | | |
| M | 31 (63) | 48 (62) | 0.92 | 48 (47) | **0.029** | 0.20 |
| F | 18 (37) | 29 (38) | | 54 (53) | | |
| Symptoms | | | | | | |
| Symptoms data available | 48 (98) | 75 (97) | 0.99 | 102 (100) | 0.99 | 0.99 |
| Fever duration, median days (IQR) | 2 (2–4) | 3 (2–5) | 0.46 | 3 (1–4) | 0.64 | 0.89 |
| Headache | 36 (75) | 60 (80) | 0.65 | 60 (59) | **0.004** | 0.05 |
| Dizziness | 33 (69) | 44 (59) | 0.23 | 49 (48) | **0.029** | **0.017** |
| Confusion | 5 (10) | 5 (7) | 0.34 | 9 (9) | 0.75 | 0.75 |
| Vision changes | 8 (17) | 10 (13) | 0.56 | 11 (11) | 0.42 | 0.31 |
| Retro-orbital pain | 11 (23) | 19 (25) | 0.99 | 22 (22) | 0.82 | 0.85 |
| Hearing loss | 7 (15) | 4 (5) | 0.11 | 2 (2) | **0.023** | **0.005** |
| Coryza | 16 (33) | 22 (30) | 0.50 | 32 (31) | 0.82 | 0.81 |
| Cough | 23 (48) | 34 (45) | 0.59 | 41 (40) | 0.48 | 0.37 |
| Dyspnea | 16 (33) | 13 (17) | **0.047** | 27 (26) | 0.64 | 0.39 |
| Joint pain | 20 (42) | 29 (39) | 0.62 | 36 (35) | 0.57 | 0.45 |
| Muscle pain | 14 (29) | 13 (17) | 0.08 | 23 (23) | 0.81 | 0.38 |
| Lethargy | 32 (67) | 45 (60) | 0.37 | 59 (58) | 0.54 | 0.30 |
| Nausea | 16 (33) | 34 (46) | 0.16 | 44 (44) | 0.71 | 0.23 |
| Vomiting | 13 (27) | 27 (36) | 0.32 | 47 (46) | **0.035** | **0.027** |
| Abdominal pain | 20 (42) | 33 (44) | 0.56 | 41 (40) | 0.48 | 0.86 |
| Loss of appetite | 34 (71) | 49 (66) | 0.43 | 70 (68) | 0.76 | 0.79 |
| Diarrhea | 12 (25) | 20 (27) | 0.67 | 32 (31) | 0.49 | 0.42 |
| Dysuria | 4 (8) | 6 (8) | 0.99 | 6 (6) | 0.61 | 0.46 |
| Signs | | | | | | |
| Conjunctival suffusion | 0/46 (0) | 0/73 (0) | NA | 2/95 (2) | 0.21 | 0.99 |
| Respiratory distress† | 10 (21) | 21 (27) | 0.67 | 34 (33) | 0.21 | 0.17 |
| Respiratory crepitations on auscultation | 5 (10) | 12/74 (16) | 0.25 | 18 (18) | 0.32 | 0.33 |
| Abnormal chest radiograph result | 8/14 (57) | 18/31 (58) | 0.50 | 23/39 (59) | 0.70 | 0.99 |
| Maculopapular rash | 4 (8) | 10/75 (13) | 0.37 | 6 (6) | 0.23 | 0.73 |
| Eschar | 0/47 (0) | 0/74 (0) | NA | 0/101 (0) | NA | NA |
| Lymphadenopathy | 0/46 (0) | 2/72 (3) | 0.53 | 3/98 (3) | 0.67 | 0.55 |
| Abdominal tenderness | 7/44 (16) | 5/49 (10) | 0.36 | 11/91 (12) | 0.76 | 0.59 |
| Hepatomegaly | 10 (21) | 9/75 (12) | 0.13 | 10 (10) | 0.17 | 0.06 |
| Splenomegaly | 3/41 (7) | 2/73 (3) | 0.33 | 2/89 (2) | 0.46 | 0.33 |

*Values are no. (%) unless indicated. Bold indicates a statistically significant difference (p<0.05). Results are from time of study enrolment unless indicated. IQR, interquartile range; NA, not applicable.
†Respiratory rate ≥30 breaths/min or tissue oxygen saturation <96% on room air.

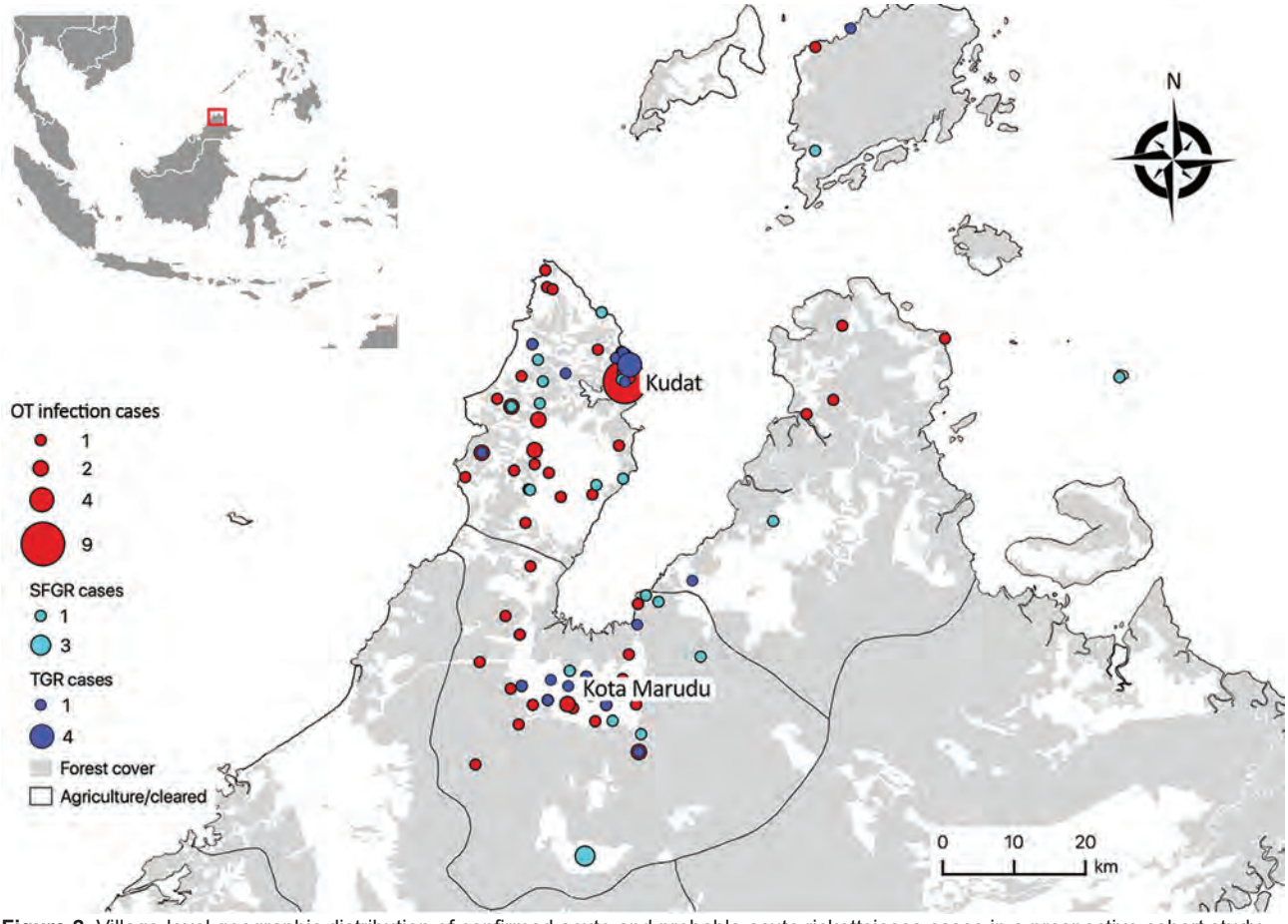


**Figure 2.** Village-level geographic distribution of confirmed acute and probable acute rickettsioses cases in a prospective cohort study of acute febrile illness attributable to rickettsioses, Sabah, East Malaysia, 2013–2015. Inset map shows study area in Sabah, Malaysia. OT, *Orientia tsutsugamushi* infection; SFGR, spotted-fever group rickettsiosis; TGR, typhus-group rickettsioses.

in the region. A large multicenter study in Thailand, Vietnam, and Indonesia showed that 6% of 1,578 enrolled patients had serologically confirmed acute rickettsioses (*20*). Other rigorous clinical and cross-sectional studies have demonstrated marked spatial heterogeneity in seroprevalence of rickettsioses (*21*), including 1% in Thailand (*22*), 33% in areas bordering Myanmar (*23*), 7% to 27% in Laos (*24*–*26*), and up to 10% in parts of Indonesia (*27*,*28*). Our study suggests that rickettsioses are at least as common (26%) in Malaysia as elsewhere in the region.

Rickettsioses are likely to be reemerging in East Malaysia. Despite the presence of a common vector of scrub typhus, *Leptotrombidium (L.) deliense* mites, being documented in coastal areas for decades (*29*), a single statewide study (including Kudat District) in the 1980s reported no acute rickettsioses among 383 febrile patients with paired serum samples tested by IFA (*30*). Sero-epidemiologic findings from 837 persons at that time demonstrated a low seroprevalence of 0.8% for *O. tsutsugamushi*, 8.6% for SFGR, and 0% for TGR (*30*). At the Sabah state tertiary referral hospital during 1994–1999, a total of 11,037 samples from febrile patients sent for acute IgG or IgM testing showed a comparatively low seroprevalence of 2.6% for *O. tsutsugamushi*, 1.3% for TGR, and 1.6% for SFGR (*5*). However, the inability to confirm acute rickettsioses, even retrospectively, if paired serum samples are not obtained has constrained broader public health understanding of their epidemiology and disease prevalence among the at-risk population in Sabah.

The epidemiology of rickettsial infections in this study is consistent with previous reports of scrub typhus and spotted fever rickettsioses described in rural areas in Southeast Asia (*31*); those reports indicated that infections were more commonly found in male adults, in agricultural, plantation, or forestry workers (*8*,*28*,*32*,*33*), and in persons with lower socio-economic status (*21*,*34*). The presence of typhus group rickettsioses in rural residents in our study

population, despite generally being reported more frequently in urban populations (*31*), highlights the need for further studies to better understand the epidemiology of rickettsioses in Malaysia and to design appropriate control measures. Because SFGR and TGR cross-reactivity by IFA is expected, testing for all 3 rickettsioses (*O. tsutsugamushi* infection, SFGR, and TGR) is important.

Factors explaining a potential increase in rickettsioses in Sabah could in part be related to changes in human land use (*10*) and the relationship with occupational or travel behavior and vector bionomics (*35*). The effect of habitat on *O. tsutsugamushi* seroprevalence has previously been evaluated in peninsular Malaysia; higher seropositivity overall was observed in indigenous adults with exposure to intact forest areas (73%) compared with forest fringe (48%) and village areas (8%) (*4*). These findings are broadly consistent with the association in our study between persons with acute or past rickettsioses and a history of extended forest exposure. Rubber plantation workers in peninsular Malaysia have been reported to have higher SFGR prevalence (40%), compared with *O. tsutsugamushi* (8%) and TGR (1%) (*36*). In contrast, although those identified as rubber tappers in our study had high seroprevalence to rickettsioses overall, most of these infections were attributable to *O. tsutsugamushi*.

We found that patients with acute rickettsioses had clinical findings similar to those without acute rickettsioses, with the exception of more frequent dizziness and hearing loss and less frequent vomiting. Detection of hearing loss might assist in clinical recognition of rickettsioses and has been reported in up to one third of patients with acute scrub typhus (*37*) as well as in those with SFGR (*38*). Eschar occurs most frequently on the anterior chest in women and the groin in men with scrub typhus (*39*); the relative rarity of eschar and higher frequency of hepatomegaly found in our study was also previously described in Malaysia (*2*). We observed severe cases of acute kidney injury in a small number of patients; however, acute kidney injury remains clinically important because of the subsequent increased risk for chronic kidney disease (*40*).

Common laboratory markers, such as abnormalities in leukocyte count, thrombocytopenia, anemia, and raised liver transaminases, were all nonspecific (*31*). Neutropenia occurred in 1 patient with acute scrub typhus, despite this sign being reported as a potentially useful clinical tool to differentiate scrub typhus from dengue (*41*). AFI was primarily attributed to dengue by treating clinicians, who initiated dengue fluid management protocols. In other cases, empiric treatment of suspected typhoid or leptospirosis was initiated with cephalosporins or penicillins, which are ineffective against rickettsioses. Treatment with doxycycline is recommended by the Malaysia Ministry of Health (*42*) because an estimated 6% of untreated scrub typhus cases in Asia are fatal (*43*); however, we found that rickettsioses were unsuspected and untreated.

Tools to support early diagnosis and local evidence-based clinical algorithms to guide directed and empirical treatment of undifferentiated AFI are needed. Diagnosis of acute rickettsioses remains problematic. *Orientia* and *Rickettsia* spp. are obligate intracellular bacteria predominantly targeting endothelial cells (*44*,*45*); hence, real-time PCR on peripheral blood is insensitive for the detection of acute rickettsioses (*15*,*19*,*46*). Incomplete follow-up meant the sensitivity of PCR could not be directly measured against gold-standard IFA serologic diagnosis for SFGR and TGR, although low PCR sensitivity of 18% has been reported (*19*). Longstanding technical difficulties with IFA also include the need for extensively trained readers and expensive equipment. Conventional use of antibody detection against only 3 major *O. tsutsugamushi* antigen groups and serologic cross-reactivity further limits accurate diagnoses; however, high antigenic variation has been observed across Southeast Asia (*47*,*48*). We found that acute-phase IgM was a poor predictor of acute rickettsial infection even in the setting of acute scrub typhus, underscoring the importance of increased clinical awareness, improved diagnostic tools, and empiric treatment of those with epidemiologic or clinical risk factors.

The main limitation of this study was the relatively low proportion (41%) of patients with both acute-phase and convalescent-phase serum samples compared with our previous studies (*17*,*18*). For this reason, we also performed PCR and tested for IgM, even though sensitivity of the former and specificity of the latter are limited for identifying acute rickettsioses (*19*). Our estimates of the seroprevalence of rickettsioses and incidence of confirmed acute rickettsioses are conservative. First, only half of patients returned for convalescent follow-up, yet most confirmed acute rickettsioses were seroconversions rather than based on 4-fold rises in titer alone. Second, over half of patients who did have a convalescent-phase serum sample obtained had it obtained earlier than the recommended ≥14 days. In experimental human SFGR infection, ≥3 weeks were required before the geometric mean titer of infected volunteers reached

diagnostic IgG titers (*49*). Third, antibody detection of different antigen groups such as that observed in *O. tsutsugamushi* was based on cross-reactivity to the single Karp strain. Finally, patients with seroconversions indicative of past infection might be missed by a screening strategy that entails testing convalescent-phase serum samples first.

To better estimate the actual prevalence of acute rickettsioses, we additionally delineated patients with confirmed rickettsioses with likely acute infection (patients with rising or single IgG titers of ≥160) as having probable acute infections. The likely underestimation of acute infections caused by diagnostic uncertainty is supported by the similarity in initial clinical and laboratory findings between confirmed and probable acute rickettsioses. The burden and clinical features of rickettsioses are likely underestimated in our study not only because of underreporting of laboratory-confirmed cases but also because persons with mild illness, nonspecific features, and limited physical or economic ability to travel to hospital and persons living in remote areas might not have sought care. Similarly, persons with severe disease might have sought care at or been transferred to a tertiary hospital before study enrollment or died before care they sought or obtained care. TGR prevalence is also potentially underestimated because our population was mainly rural rather than urban. However, our data are likely generalizable to similar populations in Sabah and potentially neighboring areas.

In conclusion, rickettsioses are prevalent among persons with nonmalarial AFI in Sabah, Malaysia. A comprehensive prospective study of rickettsial infections across Malaysia is warranted to define the totality of regional risk. Improved diagnostic tools are urgently needed; in their absence, increased clinical suspicion and empirical doxycycline might avert disease and death attributable to rickettsioses.

### Acknowledgments

We thank the participants in this study and the clinical and laboratory research staff, including Emma Istiana binti Israk, Sitti Saimah binti Sakam, Norfarain binti Mohamed Yassin, Salwah Hamit binti Hamid, Noorazela binti Mohamed Yassin, Areys Benjamin, Wilhelmina Nevir, Siti Norfazaziwantie binti Redzuan, and Maslianah binti Sintom. We express sincere appreciation also to the hospital directors at the study sites. We thank the Director-General of Health, Ministry of Health, Malaysia, for permission to publish this study. We also thank Emily Clemens and Amanda Olivier for excellent technical support with serologic and molecular testing.

This study was supported by the Malaysia Ministry of Health (grant no. 2014-26), the Australian National Health and Medical Research Council (program no. 1037304; fellowship no. 605831 to T.W.Y.; scholarship no. 1074795 and fellowship no. 1138860 to M.J.G.; fellowship no. 1135820 to N.M.A.), the US National Institutes of Allergy and Infectious Diseases (grant no. R03 AI111300 to M.E.R.), and the Uniformed Services University for the Health Sciences (grant no. PAT-74-3977 to J.S.D.).

### About the Author

Dr. Grigg is a senior research fellow at Menzies School of Health Research and Charles Darwin University, Australia. His primary research interests include the epidemiology, diagnosis and treatment of *Plasmodium knowlesi* and other *Plasmodium* species infections causing malaria in Malaysia and Indonesia; other tropical and zoonotic/vectorborne infectious diseases; and the health of Indigenous peoples in remote Northern Territory communities in Australia.

### References

1. McQuiston JH, Wiedeman C, Singleton J, Carpenter LR, McElroy K, Mosites E, et al. Inadequacy of IgM antibody tests for diagnosis of Rocky Mountain Spotted Fever. Am J Trop Med Hyg. 2014;91:767–70. https://doi.org/10.4269/ajtmh.14-0123
2. Brown GW, Robinson DM, Huxsoll DL, Ng TS, Lim KJ, Sannasey G. Scrub typhus: a common cause of illness in indigenous populations. Trans R Soc Trop Med Hyg. 1976;70:444–8. https://doi.org/10.1016/0035-9203(76)90127-9
3. Brown GW, Shirai A, Jegathesan M, Burke DS, Twartz JC, Saunders JP, et al. Febrile illness in Malaysia—an analysis of 1,629 hospitalized patients. Am J Trop Med Hyg. 1984;33:311–5. https://doi.org/10.4269/ajtmh.1984.33.311
4. Cadigan FC Jr, Andre RG, Bolton M, Gan E, Walker JS. The effect of habitat on the prevalence of human scrub typhus in Malaysia. Trans R Soc Trop Med Hyg. 1972;66:582–7. https://doi.org/10.1016/0035-9203(72)90303-3
5. Tay ST, Rohani MY. The use of the indirect immunoperoxidase test for the serodiagnosis of rickettsial diseases in Malaysia. Southeast Asian J Trop Med Public Health. 2002;33:314–20.
6. Ministry of Health Malaysia. Case definitions for infectious diseases in Malaysia. 3rd edition. 2017 Jan 1 [cited 2019 Jan 12]. http://www.moh.gov.my/index.php
7. Ministry of Health Malaysia. Health indicators (Pentunjuk Kesihatan), 2015 [cited 2019 Jan 12]. http://www.moh.gov.my/images/gallery/publications/Petunjuk%20Kesihatan%202016.pdf
8. Tay ST, Ho TM, Rohani MY, Devi S. Antibodies to *Orientia tsutsugamushi, Rickettsia typhi* and spotted fever group rickettsiae among febrile patients in rural areas of Malaysia. Trans R Soc Trop Med Hyg. 2000;94:280–4. https://doi.org/10.1016/S0035-9203(00)90322-5
9. Malaysia Government Department of Statistics. Population and housing census, Malaysia. 2010 [cited 2018 Sep 15]. https://www.statistics.gov.my/mycensus2010/images/stories/files/Laporan_Kiraan_Permulaan2010.pdf

10. Bryan JE, Shearman PL, Asner GP, Knapp DE, Aoro G, Lokes B. Extreme differences in forest degradation in Borneo: comparing practices in Sarawak, Sabah, and Brunei. PLoS One. 2013;8(7):e69679.
11. World Health Organization. Haemoglobin concentrations for the diagnosis of anaemia and assessment of severity. 2011 [cited 2018 Oct 10]. http://www.who.int/vmnis/indicators/haemoglobin.pdf
12. KDIGO clinical practice guidelines for acute kidney injury. Kidney Int Suppl. 2012;2:1–138.
13. Reller ME, Chikeka I, Miles JJ, Dumler JS, Woods CW, Mayorga O, et al. First identification and description of rickettsioses and Q fever as causes of acute febrile illness in Nicaragua. PLoS Negl Trop Dis. 2016;10:e0005185. https://doi.org/10.1371/journal.pntd.0005185
14. Reller ME, Bodinayake C, Nagahawatte A, Devasiri V, Kodikara-Arachichi W, Strouse JJ, et al. Unsuspected rickettsioses among patients with acute febrile illness, Sri Lanka, 2007. Emerg Infect Dis. 2012;18:825–9. https://doi.org/10.3201/eid1805.111563
15. Prakash JAJ, Reller ME, Barat N, Dumler JS. Assessment of a quantitative multiplex 5′ nuclease real-time PCR for spotted fever and typhus group rickettsioses and *Orientia tsutsugamushi*. Clin Microbiol Infect. 2009;15(Suppl 2):292–3. https://doi.org/10.1111/j.1469-0691.2008.02242.x
16. US Centers for Disease Control and Prevention. Spotted fever rickettsiosis (*Rickettsia* spp.) 2010 case definition. 2010 [cited 2018 Oct 5]. https://wwwn.cdc.gov/nndss/conditions/spotted-fever-rickettsiosis/case-definition/2010
17. Fletcher W, Lesslar JE. Tropical typhus in the Federated Malay States with a compilation on epidemic typhus. Bull Inst Med Res. 1925;2:88.
18. Malaysia Ministry of Health. Health indicators (Pentunjuk Kesihatan) 2016 [cited 2018 Nov 23]. http://www.moh.gov.my/images/gallery/publications/Petunjuk%20Kesihatan%202017.pdf
19. Paris DH, Dumler JS. State of the art of diagnosis of rickettsial diseases: the use of blood specimens for diagnosis of scrub typhus, spotted fever group rickettsiosis, and murine typhus. Curr Opin Infect Dis. 2016;29:433–9. https://doi.org/10.1097/QCO.0000000000000298
20. Southeast Asia Infectious Disease Clinical Research Network. Causes and outcomes of sepsis in southeast Asia: a multinational multicentre cross-sectional study. Lancet Glob Health. 2017;5:e157–67. https://doi.org/10.1016/S2214-109X(17)30007-4
21. Vallée J, Thaojaikong T, Moore CE, Phetsouvanh R, Richards AL, Souris M, et al. Contrasting spatial distribution and risk factors for past infection with scrub typhus and murine typhus in Vientiane City, Lao PDR. PLoS Negl Trop Dis. 2010;4:e909. https://doi.org/10.1371/journal.pntd.0000909
22. Pradutkanchana J, Pradutkanchana S, Kemapanmanus M, Wuthipum N, Silpapojakul K. The etiology of acute pyrexia of unknown origin in children after a flood. Southeast Asian J Trop Med Public Health. 2003;34:175–8.
23. Parola P, Miller RS, McDaniel P, Telford SR III, Rolain J-M, Wongsrichanalai C, et al. Emerging rickettsioses of the Thai–Myanmar border. Emerg Infect Dis. 2003;9:592–5. https://doi.org/10.3201/eid0905.020511
24. Syhavong B, Rasachack B, Smythe L, Rolain J-M, Roque-Afonso A-M, Jenjaroen K, et al. The infective causes of hepatitis and jaundice amongst hospitalised patients in Vientiane, Laos. Trans R Soc Trop Med Hyg. 2010;104:475–83. https://doi.org/10.1016/j.trstmh.2010.03.002
25. Phongmany S, Rolain J-M, Phetsouvanh R, Blacksell SD, Soukkhaseum V, Rasachack B, et al. Rickettsial infections and fever, Vientiane, Laos. Emerg Infect Dis. 2006;12:256–62. https://doi.org/10.3201/eid1202.050900
26. Mayxay M, Castonguay-Vanier J, Chansamouth V, Dubot-Pérès A, Paris DHP, Phetsouvanh R, et al. Causes of non-malarial fever in Laos: a prospective study. Lancet Glob Health. 2013;1:e46–54. https://doi.org/10.1016/S2214-109X(13)70008-1
27. Gasem MH, Wagenaar JFP, Goris MGA, Adi MS, Isbandrio BB, Hartskeerl RA, et al. Murine typhus and leptospirosis as causes of acute undifferentiated fever, Indonesia. Emerg Infect Dis. 2009;15:975–7. https://doi.org/10.3201/eid1506.081405
28. Richards AL, Ratiwayanto S, Rahardjo E, Kelly DJ, Dasch GA, Fryauff DJ, et al. Serologic evidence of infection with ehrlichiae and spotted fever group rickettsiae among residents of Gag Island, Indonesia. Am J Trop Med Hyg. 2003;68:480–4. https://doi.org/10.4269/ajtmh.2003.68.480
29. Dohany AL, Phang OW, Rapmund G. Chigger (Acarina: Trombiculidae) surveys of the west coast beaches of Sabah and Sarawak. Southeast Asian J Trop Med Public Health. 1977;8:200–6.
30. Taylor AC, Hii J, Kelly DJ, Davis DR, Lewis GE Jr. A serological survey of scrub, tick, and endemic typhus in Sabah, East Malaysia. Southeast Asian J Trop Med Public Health. 1986;17:613–9.
31. Aung AK, Spelman DW, Murray RJ, Graves S. Rickettsial infections in Southeast Asia: implications for local populace and febrile returned travelers. Am J Trop Med Hyg. 2014;91:451–60. https://doi.org/10.4269/ajtmh.14-0191
32. Suttinont C, Losuwanaluk K, Niwatayakul K, Hoontrakul S, Intaranongpai W, Silpasakorn S, et al. Causes of acute, undifferentiated, febrile illness in rural Thailand: results of a prospective observational study. Ann Trop Med Parasitol. 2006;100:363–70. https://doi.org/10.1179/136485906X112158
33. Suputtamongkol Y, Suttinont C, Niwatayakul K, Hoontrakul S, Limpaiboon R, Chierakul W, et al. Epidemiology and clinical aspects of rickettsioses in Thailand. Ann N Y Acad Sci. 2009;1166:172–9. https://doi.org/10.1111/j.1749-6632.2009.04514.x
34. Tay ST, Mohamed Zan HA, Lim YAL, Ngui R. Antibody prevalence and factors associated with exposure to *Orientia tsutsugamushi* in different aboriginal subgroups in West Malaysia. PLoS Negl Trop Dis. 2013;7:e2341.
35. Kilpatrick AM, Randolph SE. Drivers, dynamics, and control of emerging vector-borne zoonotic diseases. Lancet. 2012;380:1946–55. https://doi.org/10.1016/S0140-6736(12)61151-9
36. Tee TS, Kamalanathan M, Suan KA, Chun SS, Ming HT, Yasin RM, et al. Seroepidemiologic survey of *Orientia tsutsugamushi, Rickettsia typhi*, and TT118 spotted fever group rickettsiae in rubber estate workers in Malaysia. Am J Trop Med Hyg. 1999;61:73–7. https://doi.org/10.4269/ajtmh.1999.61.73
37. Noad KB, Haymaker W. The neurological features of Tsutsugamushi fever, with special reference to deafness. Brain. 1953;76:113–31. https://doi.org/10.1093/brain/76.1.113
38. Sexton DJ. Acute hearing loss and rickettsial diseases. Clin Infect Dis. 2006;42:1506. https://doi.org/10.1086/503682
39. Kim D-M, Won KJ, Park CY, Yu KD, Kim HS, Yang TY, et al. Distribution of eschars on the body of scrub typhus patients: a prospective study. Am J Trop Med Hyg. 2007;76:806–9. https://doi.org/10.4269/ajtmh.2007.76.806

40. Hsu RK, Hsu C-Y. The role of acute kidney injury in chronic kidney disease. Semin Nephrol. 2016;36:283–92. https://doi.org/10.1016/j.semnephrol.2016.05.005
41. Raby E, Dyer JR. Endemic (murine) typhus in returned travelers from Asia, a case series: clues to early diagnosis and comparison with dengue. Am J Trop Med Hyg. 2013;88:701–3. https://doi.org/10.4269/ajtmh.12-0590
42. Ministry of Health Malaysia. National Antimicrobial Guideline. 2019 [cited 2019 Feb 12]. https://www.pharmacy.gov.my/v2/sites/default/files/document-upload/national-antimicrobial-guideline-2019-full-version-3rd-edition.pdf
43. Taylor AJ, Paris DH, Newton PN. A systematic review of mortality from untreated scrub typhus (*Orientia tsutsugamushi*). PLoS Negl Trop Dis. 2015;9:e0003971.
44. Valbuena G, Walker DH. Infection of the endothelium by members of the order Rickettsiales. Thromb Haemost. 2009;102:1071–9. https://doi.org/10.1160/TH09-03-0186
45. Moron CG, Popov VL, Feng HM, Wear D, Walker DH. Identification of the target cells of *Orientia tsutsugamushi* in human cases of scrub typhus. Mod Pathol. 2001;14:752–9. https://doi.org/10.1038/modpathol.3880385
46. Paris DH, Blacksell SD, Stenos J, Graves SR, Unsworth NB, Phetsouvanh R, et al. Real-time multiplex PCR assay for detection and differentiation of rickettsiae and orientiae. Trans R Soc Trop Med Hyg. 2008;102:186–93. https://doi.org/10.1016/j.trstmh.2007.11.001
47. Kelly DJ, Fuerst PA, Ching W-M, Richards AL. Scrub typhus: the geographic distribution of phenotypic and genotypic variants of *Orientia tsutsugamushi*. Clin Infect Dis. 2009;48 Suppl 3:S203–30.
48. Tay ST, Rohani MY, Ho TM, Devi S. Antigenic types of *Orientia tsutsugamushi* in Malaysia. Southeast Asian J Trop Med Public Health. 2002;33:557–64.
49. Clements ML, Dumler JS, Fiset P, Wisseman CL Jr, Snyder MJ, Levine MM. Serodiagnosis of Rocky Mountain spotted fever: comparison of IgM and IgG enzyme-linked immunosorbent assays and indirect fluorescent antibody test. J Infect Dis. 1983;148:876–80. https://doi.org/10.1093/infdis/148.5.876

Address for correspondence: Matthew Grigg, Global and Tropical Health Division, Menzies School of Health Research, PO Box 41096, Casuarina, Darwin 0811, Northern Territory, Australia; email: matthew.grigg@menzies.edu.au; Megan E. Reller, Division of Infectious Diseases and International Health, Department of Medicine, Duke University School of Medicine, 315 Trent Dr, Hanes House, Rm 250, Durham, NC 27710, USA; email: megan.reller@duke.edu

# Meningococcal W135 Disease Vaccination Intent, the Netherlands, 2018–2019

Marion de Vries, Liesbeth Claassen,[1] Margreet J.M. te Wierik,[1] Feray Coban, Albert Wong, Danielle R.M. Timmermans, Aura Timen

To control the rise in *Neisseria meningitidis* strain W infections, during 2018–2019, the Netherlands launched a catch-up meningococcal conjugate (MenACWY) vaccination campaign for teenagers (13–18 years of age). Applying a mental models approach, we surveyed teenagers and their parents about their knowledge and beliefs about meningococcal disease, the MenACWY vaccination, vaccinations in general, and their MenACWY vaccination intentions. Using random forest analysis, we studied predictions of vaccination intentions by knowledge and beliefs. Survey response rate was 52.8% among teenagers and 59.4% among parents. MenACWY vaccination intentions were best predicted by knowledge and beliefs about vaccinations in general, surpassing knowledge and beliefs about meningococcal disease and the MenACWY vaccination. For teenagers, their parents' intention that the teenager be vaccinated was a strong predictor of the teenagers' own vaccination intention. To optimize vaccination uptake during future outbreaks, we recommend that communications emphasize the effectiveness and safety of vaccines and continue to focus on parents.

Since the end of 2015, invasive meningococcal disease (IMD) caused by *Neisseria meningitidis* strain W135 has emerged as a severe threat to public health in the Netherlands (*1*). Before 2015, IMD W135 cases occurred sporadically, averaging 4 cases per year. From 2015 on, the number of cases increased rapidly, to 103 patients in 2018 alone. Cases were reported among persons in all age groups, but the largest numbers of cases were among children <5 years of age, teenagers, and elderly persons. The case-fatality rate has been highest among teenagers/young adults 14–24 years of age (29% compared with an average case-fatality rate of 17%) (*2*).

In September 2017, the Ministry of Health, Welfare and Sport in the Netherlands decided to introduce the meningococcal conjugate (MenACWY) vaccine into the National Immunization Program for children 14 months of age (replacing the meningococcal C conjugate vaccine used until then) and to have an additional catch-up MenACWY vaccination campaign in 2018 and 2019 that focused on teenagers. The initial target groups for the catch-up vaccination campaign were teenagers ≈14 years of age (born after April 2004 and in 2005). In July 2019, because of increased vaccine accessibility, the target groups were extended to include all teenagers 14–18 years of age (cohorts 2001–2005).

Various studies have been performed to determine how persons make vaccination decisions, including those regarding vaccination against meningococcal disease (*3*–*12*). This academic interest in vaccination decisions has increased over the past few years after the gradual decline of vaccination uptake observed in many countries. Various factors play a role in this decline (*13*). Frequently mentioned causes are the lack of laypersons' familiarity with the severe consequences of vaccine-preventable diseases, increased concerns about the safety of vaccines, and decreased trust in the effectiveness of vaccines.

In contrast to most studies that have shown the influence of knowledge and beliefs on vaccination decisions (e.g., those applying the theory of planned behavior [*14*,*15*], the protection motivation theory [*16*,*17*], and the health belief model [*18*,*19*]), our aim with this study was not to fully understand vaccination behavior but to gain insights into specific aspects of knowledge and beliefs that could provide concrete

Author affiliations: National Institute for Public Health and the Environment (RIVM), Bilthoven, the Netherlands (M. de Vries, L. Claassen, M.J.M. te Wierik, F. Coban, A. Wong, A. Timen); Vrije Universiteit Amsterdam, Amsterdam, the Netherlands (D.R.M. Timmermans, A. Timen)

DOI: https://doi.org/10.3201/eid2607.191812

[1]These authors contributed equally to this article.

input for communication practices. Studies of vaccination decisions that apply behavioral models often study risk and benefit perceptions in relatively general terms (e.g., perceived vulnerability, severity, and safety). At the same time, the need to assess context-specific knowledge and beliefs when studying human behavior has been strongly emphasized (*20*). These specific beliefs are not only likely to better predict vaccination behavior (*20*), but insights into these beliefs can also provide more concrete input for communication (*21*).

The mental models approach, a method developed to improve risk communication in the field of environmental risks (*22*–*26*), focuses on assessing and comparing experts' and laypersons' knowledge and beliefs about risks. This approach has been infrequently applied in the field of infectious diseases and vaccinations (*26*–*28*). The concept of mental models suggests that persons have mental representations of risks, consisting of a complex interconnected web of both specific and more general knowledge and beliefs about the causes, effects, and risk mitigation options of that risk (*21*). Laypersons' mental models often differ largely from those of experts, which is one reason why experts' risk communications often do not have the desired effect among laypersons (*21*). Following the mental models approach, communications should be based not only on what experts consider important but also on what laypersons consider important and what they already know and believe. Communications thus need to be compatible with the mental model of the receiver, should correct misbeliefs, should add information that was previously lacking, and should be delivered in language that laypersons understand.

On the basis of the mental models approach, at the onset of the MenACWY vaccination campaign in September 2018, we explored aspects of knowledge and specific beliefs about meningococcal disease, the MenACWY vaccination, and vaccines in general among teenagers in the Netherlands invited for the MenACWY vaccination and their parents. We also investigated which of these aspects of knowledge and specific beliefs are strong predictors of MenACWY vaccination intentions. Those aspects of knowledge and specific beliefs that strongly predict vaccination intentions could be prioritized in future communications.

Two research questions were central to our study: What do teenagers and their parents know and believe about meningococcal disease, the MenACWY vaccination, and vaccinations in general? Which aspects of knowledge and specific beliefs predict MenACWY vaccination intentions by teenagers and their parents?

## Methods

### Study Population and Procedure

During September 13–26, 2018, we sent surveys to teenagers ≈14 years of age (born after April 2004 and in 2005; n = 1,923), to whom the MenACWY vaccination was initially directed; to their parents (n = 2,000); and to teenagers from the extended target group (teenagers born from 2001 through April 2004; n = 1,113) and their parents (n = 1,002). The surveys were conducted via an online survey panel (Kantar Public, http://www.niipo.nl/panel). At the time of this study, this survey panel had an active population of ≈140,000 residents in the Netherlands. Panel members gave active consent for their participation in the panel organization, including consent for data sharing.

Before actively entering the survey, all panel members invited to participate were informed about the purpose and content of the study. Teenagers' participation required additional consent from 1 of their parents. Survey completion took 15 minutes on average. The Clinical Expertise Centre RIVM determined that this research was not subject to law in the Netherlands for medical research involving human subjects and, therefore, concluded that it was exempt from needing further approval from an ethics research committee.

### Survey Development

In line with the mental models approach (*21*,*29*), we based the survey questions on basic information provided by the National Institute for Public Health and the Environment (RIVM) (*2*) and on knowledge and beliefs among teenagers and parents, which we explored with open-ended, semistructured interviews. We interviewed 12 teenagers and 10 parents during April–June 2018. The interviews started with open-ended questions about vaccinations and infectious diseases in general (e.g., "What can you tell me about vaccinations?") and consequently narrowed down to meningococcal disease and the MenACWY vaccination. In addition to the questions yielded from the RIVM information and the interviews, we supplemented the survey with questions about the safety and effectiveness of vaccines in general, derived from vaccine-skeptic websites in the Netherlands (*30*,*31*), to examine whether beliefs that contradict the RIVM information were present in the population.

### Operationalization of Concepts

The survey questions addressed MenACWY vaccination intention and various aspects of knowledge

and beliefs about meningococcal disease, the MenACWY vaccination, and vaccinations in general. MenACWY vaccination intention was assessed with the question "Do you want to be vaccinated against meningococcal disease type A, C, W, and Y?" for the teenagers and "Do you want your child to be vaccinated against meningococcal disease type A, C, W, and Y?" for parents. Respondents could answer on a 7-point semantic scale, from 0 (certainly not) to 6 (certainly yes).

We assessed aspects of knowledge and specific beliefs about meningococcal disease, the MenACWY vaccination, and vaccinations in general with 5 questions, including 42 items (Appendix, https://wwwnc.cdc.gov/EID/article/26/7/19-1812-App1.pdf). Most items assessing knowledge and beliefs were formulated as statements. Respondents were asked to indicate on a 5-point Likert scale whether they thought that these statements were true or false. Exceptions to the use of this scale were items assessing respondents' familiarity with various terms used for meningococcal disease (3-point scale) and items assessing respondents' beliefs about short-term adverse events of vaccinations (7-point scale).

### Statistical Analyses

We performed descriptive analyses for each measure within the samples of parents and teenagers. We used independent Student *t*-tests tests to study differences between parents and teenagers with regard to MenACWY vaccination intention and knowledge and belief items, measured on 5- and 7-point Likert scales. Differences between parents' and teenagers' knowledge and belief items measured on a 3-point scale were studied by using $\chi^2$ tests.

To study whether and how knowledge and beliefs predict MenACWY vaccination intentions, we applied random forest analyses (RF) (*32*) in R (*33*). RF is a nonparametric machine learning method for regression and classification based on an ensemble of decision trees. We considered RF to be appropriate because our study has a dependent variable (MenACWY vaccination intention) that is not normally distributed, a relatively large number of (partly intercorrelated) independent variables (knowledge and beliefs), and potentially nonlinear relationships between independent variables and the dependent variable.

We built separate RF models for teenagers and parents and built a third model for all teenagers in the sample for whom at least 1 parent also participated in the survey. In this model, the knowledge and beliefs variables and the dependent variable from the parents were added as independent variables to their children's model to study the interrelatedness of paired parents and children. All analyses were controlled for age, sex, education, income, social class (based on income, education, and employment), region of residence, teenager's vaccination record, whether the respondent was aware of the MenACWY vaccination campaign, and whether teenagers and their parents were part of the first target group (cohort born after April 2004 or in 2005) or the second target group (cohorts born 2001–2003 or before May 2004). We used the RF method to generate 4 types of output: 1) the variable importance ranking, which ranks the independent variables in terms of how much they contribute to the explanation of the dependent variable; 2) the marginal means (MM), which describe the relationship between the dependent variable and each independent variable; 3) the total explained variance of the model; and 4) the cumulative variance explained (CVE), which indicates how much each independent variable adds to the explained variance of the model when the independent variables are added to the model following the sequence of the variable importance matrix.

## Results

### Study Population

Response rates were 52.8% among teenagers (n = 1,603/3,036) and 59.4% among parents (n = 1,784/3,002). The sample contained 1,318 pairs of a parent and a teenager from the same household (Table).

### MenACWY Vaccination Intention

Teenagers were generally willing to be vaccinated with the MenACWY vaccine, and their parents were willing to have them vaccinated. Mean (± SD) scores were 5.0 (± 1.5) for parents and 4.4 (± 1.7) for teenagers. Parents were significantly more willing to have their teenagers vaccinated with the MenACWY vaccine than were teenagers willing to be vaccinated ($p<0.001$).

### Knowledge and Beliefs about Meningococcal Disease

Whether respondents were familiar with meningococcal disease depended on the terms used to identify it. Respondents were most familiar with the Dutch lay terms for septicemia and meningitis (Appendix). Less well known were the more expert terms for meningococci, meningococcal disease, septicemia, and meningitis. Parents were significantly more aware than teenagers of all terms used for meningococcal disease.

The average responses to most items assessing knowledge and beliefs about meningococcal disease reflected modest levels of knowledge and are mostly close to the scale median representing the "don't know" category (Appendix). Respondents generally seemed aware of the transmissibility and seriousness of IMD and of the current outbreak, reflected by the scores on the following items: "Meningococcal disease is contagious," "Meningococcal disease requires hospitalization for treatment," and "In the past couple of years, more people in the Netherlands fell ill due to one of the meningococcus types." Parents were significantly more knowledgeable than teenagers with regard to all but 1 item representing true or false statements about meningococcal disease.

### Knowledge and Beliefs about MenACWY Vaccination

In general, respondents indicated knowing that MenACWY vaccination does not confer lifelong protection against meningococcal disease (Appendix). Less well known was the fact that this vaccine does not protect against all meningococcal serogroups. Parents were significantly more knowledgeable than teenagers about the continued possibility of contracting meningococcal disease after vaccination and about the reasons why teenagers were invited to receive MenACWY vaccination.

### Knowledge and Beliefs about Vaccinations in General

On average, parents and teenagers believed that vaccinations are needed to prevent infectious diseases and are effective at doing so (Appendix). We found some misbeliefs concerning the safety of vaccines. The most prominent misbelief was represented by the relatively high scores for "Every year, a number of children in the Netherlands die from the harmful consequences of vaccines." We did not observe a clear pattern between parents and teenagers in knowledge and beliefs about vaccinations in general; for some items, parents seemed more knowledgeable, but for others, teenagers seemed to know more. Of all short-term adverse events, teenagers were significantly more concerned than their parents about the pain caused by vaccination and less concerned about the possibility of a swollen arm after vaccination.

### MenACWY Vaccination Intentions among Teenagers and Parents as Predicted by Aspects of Knowledge and Specific Beliefs

RF analyses included all respondents who reported the teenager not having received, or not remembering having received, the MenACWY vaccination before their participation in the survey (1,541 teenagers and 1,712 parents). The RF models explain 47.2% of the variance in MenACWY vaccination intentions for parents and 31.7% for teenagers. The combined model (in this model, the knowledge and beliefs items and the dependent variable from the parents were added to their children's models) explains 39.9% of the variance in MenACWY vaccination intentions among teenagers.

In the RF model for parents, 5 knowledge/belief items (plus the control variable "vaccination history teenager") are considerably stronger predictors of MenACWY vaccination intention than the other items (Figure 1). Each of these items represents a belief regarding vaccines. The item "Vaccinations are needed to prevent infectious diseases" is the strongest predictor in this model (CVE 25.8%, MM 4.33–4.90). Note that when all other variables are kept constant, the lowest value for "Vaccinations are needed to prevent infectious diseases" (0) corresponds to a mean MenACWY vaccination intention of 4.33 and the

**Table.** Description of participants in study of invasive meningococcal W135 disease vaccination intent, the Netherlands, 2018–2019*

| Participant | No. (%) |
|---|---|
| Sex | |
| Parents, n = 1,784* | |
| F | 991 (55.5) |
| M | 793 (44.5) |
| Teenagers, n = 1,603* | |
| F | 810 (50.5) |
| M | 793 (49.5) |
| Age, y† | |
| Teenagers | |
| 12 | 111 (6.9) |
| 13 | 611 (38.1) |
| 14 | 379 (23.6) |
| 15 | 175 (10.9) |
| 16 | 161 (10.0) |
| 17 | 166 (10.4) |
| Education‡ | |
| Parents | |
| Low | 252 (14.1) |
| Intermediate | 1,318 (73.9) |
| High | 214 (12.0) |
| Teenagers | |
| No current education | 8 (0.5) |
| Primary school | 12 (0.7) |
| Secondary school | 1,406 (87.7) |
| Preparing for vocational education | 552 (39.3) |
| Preparing for higher education | 809 (57.5) |
| Combination | 45 (3.2) |
| Vocational education | 129 (8.0) |
| Higher education | 48 (0.7) |
| Initial target group, born after Apr 2004 through 2005 | |
| Parents | 1,177 (66.0) |
| Teenagers | 1,010 (63.0) |
| Extended target group, cohorts born 2001 through Apr 2004 | |
| Parents | 607 (34.0) |
| Teenagers | 593 (37.0) |

*Total parent–teenager pairs = 1,318 (73.9% of parents, 82.2% of teenagers).
†Parents' age range 31–73 y; mean (± SD) age 46.5 (5.5) y.
‡Categories based on (*34*).

highest value (4) corresponds to a mean MenACWY vaccination intention of 4.90.

The next items were "Vaccination can lead to various severe health conditions" (CVE 40.0%, MM 5.12–4.77), "Vaccinations protect well against infectious diseases" (CVE 42.2%, MM 4.54–5.08), "Little is known about the possible harmful consequences of vaccination" (CVE 46.4%, following the 45.25% CVE of "vaccination history teenager," MM 5.00–4.57), and "Vaccinations weaken the immune system" (CVE 47.3%, MM 5.04–4.67).

In the model for teenagers (Figure 2), only 2 knowledge and beliefs items (plus the control variable "vaccination history teenager") have a stronger

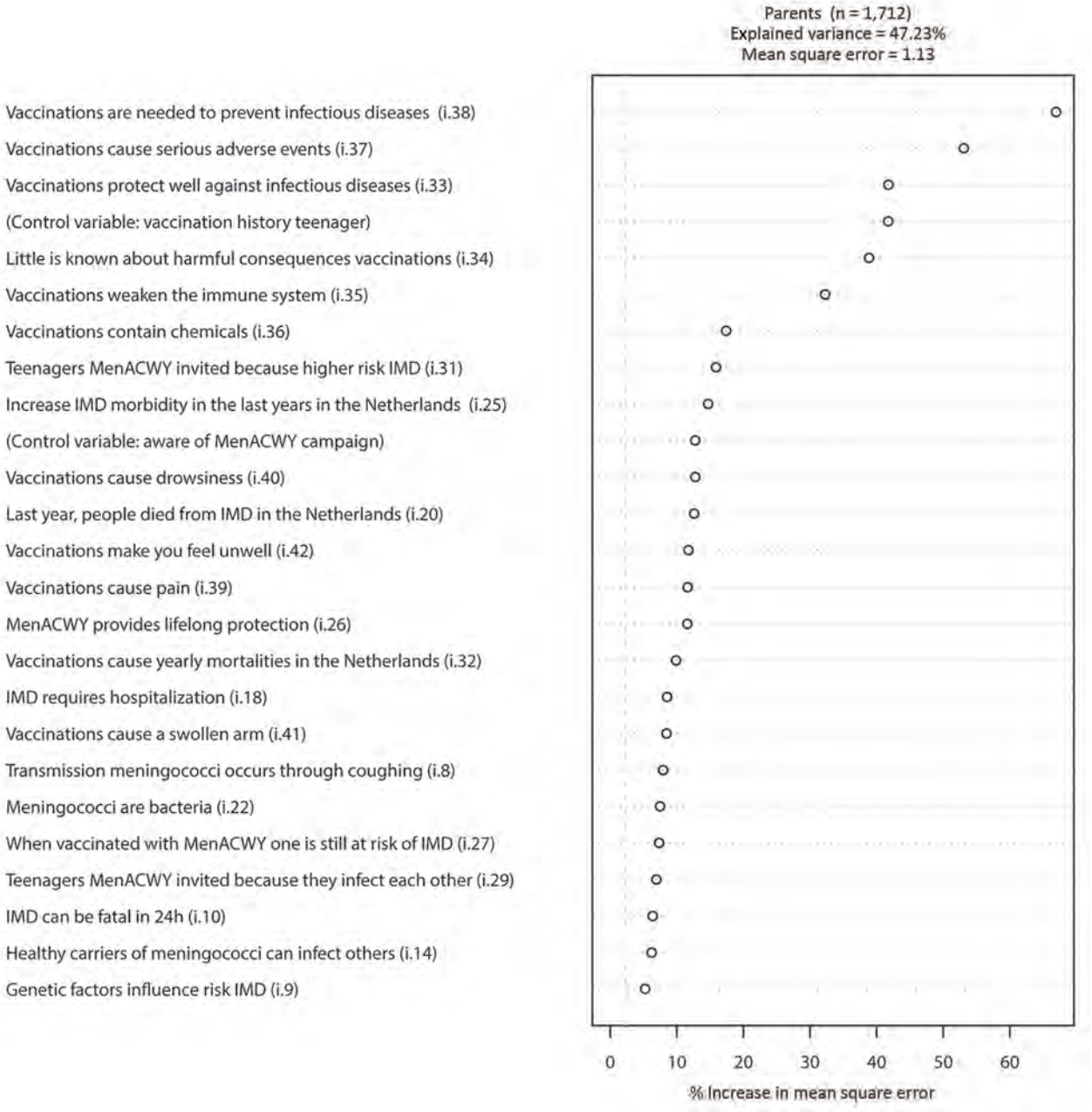


**Figure 1.** Variable importance ranking among parents in study of vaccination intent regarding IMD caused by *Neisseria meningitidis* strain W135, the Netherlands, 2018–2019. The 25 strongest predictors (i.e., knowledge and belief items [Table] and control variables), are ranked top to bottom, based on their ability to predict parental meningococcal conjugate [MenACWY] vaccination intention. Control variables are age, sex, education, income, region, social class, region of residence, vaccination record of the teenager, whether the respondent was aware of the MenACWY vaccination campaign, and whether teenagers and their parents were part of the first (cohorts 2004–2005) or the second MenACWY vaccination target group (cohorts 2001–2003). IMD, invasive meningococcal disease.

ability to predict MenACWY vaccination intention than the other items, namely, "Vaccinations are needed to prevent infectious diseases" (CVE 16.7%, MM 3.66–4.61) and "Vaccinations protect well against infectious diseases" (CVE 18.7%, MM 4.00–4.62). In the combined model for teenagers (Figure 3), only 1 considerably strong predictor was observed, namely, the MenACWY vaccination intention of the parent (CVE 29.6%, MM 3.00–4.69).

## Discussion

Our study provides insights into MenACWY vaccination intentions and underlying knowledge and beliefs among teenagers and their parents at the start of the 2018 catch-up vaccination campaign in the Netherlands. Our study shows that teenagers were generally inclined to receive the MenACWY vaccination and parents were generally inclined to have their teenagers vaccinated. Both groups

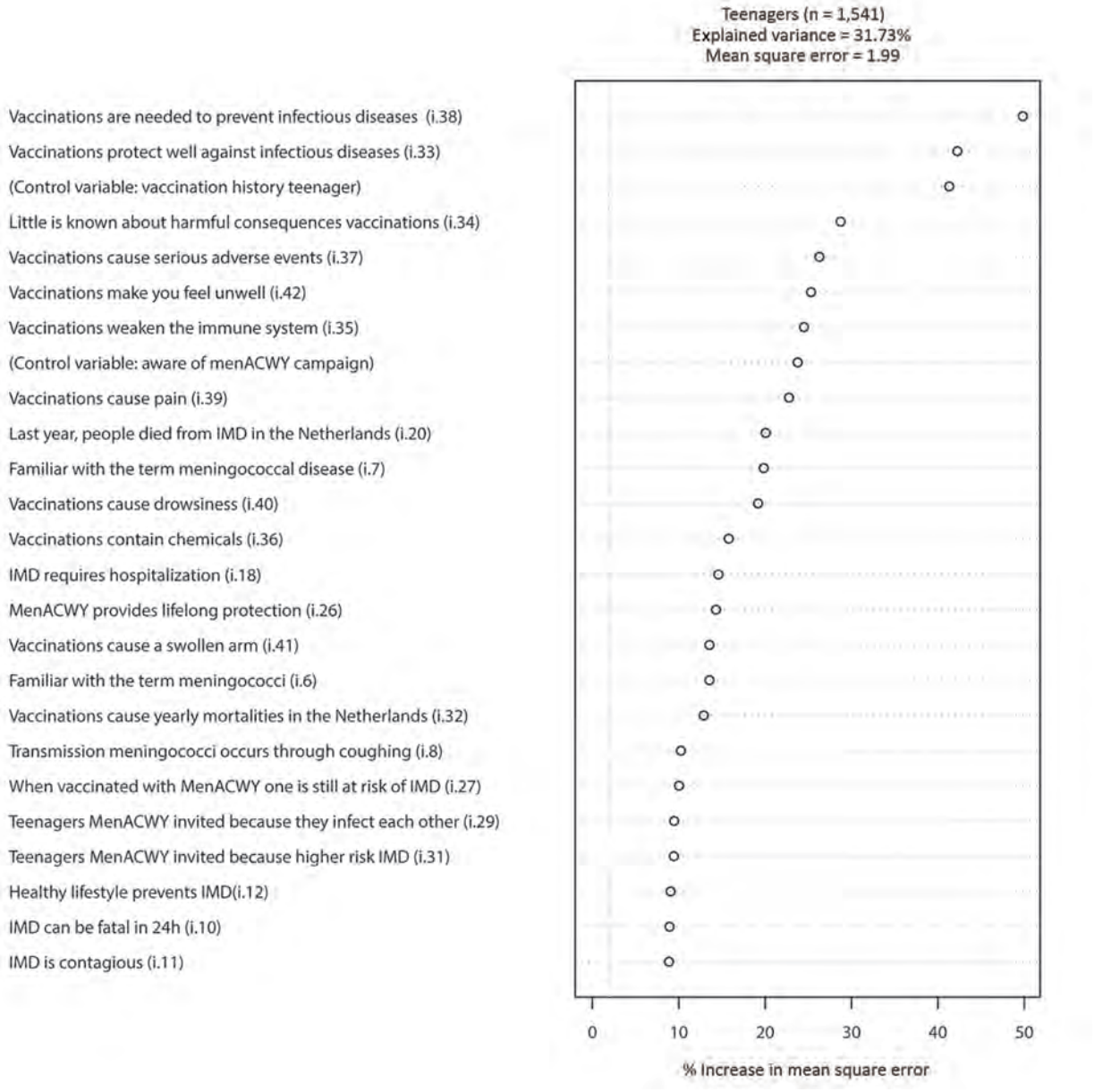


**Figure 2.** Variable importance ranking among teenagers in study of vaccination intent regarding IMD caused by *Neisseria meningitidis* strain W135, the Netherlands, 2018–2019. The 25 strongest predictors (i.e., knowledge and belief items [Table] and control variables) are ranked top to bottom, based on their ability to predict meningococcal conjugate (MenACWY) vaccination intention among teenagers. Control variables are age, sex, education, income, region, social class, region of residence, vaccination record of the teenager, whether the respondent was aware of the MenACWY vaccination campaign, and whether teenagers and their parents were part of the first (cohorts 2004–2005) or second MenACWY vaccination target group (cohorts 2001–2003). IMD, invasive meningococcal disease.

seemed aware of the severity and contagiousness of IMD, but we also identified knowledge gaps and misbeliefs. Knowledge and beliefs concerning the effectiveness of, need for, and safety of vaccines were the strongest predictors of MenACWY vaccination intentions. For teenagers, the strongest predictor of their own vaccination intention was whether their parent(s) wanted them to be vaccinated.

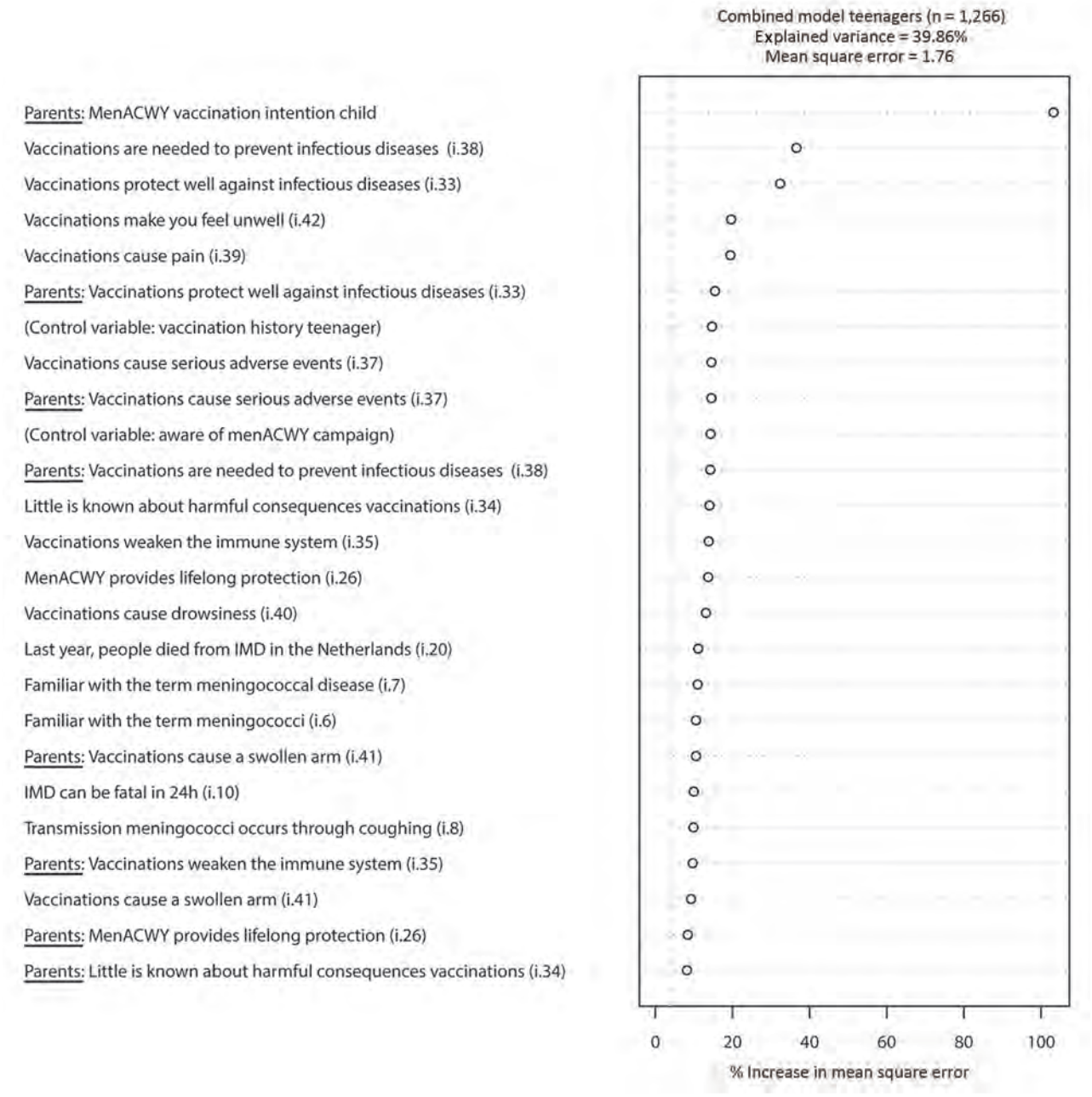


**Figure 3.** Variable importance ranking among teenagers (combined model) in study of vaccination intent regarding IMD caused by *Neisseria meningitidis* strain W135, the Netherlands, 2018–2019. The 25 strongest predictors (i.e., knowledge and belief items [Table] and control variables) are ranked top to bottom, based on their ability to predict meningococcal conjugate (MenACWY) vaccination intention among teenagers with a parent in the sample. This model includes both the knowledge and beliefs (Table) of teenagers, as well as the knowledge, beliefs, and MenACWY vaccination intention of their parents and the control variables from both groups as independent variables. Control variables are age, sex, education, income, region, social class, region of residence, vaccination record of the teenager, whether the respondent was aware of the MenACWY vaccination campaign, and whether teenagers and their parents were part of the first MenACWY vaccination target group (cohorts 2004–2005) or the second MenACWY vaccination target group (cohorts 2001–2003). IMD, invasive meningococcal disease.

Although our study showed that MenACWY vaccination intentions among teenagers and their parents were relatively high, which is also reflected in the (preliminary) MenACWY vaccination uptake of 84% among teenagers (*35*), our study also revealed knowledge gaps and misconceptions concerning IMD, the MenACWY vaccination, and vaccinations in general. We observed differences in familiarity with various terms used to indicate IMD. Although the respondents were generally familiar with Dutch lay terms for the medical conditions caused by meningococci, few were familiar with the scientific terms for meningococci and meningococcal disease, despite the fact that these latter terms were mainly used in the communication materials. Furthermore, we found misbeliefs about the safety of vaccines. For example, we found a relatively strong agreement in our study population for the misbelief that vaccines annually cause the death of several children in the Netherlands. Nevertheless, we did find that teenagers and parents generally believed that IMD is a serious and contagious disease and that vaccinations are effective, safe, and needed.

Our results additionally show which specific misbeliefs and knowledge gaps might be prioritized to increase vaccination willingness among teenagers and parents. Teenagers and parents in our study who thought that vaccinations do not offer good protection against infectious diseases and that vaccinations are not necessary to prevent infectious diseases were less willing to accept MenACWY vaccination than were those who did not harbor these beliefs. In addition, vaccination intentions were lower among parents who believed that little is known about the possible harmful consequences of vaccination, that vaccinations weaken the immune system, and that vaccination can lead to serious adverse events. These beliefs about vaccinations in general surpassed all other knowledge and beliefs in their ability to predict MenACWY vaccination intentions. Previous studies have also found an influence of beliefs about the safety and effectiveness of vaccines on meningococcal vaccination decisions, both with regard to vaccines in general and with regard to the specific vaccine (*9*–*11*).

Of note, we did not find a major role for knowledge and beliefs associated with the severity of IMD in the variation of vaccination intentions, although previous research demonstrated that severity was an important factor in decisions for vaccination against IMD (*4*,*9*,*11*). One possible explanation for this finding is that the severity of IMD is a reason for persons to get vaccinated but does not explain why they do not intend to get vaccinated (*9*,*11*). Those persons, whose intention to get vaccinated is lower than that of most persons, provide variance in the dependent variable (MenACWY vaccination intention), and this variance is best explained by knowledge and beliefs about vaccinations in general.

Our results further show that parents were more willing to have their teenagers vaccinated than were the teenagers themselves and that parents were somewhat more knowledgeable about IMD and the MenACWY vaccination. It has been argued that teenagers are less knowledgeable about health issues than adults because, among other things, teenagers have had less contact with health issues and the healthcare system (*36*,*37*). Similarly, teenagers are likely to have limited (direct or indirect) experience with IMD, whereas their parents are more likely to recall the 1999–2002 outbreak of IMD in the Netherlands, caused by group C meningococci (*38*).

The lower vaccination intentions, knowledge gaps, and misbeliefs among teenagers might suggest that, to achieve high vaccine uptake during emerging outbreaks, public health authorities should focus on risk and benefits communication about vaccine-preventable diseases and vaccines for teenagers. However, our results also indicate that teenagers' willingness to adopt vaccination is most strongly predicted by their parents' willingness to have their child vaccinated. In this light, we need to consider whether intensifying the communication for teenagers would indeed be of much help for increasing their vaccine uptake. More effective might be filling the knowledge gaps and debunking misbeliefs that underlie parental vaccination intentions. Nevertheless, the observed predictive ability of parental vaccination intention does not necessarily imply that parents decide whether their teenager should be vaccinated. It probably also reflects the commonalities in knowledge, beliefs, and norms in social groups or networks (*39*).

Our study has some limitations. First, questions from our survey were developed specifically for this population and disease and are therefore not directly applicable to study knowledge and beliefs in different population or disease contexts. Nevertheless, we believe that gaining these insights about specific knowledge and beliefs that influence vaccination decisions can provide more valuable input for communication strategies than can survey studies that assess perceptions of risk with more general constructs. Second, our study focused solely on knowledge and beliefs and their role in vaccination intentions. We did not include in our research other predictors of health behavior (e.g., the influence of subjective norm perceptions and self-efficacy

perceptions [*20*]). Last, although our study population was sampled to be representative of the larger population and the response rate was relatively high, because participation was voluntary, the final selection of participants might include more persons with a specific interest in the topic.

For future communications accompanying vaccination campaigns combating outbreaks, we recommend concentrating on filling knowledge gaps and addressing specific misbeliefs about the effectiveness and safety of vaccines. In addition, communicators should pay attention to the wording of the messages, which should ideally correspond to the lay vocabulary. As for teenagers, the strongest predictor of their own willingness to be vaccinated was their parents' vaccination intention. We therefore suggest that parents remain a target group in communications about vaccination of teenagers.

### Acknowledgments

We thank all respondents for their participation in our study.

This research was funded by the RIVM Strategic Program (project NO PANIC!, project no. S/123003).

### About the Author

Ms. de Vries is a PhD candidate at the National Institute for Public Health and the Environment (RIVM) in the Netherlands. Her academic background is in sociology and global health, and her PhD study focuses on the analysis of public perceptions of health risks during public health crises.

### References

1. Knol MJ, Ruijs WL, Antonise-Kamp L, de Melker HE, van der Ende A. Implementation of MenACWY vaccination because of ongoing increase in serogroup W invasive meningococcal disease, the Netherlands, 2018. Euro Surveill. 2018;23. https://doi.org/10.2807/1560-7917.ES.2018.23.16.18-00158
2. RIVM. Meningokokken [cited 2019 Dec 12]. https://www.rivm.nl/meningokokken
3. Basta NE, Becker AB, Li Q, Nederhoff D. Parental awareness of meningococcal B vaccines and willingness to vaccinate their teens. Vaccine. 2019;37:670–6. https://doi.org/10.1016/j.vaccine.2018.11.078
4. Dubé E, Gagnon D, Hamel D, Belley S, Gagné H, Boulianne N, et al. Parents' and adolescents' willingness to be vaccinated against serogroup B meningococcal disease during a mass vaccination in Saguenay-Lac-St-Jean (Quebec). Can J Infect Dis Med Microbiol. 2015;26:163–7. https://doi.org/10.1155/2015/732464
5. Landowska K, Waller J, Bedford H, Rockliffe L, Forster AS. Influences on university students' intention to receive recommended vaccines: a cross-sectional survey. BMJ Open. 2017;7:e016544. https://doi.org/10.1136/bmjopen-2017-016544
6. Paul B, Watson JY, Kim Chenery. Meningococcal B. Tell me everything you know and everything you don't know. New Zealanders' decision making regarding an immunisation programme. N Z Med J. 2007;120:U2751. PMID: 17972971
7. Timmermans DR, Henneman L, Hirasimg RA, van der Wal G. Parents' perceived vulnerability and perceived control in preventing meningococcal C infection: a large-scale interview study about vaccination. BMC Public Health. 2008;8:45. https://doi.org/10.1186/1471-2458-8-45
8. Timmermans DR, Henneman L, Hirasing RA, van der Wal G. Attitudes and risk perception of parents of different ethnic backgrounds regarding meningococcal C vaccination. Vaccine. 2005;23:3329–35. https://doi.org/10.1016/j.vaccine.2005.01.075
9. Breakwell L, Vogt TM, Fleming D, Ferris M, Briere E, Cohn A, et al. Understanding factors affecting University A students' decision to receive an unlicensed serogroup B meningococcal vaccine. J Adolesc Health. 2016;59:457–64. https://doi.org/10.1016/j.jadohealth.2016.06.004
10. Blagden S, Seddon D, Hungerford D, Stanistreet D. Uptake of a new meningitis vaccination programme amongst first-year undergraduate students in the United Kingdom: a cross-sectional study. PLoS One. 2017;12:e0181817. https://doi.org/10.1371/journal.pone.0181817
11. Le Ngoc Tho S, Ader F, Ferry T, Floret D, Arnal M, Fargeas S, et al. Vaccination against serogroup B *Neisseria meningitidis*: perceptions and attitudes of parents. Vaccine. 2015;33:3463–70. https://doi.org/10.1016/j.vaccine.2015.05.073
12. Trayner KM, Anderson N, Cameron JC. A mixed-methods study to identify factors associated with MenACWY vaccine uptake, barriers and motivations towards vaccination among undergraduate students. Health Educ J. 2019;78:189–202. https://doi.org/10.1177/0017896918796049
13. Larson HJ, Cooper LZ, Eskola J, Katz SL, Ratzan S. Addressing the vaccine confidence gap. Lancet. 2011;378:526–35. https://doi.org/10.1016/S0140-6736(11)60678-8
14. Wang LD-L, Lam WWT, Fielding R. Determinants of human papillomavirus vaccination uptake among adolescent girls: a theory-based longitudinal study among Hong Kong Chinese parents. Prev Med. 2017;102:24–30. https://doi.org/10.1016/j.ypmed.2017.06.021
15. Hirth JM, Batuuka DN, Gross TT, Cofie L, Berenson AB. Human papillomavirus vaccine motivators and barriers among community college students: considerations for development of a successful vaccination program. Vaccine. 2018;36:1032–7. https://doi.org/10.1016/j.vaccine.2018.01.037
16. Ling M, Kothe EJ, Mullan BA. Predicting intention to receive a seasonal influenza vaccination using protection motivation theory. Soc Sci Med. 2019;233:87–92. https://doi.org/10.1016/j.socscimed.2019.06.002
17. Camerini A-L, Diviani N, Fadda M, Schulz PJ. Using protection motivation theory to predict intention to adhere to official MMR vaccination recommendations in Switzerland. SSM Popul Health. 2018;7:005–5.
18. Scherr CL, Jensen JD, Christy K. Dispositional pandemic worry and the health belief model: promoting vaccination during pandemic events. J Public Health (Oxf). 2017;39:e242–50.
19. Wagner AL, Boulton ML, Sun X, Mukherjee B, Huang Z, Harmsen IA, et al. Perceptions of measles, pneumonia, and meningitis vaccines among caregivers in Shanghai, China, and the health belief model: a cross-sectional study. BMC Pediatr. 2017;17:143. https://doi.org/10.1186/s12887-017-0900-2
20. Fishbein M, Ajzen I. Predicting and changing behavior: the reasoned action approach. New York: Psychology Press; 2010.

21. Morgan MG. Risk communication: A mental models approach: Cambridge (UK): Cambridge University Press; 2002.
22. Claassen L, Bostrom A, Timmermans DR. Focal points for improving communications about electromagnetic fields and health: a mental models approach. J Risk Res. 2016;19:246–69. https://doi.org/10.1080/13669877.2014.961519
23. Galada HC, Gurian PL, Corella-Barud V, Pérez FG, Velázquez-Angulo G, Flores S, et al. Applying the mental models framework to carbon monoxide risk in northern Mexico. Rev Panam Salud Publica. 2009;25:242–53. https://doi.org/10.1590/S1020-49892009000300008
24. Wagner K. Mental models of flash floods and landslides. Risk Anal. 2007;27:671–82. https://doi.org/10.1111/j.1539-6924.2007.00916.x
25. Zaksek M, Arvai JL. Toward improved communication about wildland fire: mental models research to identify information needs for natural resource management. Risk Anal. 2004;24:1503–14. https://doi.org/10.1111/j.0272-4332.2004.00545.x
26. Southwell BG, Ray SE, Vazquez NN, Ligorria T, Kelly BJ. A mental models approach to assessing public understanding of Zika virus, Guatemala. Emerg Infect Dis. 2018;24:938–9. https://doi.org/10.3201/eid2405.171570
27. Downs JS, de Bruin WB, Fischhoff B. Parents' vaccination comprehension and decisions. Vaccine. 2008;26:1595–607. https://doi.org/10.1016/j.vaccine.2008.01.011
28. Bostrom A. Vaccine risk communication: lessons from risk perception, decision making and environmental risk communication research. Risk. 1997;8:173.
29. Bruine de Bruin W, Bostrom A. Assessing what to address in science communication. Proc Natl Acad Sci U S A. 2013;110(Suppl 3):14062–8. https://doi.org/10.1073/pnas.1212729110
30. Foundation Vaccine-Free. Stichting Vaccinvrij [cited 2018 Aug 10]. https://stichtingvaccinvrij.nl
31. Dutch Association Vaccine Critical. Nederlandse Vereniging Kritisch Prikken [cited 2018 Aug 10]. https://www.nvkp.nl
32. Breiman L. Random forests. Mach Learn. 2001;45:5–32. https://doi.org/10.1023/A:1010933404324
33. Liaw A, Wiener M. Classification and regression by randomForest. R News. 2002;2:18–22.
34. Centraal Bureau voor de Statistiek. Standaard Onderwijsindeling 2006 [cited 2020 Apr 28]. https://www.cbs.nl/nl-nl/onze-diensten/methoden/classificaties/onderwijs-en-beroepen/standaard-onderwijsindeling--soi--/standaard-onderwijsindeling-2006
35. Baboe Kalpoe S, Benschop KSM, van Benthem BHB, Berbers GAM, van Binnendijk R, Bodewes R, et al. The National Immunisation Programme in the Netherlands: surveillance and developments in 2018–2019 [cited 2020 Apr 24]. https://www.rivm.nl/en/bibcite/reference/327621
36. Newacheck PW, Wong ST, Galbraith AA, Hung Y-Y. Adolescent health care expenditures: a descriptive profile. J Adolesc Health. 2003;32(Suppl):3–11. https://doi.org/10.1016/S1054-139X(03)00064-8
37. Manganello JA. Health literacy and adolescents: a framework and agenda for future research. Health Educ Res. 2008;23:840–7. https://doi.org/10.1093/her/cym069
38. Bijlsma MW, Bekker V, Brouwer MC, Spanjaard L, van de Beek D, van der Ende A. Epidemiology of invasive meningococcal disease in the Netherlands, 1960-2012: an analysis of national surveillance data. Lancet Infect Dis. 2014;14:805–12. https://doi.org/10.1016/S1473-3099(14)70806-0
39. Brunson EK. The impact of social networks on parents' vaccination decisions. Pediatrics. 2013;131:e1397–404. https://doi.org/10.1542/peds.2012-2452

Address for correspondence: Marion de Vries, National Institute for Public Health and the Environment (RIVM), PO Box 1, 3720 BA Bilthoven, The Netherlands; email: marion.de.vries@rivm.nl

# Risk for Coccidioidomycosis among Hispanic Farm Workers, California, USA, 2018

Stephen A. McCurdy, Catherine Portillo-Silva, Carol L. Sipan, Heejung Bang, Kirt W. Emery

To determine occupational risk factors for coccidioidomycosis among adult Hispanic outdoor agricultural workers in California, USA, we conducted a case–control study of workers seen at the Kern County medical facility and referred to the public health laboratory for coccidioidomycosis serologic testing. Participants completed an interviewer-administered health and work questionnaire. Among 203 participants (110 case-patients with positive and 93 controls with negative serologic results), approximately half were women, and more than three quarters were born in Mexico. Associated with coccidioidomycosis were self-reported dust exposure and work with root and bulb vegetable crops. A protective factor was leaf removal, an activity associated with grape cultivation. We conclude that subjective dust exposure and work with root and bulb vegetable crops are associated with increased risk for coccidioidomycosis among Hispanic farm workers. The agricultural industry should evaluate and promote dust-reduction measures, including wetting soil and freshly harvested products.

Coccidioidomycosis (Valley fever or San Joaquin Valley fever) is a pulmonary and systemic infection that results from respiratory exposure to aerosolized arthroconidia spores of soil-dwelling species of *Coccidioides* fungi (*1*). *Coccidioides* fungi and coccidioidomycosis are strongly associated with the semiarid climate of the Lower Sonoran life zone of the southwestern United States and parts of Mexico, Central America, and South America. Most US cases occur in Arizona and California. However, the fungus and locally acquired cases have recently been reported as far north as Washington state, potentially related to changes in climate and land use patterns (*2*,*3*). In California, the species most often implicated in human infection is *C. immitis*, whereas in Arizona it is *C. posadasii* (*2*,*3*).

After an incubation period of ≈1–3 weeks, most infected persons experience few or mild symptoms, and the condition usually resolves within weeks or months, often unrecognized (*4*,*5*). Approximately 40% of infected persons experience an influenza-like illness with cough, fever, and fatigue that typically resolves without treatment. Approximately 1% of cases involve dissemination to skin, bone, meninges, and other tissues (*6*); patients with disseminated disease require long-term antifungal therapy and may die (*7*). Risk factors for disseminated disease include male sex, age >60 years, pregnancy, immunocompromise, and African and Filipino ancestry (*8*).

Case identification is based on clinically compatible illness with confirmatory laboratory evidence or skin-test conversion (*9*). Local health departments may find it impractical to obtain clinical information and thus may identify cases solely on the basis of laboratory results (*4*). Because most cases are subclinical, public health surveillance substantially underestimates infection risk. McCotter et al. estimated that the true number of cases is ≈4–6-fold greater than that captured by public health surveillance (*2*).

Residence in or visits to coccidioidomycosis-endemic areas may lead to exposure and infection. The largest outbreaks have been associated with natural phenomena. A December 1977 dust storm in California's San Joaquin Valley (an area of high coccidioidomycosis endemicity, from which the disease derives its common name) resulted in a ≥10-fold increase in incidence in 15 of the state's 58 counties (*1*,*10*). The 1994 Northridge, California, earthquake was responsible for 203 outbreak-associated cases, including 3 deaths (*11*). Occupational risk has been associated with soil-disruptive activity involving archeologists (*12*), film crews (*13*), solar power farm construction workers (*14*,*15*), roadway and construction workers

Author affiliations: University of California, Davis, California, USA (S.A. McCurdy, H. Bang); University of California, Merced, California, USA (C. Portillo-Silva, C.L. Sipan); Kern County Public Health Services Department, Bakersfield, California, USA (K.W. Emery)

DOI: https://doi.org/10.3201/eid2607.200024

(*16*,*17*), and agricultural workers (*18*). Prison inmates in the San Joaquin Valley are also at increased risk, leading to a policy of excluding inmates with nonreactive spherulin-based coccidioidomycosis skin tests from these facilities (*19*).

In recent decades, coccidioidomycosis in California has increased markedly. Since individual case reporting began in 1995, the 2 highest years on record have been 2017 (7,658 cases) and 2018 (7,515 cases) (*4*). During 2000–2013, an average of 78 deaths/year were attributed to coccidioidomycosis in California (*20*), and during 2000–2011, ≈25,000 hospitalizations were reported (*21*). The historically highest incidence among California counties has been in Kern County (2,937 cases in 2018, 323.2 cases/100,000 persons/year), and several factors may contribute. First, the county is situated within the highly coccidioidomycosis-endemic San Joaquin Valley. Second, Kern is the most productive agricultural county in the nation (*22*), so soil disruption and exposure to agricultural dust are common. Third, Kern County leads the state by having had ≈116,000 hired farm workers in 2014 (*23*). Although Hispanic origin has not been shown to be an independent risk factor for coccidioidomycosis (*8*), and to our knowledge no outbreaks in this group have been reported, ≈95% of hired crop workers in California are Hispanic (*24*) and thus represent a large occupational risk group.

Despite longstanding recognition of agricultural work as an occupational risk factor for coccidioidomycosis, little research to identify specific high-risk agricultural exposures, such as crops or tasks, has been conducted. We therefore conducted a case–control study of coccidioidomycosis in Hispanic farm workers in Kern County, California, focused on identifying occupational risks. We tested the hypothesis that subjective dust exposure is related to risk for infection and conducted exploratory analyses to identify associated crops and tasks.

## Materials and Methods

### Study Design

For this case-control study, we used data collected from June 1, 2016, through August 31, 2018. During this period, the Kern County Public Health Services Department provided a list, approximately monthly, of persons who had undergone serologic testing for coccidioidomycosis at the Kern County Public Health Laboratory after referral from Kern Medical, the county public healthcare organization where local Hispanic agricultural workers are likely to seek care. Kern Medical comprises a 222-bed teaching hospital and clinics providing primary and specialty care for an ethnically diverse population. Kern Medical has longstanding expertise with coccidioidomycosis and hosts the Valley Fever Institute (*25*) to promote education, treatment, and research on coccidioidomycosis.

### Study Sample

To assess candidacy for our study, we made up to 10 attempts to contact by telephone all persons referred from Kern Medical for coccidioidomycosis serologic testing who were ≥18 years of age and had ≥1 positive serologic test result (potential cases) and a random sample of persons with all negative serologic test results (potential controls). We invited to complete a full in-person interview those screened persons with self-declared Hispanic or Latino origin who had worked in outdoor agriculture in Kern County for ≥1 month in the preceding year, were not incarcerated, and were able to provide informed consent in Spanish or English. We initially excluded women who had been pregnant in the past year because Kern Medical uses coccidioidomycosis testing for screening of pregnant women rather than for diagnosis of suspected illness. However, because of low enrollment, we removed the pregnancy exclusion and considered as study candidates all persons who had undergone coccidioidomycosis serologic testing after referral from Kern Medical. Participants received a gift certificate for $15 in appreciation for their time. The University of California Davis Institutional Review Board approved and monitored the study (IRBNet ID 747508).

### Definitions

Serologic evaluation comprised 3 tests: immunodiffusion for IgM, immunodiffusion for IgG, and complement fixation (considered positive for dilutions ≥1:2). Case-patients were defined as persons with ≥1 positive serologic test result. Control status was assigned to persons with negative results for all 3 serologic tests.

### Questionnaire Development and Administration

We reviewed available survey instruments from previous outbreak investigations in Kern and San Joaquin Counties (*26*) and incorporated relevant material into our questionnaire. Colleagues in the California Department of Public Health and the Centers for Disease Control and Prevention reviewed questionnaire drafts. We pilot tested the questionnaire with a sample of 20 Hispanic agricultural workers in Kern County and excluded those persons from this report. The final questionnaire addressed demographic characteristics; health history; and agricultural work history with job start and end dates for the preceding

year, weekly hours, frequency of outdoor work, crop or commodity, tasks, subjective dust exposure, and frequency of use in dusty conditions for personal respiratory protective measures and soil wetting. We separated jobs by change in location and task. After obtaining informed consent, trained study staff fluent in Spanish and English and blinded to participant case status administered the questionnaire in each participant's home or in the study office.

### Exposure Assessment

Participants whose jobs involved a specific crop or task were considered to have been exposed to that crop or task; we added the total weeks of exposure over all jobs in the preceding year. We combined crops into 3 categories based on likely exposure to potentially infectious soil dusts: root and bulb vegetables growing underground (beets, carrots, garlic, onions, radishes, sweet potatoes), near-ground crops (blueberries, chili peppers, cotton, grapes, kale, lettuce, spinach, strawberries, tomatoes, watermelons), and tree crops (almonds, apples, apricots, cherries, kiwis, oranges and Mandarin oranges, pomegranates, pistachios). We also examined individual crops and tasks reported by ≥9% of participants. Dust exposure was based on response to the question: "How often did/does your work at this job generate a lot of dust?" Responses were "never/sometimes/half of the time/most of the time/always." For final analyses, we dichotomized these responses as "never/sometimes" versus "half of the time/most of the time/always." These responses were also used for mask use ("When working in dusty conditions, how often did/do you wear a mask?") and frequency of soil wetting ("When working in dusty conditions, how often is/was the soil kept wet to reduce dust?").

### Data Management and Analysis

Data from the paper questionnaires were double-entered into a computer database; discrepancies were checked against the paper questionnaire and corrected. Subsequently, a 20% sample of randomly selected questionnaires was checked against the digital database; 6 entry errors among 223 variables per questionnaire were identified and corrected (error rate <0.15%).

We analyzed data by using Stata 15.1 (https://www.stata.com). We summarized distributions of continuous variables with either means and SDs (for approximately bell-shaped distributions) or medians and interquartile ranges (IQRs). We summarized categorical variables as percentages within each category. For group comparisons, we used the Fisher exact test for nonordinal categorical variables and the Kruskal-Wallis test for continuous and ordinal categorical variables.

We initially examined 2-dimensional tables of case status by selected occupational and demographic characteristics and used the Stata logistic command to derive unadjusted odds ratios (ORs), with subsequent adjustments for age and sex. We assessed robustness by comparing adjusted odds ratios from the entire sample with those derived among men and women separately, after removing from analysis women reporting a pregnancy in the preceding year and persons reporting no symptoms.

## Results

### Study Sample and Demographic Characteristics:

We screened 1,803 (51%) of 3,509 persons selected from the Kern County Public Health Services Department periodic lists of coccidioidomycosis testing referrals. Reasons for not screening were wrong numbers or failure to connect after 10 attempts (≈75%), language or communication difficulty (≈15%), or the person declining to be screened (≈10%). Of those screened, 380 (21%) persons were eligible; of those, 215 (57%) completed an interview. Participation was higher for case-patients (70%) than for controls (48%; p = 0.0001). Of those interviewed, 203 (110 case-patients and 93 controls) were subsequently confirmed as eligible and included in our sample (Table 1). The major reasons for postinterview disqualification were lack of qualifying agricultural work and indeterminate serologic test results. Median time from testing to interview was 39 (IQR 25–55) days.

Women represented a greater proportion of controls (57%) than of case-patients (42%); p = 0.04). Female controls were also significantly younger than male controls and case-patients of each sex (p = 0.03). More than three quarters of participants were born in Mexico, and ≈85% completed the interview in Spanish. Median time living in Kern County was >10 years. Median annual family income was in the $15,001–$20,000 category, and most participants had completed ≤9 years of formal education. Pregnancy within the past year was less frequent among female case-patients (27%) than female controls (74%; p = 0.0001).

### Occupational Characteristics

Case-patients and controls were comparable for number of jobs (median 3), weeks worked in outdoor agriculture in the preceding year (median 30),

and weekly work hours in the most recent job (median 48). A significantly higher percentage of case-patients (21%) than controls (9%) worked with root and bulb vegetable crops (p = 0.02; Table 2). The most frequently worked crop was grapes, worked less frequently by case-patients (58%) than controls (72%; p = 0.06). Case-patients and controls were comparable with respect to agricultural tasks, with the exception of leaf removal, which was performed significantly less frequently by case-patients (23%) than controls (40%; p = 0.01).

Always working outdoors was reported by 94% of participants. With respect to the most recent job, significantly more case-patients (71%) than controls (56%) reported dust exposure for half of the time or more (p = 0.02), whereas mask use and soil wetting in dusty conditions on a half-time or more basis were comparable among case-patients and controls, reported by approximately half of participants. Neither mask use nor soil wetting were independently associated with self-reported dust exposure. Among 117 persons reporting any mask use, 102 (87%) reported wearing a bandana, 7 (6%) using an N95 respirator, and 1 (1%) wearing a half-face mask. Women were markedly more likely than men to report mask use (77% vs. 27%; p = 0.0001).

### Associations between Occupational Exposures and Coccidioidomycosis

Age- and sex-adjusted ORs for having coccidioidomycosis (Table 2) were significantly elevated for self-reported dust exposure (OR 1.9, 95% CI 1.0–3.5) and work with root and bulb vegetables (OR 3.0, 95% CI 1.2–7.1). Exploratory analysis of hours worked with root and bulb vegetable crops did not show a dose response, although 95% CIs were wide. For work with root and bulb vegetables, the OR for work with carrots was also elevated (OR 2.9, 95% CI 1.0–8.6). ORs were reduced for those who worked with grapes (0.6, 95% CI 0.3–1.0) and leaf removal (OR 0.4, 95% CI 0.2–0.8). Mask use and soil wetting in dusty conditions were associated with modest and statistically nonsignificant reductions in ORs. Patterns were similar for men and women separately and after excluding women pregnant in the prior year (12 cases, 39 controls) and persons reporting no clinical features of coccidioidomycosis (4 cases, 16 controls).

### Clinical Characteristics

Case-patients were significantly more likely than controls to report clinical features associated with coccidioidomycosis (Table 3); adjusted ORs ranged from 2.6 (weight loss) to 4.3 (shortness of breath). The most frequent signs/symptoms among all participants were fatigue and cough. Case-patients reported significantly greater median weight loss (10 vs. 0 lb; p = 0.003) and lost workdays (18.5 vs. 0 d; p = 0.0001) than did controls. Case-patients had >2-fold increased odds of being hospitalized.

**Table 1.** Selected demographic and health characteristics of 203 Hispanic farm workers evaluated for coccidioidomycosis, Kern County, California, USA, 2016–2018*

| Characteristic | Case-patients, n = 110 | Controls, n = 93 |
|---|---|---|
| Sex, no. (%) | | |
| F | 46 (42) | 53 (57) |
| M | 64 (58) | 40 (43) |
| Age, y | | |
| Median | | |
| M | 38.7 | 42.0 |
| F | 38.1 | 32.7 |
| IQR | | |
| M | 29.6–47.8 | 29.0–50.5 |
| F | 28.5–46.3 | 27.0–39.5 |
| Country of birth, no. (%) | | |
| Mexico | 83 (76) | 74 (80) |
| United States | 16 (15) | 16 (17) |
| Central America | 11 (10) | 3 (3) |
| Language used during interview, no. (%) | | |
| Spanish | 94 (85) | 80 (86) |
| English | 16 (15) | 13 (14) |
| Years lived in United States | | |
| Median | | |
| M | 18.7 | 23.2 |
| F | 18.0 | 16.6 |
| IQR | | |
| M | 13.2–27.4 | 14.8–32.7 |
| F | 12.5–23.3 | 9.6–20.3 |
| Years lived in Kern County | | |
| Median | | |
| M | 11.2 | 16.8 |
| F | 14.0 | 11.6 |
| IQR | | |
| M | 5.6–21.5 | 10.7–26.2 |
| F | 7.2–14.9 | 4.7–17.0 |
| Years of education | | |
| Median | 7.5 | 9.0 |
| IQR | 6–12 | 6–12 |
| Annual family income, US $, no. (%) | | |
| ≤9,000 | 17 (15) | 11 (12) |
| 9,001–12,000 | 15 (14) | 10 (11) |
| 12,001–15,000 | 13 (12) | 17 (18) |
| 15,001–20,000 | 12 (11) | 15 (16) |
| ≥20,001 | 24 (22) | 20 (22) |
| Not stated | 29 (26) | 20 (22) |
| Smoker status, no. (%) | | |
| Never | 80 (73) | 65 (70) |
| Former | 27 (25) | 22 (24) |
| Current | 3 (3) | 6 (6) |
| Selected health conditions, no. (%) | | |
| Diabetes | 20 (18) | 17 (18) |
| Asthma | 5 (5) | 7 (8) |
| Other lung conditions | 31 (28) | 17 (18) |
| Cancer | 5 (5) | 7 (8) |
| Pregnancy† | 12 (27) | 39 (74) |

*IQR, interquartile range.
†Percentage calculations based on women only.

## Discussion

We report the results of a case–control study that examined potential occupational risk factors for coccidioidomycosis among Hispanic agricultural workers in Kern County, California. Self-reported dust exposure was significantly associated with a near doubling of the odds of coccidioidomycosis, and odds were increased a significant 3-fold for those who worked with root and bulb vegetable crops. Leaf removal, a task almost uniquely limited to grape cultivation, was associated with a significant 60% reduction in odds. Mask use (chiefly cloth bandanas) and soil wetting was associated with modest and statistically nonsignificant reductions of odds of coccidioidomycosis. The clinical findings illustrate a heavy health burden. The most prevalent symptom was fatigue or weakness, reported by ≈80% of cases and associated with a median 18.5 days of lost work time. Those lost days accounted for ≈10% of the 213 average annual workdays for California farm workers in 2015–2016 (*24*) and represent an income loss few can afford.

The association with self-reported dust exposure is consistent with the mechanism of exposure, whereby aerosolized *Coccidioides* spores are inspired and establish infection in the lung. Thus, time spent outdoors, where wind may carry dust and spores from on site or afar, is an environmental risk for the general population in coccidioidomycosis-endemic areas and especially for persons whose work is outdoors or involves soil disruption (*27*). The largest occupational risk group is agricultural workers. In 2014, there were an estimated 829,300 hired agricultural workers in California (*23*); ≈95% were Hispanic (*24*). Thus, Kern County and the San Joaquin Valley represent the confluence of multiple factors contributing to the public health effects of coccidioidomycosis: environmental conditions favorable to growth and aerosolization of *Coccidioides* spores, predominance of agriculture with concomitant soil disruption in an outdoor work setting, and a large population of occupationally exposed persons.

With this study, we aimed to identify specific agricultural exposures and practices affecting risk. We observed a 3-fold increase in the odds of coccidioidomycosis among root and bulb vegetable crop workers, although a dose-response phenomenon

**Table 2.** Selected occupational exposures and associations with coccidioidomycosis among 203 Hispanic farm workers, Kern County, California, USA, 2016–2018

| Characteristic | Cases, no. (%), n = 110 | Controls, no. (%), n = 93 | Adjusted odds ratio (95% CI)* |
|---|---|---|---|
| Self-reported dust exposure for most recent job | | | |
| Never or sometimes | 32 (29) | 41 (44) | Reference |
| Half time or more | 78 (71) | 52 (56) | 1.9 (1.0–3.5) |
| Work in crop category in past year†‡ | | | |
| Root and bulb vegetable crops†‡ | 23 (21) | 8 (9) | 3.0 (1.2–7.1) |
| Near-ground crops†§ | 76 (69) | 76 (81) | 0.5 (0.3– 1.0) |
| Tree crops†¶ | 60 (55) | 41 (44) | 1.4 (0.8–2.5) |
| Work with specified crop in past year†# | | | |
| Grapes | 64 (58) | 67 (72) | 0.6 (0.3–1.0) |
| Almonds | 24 (22) | 17 (18) | 1.1 (0.5– 2.3) |
| Mandarin oranges | 23 (21) | 19 (20) | 1.1 (0.5– 2.1) |
| Carrots | 14 (13) | 5 (5) | 2.9 (1.0. 8.6) |
| Tasks performed in past year†** | | | |
| Harvest | 82 (75) | 68 (73) | 1.3 (0.7– 2.5) |
| Pruning | 40 (36) | 39 (42) | 0.7 (0.4– 1.3) |
| Packing (outdoor) | 39 (35) | 33 (35) | 1.2 (0.6– 2.1) |
| Leaf removal | 25 (23) | 37 (40) | 0.4 (0.2– 0.8) |
| Weeding | 14 (13) | 10 (11) | 1.3 (0.5– 3.1) |
| Irrigation | 15 (14) | 7 (8) | 1.6 (0.6– 4.2) |
| Mask use for most recent job | | | |
| Never or sometimes | 58 (53) | 40 (43) | Reference |
| Half the time or more | 51 (47) | 53 (57) | 0.9 (0.5– 1.7) |
| Soil wetting in dusty conditions for most recent job | | | |
| Never or sometimes | 63 (58) | 48 (52) | Reference |
| Half the time or more | 46 (42) | 45 (48) | 0.8 (0.4– 1.3) |

*Adjusted for age and sex.
†Categories are not mutually exclusive; reference group is all participants not working in specified category.
‡Root and bulb vegetables growing underground: beets, carrots, garlic, onions, radishes, sweet potatoes.
§Near-ground crops: cotton and fruits and vegetables growing above ground and near the surface, including blueberries, chili peppers, grapes, kale, lettuce, spinach, strawberries, tomatoes, watermelon.
¶Tree crops: almonds, apples, apricots, cherries, kiwi, oranges and Mandarin oranges, pomegranates, pistachios.
#Limited to crops reported by ≥9% of participants; crops are not mutually exclusive.
**Limited to tasks reported by ≥9% of participants; tasks are not mutually exclusive.

**Table 3.** Reported clinical characteristics among 203 Hispanic farm workers evaluated for coccidioidomycosis, Kern County, California, USA, 2016–2018

| Clinical characteristic | Cases, no. (%), n = 110 | Controls, no. (%), n = 93 | Adjusted odds ratio (95% CI)* |
|---|---|---|---|
| ≥1 clinical characteristic | 100 (91) | 72 (77) | 4.4 (1.4–14.2) |
| Fatigue or weakness | 91 (83) | 52 (56) | 3.7 (1.9–7.2) |
| Cough | 74 (67) | 38 (41) | 3.0 (1.6–5.3) |
| Night sweats | 73 (66) | 34 (37) | 3.2 (1.8– 5.8) |
| Weight loss† | 73 (66) | 40 (43) | 2.6 (1.4–4.7) |
| Fever | 72 (65) | 29 (31) | 4.0 (2.2–7.4) |
| Chest pain | 71 (65) | 29 (31) | 3.8 (2.1– 7.0) |
| Shortness of breath | 66 (60) | 25 (27) | 4.3 (2.3–7.9) |
| Difficulty breathing | 66 (60) | 34 (37) | 2.8 (1.5–4.9) |
| Hospitalized‡ | 52 (47) | 24 (26) | 2.3 (1.2–4.4) |
| Missed work§ | 88 (80) | 45 (48) | 4.0 (2.1–7.7) |

*Adjusted for age and sex.
†Median (interquartile [IQR]) weight loss, in pounds, by case-patients vs. controls 10 (0–18) vs. 0 (0–10); p = 0.003, Kruskal-Wallis test.
‡Median (IQR) nights hospitalized for case-patients vs. controls 0 (0–5) vs. 0 (0–1); p = 0.002, Kruskal-Wallis test.
§Median (IQR) days of work lost by case-patients vs. controls 18.5 (2–48) vs. 0 (0–24); p = 0.0001, Kruskal-Wallis test.

was not evident. The mechanism behind the observed increased risk may relate to dust exposure during cultivation and harvest. Harvest typically is mechanized, but workers may be involved in handling and shaking off surface and subsurface dirt, potentially bearing infectious *Coccidioides* spores, from freshly harvested product as it is prepared for transport and market. Similarly, reduced risk associated with leaf removal and work with grapes may be mediated through less frequent work with other crops and tasks associated with exposure to dust from surface and subsurface dirt.

Mask use and soil wetting showed modest and statistically nonsignificant protective effects. Mask use, chiefly with a pañuelo, a cloth bandana covering the mouth and nose, is primarily reported by women, here and in other studies (*28*). Cloth bandanas are of limited effectiveness for respiratory protection (*29*), and educational campaigns should focus on limiting work under dusty conditions and promoting use of National Institute for Occupational Safety and Health (NIOSH)–approved respirators with particulate filters rated N95, N99, N100, P100, or HEPA when such work is necessary. Unfortunately, compliance may be reduced by the practical challenges of using personal respiratory protection, including discomfort and interference with speed and workflow.

A limitation of this study is low power due to sample size, limiting exploration of confounding as a possible contributor to observed associations. For example, associations between crop or task and disease risk could be confounded by sociodemographic and other factors that may channel susceptible persons to certain crops and work activities. Sample size also affected precision and subgroup analyses, yet we nevertheless found statistically significant associations for subjective dust exposure, work with root and bulb vegetables, and leaf removal and nonsignificant findings in the expected direction of effect for mask use and soil wetting. These findings suggest the need for focused studies looking at dust exposure and disease risk in association with specific crops and activities and efficacy of protective programs.

We originally planned to limit participation to persons referred for *Coccidioides* serologic testing because of clinical indications of disease. However, it was not feasible for the Kern County Public Health Services Department to document clinical features as recommended by the Council of State and Territorial Epidemiologists (*9*), and case identification was based solely on serologic test results. Moreover, women seen for obstetric care at Kern Medical are referred for coccidioidomycosis serologic testing as a screening measure. However, exploratory and sensitivity analyses, in which we examined men and women separately and removed women reporting pregnancy in the preceding year and persons without reported clinical features, did not materially change our findings.

Selection bias may also have affected our results in several ways. First, the sample was limited to persons working in Kern County. Although the study population was demographically similar to published descriptions (*24*) of California Hispanic farm workers, it is possible that our population differed from those in other locales in ways that may affect risk for coccidioidomycosis. Second, the study could not include case-patients who were asymptomatic or did not seek evaluation. Our study sample probably represents persons with more severe cases because all sought medical care from Kern Medical, the county healthcare facility. Moreover, nearly half of the case-patients reported overnight hospitalization. Thus, the epidemiologic patterns observed here may not apply to persons with milder cases that are likely to remain unrecognized. In addition, the Berkson bias (*30*) may

yield observed ORs for agricultural exposures that underestimate true associations (i.e., if agricultural exposures cause pulmonary conditions other than coccidioidomycosis, such that those exposures are more prevalent in controls than they would otherwise be). Third, a low participation rate, especially among controls, may also have introduced selection bias. For example, if healthier control candidates were less likely to participate and had lower exposure levels contributing to their good health, our control sample would be biased toward higher exposures, leading to underestimation of true ORs. Alternatively, if healthier control candidates were more likely to participate and had lower exposure levels contributing to their good health, our control sample would be biased toward lower exposures, leading to overestimation of true ORs.

We were also unable to validate self-reported exposure information and clinical features. Hence, reporting bias may have affected our results, particularly if case-participants suspected that certain exposures might be important and overreported those. However, we are unaware of beliefs regarding coccidioidomycosis in this population that might affect reporting behavior, and we consider reporting bias an unlikely explanation of the observed associations.

On the basis of our findings, we recommend basic research on exposure, to include local soil sampling for *Coccidioides* spp. and area and personal respirable air sampling during harvest and other phases of cultivation, especially for root and bulb vegetable crops where exposure to surface and subsurface dust is likely. Although daunting from a practical standpoint, cohort studies of susceptible persons (i.e., based on nonreactive initial spherulin skin test) would help establish incidence and epidemiologic patterns while including persons contracting subclinical infections. Although the effectiveness of preventive recommendations remains uncertain (*8*), current recommendations (*27*,*31*) for reducing dust exposure, including wetting soil and freshly harvested products, should be followed, especially for persons working with root and bulb vegetable crops. Personal respiratory protection, using NIOSH–approved equipment, should be encouraged. Because masks are more commonly used by women, educational programs should focus on improving acceptance among men and include evaluation of program effectiveness. Programs must also account for factors interfering with education and care that are common among the Hispanic agricultural worker population, including social marginalization associated with language, culture, and legal status and low levels of health insurance (*32*).

**Acknowledgments**

Special thanks to the Kern County farm workers who participated in this study and the Kern County Public Health Services Department.

This work was sponsored by the Centers for Disease Control and Prevention and NIOSH (U01 OH010839) and the Western Center for Agricultural Health and Safety (NIOSH grant U50 OH007550). H.B. was partly supported by the National Institutes of Health (grant UL1 TR001860).

## About the Author

Dr. McCurdy is emeritus professor of public health sciences and internal medicine at the University of California, Davis, School of Medicine. His primary research interest is occupational health among agricultural workers.

## References

1. Pappagianis D, Einstein H. Tempest from Tehachapi takes toll or *Coccidioides* conveyed aloft and afar. West J Med. 1978;129:527–30.
2. McCotter OZ, Benedict K, Engelthaler DM, Komatsu K, Lucas KD, Mohle-Boetani JC, et al. Update on the epidemiology of coccidioidomycosis in the United States. Med Mycol. 2019;57(Suppl_1):S30–40. https://doi.org/10.1093/mmy/myy095
3. Pearson D, Ebisu K, Wu X, Basu R. A review of coccidioidomycosis in California: exploring the intersection of land use, population movement, and climate change. Epidemiol Rev. 2019;41:145–57. https://doi.org/10.1093/epirev/mxz004
4. California Department of Public Health. Epidemiologic summary of coccidioidomycosis in California, 2018 [cited 2019 Nov 19]. https://www.cdph.ca.gov/Programs/CID/DCDC/CDPH%20Document%20Library/CocciEpiSummary2018.pdf
5. McCotter OZ, Chiller TM. Coccidioidomycosis (Valley fever) [cited 2020 Jan 2]. https://wwwnc.cdc.gov/travel/yellowbook/2020/travel-related-infectious-diseases/coccidioidomycosis-valley-fever
6. Freedman M, Jackson BR, McCotter O, Benedict K. Coccidioidomycosis outbreaks, United States and worldwide, 1940–2015. Emerg Infect Dis. 2018;24:417–23. https://doi.org/10.3201/eid2403.170623
7. Galgiani JN, Ampel NM, Blair JE, Catanzaro A, Geertsma F, Hoover SE, et al. 2016 Infectious Diseases Society of America (IDSA) clinical practice guideline for the treatment of coccidioidomycosis. Clin Infect Dis. 2016;63:e112–46. https://doi.org/10.1093/cid/ciw360
8. Brown J, Benedict K, Park BJ, Thompson GR III. Coccidioidomycosis: epidemiology. Clin Epidemiol. 2013;5:185–97.
9. Council of State and Territorial Epidemiologists. Public health reporting and national notification for coccidioidomycosis [cited 2020 Jan 2]. https://cdn.ymaws.com/www.cste.org/resource/resmgr/PS/10-ID-04.pdf
10. Flynn NM, Hoeprich PD, Kawachi MM, Lee KK, Lawrence RM, Goldstein E, et al. An unusual outbreak of windborne coccidioidomycosis. N Engl J Med. 1979;301:358–61. https://doi.org/10.1056/NEJM197908163010705

11. Schneider E, Hajjeh RA, Spiegel RA, Jibson RW, Harp EL, Marshall GA, et al. A coccidioidomycosis outbreak following the Northridge, Calif, earthquake. JAMA. 1997;277:904–8. https://doi.org/10.1001/jama.1997.03540350054033
12. Werner SB, Pappagianis D, Heindl I, Mickel A. An epidemic of coccidioidomycosis among archeology students in northern California. N Engl J Med. 1972;286:507–12. https://doi.org/10.1056/NEJM197203092861003
13. Wilken JA, Marquez P, Terashita D, McNary J, Windham G, Materna B; Centers for Disease Control and Prevention (CDC). Coccidioidomycosis among cast and crew members at an outdoor television filming event—California, 2012. MMWR Morb Mortal Wkly Rep. 2014;63:321–4.
14. Wilken JA, Sondermeyer G, Shusterman D, McNary J, Vugia DJ, McDowell A, et al. Coccidioidomycosis among workers constructing solar power farms, California, USA, 2011–2014. Emerg Infect Dis. 2015;21:1997–2005. https://doi.org/10.3201/eid2111.150129
15. Sondermeyer Cooksey GL, Wilken JA, McNary J, Gilliss D, Shusterman D, Materna BL, et al. Dust exposure and coccidioidomycosis prevention among solar power farm construction workers in California. Am J Public Health. 2017;107:1296–303. https://doi.org/10.2105/AJPH.2017.303820
16. Nicas M. A point-source outbreak of coccidioidomycosis among a highway construction crew. J Occup Environ Hyg. 2018;15:57–62. https://doi.org/10.1080/15459624.2017.1383612
17. Cummings KC, McDowell A, Wheeler C, McNary J, Das R, Vugia DJ, et al. Point-source outbreak of coccidioidomycosis in construction workers. Epidemiol Infect. 2010;138:507–11. https://doi.org/10.1017/S0950268809990999
18. Das R, McNary J, Fitzsimmons K, Dobraca D, Cummings K, Mohle-Boetani J, et al. Occupational coccidioidomycosis in California: outbreak investigation, respirator recommendations, and surveillance findings. J Occup Environ Med. 2012;54:564–71. https://doi.org/10.1097/JOM.0b013e3182480556
19. Wheeler C, Lucas KD, Derado G, McCotter O, Tharratt RS, Chiller T, et al. Risk stratification with coccidioidal skin test to prevent Valley fever among inmates, California, 2015. J Correct Health Care. 2018;24:342–51. https://doi.org/10.1177/1078345818792679
20. Sondermeyer GL, Lee LA, Gilliss D, Vugia DJ. Coccidioidomycosis-associated deaths in California, 2000-2013. Public Health Rep. 2016;131:531–5. https://doi.org/10.1177/0033354916662210
21. Sondermeyer G, Lee L, Gilliss D, Tabnak F, Vugia D. Coccidioidomycosis-associated hospitalizations, California, USA, 2000–2011. Emerg Infect Dis. 2013;19:1590–7. https://doi.org/10.3201/eid1910.130427
22. California Department of Food and Agriculture. California County Agricultural Commissioners' Reports, crop year 2016–2017 [cited 2019 Nov 1]. https://www.cdfa.ca.gov/statistics/pdfs/2017cropyearcactb00.pdf
23. Martin P, Hooker B, Akhtar M, Stockton M. How many workers are employed in California agriculture? Calif Agric. 2016;71:30–4 https://doi.org/10.3733/ca.2016a0011
24. National Agricultural Workers Survey. Data tables 13 and 14 [cited 2019 Sep 21]. https://www.doleta.gov/naws/research/data-tables
25. Valley Fever Institute. Valley fever [cited 2019 Sep 21]. http://valleyfeverinstitute.com
26. Centers for Disease Control and Prevention (CDC). Coccidioidomycosis among persons attending the world championship of model airplane flying—Kern County, California, October 2001. MMWR Morb Mortal Wkly Rep. 2001;50:1106–7.
27. de Perio MA, Materna BL, Sondermeyer Cooksey GL, Vugia DJ, Su CP, Luckhaupt SE, et al. Occupational coccidioidomycosis surveillance and recent outbreaks in California. Med Mycol. 2019;57(Suppl_1):S41–5. https://doi.org/10.1093/mmy/myy031
28. McCurdy SA, Stoecklin-Marois MT, Tancredi DJ, Bennett DH, Schenker MB. Region of birth, sex, and agricultural work of immigrant Latino farm workers: the MICASA study. J Agric Saf Health. 2014;20:79–90.
29. Bowen LE. Does that face mask really protect you? Appl Biosaf. 2010;15:67–71. https://doi.org/10.1177/153567601001500204
30. Rothman KJ, Greenland S, Lash TL. Validity in epidemiologic studies. In: Rothman KJ, Greenland S, Lash TL, editors. Modern epidemiology. Philadelphia: Lippencott Williams & Wilkins; 2008. p 135–6.
31. Hazard Evaluation System and Information Service. Preventing work-related coccidioidomycosis (Valley fever) [cited 2019 Nov 19]. https://www.cdph.ca.gov/Programs/CCDPHP/DEODC/OHB/HESIS/CDPH%20Document%20Library/CocciFact.pdf
32. Villarejo D, McCurdy SA, Bade B, Samuels S, Lighthall D, Williams D III. The health of California's immigrant hired farmworkers. Am J Ind Med. 2010;53:387–97. https://doi.org/10.1002/ajim.20796


Address for correspondence: Stephen A. McCurdy, Department of Public Health Sciences, MS-1C Rm 126, University of California, Davis, Davis, CA 95616-8638, USA; email: samccurdy@ucdavis.edu

# Atypical Manifestations of Cat-Scratch Disease, United States, 2005–2014

Courtney C. Nawrocki, Ryan J. Max,[1] Natalie S. Marzec,[2] Christina A. Nelson

## Medscape EDUCATION ACTIVITY

In support of improving patient care, this activity has been planned and implemented by Medscape, LLC and Emerging Infectious Diseases. Medscape, LLC is jointly accredited by the Accreditation Council for Continuing Medical Education (ACCME), the Accreditation Council for Pharmacy Education (ACPE), and the American Nurses Credentialing Center (ANCC), to provide continuing education for the healthcare team.

Medscape, LLC designates this Journal-based CME activity for a maximum of 1.00 ***AMA PRA Category 1 Credit(s)™***. Physicians should claim only the credit commensurate with the extent of their participation in the activity.

Successful completion of this CME activity, which includes participation in the evaluation component, enables the participant to earn up to 1.0 MOC points in the American Board of Internal Medicine's (ABIM) Maintenance of Certification (MOC) program. Participants will earn MOC points equivalent to the amount of CME credits claimed for the activity. It is the CME activity provider's responsibility to submit participant completion information to ACCME for the purpose of granting ABIM MOC credit.

All other clinicians completing this activity will be issued a certificate of participation. To participate in this journal CME activity: (1) review the learning objectives and author disclosures; (2) study the education content; (3) take the post-test with a 75% minimum passing score and complete the evaluation at http://www.medscape.org/journal/eid; and (4) view/print certificate. For CME questions, see page 1643.

**Release date: June 17, 2020; Expiration date: June 17, 2021**

### Learning Objectives

Upon completion of this activity, participants will be able to:

- Assess the epidemiology of atypical CSD in the United States, based on an analysis of data from the 2005 to 2014 MarketScan national health insurance claims databases
- Describe the clinical features of atypical CSD in the United States, based on an analysis of data from the 2005 to 2014 MarketScan national health insurance claims databases
- Describe the clinical and public health implications of the epidemiology and clinical features of atypical CSD in the United States, based on an analysis of data from the 2005 to 2014 MarketScan national health insurance claims databases

### CME Editor

**Thomas J. Gryczan, MS,** Technical Writer/Editor, Emerging Infectious Diseases. *Disclosure: Thomas J. Gryczan, MS, has disclosed no relevant financial relationships.*

### CME Author

**Laurie Barclay, MD,** freelance writer and reviewer, Medscape, LLC. *Disclosure: Laurie Barclay, MD, has disclosed no relevant financial relationships.*

### Authors

*Disclosures:* ***Courtney C. Nawrocki, MPH; Natalie S. Marzec, MD, MPH;*** *and* ***Christina A. Nelson, MD, MPH,*** *have disclosed no relevant financial relationships.* ***Ryan J. Max, MSPH,*** *has disclosed the following relevant financial relationships: employed by a commercial interest: GlaxoSmithKline.*

Author affiliations: Oak Ridge Institute for Science and Education, Oak Ridge, Tennessee, USA (C.C. Nawrocki, R.J. Max); Centers for Disease Control and Prevention, Fort Collins, Colorado, USA (C.C. Nawrocki, R.J. Max, C.A. Nelson); University of Colorado, Aurora, Colorado, USA (N.S. Marzec)

[1]Current affiliation: University of North Carolina, Chapel Hill, North Carolina, USA.

[2]Current affiliation: Colorado Department of Public Health and Environment, Denver, Colorado, USA.

DOI: https://doi.org/10.3201/eid2607.200034

Atypical manifestations that can be severe and difficult to diagnosis develop in 5%–20% of patients with cat-scratch disease. To clarify the epidemiology of atypical cat-scratch disease in the United States, we analyzed data from the 2005–2014 MarketScan national health insurance claims databases by using the International Classification of Diseases, 9th Revision, Clinical Modification, codes for cat-scratch disease and selected atypical manifestations: retinitis/neuroretinitis, conjunctivitis, neuritis, encephalitis, hepatosplenic disease, osteomyelitis, erythema nodosum, and endocarditis. Atypical cat-scratch disease accounted for 1.5% of all cases, resulting in an average annual incidence of 0.7 cases/100,000 population. Atypical cat-scratch disease was associated with increased risk for hospitalization (risk ratios 8.77, 95% CI 6.56–11.72) and occurred most often in female patients 10–14 years of age. Ocular (48.7%), hepatosplenic (24.6%), and neurologic (13.8%) manifestations were most common among patients. A more comprehensive understanding of atypical cat-scratch disease can improve patient diagnosis and potentially elucidate pathophysiology of the disease.

Cat-scratch disease, a zoonotic bacterial infection, occurs worldwide and is caused by *Bartonella henselae*, a fastidious, intracellular gram-negative bacillus (*1*). Cats are the major reservoir of *B. henselae* and are infected by *Ctenocephalides felis* cat fleas. Although most cats infected with *B. henselae* are asymptomatic, signs such as fever and myocarditis might develop in some cats (*2*,*3*). Humans usually become infected through the scratches or bites of infected cats. *B. henselae* has also been shown to infect dogs (*4*), in some cases resulting in canine endocarditis (*5*–*7*). Although some human cases of cat-scratch disease have been linked to canine–human transmission (*8*–*12*), further research is needed to clarify the public health significance of *B. henselae* infection in dogs.

The true burden of cat-scratch disease in the United States is unknown because it is not a reportable condition; however, efforts have been made to estimate its incidence in the United States. In 1993, an analysis of hospital discharge data estimated a nationwide incidence of hospitalized cases of 0.77–0.86 cases/100,000 population annually (*13*). A subsequent study that examined a database of national health insurance claims during 2005–2013 found that incidence of cat-scratch disease in the United States was highest in southern states (6.4 cases/100,000 population) and in children 5–9 years of age (9.4 cases/100,000 population) (*14*).

Cat-scratch disease typically manifests as fever and an erythematous papule at the site of the cat scratch or bite, followed by lymphadenopathy in the regional lymph nodes that drain the area of inoculation (*15*). The papule usually appears 3–10 days after inoculation and can persist for several weeks, with regional lymphadenopathy developing 1–3 weeks postinoculation (*1*). From 80% to 95% of cases of cat-scratch disease are consistent with this typical presentation, and the remainder of cases manifest as atypical and more severe symptoms (*16*,*17*).

Atypical manifestations of cat-scratch disease can involve the eyes, nervous system, heart, liver, spleen, skin, or musculoskeletal system and might result in major illness (*1*,*15*). When cat-scratch disease involves the eye, the anterior compartment might be affected by Parinaud oculoglandular syndrome, and the posterior compartment might be affected by retinitis, retinochoroiditis, optic neuritis, uveitis, and vitritis (*18*–*20*). Nervous system involvement most commonly manifests as encephalopathy, but seizures, nerve palsies, neuritis, myelitis, and cerebellar ataxia have also been reported (*21*,*22*).

Endocarditis is more often seen in adults with cat-scratch disease than in children, although preexisting valvular disease puts children at increased risk for this complication (*1*). *Bartonella* infection can also cause abdominal pain and microabscesses in the liver and spleen (*23*), and in immunocompromised hosts can result in bacillary peliosis hepatis (*24*). In addition to the classic erythematous papule at the site of inoculation, erythema nodosum and bacillary angiomatosis are reported dermatologic manifestations of atypical infection (*25*,*26*). Osteolytic lesions, osteomyelitis, and arthritis have also been associated with cat-scratch disease (*16*,*24*,*26*). A study in 1998 found cat-scratch disease to be the third leading cause of prolonged fever of unknown origin in children, and a history of cat exposure was frequently absent (*27*).

Atypical manifestations of *B. henselae* infection can be severe, difficult to diagnose, and lead to lasting impairment. It is unclear why certain patients develop atypical cat-scratch disease, and little is known about its epidemiology. Improved understanding of atypical cat-scratch disease could lead to better recognition of cases by clinicians and inform efforts to understand the pathophysiology of this disease. The purpose of this study was to better characterize the rare and serious complications of this nonreportable zoonotic infection by using nationwide insurance claims data.

## Methods

To identify potential cases of atypical cat-scratch disease, we conducted a retrospective analysis of

persons enrolled in the Truven Health MarketScan Commercial Claims and Encounters Database (Truven Health Analytics, https://www.ibm.com) during 2005–2014. The MarketScan Commercial Claims and Encounters Database includes persons <65 years of age covered by select employer-sponsored health insurance plans in all 50 states and contains administrative claims data on outpatient visits, inpatient admissions, and emergency department visits. Demographically, the MarketScan population generally mirrors the US population, with a slight overrepresentation of persons 50–59 years of age and a slight underrepresentation of persons 20–29 years of age (*28*).

Billing codes from outpatient, inpatient, and emergency department visits are assigned by either a clinician or billing specialist according to the International Classification of Diseases, 9th Revision, Clinical Modification (ICD-9-CM), and procedures are captured as either ICD-9-CM codes, Current Procedure Terminology codes, or Healthcare Common Procedure Coding System codes. Because the International Classification of Diseases, 10th Revision, Clinical Modification, was not officially adopted in the United States until 2015, those codes were not included.

We identified cat-scratch disease cases by extracting all enrollee visit records during the study period with an ICD-9-CM code for cat-scratch disease (078.3). The first instance of a 078.3 diagnosis code in a patient record was considered the index event. Atypical manifestations of interest were selected for analysis if they had recorded precedent in the literature as a complication of cat-scratch disease and distinct, clearly discernable ICD-9-CM codes associated with the specific manifestation. Based on these criteria, the known complications of cat-scratch diseases included for analysis were endocarditis, osteomyelitis, erythema nodosum, conjunctivitis, retinitis/neuroretinitis, encephalitis, neuritis, and hepatosplenic disease.We included ICD-9-CM codes associated with optic neuritis in the retinitis/neuroretinitis category. Encounters with an ICD-9-CM code for cat-scratch disease and an accompanying diagnostic code to indicate the anatomic location of a wound or inoculation site for *B. henselae* were also flagged for analysis and were categorized as either head or neck region, arm or shoulder region, leg or hip region, or torso region. We compiled a detailed list of all ICD-9-CM codes used to identify atypical manifestations of cat-scratch disease (Appendix Table, https://wwwnc.cdc.gov/EID/article/26/7/20-0034-App1.pdf).

We extracted insurance billing records of enrollees with ICD-9-CM codes for cat-scratch disease and selected manifestations at either the same encounter or within a 30-day window of one another. These records were evaluated along with previous and subsequent records by 2 independent reviewers (R.J.M. and C.A.N.) to ensure that the clinical picture was consistent with the coded atypical manifestation based on diagnosis codes, procedure codes, and provider types. If plausible alternative causes of the selected manifestation or likely coding errors were identified, we did not include the enrollee record as an atypical case. In cases of discordance, a third reviewer (Paul Mead) determined final categorization based on record review.

We included persons with an ICD-9-CM code for cat-scratch disease but without accompanying atypical manifestation as typical cases for comparison. Residence in a rural area was assigned if an enrollee did not reside in a metropolitan statistical area, as designated by the US Office of Management and Budget. Because previous research has identified increases in cat-scratch disease in late summer, fall, and January (*13*,*14*,*29*), we categorized month of onset as either late summer and fall, January, or all other months for analysis.

We performed descriptive and comparative statistical analyses by using JMP version 13.2.1 (https://www.jmp.com) and SAS version 9.3 (https://www.sas.com). We used Pearson $\chi^2$ tests or Fisher exact tests for comparisons of categorical variables. To compare the conditional probability of having atypical cat-scratch disease across strata of potential variables of interest (e.g., sex, age category), we calculated risk ratios (RRs) and associated 95% CIs. Human subjects review at the Centers for Disease Control and Prevention determined that institutional review board approval was not required for this study.

## Results

### Study Population and Incidence

During 2005–2014, the MarketScan database contained a median of 44,488,485 (range 16,159,068–53,131,420) enrollees each year. Of 14,824 cat-scratch disease cases identified from MarketScan during this period, 224 (1.5%) cases were classified as atypical (Table 1). The average annual incidence of atypical cat-scratch disease diagnoses during the study period was 0.7 cases/100,000 population.

Atypical cat-scratch disease was most common among adults 15–49 years of age (47.3%), and patients with atypical cat-scratch disease were more likely to be hospitalized than those with typical manifestations ($p<0.0001$).

**Table 1.** Characteristics of patients with cat-scratch disease and risk factors for development of atypical cat-scratch disease, United States, 2005–2014

| Characteristic | Typical disease, no. (%), n = 14,600 | Atypical disease, no. (%), n = 224 | Risk ratio (95% CI)* |
|---|---|---|---|
| Sex | | | |
| M | 5,583 (38.2) | 94 (42.0) | 1.17 (0.90–1.52) |
| F | 9,017 (61.8) | 130 (58.0) | Referent |
| Age, y | | | |
| Child ≤14 | 4,678 (32.0) | 81 (36.2) | 1.20 (0.91–1.57) |
| Adult, 15–49 | 6,421 (44.0) | 106 (47.3) | Referent |
| Adult, 50–64 | 3,501 (24.0) | 37 (16.5) | 0.63 (0.44–0.90) |
| Month of onset | | | |
| Late summer and fall† | 5,470 (37.5) | 93 (41.5) | 1.18 (0.90–1.56) |
| January | 1,490 (10.2) | 22 (9.8) | 1.03 (0.65–1.64) |
| All other months‡ | 7,640 (52.3) | 109 (48.7) | Referent |
| Hospitalized | 487 (3.3) | 56 (25) | 8.77 (6.56–11.72) |
| Residence in southern state | 7,732 (53.0) | 129 (57.6) | 1.20 (0.93–1.57) |
| Residence in rural area | 3,235 (22.1) | 51 (22.8) | 1.06 (0.78–1.45) |

*Outcome for risk ratio calculations was development of atypical cat-scratch disease.
†August, September, October, and November.
‡February, March, April, May, June, July, and December.

### Distribution by Age and Sex

Children ≤14 years of age accounted for 36.2% of atypical cat-scratch disease diagnoses overall; 26 cases (11.4%) were in female patients 10–14 years of age (Figure 1). Among female patients 10–14 years of age, 16 patients (61.5%) had ocular manifestations (13 retinitis/neuroretinitis and 3 conjunctivitis), and 6 patients (23.1%) had hepatosplenic disease.

Nearly half of all patients with atypical cat-scratch disease were younger adults (15–49 years of age). When we compared older adults with younger adults, older adults (50–64 years of age) had a decreased risk for having atypical cat-scratch disease (RR 0.63, 95% CI 0.44–0.90) (Table 1).

### Seasonality

Atypical cat-scratch disease diagnoses increased from August through March, and diagnoses were concentrated during August–October (33.5% of diagnoses) and January–March (29.5% of diagnoses) (Figure 2), although neither diagnosis in late summer and fall or diagnosis in January were found to be risk factors for development of atypical cat-scratch disease (Table 1). Trends in atypical cat-scratch disease diagnoses were similar to trends in typical cat-scratch disease diagnoses. However, typical cat-scratch disease had less defined peak periods, and diagnoses decreased sharply after January.

### Geographic Distribution and Residence in Rural Area

Most (57.6%) cases of atypical cat-scratch disease occurred in the southern region of the United States (57.6%), followed by the midwest (16.5%) and northeast (12.5%) regions (Figure 3). The geographic distribution of atypical cases did not differ significantly from cases of typical cat-scratch disease.

Residence in a rural area was not a risk factor for development of atypical cat-scratch disease (RR 1.06, 95% CI 0.78–1.45). Also, the proportion of patients with atypical cat-scratch disease living in a rural area did not differ from the proportion of patients with typical cat-scratch disease living in a rural area (p = 0.70).

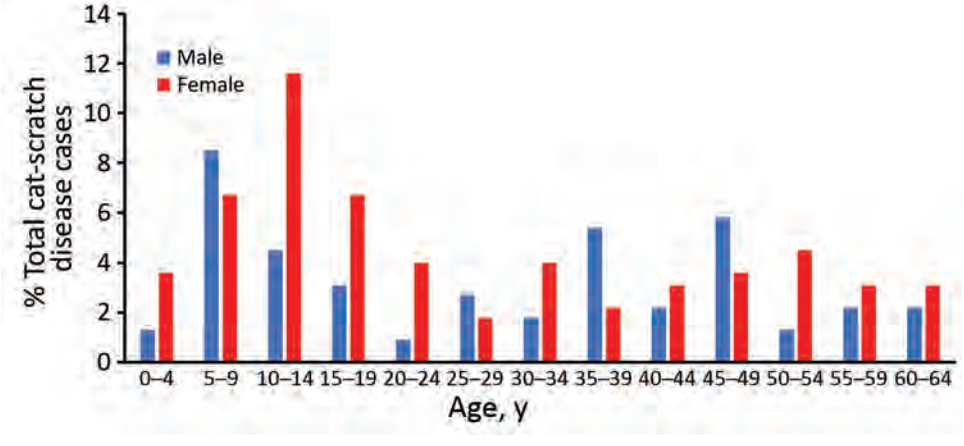


**Figure 1.** Age and sex distribution of patients with atypical cat-scratch disease, United States, 2005–2014.

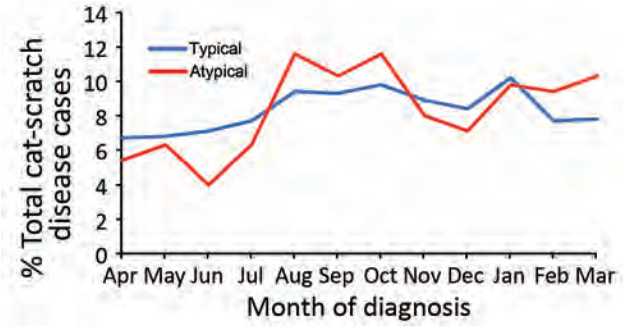


**Figure 2.** Seasonal variation of atypical and typical cat-scratch disease by month of diagnosis, United States, 2005–2014.

### Atypical Manifestations by Type

Among 224 patients with atypical cat-scratch disease, 109 (48.7%) had ocular manifestations (retinitis/neuroretinitis or conjunctivitis), 55 (24.6%) had hepatosplenic disease, and 31 (13.8%) had neurologic manifestations (neuritis or encephalitis). The remaining 33 (14.7%) case-patients had osteomyelitis, erythema nodosum, or endocarditis (Table 2). Among patients with ocular manifestations, 82.6% had retinitis/neuroretinitis; most (64.5%) patients with neurologic manifestations had encephalitis. Three (1.3%) patients with atypical cat-scratch disease had >1 manifestation: 1 patient with osteomyelitis and hepatosplenic disease; 1 patient with endocarditis and hepatosplenic disease; and 1 patient with osteomyelitis, encephalitis, and hepatosplenic disease.

Children ≤14 years of age were at increased risk for hepatosplenic disease (RR 1.76, 95% CI 1.04–2.99) and osteomyelitis (RR 3.81, 95% CI 1.28–11.37) compared with persons ≥15 years of age. Older adults (50–64 years of age) were less likely to show development of ocular manifestations (retinitis/neuroretinitis and conjunctivitis) than younger adults (15–49 years of age) (RR 0.49, 95% CI 0.28–0.85).

Among persons with ocular (retinitis/neuroretinitis and conjunctivitis) manifestations, most diagnoses were made during August–October (31.2%) and January–March (35.8%). Among persons with neurologic (neuritis and encephalitis) manifestations, diagnoses were concentrated during October (22.6%). We observed no notable trends in seasonality of diagnoses for other manifestations of atypical cat-scratch disease (Figure 4). We also observed no differences in geographic distribution or rurality by manifestation of atypical cat-scratch disease.

### Hospitalization of Atypical Case-Patients

Patients with atypical cat-scratch disease were more likely to be hospitalized than patients with typical cat-scratch disease (RR 8.77, 95% CI 6.56–11.72) (Table 1). Among patients with atypical cat-scratch disease, children ≤14 years of age accounted for 60.7% of hospitalizations and had an increased risk for hospitalization compared with adults 15–49 years of age (RR 2.34, 95% CI 1.44–3.79). A total of 57.1% of the hospitalizations occurred during August–November, and we found an overall increased risk for hospitalization during this period when compared with all other months, except for January (RR 1.88, 95% CI 1.15–3.05) (Table 3).

Increased risks of hospitalization were found for neurologic manifestations (neuritis and encephalitis) (RR 1.88, 95% CI 1.15–3.08), hepatosplenic disease (RR 2.30, 95% CI 1.49–3.55), and osteomyelitis (RR 2.13, 95% CI 1.20–3.82). Ocular manifestations (retinitis/neuroretinitis and conjunctivitis) were associated with decreased risk for hospitalization (RR 0.23, 95% CI 0.12–0.43).

### Location of Wound

Information on wound location was available for only 10 (4.5%) patients with atypical cat-scratch disease. Among these persons, 2 with conjunctivitis, 1 with encephalitis, and 2 with hepatosplenic disease had a wound on the head or neck; 1 with osteomyelitis and 3 with hepatosplenic manifestations had a wound on the arm or shoulder; 1 with endocarditis had a wound on the leg or hip;

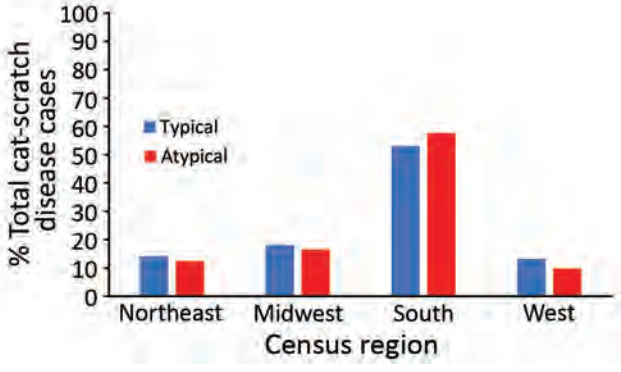


**Figure 3.** Proportions of typical and atypical cat-scratch disease by US Census region, United States, 2005–2014. Northeast: Connecticut, Maine, Massachusetts, New Hampshire, Rhode Island, Vermont, New Jersey, New York, Pennsylvania. Midwest: Illinois, Indiana, Iowa, Kansas, Michigan, Minnesota, Missouri, Nebraska, North Dakota, South Dakota, Ohio, Wisconsin. South: Arkansas, Delaware, Florida, Georgia, Louisiana, Maryland, North Carolina, Oklahoma, South Carolina, Texas, Virginia, West Virginia, Alabama, Hawaii, Kentucky, Mississippi, Oregon, Tennessee. West: Alaska, Arizona, California, Colorado, Idaho, Montana, Nevada, New Mexico, Utah, Washington, Wyoming, Puerto Rico, Virgin Islands.

**Table 2.** Demographic characteristics for patients by manifestation of atypical cat-scratch disease, United States, 2005–2014

| Characteristic | No. (%) | Sex, no. (%) | | Age category, y, no. (%) | | | Hospitalized, no. (%) |
|---|---|---|---|---|---|---|---|
| | | M | F | 0–14 | 15–49 | 50–64 | |
| Atypical disease | 224* | 94 (42.0) | 130 (58.0) | 81 (36.2) | 106 (47.3) | 37 (16.5) | 56 (25.0) |
| Ocular disease | 109 (48.7) | 46 (48.9) | 63 (48.5) | 33 (40.7) | 60 (56.6) | 16 (43.2) | 10 (17.9) |
| Retinitis/neuroretinitis | 90 (40.2) | 36 (38.3) | 54 (41.5) | 23 (28.4) | 53 (50.0) | 14 (37.8) | 8 (14.3) |
| Conjunctivitis | 19 (8.5) | 10 (10.6) | 9 (6.9) | 10 (12.3) | 7 (6.6) | 2(5.4) | 2 (3.6) |
| Hepatosplenic disease | 55 (24.6) | 24 (25.5) | 31 (23.8) | 25 (30.9) | 21 (19.8) | 9 (24.3) | 24 (42.9) |
| Neurologic disease | 31 (13.8) | 13 (13.8) | 18 (13.8) | 12 (14.8) | 13 (12.3) | 6 (16.2) | 13 (23.2) |
| Encephalitis | 20 (8.9) | 12 (12.8) | 8 (6.2) | 12 (14.8) | 8 (7.5) | 0 (0) | 13 (23.2) |
| Neuritis | 11 (4.9) | 1 (1.1) | 10 (7.7) | 0 (0) | 5 (4.7) | 6 (16.2) | 0 (0) |
| Osteomyelitis | 14 (6.3) | 6 (6.4) | 8 (6.2) | 9 (11.1) | 4 (3.8) | 1 (2.7) | 7 (12.5) |
| Erythema nodosum | 11 (4.9) | 2 (2.1) | 9 (6.9) | 4 (4.9) | 5 (4.7) | 2 (5.4) | 4 (7.1) |
| Endocarditis | 8 (3.6) | 4 (4.3) | 4 (3.1) | 1 (1.2) | 4 (3.8) | 3 (8.1) | 2 (3.6) |

*A total of 228 manifestations of atypical cat-scratch disease were seen among 224 patients. Three patients had >1 manifestation; 1 patient had osteomyelitis and hepatosplenic disease;1 patient had endocarditis and hepatosplenic disease; and 1 patient had osteomyelitis, encephalitis, and hepatosplenic disease.

and 1 with endocarditis had a wound on an unspecified limb.

## Discussion

Using US nationwide insurance claims data, we identified and characterized 224 atypical cases of cat-scratch disease during 2005–2014 and estimated an average annual incidence of 0.7 cases/100,000 population. Nearly half of all atypical cat-scratch disease cases had ocular manifestations, most of which were retinitis/neuroretinitis. Atypical cat-scratch disease was most prevalent among female patients 10–14 years of age, who most commonly had ocular manifestations.

Trends in hospitalizations of patients with cat-scratch disease highlight the severity of atypical cat-scratch disease compared with typical cat-scratch disease. Atypical cat-scratch disease appears to be particularly severe among children ≤14 years of age, who had an increased risk for hospitalization. Adults 50–64 years of age had the lowest risk for development of atypical cat-scratch disease and specifically ocular manifestations. Reasons that older adults might have complications associated with cat-scratch disease less often than other age groups are unclear and require further study.

Severity of cat-scratch disease in children has been previously documented. In a study conducted by Reynolds et al., ≈25% of hospitalizations of children for cat-scratch disease were caused by complications associated with atypical cat-scratch disease; neurologic and hepatosplenic complications were most common (*30*). Although children in our study were also particularly at risk for hepatosplenic disease, neurologic and hepatosplenic complications were associated with increased risk for hospitalization in our overall study population, indicating that these manifestations are particularly severe for all age groups. Encephalitis was the most common neurologic manifestation in our population, which was also consistent with findings of Reynolds et al., in which most hospitalizations of children for neurologic complications of cat-scratch disease were caused by encephalitis or encephalopathy (*30*). Thus, physicians should consider cat-scratch disease in patients who have encephalitis or new onset hepatosplenic abnormalities, especially children.

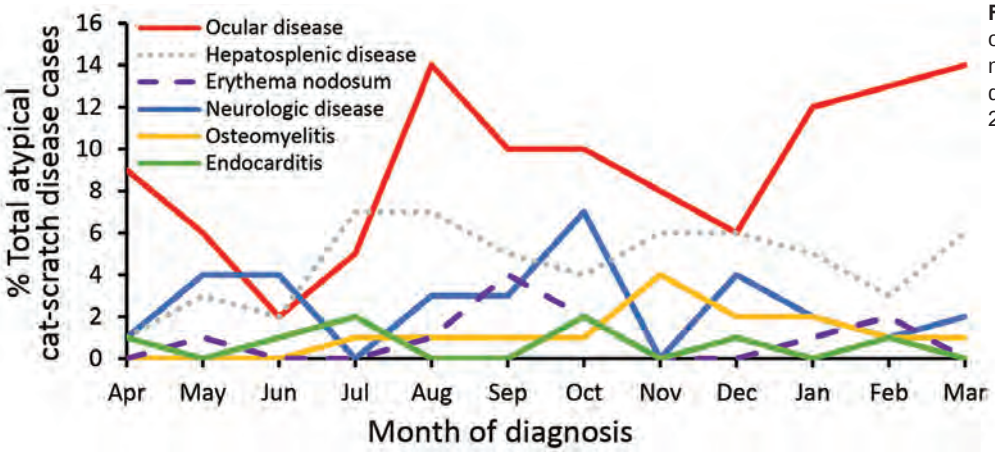


**Figure 4.** Seasonal variation of atypical cat-scratch disease manifestations by month of diagnosis, United States, 2005–2014.

**Table 3.** Demographic characteristics for patients hospitalized with atypical cat-scratch disease and associated risk factors for hospitalization, United States, 2005–2014

| Characteristic | Hospitalized, no. (%), n = 56 | Not hospitalized, no. (%), n = 168 | Risk ratio (95% CI) |
|---|---|---|---|
| Sex | | | |
| M | 26 (46.4) | 68 (40.5) | 1.19 (0.76–1.89) |
| F | 30 (53.6) | 100 (59.5) | Referent |
| Age, y | | | |
| Child ≤14 | 34 (60.7) | 47 (28.0) | 2.34 (1.44–3.79) |
| Younger adult, 15–49 | 19 (33.9) | 87 (51.8) | Referent |
| Older adult, 50–64 | 3 (5.4) | 34 (20.2) | 0.45 (0.14–1.44) |
| Month of onset | | | |
| Late summer and fall* | 32 (57.1) | 61 (36.3) | 1.88 (1.15–3.05) |
| January | 4 (7.1) | 18 (10.7) | 0.99 (0.38–2.62) |
| All other months† | 20 (35.7) | 89 (53.0) | Referent |
| Residence in southern state | 36 (64.3) | 93 (55.4) | 1.33 (0.82–2.14) |
| Residence in rural area | 11 (19.6) | 40 (23.8) | 1.26 (0.71–2.26) |

*August, September, October, and November.
†February, March, April, May, June, July, and December.

Previous studies have documented the highest rates of cat-scratch disease in late summer and fall and a separate peak often seen in January (*13*,*14*,*29*). One such study found that rates of *B. henselae* seropositivity among samples submitted to Mayo Clinic Laboratories over a 10-year period were highest during September–January, with the highest annual rates in January (*29*). Typical cat-scratch disease diagnoses in our study followed similar seasonal patterns to those previously reported. However, atypical cat-scratch disease appeared more concentrated during August–October and January–March. The reasons for this finding are unclear but might include delays in diagnosis of atypical cat-scratch disease. For example, patients who contract cat-scratch disease and had complications during January might not be given a diagnosis of atypical cat-scratch disease at that time because they do not show classic symptoms or their symptoms take time to develop and care-seeking is delayed.

Furthermore, a recent case series of ocular manifestations of cat-scratch disease reported that 9 of 10 patients had symptoms ≤3 months before showing development of ocular complications and that 3 patients had been originally given misdiagnoses of etiologies other than cat-scratch disease (*31*). Given that ocular manifestations of cat-scratch disease were most common in our study, increased diagnoses of atypical cat-scratch disease through March could be a sign of delayed diagnoses, particularly for manifestations that are less severe, such as those involving the eye.

Trends related to geographic distribution of cases did not differ between atypical and typical cat-scratch disease. Similar to findings from 3 previous studies that reported the highest incidences of cat-scratch disease in the southern United States (*13*,*14*,*30*), in our study, most typical (53.0%) and atypical (57.6%) cat-scratch disease cases occurred in patients residing in this region. In addition, a national survey of US healthcare providers found that those in the Pacific and southern regions of the United States were more likely to have been given a diagnosis of cat-scratch disease than in other regions (*32*). These findings are further supported by studies that have found higher average *B. henselae* seroprevalences and active bacteremia in pet cats from warmer, more humid climates, including the southern United States (*33*,*34*). Thus, healthcare providers in regions with climates that support flea abundance should be aware of the risk for cat-scratch disease and be able to recognize its atypical manifestations.

This study had several limitations. First, although MarketScan is a large database of insurance claims data from persons covered by employer-sponsored insurance, it is a convenience sample and may not accurately represent the characteristics of all persons in the United States. For example, trends we see in atypical cat-scratch disease by geographic region and rural residence might be biased by differences in coverage and access to care that are not accounted for here. Furthermore, MarketScan does not include data for adults ≥65 years of age, military personnel, uninsured persons, or Medicaid/Medicare enrollees. These specific populations might show varying degrees of cat-scratch disease severity or risk that are not captured in our results. In addition, because only persons <65 years of age are included in the database, the proportion of children who have cat-scratch disease might be artificially inflated. The number of patients who had atypical cat-scratch disease was small, especially when broken down by manifestation. Thus, it is difficult to draw conclusions regarding risk factors for specific manifestations of atypical cat-scratch disease and hospitalization within these groups.

Furthermore, misclassification could have occurred when ICD-9-CM codes were used to classify atypical cat-scratch disease for several reasons. ICD-9-CM codes are subject to error from the clinicians and billing specialists who enter them. In addition, we excluded records that fit our criteria for manifestations of atypical cat-scratch disease but lacked additional supporting information, which could have caused us to underestimate the true burden of atypical cat-scratch disease. Last, codes for some known atypical cat-scratch disease manifestations, such as pulmonary complications and thrombocytopenia, were excluded because of etiologic ambiguity in enrollee records.

In conclusion, our findings indicate that atypical cat-scratch disease in the United States follows trends similar to those for typical cat-scratch disease but is more prevalent and severe among children ≤14 years of age and is least likely to occur in older adults (50–64 years of age). In addition, differences in seasonality of diagnoses were seen, which might be an indication that diagnosis of atypical cat-scratch disease is often delayed. Ocular (retinitis/neuroretinitis and conjunctivitis) and hepatosplenic complications were the most common manifestations of atypical cat-scratch disease. Improved understanding of atypical cat-scratch disease might lead to better recognition of cases by clinicians, as well as inform efforts to clarify the pathophysiology of this disease.

### Acknowledgments

We thank Paul Mead for serving as the third reviewer of insurance billing records of enrollees with ICD-9-CM codes in cases of discordance between the 2 reviewers and Dan Pastula for providing assistance with defining neurologic manifestations of cat-scratch disease.

## About the Author

Ms. Nawrocki is an Oak Ridge Institute for Science and Education epidemiology fellow in the Bacterial Diseases Branch, Division of Vector-Borne Diseases, National Center for Emerging and Zoonotic Infectious Diseases, Centers for Disease Control and Prevention, Fort Collins, CO. Her primary research interests include how interactions between humans, animals, and the environment facilitate the spread of infectious diseases, and the epidemiology and prevention of vector-borne diseases.

### References

1. Florin TA, Zaoutis TE, Zaoutis LB. Beyond cat scratch disease: widening spectrum of *Bartonella henselae* infection. Pediatrics. 2008;121:e1413–25. https://doi.org/10.1542/peds.2007-1897
2. Perez C, Hummel JB, Keene BW, Maggi RG, Diniz PP, Breitschwerdt EB. Successful treatment of *Bartonella henselae* endocarditis in a cat. J Feline Med Surg. 2010;12:483–6. https://doi.org/10.1016/j.jfms.2009.12.018
3. Varanat M, Broadhurst J, Linder KE, Maggi RG, Breitschwerdt EB. Identification of *Bartonella henselae* in 2 cats with pyogranulomatous myocarditis and diaphragmatic myositis. Vet Pathol. 2012;49:608–11. https://doi.org/10.1177/0300985811404709
4. Solano-Gallego L, Bradley J, Hegarty B, Sigmon B, Breitschwerdt E. *Bartonella henselae* IgG antibodies are prevalent in dogs from southeastern USA. Vet Res. 2004;35:585–95. https://doi.org/10.1051/vetres:2004034
5. Donovan TA, Fox PR, Balakrishnan N, Ericson M, Hooker V, Breitschwerdt EB. Pyogranulomatous pancarditis with intramyocardial *Bartonella henselae* San Antonio 2 (BhSA2) in a dog. J Vet Intern Med. 2017;31:142–8. https://doi.org/10.1111/jvim.14609
6. MacDonald KA, Chomel BB, Kittleson MD, Kasten RW, Thomas WP, Pesavento P. A prospective study of canine infective endocarditis in northern California (1999–2001): emergence of *Bartonella* as a prevalent etiologic agent. J Vet Intern Med. 2004;18:56–64.
7. Pesavento PA, Chomel BB, Kasten RW, McDonald KA, Mohr FC. Pathology of *Bartonella* endocarditis in six dogs. Vet Pathol. 2005;42:370–3. https://doi.org/10.1354/vp.42-3-370
8. Chen TC, Lin WR, Lu PL, Lin CY, Chen YH. Cat scratch disease from a domestic dog. J Formos Med Assoc. 2007;106(Suppl):S65–8. https://doi.org/10.1016/S0929-6646(09)60356-9
9. Chung JY, Han TH, Kim BN, Yoo YS, Lim SJ. Detection of *Bartonella henselae* DNA by polymerase chain reaction in a patient with cat scratch disease: a case report. J Korean Med Sci. 2005;20:888–91. https://doi.org/10.3346/jkms.2005.20.5.888
10. Keret D, Giladi M, Kletter Y, Wientroub S. Cat-scratch disease osteomyelitis from a dog scratch. J Bone Joint Surg Br. 1998;80:766–7. https://doi.org/10.1302/0301-620X.80B5.0800766
11. Schiellerup P, Krogfelt KA, Andersen AB. *Bartonella henselae* causing severe and protracted illness in an otherwise healthy person. Scand J Infect Dis. 2004;36:316–8. https://doi.org/10.1080/00365540410019516
12. Tsukahara M, Tsuneoka H, Iino H, Ohno K, Murano I. *Bartonella henselae* infection from a dog. Lancet. 1998;352:1682. https://doi.org/10.1016/S0140-6736(05)61455-9
13. Jackson LA, Perkins BA, Wenger JD. Cat scratch disease in the United States: an analysis of three national databases. Am J Public Health. 1993;83:1707–11. https://doi.org/10.2105/AJPH.83.12.1707
14. Nelson CA, Saha S, Mead PS. Cat-scratch disease in the United States, 2005–2013. Emerg Infect Dis. 2016;22:1741–6. https://doi.org/10.3201/eid2210.160115
15. Spach DH, Koehler JE. *Bartonella*-associated infections. Infect Dis Clin North Am. 1998;12:137–55. https://doi.org/10.1016/S0891-5520(05)70414-1
16. Carithers HA. Cat-scratch disease. An overview based on a study of 1,200 patients. Am J Dis Child. 1985;139:1124–33. https://doi.org/10.1001/archpedi.1985.02140130062031
17. Murakami K, Tsukahara M, Tsuneoka H, Iino H, Ishida C, Tsujino K, et al. Cat scratch disease: analysis of 130 seropositive cases. J Infect Chemother. 2002;8:349–52. https://doi.org/10.1007/s10156-002-0194-6

18. Cunningham ET Jr, Koehler JE. Ocular bartonellosis. Am J Ophthalmol. 2000;130:340–9. https://doi.org/10.1016/S0002-9394(00)00573-0
19. Amer R, Tugal-Tutkun I. Ophthalmic manifestations of *Bartonella* infection. Curr Opin Ophthalmol. 2017;28:607–12. https://doi.org/10.1097/ICU.0000000000000419
20. Habot-Wilner Z, Trivizki O, Goldstein M, Kesler A, Shulman S, Horowitz J, et al. Cat-scratch disease: ocular manifestations and treatment outcome. Acta Ophthalmol. 2018;96:e524–32. https://doi.org/10.1111/aos.13684
21. Carithers HA, Margileth AM. Cat-scratch disease. Acute encephalopathy and other neurologic manifestations. Am J Dis Child. 1991;145:98–101. https://doi.org/10.1001/archpedi.1991.02160010104026
22. Marra CM. Neurologic complications of *Bartonella henselae* infection. Curr Opin Neurol. 1995;8:164–9. https://doi.org/10.1097/00019052-199506000-00002
23. Arisoy ES, Correa AG, Wagner ML, Kaplan SL. Hepatosplenic cat-scratch disease in children: selected clinical features and treatment. Clin Infect Dis. 1999;28:778–84. https://doi.org/10.1086/515197
24. Anderson BE, Neuman MA. *Bartonella* spp. as emerging human pathogens. Clin Microbiol Rev. 1997;10:203–19. https://doi.org/10.1128/CMR.10.2.203
25. Bass JW, Vincent JM, Person DA. The expanding spectrum of *Bartonella* infections: II. Cat-scratch disease. Pediatr Infect Dis J. 1997;16:163–79. https://doi.org/10.1097/00006454-199702000-00002
26. Margileth AM, Wear DJ, English CK. Systemic cat scratch disease: report of 23 patients with prolonged or recurrent severe bacterial infection. J Infect Dis. 1987;155:390–402. https://doi.org/10.1093/infdis/155.3.390
27. Jacobs RF, Schutze GE. *Bartonella henselae* as a cause of prolonged fever and fever of unknown origin in children. Clin Infect Dis. 1998;26:80–4. https://doi.org/10.1086/516256
28. Nelson CA, Saha S, Kugeler KJ, Delorey MJ, Shankar MB, Hinckley AF, et al. Incidence of clinician-diagnosed Lyme disease, United States, 2005–2010. Emerg Infect Dis. 2015;21:1625–31. https://doi.org/10.3201/eid2109.150417
29. Theel ES, Ross T. Seasonality of *Bartonella henselae* IgM and IgG antibody positivity rates. J Clin Microbiol. 2019;57:e01263-19. https://doi.org/10.1128/JCM.01263-19
30. Reynolds MG, Holman RC, Curns AT, O'Reilly M, McQuiston JH, Steiner CA. Epidemiology of cat-scratch disease hospitalizations among children in the United States. Pediatr Infect Dis J. 2005;24:700–4. https://doi.org/10.1097/01.inf.0000172185.01939.fc
31. Oray M, Önal S, Koç Akbay A, Tuğal Tutkun İ. Diverse clinical signs of ocular involvement in cat scratch disease. Turk J Ophthalmol. 2017;47:9–17. https://doi.org/10.4274/tjo.28009
32. Nelson CA, Moore AR, Perea AE, Mead PS. Cat scratch disease: U.S. clinicians' experience and knowledge. Zoonoses Public Health. 2018;65:67–73. https://doi.org/10.1111/zph.12368
33. Guptill L, Wu CC, HogenEsch H, Slater LN, Glickman N, Dunham A, et al. Prevalence, risk factors, and genetic diversity of *Bartonella henselae* infections in pet cats in four regions of the United States. J Clin Microbiol. 2004;42:652–9. https://doi.org/10.1128/JCM.42.2.652-659.2004
34. Jameson P, Greene C, Regnery R, Dryden M, Marks A, Brown J, et al. Prevalence of *Bartonella henselae* antibodies in pet cats throughout regions of North America. J Infect Dis. 1995;172:1145–9. https://doi.org/10.1093/infdis/172.4.1145


Address for correspondence: Courtney C. Nawrocki, Centers for Disease Control and Prevention, 3156 Rampart Rd, Fort Collins, CO 80521, USA; email: osm9@cdc.gov

# Paradoxal Trends in Azole-Resistant *Aspergillus fumigatus* in a National Multicenter Surveillance Program, the Netherlands, 2013–2018

Pieter P.A. Lestrade, Jochem B. Buil, Martha T. van der Beek, Ed J. Kuijper, Karin van Dijk, Greetje A. Kampinga, Bart J.A. Rijnders, Alieke G. Vonk, Sabine C. de Greeff, Annelot F. Schoffelen, Jaap van Dissel, Jacques F. Meis, Willem J.G. Melchers, Paul E. Verweij

We investigated the prevalence of azole resistance of *Aspergillus fumigatus* isolates in the Netherlands by screening clinical *A. fumigatus* isolates for azole resistance during 2013–2018. We analyzed azole-resistant isolates phenotypically by in vitro susceptibility testing and for the presence of resistance mutations in the *Cyp51A* gene. Over the 6-year period, 508 (11%) of 4,496 culture-positive patients harbored an azole-resistant isolate. Resistance frequency increased from 7.6% (95% CI 5.9%–9.8%) in 2013 (58/760 patients) to 14.7% (95% CI 12.3%–17.4%) in 2018 (112/764 patients) (p = 0.0001). $TR_{34}$/L98H (69%) and $TR_{46}$/Y121F/T289A (17%) accounted for 86% of Cyp51A mutations. However, the mean voriconazole MIC of $TR_{34}$/L98H isolates decreased from 8 mg/L (2013) to 2 mg/L (2018), and the voriconazole-resistance frequency was 34% lower in 2018 than in 2013 (p = 0.0001). Our survey showed changing azole phenotypes in $TR_{34}$/L98H isolates, which hampers the use of current PCR-based resistance tests.

Author affiliations: VieCuri Hospital, Venlo, the Netherlands (P.P.A. Lestrade); Center of Expertise in Mycology Radboud University Medical Center/Canisius-Wilhelmina Hospital, Nijmegen, the Netherlands (J.B. Buil, J.F. Meis, W.J.G. Melchers, P.E. Verweij); Leiden University Medical Center, Leiden, the Netherlands (M.T. van der Beek, E.J. Kuijper); Amsterdam University Medical Center, Vrije Universiteit Amsterdam, Amsterdam, the Netherlands (K. van Dijk); University of Groningen, University Medical Center Groningen, Groningen, the Netherlands (G.A. Kampinga); Erasmus Medical Center, Rotterdam, the Netherlands (B.J.A. Rijnders, A.G. Vonk); Center for Infectious Disease Control, Dutch National Institute for Public Health and the Environment, Bilthoven, the Netherlands (S.C. de Greeff, A.F. Schoffelen, J. van Dissel)

DOI: https://doi.org/10.3201/eid2607.200088

*Aspergillus fumigatus* is a saprobic mold that thrives on decaying plant material. The fungus is thermotolerant and exhibits optimum growth at 37°C. *A. fumigatus* has evolved into an major cause of pulmonary infections, especially in immunocompromised persons. Patients at risk for invasive aspergillosis include patients with hematologic malignancy, solid organ transplant recipients, and patients receiving corticosteroids. In addition, new risk groups are being recognized, including patients treated with ibrutinib (*1*) and patients with severe influenza (*2*,*3*). The fungus might also cause chronic pulmonary infections, chronic lung colonization, and allergic syndromes (*4*).

Azoles represent the most important class of antifungal agents that are used for the management of *Aspergillus* diseases. Triazoles with activity against aspergilli include itraconazole, voriconazole, posaconazole, and isavuconazole. However, use of this drug class has been threatened by the emergence of azole resistance, which was first reported in 1997 (*5*). Although resistance might be selected during azole therapy, resistance selection in the environment through exposure to azole fungicides has been shown to be the most important route for resistance selection (*6*). The environmental route of resistance selection poses numerous challenges for patient management because two thirds of patients with azole-resistant invasive aspergillosis have no previous history of azole therapy (*7*). A recent cohort study showed that voriconazole resistance resulted in 21% lower day-42 survival in patients with culture-positive invasive aspergillosis compared with voriconazole-susceptible infection, indicating a major effect of resistance on patient survival (*8*). Because most patients with invasive aspergillosis are culture

negative, sensitive non–culture-based resistance tests are urgently needed (*9*).

Although azole-resistant *A. fumigatus* was recently added to the antibiotic threats list of the US Centers for Disease Control and Prevention (*10*), systematic resistance surveillance programs are currently lacking. Surveillance is hampered by low numbers of culture-positive patients, difficulty in diagnosing and classifying patients with *Aspergillus* diseases, low awareness of fungal resistance, and limited prioritization of fungal resistance research. Furthermore, unlike bacteria, molds do not routinely undergo resistance testing in most clinical microbiology laboratories, thus necessitating the implementation of specific laboratory protocols. Early reports on azole resistance in the Netherlands prompted the national Center for Infectious Disease Control (Cib) to support a reference laboratory to set up a surveillance network to monitor trends in azole-resistance frequency in *A. fumigatus*. Our aim was to determine the resistance frequency over a period of 6 years to describe resistance phenotypes and to analyze underlying resistance mutations and trends.

## Methods

Five University Medical Centers (UMCs) participated in the surveillance network, including Leiden UMC (Leiden), Erasmus Medical Center (Rotterdam), Amsterdam UMC, VU Medical Center (Amsterdam), UMC Groningen (Groningen), and Radboud UMC (Nijmegen). The geographic regions include the west of the Netherlands (Rotterdam, Leiden, and Amsterdam), which is the most heavily populated region; the north (Groningen); and the east (Nijmegen). The centers were asked to screen *A. fumigatus* isolates cultured from clinical specimens by using an agar-based screening test (VIPcheck; MediaProducts, https://www.mediaproductsbv.nl). VIPcheck contains 3 agar wells supplemented with itraconazole, voriconazole, and posaconazole, and a growth control well (*11*). *A. fumigatus* colonies from the primary culture were inoculated on the 4-wells plate, incubated for up to 48 hours, and inspected for growth. If an isolate grew on any of the azole-containing wells, the isolate was sent anonymously to Radboud UMC for MIC testing and genotypic characterization. MIC testing was performed according to the European Committee on Antimicrobial Susceptibility Testing (EUCAST) broth microdilution reference method (*12*–*14*) for amphotericin B (AmB), itraconazole, voriconazole, posaconazole, and isavuconazole (added in 2015 after the drug was clinically licensed). Azole resistance was defined as resistance to ≥1 azole drug, according to EUCAST clinical breakpoints (itraconazole, >2 mg/L; voriconazole, >2 mg/L; posaconazole, >0.25 mg/L, and isavuconazole, >1 mg/L). EUCAST broth microdilution plates were made at Radboud UMC in batches of 250 96-well plates and complied with the recommended quality control standards (*11*–*13*). For *A. fumigatus* isolates with a confirmed azole-resistant phenotype, the full *Cyp51A* gene was analyzed by PCR amplification and sequencing (*7*). The Cyp51A sequence (GenBank accession no. AF338659) was used for mutation analysis. A spore suspension of all isolates was stored at –80°C in 10% glycerol.

Results of phenotypic testing were sent to the surveillance laboratories as soon as these were available. Analysis of the resistance genotypes was batched, and once a year each center received a list of isolates with resistance genotype and phenotype. The list of isolates was checked by the centers, who also provided the number of *A. fumigatus* culture-positive patients who had been screened for azole resistance during the year and the number of patients who harbored an azole-resistant isolate. Clinical information regarding underlying disease and classification of *Aspergillus* disease was not collected. Data on *A. fumigatus* resistance epidemiology are reported and published annually (*15*).

We calculated mean MICs with 95% CIs with GraphPad Prism 5.03 (https://www.graphpad.com). For calculations, we recoded MICs >16 mg/L as 32 mg/L. We calculated statistical tests on differences in MIC distributions by using Kruskal-Wallis test and tests on differences in classification according to clinical breakpoints by using the Fisher exact test.

## Results

### General Epidemiology

During 2013–2018, *A. fumigatus* isolates from 4,518 culture-positive patients were screened for the presence of azole-resistance. In 1 center, prospective screening was not performed in 2015, but only selected isolates from 22 patients were analyzed (Table 1). Therefore, we excluded these patients from calculation of the azole-resistance frequency, leaving 4,496 patients who had been screened for azole resistance. In total, 508 patients (11%) harbored an azole-resistant *A. fumigatus* isolate. Over the 6-year period, the overall resistance frequency increased from 7.6% (95% CI 5.9%–9.8%) in 2013 (58/760 patients) to 14.7% (95% CI 12.3%–17.4%) in 2018 (112/764 patients; p = 0.0001).

### Triazole-Resistance Genotypes

Overall, 640 *A. fumigatus* isolates (obtained from 508 patients) exhibited phenotypical resistance for

**Table 1.** Number of *Aspergillus fumigatus* culture-positive patients screened for azole resistance and azole resistance frequency in clinical *A. fumigatus* isolates in 5 University Medical Centers in the Netherlands*

| Surveillance center | No. resistant/no. screened (%) | | | | | |
|---|---|---|---|---|---|---|
| | 2013 | 2014 | 2015 | 2016 | 2017 | 2018 |
| Erasmus MC, Rotterdam | 10/231 (4.3) | 10/265 (3.8) | 7/22 (31.8)† | 24/186 (12.9) | 19/147 (12.9) | 17/129 (13.2) |
| LUMC, Leiden | 19/99 (19.2) | 15/113 (13.3) | 23/141 (16.3) | 18/88 (20.5) | 27/114 (23.7) | 25/120 (20.8) |
| Radboud UMC, Nijmegen | 6/123 (4.9) | 7/143 (4.9) | 12/145 (8.3) | 20/210 (9.5) | 21/198 (10.6) | 23/196 (11.7) |
| UMCG, Groningen | 16/194 (8.2) | 18/191 (9.4) | 15/225 (6.7) | 26/215 (12.1) | 35/240 (14.6) | 34/238 (14.3) |
| VUMC, Amsterdam | 8/113 (7.1) | 9/104 (8.7) | 14/89 (15.7) | 13/85 (15.3) | 12/75 (16.0) | 13/81 (16.0) |
| Total | 58/760 (7.6) | 59/814 (7.2) | 64/600 (10.7)‡ | 101/784 (12.9) | 114/774 (14.7) | 112/764 (14.7) |

*MC, medical center; UMC, university medical center.
†Only a limited number of patients was screened for azole resistance.
‡Calculation of resistance frequency did not include the cases of Erasmus MC.

≥1 triazole. $TR_{34}$/L98H was the most frequently observed resistance mechanism and was present in 445 (69%) azole-resistant *A. fumigatus* isolates, whereas $TR_{46}$/Y121F/T289A was present in 111 (17%) isolates. Of 445 $TR_{34}$/L98H isolates, 24 had ≥1 additional polymorphisms in the *Cyp51A* gene (F495I, n = 9; Q259H, n = 5; S297T, n = 4; D262N, n = 1; N326H, n = 1; P337L, n = 1; Y341H, n = 1; I364V, n = 1; G328A, n = 1; and L399V, n = 1). In addition, 8 $TR_{34}$/L98H isolates harbored a T67G substitution in the gene promotor region, which has not been associated with azole resistance. TR-mediated resistance mutations are associated with resistance selection in the environment, which thus accounted for 86% of resistance mutations. In 76 azole-resistant isolates (12%), no mutations were found in the *Cyp51A* gene, indicating that other, yet uncharacterized, resistance mechanisms might be present. Over the 6-year observation period, no significant trends in the distribution of resistance mutations was observed (Figure 1).

### Triazole-Resistance Phenotypes

Resistance mutations most commonly affected the activity of all 4 mold-active azoles. Among the 640 azole-resistant *A. fumigatus* isolates, 413 (65%) isolates exhibited a panazole-resistant phenotype, 51 (8%) a multiazole-resistant phenotype, and 176 (28%) resistance to a single azole.

Because voriconazole is the treatment of choice for invasive aspergillosis, the azole resistance phenotypes were categorized according to voriconazole clinical breakpoints. Overall, 498 (77.8%) *A. fumigatus* isolates were voriconazole-resistant (Table 2). Although most voriconazole-resistant isolates exhibited a panazole-resistant phenotype, 50 (10%) voriconazole-resistant isolates were itraconazole-susceptible, of which 8 were also susceptible to posaconazole. Isolated posaconazole susceptibility in voriconazole-resistant isolates was not observed. The underlying resistance mutations detected in these 50 isolates included $TR_{46}$/Y121F/T289A (35 isolates) and G448S (3 isolates), whereas *Cyp51A* mutations were not detected in 12 isolates. All voriconazole-resistant isolates were also resistant to isavuconazole.

In 124 (19%) *A. fumigatus* isolates, a voriconazole MIC of 2 mg/L was measured (Table 2); of these, 120 (97%) were resistant against either itraconazole, posaconazole, or both. The 4 remaining isolates were

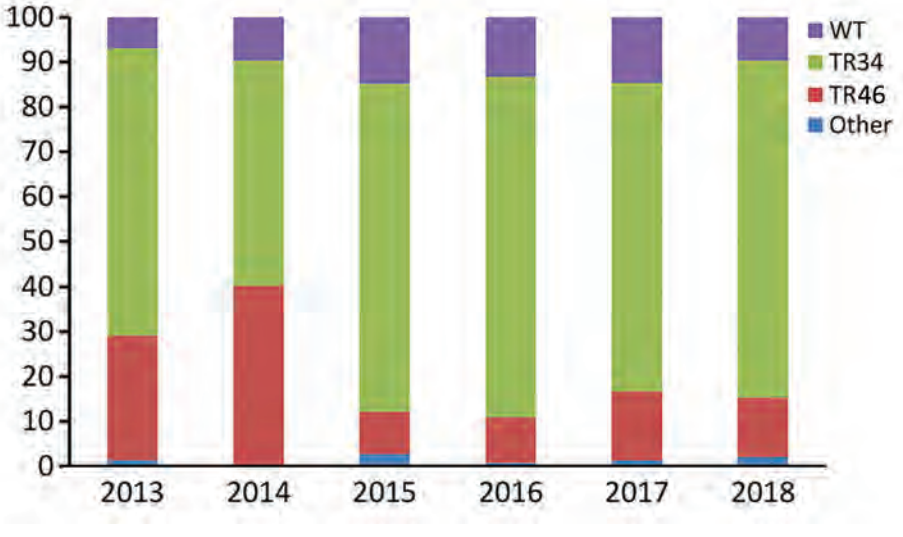


**Figure 1.** Distribution of *Cyp51A*-mediated resistance mutations in *Aspergillus fumigatus*, as observed in a national multicenter surveillance program in the Netherlands, 2013–2018. WT, wildtype *Cyp51A*; TR34, $TR_{34}$/L98H; TR46, $TR_{46}$/Y121F.

**Table 2.** Resistance profiles of 640 azole-resistant *Aspergillus fumigatus* isolates classified according to voriconazole clinical breakpoints in a national multicenter surveillance program in the Netherlands, 2013–2018*

| Voriconazole classification (no. isolates) | No. (%) isolates | | |
|---|---|---|---|
| | Itraconazole | Posaconazole | Isavuconazole |
| Voriconazole-susceptible (18) | | | |
| Susceptible | 0 | 1 (5.6) | 6/16 (37.5) |
| Intermediate | 1 (5.6) | 2 (11.1) | NA |
| Resistant | 17 (94.4) | 15 (83.3) | 10/16 (62.5) |
| Voriconazole-intermediate (124) | | | |
| Susceptible | 0 | 4 (3.2) | 2/121 (1.7) |
| Intermediate | 6 (4.8) | 19 (15.3) | NA |
| Resistant | 118 (95.2) | 101 (81.5) | 119/121 (98.3) |
| Voriconazole-resistant (498) | | | |
| Susceptible | 50 (10) | 8 (1.6) | 0/396 (0) |
| Intermediate | 25 (5) | 28 (5.6) | NA |
| Resistant | 423 (85) | 462 (92.8) | 396/396 (100) |

*Isavuconazole was not measured before 2014; therefore, denominator is different in comparison with itraconazole and posaconazole. NA, not applicable (no intermediate susceptibility category defined for isavuconazole).

itraconazole- and posaconazole-susceptible but isavuconazole-resistant. Three of these isolates harbored the $TR_{34}$/L98H mutation, and in the fourth isolate, no *Cyp51A* mutations were found. An underlying resistance mutation was detected in 99 (80%) of the 124 isolates with voriconazole-intermediate susceptibility.

Overall, 18 (3%) azole-resistant isolates were phenotypically voriconazole-susceptible, although these isolates were resistant to either itraconazole, posaconazole, or both (Table 2). Isavuconazole MICs were available for 16 phenotypically voriconazole-susceptible isolates, and isavuconazole resistance was found in 10 (63%) of these, with a mean isavuconazole MIC of 11 mg/L (range 2 to >16 mg/L). Underlying *Cyp51A*-mediated resistance mutations in these 10 isavuconazole-resistant, voriconazole-susceptible isolates included 6 isolates with a $TR_{34}$/L98H genotype, although in 4 isolates no *Cyp51A* mutations were detected.

$TR_{34}$/L98H is associated with high resistance to itraconazole, which was the case in 438 of 445 (98%) isolates, although $TR_{46}$/Y121F/T289A is associated with high voriconazole resistance, which was found in all 111 $TR_{46}$/Y121F/T289A isolates (Figure 2). Thirty-five of 111 (32%) $TR_{46}$/Y121F/T289A isolates were susceptible to itraconazole, although 3 of these isolates were also susceptible to posaconazole.

### Trends in Voriconazole Resistance

In 2013, voriconazole resistance was detected in 94% (68/72) of azole-resistant *A. fumigatus* isolates, but in 2018 voriconazole resistance was detected for only 60% (87/144) azole-resistant *A. fumigatus* isolates (p = 0.0001) (Figure 3). The trend toward lower voriconazole MICs was not attributable to a shift in resistance mutations but was apparent mainly in isolates harboring $TR_{34}$/L98H (Figure 4, panel A). Voriconazole MIC distributions were significantly different when 2013 (mean voriconazole MIC 8 mg/L) was compared with 2018 (mean voriconazole MIC 2 mg/L) (p<0.001). In 2013, 2 (4%) of 46 $TR_{34}$/L98H isolates were not classified as voriconazole-resistant, whereas 49 (4%) of 108 (45%) $TR_{34}$/L98H isolates exhibited a voriconazole-nonresistant phenotype in 2018 (p = 0.0001), of which most exhibited a MIC of 2 mg/L (intermediate). Because a F495I mutation in $TR_{34}$/L98H isolates was shown to be associated with reduced resistance to voriconazole (*16*), all 106 voriconazole-nonresistant $TR_{34}$/L98H isolates were checked for the presence of this mutation. Only 8 $TR_{34}$/L98H isolates were found to harbor the F495I mutation.

Because MIC testing was performed on receipt of the isolate over a 6-year period and thus involved various batches of MIC plates, all 46 $TR_{34}$/L98H isolates from 2013 and 106 isolates (2 isolates were not available) from 2018 were retested for voriconazole and isavuconazole by using a single batch of MIC plates. Retesting confirmed the initial observation showing a 45% lower voriconazole-resistance frequency among $TR_{34}$/L98H isolates in 2018 compared with 2013 (46/46 in 2013 vs. 58/106 in 2018; p = 0.0001) (Appendix Figure, https://wwwnc.cdc.gov/EID/article/26/7/20-0088-App1.pdf). In 2013, the overall azole-resistance frequency was 7.6% at the patient level and voriconazole-resistance frequency was 7.2%, whereas in 2018 the azole-resistance frequency was 14.7% compared with 8.8% voriconazole resistance (Table 1 [estimated voriconazole resistance frequencies not shown]).

We observed a similar decreasing trend of MICs for isavuconazole (Figure 4, panel B; Appendix Figure). However, the decrease in MICs did not result in an increase of susceptible isolates because all but 2 $TR_{34}$/L98H isolates remained isavuconazole-resistant based on the EUCAST breakpoint. The isavuconazole MIC distributions were significantly different when

the distribution of 2015 was compared with that of 2018 (p<0.001). No trends in phenotype changes were observed for itraconazole and posaconazole.

## Discussion

Our resistance surveillance showed an increasing frequency of azole resistance in clinical *A. fumigatus* isolates during 2013–2018 in the Netherlands. Although the resistance frequency varied between the 5 UMCs, the increasing trend was observed in all centers. In 2017 and 2018, the azole-resistance frequency exceeded 10% in all centers, a threshold above which experts recommend reconsidering the use of first-line voriconazole monotherapy (*17*,*18*). Alternative regimens that cover resistance include voriconazole/isavuconazole in combination with liposomal-AmB or an echinocandin, or monotherapy with liposomal-AmB. As such, the Netherlands national guideline was revised and now recommends combination therapy in patients with suspected invasive aspergillosis, in particular for critically ill patients or when azole resistance cannot be excluded (*19*).

How the 10% resistance threshold should be determined remains unclear (*17*,*18*). Our study indicated that despite the increasing azole-resistance frequency, the resistance frequency of voriconazole remained below this threshold (8.8% in 2018). This observation warrants the question of which threshold (i.e., azole resistance or voriconazole resistance) should be used to guide decisions regarding primary treatment choices. The trend toward lower voriconazole MICs was observed mainly in $TR_{34}$/L98H isolates, whereas most nonresistant isolates exhibited a voriconazole MIC of 2 mg/L (intermediate). The optimal management of voriconazole-intermediate invasive aspergillosis remains unclear, but an increased failure rate is anticipated in patients treated with voriconazole monotherapy at the standard dose. An increased voriconazole trough level target of 2–6 mg/L is recommended or combining voriconazole with an echinocandin or liposomal-AmB monotherapy (*18*). Furthermore, there is currently insufficient evidence that infection caused by azole-susceptible or intermediate susceptible *A. fumigatus* isolates that harbor a resistance mutation can safely be treated with azole monotherapy.

Resistance was highly dominated by environmental resistance mutations, such as $TR_{34}$/L98H and $TR_{46}$/Y121F/T289A. Indeed, a recent study identified sites at high risk for resistance selection in the environment, referred to as hotspots (*20*). Particularly, stockpiling of decaying plant waste containing azole fungicide residues was found to harbor high numbers of resistant *A. fumigatus*, and isolates with identical resistance mutations to those recovered from clinical specimens were cultured from these hotspots (*20*,*21*). The observations support a strong link between environmental resistance selection and azole-resistant disease in humans. The increasing trend in azole-resistance frequency and the emergence of new resistance mutations indicate that the current use of azole fungicides is not sustainable and over time the medical use of azoles will be further

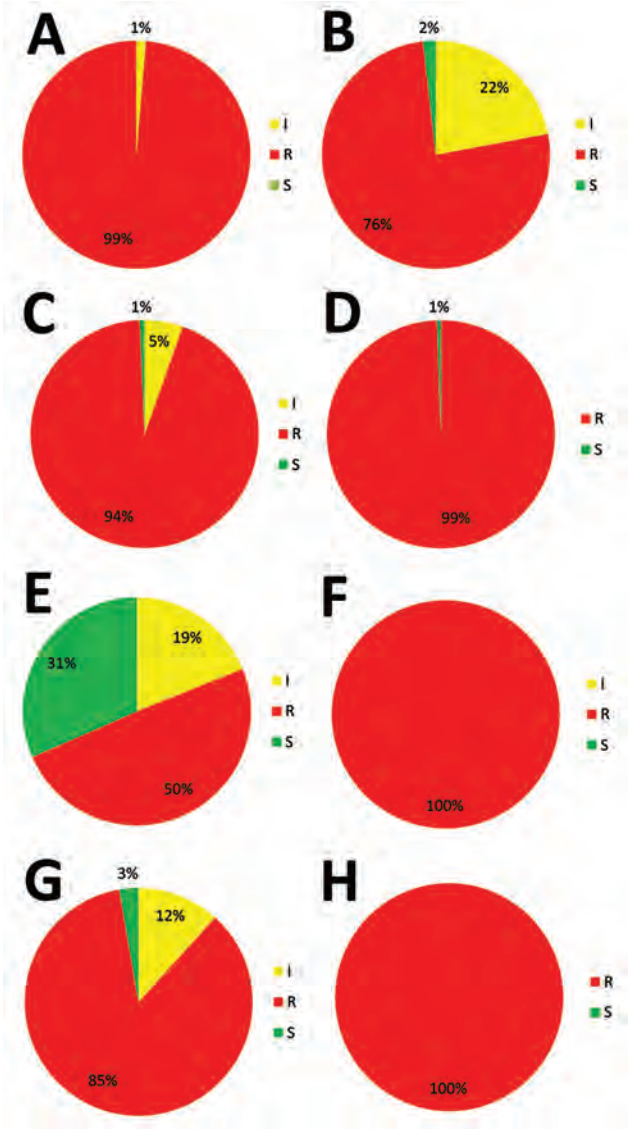


**Figure 2.** Triazole-resistance classification in 555 *Aspergillus fumigatus* isolates harboring $TR_{34}$/L98H and $TR_{46}$/Y121F/T289A resistance mutations, as observed in a national multicenter surveillance program in the Netherlands, 2013–2018. A) Itraconazole $TR_{34}$/L98H. B) Voriconazole $TR_{34}$/L98H. C) Posaconazole $TR_{34}$/L98H. D) Isavuconazole $TR_{34}$/L98H. E) Itraconazole $TR_{46}$/Y121F/T289A. F) Voriconazole, $TR_{46}$/Y121F/T289A. G) Posaconazole $TR_{46}$/Y121F/T289A. H) Isavuconazole $TR_{46}$/Y121F/T289A. I, intermediate; R, resistant; S, susceptible.

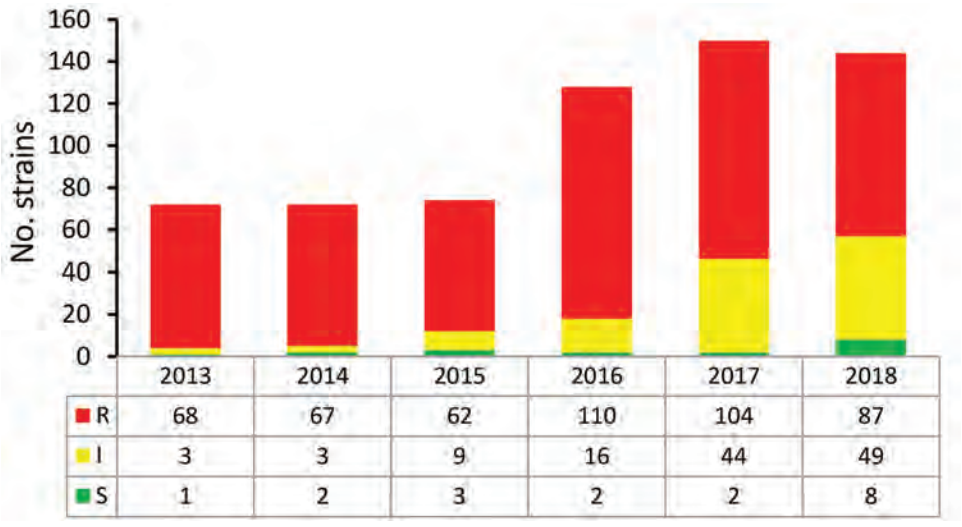


| | 2013 | 2014 | 2015 | 2016 | 2017 | 2018 |
|---|---|---|---|---|---|---|
| R | 68 | 67 | 62 | 110 | 104 | 87 |
| I | 3 | 3 | 9 | 16 | 44 | 49 |
| S | 1 | 2 | 3 | 2 | 2 | 8 |

**Figure 3.** Trends in voriconazole-susceptibility classification of 640 *Aspergillus fumigatus* isolates, by year, as observed in a national multicenter surveillance program in the Netherlands, 2013–2018. I, intermediate; R, resistant; S, susceptible.

threatened. Given the limited alternative treatment options for *Aspergillus* diseases, further research aimed at reducing the burden of azole resistance in the environment is urgently needed.

An important question is how the changing voriconazole phenotype in $TR_{34}$/L98H isolates can be explained. One possibility is that $TR_{34}$/L98H isolates harbor additional mechanisms or compensatory mutations that affect the overall azole-resistance phenotype. Additional changes in peptide sequence of the 14-α-sterol demethylase enzyme have been reported in $TR_{34}$/L98H isolates, such as F495I, which confers resistance to imidazole (*16*). Recombination experiments showed that recombinants with S297T/F495I in the $TR_{34}$/L98H background conferred high resistance to imidazole but also produced lower voriconazole MICs compared with the $TR_{34}$/L98H parent strain (*16*). Because $TR_{34}$ isolates originate in the environment through exposure to azole fungicides, changes in azole fungicide exposures could prompt changes in resistance phenotypes. However, only 9 isolates with an additional F495I mutation in the *Cyp51A* gene were found, of which 8 were voriconazole-susceptible, indicating that other or multiple factors might have contributed to the observed phenotype change.

Another possibility is the presence of other resistance mechanisms in $TR_{34}$/L98H isolates. Recent studies analyzing transcriptional control mechanisms of *Cyp51A*, have identified transcription factors, such as ABC transporter regulator, which was found to regulate many different processes involved in drug resistance, metabolism, and virulence (*22*). Furthermore, other steps in the ergosterol biosynthesis might be affected, for example, through mutations in the 3-hydroxy-3-methyl-glutaryl-coenzyme A reductase-encoding gene (*hmg1*) (*23*). Mutations in the *hmg1* gene resulting in peptide sequence changes were found to be frequent in $TR_{34}$/L98H isolates, possibly affecting the azole phenotype (*23*). These recent insights indicate that the resistance phenotype is likely to be multifactorial and that more research is needed to characterize possible mechanisms that explain the observed variation in $TR_{34}$/L98H phenotypes.

The main clinical implication of the observed phenotypic variation in $TR_{34}$/L98H relates to direct detection of resistance mutations through PCR tests. Several commercial PCR tests are available that enable detection of $TR_{34}$/L98H and $TR_{46}$/Y121F/T289A directly in clinical specimens (*24*,*25*), which are used to guide selection of antifungal drugs. However, this approach can only be used if the resistance genotype predicts the azole phenotype. Although $TR_{46}$/Y121F/T289A mutation detection is uniformly associated with resistance to voriconazole, the wide spectrum of voriconazole MICs in $TR_{34}$/L98H isolates hampers the use of direct detection of this mutation because voriconazole therapy might be withheld in cases of voriconazole-susceptible infection. However, as stated previously, the efficacy of voriconazole in voriconazole-susceptible and voriconazole-intermediate $TR_{34}$/L98H infection would need to be investigated before any treatment recommendations involving azole monotherapy can be implemented.

Our resistance surveillance had several limitations. All *A. fumigatus* isolates cultured from clinical specimens were screened for azole resistance, involving diverse patient groups and isolates not regarded clinically relevant. Including all isolates has the advantage of collecting a meaningful number

of isolates, but the resistance frequency might not be representative for specific patient groups such as those with invasive aspergillosis. Furthermore, within hospitals the resistance frequency might vary between years (*26*), thus further complicating establishing a meaningful (local) resistance frequency. Another limitation was the lack of clinical information and *Aspergillus* disease classification. Such information would be more suitable to guide treatment decisions and local antifungal guidelines, but gathering the data is laborious, given that all aspergillosis cases need to be identified and classified. Various cohort studies have been performed in the Netherlands showing differences in resistance rates between patient groups. A resistance frequency of 26% (10 of 38 patients) was reported in *A. fumigatus* culture-positive intensive-care unit patients in a single hospital (*27*) and 29% (4 of 14 patients) in a national study of intensive-care unit patients with influenza-associated aspergillosis (*2*). In contrast, a low resistance frequency was reported in a 5 year single-center cohort of patients with hematologic malignancy (*28*), but the culture-positivity rate was only 6% and thus, in most patients, the presence of resistance remained unknown. To date, only few studies have determined the frequency of resistance mutations in culture-negative patients. In 1 study, the rate was found to be similar to that observed in culture-positive patients (*29*), although higher resistance rates were reported in culture-negative patients in comparison with the rates found by culture in another study on patients with chronic rather than acute invasive aspergillosis (*30*). Differences could be explained in part by coincidence because the number of cases in these single-center studies is small. Another explanation might be the number of *A. fumigatus* colonies that were tested for resistance, given that clinical cultures might contain azole-susceptible and azole-resistant colonies in cases of mixed infection (*31*,*32*).

In conclusion, azole resistance in *A. fumigatus* has been reported worldwide and provides major

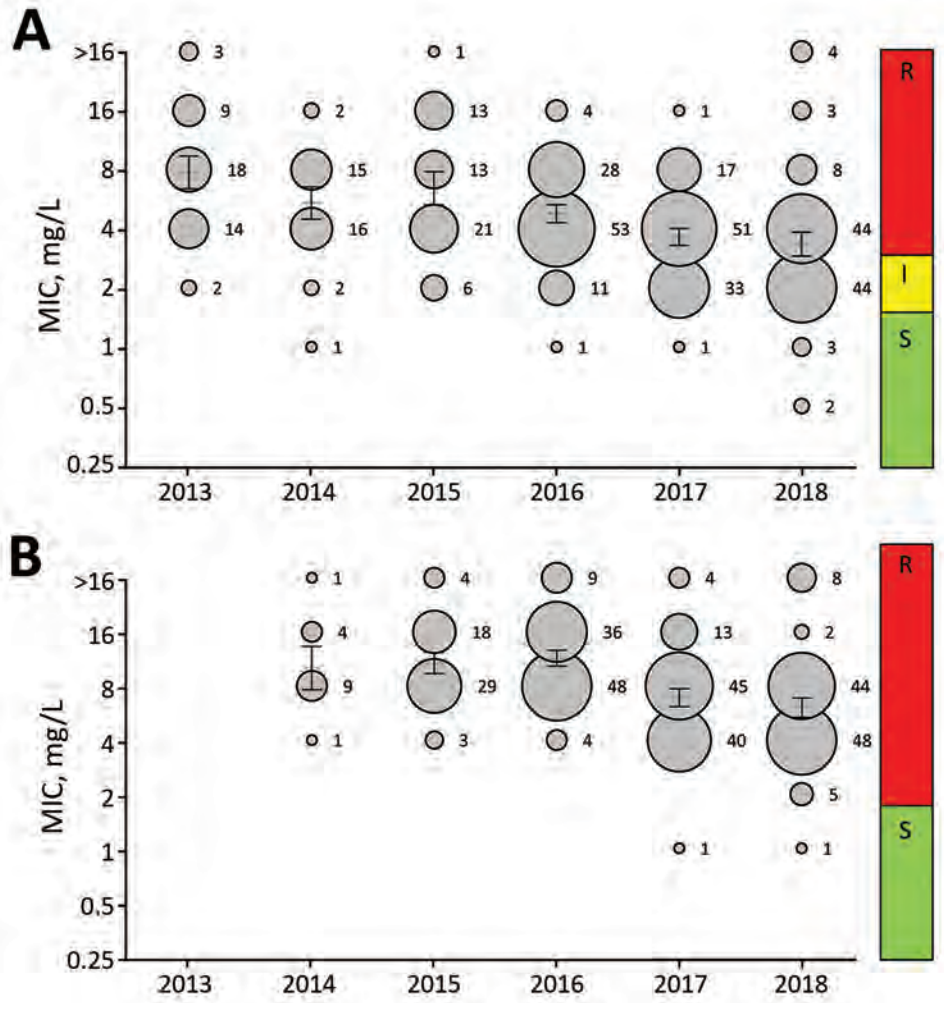


**Figure 4.** Trends in voriconazole (A) and isavuconazole (B) MIC distributions in *Aspergillus fumigatus* harboring $TR_{34}$/L98H, as observed in a national multicenter surveillance program in the Netherlands, 2013–2018. MIC distribution is displayed as a bubble graph for each year, where the diameter corresponds with the number of isolates with the corresponding MIC. The number of isolates is presented for each MIC. Mean MIC with 95% CIs are plotted for each year as a line with error bars. The clinical interpretation is shown on the right of the diagram. I, intermediate; R, resistant; S, susceptible.

challenges regarding management of invasive aspergillosis and other *Aspergillus* diseases (*9*,*32*). Nevertheless, *A. fumigatus* is not included in global action plans to combat antimicrobial resistance (*33*), and no international surveillance programs monitor resistance in *A. fumigatus.* As a consequence, the presence and frequency of azole resistance remains unknown in most countries (*34*,*35*). Despite the challenges we face in performing resistance surveillance in *A. fumigatus*, our national surveillance has proved important to guide the national treatment guideline and provided insights in trends in resistance genotypes and phenotypes. Furthermore, continued surveillance will help to monitor effects of interventions aimed at reducing the resistance burden in the environment. We believe that global *A. fumigatus* resistance surveillance programs are warranted and should be implemented in initiatives to combat antimicrobial resistance.

### Acknowledgments

We thank our mycology technicians for their dedicated work.

### About the Author

Mr. Lestrade currently works in VieCuri Medical Centre as a clinical microbiologist. His primary research interest is triazole resistance in *Aspergillus fumigatus*.

### References

1. Ghez D, Calleja A, Protin C, Baron M, Ledoux MP, Damaj G, et al.; French Innovative Leukemia Organization (FILO) CLL group. Early-onset invasive aspergillosis and other fungal infections in patients treated with ibrutinib. Blood. 2018; 131:1955–9. https://doi.org/10.1182/blood-2017-11-818286
2. van de Veerdonk FL, Kolwijck E, Lestrade PPA, Hodiamont CJ, Rijnders BJA, van Paassen J, et al.; Dutch Mycoses Study Group. Influenza-associated aspergillosis in critically ill patients. Am J Respir Crit Care Med. 2017;196:524–7. https://doi.org/10.1164/rccm.201612-2540LE
3. Schauwvlieghe AFAD, Rijnders BJA, Philips N, Verwijs R, Vanderbeke L, Van Tienen C, et al.; Dutch-Belgian Mycosis Study Group. Invasive aspergillosis in patients admitted to the intensive care unit with severe influenza: a retrospective cohort study. Lancet Respir Med. 2018;6:782–92. https://doi.org/10.1016/S2213-2600(18)30274-1
4. Kosmidis C, Denning DW. The clinical spectrum of pulmonary aspergillosis. Thorax. 2015;70:270–7. https://doi.org/10.1136/thoraxjnl-2014-206291
5. Verweij PE, Chowdhary A, Melchers WJG, Meis JF. Azole resistance in *Aspergillus fumigatus*: can we retain the clinical use of mold-active antifungal azoles? Clin Infect Dis. 2016;62:362–8. https://doi.org/10.1093/cid/civ885
6. Snelders E, van der Lee HAL, Kuijpers J, Rijs AJMM, Varga J, Samson RA, et al. Emergence of azole resistance in *Aspergillus fumigatus* and spread of a single resistance mechanism. PLoS Med. 2008;5:e219. https://doi.org/10.1371/journal.pmed.0050219
7. van der Linden JWM, Snelders E, Kampinga GA, Rijnders BJA, Mattsson E, Debets-Ossenkopp YJ, et al. Clinical implications of azole resistance in *Aspergillus fumigatus*, the Netherlands, 2007–2009. Emerg Infect Dis. 2011;17:1846–54. https://doi.org/10.3201/eid1710.110226
8. Lestrade PPA, Bentvelsen RG, Schauwvlieghe AFAD, Schalekamp S, van der Velden WJFM, Kuiper EJ, et al. Voriconazole resistance and mortality in invasive aspergillosis: a multicenter retrospective cohort study. Clin Infect Dis. 2019;68:1463–71. https://doi.org/10.1093/cid/ciy859
9. Buil JB, Zoll J, Verweij PE, Melchers WJG. Molecular detection of azole-resistant *Aspergillus fumigatus* in clinical samples. Front Microbiol. 2018;9:515. https://doi.org/10.3389/fmicb.2018.00515
10. US Centers for Disease Control and Prevention. Antibiotic resistance threats in the United States 2019 [cited 2019 Nov 29]. https://www.cdc.gov/drugresistance/pdf/threats-report/2019-ar-threats-report-508.pdf
11. Arendrup MC, Verweij PE, Mouton JW, Lagrou K, Meletiadis J. Multicentre validation of 4-well azole agar plates as a screening method for detection of clinically relevant azole-resistant *Aspergillus fumigatus*. J Antimicrob Chemother. 2017;72:3325–33. https://doi.org/10.1093/jac/dkx319
12. Hope WW, Cuenca-Estrella M, Lass-Flörl C, Arendrup MC; European Committee on Antimicrobial Susceptibility Testing Subcommittee on Antifungal Susceptibility Testing. EUCAST technical note on voriconazole and *Aspergillus spp.* Clin Microbiol Infect. 2013;19:E278–80. https://doi.org/10.1111/1469-0691.12148
13. Arendrup MC, Meletiadis J, Mouton JW, Guinea J, Cuenca-Estrella M, Lagrou K, et al.; Subcommittee on Antifungal Susceptibility Testing of the ESCMID European Committee for Antimicrobial Susceptibility Testing. EUCAST technical note on isavuconazole breakpoints for *Aspergillus*, itraconazole breakpoints for *Candida* and updates for the antifungal susceptibility testing method documents. Clin Microbiol Infect. 2016;22:571.e1–4. https://doi.org/10.1016/j.cmi.2016.01.017
14. Arendrup MC, Cuenca-Estrella M, Lass-Flörl C, Hope WW; European Committee on Antimicrobial Susceptibility Testing Subcommittee on Antifungal Susceptibility Testing. EUCAST technical note on *Aspergillus* and amphotericin B, itraconazole, and posaconazole. Clin Microbiol Infect. 2012; 18:E248–50. https://doi.org/10.1111/j.1469-0691.2012.03890.x
15. de Greeff SC, Mouton JW, Schoffelen AF, Verduin CM. Nethmap 2019: consumption of antimicrobial agents and antimicrobial resistance among medically important bacteria in the Netherlands [cited 2019 Nov 29]. https://www.rivm.nl/publicaties/nethmap-2019-consumption-of-antimicrobial-agents-and-antimicrobial-resistance-among
16. Chen Y, Li Z, Han X, Tian S, Zhao J, Chen F, et al. Elevated MIC values of imidazole drugs against *Aspergillus fumigatus* isolates with $TR_{34}$/L98H/S297T/F495I mutation. Antimicrob Agents Chemother. 2018;62:1–10. https://doi.org/10.1128/AAC.01549-17
17. Verweij PE, Ananda-Rajah M, Andes D, Arendrup MC, Brüggemann RJ, Chowdhary A, et al. International expert opinion on the management of infection caused by azole-resistant *Aspergillus fumigatus*. Drug Resist Updat. 2015;21–22:30–40. https://doi.org/10.1016/j.drup.2015.08.001
18. Ullmann AJ, Aguado JM, Arikan-Akdagli S, Denning DW, Groll AH, Lagrou K, et al. Diagnosis and management of *Aspergillus* diseases: executive summary of the 2017

ESCMID-ECMM-ERS guideline. Clin Microbiol Infect. 2018; 24(Suppl 1):e1–38. https://doi.org/10.1016/j.cmi.2018.01.002
19. Stichting Werkgroep AntibioticaBeleid. SWAB guidelines for the management of invasive fungal infections [cited 2019 Nov 29]. https://swab.nl/richtlijnen
20. Schoustra SE, Debets AJM, Rijs AJMM, Zhang J, Snelders E, Leendertse PC, et al. Environmental hotspots for azole resistance selection of *Aspergillus fumigatus*, the Netherlands. Emerg Infect Dis. 2019;25:1347–53. https://doi.org/10.3201/eid2507.181625
21. Zhang J, Snelders E, Zwaan BJ, Schoustra SE, Meis JF, van Dijk K, et al. A novel environmental azole resistance mutation in *Aspergillus fumigatus* and a possible role of sexual reproduction in its emergence. MBio. 2017;8:e00791–17. https://doi.org/10.1128/mBio.00791-17
22. Paul S, Stamnes M, Thomas GH, Liu H, Hagiwara D, Gomi K, et al. AtrR is an essential determinant of azole resistance in *Aspergillus fumigatus*. MBio. 2019;10:1–19. https://doi.org/10.1128/mBio.02563-18
23. Rybak JM, Ge W, Wiederhold NP, Parker JE, Kelly SL, Rogers PD, et al. Mutations in *hmg1*, challenging the paradigm of clinical triazole resistance in *Aspergillus fumigatus*. MBio. 2019;10:1–19. https://doi.org/10.1128/mBio.00437-19
24. Dannaoui E, Gabriel F, Gaboyard M, Lagardere G, Audebert L, Quesne G, et al. Molecular diagnosis of invasive aspergillosis and detection of azole resistance by a newly commercialized PCR kit. J Clin Microbiol. 2017;55:3210–8. https://doi.org/10.1128/JCM.01032-17
25. Chong GM, van der Beek MT, von dem Borne PA, Boelens J, Steel E, Kampinga GA, et al. PCR-based detection of *Aspergillus fumigatus Cyp51A* mutations on bronchoalveolar lavage: a multicentre validation of the AsperGenius assay® in 201 patients with haematological disease suspected for invasive aspergillosis. J Antimicrob Chemother. 2016;71:3528–35. https://doi.org/10.1093/jac/dkw323
26. Buil JB, Snelders E, Denardi LB, Melchers WJG, Verweij PE. Trends in azole resistance in *Aspergillus fumigatus*, the Netherlands, 1994–2016. Emerg Infect Dis. 2019;25:176–8. https://doi.org/10.3201/eid2501.171925
27. van Paassen J, Russcher A, In 't Veld-van Wingerden AW, Verweij PE, Kuijper EJ. Emerging aspergillosis by azole-resistant *Aspergillus fumigatus* at an intensive care unit in the Netherlands, 2010 to 2013. Euro Surveill. 2016;21:30300. https://doi.org/10.2807/1560-7917.ES.2016.21.30.30300
28. Lestrade PP, van der Velden WJFM, Bouwman F, Stoop FJ, Blijlevens NMA, Melchers WJG, et al. Epidemiology of invasive aspergillosis and triazole-resistant *Aspergillus fumigatus* in patients with haematological malignancies: a single-centre retrospective cohort study. J Antimicrob Chemother. 2018;73:1389–94. https://doi.org/10.1093/jac/dkx527
29. Montesinos I, Argudín MA, Hites M, Ahajjam F, Dodémont M, Dagyaran C, et al. Culture-based methods and molecular tools for azole-resistant *Aspergillus fumigatus* detection in a Belgian university hospital. J Clin Microbiol. 2017;55:2391–9. https://doi.org/10.1128/JCM.00520-17
30. Denning DW, Park S, Lass-Florl C, Fraczek MG, Kirwan M, Gore R, et al. High-frequency triazole resistance found in nonculturable *Aspergillus fumigatus* from lungs of patients with chronic fungal disease. Clin Infect Dis. 2011;52:1123–9. https://doi.org/10.1093/cid/cir179
31. Ahmad S, Joseph L, Hagen F, Meis JF, Khan Z. Concomitant occurrence of itraconazole-resistant and -susceptible strains of *Aspergillus fumigatus* in routine cultures. J Antimicrob Chemother. 2015;70:412–5. https://doi.org/10.1093/jac/dku410
32. Kolwijck E, van der Hoeven H, de Sévaux RGL, ten Oever J, Rijstenberg LL, van der Lee HAL, et al. Voriconazole-susceptible and voriconazole-resistant *Aspergillus fumigatus* coinfection. Am J Respir Crit Care Med. 2016;193:927–9. https://doi.org/10.1164/rccm.201510-2104LE
33. World Health Organization. Global action plan on antimicrobial resistance [cited 2019 Nov 29]. https://www.who.int/antimicrobial-resistance/global-action-plan
34. van der Linden JWM, Arendrup MC, Warris A, Lagrou K, Pelloux H, Hauser PM, et al. Prospective multicenter international surveillance of azole resistance in *Aspergillus fumigatus*. Emerg Infect Dis. 2015;21:1041–4. https://doi.org/10.3201/eid2106.140717
35. Lestrade PPA, Meis JF, Melchers WJG, Verweij PE. Triazole resistance in *Aspergillus fumigatus*: recent insights and challenges for patient management. Clin Microbiol Infect. 2019;25:799–806. https://doi.org/10.1016/j.cmi.2018.11.027

Address for correspondence: Paul E. Verweij, Medical Microbiology, Internal postal code: 777, Geert Grooteplein 10, 6525 GA Nijmegen, the Netherlands; email: paul.verweij@radboudumc.nl

# Large Nationwide Outbreak of Invasive Listeriosis Associated with Blood Sausage, Germany, 2018–2019

Sven Halbedel,[1] Hendrik Wilking,[1] Alexandra Holzer, Sylvia Kleta, Martin A. Fischer, Stefanie Lüth, Ariane Pietzka, Steliana Huhulescu, Raskit Lachmann, Amrei Krings, Werner Ruppitsch, Alexandre Leclercq, Rolf Kamphausen, Maylin Meincke, Christiane Wagner-Wiening, Matthias Contzen, Iris Barbara Kraemer, Sascha Al Dahouk, Franz Allerberger, Klaus Stark,[2] Antje Flieger[2]

Invasive listeriosis is a severe foodborne infection in humans and is difficult to control. Listeriosis incidence is increasing worldwide, but some countries have implemented molecular surveillance programs to improve recognition and management of listeriosis outbreaks. In Germany, routine whole-genome sequencing, core genome multilocus sequence typing, and single nucleotide polymorphism calling are used for subtyping of *Listeria monocytogenes* isolates from listeriosis cases and suspected foods. During 2018–2019, an unusually large cluster of *L. monocytogenes* isolates was identified, including 134 highly clonal, benzalkonium-resistant sequence type 6 isolates collected from 112 notified listeriosis cases. The outbreak was one of the largest reported in Europe during the past 25 years. Epidemiologic investigations identified blood sausage contaminated with *L. monocytogenes* highly related to clinical isolates; withdrawal of the product from the market ended the outbreak. We describe how epidemiologic investigations and complementary molecular typing of food isolates helped identify the outbreak vehicle.

Listeriosis is a severe, mainly foodborne, human infection associated with higher case-fatality and hospitalization rates than other bacterial gastrointestinal pathogens (*1*). The causative agent, *Listeria monocytogenes*, occurs ubiquitously in the environment and disseminates into the food production chain. Patients develop either self-limiting noninvasive gastroenteritis or invasive listeriosis (*2*,*3*). Listeriosis adversely affects older and immunocompromised persons, as well as pregnant women, causing a severe invasive form of the disease that leads to sepsis, meningitis, and encephalitis, as well as neonatal infections and miscarriage (*4*). Case-fatality rates of invasive listeriosis are ≈30% for neurolisteriosis and even higher in septic patients (*5*). In Europe and North America, invasive listeriosis affects 0.3–0.6 persons/100,000 population/year (*6*,*7*).

*L. monocytogenes* forms hard-to-remove biofilms in food-processing plants, can acquire tolerance to sanitizers, and multiplies even at temperatures used for refrigeration (*8*). These properties complicate efficient prevention of *L. monocytogenes* contaminations in different types of ready-to-eat products, including dairy, meat, and fish, and in fruits and vegetables, all of which have been vehicles for listeriosis outbreaks in the past (*9*–*12*).

Author affiliations: Robert Koch Institute, Wernigerode, Germany (S. Halbedel, M.A. Fischer, A. Flieger); Robert Koch Institute, Berlin, Germany (H. Wilking, A. Holzer, R. Lachmann, A. Krings, M. Meincke, K. Stark); German Federal Institute for Risk Assessment, Berlin (S. Kleta, S. Lüth, S.A. Dahouk); Freie Universität Berlin, Berlin (S. Lüth); Austrian Agency for Health and Food Safety, Vienna, Austria (A. Pietzka, S. Huhulescu, W. Ruppitsch, F. Allerberger); European Centre for Disease Prevention and Control, Stockholm, Sweden (A. Krings, M. Meincke); Institut Pasteur, Paris, France (A. Leclercq); Ministry for Environment, Agriculture, Conservation and Consumer Protection of the State of North Rhine-Westphalia, Düsseldorf, Germany (R. Kamphausen); State Health Office Baden-Wuerttemberg, Stuttgart, Germany (M. Meincke, C. Wagner-Wiening); Chemical and Veterinary Investigations Office, Fellbach, Germany (M. Contzen); Bavarian Health and Food Safety Authority, Oberschleißheim, Germany (I.B. Kraemer); Rheinisch-Westfälische Technische Hochschule, Aachen, Germany (S.A. Dahouk)

DOI: https://doi.org/10.3201/eid2607.200225

[1]These authors contributed equally to this article.

[2]These authors contributed equally to this article.

Outbreaks of listeriosis are difficult to control for several reasons. First, case numbers are low, impairing the generation of valid hypotheses about possible food sources through patient interviews. Second, incubation time can be long, 1–67 days (*13*), and patients often are seriously ill, further complicating patient interviews. Third, the large variety of possible food sources makes pinpointing through patient interviews and follow-up tracing of food difficult. Moreover, listeriosis outbreaks can be geographically widespread due to long-distance food trade connections, e-commerce, and travel, thus hampering outbreak recognition by local authorities (*10*,*14*,*15*). In addition, listeriosis outbreaks can be protracted and last for several years (*16*), making it difficult to correctly identify affected patient groups and the common source of infection.

Nationwide systematic collection of *L. monocytogenes* isolates from human listeriosis cases and subtyping by using high-resolution whole-genome sequencing (WGS)–based typing techniques can aid in rapid and reliable detection of outbreak clusters (*3*,*17*–*22*), some of which were not detectable in the past. At the same time, systematic and on-demand typing of food-associated *L. monocytogenes* isolates assist in detecting outbreak sources. In a recent molecular surveillance study in France, one third of all isolates were grouped into WGS clusters, and most clusters contained <5 isolates (*20*). Larger outbreaks of invasive listeriosis occur, although infrequently, and 2 of the world's largest outbreaks in the recent past included 147 cases in a multistate outbreak associated with cantaloupes in the United States in 2011 (*10*) and 1,060 cases in an outbreak associated with French polony sausage in South Africa during 2017–2018 (*11*). Since August 2019, Spain has been experiencing another large listeriosis outbreak (*23*), but the scientific evaluation of this outbreak is ongoing.

We describe an exceptionally large nationwide outbreak that included 134 laboratory-confirmed *L. monocytogenes* isolates from 112 patients with epidemiologic investigations and complementary WGS-based typing of food isolates identifying the outbreak vehicle. This outbreak represents one of the largest outbreaks of invasive listeriosis in Europe documented in the scientific literature during the past 25 years.

## Methods and Materials

### Isolation, Growth, and Serotyping of *L. monocytogenes*

We isolated *L. monocytogenes* from 184 specimens from human cases and food sources (Appendix Table 1, http://wwwnc.cdc.gov/EID/article/26/7/20-0225-App1.pdf). We performed routine *L. monocytogenes* cultures in brain heart infusion (BHI) broth, or on BHI or sheep blood agar plates at 37°C. We detected and enumerated *L. monocytogenes* from food samples according to International Organization for Standardization (ISO) methods EN ISO 11290–1:2017 and EN ISO 11290–2:2017 (*24*,*25*). We confirmed the species by using EN ISO 11290–1:2017 or matrix-assisted laser desorption/ionization time-of-flight mass spectrometry, and a previously described multiplex PCR (*26*). We used the GenElute Bacterial Genomic DNA Kit (SigmaAldrich, https://www.sigmaaldrich.com) or the QIAamp DNA Mini Kit (QIAGEN, https://www.qiagen.com) to isolate chromosomal DNA and determined molecular serogroups by using multiplex PCR (*27*).

### Genome Sequencing, Multilocus Sequence Typing, and Core Genome MLST

We quantified DNA by using the Qubit dsDNA BR or HS Assay Kit and Qubit fluorometers (Invitrogen, https://www.thermofisher.com). We prepared libraries by using the Nextera XT DNA Library Prep Kit (Illumina, https://www.illumina.com) and sequenced isolates on MiSeq, HiSeq, or NextSeq sequencers (Illumina). We trimmed and assembled raw reads in SeqSphere (Ridom, https://www.ridom.de) by using the Velvet assembler. We extracted in silico serogroups, multilocus sequence types (STs), and 1,701 locus core genome multilocus sequence typing (cgMLST) complex types (CTs) by using SeqSphere and automated allele submission to the *L. monocytogenes* cgMLST server (http://www.cgmlst.org/ncs/schema/690488) (*28*). We deposited genome sequences in the European Nucleotide Archive (https://www.ebi.ac.uk/ena; accession numbers in Appendix Table 1). Coverage ranged between 22- and 116-fold (median 54-fold). We defined cgMLST clusters as groups of isolates with ≤10 different alleles between neighboring isolates. We used SeqSphere in the pairwise ignore missing values mode and an unweighted pair group method with arithmetic mean to generate phylogenetic trees.

### Single-Nucleotide Polymorphism–Based Alignments

We used pipelines developed in-house to map sequencing reads, generate consensus sequences, calculate alignment, and filter single-nucleotide polymorphisms (SNPs) using an exclusion distance of 300 bps (*17*). We used the 10-092876-0769 LM12 genome (GenBank accession no. CP019625) a member of serogroup IVb, ST6, and CT6304, as the reference. We

generated maximum likelihood trees by using the Geneious 9.1.3 Tree Builder (https://www.geneious.com) and the randomized axelerated maximum likelihood plugin.

### Virulome and Resistome Analyses and Susceptibility Testing

We included virulence and resistance genes of *L. monocytogenes* as target loci in SeqSphere task templates, as previously described (*17*,*29*). We extracted targets from assembled contigs by using SeqSphere and considered alleles present when identity was >90% and the query sequence aligned ≥99% with the reference sequence.

We performed antimicrobial drug susceptibility testing by using a microdilution assay in a 96-well plate format adapted from a study by Noll et al. (*30*). All susceptibility testing was performed in accordance with European Committee on Antimicrobial Susceptibility Testing guidelines in Mueller Hinton fastidious (MH-F) broth (*31*).

We spread *L. monocytogenes* isolates on BHI agar plates and placed 6 mm cellulose discs loaded with 10 μL of a 10 mg/mL aqueous benzalkonium chloride solution on top of the agar plate. We incubated plates at 37°C overnight, then determined growth inhibition zone diameters. We used the Student *t*-test to assess statistical significance.

### Case-Control Study

We defined outbreak cases as patients reported to public health authorities with disease onset during August 2018–June 2019 and isolation of *L. monocytogenes* from normally sterile body fluids and confirmation by cgMLST and SNP analysis. *L. monocytogenes* isolates were sent to the Robert Koch Institute (Wernigerode, Germany) and notification and typing data were merged for investigation. After the outbreak was identified, patients were interviewed by using a standardized questionnaire on food consumption during the 2 weeks before illness onset, general eating habits, and food purchasing behaviors. These data identified 40 food items for inclusion in the case-control study.

We collaborated with a survey institute to contact and interview case-controls. We frequency matched case-controls to case-patients for age, gender, and federal state of residence. We considered food items with $p \leq 0.05$ consumed by ≥50% of participants for multivariable analysis. We used a stepwise-backward approach for model formation to consecutively exclude food items that were no longer significantly associated from the multivariable model until only significantly associated foods and their confounders remained. We determined risk measures, including odds, univariable, and multivariable ratios, in the statistical analysis.

## Results

### Molecular Surveillance

The binational German–Austrian Consultant Laboratory for *L. monocytogenes* collects and sequences genomes of isolates from approximately two thirds of all mandatorily notified listeriosis cases in Germany; 699 cases were notified in 2018 and 593 in 2019. A phylogenetically diverse cluster, designated Epsilon1, was identified by using cgMLST. Epsilon1 included 46 PCR serogroup IVb isolates belonging to ST6 and CT90, CT2981, CT3803, CT3805, CT3806, CT3921, CT4083, CT4465, CT6236, CT6331, CT7353, and CT7451, all of which had specific allelic profiles within a CT threshold of ≤10 different alleles (*17*,*28*). The Epsilon1 cluster included isolates collected from all over Germany during 2011–2019 with no apparent geographic concentration. Allelic distances between isolates varied from 0–25 (median 11). In autumn 2018, a sudden increase of CT4465 and CT7353 isolates belonging to the Epsilon1 cluster was detected. Furthermore, the number of listeriosis cases reported in calendar weeks 34–43, 46, 48, and 50 exceeded the median of the 5 previous years (Appendix Figure 1). To identify the outbreak clone among all incoming serogroup IVb isolates, we developed a clone-specific PCR (Appendix). Altogether, 134 clinical CT4465 and CT7353 isolates were collected during August 2018–April 2019. These isolates formed a remarkably homogenous cluster with 0–5 (median 0) different cgMLST alleles (Figure 1). In contrast, 2 CT4465 isolates collected earlier, in July 2017 and June 2018, differed in 9–15 alleles (Figure 1).

We mapped raw sequence reads of all Epsilon1 strains against the 10-092876-0769 LM12 genome, the most closely related complete genome available. SNP calling separated the Epsilon1 cluster into several subclusters, but all CT4465 and CT7353 isolates collected from August 2018 onwards formed a single cluster (Appendix Figure 2). This subcluster was named Epsilon1a, and SNP distances in this cluster ranged from 0–3 SNPs (median 0). The 2 earlier CT4465 isolates were separated from the Epsilon1a cluster by 6–10 SNPs difference (median 8). Thus, SNP calling supported detection of a cluster of closely related CT4465 and CT7353 strains. Of note, only 21–29 cgMLST alleles (median 26) and 8–12 SNPs (median 8) differed between the Epsilon1a clone and the outbreak strain from South Africa (*11*), CT5886 (Figure 1; Appendix Figure 2).

### Case Cohort

We collected 134 isolates from 112 patients who met the case definition. Initial cases were reported in August 2018, and the outbreak peaked in September 2018 (Figure 2, panel A); the last notified case was in April 2019. Cases occurred in 11/16 federal states in Germany; most cases occurred in western and southern Germany (Figure 2, panel B). This outbreak and the assembled genome of 1 representative isolate (isolate no. 18-04540) were shared via the Epidemic Intelligence Information System platform of the European Centre for Disease Prevention and Control on October 23, 2018 (UI-516, https://www.ecdc.europa.eu). France, the only other country involved, reported an Epsilon1a listeriosis case in a patient who had traveled to and purchased food in Germany. Sequence data of isolate 18-04540 was submitted to the European Nucleotide Archive (https://www.ebi.ac.uk/ena; accession no. SAMEA5041142). However, the closest related isolate available at the National Center for Biotechnology Information (https://www.ncbi.nlm.nih.gov) pathogen detection pipeline was a 2016 clinical isolate from the Netherlands with an SNP distance of 12, which is clearly above the SNP distances observed in the Epsilon1a cluster.

One (0.9%) case-patient was pregnant, but the gestational age and health outcome of her newborn were not reported. The remaining 111 case-patients were 53–98 (median 79) years of age; 66 (59%) were men, 45 (41%) were women. Seven (6.3%) case-patients died, 2 of whom had listeriosis as the primary cause of death. The age distribution was not noticeably different from other notified listeriosis outbreaks. Of the 134 Epsilon1a isolates, 99 were from blood samples, 13 from cerebrospinal fluid, and 1 each from lymph nodes, ascites, sputum, pleura, joints, abscesses, or a superficial wound (Appendix Table 1). The isolation source was not reported for the remaining 15 isolates.

### Properties of the Outbreak Clone

Virulome analysis revealed the presence of *Listeria* pathogenicity island 1 (LIPI-1) in all Epsilon1a outbreak isolates and detected the complete listeriolysin S-encoding LIPI-3 in 64% (Appendix Figure 3). However, we did not detect LIPI-4, which encodes a putative phosphotransferase system associated with neurolisteriosis (*32*). Epsilon1a clones carried the same complement of internalin genes as other serogroup IVb strains (Appendix Figure 3).

Susceptibility testing revealed sensitivity toward most clinically relevant antimicrobial drugs, but all tested isolates were fully resistant to ceftriaxone and daptomycin (Appendix Table 2), which is consistent with the intrinsic resistance of *L. monocytogenes* and the absence of additional resistance determinants, as suggested by the resistome

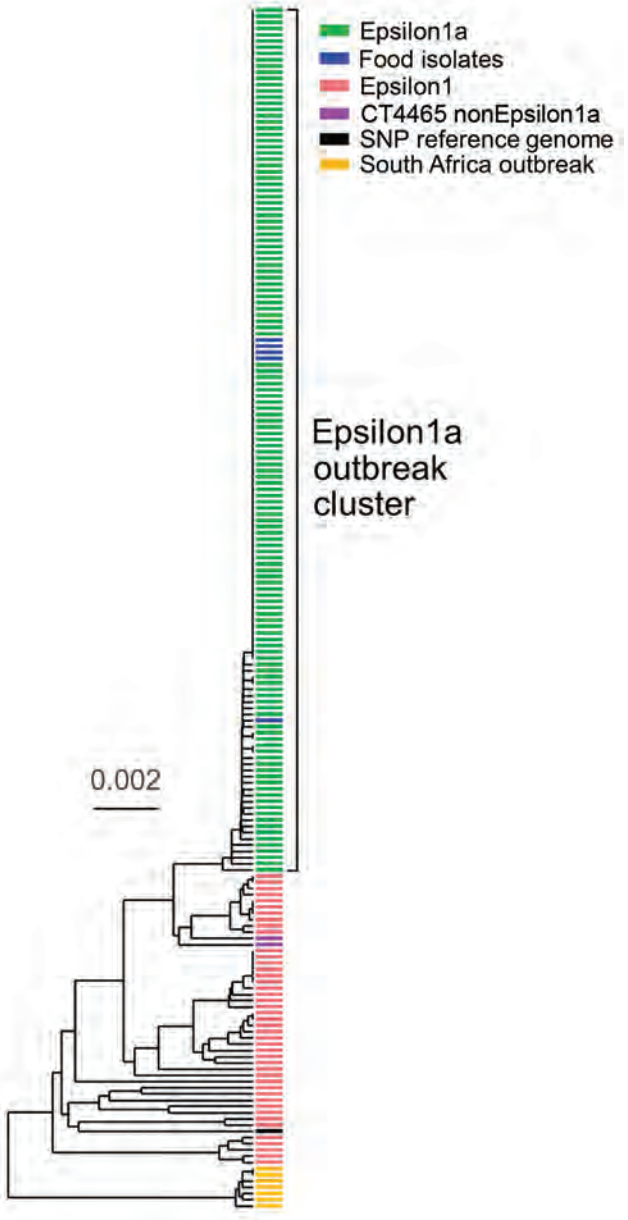


**Figure 1.** Phylogenic tree constructed by using unweighted pair group method with arithmetic mean and core genome multilocus sequence typing data of *Listeria monocytogenes* isolates from a large listeriosis outbreak, Germany. Green indicates clinical isolates of Epsilon1a subcluster; blue indicates food isolates of Epsilon1a subcluster; pink indicates isolates from the Epsilon1 cluster; violet indicates 2 complex type 4465 isolates not belonging to Epsilon1a from earlier listeriosis cases in July 2017 and June 2018; yellow indicates isolates from a listeriosis outbreak in South Africa (*11*); black indicates reference strain 10-092876-0769 LM12 used for SNP calling (Appendix Figure 2, https://wwwnc.cdc.gov/EID/article/26/7/20-0225-App1.pdf). Scale bar indicates allelic substitutions per site. SNP, single-nucleotide polymorphism.

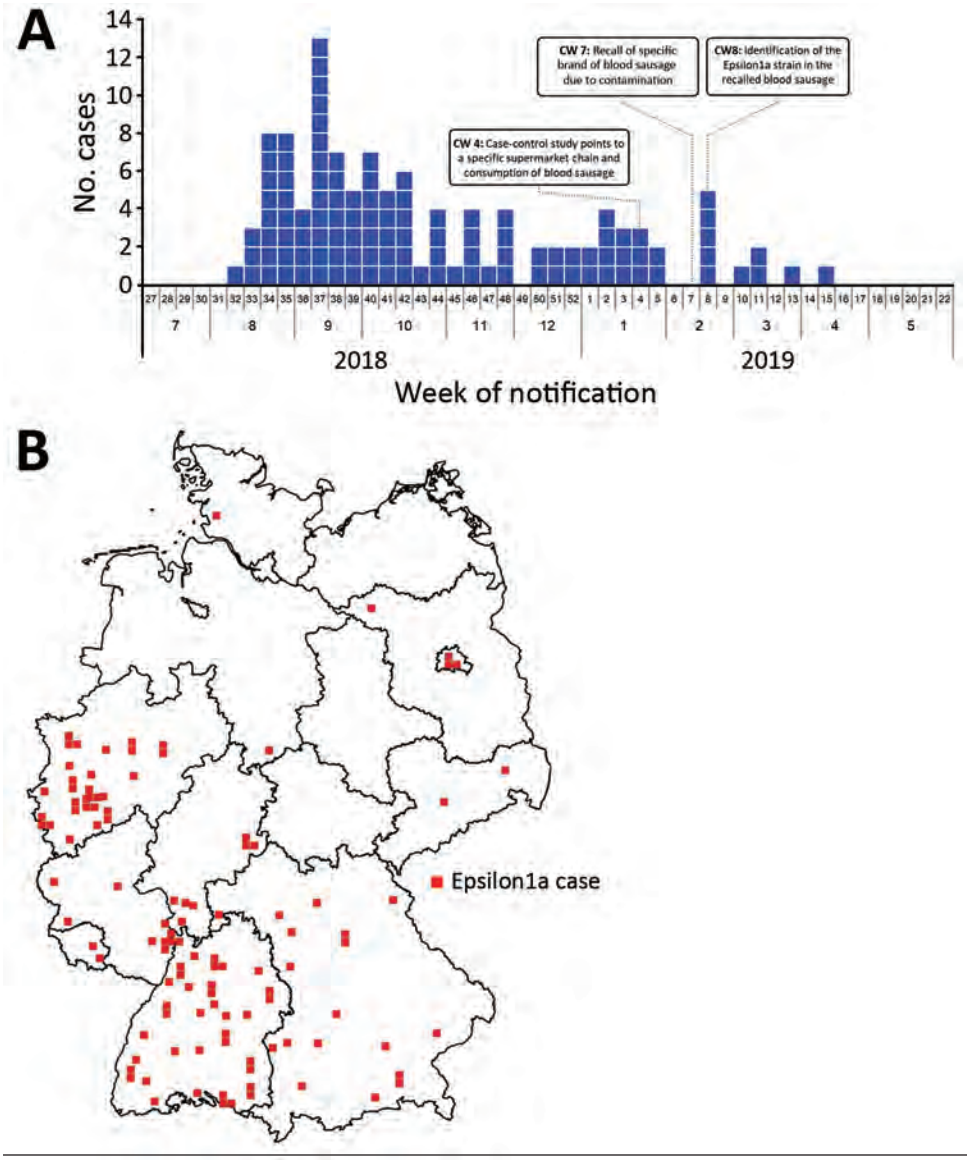


**Figure 2.** Spatial and temporal distribution of cases during a large listeriosis outbreak, Germany. A) Number of *Listeria monocytogenes* isolates from subcluster Epsilon1a received by the consulting laboratory per week during the outbreak. B) Geographic distribution of laboratory-confirmed Epsilon1a cases in Germany during the outbreak. CW, calendar week.

approach (Appendix Figure 4). Further resistome analysis demonstrated the prevalence of the *emrC* gene, which is associated with benzalkonium chloride tolerance (Appendix Figure 4). In full agreement with this observation, Epsilon1a and Epsilon1 isolates demonstrated increased tolerance to benzalkonium chloride compared with ST6 or serogroup IVb isolates from other outbreak clusters (Figure 3).

### Identification the Outbreak Vehicle

Our case-control study included 41 case-patients and 155 controls. A total of 40/41 (98%) case-patients reported that they purchased food in a single specific supermarket chain, compared with 99/154 controls (64.3%; odds ratio [OR] 22.5, 95% CI 2.9–174.9; p = 0.003). No other supermarket chains were associated with outbreak cases, and we only included case-patients and controls that had purchased food from the specific supermarket chain in further analyses. In the fourth calendar week of 2019, we detected a strong association between cases and consumption of minced meat (OR 42.4, 95% CI 4.3–415.4; p = 0.001) and blood sausage (OR 23.1, 95% CI 4.3–123.5; p<0.001; Table). Among case-patients, 90% reported consuming minced meat and 80% reported consuming blood sausage compared with 23% of controls who consumed minced meat and 45% who consumed blood sausage. None of the case-patients were vegetarians.

To perform risk-oriented screening, food samples were collected in supermarkets and the house-

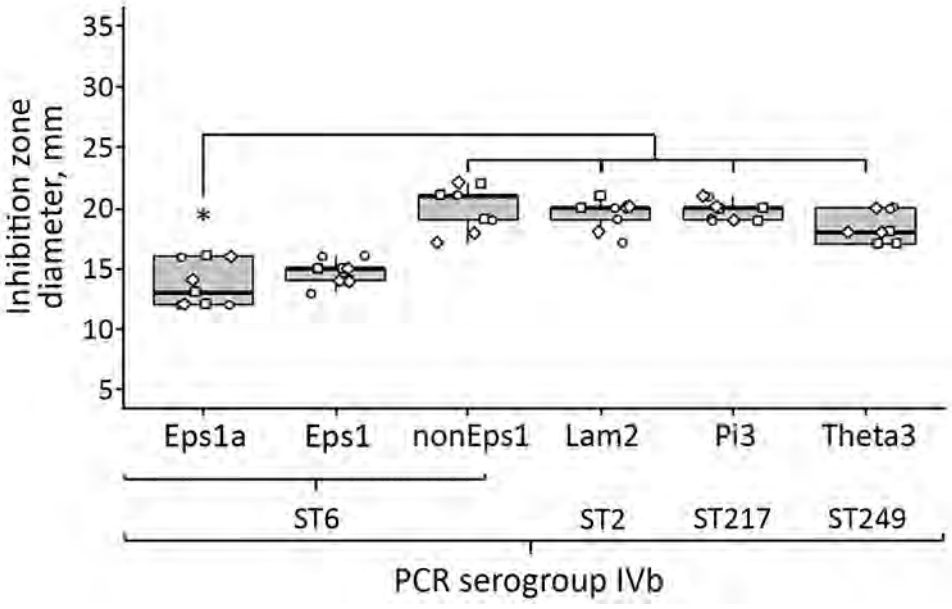


**Figure 3.** Tolerance of isolates of *Listeria monocytogenes* from subcluster Epsilon1a in Germany to benzalkonium chloride. Three representative isolates from human listeriosis clusters Epsilon1a, Epsilon1, and distinct listeriosis clusters Lambda2 (ST2, CT2402), (*17*) Pi3 (ST217, CT5744), or Theta3 (ST249, CT4449) were tested for resistance to benzalkonium chloride by disc diffusion, along with 3 representative ST6 isolates, not belonging to Epsilon1. Epsilon1a and Epsilon1 isolates showed increased resistance to benzalkonium chloride. Circles, squares, and diamonds represent results of 3 independent replicates for 3 isolates per group. Asterisk indicates statistically significant differences to Epsilon1a ($p \leq 0.01$) calculated by using the Student *t*-test. CT, complex type; Eps1, Epsilon1; Eps1a, Epsilon1a; Lam2, Lambda2; nonEps1, nonEpsilon1; ST, sequence type.

holds of some patients, according to the results of the epidemiologic investigations. In 1 case, *L. monocytogenes* was detected in 3 open samples from a patient's refrigerator. Among these, sliced blood sausage purchased at the implicated supermarket chain showed the highest contamination (>3 × $10^6$ CFU/g). This finding led to another round of intensified screening of prepackaged blood sausage. In calendar week 7 of 2019, *L. monocytogenes* was found in an original sealed package of sliced blood sausage (<10 CFU/g) and in a second sample of blood sausage from the same manufacturer. In total, 5 isolates from patients' household food items and from blood sausage samples grouped with clinical Epsilon1a isolates after cgMLST (0–3 different alleles, median = 0) and SNP calling (0–2 SNPs, median = 0) (Figure 1; Appendix Figure 2).

The blood sausage was produced by a large meat and sausage manufacturer in Germany and sold in many parts of the country. The product was withdrawn from the market on February 12, 2019. The last clinical Epsilon1a isolate was collected on April 18, 2019. In contrast, Epsilon1 isolates not belonging to the Epsilon1a cluster caused disease even after the end of the Epsilon1a outbreak. The plant was cleaned and disinfected. Thereafter, *L. monocytogenes* was not detected from products or the production site among several hundred samples collected by food safety inspectors and ≈2,500 control samples collected by the manufacturer.

## Discussion

The Epsilon1a outbreak is the largest identified outbreak of listeriosis in Germany and one of the largest documented outbreaks of invasive listeriosis in Europe in >25 years. The last reported outbreak of invasive listeriosis of this size in Europe was during 1992–1993 when 247 patients were infected in France with a serotype IVb clone from contaminated pork tongue in aspic (*33*). Cantaloupe was the vehicle in the large outbreak in the United States in 2011 that was caused by 5 different clones (*10*). In contrast, the single clone that caused a large outbreak in South Africa showed strong clonality and the genomes of 326 isolates differed in ≤4 cgMLST alleles (*11*). Likewise, the Epsilon1a outbreak was caused by a single clone, and we observed high clonality among isolates. The mutation rate in the natural *L. monocytogenes* population is 2.6 × $10^{-7}$ substitutions per site per year (*29*). On average, 1 SNP/year can be expected for *L. monocytogenes* strains under natural conditions. The high clonality of Epsilon1a could imply that the outbreak clone only persisted in the production facility and did not undergo rapid multiplication.

Purchases in a particular supermarket chain and consumption of blood sausage were strongly associated with listeriosis in the case-control study, and the outbreak clone was identified in blood sausage samples from a patient's household and from the implicated supermarket chain. Blood sausage is heat-treated during production, so contamination likely

**Table.** Results of multivariable analysis of risk for infection by food consumption from a case-control study during listeriosis outbreak, Germany 2018–2019*

| Food item | Odds ratio (95% CI)† | p value |
|---|---|---|
| Minced meat | 42.4 (4.3–415.1) | 0.001 |
| Blood sausage | 23.1 (4.3–123.5) | <0.001 |
| Cold cuts, including roast pork and Kassler | 15.4 (2.9–82.1) | 0.001 |
| Edamer cheese | 7.3 (1.6–32.8) | 0.009 |
| Smoked ham‡ | 0.06 (0.0–0.4) | 0.003 |
| Hard cheese‡ | 0.2 (0.0–0.9) | 0.038 |

*Includes 40/41 cases and 99/155 controls that confirmed shopping at the implicated supermarket chain.
†Adjusted for age, gender, and residence in northern or southern region.
‡Smoked ham and hard cheese are confounders for cold cuts and Edamer cheese.

occurred after production, possibly during slicing or packaging. The shelf-life of sliced blood sausage is several days to a few weeks (*34*) and the amount of *L. monocytogenes* found in unopened blood sausage samples was below the limit of 100 CFU/g. Storage beyond the anticipated shelf-life or insufficient refrigeration might have allowed *L. monocytogenes* to multiply inside the vehicle, which would only be prevented by a zero-tolerance policy.

Typically, pregnancy-related listeriosis accounts for ≈7% of all listeriosis cases (*35*). However, in this outbreak only 1/112 (0.8%) cases was in a pregnant woman. Official recommendations for pregnant women to apply special hygiene practices to sliced sausage products likely had an effect (*36*).

Analysis of the Epsilon1a genome has yielded some insights into the infectivity of this ST6 clone. *L. monocytogenes* ST6 clones were first isolated in 1990 (*37*), have caused various outbreaks in the past, including the large outbreak in South Africa (*11*), and are associated with increased rates of meningitis (*38*). The Epsilon1a clone and the outbreak strain from South Africa are closely related. Thus, 2 descendants of the same historic *L. monocytogenes* ancestor have spread globally and contaminated food production facilities on 2 different continents. The Epsilon1a clone carried the *emrC* gene, which presumably caused its increased tolerance to benzalkonium chloride (*39*). Europe banned use of benzalkonium chloride as a disinfectant in 2016 (*40*), but its past use might have selected tolerant strains.

The identification of this outbreak and its vehicle resulted from an efficient collaboration between public health and food safety authorities in Germany. Several requirements had to be met for successful outbreak clarification: development of a mandatory notification system for systematic patient interviews and an efficient questionnaire to generate hypotheses on possible food sources; implementation of a WGS-based molecular surveillance program for reliable identification of outbreak clusters by public health authorities; systematic collection of food isolates from internal controls and on-demand investigations and use of a harmonized WGS-based subtyping methodology by food safety authorities; and a continuous exchange of information on outbreak clusters between the institutions involved. These prerequisites have identified the causative food vehicles for 5 of 6 large listeriosis clusters that occurred in Germany during 2014–2019, which likely would not have been possible before use of WGS in outbreak investigations. However, introduction of routine interviews of listeriosis patients, regardless of outbreaks, probably could further accelerate identification of outbreak vehicles. In our opinion, the Epsilon1a outbreak demonstrates how WGS-based pathogen surveillance combined with efficient interventions of the involved stakeholders can improve management and prevention of foodborne infectious diseases.

### Acknowledgments

We thank Andrea Thürmer and her team for sequencing support, Birgitt Hahn and Simone Dumschat for excellent technical assistance, and Yvonne Pfeiffer for help with some experiments. We also thank Karan Gautam Kaval for the critical review of the manuscript.

This project was supported by the intensified molecular surveillance initiative of the Robert Koch Institute to A.F. and K.S. (2016–2018, grant no. 832133) and grants of the German Ministry of Health to S.H. (grant no. ZMVI1-2518NIK703) and to A.F. and S.K. (grant no. MolTypList). The funders had no role in study design, data collection and analysis, decision to publish, or preparation of the manuscript.

### About the Author

Dr. Halbedel is a molecular microbiologist in the Division of Enteropathogenic Bacteria and *Legionella* at the Robert Koch Institute in Wernigerode, Germany, and the deputy head of the consultant laboratory for *Listeria*. His research focuses on physiology, virulence, and epidemiology of *Listeria monocytogenes*.

### References

1. Werber D, Hille K, Frank C, Dehnert M, Altmann D, Müller-Nordhorn J, et al. Years of potential life lost for six major enteric pathogens, Germany, 2004–2008. Epidemiol Infect. 2013;141:961–8. https://doi.org/10.1017/S0950268812001550
2. Ooi ST, Lorber B. Gastroenteritis due to *Listeria monocytogenes*. Clin Infect Dis. 2005;40:1327–32. https://doi.org/10.1086/429324

3. Halbedel S, Prager R, Banerji S, Kleta S, Trost E, Nishanth G, et al. A *Listeria monocytogenes* ST2 clone lacking chitinase ChiB from an outbreak of non-invasive gastroenteritis. Emerg Microbes Infect. 2019;8:17–28. https://doi.org/10.1080/22221751.2018.1558960
4. Allerberger F, Wagner M. Listeriosis: a resurgent foodborne infection. Clin Microbiol Infect. 2010;16:16–23. https://doi.org/10.1111/j.1469-0691.2009.03109.x
5. Charlier C, Perrodeau É, Leclercq A, Cazenave B, Pilmis B, Henry B, et al.; MONALISA study group. Clinical features and prognostic factors of listeriosis: the MONALISA national prospective cohort study. Lancet Infect Dis. 2017;17:510–9. https://doi.org/10.1016/S1473-3099(16)30521-7
6. de Noordhout CM, Devleesschauwer B, Angulo FJ, Verbeke G, Haagsma J, Kirk M, et al. The global burden of listeriosis: a systematic review and meta-analysis. Lancet Infect Dis. 2014;14:1073–82. https://doi.org/10.1016/S1473-3099(14)70870-9
7. European Centre for Disease Prevention and Control. Surveillance atlas of infectious diseases. 2018 [cited 2020 Mar 16]. https://atlas.ecdc.europa.eu/public/index.aspx
8. Ferreira V, Wiedmann M, Teixeira P, Stasiewicz MJ. *Listeria monocytogenes* persistence in food-associated environments: epidemiology, strain characteristics, and implications for public health. J Food Prot. 2014;77:150–70. https://doi.org/10.4315/0362-028X.JFP-13-150
9. Swaminathan B, Gerner-Smidt P. The epidemiology of human listeriosis. Microbes Infect. 2007;9:1236–43. https://doi.org/10.1016/j.micinf.2007.05.011
10. McCollum JT, Cronquist AB, Silk BJ, Jackson KA, O'Connor KA, Cosgrove S, et al. Multistate outbreak of listeriosis associated with cantaloupe. N Engl J Med. 2013;369:944–53. https://doi.org/10.1056/NEJMoa1215837
11. Smith AM, Tau NP, Smouse SL, Allam M, Ismail A, Ramalwa NR, et al. Outbreak of *Listeria monocytogenes* in South Africa, 2017–2018: laboratory activities and experiences associated with whole-genome sequencing analysis of isolates. Foodborne Pathog Dis. 2019;16:524–30. https://doi.org/10.1089/fpd.2018.2586
12. Stephan R, Althaus D, Kiefer S, Lehner A, Hatz C, Schmutz C, et al. Foodborne transmission of *Listeria monocytogenes* via ready-to-eat salad: A nationwide outbreak in Switzerland, 2013–2014. Food Control. 2015;57:14–7. https://doi.org/10.1016/j.foodcont.2015.03.034
13. Goulet V, King LA, Vaillant V, de Valk H. What is the incubation period for listeriosis? BMC Infect Dis. 2013;13:11. https://doi.org/10.1186/1471-2334-13-11
14. Heiman KE, Garalde VB, Gronostaj M, Jackson KA, Beam S, Joseph L, et al. Multistate outbreak of listeriosis caused by imported cheese and evidence of cross-contamination of other cheeses, USA, 2012. Epidemiol Infect. 2016;144:2698–708. https://doi.org/10.1017/S095026881500117X
15. European Centre for Disease Prevention and Control and European Food Safety Authority. Multi-country outbreak of Listeria monocytogenes sequence type 8 infections linked to consumption of salmon products—25 October 2018. Stockholm and Parma: ECDC/EFSA; 2018 [cited 2019 Dec 17]. https://www.ecdc.europa.eu/sites/default/files/documents/listeria-multi-country-outbreak-october-2018.pdf
16. Ruppitsch W, Prager R, Halbedel S, Hyden P, Pietzka A, Huhulescu S, et al. Ongoing outbreak of invasive listeriosis, Germany, 2012 to 2015. Euro Surveill. 2015;20:30094. https://doi.org/10.2807/1560-7917.ES.2015.20.50.30094
17. Halbedel S, Prager R, Fuchs S, Trost E, Werner G, Flieger A. Whole-genome sequencing of recent *Listeria monocytogenes* isolates from Germany reveals population structure and disease clusters. J Clin Microbiol. 2018;56:e00119–18. https://doi.org/10.1128/JCM.00119-18
18. Kleta S, Hammerl JA, Dieckmann R, Malorny B, Borowiak M, Halbedel S, et al. Molecular tracing to find source of protracted invasive listeriosis outbreak, southern Germany, 2012–2016. Emerg Infect Dis. 2017;23:1680–3. https://doi.org/10.3201/eid2310.161623
19. Jackson BR, Tarr C, Strain E, Jackson KA, Conrad A, Carleton H, et al. Implementation of nationwide real-time whole-genome sequencing to enhance listeriosis outbreak detection and investigation. Clin Infect Dis. 2016;63:380–6. https://doi.org/10.1093/cid/ciw242
20. Moura A, Tourdjman M, Leclercq A, Hamelin E, Laurent E, Fredriksen N, et al. Real-time whole-genome sequencing for surveillance of *Listeria monocytogenes*, France. Emerg Infect Dis. 2017;23:1462–70. https://doi.org/10.3201/eid2309.170336
21. Kwong JC, Mercoulia K, Tomita T, Easton M, Li HY, Bulach DM, et al. Prospective whole-genome sequencing enhances national surveillance of *Listeria monocytogenes*. J Clin Microbiol. 2016;54:333–42. https://doi.org/10.1128/JCM.02344-15
22. Chen Y, Gonzalez-Escalona N, Hammack TS, Allard MW, Strain EA, Brown EW. Core genome multilocus sequence typing for identification of globally distributed clonal groups and differentiation of outbreak strains of *Listeria monocytogenes*. Appl Environ Microbiol. 2016;82:6258–72. https://doi.org/10.1128/AEM.01532-16
23. World Health Organization. Listeriosis–Spain, disease outbreak news. Geneva: the Organization; updated 2019 Sep 16 [cited 2019 Oct 1]. https://www.who.int/csr/don/16-september-2019-listeriosis-spain
24. International Organization for Standardization. ISO 11290-1:2017. Microbiology of the food chain—Horizontal method for the detection and enumeration of *Listeria monocytogenes* and of *Listeria* spp.—part 1: detection method. Geneva: The Organization; 2017 [cited 2019 Dec 17]. https://www.iso.org/standard/60313.html
25. International Organization for Standardization. ISO 11290-2:2017. Microbiology of the food chain—horizontal method for the detection and enumeration of *Listeria monocytogenes* and of *Listeria* spp.—part 2: enumeration method. Geneva: The Organization; 2017 [cited 2019 Dec 17]. https://www.iso.org/standard/60314.html
26. Bubert A, Hein I, Rauch M, Lehner A, Yoon B, Goebel W, et al. Detection and differentiation of *Listeria* spp. by a single reaction based on multiplex PCR. Appl Environ Microbiol. 1999;65:4688–92. https://doi.org/10.1128/AEM.65.10.4688-4692.1999
27. Kérouanton A, Marault M, Petit L, Grout J, Dao TT, Brisabois A. Evaluation of a multiplex PCR assay as an alternative method for *Listeria monocytogenes* serotyping. J Microbiol Methods. 2010;80:134–7. https://doi.org/10.1016/j.mimet.2009.11.008
28. Ruppitsch W, Pietzka A, Prior K, Bletz S, Fernandez HL, Allerberger F, et al. Defining and evaluating a core genome multilocus sequence typing scheme for whole-genome sequence-based typing of *Listeria monocytogenes*. J Clin Microbiol. 2015;53:2869–76. https://doi.org/10.1128/JCM.01193-15
29. Moura A, Criscuolo A, Pouseele H, Maury MM, Leclercq A, Tarr C, et al. Whole genome-based population biology and epidemiological surveillance of *Listeria monocytogenes*. Nat Microbiol. 2016;2:16185. https://doi.org/10.1038/nmicrobiol.2016.185

30. Noll M, Kleta S, Al Dahouk S. Antibiotic susceptibility of 259 *Listeria monocytogenes* strains isolated from food, food-processing plants and human samples in Germany. J Infect Public Health. 2018;11:572–7. https://doi.org/10.1016/j.jiph.2017.12.007
31. European Committee on Antimicrobial Susceptibility Testing. Breakpoint tables for interpretation of MICs and zone diameters. Version 9.0, 2019. Basal (Switzerland): EUCAST; 2019 Jan 1 [cited 2019 Dec 5]. http://www.eucast.org/fileadmin/src/media/PDFs/EUCAST_files/Breakpoint_tables/v_9.0_Breakpoint_Tables.pdf
32. Maury MM, Tsai YH, Charlier C, Touchon M, Chenal-Francisque V, Leclercq A, et al. Uncovering *Listeria monocytogenes* hypervirulence by harnessing its biodiversity. Nat Genet. 2016;48:308–13. https://doi.org/10.1038/ng.3501
33. Jacquet C, Catimel B, Brosch R, Buchrieser C, Dehaumont P, Goulet V, et al. Investigations related to the epidemic strain involved in the French listeriosis outbreak in 1992. Appl Environ Microbiol. 1995;61:2242–6. https://doi.org/10.1128/AEM.61.6.2242-2246.1995
34. Pereira JA, Silva P, Matos TJ, Patarata L. Shelf life determination of sliced Portuguese traditional blood sausage—Morcela de Arroz de Monchique through microbiological challenge and consumer test. J Food Sci. 2015;80:M642–8. https://doi.org/10.1111/1750-3841.12782
35. Allerberger F, Huhulescu S. Pregnancy related listeriosis: treatment and control. Expert Rev Anti Infect Ther. 2015;13:395–403. https://doi.org/10.1586/14787210.2015.1003809
36. Groeneveld M, Wichmann-Schauer H, Oehlenschläger J, Werber D, Maschkowski G; Federal Institute of Agriculture and Food. Listeriosis and toxoplasmosis-safe eating during pregnancy, 2nd edition; B. Klein editor [in German]. Bonn, Germany: Bundesanstalt für Landwirtschaft und Ernährung; 2017 [cited 2019 Dec 17]. https://www.ble-medienservice.de/frontend/esddownload/index/id/513/on/0346_DL/act/dl
37. Cantinelli T, Chenal-Francisque V, Diancourt L, Frezal L, Leclercq A, Wirth T, et al. "Epidemic clones" of *Listeria monocytogenes* are widespread and ancient clonal groups. J Clin Microbiol. 2013;51:3770–9. https://doi.org/10.1128/JCM.01874-13
38. Koopmans MM, Brouwer MC, Bijlsma MW, Bovenkerk S, Keijzers W, van der Ende A, et al. *Listeria monocytogenes* sequence type 6 and increased rate of unfavorable outcome in meningitis: epidemiologic cohort study. Clin Infect Dis. 2013;57:247–53. https://doi.org/10.1093/cid/cit250
39. Kremer PH, Lees JA, Koopmans MM, Ferwerda B, Arends AW, Feller MM, et al. Benzalkonium tolerance genes and outcome in *Listeria monocytogenes* meningitis. Clin Microbiol Infect. 2017;23:265.e1–e7. PubMed https://doi.org/10.1016/j.cmi.2016.12.008
40. European Union. Commission implementing decision (EU) 2016/1950 of 4 November 2016 on the non-approval of certain biocidal active substances pursuant to Regulation (EU) No. 528/2012 of the European Parliament and of the Council. Official Journal of the European Union 2016. p. 16–20 [cited 2019 Dec 17]. https://www.helpdesk-biocides.fr/files/PDF/reglementation_europe/en_non_inscription_sa/20161104_decision_2016_1950_eu_non_approval_susbtances_bpr.pdf

Addresses for correspondence: Sven Halbedel or Antje Flieger, FG11 Division of Enteropathogenic Bacteria and Legionella, Robert Koch Institute, Burgstrasse 37, 38855 Wernigerode, Germany; email: halbedels@rki.de or fliegera@rki.de

# Identifying Locations with Possible Undetected Imported Severe Acute Respiratory Syndrome Coronavirus 2 Cases by Using Importation Predictions

Pablo Martinez De Salazar,[1] René Niehus,[1] Aimee Taylor,[1] Caroline O'Flaherty Buckee, Marc Lipsitch

Cases of severe acute respiratory syndrome coronavirus 2 (SARS-CoV-2) infection exported from mainland China could lead to self-sustained outbreaks in other countries. By February 2020, several countries were reporting imported SARS-CoV-2 cases. To contain the virus, early detection of imported SARS-CoV-2 cases is critical. We used air travel volume estimates from Wuhan, China, to international destinations and a generalized linear regression model to identify locations that could have undetected imported cases. Our model can be adjusted to account for exportation of cases from other locations as the virus spreads and more information on importations and transmission becomes available. Early detection and appropriate control measures can reduce the risk for transmission in all locations.

A novel coronavirus, later named severe acute respiratory syndrome coronavirus 2 (SARS-CoV-2), was identified in December 2019 in the city of Wuhan, capital of Hubei Province, China, where cases were first confirmed (*1*). During December 2019–February 2020, the number of confirmed cases increased drastically. Model estimates suggested that >75,000 persons were infected by January 25, 2020, and the epidemic had a doubling time of ≈6 days (*2*). By the end of January 2020, travel restrictions were implemented for Wuhan and neighboring cities. Nonetheless, the virus spread from Wuhan to other cities in China and outside the country. By February 4, 2020, a total of 23 locations outside mainland China reported cases, 22 of which reported imported cases; Spain reported a case caused by secondary transmission (*3*).

Author affiliation: Harvard T.H. Chan School of Public Health, Boston, Massachusetts, USA

DOI: https://doi.org/10.3201/eid2607.200250

Most cases imported to other locations have been linked to recent travel history from China (*3*), suggesting that air travel plays a major role in exportation of cases to locations outside of China. To prevent other cities and countries from becoming epicenters of the SARS-CoV-2 epidemic, substantial targeted public health interventions are required to detect cases and control local spread of the virus. We collected estimates of air travel volume from Wuhan to the 27 most connected locations outside of China from a total of 194 international destinations. We then identified 49 locations with high surveillance capacity according to the Global Health Security (GHS) Index (*4*). We assumed these locations would have relatively high proficiency in detecting SARS-CoV-2 and reporting confirmed imported cases, which we refer to as imported-and-reported cases. We fitted a generalized linear regression model on this subset of locations; based on this model fit, we generated predictions for all international locations. Using these predictions, we identified locations that might not be detecting imported cases.

## Methods

To identify locations reporting fewer than predicted imported SARS-CoV-2 infected cases, we fit a model to data from 49 locations outside mainland China that had a score of >49.2/100 (the 75th quantile) of the GHS Index's category 2 (Early Detection and Reporting of Epidemics of Potential International Concern) (*4*). Among these, 17 had high travel connectivity to Wuhan and 32 had low connectivity to Wuhan (S. Lai et al., unpub. data, https://doi.org/10.1101/2020.02.04.20020479). We considered locations to be countries without taking any position on territorial

[1]These authors contributed equally to this article.

claims. We performed a Poisson regression by using the cumulative number of imported-and-reported SARS-CoV-2 cases in these 49 countries and the estimated number of daily airline passengers from the Wuhan airport. We then compared predictions from this model with imported-and-reported cases across 194 locations from the GHS Index, excluding China as the epicenter of the outbreak.

The model requires data on imported-and-reported cases of SARS-CoV-2 infection, daily air travel volume, and surveillance capacity. We obtained data on imported-and-reported cases aggregated by destination from the World Health Organization technical report issued February 4, 2020 (*3*). We assumed a case count of 0 for locations not listed. We used February 4 as the cutoff for cumulative imported-and-reported case counts because exported cases from Hubei Province dropped rapidly after this date (*3*), likely because of travel restrictions for the province were implemented on January 23. We defined imported-and-reported cases as those with known travel history from China; of those, 83% had a travel history from Hubei Province and 17% traveled from unknown locations in China (*3*). We excluded reported cases likely caused by transmission outside of China or cases in which the transmission source was still under investigation (*3*). In addition, we excluded Hong Kong, Macau, and Taiwan from our model because locally transmitted and imported cases were not disaggregated in these locations.

We obtained data on daily air travel from a network-based modeling study (S. Lai et al., unpub. data, https://doi.org/10.1101/2020.02.04.20020479) that reported monthly air travel volume estimates for the 27 locations outside mainland China that are most connected to Wuhan. These estimates were calculated from International Air Travel Association data from February 2018, which includes direct and indirect flight itineraries from Wuhan. For these 27 locations, estimated air travel volumes are ≥6 passengers/day. We assumed that travel volumes for locations not among the most connected are censored by a detection limit. We used a common method of dealing with censored data from environmental sampling (*5*), or metabolomics (*6*), and set the daily air travel volume to half the minimum value. Therefore, we used 3 passengers/day for estimated travel volumes for the 167 locations from the GHS Index not listed by Lai et al. We tested the robustness of our results by using a set of alternative values of 0.1, 1, and 6 passengers/day for the censored data.

As noted, we defined high surveillance locations as those with a GHS Index for category 2 above the 75th quantile (*4*). We assessed among the high and low surveillance locations the numbers of zero and of nonzero imported-and-reported case counts (Table).

**Table.** Surveillance capacity of locations with and without imported-and-reported cases of severe acute respiratory syndrome coronavirus 2, 2020*

| Surveillance capacity | No. locations | | Total |
|---|---|---|---|
| | 0 cases | ≥1 case | |
| High | 35 | 14 | 49 |
| Low | 138 | 7 | 145 |
| Total | 173 | 21 | 194 |

*Aggregated case counts collected during January 20–February 4, 2020. Surveillance capacity reported by category 2, Early Detection and Reporting of Epidemics of Potential International Concern, of the Global Health Security (GHS) Index (*3*). High surveillance capacity is defined as a GHS Index above the 75th quantile; low surveillance capacity is defined as a GHS Index below the 75th quantile.

For our model, we assumed that the cumulative imported-and-reported case counts across 49 high surveillance locations follow a Poisson distribution from the beginning of the epidemic until February 4, 2020. Then the expected case count is linearly proportional to the daily air travel volume in the following formula:

$$C_i \sim Poisson(\lambda_i)$$
$$\lambda_i = \beta x_i, \text{for } i = 1, \ldots, n$$

where $i$ denotes location, $C_i$ denotes the imported-and-reported case count in a location, $\lambda_i$ denotes the expected case count in a location, $\beta$ denotes the regression coefficient, and $x_i$ denotes the daily air travel volume from Wuhan to a location. The Poisson model assumes cases are independent and that the variance is equal to the expected case count. Imported-and-reported cases likely meet the independence assumption because the value excludes cases with local transmission. We also checked the robustness of our results by using an over dispersed model with a negative binomial likelihood. We computed the p value of the overdispersion parameter as shown in Gelman and Hill (*7*).

We used R version 3.6.1 (https://www.r-project.org) to compute $\hat{\beta}$, the maximum likelihood estimate of $\beta$, and the expected imported-and-reported case count given high surveillance (Figure 1). We also computed the 95% prediction interval (PI) bounds under this model of high surveillance for all 194 locations of daily air travel volume (Figure 1). First, we generated a bootstrapped dataset by sampling $n$ locations with replacement among high surveillance locations. Then, we re-estimated $\beta$ by using the bootstrapped dataset. Finally, we simulated imported-and-reported case counts for all 194 locations under our model by using the estimate of $\beta$ from the bootstrapped dataset. We repeated the 3 steps 50,000 times to generate 50,000 simulated imported-and-reported case counts for each of the locations and computed to the lower and upper PI bounds (PI 2.5%–97.5%). We smoothed the 95% PI bounds by us-

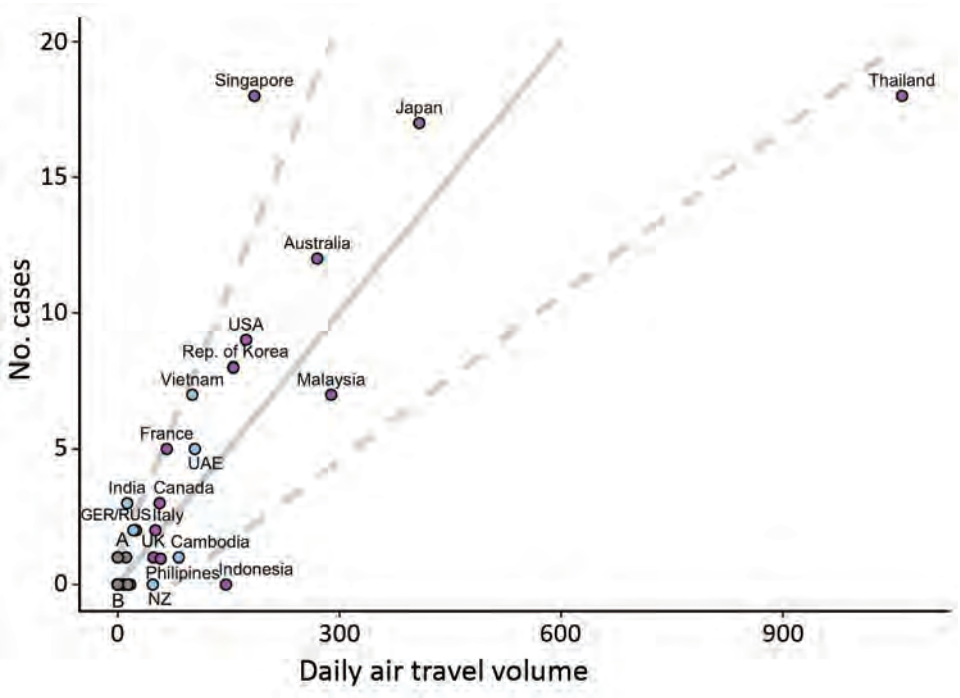


**Figure 1.** Plot showing imported-and-reported cases of severe acute respiratory syndrome coronavirus 2 (SARS-CoV-2) against air travel volume (no. persons/day) from Wuhan, China. No. cases refers to possible imported-and-reported SARS-CoV-2 cases. Solid line indicates the expected imported-and-reported case counts for locations based on the model fit to high surveillance locations (slope = 3.3 cases/100 passengers; p<0.001). Dashed lines represent for the same model the smoothed 95% prediction interval bounds. Purple dots indicate locations with high surveillance capacity according to category 2 of the Global Health Security Index. Cluster A is composed of Nepal, Sri Lanka, Finland, and Sweden, locations with 1 imported-and-reported case and air travel volume of <20 passengers per day. Cluster B is composed of 161 locations with no imported-and-reported cases and estimated air travel <10 passengers per day. GER, Germany; NZ, New Zealand; RUS, Russia; UAE, United Arab Emirates; UK, United Kingdom; USA, United States of America.

ing ggplot2 in R (*8*). We fit the imported-and-reported case counts of the 49 high surveillance locations to the model and plotted these alongside 145 locations with low surveillance capacity (Figure 1). We noted some overlap between high and low surveillance locations (Figure 1).

To assess the robustness of our results we ran 8 additional regression analyses by implementing a series of changes to the analysis. These changes included the following: setting the daily air travel volume to 0.1, 1, or 6 passengers/day for locations not listed by Lai et al. (unpub. data, https://doi.org/10.1101/2020.02.04.20020479) (Figure 2, panels A–C); removing all locations not listed by Lai et al. before fitting (Figure 2, panel D); defining high surveillance locations by using a more lenient GHS Index criterion, 50th quantile (Figure 2, panel E), and a more stringent criterion, 95th quantile (Figure 2, panel F); excluding Thailand from the model because it is a high-leverage point (Figure 2, panel G); and using an overdispersed Poisson likelihood (i.e., a negative-binomial likelihood) (Figure 2, panel H). We provide code for these analyses on GitHub (https://github.com/c2-d2/cov19flightimport).

## Results

We found that daily air travel volume positively correlates with imported-and-reported case counts of SARS-CoV-2 infection among high surveillance locations (Figure 1). We noted that increasing flight volume by 31 passengers/day is associated with 1 additional expected imported-and-reported case. In addition, Singapore and India lie above the 95% PI in our model; Singapore had 12 more imported-and-reported cases (95% PI 6–17 cases) than expected and India had 3 (95% PI 1–3 cases) more than expected. Thailand has a relatively high air travel volume compared with other locations, but it lies below the 95% PI, reporting 16 (95% PI 1–40 cases) fewer imported-and-reported cases than expected under the model. Indonesia lies below the PI and has no imported-and-reported cases, but the expected case count is 5 (95% PI 1–10 cases) in our model. Across all 8 robustness regression analyses, we consistently observed that Singapore lies above the 95% PI and Thailand and Indonesia lie below (Figure 2). India remains above the 95% PI in all robustness analyses except when we used the more stringent GHS Index, 95th quantile, for fitting; then India lies on the upper bound of the 95% PI (Figure 2, panel F).

## Discussion

We aimed to identify locations with likely undetected or underdetected imported cases of SARS-CoV-2 by fitting a model to the case counts in locations with high surveillance capacity and Wuhan-to-location air travel volumes. Our model can be adjusted to account

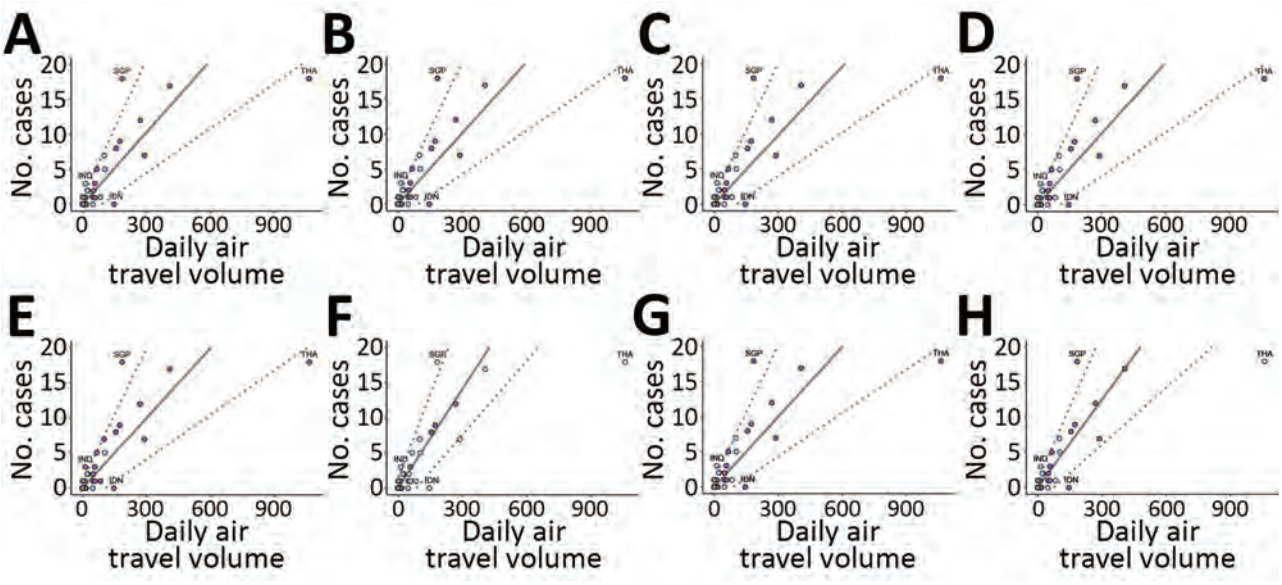


**Figure 2.** Analyses of imported-and-reported cases and daily air travel volume using a model to predict locations with potentially undetected cases of severe acute respiratory virus 2 (SARS-CoV-2). Air travel volume measured in number of persons/day. No. cases refers to possible undetected imported SARS-CoV-2 cases. Solid line shows the expected imported-and-reported case counts based on our model fitted to high surveillance locations, indicated by purple dots. Dashed lines indicate the 95% prediction interval bounds smoothed for all locations, including those with low surveillance capacity, indicated by light blue dots. A–C) Regressions that set the daily air travel volume for locations not listed by S. Lai et al. (unpub. data, https://doi.org/10.1101/2020.02.04.20020479): A) air travel volume set to 0.1 passenger/day; B) volume set to 1 pas sengers/day; C) volume set to 6 passengers/day. D) Regression removing locations not listed by Lai et al. before fitting. E) Regression defining high surveillance locations by using a more lenient Global Health Security (GHS) Index criterion (50th quantile) for category 2, Early Detection and Reporting of Epidemics of Potential International Concern, to define high surveillance locations. F) A more stringent GHS Index criterion (95th quantile) to define high surveillance locations. G) Regression using a negative binomial likelihood and estimated dispersion parameter of 1.27 ($p = 0.097$). H) Regression excluding Thailand from the model fit. Across all 8 regression analyses, Singapore lies above the 95% PI and Thailand and Indonesia lie below. India remained above 95% PI for all regressions, except when we used a more stringent GHS Index criterion (panel F). IDN, Indonesia; IND, India; SGP, Singapore; THA, Thailand.

for exportation of cases from locations other than Wuhan as the outbreak develops and more information on importations and self-sustained transmission becomes available. One key advantage of this model is that it does not rely on estimates of incidence or prevalence in the epicenter of the outbreak. Also, we intentionally used a simple generalized linear model. The linearity of the expected case count means that we have only 1 regression coefficient in the model and no extra parameters. The Poisson likelihood then captures the many 0-counts observed for less highly connected locations but also describes the slope between case-count and flight data among more connected locations. We believe this model provides the most parsimonious phenomenologic description of the data.

According to our model, locations above the 95% PI of imported-and-reported cases could have higher case-detection capacity. Locations below the 95% PI might have undetected cases because of expected imported-and-reported case counts under high surveillance. Underdetection of cases could increase the international spread of the outbreak because the transmission chain could be lost, reducing opportunities to deploy case-based control strategies. We recommend rapid strengthening of outbreak surveillance and control efforts in locations below the 95% PI lower bound, particularly Indonesia, to curb potential local transmission. Early detection of cases and implantation of appropriate control measures can reduce the risk for self-sustained transmission in all locations.

**Acknowledgment**

We thank Pamela Martinez, Nicholas Jewell, and Stephen Kissler for valuable feedback.

This work was supported by US National Institute of General Medical Sciences (award no. U54GM088558). P.M.D was supported by the Fellowship Foundation Ramon Areces. A.R.T. and C.O.B. were supported by a Maximizing Investigator's Research Award (no. R35GM124715-02) from the US National Institute of General Medical Sciences.

The authors are solely responsible for this content and it does not necessarily represent the official views of the National Institute of General Medical Sciences or the National Institutes of Health.

Declaration of interests: Marc Lipsitch has received consulting fees from Merck. All other authors declare no competing interests.

### About the Author

Dr. De Salazar is a research fellow at Harvard T.H. Chan School of Public Health, working on multiscale statistical models of infectious diseases within host, population, and metapopulation models. His research interests include diagnostic laboratory methods and public health response.

### References:


1. Zhou P, Yang XL, Wang XG, Hu B, Zhang L, Zhang W, et al. A pneumonia outbreak associated with a new coronavirus of probable bat origin. Nature. 2020;579:270–3. https://doi.org/10.1038/s41586-020-2012-7
2. Wu JT, Leung K, Leung GM. Nowcasting and forecasting the potential domestic and international spread of the 2019-nCoV outbreak originating in Wuhan, China: a modelling study. Lancet. 2020;395:689–97. https://doi.org/10.1016/S0140-6736(20)30260-9
3. World Health Organization. Coronavirus disease 2019 (COVID-19) situation report—15, 4 Feb 2020 [cited 2020 Feb 14]. https://www.who.int/docs/default-source/coronaviruse/situation-reports/20200204-sitrep-15-ncov.pdf
4. Nuclear Threat Initiative and Johns Hopkins Center for Health Security. Global health security index [cited 2020 Feb 14]. https://www.ghsindex.org
5. US Environmental Protection Agency. Data quality assessment: statistical methods for practitioners EPA QA/G9-S [cited 2020 Feb 14]. Washington: The Agency; 2006. https://www.epa.gov/sites/production/files/2015-08/documents/g9s-final.pdf
6. Lamichhane S, Sen P, Dickens AM, Hyötyläinen T, Orešič M. An overview of metabolomics data analysis: current tools and future perspectives. In: Jaumot J, Bedia C, Tauler R, editors. Comprehensive analytical chemistry. Vol. 82. Amsterdam: Elsevier; 2018. p. 387–413.
7. Gelman A, Hill J. Analytical methods for social research. In: Data analysis using regression and multilevel/hierarchical models. Cambridge: Cambridge University Press; 2006. p. 235–236. https://doi.org/10.1017/cbo9780511790942.014
8. Wickham H. ggplot2: elegant graphics for data analysis. New York: Springer; 2016.


Address for correspondence: Pablo M. De Salazar or Marc Lipsitch, Center for Communicable Disease Dynamics, Department of Epidemiology, Harvard T.H. Chan School of Public Health, 677 Huntington Ave, Boston, MA 02115, USA; email: pablom@hsph.harvard.edu or mlipsitch@hsph.harvard.edu

# High Contagiousness and Rapid Spread of Severe Acute Respiratory Syndrome Coronavirus 2

Steven Sanche[1], Yen Ting Lin[1], Chonggang Xu, Ethan Romero-Severson, Nick Hengartner, Ruian Ke

Severe acute respiratory syndrome coronavirus 2 is the causative agent of the ongoing coronavirus disease pandemic. Initial estimates of the early dynamics of the outbreak in Wuhan, China, suggested a doubling time of the number of infected persons of 6–7 days and a basic reproductive number ($R_0$) of 2.2–2.7. We collected extensive individual case reports across China and estimated key epidemiologic parameters, including the incubation period (4.2 days). We then designed 2 mathematical modeling approaches to infer the outbreak dynamics in Wuhan by using high-resolution domestic travel and infection data. Results show that the doubling time early in the epidemic in Wuhan was 2.3–3.3 days. Assuming a serial interval of 6–9 days, we calculated a median $R_0$ value of 5.7 (95% CI 3.8–8.9). We further show that active surveillance, contact tracing, quarantine, and early strong social distancing efforts are needed to stop transmission of the virus.

Severe acute respiratory syndrome coronavirus 2 (SARS-CoV-2) is the etiologic agent of the current rapidly growing outbreak of coronavirus disease (COVID-19), originating from the city of Wuhan, Hubei Province, China (*1*). Initially, 41 cases of "pneumonia of unknown etiology" were reported to the World Health Organization by the Wuhan Municipal Health Committee at the end of December 2019 (*2*). On January 8, 2020, the pathogen was identified (*1*), and human-to-human transmission was reported soon after. By January 21, most provinces of China had reported COVID-19 cases. By March 16, the outbreak had led to >170,000 total confirmed cases and >6,500 deaths globally. In a period of 3 months, an outbreak of apparent idiopathic pneumonia had become the COVID-19 pandemic.

Studying dynamics of a newly emerged and rapidly growing infectious disease outbreak, such as COVID-19, is important but challenging because of the limited amount of data available. In addition, unavailability of diagnostic reagents early in the outbreak, changes in surveillance intensity and case definitions, and overwhelmed healthcare systems confound estimates of the growth of the outbreak based on data. Initial estimates of the exponential growth rate of the outbreak were 0.1–0.14/day (a doubling time of 6–7 days), and a basic reproductive number ($R_0$; defined as the average number of secondary cases attributable to infection by an index case after that case is introduced into a susceptible population) ranged from 2.2 to 2.7 (*1*,*3*–*5*). These estimates were based on 2 broad strategies. First, Li et al. used very early case count data in Wuhan before January 4 (*1*). However, case count data can be confounded by reservoir spillover events, stochasticities in the initial phase of the outbreak, and low surveillance intensity. The epidemic curve based on symptom onset after January 4 showed a very different growth rate (*6*). Second, inference was performed by using international flight data and infected persons reported outside of China (*3*–*5*). Because of the low numbers of persons traveling abroad compared with the total population size in Wuhan, this approach leads to substantial uncertainties (*7*,*8*). Inferences based on a low number of observations are prone to measurement error when data are incomplete or model assumptions are not fully justified; both conditions are common challenges associated with rapid and early outbreak analyses of a new pathogen.

We collected an expanded set of case reports across China on the basis of publicly available information, estimated key epidemiologic parameters, and provided a new estimate of the early epidemic growth rate and $R_0$ in Wuhan. Our approaches are based on integration of high-resolution domestic travel data and early infection data reported in provinces other than Hubei to infer outbreak dynamics in

Author affiliation: Los Alamos National Laboratory, Los Alamos, New Mexico, USA

DOI: https://doi.org/10.3201/eid2607.200282

[1]These first authors contributed equally to this article.

Wuhan. They are designed to be less sensitive to biases and confounding factors in the data and model assumptions. Without directly using case confirmation data in Wuhan, we avoid the potential biases in reporting and case confirmation in Wuhan, whereas because of the high level of domestic travel before the Lunar New Year in China, inference based on these data minimizes uncertainties and risk for potential misspecifications and biases in data and model assumptions.

## Methods

### Methodologic Overview

We developed 2 modeling approaches to infer the growth rate of the outbreak in Wuhan from data from provinces other than Hubei. In the first model, the first arrival model, we computed the likelihood of the arrival times of the first known cases in provinces outside of Hubei as a function of the exponential growing population of infected persons in Wuhan before late January. This calculation involved using domestic travel data to compute the probability that an infected person traveled from Wuhan to a given province as a function of the unknown actual number of infected persons in Wuhan and the probability that they traveled. The timings of the arrivals of the first infected persons in different provinces would reflect the rate of the epidemic growth in Wuhan.

In the second model, the case count model, we accounted for the detection of additional persons who were infected in Wuhan and received their diagnoses in other provinces and explicitly modeled those persons by using a hybrid deterministic–stochastic SEIR (susceptible-exposed-infectious-recovered) model. We then fitted this model to new daily case count data reported outside Hubei Province during the period before substantial transmission occurred outside of the province.

By using data collected outside Hubei Province, we minimized the effect of changes in surveillance intensity. By the time cases were confirmed in provinces outside Hubei, all of the provinces of China had access to diagnostic kits and were engaging in active surveillance of travelers out of Wuhan (e.g., using temperatures detectors and digital data to identify infected persons [*9*]) as the outbreak unfolded. Furthermore, the healthcare systems outside Hubei were not yet overwhelmed with cases and were actively searching for the first positive case, leading to much lower bias in the reporting in each province compared with the time series of confirmed cases in Wuhan.

### Data

#### Individual Case Reports

We collected publicly available reports of 140 confirmed COVID-19 cases (mostly outside Hubei Province). These reports were published by the Chinese Centers for Disease Control and Prevention (China CDC) and provincial health commissions; accession dates were January 15–30, 2020 (Appendix 1 Table 1, https://wwwnc.cdc.gov/EID/article/26/7/20-0282-App1.xlsx). Many of the individual reports were also published on the China CDC official website (http://www.chinacdc.cn/jkzt/crb/zl/szkb_11803) and the English version of the China CDC weekly bulletin (http://weekly.chinacdc.cn/news/TrackingtheEpidemic.htm). These reports include demographic information as well as epidemiologic information, including potential periods of infection, and dates of symptom onset, hospitalization, and case confirmation. Most of the health commissions in provinces and special municipalities documented and published detailed information of the first or the first few patients with confirmed COVID-19. As a result, a unique feature of this dataset includes case reports of many of the first or the first few persons who were confirmed to have SARS-CoV-2 virus infection in each province, where dates of departure from Wuhan were available.

#### Travel Data

We used the Baidu Migration server (https://qianxi.baidu.com) to estimate the number of daily travelers in and out of Wuhan (Appendix 1 Table 2).
The server is an online platform summarizing mobile phone travel data hosted by Baidu Huiyan (https://huiyan.baidu.com).

#### Calculations of $R_0$ and Effect of Intervention Strategies

We considered realistic distributions for the latent and infectious periods to calculate $R_0$. We described the methods we used to calculate $R_0$ and the effect of intervention strategies on the outbreak (Appendix 2, https://wwwnc.cdc.gov/EID/article/26/7/20-0282-App2.pdf).

## Results

### Estimating Distributions of Epidemiologic Parameters

We first translated reports from documents or news reports published daily from the China CDC website and official websites of health commissions across provinces and special municipalities in China during January 15–30, 2020. Altogether, we collected

137 individual case reports from China and 3 additional case reports from outside of China (Appendix 1 Table 1).

By using this dataset, we estimated the basic parameter distributions of durations from initial exposure to symptom onset to hospitalization to discharge or death. Our estimate of the time from initial exposure to symptom onset (i.e., the incubation period) is 4.2 days (95% CI 3.5–5.1 days) (Figure 1, panel A), based on 24 case reports. This estimated duration is generally consistent with a recent report by Guan et al. (*10*) showing that the median incubation period is 4 days. Our estimate is ≈1 day shorter than 2 previous estimates (*1*,*11*). One potential caveat of our estimation is that because most of the case reports we collected were from the first few persons detected in each province, this estimation might be biased toward patients with more severe symptoms if they are more likely to be detected.

The time from symptom onset to hospitalization showed evidence of time dependence (Figure 1, panel B; Appendix 2 Figure 1). Before January 18, the time from symptom onset to hospitalization was 5.5 days (95% CI 4.6–6.6 days), whereas after January 18, the duration shortened significantly to 1.5 days (95% CI 1.2–1.9 days) ($p<0.001$ by Mann–Whitney U test). The change in the distribution coincides with news reports of potential human-to-human transmission and upgrading of emergency response level to Level 1 by the China CDC. The emerging consensus about the risk for COVID-19 probably led to substantial behavior changes among symptomatic persons, in terms of seeking more timely medical care during this period. However, because most of the individual reports were collected in provinces other than Hubei, the change in durations might only reflect changes in the rest of China (rather than in Hubei). We also found that the time from initial hospital admittance to discharge was 11.5 days (95% CI 8.0–17.3 days) (Figure 1, panel C) and from initial hospital admittance to death was 11.2 days (95% CI 8.7–14.9 days) (Figure 1, panel D). The time from symptom onset to death was estimated to be 16.1 days (95% CI 13.1–20.2 days).

### Estimating the Growth Rate of the Outbreak in Wuhan in January 2020

Moving from empirical estimates of basic epidemiologic parameters to an understanding of the early growth rates of COVID-19 requires model-based inference and data. We first collected real-time travel data during the epidemic by using the Baidu Migration server, which provides real-time travel patterns in China based on mobile-phone positioning services (Figure 2, panel A; Appendix 1 Methods, Table 2). We estimated that, before the January 23 lockdown of the city, ≈40,000–140,000 people in Wuhan traveled to destinations outside Hubei Province each day (Figure 2, panel B). The extensive travel before the Lunar New Year was probably an important driver of the spread of COVID-19 in China.

We then integrated spatiotemporal domestic travel data to infer the outbreak dynamics in Wuhan by using two mathematical approaches (Appendix 2; conceptual framework depicted in Figure 3, panel A). The first-arrival model uses a unique feature of our case report dataset whereby the dates of departure from Wuhan for many of the first persons who were confirmed with SARS-CoV-2 infection in each province were known (Appendix 1 Table 1). We assumed an exponential growth for the total infected

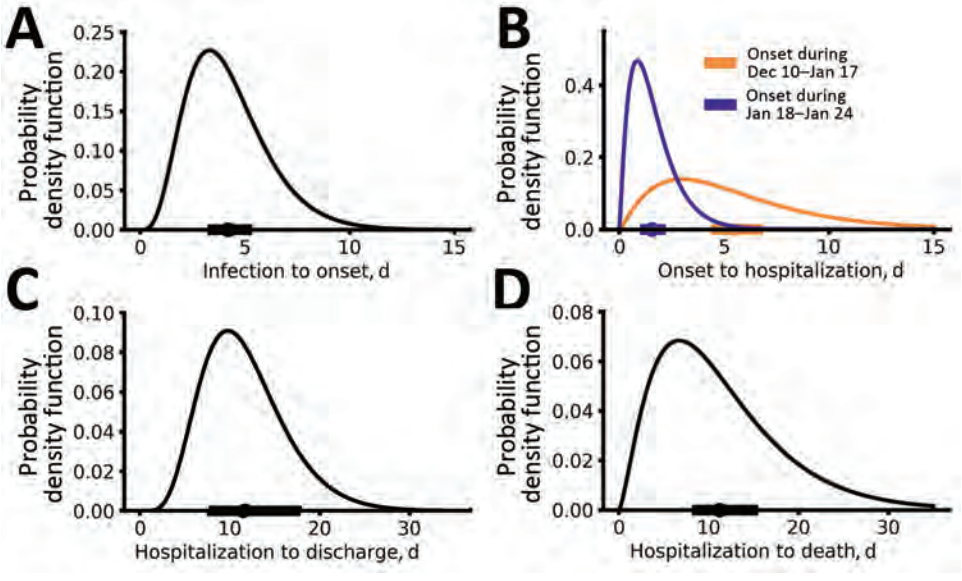


**Figure 1.** Epidemiologic characteristics of early dynamics of coronavirus disease outbreak in China. Distributions of key epidemiologic parameters: durations from infection to symptom onset (A), from symptom onset to hospitalization (B), from hospitalization to discharge (C), and from hospitalization to death (D). Filled circles and bars on *x*-axes denote the estimated means and 95% CIs.

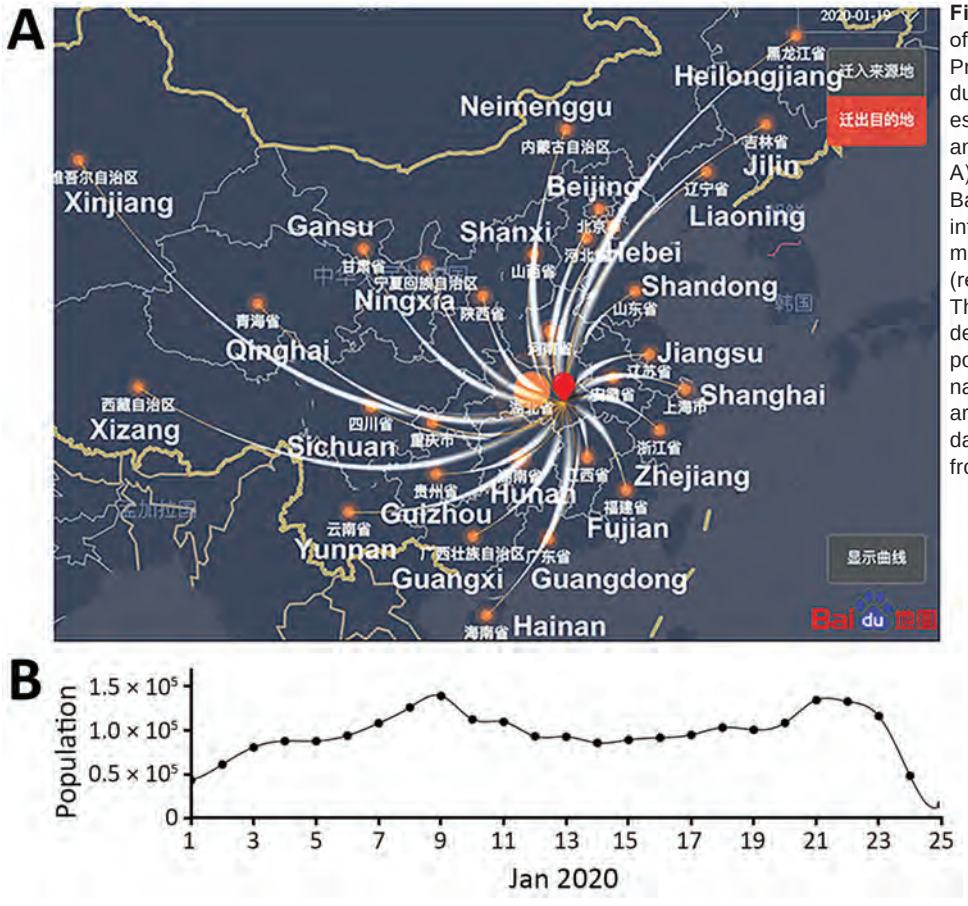


**Figure 2.** Extremely high level of travel from Wuhan, Hubei Province, to other provinces during January 2020, as estimated by using high-resolution and real-time travel data, China. A) A modified snapshot of the Baidu Migration online server interface showing the human migration pattern out of Wuhan (red dot) on January 19, 2020. Thickness of curved white lines denotes the size of the traveler population to each province. The names of most of the provinces are shown in white. B) Estimated daily population sizes of travelers from Wuhan to other provinces.

population $I^*$ in Wuhan, $I^*(t) = e^{r(t-t_0)}$, where $I^*$ includes infected persons who are asymptomatic or symptomatic, $r$ is the exponential growth rate, and $t_0$ is the theoretical time of the exponential growth initiation, so that $I^*(t_0) = 1$ in the deterministic model. We call $t_0$ a "theoretical" time in the sense that it should not be interpreted as the time of first infection in a population. We should expect that $t_0$ is later than the date of the first infection because multiple spillover events from the animal reservoir might be needed to establish sustained transmission and stochasticity might play a large role in initial dynamics before the onset of exponential growth (*12*–*14*).

We used travel data for each of the provinces (Appendix 1 Table 3) and the earliest times that an infected person arrived in a province, across a total of 26 provinces (Figure 3, panel B), to infer $r$ and $t_0$ (Appendix 2). Model predictions of arrival times in the 26 provinces fitted the actual data well (Appendix 2 Figure 2). The growth rate $r$ is estimated to be 0.29/day (95% CI 0.21–0.37/day), corresponding to a doubling time of 2.4 days (95% CI 1.9–3.3 days). $t_0$ is estimated to be December 20, 2019 (95% CI December 11–26). As we show later, there exist larger uncertainties in the estimation of $t_0$.

We further estimated that the total infected population size in Wuhan was ≈4,100 (95% CI 2,423–6,178) on January 18 (Appendix 2 Figure 3), which is consistent with a recently posted estimate (*7*). The estimated number of infected persons was ≈18,700 (95% CI 7,147–38,663) on January 23 (i.e., the date when Wuhan started its lockdown). We projected that without any control measures, the infected population would be ≈233,400 (95% CI 38,757–778,278) by the end of January.

An alternative model, the case count approach, used daily new case counts of persons who had COVID-19 diagnosed in other provinces but who had been in Hubei Province within 14 days of becoming symptomatic. This model uses data beyond the first appearance of an infected person from Wuhan but also accounts for the stochastic nature of the process by using a hybrid model. In this model, the infected population in Wuhan was described with a deterministic model, whereas the infected persons who traveled from Wuhan to other provinces were tracked with a stochastic SEIR (susceptible-exposed-infectious-recovered) model (*12*). We restricted the data to the period of January

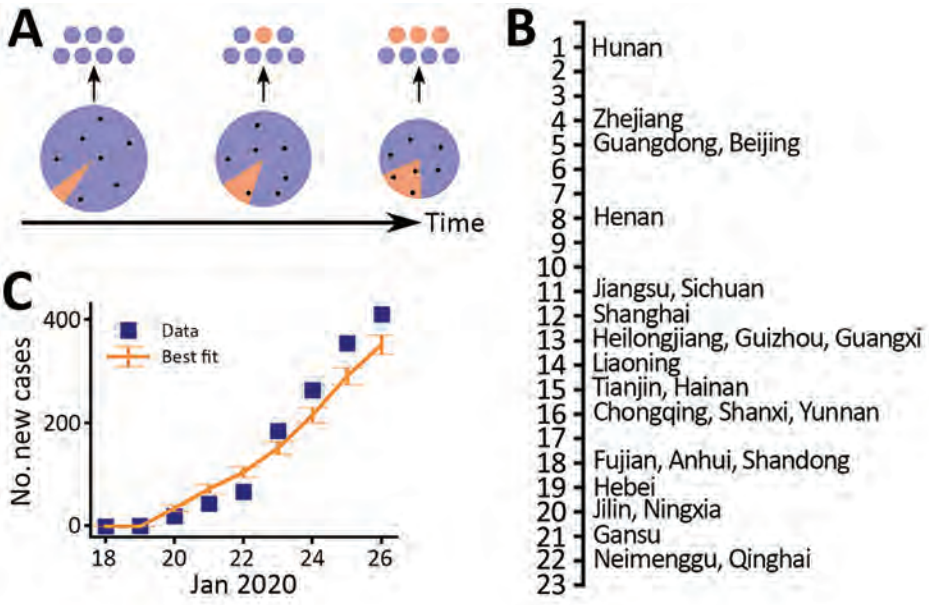


**Figure 3.** Estimates of the exponential growth rate and the date of exponential growth initiation of the coronavirus disease outbreak in China based on 2 different approaches. A) Schematic illustrating the export of infected persons from Wuhan. Travelers (dots) are assumed to be random samples from the total population (whole pie). Because of the growth of the infected population (orange pie) and the shrinking size of the total population in Wuhan over time, probability of infected persons traveling to other provinces increases (orange dots). B) The dates of documented first arrivals of infected persons in 26 provinces. C) Best fit of the case count model to daily counts of new cases (including only imported cases) in provinces other than Hubei. Error bars indicate SDs.

19–26, when new cases reported were mostly infections imported from Wuhan (i.e., indicative of the dynamics in Wuhan). The transitions of the infected persons from symptom onset to hospitalization and then to case confirmation were assumed to follow the distributions inferred from the case report data (Appendix 2). Simulation of the model using best-fit parameters showed that the model described the observed case counts over time well (Figure 3, panel C). The estimated theoretical time ($t_0$) is December 16, 2019 (95% CI December 12–21), and the exponential growth rate is 0.30/day (95% CI 0.26–0.34/day). These estimates are consistent with estimates in the first arrival approach (Figure 4; Appendix 2 Figure 4).

In both models, we assumed perfect detection (i.e., of infected cases outside of Hubei Province). However, a certain fraction of cases probably was not reported. To investigate the robustness of our estimates, we performed extensive sensitivity analyses to test 23 different scenarios of surveillance intensity (Appendix 2). First, we tested the assumption that a constant fraction of infected persons (e.g., persons with mild or no symptoms) (*15*) were not detected. We found that under this assumption, $t_0$would be earlier than our estimate but the estimation of the growth rate remained the same (Appendix 1 Table 4). Second, we tested the assumption that the intensity of surveillance increases over the period of data collection, although this scenario is less likely because of the intensive surveillance implemented outside Hubei Province. We found that our data in general do not support this hypothesis on the basis of corrected Akaike Information criterion scores (Appendix 1 Table 4). However, if the intensity of surveillance outside Hubei Province increased over the period of January, we would predict a lower growth rate than the estimate we just described. For the worst-case scenario considered, we estimated the growth rate of the outbreak to be 0.21/day (Appendix 2).

### Other Evidence of a High Growth Rate of the Outbreak in Wuhan

In addition to using 2 modeling approaches, we looked for other evidence of a high outbreak growth rate to cross-validate our estimations. We found that the time series of reported deaths in Hubei, which is less subject to the biases of the confirmed case counts, is simply not consistent with a growth rate of 0.1/day (Appendix 2 Figure 5). As the infected population grows, the number of death cases will grow at the same rate but with a delayed onset corresponding to the time from infection to death. Fitting a simple exponential growth model to the number of reported deaths in Hubei during late January 2020 yields an estimate of 0.22–0.27/day, which is within the 95% CI of the estimation we previously described.

Overall, these analyses suggest that although there exist uncertainties depending on the level of surveillance, the exponential growth rate of the outbreak is probably 0.21–0.3/day. This estimation is much higher than previous reports, in which the growth rate was estimated to be 0.1–0.14/day (*1*,*3*–*5*).

### Estimating $R_0$

The basic reproductive number, $R_0$, is dependent on the exponential growth rate of an outbreak, as well as additional factors such as the latent period (the time from infection to infectiousness) and the infectious period (*16*,*17*), both of which cannot be estimated directly from the data. Following the approach by Wearing and Rohani (*16*), we found that with a high growth rate of the outbreak, $R_0$ is in general high and the longer the latent and the infectious periods, the higher the estimated $R_0$ (Appendix 2 Figure 6).

To derive realistic values of $R_0$, we used previous estimates of serial intervals for COVID-19. The serial interval is estimated to be ≈7–8 days based on data collected early in the outbreak in Wuhan (*1*). More recent data collected in Shenzhen Province, China, suggests that the serial interval is dependent on the time to hospital isolation (Q. Bi et al., unpub. data, https://doi.org/10.1101/2020.03.03.20028423). When infected persons are isolated after 5 days of symptoms (a probable scenario for the early outbreak in Wuhan, where the public was not aware of the virus and few interventions were implemented), the serial interval is estimated to be 8 days (Q. Bi et al., unpub. data). Thus, these results suggest a serial interval of 7–8 days. With this serial interval, we sampled latent and infectious periods within wide biologically plausible ranges (Appendix 2) and estimated the median $R_0$ to be 5.8 (95% CI 4.4–7.7) (Figure 5, panel A). To include a wider range of serial interval (i.e., 6–9 days) (Figure 5, panel A; Appendix 2 Figure 6), given the uncertainties in these estimations, we estimated that the median of estimated $R_0$ is 5.7 (95% CI of 3.8–8.9) (Figure 5, panel B). The estimated $R_0$ can be lower if the serial interval is shorter. However, recent studies reported that persons can be infectious for a long period, such as 1–3 weeks after symptom onset (*18*; R. Woelfel et al., unpub data. https://doi.org/10.1101/2020.03.05.20030502); thus, we believe that a mean serial interval shorter than 6 days is unlikely during the early outbreak in Wuhan, where infected persons were not rapidly hospitalized.

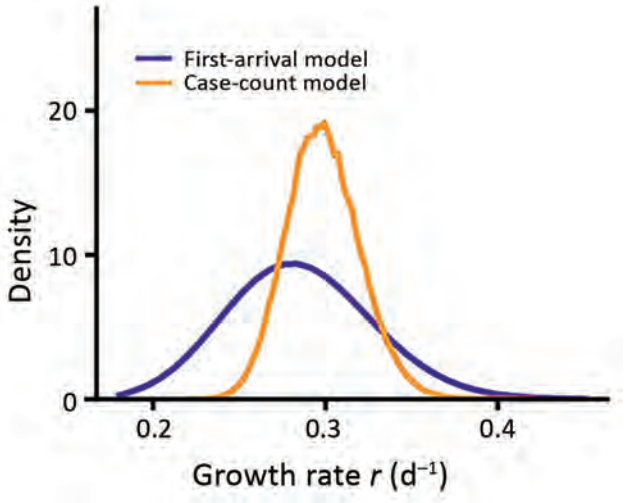


**Figure 4.** Marginalized likelihoods of growth rate (*r*) for 2 inference approaches to estimates the exponential growth rate of the coronavirus disease outbreak in China.

### Implications for Intervention Strategies

The $R_0$ values we estimated have important implications for predicting the effects of pharmaceutical and nonpharmaceutical interventions. For example, the threshold for combined vaccine efficacy and herd immunity needed for disease extinction is calculated as $1 - 1/R_0$. At $R_0 = 2.2$, this threshold is only 55%. But at $R_0 = 5.7$, this threshold rises to 82% (i.e., >82% of the population has to be immune, through either vaccination or prior infection, to achieve herd immunity to stop transmission).

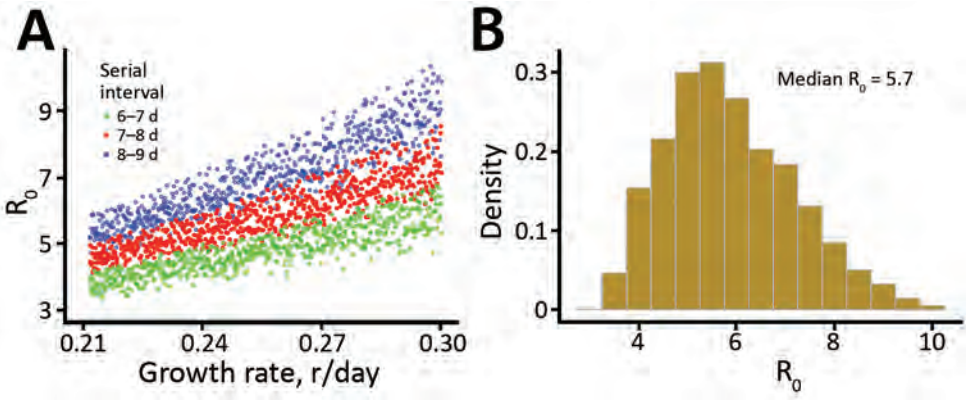


**Figure 5.** Estimation of the basic reproductive number ($R_0$), derived by integrating uncertainties in parameter values, during the coronavirus disease outbreak in China. A) Changes in $R_0$ based on different growth rates and serial intervals. Each dot represents a calculation with mean latent period (range 2.2–6 days) and mean infectious periods (range 4–14 days). Only those estimates falling within the range of serial intervals of interests were plotted. B) Histogram summarizing the estimated $R_0$ of all dots in panel A (i.e., serial interval ranges of 6–9 days). The median $R_0$ is 5.7 (95% CI 3.8–8.9).

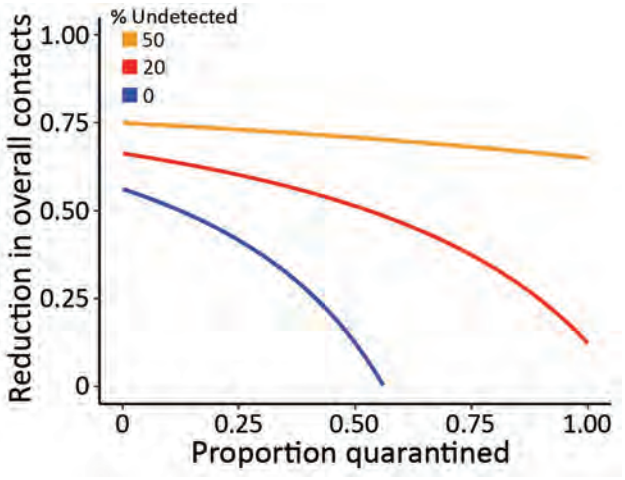


**Figure 6.** Levels of minimum efforts of intervention strategies needed to control the spread of severe acute respiratory syndrome coronavirus 2, (i.e. reducing the reproductive number to <1), during the coronavirus disease outbreak in China. Strategies considered were quarantine of infected persons and persons who had contact with them (*x*-axis) and population-level efforts to reduce overall contact rates (*y*-axis). Percentages denote the percentages of transmissions driven by infected persons that were not detected by surveillance as a result of asymptomatic infection, mild-to-moderate illness or low surveillance intensity.

We then evaluated the effectiveness for nonpharmaceutical interventions, such as contact tracing, quarantine, and social distancing, by using the framework by Lipsitch et al. (*19*) (Appendix 2). We extended the framework to consider a fraction of transmission occurring from infected persons who would not be identified by surveillance and can transmit effectively (*15*). This fraction is determined by the fraction of actual asymptomatic persons and the extent of surveillance efforts to identify these persons and persons with mild-to-moderate symptoms. Results show that quarantine and contact tracing of symptomatic persons can be effective when the fraction of unidentified persons is low. However, when 20% of transmission is driven by unidentified infected persons, high levels of social distancing efforts will be needed to contain the virus (Figure 6), highlighting the importance of early and effective surveillance, contact tracing, and quarantine. Future field, laboratory, and modeling studies aimed to address the unknowns, such as the fraction of asymptomatic persons, the extent of their transmissibility depending on symptom severity, the time when persons become infectious, and the existence of superspreaders are needed to accurately predict the impact of various control strategies (*20*).

## Discussion

In this study, we estimated several basic epidemiologic parameters, including the incubation period (4.2 days), a time dependent duration from symptom onset to hospitalization (changing from 5.5 days in early January to 1.5 days in late January outside Hubei Province), and the time from symptom onset to death (16.1 days). By using 2 distinct approaches, we estimated the growth rate of the early outbreak in Wuhan to be 0.21–0.30 per day (a doubling time of 2.3–3.3 days), suggesting a much faster rate of spread than initially measured. This finding would have important implications for forecasting epidemic trajectories and the effect on healthcare systems as well as for evaluating the effectiveness of intervention strategies.

We found $R_0$ is likely to be 5.7 given our current state of knowledge, with a broad 95% CI (3.8–8.9). Among many factors, the lack of awareness of this new pathogen and the Lunar New Year travel and gathering in early and mid-January 2020 might or might not play a role in the high $R_0$. A recent study based on structural analysis of the virus particles suggests SARS-CoV-2 has a much higher affinity to the receptor needed for cell entry than the 2003 SARS virus (*21*), providing a molecular basis for the high infectiousness of SARS-CoV-2.

How contagious SARS-CoV-2 is in other countries remains to be seen. Given the rapid rate of spread as seen in current outbreaks in Europe, we need to be aware of the difficulty of controlling SARS-CoV-2 once it establishes sustained human-to-human transmission in a new population (*20*). Our results suggest that a combination of control measures, including early and active surveillance, quarantine, and especially strong social distancing efforts, are needed to slow down or stop the spread of the virus. If these measures are not implemented early and strongly, the virus has the potential to spread rapidly and infect a large fraction of the population, overwhelming healthcare systems. Fortunately, the decline in newly confirmed cases in China and South Korea in March 2020 and the stably low incidences in Taiwan, Hong Kong, and Singapore strongly suggest that the spread of the virus can be contained with early and appropriate measures.

### Acknowledgments

We thank Alan Perelson, Christiaan van Dorp, and Ruy Ribeiro for suggestions and critical reading of the manuscript and Weili Yin for help with collecting and translating documents from provincial health commission websites.

S.S. and R.K. received funding from the Defense Advanced Research Projects Agency (grant no. HR0011938513) and the Laboratory Directed Research and Development Rapid

Response Program through the Center for Nonlinear Studies at Los Alamos National Laboratory. C.X. received funding from Laboratory Directed Research and Development Program. E.R.S. received funding from the National Institutes of Health (grant no. R01AI135946). The funders had no role in study design, data collection and analysis, decision to publish, or preparation of the manuscript.

Author contributions: R.K. and N.H. conceived the project; R.K. collected data; S.S., Y.T.L., C.X., and R.K. performed analyses; S.S., Y.T.L., E.R.S., N.H., and R.K. wrote and edited the manuscript.

Authors declare no competing interests. All data are available in the main text and in Appendices 1 and 2.

## About the Author

Dr. Sanche is a postdoctoral research associate at Los Alamos National Laboratory, Los Alamos, New Mexico, USA. His primary research interest lies in complex disease dynamics inferred from data science and mathematical modeling. Dr. Lin is also a postdoctoral research associate at Los Alamos National Laboratory. His primary research interest lies in applied stochastic processes, biological physics, statistical inference, and computational system biology.

## References

1. Li Q, Guan X, Wu P, Wang X, Zhou L, Tong Y, et al. Early transmission dynamics in Wuhan, China, of novel coronavirus-infected pneumonia. N Engl J Med. 2020;382:1199–207. https://doi.org/10.1056/NEJMoa2001316
2. WHO. Pneumonia of unknown cause—China [cited 2020 Jan 30]. https://www.who.int/csr/don/05-january-2020-pneumonia-of-unkown-cause-china
3. Wu JT, Leung K, Leung GM. Nowcasting and forecasting the potential domestic and international spread of the 2019-nCoV outbreak originating in Wuhan, China: a modelling study. Lancet. 2020;395:689–97. https://doi.org/10.1016/S0140-6736(20)30260-9
4. Riou J, Althaus CL. Pattern of early human-to-human transmission of Wuhan 2019 novel coronavirus (2019-nCoV), December 2019 to January 2020. Euro Surveill. 2020;25:25. https://doi.org/10.2807/1560-7917.ES.2020.25.4.2000058
5. Du Z, Wang L, Cauchemez S, Xu X, Wang X, Cowling BJ, et al. Risk for transportation of coronavirus disease from Wuhan to other cities in China. Emerg Infect Dis. 2020;26:1049–52. https://doi.org/10.3201/eid2605.200146
6. Novel Coronavirus Pneumonia Emergency Response Epidemiology Team. The epidemiological characteristics of an outbreak of 2019 novel coronavirus diseases (COVID-19) in China [in Chinese]. Zhonghua Liu Xing Bing Xue Za Zhi. 2020;41:145–51.
7. Imai N, Dorigatti I, Cori A, Donnelly C, Riley S. Ferguson. Report 2: estimating the potential total number of novel coronavirus cases in Wuhan City, China [cited 2020 Feb 2]. https://www.imperial.ac.uk/media/imperial-college/medicine/sph/ide/gida-fellowships/Imperial-College-COVID19-update-epidemic-size-22-01-2020.pdf
8. Imai N, Dorigatti I, Cori A, Riley S, Ferguson NM. Estimating the potential total number of novel coronavirus cases in Wuhan City, China [cited 2020 Feb 2]. https://www.imperial.ac.uk/media/imperial-college/medicine/sph/ide/gida-fellowships/2019-nCoV-outbreak-report-17-01-2020.pdf
9. Hongyang L. Railway corporation using big data to trace potential virus carrier. ChinaDailyNews [cited 2020 Feb 1]. https://www.chinadaily.com.cn/a/202001/30/WS5e329ca2a310128217273b89.html
10. Guan WJ, Ni ZY, Hu Y, Liang WH, Ou CQ, He JX, et al.; China Medical Treatment Expert Group for Covid-19. Clinical characteristics of coronavirus disease 2019 in China. N Engl J Med. 2020 Feb 28 [Epub ahead of print]. https://doi.org/10.1056/NEJMoa2002032
11. Lauer SA, Grantz KH, Bi Q, Jones FK, Zheng Q, Meredith HR, et al. The incubation period of coronavirus disease 2019 (COVID-19) from publicly reported confirmed cases: estimation and application. Ann Intern Med. 2020 Mar 10 [Epub ahead of print]. https://doi.org/10.7326/M20-0504
12. Anderson RM, May RM. Infectious diseases of humans: dynamics and control. Oxford Science Publications. Oxford: Oxford University Press; 1991. p. 768.
13. Lloyd-Smith JO, Schreiber SJ, Kopp PE, Getz WM. Superspreading and the effect of individual variation on disease emergence. Nature. 2005;438:355–9. https://doi.org/10.1038/nature04153
14. Romero-Severson EO, Ribeiro RM, Castro M. Noise is not error: detecting parametric heterogeneity between epidemiologic time series. Front Microbiol. 2018;9:1529. https://doi.org/10.3389/fmicb.2018.01529
15. Rothe C, Schunk M, Sothmann P, Bretzel G, Froeschl G, Wallrauch C, et al. Transmission of 2019-nCoV infection from an asymptomatic contact in Germany. N Engl J Med. 2020;382:970–1. https://doi.org/10.1056/NEJMc2001468
16. Wearing HJ, Rohani P, Keeling MJ. Appropriate models for the management of infectious diseases. PLoS Med. 2005;2:e174. https://doi.org/10.1371/journal.pmed.0020174
17. Lloyd AL. The dependence of viral parameter estimates on the assumed viral life cycle: limitations of studies of viral load data. Proc Biol Sci. 2001;268:847–54. https://doi.org/10.1098/rspb.2000.1572
18. Zhou F, Yu T, Du R, Fan G, Liu Y, Liu Z, et al. Clinical course and risk factors for mortality of adult inpatients with COVID-19 in Wuhan, China: a retrospective cohort study. Lancet. 2020;395:1054–62. https://doi.org/10.1016/S0140-6736(20)30566-3
19. Lipsitch M, Cohen T, Cooper B, Robins JM, Ma S, James L, et al. Transmission dynamics and control of severe acute respiratory syndrome. Science. 2003;300:1966–70. https://doi.org/10.1126/science.1086616
20. Fraser C, Riley S, Anderson RM, Ferguson NM. Factors that make an infectious disease outbreak controllable. Proc Natl Acad Sci U S A. 2004;101:6146–51. https://doi.org/10.1073/pnas.0307506101
21. Wrapp D, Wang N, Corbett KS, Goldsmith JA, Hsieh CL, Abiona O, et al. Cryo-EM structure of the 2019-nCoV spike in the prefusion conformation. Science. 2020;367:1260–3. https://doi.org/10.1126/science.abb2507

Address for correspondence: Ruian Ke, T-6 Theoretical Biology and Biophysics, Mailstop K710, Los Alamos National Laboratory, NM 87544, USA; email: rke@lanl.gov

# Severe Acute Respiratory Syndrome Coronavirus 2–Specific Antibody Responses in Coronavirus Disease Patients

Nisreen M.A. Okba,[1] Marcel A. Müller,[1] Wentao Li,[1] Chunyan Wang, Corine H. GeurtsvanKessel, Victor M. Corman, Mart M. Lamers, Reina S. Sikkema, Erwin de Bruin, Felicity D. Chandler, Yazdan Yazdanpanah, Quentin Le Hingrat, Diane Descamps, Nadhira Houhou-Fidouh, Chantal B.E.M. Reusken, Berend-Jan Bosch, Christian Drosten, Marion P.G. Koopmans, Bart L. Haagmans

A new coronavirus, severe acute respiratory syndrome coronavirus 2 (SARS-CoV-2), has recently emerged to cause a human pandemic. Although molecular diagnostic tests were rapidly developed, serologic assays are still lacking, yet urgently needed. Validated serologic assays are needed for contact tracing, identifying the viral reservoir, and epidemiologic studies. We developed serologic assays for detection of SARS-CoV-2 neutralizing, spike protein–specific, and nucleocapsid-specific antibodies. Using serum samples from patients with PCR-confirmed SARS-CoV-2 infections, other coronaviruses, or other respiratory pathogenic infections, we validated and tested various antigens in different in-house and commercial ELISAs. We demonstrated that most PCR-confirmed SARS-CoV-2–infected persons seroconverted by 2 weeks after disease onset. We found that commercial S1 IgG or IgA ELISAs were of lower specificity, and sensitivity varied between the 2 assays; the IgA ELISA showed higher sensitivity. Overall, the validated assays described can be instrumental for detection of SARS-CoV-2–specific antibodies for diagnostic, seroepidemiologic, and vaccine evaluation studies.

Author affiliations: Erasmus Medical Center, Rotterdam, the Netherlands (N.M.A. Okba, C.H. GeurtsvanKessel, M.M. Lamers, R.S. Sikkema, E. deBruin, F.D. Chandler, C.B.E.M. Reusken, M.P.G. Koopmans, B.L. Haagmans); Charité-Universitätsmedizin Berlin, Berlin, Germany (M.A. Müller, V.M. Corman, C. Drosten); German Centre for Infection Research, Berlin (M.A. Müller, V.M. Corman, C. Drosten); Utrecht University, Utrecht, the Netherlands (W. Li, C. Wang, B.-J. Bosch); Université de Paris, Paris, France (Y. Yazdanpanah, Q. Le Hingrat, D. Descamps); Hôpital Bichat-Claude Bernard, Paris (Y. Yazdanpanah, Q. Le Hingrat, D. Descamps, N. Houhou-Fidouh); RIVM, Bilthoven, the Netherlands (C.B.E.M. Reusken)

DOI: https://doi.org/10.3201/eid2607.200841

In December 2019, a new coronavirus emerged in China and caused an acute respiratory disease now known as coronavirus disease 2019 (COVID-19) (*1*). The virus was identified to be a betacoronavirus related to severe acute respiratory syndrome coronavirus (SARS-CoV) and thus was named SARS-CoV-2 (*2*). In <2 decades, this virus is the third known coronavirus to cross the species barrier and cause severe respiratory infections in humans after SARS-CoV in 2003 and Middle East respiratory syndrome coronavirus (MERS-CoV) in 2012, yet with unprecedented spread compared with the earlier 2 viruses.

Because of the rapid increase in number of cases and uncontrolled and vast spread worldwide, the World Health Organization has declared SARS-CoV-2 a pandemic. As of March 14, 2020, the virus had infected >130,000 persons in 122 countries, 3.7% of whom had died. (*3*). Rapid identification of the etiology and sharing of the genetic sequence of the virus, followed by international collaborative efforts initiated because of emergence of SARS-CoV-2, has led to rapid availability of real-time PCR diagnostic assays that support case ascertainment and tracking of the outbreak (*4*). Availability of these assays has helped in patient detection and efforts to contain the virus. However, validated serologic assays are still lacking and are urgently needed.

Validated serologic assays are crucial for patient contact tracing, identifying the viral reservoir hosts, and epidemiologic studies. Epidemiologic studies are urgently needed to help uncover the burden of disease, in particular the rate of asymptomatic infections, and to get better estimates on illness and death. In ad-

[1]These authors contributed equally to this article.

dition, these epidemiologic studies can help identify the extent of virus spread in households, communities, and specific settings, which could help guide control measures. Serologic assays are also needed for evaluation of results of vaccine trials and development of therapeutic antibodies.

Among the 4 coronavirus structural proteins, the spike (S) and nucleocapsid (N) proteins are the main immunogens (*5*). We describe development of serologic assays for detection of virus neutralizing antibodies and antibodies to the N protein and various S protein domains, including the S1 subunit, and the receptor-binding domain (RBD) of SARS-CoV-2 in an ELISA format. Using a well-characterized cohort of serum samples from PCR-confirmed SARS-CoV-2 and patients PCR-confirmed to be infected with seasonal coronaviruses and other respiratory pathogens, we validated and tested various antigens in different platforms developed in-house, as well as a commercial platform.

## Materials and Methods

### Serum Samples

#### Erasmus Medical Center Samples

We used serum samples (n = 10) collected from 3 PCR-confirmed patients: 2 with mild COVID-19 and 1 with severe COVID-19 (Table 1) from France in accordance with local ethics approvals (F.-X. Lescure et al., unpub. data, https://doi.org/10.1101/2020.03.11.987958). For assay validation, we used samples obtained from persons who had PCR-diagnosed infections with human coronaviruses (HCoV-229E, NL63, or OC43), SARS-CoV, MERS-CoV, or other respiratory viruses (Table 1) as reported (*6*). We also included samples from patients who had recent infections with cytomegalovirus, Epstein-Barr virus, or *Mycoplasma pneumoniae* because these pathogens have a higher likelihood of causing false-positive results. As negative controls, we used serum samples from 45 healthy blood donors (Sanquin Blood Bank, https://www.sanquin.nl) (cohort A). We also tested serum samples from SARS patients (*7*). All samples were stored at -20°C until use. The Sanquin Blood Bank obtained written informed consent for research use of samples from blood donors. Use of serum samples from the Netherlands was approved by the local medical ethics committee (approval no. 2014–414).

#### Berlin Samples

All serum samples (n = 31) from patients with PCR-confirmed cases of COVID-19 cases were previously analyzed by a recombinant SARS-CoV-2 S protein–based immunofluorescence test and plaque reduction neutralization (R. Wölfel et al., unpub.

**Table 1.** Cohorts used to validate specificity and sensitivity of assays for SARS-CoV-2*

| Cohort | Country | Sample source | Infection | No. samples | Postdiagnosis range or time |
|---|---|---|---|---|---|
| A | The Netherlands | Healthy blood donors (negative cohort) | NA | 45 | NA |
| B | The Netherlands | Non-CoV respiratory infections† | Adenovirus | 5 | 2–4 wk |
| | | | Bocavirus | 2 | 2–4 wk |
| | | | Enterovirus | 2 | 2–4 wk |
| | | | HMPV | 9 | 2–4 wk |
| | | | Influenza A | 13 | 2–4 wk |
| | | | Influenza B | 6 | 2–4 wk |
| | | | Rhinovirus | 9 | 2–4 wk |
| | | | RSV | 9 | 2–4 wk |
| | | | PIV-1 | 4 | 2–4 wk |
| | | | PIV-3 | 4 | 2–4 wk |
| | | | *Mycoplasma pneumoniae* | 1 | 2–4 wk |
| | | | CMV | 5 | 2–4 wk |
| | | | EBV | 7 | 2–4 wk |
| C | The Netherlands | HCoV infections† | α-CoV HCoV-229E | 19 | 2 w–1 y |
| | | | α-CoV HCoV-NL63 | 18 | 2 w–1 y |
| | | | β-CoV HCoV-OC43 | 38 | 2 w–1 y |
| D | The Netherlands | Zoonotic CoV infections† | MERS-CoV | 2 | 10,228 d |
| | South Korea | | | 5 | 9 mo |
| E | Hong Kong, China | Zoonotic CoV infection† | SARS-CoV | 2 | >14 d |
| F | France | RT-PCR confirmed SARS-CoV-2 infections | Mild infection | 6‡ | 3–27 d |
| | | | Severe infection | 4§ | 6–31 d |

*Cohorts A–E were used to test assay specificity; cohort F was used to test assay sensitivity. α-CoV, alphacoronavirus; β-CoV, betacoronavirus; CoV, coronavirus; CMV, cytomegalovirus; EBV, Epstein-Barr virus; HCoV, human coronavirus; HMPV, human metapneumovirus; MERS, Middle East respiratory syndrome; NA, not applicable; PIV, parainfluenza virus; RSV, respiratory syncytial virus; RT-PCR, reverse transcription PCR.
†Cross-reactivity.
‡Samples taken from 2 patients at different time points.
§Samples taken from 1 patient at different time points.

data, https://doi.org/10.1101/2020.03.05.20030502). We tested serum samples as part of an extended diagnostic regimen after we obtained informed written consent from patients. We obtained non–SARS-CoV-2–infected serum samples (n = 31) from the serum collection of the National Consiliary Laboratory for Coronavirus Detection at Charité–Universitätsmedizin Berlin (Berlin, Germany). Samples were collected after we obtained informed written consent. The collection contained follow-up antibody-positive serum samples from PCR-confirmed virus-infected cases: HCoV-229E (n = 4), HCoV-HKU1 (n = 3), HCoV-OC43 (n = 7), MERS-CoV (n = 3), HCoV-NL63 (n = 6), SARS-CoV (n = 3), and common cold CoV (n = 6).

### Protein Expression

We expressed the S ectodomains of SARS-CoV-2 (residues 1–1,213, strain Wuhan-Hu-1, GenBank accession no. QHD43416.1), SARS-CoV (residues 1–1,182, strain CUHK-W1, accession no. AAP13567.1), and MERS-CoV (residues 1–1262, strain EMC, accession no. YP_009047204.1) in HEK-293T cells by using a C-terminal trimerization motif, Strep-tag, and the pCAGGS expression plasmid. Likewise, we expressed the SARS-CoV-2 S1 subunit or its subdomains (S;S1, residues 1–682; $S1^A$, residues 1–294; RBD, residues 329–538; accession no. QHD43416.1) in 293T cells, as described (C. Wang et al., unpub. data, https://doi.org/10.1101/2020.03.11.987958).

We produced S1 proteins of other HCoVs: HKU1 (residues 1–750), OC43 (residues 1–760), NL63 (residues 1–717), 229E (residues 1–537), SARS-CoV (residues 1–676), and MERS-CoV as described (*6*,*8*). We affinity purified all recombinant proteins from culture supernatant by using Protein-A Sepharose beads (catalog no. 17–0780–01; GE Healthcare, GE Healthcare, https://www.gehealthcare.com) or strep-tactin beads (catalog no. 2–1201–010; IBA Lifesciences, https://www.iba-lifesciences.com). We checked purity and integrity of all purified recombinant proteins by using sodium dodecyl sulfate–polyacrylamide gel electrophoresis and staining with Coomassie blue.

### Plaque Reduction Neutralization Test

We used the plaque reduction neutralization test (PRNT) as a reference for this study because neutralization assays are the standard for coronavirus serologic analysis. We tested serum samples for their neutralization capacity against SARS-CoV-2 (German isolate; GISAID ID EPI_ISL 406862; European Virus Archive Global #026V-03883) by using PRNT as described with some modifications (*9*). We 2-fold serially diluted heat-inactivated samples in *Dulbecco modified Eagle medium* supplemented with $NaHCO_3$, HEPES buffer, penicillin, streptomycin, and 1% fetal bovine serum, starting at a dilution of 1:10 in 50 μL. We then added 50 μL of virus suspension (400 plaque-forming units) to each well and incubated at 37°C for 1 h before placing the mixtures on Vero-E6 cells. After incubation for 1 h, we washed, cells supplemented with medium, and incubated for 8 h. After incubation, we fixed the cells with 4% formaldehyde/phosphate-buffered saline (PBS) and stained the cells with polyclonal rabbit anti-SARS-CoV antibody (Sino Biological, https://www.sinobiological.com) and a secondary peroxidase-labeled goat anti-rabbit IgG (Dako, https://www.agilent.com). We developed signal by using a precipitate forming 3,3′,5,5′-tetramethylbenzidine substrate (True Blue; Kirkegaard and Perry Laboratories, https://www.seracare.com) and counted the number of infected cells per well by using an ImmunoSpot Image Analyzer (CTL Europe GmbH, https://www.immunospot.eu). The serum neutralization titer is the reciprocal of the highest dilution resulting in an infection reduction of >50% ($PRNT_{50}$). We considered a titer >20 to be positive.

We performed the PRNT for serum samples from Germany by using Vero E6 cells, as described (R. Wölfel et al., unpub. data, https://doi.org/10.1101/2020.03.05.20030502) (*10*) and 24-well plates. Before the PRNT, we heat-inactivated patient serum samples at 56°C for 30 min. For each dilution step (in duplicate), we diluted patient serum samples in 200 μL of OptiPro serum-free medium (https://www.thermofisher.com) and mixed 1:1 with 200 μL of virus solution containing 100 PFUs. We vortexed the 400-μL serum–virus solution gently, incubated at 37°C for 1 h, and then incubated each 24-well plate with 200 μL serum–virus solution. After incubation for 1 h at 37°C, we discarded supernatants, washed cells once with PBS, and supplemented them with 1.2% microcrystalline cellulose solution in Dulbecco modified Eagle medium. After 3 days, we fixed and inactivated the plates by using a 6% formaldehyde/PBS solution and stained with crystal violet.

### ELISA

We performed anti-SARS-CoV-2 S1 IgG and IgA ELISAs by using β-versions of 2 commercial kits (EUROIMMUN Medizinische Labordiagnostika AG, https://www.euroimmun.com) and performed the assay according to the manufacturer's protocol. We detected optical density (OD) at 450 nm and calculated a ratio of the reading of each sample to the reading of the calibrator, included in the kit, for each sample

(OD ratio). Because the β-version of the kit awaits validation and marking, we determined an in-house cutoff value based on the mean background reactivity of all SARS-CoV-2–negative serum samples in the study multiplied by 3. The OD ratio was 0.9 for IgA and 0.3 for IgG.

We performed the in-house ELISAs by coating 96-well microtiter ELISA plates with in-house–produced S antigens (S or S1 of SARS-CoV-2, SARS-CoV or MERS-CoV; SARS-CoV-2 $S1^A$; or RBD proteins) or SARS-CoV N protein (Sino Biological) in PBS overnight at 4°C. After blocking, we added diluted serum (diluted 1:100 or 2-fold serially diluted for titers) and incubated at 37°C for 1 h. Antigen-specific antibodies were detected by using peroxidase-labeled rabbit anti-human IgG (Dako) and 3,3′,5,5′-tetramethylbenzidine as a substrate. The absorbance of each sample was measured at 450 nm, and we set the cutoff value at 6 SD above the mean value for the negative cohort.

### S1 Protein Microarray

Serum samples were previously tested for antibodies against S1 of different coronaviruses. We used a protein microassay that has been described (*6*).

### Statistical Analysis

We analyzed the correlations between antibody responses detected by different ELISAs and those detected by PRNT, which is the standard for coronavirus serologic analysis. We used GraphPad Prism version 8 (https://www.graphpad.com) for this analysis.

## Results

We evaluated SARS-CoV-2–specific antibody responses in severe and mild cases by using serum samples collected at different times postonset of disease from 3 PCR-confirmed COVID-19 patients from France. We tested serum samples for SARS-CoV-2–specific antibodies by using different ELISAs. After infection, all 3 patients seroconverted between days 13 and 21 after onset of disease (Figure 1), and antibodies were elicited against the SARS-CoV-2 S, S1 subunit, and RBD, but only 2/3 patients had detectable antibodies to the N-terminal ($S1^A$) domain. Because the N protein of SARS-CoV-2 is 90% similar to that of SARS-CoV (Table 2), we used SARS-CoV N protein as an antigen to test for SARS-CoV-2 N protein–directed antibodies in an ELISA format. We found that antibodies were elicited against the N protein in all three patients. When tested in a PRNT, serum samples from all three patients neutralized SARS-CoV-2 infection. Antibody responses detected by different assays correlated strongly with neutralizing antibody responses (Figure 2). We observed cross-reactivity with the SARS-CoV S and S1 proteins, and to a lower extent with MERS-CoV S protein, but not with the MERS-CoV S1 protein (Figure 1, panels G, H). This finding was evident from analyzing the degree of similarity of the different coronavirus S protein domains to their corresponding SARS-CoV-2 proteins (Table 2). This analysis showed that the S2 subunit is more conserved and thus plays a role in the cross-reactivity seen when the whole S was used as antigen. Thus, S1 is more specific than S as an antigen for SARS-CoV-2 serologic diagnosis.

We further assessed the specificity of the S1 assay by using cohorts A–E (Table 1), which were composed of serum samples from healthy blood donors (A), PCR-confirmed acute respiratory non-CoV infections (B), acute-phase and convalescent-phase PCR-confirmed α- and β-HCoV infections (C), PCR-confirmed MERS-CoV infections (D), and PCR-confirmed SARS-CoV infections (E). None of the serum samples from specificity cohorts A–D were reactive in our in-house S1 ELISA at the set cutoff value, indicating 100% specificity, whereas serum samples from SARS-CoV patients cross-reacted (Figure 3, panel A). The specificity of S1 as an antigen for SARS-CoV-2 serologic analysis was further supported by the fact that 87%–100% of serum samples in cohorts A–C included in this study were seropositive for endemic HCoVs (HCoV-HKU1, HCoV-OC43, HCoV-NL63, and HCoV-229E), as determined by the S1 protein microarray (Figure 3, panel B). Nonetheless, all serum samples were seronegative for SARS-CoV and MERS-CoV.

Using the same cohort, we also validated the specificity of the N protein IgG and RBD IgG ELISAs for detecting SARS-CoV-2–specific antibodies. At the set cutoff, except for serum samples from SARS-CoV patients, none of the control serum samples was positive for RBD antibodies, and 1 MERS-CoV–positive serum sample was weakly positive for N protein antibodies (Figure 3, panels C, D). We also detected seroconversion among the 3 patients with COVID-19. Because serum samples from the 3 patients were collected at a limited number of time points, it was difficult to accurately assess time for seroconversion. To accurately assess time of seroconversion, a larger number of longitudinal samples is needed. Overall, these validated ELISAs for different antigens can be useful for epidemiologic studies and for evaluation of vaccine-induced immune responses.

Next, we validated the sensitivity and specificity of 2 commercial ELISA kits for detecting S1-specific IgG and IgA by using the same cohort (Table 1;

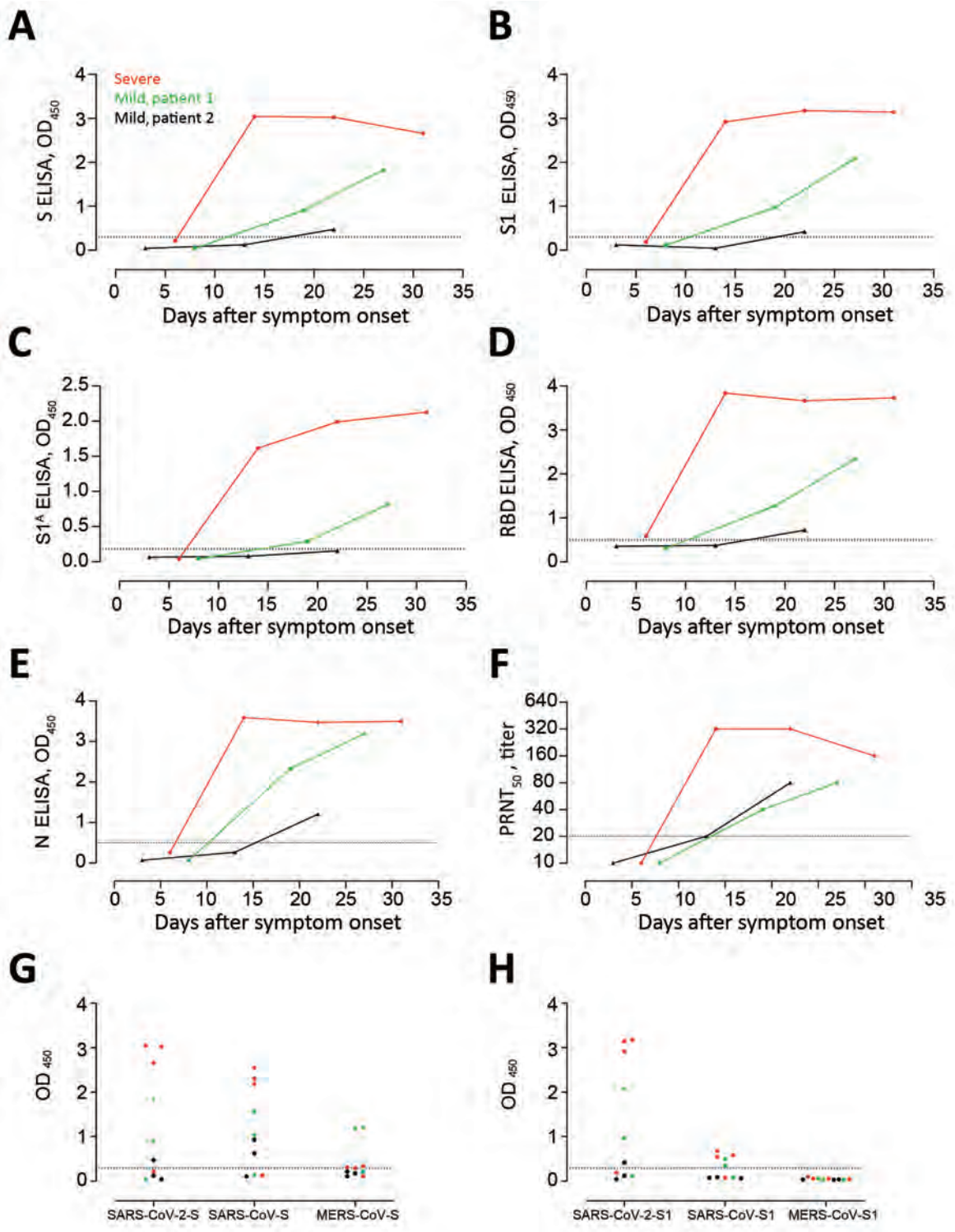


**Figure 1.** Kinetics of antibody responses against SARS-CoV-2 after infection. We tested 1 patient who had severe coronavirus disease 2019 (red) and 2 patients who had mild coronavirus disease 2019 (green and black) for antibody responses against A) S protein, B) S protein S1 subunit, C) S N-terminal ($S1^A$) domain, D) RDB, and E) N protein by using ELISAs. F) Virus-neutralizing antibodies were tested by using a $PRNT_{50}$. G, H) Reactivities of serum samples from the 3 patients at different time points against whole S (G) and S1 (H) of SARS-CoV-2, SARS-CoV, and MERS-CoV were tested by ELISAs. Dotted horizontal lines indicate ELISA cutoff values. MERS-CoV, Middle East respiratory syndrome coronavirus; N, nucleocapsid; OD, optical density; $PRNT_{50}$, 50% plaque reduction neutralization test; RBD, receptor-binding domain; S, spike; SARS-CoV, severe acute respiratory syndrome coronavirus; SARS-CoV-2, severe acute respiratory syndrome coronavirus 2.

**Table 2.** Percentage amino acid identity of coronavirus spike and nucleocapsid proteins with SARS-CoV-2 proteins*

| Virus type | Virus | Nucleocapsid | S | S1 | S2 | S1$^{A}$ | RBD |
|---|---|---|---|---|---|---|---|
| Betacoronavirus | SARS-CoV | 90 | 77 | 66 | 90 | 52 | 73 |
| | MERS-CoV | 49 | 33 | 24 | 43 | ND | ND |
| | HCoV-OC43 | 34 | 33 | 25 | 42 | ND | ND |
| | HCoV-HKU1 | 34 | 32 | 25 | 40 | ND | ND |
| Alphacoronavirus | HCoV-229E | 28 | 30 | 24 | 35 | ND | ND |
| | HCoV-NL63 | 29 | 28 | 21 | 36 | ND | ND |

*SARS-CoV-2, HCoV-OC43, MERS-CoV, HCoV-HKU1, HCoV-NL63, SARS-CoV, HCoV-229E (GenBank accession nos. NC_045512.2, NC_006213.1, NC_019843.3, NC_006577.2, NC_005831.2, NC_004718.3, and NC_002645.1). Protein sequences were aligned by using ClustalW (https://www.genome.jp/tools-bin/clustalw). RBD, receptor-binding domain; ND, not done; S, spike; S1, N-terminal subunit of the spike protein; S2, C-terminal subunit of the spike protein; S1$^{A}$, domain A of the spike S1 subunit; SARS-CoV, severe acute respiratory syndrome coronavirus; SARS-CoV-2, severe acute respiratory syndrome coronavirus 2.

Figure 4). All 3 COVID-19 patients had reactive antibodies detected by the IgG (6/10 serum samples) and IgA (7/10 serum samples) ELISAs (Figure 4). We also detected reactivity of serum samples from the validation cohorts A–D; 11/203 for IgA and 8/203 for IgG ELISAs. Serum samples from 2 patients infected with HCoV-OC43 (a betacoronavirus) were reactive in both IgG and IgA ELISA kits. We have reported the cross-reactivity of these serum samples in a MERS-CoV S1 IgG ELISA kit (*6*). We confirmed the cross-reactivity of the 2 serum samples by testing 12 serum samples from both patients that were collected at different time points (pre-OC43 and post-OC43 infection). Although all preinfection serum samples were negative, all postinfection serum samples were reactive in the IgG and IgA ELISAs.

Further validation was also made in a different laboratory by using 31 serum samples collected from 9 COVID-19 patients in Germany (R. Wölfel et al., unpub. data, https://doi.org/10.1101/2020.03.05.20030502) at different time points (3–23 days after disease onset); a specificity cohort composed of 18 serum samples from persons infected with HCoV (4 samples from persons infected with HCoV-229E, 3 from persons infected with HCoV-HKU1, 4 from persons infected with HCoV-NL63, and 7 from persons infected with HCoV-OC43); and 3 serum samples from persons infected with MERS-CoV and 3 samples from persons infected with SARS-CoV whose samples

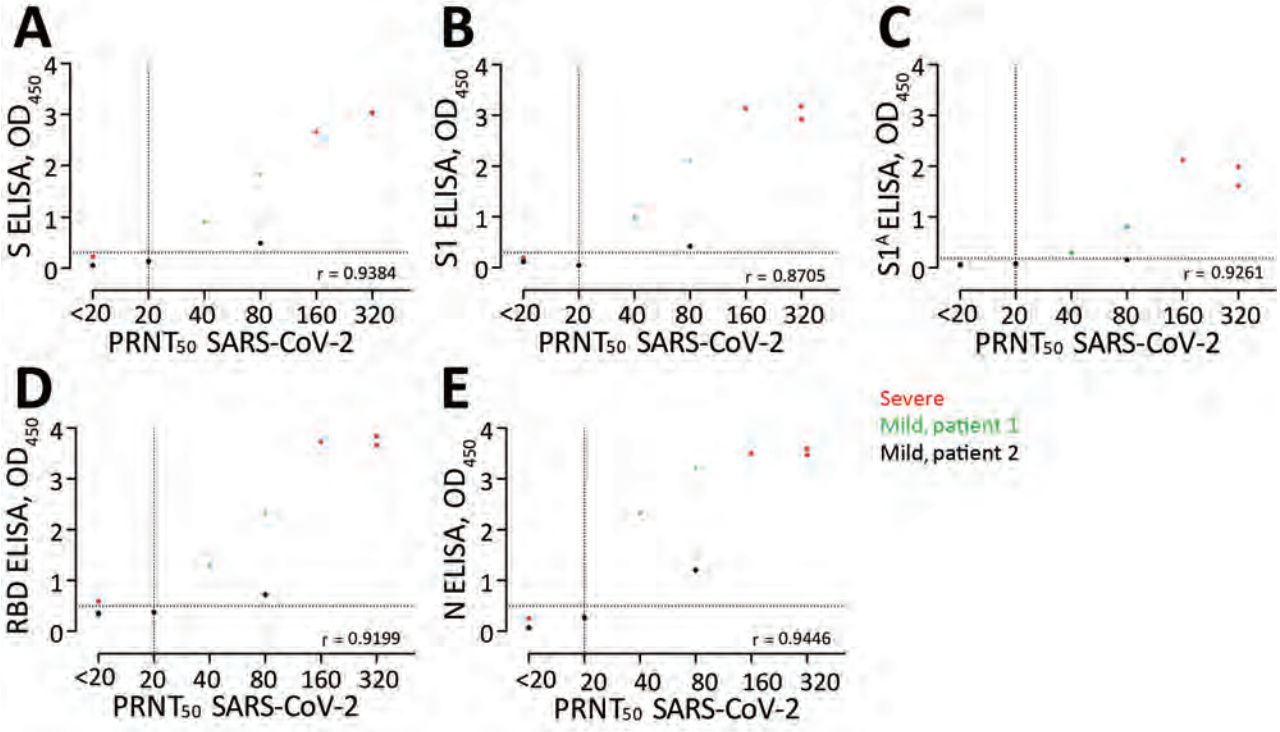


**Figure 2.** Correlations between ODs of ELISAs and PRNT results for PCR-confirmed COVID-19 patients. A) S; B) S1; C) S1$^{A}$; D) RBD; E) N. Ten serum samples were collected 6–27 days after diagnosis from 3 COVID-19 patients in France. Dots indicate patients. Dotted horizontal lines indicate ELISA cutoff values. COVID-19, coronavirus disease 2019; N, nucleocapsid; OD, optical density; PRNT$_{50}$, 50% plaque reduction neutralization test; RBD, receptor-binding domain; S, spike; SARS-CoV-2, severe acute respiratory syndrome coronavirus 2.

were collected 4–56 days after onset of disease onset (Figure 5). All 9 COVID-19 patients were previously confirmed to seroconvert at days 6–15 after onset of disease by use of a recombinant immunofluorescence test and PRNT. A total of 8/9 seroconverted patients showed reactivity above the implemented cutoff values in the IgG and IgA ELISA. A serum sample from 1 patient (Figure 5, panels A, B) had an antibody level slightly below the cutoff value, which might be explained by an overall reduced antibody response of this patient ($PRNT_{90}$ = 10). Overall, the IgA-based ELISA kit was more sensitive but less specific than the IgG-based ELISA kit.

Finally, we compared the performance of different ELISAs for detection of antibodies among PCR-confirmed COVID-19 patients with that of PRNT, which is the standard for coronavirus serologic analysis (Tables 3, 4). The $PRNT_{50}$ correlated strongly with different ELISAs; the commercial IgA ELISA showed the strongest correlation, followed by the S and N ELISA, which indicated their capacity to detect SARS-CoV-2–specific antibodies. However, a larger patient cohort is needed to assess the sensitivities of these platforms.

## Discussion

Validated SARS-CoV-2 serologic assays are urgently needed for contact tracing, epidemiologic and vaccine evaluation studies. Because the N and S proteins are the main immunogenic coronavirus proteins, we developed ELISA-based assays that were able to detect antibodies to these 2 proteins, and to the 2 S domains, $S1^A$, and RBD. Results for these assays correlated strongly with results of the $PRNT_{50}$. Because most humans have antibodies against the 4 endemic human coronaviruses, it was crucial to verify the specificity of these assays to avoid false-positive results. In addition, the 2 zoonotic coronaviruses, SARS-CoV and MERS-CoV, are also betacoronaviruses, increasing the potential for cross-reactivity. Among the S antigens tested, S1 was more specific than S in detecting SARS-CoV-2 antibodies, as MERS-CoV S cross-reactive antibodies were detected in serum of 1 of the COVID-19 patients, which was not seen when MERS-CoV S1 was used for testing. This finding could be explained by the high degree of conservation in the coronavirus S2 subunit relative to S1 (Table 2). Therefore, consistent with our earlier findings for serologic analysis of MERS-CoV (*6*), S1 is a specific antigen for SARS-CoV-2 diagnostics.

When testing the specificity of S1 or its RBD for detecting SARS-CoV-2 antibodies, none of the serum samples from the validation cohorts (A–E) showed any reactivity, except for serum samples from patients with SARS-CoV. This finding is not unexpected because cross-reactivity resulted from the high degree of similarity between S1 and RBD of SARS-CoV and SARS-CoV-2 (Table 2). However, SARS-CoV has not

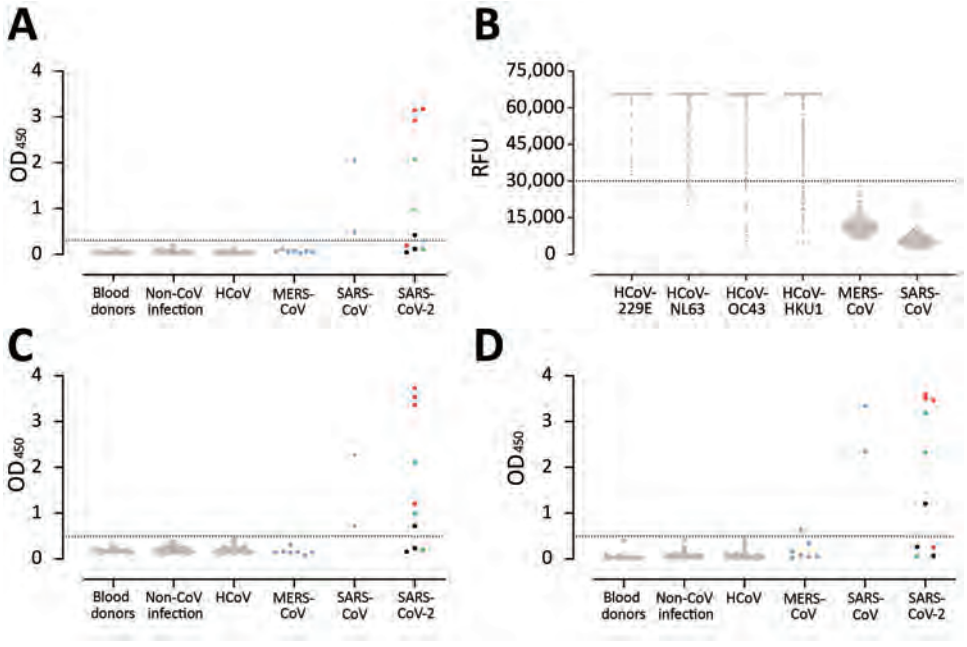


**Figure 3.** Validation of use of S1 (A, B), RBD (C), and N protein (D) ELISAs for detection of SARS-CoV-2–specific antibodies infections. Gray dots indicate specificity cohorts A–C, including healthy blood donors (n = 45), non-CoV respiratory infections (n = 76), and HCoV infections (n = 75); blue dots indicate non-SARS-CoV-2 zoonotic coronavirus infections (i.e., MERS-CoV [n = 7] and SARS-CoV [n = 2]); red dots indicate patients with severe COVID-19; and green and black dots indicate patients with mild COVID-19. Dotted horizontal lines indicate ELISA cutoff values. CoV, coronavirus; COVID-19, coronavirus disease 2019; HCoV, human coronavirus; MERS-CoV, Middle East respiratory syndrome coronavirus; N, nucleocapsid; OD, optical density; RBD, receptor-binding domain; RFU, relative fluorescence unit; S, spike; SARS-CoV, severe acute respiratory syndrome coronavirus; SARS-CoV-2; severe acute respiratory syndrome coronavirus 2.

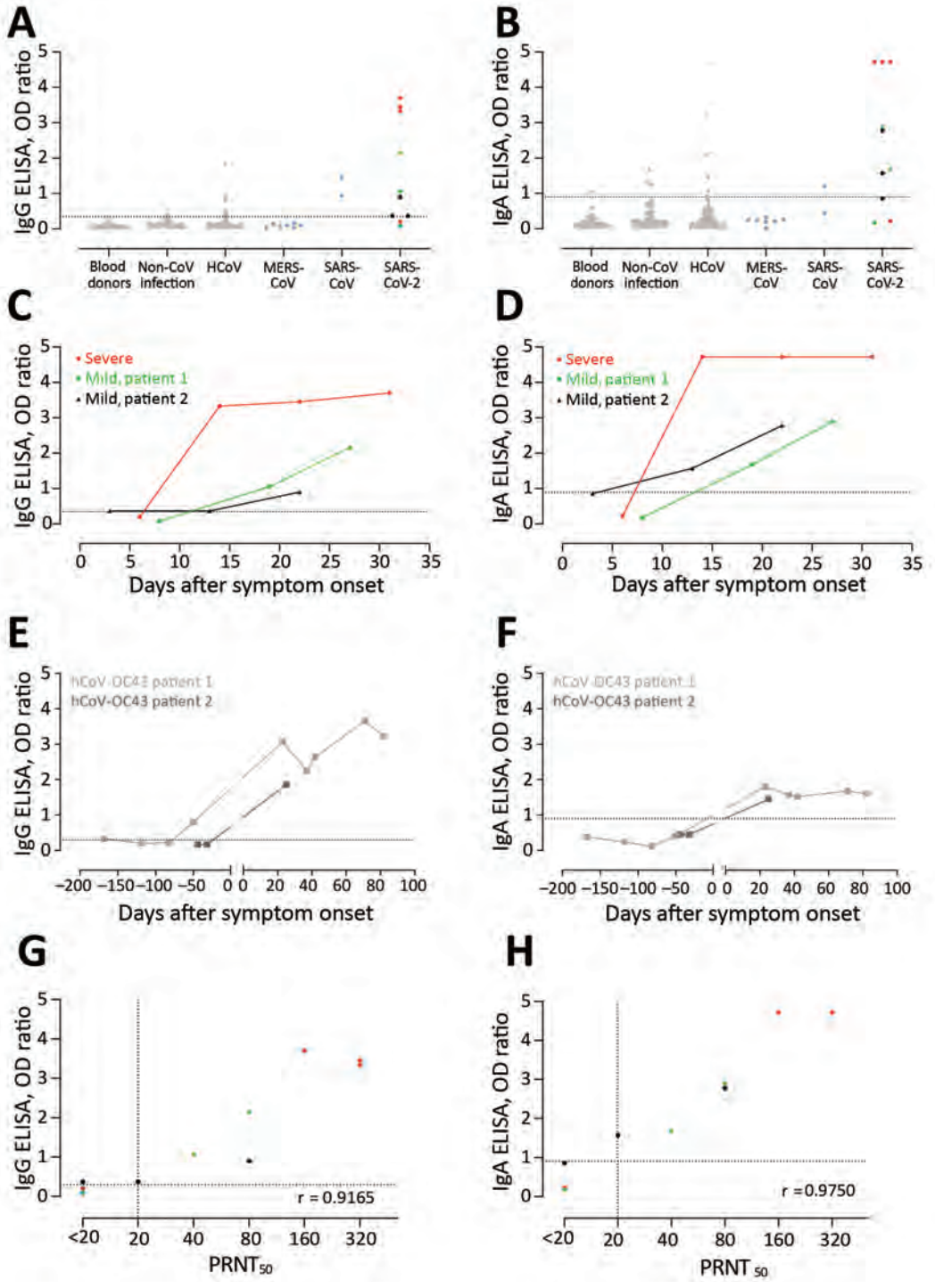


**Figure 4.** Validation of 2 commercial ELISAs for detection of SARS-CoV-2–specific IgG (A, C, E, G) and IgA (B, D, F, H). A, B) Validation of the specificity of the 2 ELISA platforms; C, D) kinetics of antibody responses in 3 COVID-19 patients; E, F) cross-reactivity of HCoV-OC43 serum samples in commercial platforms; G, H) correlation between antibody responses detected by the ELISAs and the plaque reduction neutralization assay. Gray dots indicate specificity cohorts A–C, including healthy blood donors (n = 45), non-CoV respiratory infections (n = 76), and HCoV infections (n = 75); blue dots indicate non-SARS-CoV-2 zoonotic coronavirus infections (i.e., MERS-CoV [n = 7] and SARS-CoV [n = 2]); red dots indicate patients with severe COVID-19; and green and black dots indicate patients with mild COVID-19. Dotted horizontal lines indicate ELISA cutoff values. CoV, coronavirus; COVID-19, coronavirus disease 2019; HCoV, human coronavirus; MERS-CoV, Middle East respiratory syndrome coronavirus; N, nucleocapsid; OD, optical density; $PRNT_{50}$, plaque reduction neutralization assay; RBD, receptor-binding domain; RFU, relative fluorescence unit; S, spike; SARS-CoV-2; severe acute respiratory syndrome coronavirus 2.

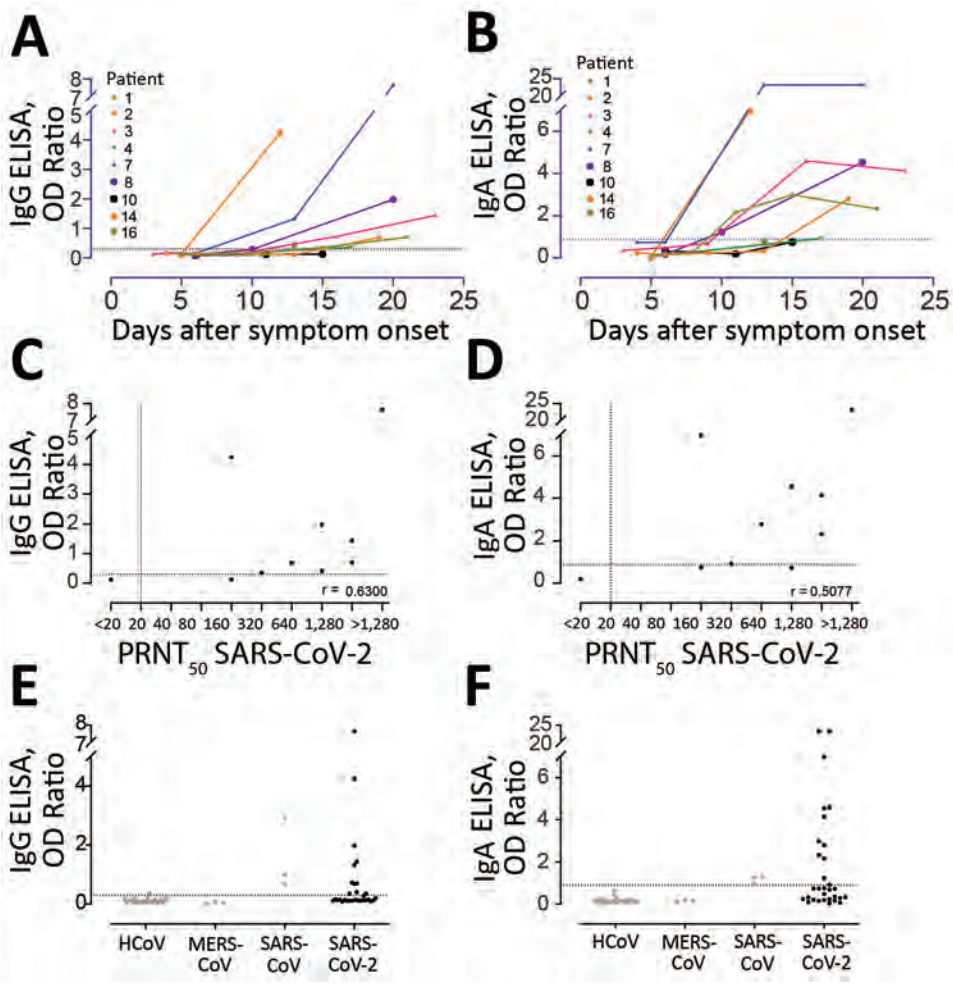


Figure 5. Sensitivity of 2 commercial ELISAs for detection of SARS-CoV-2 specific IgG (A, C, E) and IgA (B, D, F). A, B) Kinetics of antibody responses in 9 COVID-19 patients from Germany; C, D) correlation between antibody responses detected by the ELISAs and the plaque reduction neutralization assay; E, F) kits were tested for specificity by using 18 serum samples from patients infected with HCoV (4 from patients infected with HCoV-229E, 3 from patients infected with HCoV-HKU1, 4 from patients infected with HCoV-NL63, and 7 from patients infected with HCoV-OC43), MERS-CoV (n = 3), and SARS-CoV (n = 3). Dotted horizontal lines indicate ELISA cutoff values. COVID-19, coronavirus disease 2019; HCoV, human coronavirus; MERS-CoV, Middle East respiratory syndrome coronavirus; N, nucleocapsid; OD, optical density; PRNT50, plaque reduction neutralization assay; RBD, receptor-binding domain; RFU, relative fluorescence unit; S, spike; SARS-CoV, severe acute respiratory syndrome coronavirus; SARS-CoV-2; severe acute respiratory syndrome coronavirus 2.

circulated in the human population since 2003 (i.e., 17 years ago), and an earlier study reported waning of SARS-CoV–specific antibodies, which made them undetectable in 21 (91%) of 23 serum samples tested 6 years after infection (*11*). It is therefore unlikely that antibodies to this virus are present in the population, and thus it is unlikely that false-positives results are caused by reactivity of SARS-CoV antibodies.

We used the high degree of similarity between the SARS-CoV and SARS-CoV-2 proteins to develop a new in-house N protein ELISA, in which we used SARS-CoV N protein (90% similar to SARS-CoV-2 N protein) as antigen. The N protein ELISA could detect SARS-CoV-2–specific antibodies with high specificity and sensitivity. Using the 3 different validated ELISAs, we found that antibody levels were higher after severe infection than after mild infections; similar findings have been reported earlier for MERS-CoV (*12*,*13*). However, this finding needs to be confirmed in a larger cohort of patients with various degrees of disease severity, and it highlights the potential need for a sensitive

**Table 3.** Correlations between ODs/OD ratios and PRNT results of 10 serum samples obtained from 3 PCR-confirmed COVID-19 patients from France and tested in Rotterdam, the Netherlands, 6–27 d after diagnosis*

| | | In-house ELISAs | | | | | Euroimmun ELISAs | |
|---|---|---|---|---|---|---|---|---|
| Test, virus | Correlations | S1 | N | RBD | S | S1A | IgA | IgG |
| $PRNT_{50}$, SARS-CoV-2 | Spearman ρ value | 0.87 | 0.94 | 0.92 | 0.94 | 0.93 | 0.98 | 0.92 |
| | 2-tailed p value | 0.0021 | 0.0002 | 0.0005 | 0.0002 | 0.0003 | <0.0001 | 0.0005 |
| | p value summary | ≤0.01 | ≤0.001 | ≤0.001 | ≤0.001 | ≤0.001 | ≤0.0001 | ≤0.001 |
| $PRNT_{90}$, SARS-CoV-2 | Spearman ρ value | 0.88 | 0.88 | 0.88 | 0.88 | 0.88 | 0.93 | 0.88 |
| | 2-tailed p value | 0.0024 | 0.0024 | 0.0024 | 0.0024 | 0.0024 | 0.0008 | 0.002 |
| | p value summary | ≤0.01 | ≤0.01 | ≤0.01 | ≤0.01 | ≤0.01 | ≤0.001 | ≤0.01 |

*COVID-19, coronavirus disease 2019; OD, optical density; N, nucleocapsid; $PRNT_{50}$, 50% plaque reduction neutralization test; $PRNT_{90}$, 90% plaque reduction neutralization test; RBD, receptor-binding domain; S, spike; SARS-CoV-2, severe acute respiratory syndrome coronavirus 2.

**Table 4.** Correlations between ODs/OD ratios and PRNT results of 31 serum samples from 9 PCR-confirmed COVID-19 patients tested from Germany and tested in in Berlin, Germany, 3–23 d after disease onset*

| Test, virus | Correlation | Euroimmun ELISAs | |
|---|---|---|---|
| | | IgA | IgG |
| $PRNT_{50}$, SARS-CoV-2 | Spearman ρ value | 0.63 | 0.5077 |
| | 2-tailed p value | 0.056 | 0.1368 |
| | p value summary | NS | NS |
| $PRNT_{90}$, SARS-CoV-2 | Spearman ρ value | 0.7922 | 0.8525 |
| | 2-tailed p value | 0.0004 | <0.0001 |
| | p value summary | ≤0.001 | ≤0.0001 |

*COVID-19, coronavirus disease 2019; NS, not significant; OD, optical density; $PRNT_{50}$, 50% plaque reduction neutralization test; $PRNT_{90}$, 90% plaque reduction neutralization test; SARS-CoV-2, severe acute respiratory syndrome coronavirus 2.

assay to avoid missing persons who have milder infections in epidemiologic studies.

In addition, IgG seroconversion can be reliably confirmed in the second week after disease onset. However, because of the limited number of longitudinal serum samples from COVID-19 patients tested by the in-house assays, it was difficult to accurately assess time for seroconversion. For this assessment, a larger number of longitudinal samples is needed. In the 3 in-house ELISAs tested, the RBD and N protein ELISAs were more sensitive than S1 ELISA in detecting antibodies in mildly infected patients and showed stronger correlations with $PRNT_{50}$ titers. Therefore, detecting antibodies against 2 different antigens might be needed to confirm the findings and avoid false-negative results in surveillance studies. However, the sensitivities of the assays need to be further validated with a larger cohort.

We validated β-versions of IgA and S1 IgG commercial ELISAs in 2 different laboratories. The IgA-based ELISA showed higher sensitivity than the IgG-based ELISA, whereas the IgG ELISA showed higher specificity than the IgA ELISA. The IgA and IgG assays can be used for serologic diagnosis, IgG is longer lived (*14*) and thus is preferred for serosurveillance studies. We observed some cross-reactivity in both ELISAs with serum samples from the same 2 HCoV-OC43 patients in which these samples showed cross-reactivity in a MERS-CoV S1 IgG ELISA (*6*) despite the different antigen used. This finding indicates a response to another protein that could be in the blocking or coating matrix, apart from the specific antigen coated, resulting in this consistent false-positive result.

Overall, the assays developed and validated in this study could be instrumental for patient contact tracing, serosurveillance studies, and vaccine evaluation studies. However, because various studies will be conducted in different laboratories, it is crucial to calibrate and standardize assays developed by different laboratories by using well-defined standard references as part of diagnostic assay validation. This standardization is not only needed to reduce interassay variability, but to also correlate results obtained from different laboratories that use various assays (*15*). This correlation is crucial for better comparison and interpretation of results from different studies; evaluating vaccine trials; enabling uniform assessment of immunogenicity, efficacy; and better understanding of correlates of immune protection (*16*). Thus, setting up reference panels is a vital element in our preparedness approaches to emerging viruses.

### Acknowledgment

We thank Malik Peiris for providing serum samples from SARS patients.

This study was supported by the Zoonoses Anticipation and Preparedness Initiative (project Innovative Medicines Initiative grant no. 115760), the Innovative Medicines Initiative; the European Commission, and partners of the European Federation of Pharmaceutical Industries and Associations.

## About the Author

Dr. Okba is a postdoctoral researcher in the Viroscience Department, Erasmus Medical Center, Rotterdam, the Netherlands. Her primary research interest is development of diagnostic and intervention strategies for emerging viruses.

### References

1. Zhou P, Yang XL, Wang XG, Hu B, Zhang L, Zhang W, et al. A pneumonia outbreak associated with a new coronavirus of probable bat origin. Nature. 2020;579:270–3. https://doi.org/10.1038/s41586-020-2012-7
2. Coronaviridae Study Group of the International Committee on Taxonomy of Viruses. The species severe acute respiratory syndrome-related coronavirus: classifying 2019-nCoV and naming it SARS-CoV-2. Nat Microbiol. 2020 Mar 2: [Epub ahead of print].
3. World Health Organization. Coronavirus disease (COVID-2019) situation reports [cited 2020 Mar 14]. https://www.who.int/emergencies/diseases/novel-coronavirus-2019/situation-reports
4. Corman VM, Landt O, Kaiser M, Molenkamp R, Meijer A, Chu DK, et al. Detection of 2019 novel coronavirus

(2019-nCoV) by real-time RT-PCR. Euro Surveill. 2020;25:2000045. https://doi.org/10.2807/1560-7917.ES.2020.25.3.2000045
5. Meyer B, Drosten C, Müller MA. Serological assays for emerging coronaviruses: challenges and pitfalls. Virus Res. 2014;194:175–83. https://doi.org/10.1016/j.virusres.2014.03.018
6. Okba NM, Raj VS, Widjaja I, GeurtsvanKessel CH, de Bruin E, Chandler FD, et al. Sensitive and specific detection of low-level antibody responses in mild Middle East respiratory syndrome coronavirus infections. Emerg Infect Dis. 2019;25:1868–77. https://doi.org/10.3201/eid2510.190051
7. Kuiken T, Fouchier RA, Schutten M, Rimmelzwaan GF, van Amerongen G, van Riel D, et al. Newly discovered coronavirus as the primary cause of severe acute respiratory syndrome. Lancet. 2003;362:263–70. https://doi.org/10.1016/S0140-6736(03)13967-0
8. Raj VS, Mou H, Smits SL, Dekkers DH, Müller MA, Dijkman R, et al. Dipeptidyl peptidase 4 is a functional receptor for the emerging human coronavirus-EMC. Nature. 2013;495:251–4. https://doi.org/10.1038/nature12005
9. Rodon J, Okba NM, Te N, van Dieren B, Bosch B-J, Bensaid A, et al. Blocking transmission of Middle East respiratory syndrome coronavirus (MERS-CoV) in llamas by vaccination with a recombinant spike protein. Emerg Microbes Infect. 2019;8:1593–603. https://doi.org/10.1080/22221751.2019.1685912
10. Drosten C, Meyer B, Müller MA, Corman VM, Al-Masri M, Hossain R, et al. Transmission of MERS-coronavirus in household contacts. N Engl J Med. 2014;371:828–35. https://doi.org/10.1056/NEJMoa1405858
11. Tang F, Quan Y, Xin ZT, Wrammert J, Ma MJ, Lv H, et al. Lack of peripheral memory B cell responses in recovered patients with severe acute respiratory syndrome: a six-year follow-up study. J Immunol. 2011;186:7264–8. https://doi.org/10.4049/jimmunol.0903490
12. Choe PG, Perera RA, Park WB, Song KH, Bang JH, Kim ES, et al. MERS-CoV antibody responses 1 year after symptom onset, South Korea, 2015. Emerg Infect Dis. 2017;23:1079–84. https://doi.org/10.3201/eid2307.170310
13. Alshukairi AN, Khalid I, Ahmed WA, Dada AM, Bayumi DT, Malic LS, et al. Antibody response and disease severity in healthcare worker MERS survivors. Emerg Infect Dis. 2016;22:1113–5. https://doi.org/10.3201/eid2206.160010
14. Hsueh PR, Huang LM, Chen PJ, Kao CL, Yang PC. Chronological evolution of IgM, IgA, IgG and neutralisation antibodies after infection with SARS-associated coronavirus. Clin Microbiol Infect. 2004;10:1062–6. https://doi.org/10.1111/j.1469-0691.2004.01009.x
15. Harvey R, Mattiuzzo G, Hassall M, Sieberg A, Müller MA, Drosten C, et al.; Study Participants. Comparison of serologic assays for Middle East respiratory syndrome coronavirus. Emerg Infect Dis. 2019;25:1878–83. https://doi.org/10.3201/eid2510.190497
16. Rampling T, Page M, Horby P. International biological reference preparations for epidemic infectious diseases. Emerg Infect Dis. 2019;25:205–11. https://doi.org/10.3201/eid2502.180798

Address for correspondence: N.M.A. Okba or Bart L. Haagmans, Department of Viroscience, Erasmus Medical Center, PO Box 2040, 3000 CA Rotterdam, the Netherlands; emails: n.okba@erasmusmc.nl or b.haagmans@erasmusmc.nl

# Burden and Cost of Hospitalization for Respiratory Syncytial Virus in Young Children, Singapore

Clarence C. Tam, Kee Thai Yeo, Nancy Tee, Raymond Lin, Tze Minn Mak, Koh Cheng Thoon, Mark Jit, Chee Fu Yung

Respiratory syncytial virus (RSV) is the most common cause of pediatric acute lower respiratory tract infection worldwide. Detailed data on the health and economic burden of RSV disease are lacking from tropical settings with year-round RSV transmission. We developed a statistical and economic model to estimate the annual incidence and healthcare cost of medically attended RSV disease among young children in Singapore, using Monte Carlo simulation to account for uncertainty in model parameters. RSV accounted for 708 hospitalizations in children <6 months of age (33.5/1,000 child-years) and 1,096 in children 6–29 months of age (13.2/1,000 child-years). The cost of hospitalization was SGD 5.7 million (US $4.3 million) at 2014 prices; patients bore 60% of the cost. RSV-associated disease burden in tropical settings in Asia is high and comparable to other settings. Further work incorporating efficacy data from ongoing vaccine trials will help to determine the potential cost-effectiveness of different vaccination strategies.

Respiratory syncytial virus (RSV) is the commonest cause of acute lower respiratory tract infection in children <5 years of age worldwide, causing an estimated 33 million cases, 3 million hospitalizations, and 60,000 deaths annually (*1*). In young children and infants, RSV infections can cause bronchiolitis and pneumonia requiring hospitalization. In the United States, RSV accounts for 40% of respiratory hospitalizations in all age groups (*2*); children <5 years of age account for two thirds of this burden. Similarly, in the United Kingdom, RSV accounts for 28% of hospitalizations for lower respiratory tract infection in children <5 years of age (*3*).

Several RSV vaccines are in development. Potential immunization strategies include vaccination of children, pregnant mothers, and older adults. Assessing the potential impact and cost-effectiveness of future vaccination strategies relies on robust estimates of RSV-related health burden and cost, to inform national procurement and prioritization decisions. We present estimates of RSV-related primary care consultations, hospitalizations, and associated healthcare costs among children <30 months of age in Singapore.

## Methods

### Study Setting

Singapore, a high-income tropical country, has year-round RSV circulation. Compared with the distinct winter seasonal peaks in temperate settings, the RSV season is longer, peaking in May–September (*4*–*6*). Hospitalization costs in Singapore are borne by a mix of public and private insurance, out-of-pocket financing, and means-tested subsidies for lower-income patients. KK Women's and Children's Hospital (KKH) is the largest specialist women's and children's hospital in Singapore. All children admitted to KKH with respiratory symptoms, regardless of clinical severity, are tested by nasopharyngeal swab sampling for a panel of respiratory viruses using direct immunofluorescence antibody (DFA). Primary care is available through public polyclinics, private general practices, and pediatric clinics. Polyclinics are subsidized, and patients contribute a co-payment; consultations in private practices are paid out of pocket or through individual insurance. Approximately 80% of primary care consultations occur in the private sector (*7*).

Author affiliations: National University Health System, Singapore (C.C. Tam, N. Tee); National University of Singapore, Singapore (C.C. Tam, K.C. Thoon); London School of Hygiene and Tropical Medicine, London, UK (C.C. Tam, M. Jit); KK Women's and Children's Hospital, Singapore (K.T. Yeo, N. Tee, K.C. Thoon, C.F. Yung); Duke-National University of Singapore Graduate Medical School, Singapore (K.T. Yeo, K.C. Thoon, C.F. Yung); National Public Health Laboratory, Singapore (R. Lin, T.M. Mak); Nanyang Technological University, Singapore (C.F. Yung)

DOI: https://doi.org/10.3201/eid2607.190539

### Approach

We used data on primary care consultations for acute respiratory illness (ARI) and hospital admissions for bronchiolitis and pneumonia in children <30 months of age, together with data on laboratory testing for RSV and healthcare bill sizes, to estimate incidence of medically attended RSV and associated healthcare costs from a societal perspective. We used Monte Carlo simulations to estimate numbers of primary care consultations and numbers of hospitalizations for bronchiolitis, pneumonia without complications, and pneumonia with complications. We developed 2 cost models: the full-cost model estimated the total cost of RSV-related healthcare, whereas the subsidized cost estimated the share of healthcare costs paid by patients after accounting for public subsidies.

### Data Sources

#### Bronchiolitis and Pneumonia Admissions

We obtained data on bronchiolitis and pneumonia hospitalizations in children <72 months of age during 2005–2014 from electronic inpatient admission records at KKH. We selected all admissions with diagnostic codes for pneumonia and bronchiolitis in any diagnostic field (International Classification of Diseases, 9th Revision [ICD-9], codes 480–486 and 466, or ICD, 10th Revision [ICD-10], codes J12–18 and J21). We excluded records for which a pathogen other than RSV was mentioned as the cause of bronchiolitis or pneumonia in the medical code description.

#### RSV and Influenza Positive Identifications

We extracted data on positive identifications of RSV and influenza at KKH from laboratory diagnostic records for children <30 months of age for the period 2005–2014. Viral infections were detected using DFA for influenza A and B viruses, RSV, adenovirus, parainfluenza viruses 1–3, and human metapneumovirus ($D^3$ Double Duet DFA Respiratory Virus Screening and ID Kit; Diagnostic Hybrids; Quidel Corporation, https://www.quidel.com). The positive and negative percent agreements of virus detection by this test against a predicate test are 100%.

#### Rotavirus Positive Identifications

We used rotavirus as a negative control, to rule out spurious associations related to secular changes in recording of diagnoses or laboratory investigations. We extracted all positive identifications of rotavirus in children <30 months of age hospitalized for gastroenteritis during 2005–2014. Rotavirus detection in stool samples was done via an immunochromatographic assay (Simple Rotavirus/Stick Rotavirus; Operon, https://operon.es).

#### Public Primary Care Consultations

We obtained data on polyclinic consultations for ARI among children <5 years of age in 2014 from the Ministry of Health; the National Public Health Laboratory additionally tests for a range of respiratory pathogens in a subset of primary care ARI samples. We obtained data on the proportion of samples, by age group, in which RSV was detected as the sole pathogen as determined by a commercial multiplex assay (Seegene Allplex Respiratory Panel; Seegene Inc., http://www.seegene.com).

#### Costs of Hospitalization and Primary Care Consultation

Singapore Ministry of Health (MOH) standardized unit costs of hospitalization by condition, healthcare institution, and ward class, together with average length of stay (LOS), are published annually (*8*). Wards are categorized into 5 classes, A, B1, B2+, B2, and C, with A being unsubsidized and C being the most highly subsidized. We obtained published costs of an admission to KKH for bronchiolitis, pneumonia, and pneumonia with complications from the MOH website for the 5 different ward classes (Appendix Table 5, https://wwwnc.cdc.gov/EID/article/26/7/19-0539-App1.pdf). We determined the cost of a primary care consultation on the basis of the average cost of a polyclinic visit, which we obtained from the respective providers (*9*,*10*) (Appendix Table 4).

### Data Analysis

#### Proportion of Bronchiolitis and Pneumonia Admissions Attributed to RSV

We estimated the proportion of RSV-related bronchiolitis and pneumonia admissions using a seasonal regression method (*11*,*12*). We used a negative binomial model with an identity link to model weekly counts of bronchiolitis and pneumonia admissions against weekly counts of RSV-positive identifications for the years 2005–2013. We included an intercept term to account for admissions not explained by RSV. We fitted separate models for children <6 months of age and children 6–30 months of age. We used the model coefficients to predict the proportion of bronchiolitis and pneumonia admissions in 2014 attributable to RSV. We tested the model's validity by comparing the model-predicted and observed values for 2014 and calculating the correlation coefficient (ρ), root mean squared error

(RMSE), and mean absolute error (MAE) (Appendix Figure 1). In a sensitivity analysis, we ran additional regressions individually, adjusting for the following: linear and quadratic trend terms, weekly influenza positive identifications, weekly rotavirus positive identifications, and weekly gastrointestinal admissions (Appendix).

#### Percentage of Admissions for Pneumonia

Of admissions for bronchiolitis and pneumonia, the percentage specifically for pneumonia-related codes increased with age, which has implications for the cost of treatment; pneumonia incurs higher treatment costs. We used a logistic regression model with natural cubic splines of age and internal knots at 9-month age intervals to predict the age-specific proportion of pneumonia-related admissions in 2014.

#### LOS and Pneumonia with Complications

We modeled LOS in 2005–2013 by fitting an exponential regression to the percentage distribution of LOS separately for bronchiolitis and pneumonia admissions (Appendix Figure 4). We used the model coefficients to predict the LOS distribution for 2014.

We defined pneumonia with complications as pneumonia with LOS >5 days, assuming that pneumonia with complications results in longer hospitalization. Approximately 8% of admissions for bronchiolitis and pneumonia had a LOS >5 days, matching the percentage of admissions categorized as pneumonia with complications in MOH billing data.

#### Burden and Cost of RSV Hospitalization

We developed a model to estimate the annual number of hospitalizations for bronchiolitis, pneumonia, and pneumonia with complications and their associated cost, estimated separately for children <6 months and 6–29 months of age (Appendix). In the model, number of RSV-positive identifications in KKH in 2014 for each age group are inputs. We used the coefficients from the 3 regressions to estimate the overall number of bronchiolitis and pneumonia admissions attributable to RSV; the number of admissions that were bronchiolitis versus pneumonia by patient's age in months; the number of admissions for pneumonia with complications, based on the predefined cutoff for LOS; and the total number of days of hospitalization for bronchiolitis, pneumonia, and pneumonia with complications. We extrapolated hospitalization estimates to the whole of Singapore by applying inflation factors to account for the proportion of hospitalizations occurring in other hospitals (Appendix Equations 4.1–4.3).

To estimate the full hospitalization costs, we applied the average daily bill size in a class A (unsubsidized) ward to the total hospitalization days for bronchiolitis, pneumonia, and pneumonia with complications (Appendix Equation 5). To estimate the subsidized cost (the cost borne by patients), we applied the average daily bill size for each ward class to the number of hospitalization days spent by patients in each type of ward (Appendix Equation 6). We estimated costs separately for bronchiolitis, pneumonia, and pneumonia with complications.

#### Burden and Cost of RSV Primary Care Consultations

Because fine age stratification of primary care consultations was not available, we used the age distribution of RSV-positive identifications from KKH to infer the number of polyclinic consultations in children <6 months and 6–29 months of age (Appendix Equation 7). To estimate the number of consultations occurring in the private sector, we used the ratio of pediatric consultations (for children <5 years of age) in polyclinics versus private GPs, published in the 2014 Primary Care Survey (*7*). We estimated the proportion of respiratory consultations due to RSV using National Public Health Laboratory ARI testing data, in which 8% of ARI samples from children <5 years had RSV as the sole identified pathogen. We estimated the full cost of primary care consultations for RSV by applying the cost of an unsubsidized polyclinic consultation to the estimated number of consultations. To estimate the subsidized cost, we applied the cost of a pediatric polyclinic consultation to the subset of consultations occurring in government polyclinics (Appendix Equations 8.1–8.2).

### Monte Carlo Simulation

To account for uncertainty in model parameters, we used Monte Carlo methods to sample parameter values at random from their assumed distributions. We performed 10,000 simulations. For each output parameter, we used the median and 2.5th and 97.5th percentiles of the sampled distributions as the point estimate and corresponding 95% CI.

To assess the influence of our definition of pneumonia with complications, we repeated the analyses varying the LOS cutoff used to define pneumonia with complications ($\pm$ 1 day). We adjusted costs to 2014 prices using the healthcare domain of the Consumer Price Index (*13*). We rounded cumulative healthcare costs to the nearest SGD 1,000.

We performed all analyses using Stata version 12 (Stata Corporation, https://www.stata.com) and R version 3.4.1 (*14*). The SingHealth Centralized

Institutional Review Board approved this study (application 2017/2223).

## Results

During 2005–2013, there were 18,323 bronchiolitis and pneumonia admissions in children <30 months of age at KKH, an average of 39 weekly admissions, and 7,691 RSV-positive identifications, a weekly average of 16. There was substantial temporal agreement between the two time-series, with a marked peak in RSV identifications in May–September in most years (Figure 1). Model validation showed high correlation between model-predicted and observed bronchiolitis admissions for 2014 ($\rho = 0.88$ for children <6 months of age; $\rho = 0.81$ for children 6–29 months of age) (Appendix Table 1).

### Hospitalizations Attributable to RSV

The negative binomial model with an intercept and a linear term for weekly RSV-positive identifications provided the best fit to the data. From this model, RSV accounted for 47.0% (95% CI 42.4%–51.5%) of bronchiolitis and pneumonia admissions among children <6 months of age, and 34.3% (95% CI 25.0%–33.1%) among children 6–29 months. The estimated yearly number of RSV-associated bronchiolitis admissions was 135–340 among children <6 months of age and 271–680 among children 6–29 months of age (Appendix Table 1).

Adjusting for linear or quadratic trend terms, influenza positive identifications, rotavirus positive identifications, and gastrointestinal admissions resulted in small changes to the RSV-attributable percentage. However, none of these more complex models provided a better fit to the data (Appendix Table 2).

### Percentage of Pneumonia Hospitalizations by Age

Based on the regression with natural cubic splines, the percentage of pneumonia admissions was estimated to be 18.6% for children hospitalized in the first month of life. This percentage decreased to 5.5% by 4 months of age but rose to 74.0% by 29 months of age (Figure 2).

### Bronchiolitis and Pneumonia Hospitalization Rates

An estimated 708 (95% CI 664–765) bronchiolitis and pneumonia admissions due to RSV occurred in 2014 among children <6 months of age, a rate of 33.5 hospitalizations/1,000 child-years. For children 6–29 months, the corresponding number was 1,096 (95% CI 998–1,273), or 13.2 hospitalizations/1,000 child-years (Table 1). Among children <6 months of age, the number of admissions was 637 for bronchiolitis, 54 for pneumonia without complications, and 15 for pneumonia with complications. In children aged 6–29 months, the corresponding numbers were 826 for bronchiolitis, 203 for pneumonia without complications, and 63 for pneumonia with complications.

### Primary Care Consultation Rates

The number of estimated primary care consultations for RSV among children <6 months of age was 3,600 (95% CI 3,120–4,130) or 170.5 consultations/1,000 child-years. The corresponding number of consultations in children 6–29 months was 5,700 (95% CI 5,010–6,450), for a rate of 68.6 consultations/1,000 child-years (Table 1).

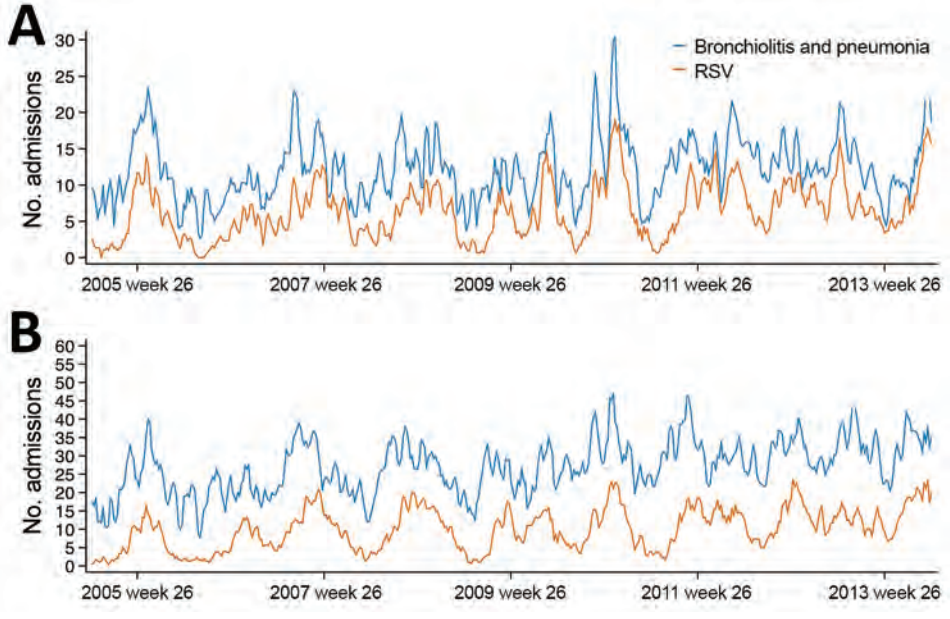


**Figure 1.** Hospital admissions for respiratory syncytial virus and for bronchiolitis and pneumonia over time by age group, Singapore, 2005–2013.

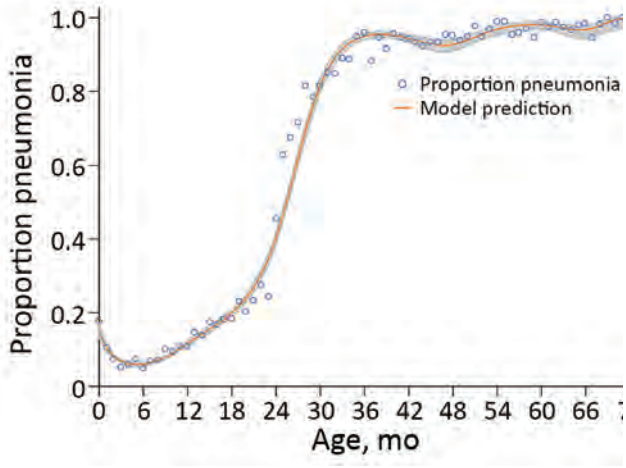


**Figure 2.** Proportion of bronchiolitis and pneumonia admissions for pneumonia-related codes as contrasted with model predictions by age, Singapore, 2005–2013. Gray shading along the curve indicates 95% CI.

### Hospitalization Costs

The annual unsubsidized cost of RSV-associated bronchiolitis and pneumonia hospitalizations among children <30 months of age was SGD 5.7 million (95% CI SGD 5.2 – SGD 6.4 million). Patients bore SGD 3.6 million (US $2.6 million), or 63%, of the total cost (Table 2). Approximately 40% of admissions occurred in maximally subsidized class C wards and 30% in unsubsidized class A wards (Figure 3).

Among children <6 months of age, average cost per bronchiolitis hospitalization was SGD 2,953 (US $2,209), rising to SGD 7,944 (US $5,942) for a hospitalization for pneumonia with complications. Among children 6–29 months of age, average costs were SGD 2,949 (US $2,206) for bronchiolitis and SGD 8,300 (US $6,208) for pneumonia with complications. Varying the definition of pneumonia with complications by ±1 day from the 5-day cutoff had negligible effect on estimates of case counts or overall cost (Appendix Figure 5).

### Primary Care Costs and Costs per Child

The annual cost of primary care consultations was SGD 0.46 million (US $0.34 million), of which 38% was incurred for children <6 months of age. The mean cost per case was SGD 49 (US $37).

The overall cost of RSV-related hospitalizations and primary care consultations was SGD 6.2 million (US $4.7 million). This total is equivalent to SGD 60 annually per birth (US $45), of which SGD 55 represents hospitalization costs.

## Discussion

RSV causes substantial pediatric health and economic burden in Singapore, accounting for 33.5 hospitalizations/1,000 child-years among children <6 months of age and 13.2 hospitalizations/1,000 child-years in children 6–29 months of age. The annual healthcare cost attributable to RSV is SGD 6.2 million (US $4.7 million), or SGD 60 (US $45) per birth, the bulk of which is for acute hospital care. Our findings help to address the gap in information to support the cost-effectiveness evaluations of future RSV vaccination strategies in tropical settings.

Shi et al. reported similar estimates on community incidence of RSV disease (66/1,000 children) and hospitalization (26/1,000 children) for infants <6 months in high-income countries (*1*). RSV hospitalization rates in children <6 months from 4 East Asia and Asia-Pacific studies ranged from 14 hospitalizations/1,000 children/year in 2 rural provinces in Thailand to 42.7/1,000/year in Alice Springs, Northern Territory, Australia (*1*). Homaira et al., using linked administrative health data from Australia, estimated a hospitalization rate of 26/1,000 children <3 months (*15*). RSV hospitalization rates of ≈45/1,000 children <6 months of age have been reported in England and Wales (*11*) and Denmark (*16*). Our estimate is somewhat lower, at 33/1,000 children. This difference could reflect differences in estimation methods

**Table 1.** Estimated RSV-associated hospitalizations and primary care consultations, Singapore, 2014

| Age, mo | Outcome | Total no. cases (95% CI) | No. cases/1,000 person-years (95% CI) |
|---|---|---|---|
| Hospitalizations | | | |
| <6 | All diagnoses | 708 (664–765) | 33.5 (31.4–36.2) |
| | Bronchiolitis | 637 (604–671) | 30.2 (28.6–31.8) |
| | Pneumonia | 54 (30–99) | 2.6 (1.4–4.7) |
| | Pneumonia with complications | 15 (7–29) | 0.7 (0.3–1.4) |
| 6–29 | All diagnoses | 1,096 (994–1,269) | 13.2 (12–15.3) |
| | Bronchiolitis | 826 (793–862) | 9.9 (9.5–10.4) |
| | Pneumonia | 203 (115–372) | 2.4 (1.4–4.5) |
| | Pneumonia with complications | 63 (38–110) | 0.8 (0.5–1.3) |
| Primary care consultations | | | |
| <6 | ARI | 3,600 (3,120–4,130) | 170.5 (147.8–195.6) |
| 6–29 | ARI | 5,700 (5,010–6,450) | 68.6 (60.3–77.6) |

*Estimates are expressed as the medians from 10,000 Monte Carlo simulations. Note that the sum of medians from individual diagnoses does not equal the median for all diagnoses combined. ARI, acute respiratory illness; RSV, respiratory syncytial virus.

**Table 2.** Cost of RSV-associated hospitalizations and primary care consultations, Singapore, 2014*

| Age, mo | Outcome | Full cost (95% CI) | Subsidized cost (95% CI) |
|---|---|---|---|
| Hospitalizations | | | |
| <6 | All | $2,160,000 ($2,002,000–$2,352,000) | $1,321,000 ($1,168,000–$1,492,000) |
| | Bronchiolitis | $1,881,000 ($1,771,000–$1,995,000) | $1,127,000 ($1,006,000–$1,250,000) |
| | Pneumonia | $152,000 ($82,000–$278,000) | $106,000 ($53,000–$198,000) |
| | Pneumonia with complications | $119,000 ($55,000–$220,000) | $80,000 ($25,000–$167,000) |
| 6–29 | All | $3,554,000 ($3,175,000–$4,118,000) | $2,236,000 ($1,932,000–$2,651,000) |
| | Bronchiolitis | $2,436,000 ($2,319,000–$2,563,000) | $1,459,000 ($1,328,000–$1,600,000) |
| | Pneumonia | $573,000 ($321,000–$1,041,000) | $401,000 ($217,000–$729,000) |
| | Pneumonia with complications | $523,000 ($322,000–$857,000) | $358,000 ($191,000–$610,000) |
| Primary care consultations | | | |
| <6 | Primary care attendances | $177,000 ($153,000–$203,000) | $118,000 ($102,000–$136,000) |
| 6–29 | Primary care attendances | $280,000 ($246,000–$317,000) | $187,000 ($163,000–$213,000) |
| Hospitalizations and primary care consultations | | | |
| <6 | All | $2,337,000 ($2,175,000–$2,530,000) | $1,440,000 ($1,285,000–$1,611,000) |
| 6–29 | All | $3,833,000 ($3,454,000–$4,399,000) | $2,423,000 ($2,115,000–$2,838,000) |
| <30 | All | $6,228,000 ($5,734,000–$6,950,000) | $3,899,000 ($3,506,000–$4,432,000) |

*Estimates are expressed as the medians from 10,000 Monte Carlo simulations. Note that the sum of medians from individual diagnoses does not equal the median for all diagnoses combined. All costs are in Singapore dollars. RSV, respiratory syncytial virus.

or the lower fertility rates in Singapore, which might result in reduced transmission of RSV among very young children.

Hospitalization costs are difficult to compare because of differences between countries in healthcare financing. In our analysis, the hospitalization cost per child was ≈US $41, higher than in Denmark (≈US $25) (*16*) but lower than in England and Wales (≈US $82) (*11*). In our analysis, two thirds of hospitalization costs were borne by patients through personal insurance, Medisave (a national medical savings scheme), or out-of-pocket payments. In health systems with shared financing, determining the share of the cost borne by different sectors can be relevant for policy decisions. Although the healthcare costs of disease are shared by patients, insurers, and governments, it is a country's government that is generally responsible for decisions about vaccine introduction and financing. Clarifying how the costs of averted illness affect different parties can help to inform vaccine policy decisions.

A limitation of our analysis is a lack of openly available information on how closely hospital bill amounts reflect actual treatment costs for RSV disease. We used average bill sizes for services in public-sector hospitals and polyclinics, which are likely to reflect treatment costs more closely than do bills for services from private healthcare providers, which are likely to include additional profit margins. Despite the large burden and cost we identified, our figures are likely to be underestimates. First, we limited our analysis to children <30 months of age because we lacked data on positive RSV identifications in older children. Second, our primary care estimates exclude consultations to private pediatricians, which were not included in the Primary Care Survey. Third, although we obtained detailed estimates of RSV hospitalization costs by ward class, our estimates of bill sizes in private hospitals is conservative. Because hospital billing data were not available by age group, we estimated the proportion of pediatric RSV admissions in private hospitals using the distribution of bronchiolitis admissions treated in different ward types, because bronchiolitis is primarily a pediatric diagnosis. We could not apply hospital-specific bill sizes because the cost of pneumonia admissions is usually heavily influenced by adult admissions; therefore, we applied KKH bill sizes for (unsubsidized) class A wards to all ward types as a proxy for the actual cost to providers of hospital care. Finally, we did not consider societal costs resulting from time taken off work by caretakers or nonhealthcare expenditure resulting from illness.

We did not estimate the fraction of RSV burden that occurs in higher-risk groups, such as preterm babies or children with underlying conditions, which could have implications for subsequent assessment of vaccination strategies. However, the overall healthcare cost is unlikely to be affected. Although we might have overestimated the burden attributable to RSV because of possible concurrent infections with other pathogens causally related to respiratory illness, we believe this is unlikely. We estimated RSV impact on primary care using the proportion of ARI samples in which RSV was identified as the sole pathogen (≈75% of samples in which RSV was detected). In estimating hospitalization burden, we used a regression approach

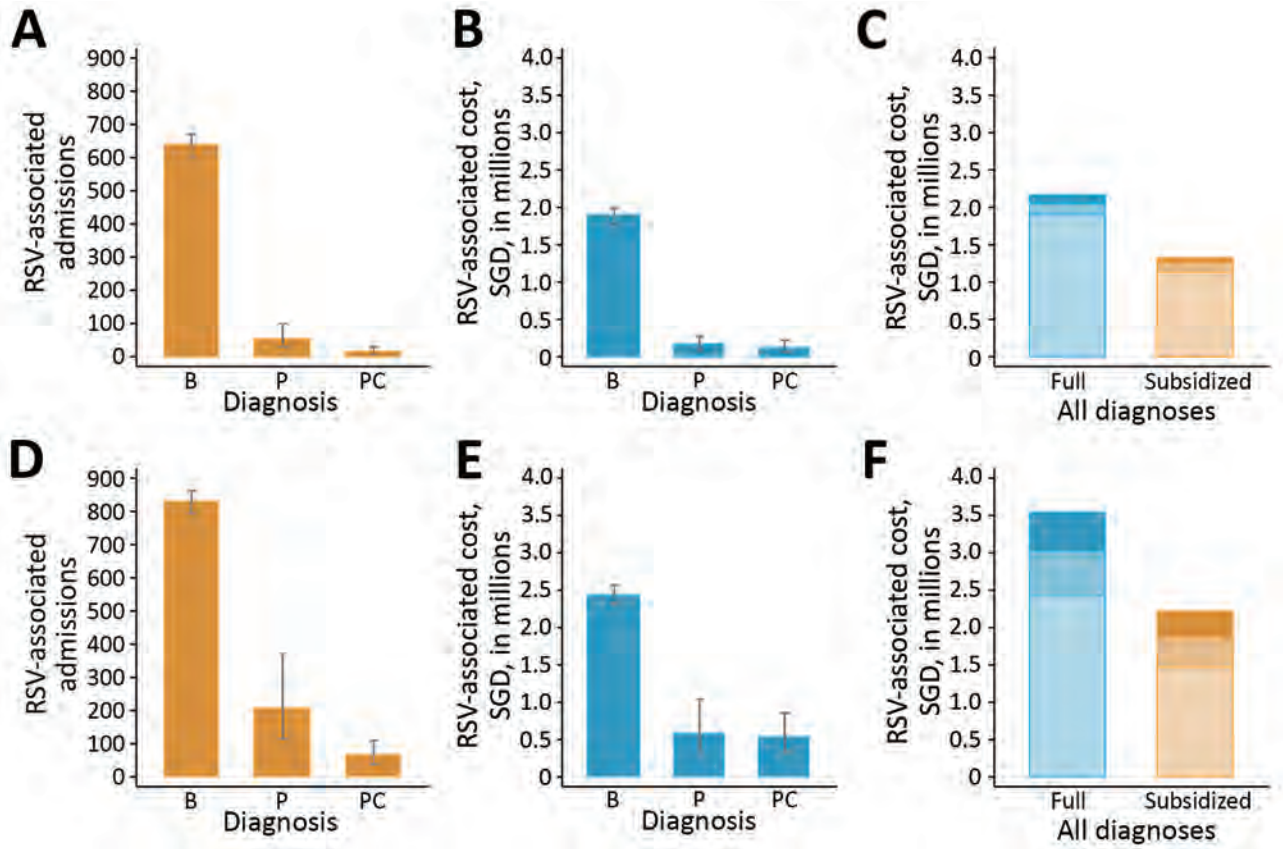


**Figure 3.** Estimated annual RSV-associated hospital admissions and costs for children ≤5 months of age (A–C) and children 6–29 months (D–F), Singapore, 2005–2013. Panels show estimated annual RSV-associated hospital admissions (panels A, D), total hospitalization costs by diagnosis (B, E), and full vs. subsidized costs (C, F). For panels C and F, shading indicates, from lightest to darkest: bronchiolitis, pneumonia without complications, pneumonia with complications. Point estimates and error bars representing medians and central 95% CI distributions were generated from 10,000 Monte Carlo simulations. B, bronchiolitis; P, pneumonia; PC, pneumonia with complications; RSV, respiratory syncytial virus; SGD, Singapore dollars.

that accounts for the seasonal correlation between hospital admissions and RSV-positive tests. To substantially affect our estimates, much of this seasonal variability would need to result from infections with other pathogens sharing similar seasonal patterns, but that is highly unlikely. Influenza showed very little correlation with bronchiolitis and pneumonia hospitalization data, whereas pneumococcal disease, also important in this age group, accounts for only a modest number of hospitalizations in Singapore (≈150 annually).

Strengths of our analysis include the availability of a long time-series of RSV-positive identifications based on routine, systematic diagnostic testing of pediatric respiratory admissions, and on patient-level data for diagnosis and length of hospitalization. The average hospitalization cost was US $2,200 for bronchiolitis and $6,000 for pneumonia. Studies of RSV-associated healthcare costs in similar Asia settings are lacking; Sruamsiri et al. estimated the average cost of RSV-associated hospitalization in Japan at US $3,300 (*17*) and Homaira et al. in Australia at US $4,500 (*15*). Of note, we estimated the cost borne by patients and the health sector; in hybrid public–private healthcare financing systems, future vaccination policy options may be better informed by understanding how avoidable costs affect different sectors of society. Our results indicate that patients bear >60% of hospitalization costs either through health insurance schemes or out-of-pocket payments.

Our findings add to the increasing body of data on the burden of RSV in infants and young children in both high- and low-income settings, and point to the need and potential for RSV vaccines to reduce neonatal disease burden. As evidence for the efficacy of new RSV vaccines emerges from ongoing trials, these data will provide a much-needed baseline against which to measure the cost effectiveness of different vaccination strategies.

C.C.T. performed the analysis and drafted the manuscript. M.J. and C.F.Y. provided technical input into the development and refinement of the modeling strategy and the interpretation of results. All authors critically reviewed and contributed to the drafting of the manuscript.

## About the Author

Dr. Tam is an epidemiologist with faculty positions at the Saw Swee Hock School of Public Health, National University of Singapore, and the London School of Hygiene & Tropical Medicine, United Kingdom. His research focuses on the epidemiology and transmission of infectious diseases, and sociobehavioral determinants of vaccination and antimicrobial use.

## References


1. Shi T, McAllister DA, O'Brien KL, Simoes EAF, Madhi SA, Gessner BD, et al.; RSV Global Epidemiology Network. Global, regional, and national disease burden estimates of acute lower respiratory infections due to respiratory syncytial virus in young children in 2015: a systematic review and modelling study. Lancet. 2017;390:946–58. https://doi.org/10.1016/S0140-6736(17)30938-8
2. Matias G, Taylor R, Haguinet F, Schuck-Paim C, Lustig R, Shinde V. Estimates of hospitalization attributable to influenza and RSV in the US during 1997-2009, by age and risk status. BMC Public Health. 2017;17:271. https://doi.org/10.1186/s12889-017-4177-z
3. Reeves RM, Hardelid P, Gilbert R, Warburton F, Ellis J, Pebody RG. Estimating the burden of respiratory syncytial virus (RSV) on respiratory hospital admissions in children less than five years of age in England, 2007-2012. Influenza Other Respir Viruses. 2017;11:122–9. https://doi.org/10.1111/irv.12443
4. Loh TP, Lai FYL, Tan ES, Thoon KC, Tee NWS, Cutter J, et al. Correlations between clinical illness, respiratory virus infections and climate factors in a tropical paediatric population. Epidemiol Infect. 2011;139:1884–94. https://doi.org/10.1017/S0950268810002955
5. Chew FT, Doraisingham S, Ling AE, Kumarasinghe G, Lee BW. Seasonal trends of viral respiratory tract infections in the tropics. Epidemiol Infect. 1998;121:121–8. https://doi.org/10.1017/S0950268898008905
6. Bloom-Feshbach K, Alonso WJ, Charu V, Tamerius J, Simonsen L, Miller MA, et al. Latitudinal variations in seasonal activity of influenza and respiratory syncytial virus (RSV): a global comparative review. PLoS One. 2013;8:e54445. https://doi.org/10.1371/journal.pone.0054445
7. Singapore Ministry of Health. Primary care survey 2014. Singapore; 2017 [cited 2019 Jan 16]. https://www.moh.gov.sg/resources-statistics/reports/primary-care-survey-2014-report
8. Singapore Ministry of Health. Fee benchmarks and bill amount information [cited 2018 Dec 4]. https://www.moh.gov.sg/cost-financing/fee-benchmarks-and-bill-amount-information
9. National Healthcare Group. National Healthcare Group polyclinics. 2017 [cited 2018 Dec 4]. https://www.nhgp.com.sg/Our_Services/General_Medical_Services/Acute_Primary_Care
10. National University Health System. National University polyclinics. 2018 [cited 2018 Dec 4]. https://www.nup.com.sg/Pages/Our Clinics/nup.aspx
11. Cromer D, van Hoek AJ, Newall AT, Pollard AJ, Jit M. Burden of paediatric respiratory syncytial virus disease and potential effect of different immunisation strategies: a modelling and cost-effectiveness analysis for England. Lancet Public Health. 2017;2:e367–74. https://doi.org/10.1016/S2468-2667(17)30103-2
12. Harris JP, Jit M, Cooper D, Edmunds WJ. Evaluating rotavirus vaccination in England and Wales. Part I. Estimating the burden of disease. Vaccine. 2007;25:3962–70. https://doi.org/10.1016/j.vaccine.2007.02.072
13. Department of Statistics Singapore. Prices and price indices. 2018 [cited 2018 Aug 21]. https://www.singstat.gov.sg/find-data/search-by-theme/economy/prices-and-price-indices/latest-data
14. R Core Team. R: a language and environment for statistical computing. Vienna: R Foundation for Statistical Computing; 2018.
15. Homaira N, Oei J-L, Mallitt K-A, Abdel-Latif ME, Hilder L, Bajuk B, et al. High burden of RSV hospitalization in very young children: a data linkage study. Epidemiol Infect. 2016;144:1612–21. https://doi.org/10.1017/S0950268815003015
16. Jepsen MT, Trebbien R, Emborg HD, Krause TG, Schønning K, Voldstedlund M, et al. Incidence and seasonality of respiratory syncytial virus hospitalisations in young children in Denmark, 2010 to 2015. Euro Surveill. 2018;23:17-00163. https://doi.org/10.2807/1560-7917.ES.2018.23.3.17-00163
17. Sruamsiri R, Kubo H, Mahlich J. Hospitalization costs and length of stay of Japanese children with respiratory syncytial virus: A structural equation modeling approach. Medicine (Baltimore). 2018;97:e11491. https://doi.org/10.1097/MD.0000000000011491


Address for correspondence: Clarence C. Tam, Saw Swee Hock School of Public Health Tahir Foundation Building, National University of Singapore, 12 Science Dr 2, Singapore 117549, Singapore, email: clarence.tam@nus.edu.sg

# Human Adenovirus Type 55 Distribution, Regional Persistence, and Genetic Variability

Jun Hang, Adriana E. Kajon, Paul C.F. Graf,[1] Irina Maljkovic Berry, Yu Yang, Mark A. Sanborn, Christian K. Fung, Anima Adhikari, Melinda S. Balansay-Ames, Christopher A. Myers, Leonard N. Binn, Richard G. Jarman, Robert A. Kuschner, Natalie D. Collins

Human adenovirus type 55 (HAdV-55) causes acute respiratory disease of variable severity and has become an emergent threat in both civilian and military populations. HAdV-55 infection is endemic to China and South Korea, but data from other regions and time periods are needed for comprehensive assessment of HAdV-55 prevalence from a global perspective. In this study, we subjected HAdV-55 isolates from various countries collected during 1969–2018 to whole-genome sequencing, genomic and proteomic comparison, and phylogenetic analyses. The results show worldwide distribution of HAdV-55; recent strains share a high degree of genomic homogeneity. Distinct strains circulated regionally for several years, suggesting persistent local transmission. Several cases of sporadic introduction of certain strains to other countries were documented. Among the identified amino acid mutations distinguishing HAdV-55 strains, some have potential impact on essential viral functions and may affect infectivity and transmission.

Acute respiratory diseases (ARD) are caused by numerous viral pathogens, including several human adenovirus (HAdV) types. Respiratory HAdV infections range from mild to severe and are fatal in some cases. HAdV-associated respiratory disease has threatened military readiness, and an increasing number of outbreaks and isolated cases documented in civilian communities in the United States and other countries (*1*–*4*) indicate that it is an emerging threat to public health. The live oral HAdV type 4 and type 7 vaccines are highly effective against the 2 dominant types causing ARD outbreaks in the military environment, but they elicit type-specific immunity and are restricted to use in the US military (*5*–*7*). ARD caused by other HAdV types, such as HAdV types 3, 14, and 21, occurs sporadically in military basic training facilities (*8*–*10*). An increasing number of new HAdV types have been described, indicating the potential emergence of new HAdV-associated diseases (*11*–*13*).

HAdV-55 was initially identified in respiratory isolates originating in China during 1965–1981 as serotype 11a, a distinct genomic variant of serotype 11, by its distinct *Bam*HI digestion profile compared with the HAdV-11 prototype strain Slobitski (*14*). This unique subspecies HAdV-B2 genotype was designated HAdV-55 (P14H11F14) in 2013 after the bioinformatics analysis of complete genome sequences revealed that the genome consists of a HAdV-14 backbone with a portion of the hexon gene from HAdV-11 (*15*–*17*). HAdV-55 has reemerged as a prevalent ARD pathogen, with endemic circulation reported in China and South Korea since 2006 (*18*–*21*). HAdV-55 whole-genome sequences (WGS) available in GenBank are mainly representative of strains from China and South Korea, but also include strains from Argentina, Egypt, and Singapore (Table 1) (*22*–*25*). More data for HAdV-55 isolates from other global locations and years are needed to enable a comprehensive investigation of the spectrum of intratypic genetic variability, phylogeny, and evolution of HAdV-55, and to apply the knowledge to epidemiology and preventive measures. We acquired WGSs of 72 HAdV-55 clinical isolates from 1969–2018 in 6 countries, and conducted genomic, proteomic, and phylogenetic analyses to reveal unique characteristics of HAdV-55 and identify amino acid residue differences between strains.

Author affiliations: Walter Reed Army Institute of Research, Silver Spring, Maryland, USA (J. Hang, I.M. Berry, Y. Yang. M.A. Sanborn, C.K. Fung, A. Adhikari, L.N. Binn, R.G. Jarman, R.A. Kuschner, N.D. Collins); Lovelace Respiratory Research Institute, Albuquerque, New Mexico, USA (A.E. Kajon); US Naval Health Research Center, San Diego, California, USA (P.C.F. Graf, M.S. Balansay-Ames, C.A. Myers)

DOI: https://doi.org/10.3201/eid2607.191707

[1]Current affiliation: US Naval Medical Research Unit 6, Lima, Peru.

**Table 1.** HAdV type 55 strains from other studies used in genomic analysis for study of virus distribution, regional persistence, and genetic variability

| HAdV-55 strain | Collection year | Collection date | Country | GenBank accession no. |
|---|---|---|---|---|
| Human/EGY/ak37_AdV11a/2001/55[P14H11F14] | 2001 | May 1 | Egypt | JX423385 |
| Human/ARG/ak36_AdV11a/2005/55[P14H11F14] | 2005 | Jan 1 | Argentina | JX423384 |
| SGN1222 | 2005 | May 26 | Singapore | FJ597732 |
| QS-DLL | 2006 | Apr | China | FJ643676 |
| CQ-814 | 2010 | Aug 18 | China | JX123027 |
| HAdV-B/CHN/BJ01/2011/55[P14H11F14] | 2011 | Mar 24 | China | JX491639 |
| Shanxi/QZ01/2011 | | Dec 5 | China | KJ883522 |
| CQ-1657 | | Apr 22 | China | JX123028 |
| Shanxi-Y16 | | UNK | China | MK123979 |
| Human/CHN/AQ-1/2012/55[P14/H11/F14] | 2012 | Apr 18 | China | KP279748 |
| HAdV-B55 XZ2012-492 | | Apr 26 | China | KC857701 |
| CQ-2903 | | Jan 8 | China | JX123029 |
| Hebei/BD01/2012 | | Feb 11 | China | KP896478 |
| Hebei/BD6728/2013 | 2013 | Apr 6 | China | KJ883520 |
| TJ-2013-90 | | Jan 14 | China | KF908851 |
| TY12 | | UNK | China | MK123980 |
| TY26 | | UNK | China | MK123981 |
| Liaoning/LS01/2013 | | Feb 25 | China | KP896483 |
| Tianjin/TJ01/2013 | | Jan 15 | China | KP896484 |
| Hebei/BD6729/2013 | | Apr 7 | China | KJ883521 |
| JS201501 | 2015 | Nov 12 | China | KX289874 |
| 100-GD_CHN_2016 | 2016 | Jun | China | KY780931 |
| 73-GD_CHN_2016 | | Jun | China | KY780933 |
| 60-GD-2016 | | Jun 30 | China | KY070248 |
| Yunnan/KM04/2016 | | Jun 8 | China | KY002685 |
| AFMC 16-0011 | 2016 | Feb 23 | South Korea | KX494979 |
| 267 | 2018 | Jun | China (Guangzhou) | MK123978 |

*HAdV, human adenovirus; UNK, unknown.

## Materials and Methods

### HAdV-55 Strains, DNA Extraction, Genome Sequencing

The HAdV-55 isolates included in this study were acquired from 2 main sources: the archival collection of isolates at Lovelace Respiratory Research Institute (LRRI), Albuquerque, NM, USA, gathered through collaborative surveillance efforts funded by the US Department of Defense's Global Emerging Infections Surveillance and Response System; and the HAdV-positive specimen collection of the Naval Health Research Center—Operational Infectious Disease (NHRC-OID, San Diego, CA, USA), NHRC-OID conducts surveillance of febrile respiratory illness among military personnel and their dependents in the Pacific Rim at Commander US Fleet Activities Yokosuka, Yokosuka, Japan (Table 2). At LRRI, we performed viral isolation in A549 cell cultures, purification of HAdV genomic DNA, and molecular typing by restriction enzyme analysis or by PCR and Sanger sequencing of hexon and fiber genes as previously described (*8*,*16*). At Walter Reed Army Institute of Research (Silver Spring, MD, USA), viral DNA samples received from LRRI were subjected to next-generation sequencing (NGS) fragment library preparation using QIAseq FX DNA Library Kit (QIAGEN, https://www.qiagen.com), followed by sequencing by using MiSeq Reagent Kit version 3 (600-cycle) and MiSeq sequencer (Illumina, https://www.illumina.com) (*26*). At the Pacific Rim Surveillance Hub (PRSH) of NHRC-OID, respiratory samples collected from persons meeting case definition for febrile respiratory illness were tested on the FilmArray Respiratory Pathogen Panel (Biofire Diagnostics, https://www.biofiredx.com), a multiplex panel consisting of 21 respiratory viral and bacterial pathogens. Adenovirus-positive samples were submitted to OID from Brian Allgood Army Community Hospital (BAACH), Seoul, South Korea. All samples from PRSH and BAACH sent to OID underwent further characterization that included additional typing by PCR amplification and sequencing of hypervariable region 7 of the hexon gene HVR7 as previously described (*27*). Clinical samples that failed to sequence were reflex-tested on type-specific assays that targeted the hexon gene, and were also inoculated in A549 cells to attempt viral isolation. We subjected all confirmed HAdV isolates to whole-genome NGS using Illumina Nextera XT library preparation kit and MiSeq System.

### Whole-Genome Sequence Assembly, Annotation, and Comparison

We first analyzed NGS data acquired at Walter Reed Army Institute of Research with an in-house de novo pathogen discovery pipeline to identify possible

**Table 2.** HAdV type 55 strains used for genomic analysis for study of vius distribution, regional persistence, and genetic variability*

| Strain | Collection year | Collection site | Country | Source | GenBank accession no. |
|---|---|---|---|---|---|
| HAdV-11/14 strain 273 | 1969 | Military camp | Spain | LRRI§ | MN654395 |
| CADOH VRDL 76–0669 | 1976 | California | USA | LRRI | MN654394 |
| CDC 97026382 | 1997 | South Dakota | USA | LRRI | MN654392 |
| NAMRU3-E3 | 2000 | Alexandria | Egypt | LRRI | MN654380 |
| NAMRU3-E4 | 2000 | Alexandria | Egypt | LRRI | MN654381 |
| NAMRU3-E6 | 2000 | Alexandria | Egypt | LRRI | MN654385 |
| NAMRU3-E66 | 2002 | Alexandria | Egypt | LRRI | MN654382 |
| NAMRU3-E72 | 2000 | Alexandria | Egypt | LRRI | MN654383 |
| NAMRU3 2005–909685 | 2005 | Cairo | Egypt | LRRI | MN654390 |
| NAMRU3 2005–908017 | 2005 | Cairo | Egypt | LRRI | MN654391 |
| NAMRU3 2007–905716 | 2007 | Cairo | Egypt | LRRI | MN654386 |
| NAMRU3 2008–905223 | 2008 | Cairo | Egypt | LRRI | MN654384 |
| NAMRU3 2009–908968 | 2009 | Cairo | Egypt | LRRI | MN654387 |
| SNG1218 | 2005 | Singapore | Singapore | LRRI | MN654388 |
| SNG1223 | 2005 | Singapore | Singapore | LRRI | MN654389 |
| WPAFB24 | 2009 | BAACH† | South Korea | LRRI | MN654379 |
| WPAFB25 | 2009 | BAACH | South Korea | LRRI | MN654378 |
| WPAFB48 | 2009 | BAACH | South Korea | LRRI | MN654377 |
| WPAFB69 | 2009 | BAACH | South Korea | LRRI | MN654375 |
| WPAFB75 | 2009 | BAACH | South Korea | LRRI | MN654376 |
| WPAFB415 | 2012 | Misawa AB‡ | Japan | LRRI | MN654393 |
| NHRC557006 | 2017 | CFA Yokosuka¶ | Japan | NHRC | NA# |
| NHRC isolates, n = 50 | 2017, 2018 | BAACH | South Korea | NHRC | NA# |

*An additional 27 full genome sequences from GenBank included in the analysis are listed in the Appendix Table 1. HAdV, human adenovirus.
†Brian Allgood Army Community Hospital at US Army Garrison Yongsan, Seoul, South Korea.
‡Misawa Air Base, Misawa, Aomori, Japan.
§LRRI archival collection of isolates generated through collaborations with NHRC, United States Air Force School of Aerospace Medicine, US Naval Medical Research Unit No. 3, US Centers for Disease Control and Prevention, and California Department of Health.
¶Commander US Fleet Activities Yokosuka, Yokosuka, Japan.
#Isolates were fully genome sequenced and found to be identical to the South Korea HAdV-55 strains.

mix of viruses (*28*). We assembled full genome sequences using NGS_Mapper (https://github.com/UDBWRAIR/ngs_mapper) an in-house reference mapping pipeline built on BWA-MEM assembler (H. Li, unpub. data, https://arxiv.org/abs/1303.3997v2). We used Geneious R10 (Biomatters Ltd., https://www.geneious.com) and Integrative Genomics Viewer (IGV) software (Broad Institute, https://igv.org) for manual curation of the assembly, sequence alignment, annotation of genes, etc. We used the complete genome sequence of HAdV-55 strain QS-DLL/China/2006 (GenBank accession no. FJ643676) (*29*,*30*) as reference in reference mapping, annotation, and sequence comparison. We analyzed NGS data acquired at NHRC using the EDGE (Empowering the Development of Genomics Expertise) Bioinformatics Platform (https://edge.readthedocs.io) (*31*) and Lasergene software suite (DNASTAR, Inc., https://www.dnastar.com), and performed sequence alignment using BLAST (http://blast.ncbi.nlm.nih.gov/Blast.cgi).

### Phylogenetic and Proteomic Analysis

We used MAFFT and MEGA7 (*32*) to align HAdV-55 genomic sequences. We determined general time reversible gamma-distributed invariant models of evolution using jModelTest2 (https://github.com/ddarriba/jmodeltest2), and inferred a maximum likelihood phylogenetic tree using PhyML in MEGA7 (http://www.megasoftware.net), with subtree pruning and regrafting and nearest-neighbor interchange tree search and Shimodiara-Hasegawa approximate likelihood ratio test for node confidence values.

We input the nucleotide sequence alignment and the GenBank feature table for the reference strain QS-DLL/China/2006 (FJ643676) into an in-house pipeline that annotates the sequences. To aid in visualization and comparison, we concatenated and aligned the annotated protein sequences using MUSCLE (http://www.drive5.com/muscle) in Geneious R10. We removed redundant identical sequences for further analysis. We visualized mismatches with an augmented version of the output using Highlighter software (https://www.hiv.lanl.gov/content/sequence/HIGHLIGHT/highlighter_top.html) (*33*).

## Results

HAdV55 has been detected worldwide for decades (Table 1). We obtained complete genome sequences for a set of diverse HAdV-55 strains originating in 6 countries over many years and deposited them in GenBank under accession nos. MN654375–MN654395 (Table 2). The characterized strains include strain 273/Spain/1969, originally identified as an intermediate variant 11/14 and isolated during an outbreak of ARD

in the Spanish military (*34*); it is the earliest available HAdV-55 isolate and is therefore considered the prototype strain. In addition, the examined collection includes 2 strains isolated from civilians in the United States, 76-0669/USA/CA/1976 and 97026382/USA/SD/1997, the strain isolated during a large ARD outbreak in a civilian job training facility in South Dakota (*35*); 10 HAdV-55 strains from 2 major cities in Egypt; 2 strains from a Singapore military base; 2 HAdV-55 strains isolated in different locations and years in Japan; and 50 recent strains from South Korea.

The genome sequences of HAdV-55 strains are highly similar, with 132 or fewer nucleotide differences out of the 34.8 kb genome (i.e., genomic nucleotide divergence ≤0.38% among all the strains). The inferred phylogenetic tree of HAdV-55 lineage shows the examined strains mostly clustered together by collection country (South Korea, China, Singapore, and Egypt), rather than collection year (Figure 1). The results demonstrate the long-term regional persistence of HAdV-55 infection, which appears to span for years. The 3 isolates collected in 2005 from Singapore were identical to each other and located within the clade of Egypt isolates from 2000–2009. We detected <9 nt differences among all 14 Egypt and Singapore isolates examined (12 from this study; 2 from GenBank). The genome sequences of isolate NHRC557006/Japan/2017 and all the South Korea isolates from this study and in GenBank were found to be identical, except for the differences in the length of the noncoding poly(A) or poly(T) sequences. A previous isolate, WPAFB415/Japan/2012, was phylogenetically distinct from isolate NHRC557006/Japan/2017 and South Korea strains, with proximity with the Egypt strains. Likewise, isolates from South Korea clustered in a monophyletic clade located proximate to the clade of China strains. Another isolate from China was found outside of the Chinese clade and was more related to a strain from Argentina. Nevertheless, we show a highly localized persistence of HAdV-55. GenBank had 1 available genome sequence for an HAdV-55 strain from Argentina, ak36_AdV11a/ARG/2005 (accession no. JX423384); however, Kajon et al. (*16*) performed thorough restriction enzyme analysis characterization and compared hexon and fiber gene sequences for 7 Argentina HAdV-55 isolates collected in 2000–2005. Their results suggest these are isolates of a single strain. Of interest, we found the virtual restriction profiles with *Bam*HI, *Bcl*I, *Bgl*II, *Bst*EII, *Hind*III, *Hpa*I, *Pst*I, *Sma*I, and *Xba*I derived from genome sequence JX423384 to be 100% identical to the patterns reported for HAdV-55 strains by Kajon et al., suggesting a single strain was responsible for multiple ARD cases in Argentina.

We compared amino acid sequences of all open reading frames (ORF) among HAdV-55 strains (Figure 2; Appendix Table, https://wwwnc.cdc.gov/EID/article/26/7/19-1707-App1.xlsx) and found very few amino acid differences. Out of 10,925 aa in the annotated 37 proteins, only 2–15 aa residues in each strain are different from consensus protein sequences (amino acid variation ≤0.14%) among the HAdV-55 strains. No single annotated protein had >2 amino acid differences compared with the consensus except BJ01/CHN/2011 (GenBank accession no. JX491639), which had 6 amino acid substitutions in the 246 aa L3 pVI 26.6 kDa protein and 3 amino acid mutations in the 812 aa L4 100K protein (Appendix Table). Seven proteins, L2 pVII 21.3 kDa protein, L3 pVI 26.6 kDa protein, L3 23K 23.7 kDa protein, E2A 58.3 kDa DNA binding protein, L4 pVIII 25 kDa protein, E4 ORF3 13.6 kDa protein, and E4 ORF2 14.3 kDa protein, were identical among all the examined strains.

Our analyses showed that hexon, fiber, and penton base proteins do not have more amino acid residue changes when compared with other proteins (Figure 2). We detected a few insertions and deletions in intergenic untranslated regions in several genomes. The strain USA/1976 has 2 deletions (of 3 aa each) in the coding sequences for L4 100K/91 kDa protein and L4 22K/21.6 kDa protein (Appendix Table). It is remarkable that there were no amino acid differences among South Korea isolates from 2009–2018. Despite the very few amino acid substitutions, most residue changes resulted in amino acids of different chemical structures, which may potentially affect protein functionality (Appendix Table). Several amino acid mutations were strain-specific and not seen in other strains or other related HAdV types. One specific example is that the P18S mutation in the terminal protein precursor (pTP) was only found in the South Korea strain. This position was highly conserved (a proline) in all other examined adenoviruses including HAdVs of species B and related simian or gorilla adenoviruses (GenBank accession nos. AP_000267, AP_000305, YP_006272955, ADQ38372). The strain BJ01/CHN/2011 was phylogenetically more closely related to the South Korea strain and had the same pTP sequence with the P18S mutation.

We obtained a total of 51 HAdV-55 isolates, 50 recovered from US military active duty personnel in South Korea and 1 from a US military dependent in Japan, through PRSH efforts. Whole-genome sequencing and sequence data analysis confirmed all strains to be identical to the South Korea strain in full agreement with the recent reports on HAdV-55 circulation in South Korea and the high number of ARD cases documented among the South Korea military (*18*,*36*).

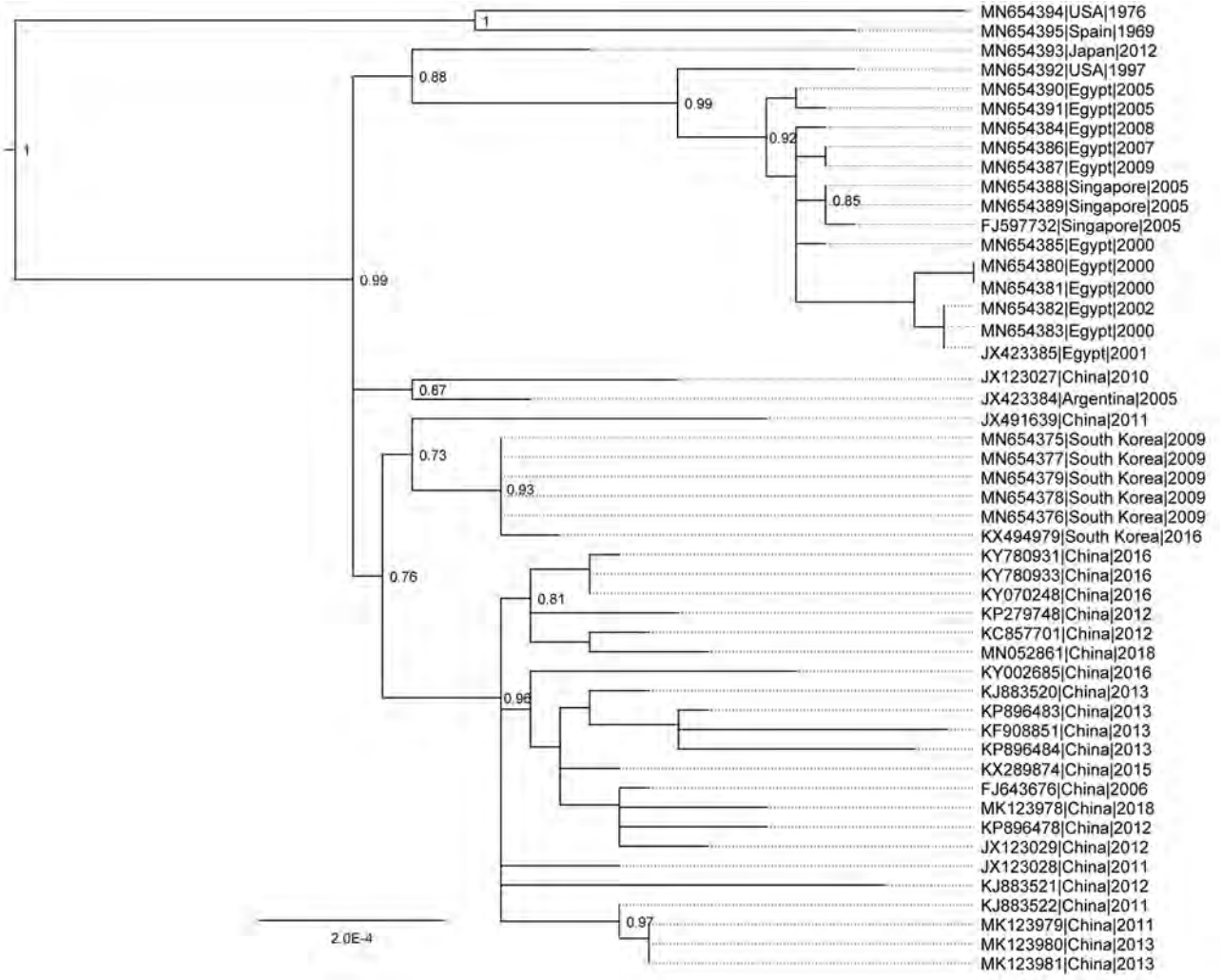


**Figure 1.** Phylogeny of HAdV-55 based on whole-genome sequences for study of virus distribution, regional persistence, and genetic variability. The phylogenetic tree was generated using the maximum-likelihood method with subtree pruning and regrafting and nearest-neighbor interchange tree search and the Shimodiara-Hasegawa approximate likelihood ratio test for node confidence values. Node confidence values were estimated using approximate likelihood ratio test and the tree was rooted on a HAdV-14 clade as an outgroup (not shown). GenBank accession numbers for isolates are provided. Scale bar indicates node confidence value. HAdV, human adenovirus.

## Discussion

Recent reports describing large numbers of HAdV-55-associated ARD cases in both China and South Korea, including outbreaks and some deaths in both civilian and military communities, have raised concerns about the possibility of global transmission events, similar to those described for severe acute respiratory syndrome or Middle East respiratory syndrome (*21*,*37*–*43*). Outbreaks and isolated cases of HAdV-55-associated ARD have been reported in the literature in other countries, such as Turkey (*44*), Israel (*45*), and France (*46*) since 2005. Possible reasons for underdetection and underreporting of HAdV-55 are its recent designation in 2013 as a discrete adenovirus type, following its recognition as an intertypic recombinant (P14H11F14) (*17*), and probably also molecular typing practices based solely on partial sequencing of the hexon gene. Molecular diagnosis of HAdV-55 and other intertypic recombinant HAdV genotypes requires a PCR-based assay targeting ≥2 regions of the genome, the penton base and hexon or the hexon and fiber genes; such assays would greatly improve molecular surveillance practices. The prototype strain, 273/Spain/1969, was detected in association with a severe ARD outbreak involving military recruits in Spain and reported as a serologically intermediate variant 11/14 (*34*). The US strain 97026382/South Dakota/1997, originally reported as HAdV-11 (*35*) and subsequently described as genome type 11a (*16*), caused a large ARD outbreak in a job

training center. It is notable that the circulation of these viruses was not detected or reported in Europe or North America in the years following the detection of either the prototype or US strain. On the other hand, the long persistence of HAdV-55 in China and South Korea suggests continuous transmission and endemicity. If strains circulating in China or South Korea can cause repeated outbreaks, that indicates an important change in the epidemiologic pattern of HAdV-55 infection: from sporadic epidemic outbreak to persistent endemicity. The identification of factors that affect HAdV-55 transmission, from novel functional changes in the viruses to social or environmental changes, warrants further investigation.

Our study and others have shown that recent HAdV-55 genomes share a nucleotide identity >99.7% (*22*,*23*,*29*). The nucleotide variations are located all over the genome and are not concentrated in any particular genomic regions. We noted amino acid substitutions on proteins essential for viral replication, such as L4 100K, which may affect virus growth phenotype, antigenicity, infectivity, or virulence. Terminal protein precursor (pTP) and its protease-processed derivatives, intermediate terminal protein (iTP) and mature terminal protein (TP), play crucial and complex roles in adenovirus genome replication and virus maturation. The mutation P18S is unique to South Korea strains and located in a conserved region of pTP. Because the structure of pTP protein of adenovirus has not been resolved, it is unknown whether the P to S mutation will affect pTP structure and consequently change protease cleavage pattern of pTP, DNA replication, and genome packaging. Earlier work by Hay et al. (*47*,*48*) demonstrated that point mutations and deletions generated on pTP affect DNA replication activity in vitro. Flint et al. (*49*) showed that G315V substitution in pTP of HAdV-5 impaired pTP maturation leading to reduced infectivity. The remaining genomic changes of HAdV-55 appear to be largely trivial and not likely responsible

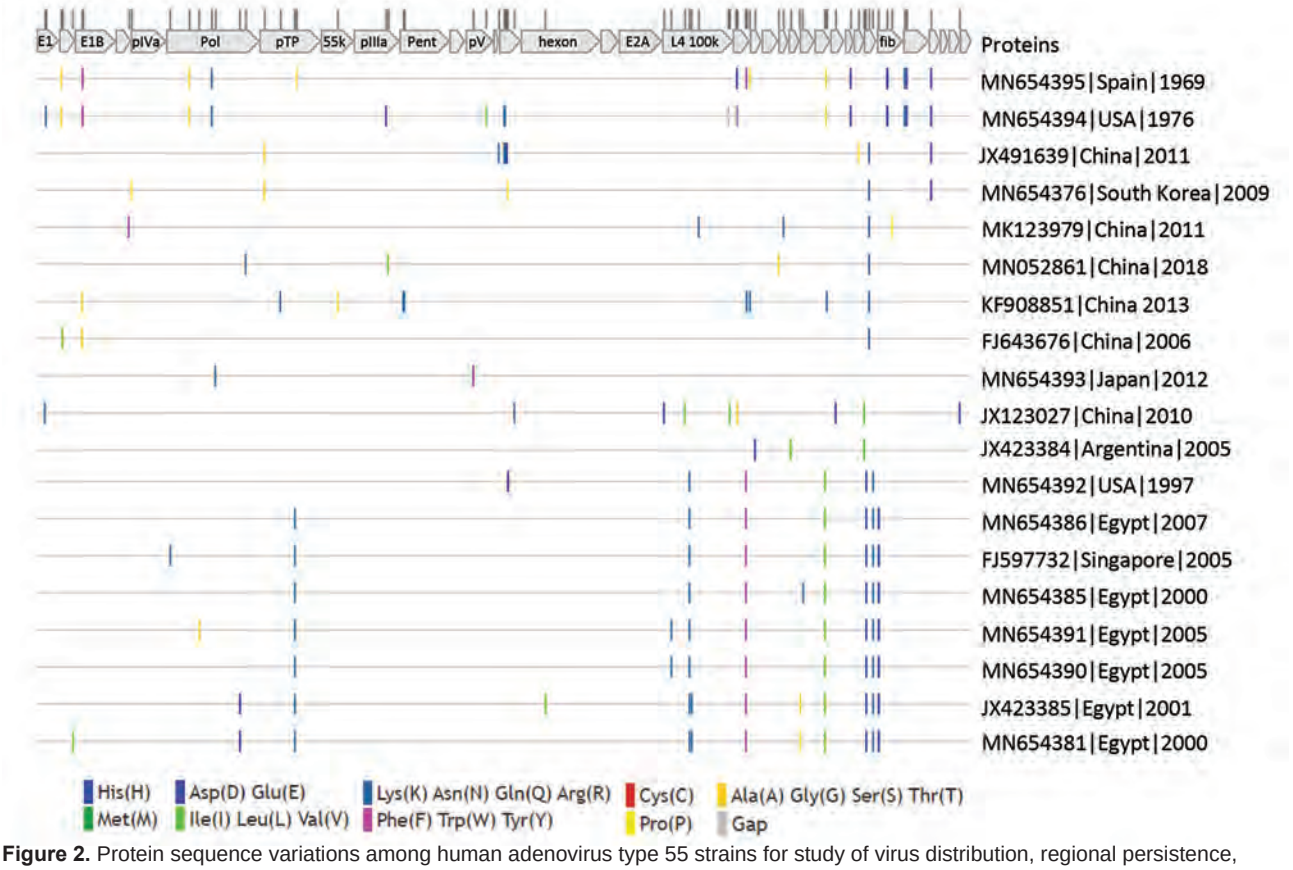


**Figure 2.** Protein sequence variations among human adenovirus type 55 strains for study of virus distribution, regional persistence, and genetic variability. Protein sequences were concatenated and aligned. Amino acid differences compared with the consensus were visualized with Highlighter software (https://www.hiv.lanl.gov/content/sequence/HIGHLIGHT/highlighter_top.html). Redundant sequences are not shown. The locations of proteins and variant amino acid residues are shown at top. GenBank accession numbers for isolates are provided. Ala, alanine; Arg, arginine; Asn, asparagine; Asp, aspartate; Cys, cysteine; Gln, glutamine; Glu, glutamate; Gly, glycine; His, histidine; Ile, isoleucine; Leu, leucine; Lys, lysine; Met, methionine; Phe, phenylalanine, Pro, proline; Ser, serine; Thr, threonine; Trp, tryptophan; Tyr, tyrosine; Val, valine.

for the increased incidence of outbreaks and disease severity. Further investigation and comparison of these strains on virology, molecular biology, and biochemistry perspectives will provide solid evidence to clarify whether some of the current strains are more infectious or virulent and therefore pose higher risks to human health. Detailed molecular epidemiology study, such as reported by Jing et al. on household HAdV-55 transmission (*50*), is warranted to enhance etiologic understanding of HAdV-55–caused ARD for accurate and timely diagnosis and disease prevention.

The United States has the highest number of domestic and international trade and travel visits in the world and is therefore highly susceptible to importation and dispersion of incoming pathogens such as HAdV-55. Indeed, isolated HAdV-55 cases and at least one outbreak have occurred in the United States with no clear identification of the source. Of interest, as suggested by the results of our phylogenetic analysis, the 2 US strains were not apparently related to each other. Therefore, implementation of enhanced surveillance, including typing of clinically relevant HAdV strains, is needed, along with proper design of countermeasures such as rapid diagnostics, treatments, and novel vaccines.

A limitation of this study is the lack of detailed clinical data and travel history. More information is needed for accurate risk assessment of disease transmission. It is unclear whether NHRC557006/Japan/2017 was introduced from South Korea by travel, or whether a cryptic circulation of the South Korea strain in Japan has yet to be detected. Similarly, without reports on additional HAdV-55 cases in Japan, it remains unknown which HAdV-55 strain, the South Korea strain, WPAFB415/Japan/2012, or other unknown strains, are circulating in Japan. A large number of HAdV-55-associated ARD cases were detected in both South Korea military personnel and US military personnel stationed in South Korea. Determining whether infected persons trained together or participated in same military events, how long and how often they were in close contact, the timeline of infection, and whether ARD outbreaks during an extended training period were underreported is important. It is worth noting that US active duty military in South Korea were vaccinated against HAdV-4 and HAdV-7, which suggests that the HAdV-4 and HAdV-7 vaccine formulation does not confer adequate protection against HAdV-55. Our ongoing and planned studies on HAdV-55–specific serologic surveys before, during, and after military deployment, as well as local serologic surveys in South Korea and Japan, will contribute to comprehensive understanding of HAdV-55 prevalence and enable data-driven decisions on the necessity of enhanced surveillance and development of effective prophylaxes.

### Acknowledgment

We thank research collaborators for generous sharing of specimens which made this study possible. We also thank James S. Hilaire, Nicole R. Nicholas, Tuan K. Nguyen, and April N. Griggs for their assistance in project management and sample tracking, storage, and retrieval. Finally, we thank the Defense Health Agency Immunization Healthcare Division (DHA-IHD), Global Emerging Infections Surveillance and Response System (GEIS), Division of the Armed Forces Health Surveillance Branch.

## About the Author

Dr. Hang is a molecular microbiologist at Walter Reed Army Institute of Research, Silver Spring, Maryland, USA. His primary research interest is pathogen discovery in clinical and environmental specimens.

### References

1. Sanchez JL, Binn LN, Innis BL, Reynolds RD, Lee T, Mitchell-Raymundo F, et al. Epidemic of adenovirus-induced respiratory illness among US military recruits: epidemiologic and immunologic risk factors in healthy, young adults. J Med Virol. 2001;65:710–8. https://doi.org/10.1002/jmv.2095
2. Kolavic-Gray SA, Binn LN, Sanchez JL, Cersovsky SB, Polyak CS, Mitchell-Raymundo F, et al. Large epidemic of adenovirus type 4 infection among military trainees: epidemiological, clinical, and laboratory studies. Clin Infect Dis. 2002;35:808–18. https://doi.org/10.1086/342573
3. Padin DS, Faix D, Brodine S, Lemus H, Hawksworth A, Putnam S, et al. Retrospective analysis of demographic and clinical factors associated with etiology of febrile respiratory illness among US military basic trainees. BMC Infect Dis. 2014;14:576. https://doi.org/10.1186/s12879-014-0576-2
4. Kajon AE, Lamson DM, St George K. Emergence and re-emergence of respiratory adenoviruses in the United States. Curr Opin Virol. 2019;34:63–9. https://doi.org/10.1016/j.coviro.2018.12.004
5. Gray GC, Goswami PR, Malasig MD, Hawksworth AW, Trump DH, Ryan MA, et al.; Adenovirus Surveillance Group. Adult adenovirus infections: loss of orphaned vaccines precipitates military respiratory disease epidemics. Clin Infect Dis. 2000;31:663–70. https://doi.org/10.1086/313999
6. Blasiole DA, Metzgar D, Daum LT, Ryan MA, Wu J, Wills C, et al. Molecular analysis of adenovirus isolates from vaccinated and unvaccinated young adults. J Clin Microbiol. 2004;42:1686–93. https://doi.org/10.1128/JCM.42.4.1686-1693.2004
7. Kuschner RA, Russell KL, Abuja M, Bauer KM, Faix DJ, Hait H, et al.; Adenovirus Vaccine Efficacy Trial Consortium. A phase 3, randomized, double-blind, placebo-controlled study of the safety and efficacy of the live, oral adenovirus type 4 and type 7 vaccine, in U.S. military recruits. Vaccine. 2013;31:2963–71. https://doi.org/10.1016/j.vaccine.2013.04.035

8. Kajon AE, Hang J, Hawksworth A, Metzgar D, Hage E, Hansen CJ, et al. Molecular epidemiology of adenovirus type 21 respiratory strains isolated from US military trainees (1996–2014). J Infect Dis. 2015;212:871–80. https://doi.org/10.1093/infdis/jiv141
9. Sanchez JL, Cooper MJ, Myers CA, Cummings JF, Vest KG, Russell KL, et al. Respiratory infections in the U.S. military: recent experience and control. Clin Microbiol Rev. 2015;28:743–800. https://doi.org/10.1128/CMR.00039-14
10. Clemmons NS, McCormic ZD, Gaydos JC, Hawksworth AW, Jordan NN. Acute respiratory disease in US Army trainees 3 years after reintroduction of adenovirus vaccine. Emerg Infect Dis. 2017;23:95–8. https://doi.org/10.3201/eid2301.161297
11. Ismail AM, Cui T, Dommaraju K, Singh G, Dehghan S, Seto J, et al. Genomic analysis of a large set of currently-and historically-important human adenovirus pathogens. Emerg Microbes Infect. 2018;7:10. https://doi.org/10.1038/s41426-017-0004-y
12. Dhingra A, Hage E, Ganzenmueller T, Böttcher S, Hofmann J, Hamprecht K, et al. Molecular evolution of human adenovirus (HAdV) species C. Sci Rep. 2019;9:1039. https://doi.org/10.1038/s41598-018-37249-4
13. Ismail AM, Lee JS, Lee JY, Singh G, Dyer DW, Seto D, et al. Adenoviromics: mining the human adenovirus species D genome. Front Microbiol. 2018;9:2178. https://doi.org/10.3389/fmicb.2018.02178
14. Li QG, Hambraeus J, Wadell G. Genetic relationship between thirteen genome types of adenovirus 11, 34, and 35 with different tropisms. Intervirology. 1991;32:338–50. https://doi.org/10.1159/000150218
15. Hierholzer JC, Pumarola A. Antigenic characterization of intermediate adenovirus 14-11 strains associated with upper respiratory illness in a military camp. Infect Immun. 1976;13:354–9. https://doi.org/10.1128/IAI.13.2.354-359.1976
16. Kajon AE, de Jong JC, Dickson LM, Arron G, Murtagh P, Viale D, et al. Molecular and serological characterization of species B2 adenovirus strains isolated from children hospitalized with acute respiratory disease in Buenos Aires, Argentina. J Clin Virol. 2013;58:4–10. https://doi.org/10.1016/j.jcv.2013.06.030
17. Seto D, Jones MS, Dyer DW, Chodosh J. Characterizing, typing, and naming human adenovirus type 55 in the era of whole genome data. J Clin Virol. 2013;58:741–2. https://doi.org/10.1016/j.jcv.2013.09.025
18. Ko JH, Woo HT, Oh HS, Moon SM, Choi JY, Lim JU, et al. Ongoing outbreak of human adenovirus-associated acute respiratory illness in the Republic of Korea military, 2013 to 2018. Korean J Intern Med (Korean Assoc Intern Med). 2019;kjim.2019.092.
19. Gao HW, Wei MT, Fan HJ, Ding H, Wei W, Liu ZQ, et al. Dynamic changes in clinical characteristics during an outbreak of human adenovirus serotype 55 in China. Disaster Med Public Health Prep. 2018;12:464–9. https://doi.org/10.1017/dmp.2015.185
20. Zheng X, Rong X, Feng Y, Sun X, Li L, Wang Q, et al. Seroprevalence of neutralizing antibodies against adenovirus type 14 and 55 in healthy adults in Southern China. Emerg Microbes Infect. 2017;6:e43. https://doi.org/10.1038/emi.2017.29
21. Lu QB, Tong YG, Wo Y, Wang HY, Liu EM, Gray GC, et al. Epidemiology of human adenovirus and molecular characterization of human adenovirus 55 in China, 2009-2012. Influenza Other Respir Viruses. 2014;8:302–8. https://doi.org/10.1111/irv.12232
22. Cheng Z, Yan Y, Jing S, Li WG, Chen WW, Zhang J, et al. Comparative genomic analysis of re-emergent human adenovirus type 55 pathogens associated with adult severe community-acquired pneumonia reveals conserved genomes and capsid proteins. Front Microbiol. 2018;9:1180. https://doi.org/10.3389/fmicb.2018.01180
23. Wang W, Liu Y, Zhou Y, Gu L, Zhang L, Zhang X, et al. Whole-genome analyses of human adenovirus type 55 emerged in Tibet, Sichuan and Yunnan in China, in 2016. PLoS One. 2017;12:e0189625. https://doi.org/10.1371/journal.pone.0189625
24. Gu SH, Song DH, Lee D, Huh K, Yoo H, Oh HS, et al. Complete genome sequence of human adenovirus type 55 associated with acute respiratory disease, isolated from a military base in the Republic of Korea. Genome Announc. 2017;5:5. https://doi.org/10.1128/genomeA.01565-16
25. Zhang Q, Seto D, Cao B, Zhao S, Wan C. Genome sequence of human adenovirus type 55, a re-emergent acute respiratory disease pathogen in China. J Virol. 2012;86:12441–2. https://doi.org/10.1128/JVI.02225-12
26. Hang J, Vento TJ, Norby EA, Jarman RG, Keiser PB, Kuschner RA, et al. Adenovirus type 4 respiratory infections with a concurrent outbreak of coxsackievirus A21 among United States Army Basic Trainees, a retrospective viral etiology study using next-generation sequencing. J Med Virol. 2017;89:1387–94. https://doi.org/10.1002/jmv.24792
27. Sarantis H, Johnson G, Brown M, Petric M, Tellier R. Comprehensive detection and serotyping of human adenoviruses by PCR and sequencing. J Clin Microbiol. 2004; 42:3963–9. https://doi.org/10.1128/JCM.42.9.3963-3969.2004
28. Kilianski A, Carcel P, Yao S, Roth P, Schulte J, Donarum GB, et al. Pathosphere.org: pathogen detection and characterization through a web-based, open source informatics platform. BMC Bioinformatics. 2015;16:416. https://doi.org/10.1186/s12859-015-0840-5
29. Yang Z, Zhu Z, Tang L, Wang L, Tan X, Yu P, et al. Genomic analyses of recombinant adenovirus type 11a in China. J Clin Microbiol. 2009;47:3082–90. https://doi.org/10.1128/JCM.00282-09
30. Walsh MP, Seto J, Jones MS, Chodosh J, Xu W, Seto D. Computational analysis identifies human adenovirus type 55 as a re-emergent acute respiratory disease pathogen. J Clin Microbiol. 2010;48:991–3. https://doi.org/10.1128/JCM.01694-09
31. Li PE, Lo CC, Anderson JJ, Davenport KW, Bishop-Lilly KA, Xu Y, et al. Enabling the democratization of the genomics revolution with a fully integrated web-based bioinformatics platform. Nucleic Acids Res. 2017;45:67–80. https://doi.org/10.1093/nar/gkw1027
32. Kumar S, Stecher G, Tamura K. MEGA7: Molecular Evolutionary Genetics Analysis version 7.0 for bigger datasets. Mol Biol Evol. 2016;33:1870–4. https://doi.org/10.1093/molbev/msw054
33. Keele BF, Giorgi EE, Salazar-Gonzalez JF, Decker JM, Pham KT, Salazar MG, et al. Identification and characterization of transmitted and early founder virus envelopes in primary HIV-1 infection. Proc Natl Acad Sci U S A. 2008;105:7552–7. https://doi.org/10.1073/pnas.0802203105
34. Hierholzer JC, Pumarola A, Rodriguez-Torres A, Beltran M. Occurrence of respiratory illness due to an atypical strain of adenovirus type 11 during a large outbreak in Spanish military recruits. Am J Epidemiol. 1974;99:434–42. https://doi.org/10.1093/oxfordjournals.aje.a121632
35. Centers for Disease Control and Prevention (CDC). Civilian outbreak of adenovirus acute respiratory disease—South Dakota, 1997. MMWR Morb Mortal Wkly Rep. 1998;47:567–70.
36. Yoo H, Gu SH, Jung J, Song DH, Yoon C, Hong DJ, et al. Febrile respiratory illness associated with human adenovirus type 55 in South Korea military, 2014–2016. Emerg Infect Dis. 2017;23:1016–20. https://doi.org/10.3201/eid2306.161848

37. Heo JY, Noh JY, Jeong HW, Choe KW, Song JY, Kim WJ, et al. Molecular epidemiology of human adenovirus-associated febrile respiratory illness in soldiers, South Korea. Emerg Infect Dis. 2018;24:1221–7. https://doi.org/10.3201/eid2407.171222
38. Yoon H, Jhun BW, Kim H, Yoo H, Park SB. Characteristics of adenovirus pneumonia in Korean military personnel, 2012–2016. J Korean Med Sci. 2017;32:287–95. https://doi.org/10.3346/jkms.2017.32.2.287
39. Park JY, Kim BJ, Lee EJ, Park KS, Park HS, Jung SS, et al. Clinical features and courses of adenovirus pneumonia in healthy young adults during an outbreak among Korean military personnel. PLoS One. 2017;12:e0170592. https://doi.org/10.1371/journal.pone.0170592
40. Dongliu Y, Guoliang Y, Haocheng X, Shuaijia Q, Li B, Yanglei J. Outbreak of acute febrile respiratory illness caused by human adenovirus B P14H11F14 in a military training camp in Shandong China. Arch Virol. 2016;161:2481–9. https://doi.org/10.1007/s00705-016-2949-x
41. Li X, Kong M, Su X, Zou M, Guo L, Dong X, et al. An outbreak of acute respiratory disease in China caused by human adenovirus type B55 in a physical training facility. Int J Infect Dis. 2014;28:117–22. https://doi.org/10.1016/j.ijid.2014.06.019
42. Gu L, Qu J, Sun B, Yu X, Li H, Cao B. Sustained viremia and high viral load in respiratory tract secretions are predictors for death in immunocompetent adults with adenovirus pneumonia. PLoS One. 2016;11:e0160777. https://doi.org/10.1371/journal.pone.0160777
43. Zhang SY, Luo YP, Huang DD, Fan H, Lu QB, Wo Y, et al. Fatal pneumonia cases caused by human adenovirus 55 in immunocompetent adults. Infect Dis (Lond). 2016;48:40–7. https://doi.org/10.3109/23744235.2015.1055585
44. Chmielewicz B, Benzler J, Pauli G, Krause G, Bergmann F, Schweiger B. Respiratory disease caused by a species B2 adenovirus in a military camp in Turkey. J Med Virol. 2005;77:232–7. https://doi.org/10.1002/jmv.20441
45. Salama M, Amitai Z, Amir N, Gottesman-Yekutieli T, Sherbany H, Drori Y, et al. Outbreak of adenovirus type 55 infection in Israel. J Clin Virol. 2016;78:31–5. https://doi.org/10.1016/j.jcv.2016.03.002
46. Lafolie J, Mirand A, Salmona M, Lautrette A, Archimbaud C, Brebion A, et al. Severe pneumonia associated with adenovirus type 55 infection, France, 2014. Emerg Infect Dis. 2016;22:2012–4. https://doi.org/10.3201/eid2211.160728
47. Botting CH, Hay RT. Role of conserved residues in the activity of adenovirus preterminal protein. J Gen Virol. 2001;82:1917–27. https://doi.org/10.1099/0022-1317-82-8-1917
48. Liu H, Naismith JH, Hay RT. Adenovirus DNA replication. Curr Top Microbiol Immunol. 2003;272:131–64. https://doi.org/10.1007/978-3-662-05597-7_5
49. Kato SE, Chahal JS, Flint SJ. Reduced infectivity of adenovirus type 5 particles and degradation of entering viral genomes associated with incomplete processing of the preterminal protein. J Virol. 2012;86:13554–65. https://doi.org/10.1128/JVI.02337-12
50. Jing S, Zhang J, Cao M, Liu M, Yan Y, Zhao S, et al. Household transmission of human adenovirus type 55 in case of fatal acute respiratory disease. Emerg Infect Dis. 2019;25:1756–8. https://doi.org/10.3201/eid2509.181937


Address for correspondence: Jun Hang, Viral Diseases Branch, Walter Reed Army Institute of Research, Silver Spring, MD 20910, USA; email: jun.hang.civ@mail.mil

# Policy Decisions and Use of Information Technology to Fight COVID-19, Taiwan

Cheryl Lin, Wendy E. Braund, John Auerbach, Jih-Haw Chou, Ju-Hsiu Teng, Pikuei Tu, Jewel Mullen

Because of its proximity to and frequent travelers to and from China, Taiwan faces complex challenges in preventing coronavirus disease (COVID-19). As soon as China reported the unidentified outbreak to the World Health Organization on December 31, 2019, Taiwan assembled a taskforce and began health checks onboard flights from Wuhan. Taiwan's rapid implementation of disease prevention measures helped detect and isolate the country's first COVID-19 case on January 20, 2020. Laboratories in Taiwan developed 4-hour test kits and isolated 2 strains of the coronavirus before February. Taiwan effectively delayed and contained community transmission by leveraging experience from the 2003 severe acute respiratory syndrome outbreak, prevalent public awareness, a robust public health network, support from healthcare industries, cross-departmental collaborations, and advanced information technology capacity. We analyze use of the National Health Insurance database and critical policy decisions made by Taiwan's government during the first 50 days of the COVID-19 outbreak.

On December 31, 2019, China reported 27 cases of an unidentified viral pneumonia outbreak in Wuhan, Hubei Province, to the World Health Organization (WHO; *1*). During the 2003 outbreak of severe acute respiratory syndrome (SARS), Taiwan experienced 346 cases and 37 deaths (*2*). Considering >8,000 cases of SARS occurred globally in 2003 and the outbreak claimed 774 lives worldwide, the Taiwan government was particularly cautious about the emerging infectious disease in nearby China in 2019. Taiwan's proximity to China and the frequency of travelers between the 2 countries created concern the virus could spread. Because millions of Taiwan citizens living and studying in China were expected to return home for the January 11 presidential election and impending Lunar New Year holiday and Taiwan is a favorite destination for tourists from China (*3*), intensified public anxiety warranted heightened disease prevention measures.

Informed by lessons from the 2003 SARS outbreak, Taiwan had systems in place to fight the potential new epidemic. The country has a robust nationwide public health network, comprehensive universal healthcare for all citizens, vibrant medical research and pharmaceutical industries, and improved infection control practices. We delineate and analyze the critical policy decisions and cross-departmental collaborations in the Taiwan government and Taiwan Centers for Disease Control (Taiwan CDC) during the first 50 days of the COVID-19 epidemic. Of note, the centralized, real-time database of the country's National Health Insurance (NHI) helped support disease surveillance and case detection. Taiwan CDC's comprehensive response and innovative use of the NHI database effectively delayed and contained community transmission in the country, even as the number of confirmed cases surged in neighboring countries in Asia starting in mid-February.

## Devising and Updating Travel and Disease Control Policies

While most of the world was preparing for the 2020 New Year, Taiwan CDC began health screening of passengers on flights arriving from Wuhan. Within a week, the government assembled a cross-departmental taskforce and an expert team of leaders in infectious diseases, public health, and laboratory sciences. The government raised the travel advisory to Wuhan to level I–watch and alerted the healthcare community to report to Taiwan CDC on patients with respiratory symptoms and fever or presumptive pneumonia who had recently traveled to Wuhan. At the same time, the Taiwan CDC epidemiology laboratory started developing and

Author affiliations: Duke University, Durham, North Carolina, USA (C. Lin, P. Tu); University of Pittsburgh, Pittsburgh, Pennsylvania, USA (W.E. Braund); Trust for America's Health, Washington, DC, USA (J. Auerbach); Taiwan Centers for Disease Control, Taipei, Taiwan (J.-H. Chou, J.-H. Teng); University of Texas, Austin, Texas, USA (J. Mullen)

DOI: https://doi.org/10.3201/eid2607.200574

producing test kits adapted from existing diagnostic modalities for pneumonia of unknown etiology.

As Taiwan CDC took the lead, public and private healthcare providers, local governments, and health departments looked to the central government for guidance regarding preparedness and response. The country quickly updated infection control practices and strategies established during the 2003 SARS epidemic, such as installation of infrared temperature checkpoints and border quarantine at airports and seaports. Following Taiwan CDC's outbreak prevention guidelines, hospitals swiftly instituted screening booths to monitor the temperature of persons entering the facility, offer hand sanitizer, and separate persons with fever or related ailments. In addition, Taiwan increased stockpiles of personal protective equipment (PPE) for healthcare workers, predesignated potential isolation wings and hospitals, and created a daily nationwide inventory of available intensive care and negative-pressure isolation rooms, including the number that could be refitted when needed.

On January 15, 2020, Taiwan CDC classified the novel coronavirus as a class-V communicable disease, which institutes legal measures, including mandated reporting and quarantine. For instance, under class-V, healthcare providers are required by law to report suspected cases to Taiwan CDC within 24 hours, and the government can isolate or quarantine persons confirmed or suspected to be infected at designated sites. The Wuhan travel advisory was elevated to level II–alert the next day and later to level III–warning (Figure; Appendix Table, https://wwwnc.cdc.gov/EID/article/26/7/20-0574-App1.pdf). Reporting criteria were broadened to include persons showing symptoms who had not traveled to China recently but had close contact with persons who had confirmed or suspected cases. In addition, specimen testing parameters were expanded. On January 20, Taiwan activated its Central Epidemic Command Center (CECC), which is equivalent to an Emergency Operations Center in the United States.

### Border Quarantine

Border quarantine procedures are managed by staff from regional offices of Taiwan CDC stationed at airports and seaports. Staff screen all incoming passengers by using no-touch, video-recordable infrared thermometers, which were installed during the 2003 SARS outbreak. Staff also monitor passengers for specific symptoms, provide timely health education, and conduct health evaluations, including sample collection or testing, as needed. In addition, staff report suspected cases to the centralized database of Taiwan CDC and to local health departments for follow-up monitoring or care and refer or transport symptomatic persons to hospitals according to infectious disease regulations, when needed.

Beginning December 31, 2019, Taiwan CDC implemented enhanced border quarantine measures, which included temporary onboard health checks on persons arriving on flights from Wuhan. As the outbreak spread internationally, in late January 2020, Taiwan began requiring passengers to manually or electronically complete a health declaration card detailing any symptoms or diseases, and travel and contact histories for case investigation or contact tracing, if necessary. In addition, Taiwan CDC staff determined the need and gave instructions for self-monitoring or home quarantine, depending on current policies and any special situations.

### Case Detection

The enhanced border quarantine procedures led to early detection of a suspected case of COVID-19. On January 20, a 55-year-old woman reported fever, cough, and shortness of breath at her airport health screening upon arrival from Wuhan. She was transported directly to the hospital, averting local exposure. She reported that she wore a mask and remained in her seat for the duration of the flight. The crew and other passengers, who had no prolonged direct interaction with her, passed the health evaluation at the airport and were directed to complete a 14-day self-monitoring regimen at home. During self-monitoring, passengers and crew were required to record their temperature twice daily, stay home, or wear a mask if they had to go out; as an extra measure, they had to respond to daily telephone checks by infectious disease staff.

On January 21, the passenger with symptoms was confirmed to have COVID-19, the first known imported case in Taiwan. The same day, the United States announced its first case in a 35-year-old man who had returned from Wuhan on January 15 and was later admitted to a hospital in Washington State on January 19 (*4*,*5*).

With confirmed cases reaching 1,400 globally, including cases in Europe (*6*), Taiwan's disease investigation teams worked through the week-long Lunar New Year holiday. Beginning on January 24, Lunar New Year's Eve, all passengers traveling from China, Hong Kong, and Macau were required to complete a health declaration card and travel history upon arrival in Taiwan. Arriving passengers were given instructions for self-monitoring and a phone number for inquiries or concerns; this procedure was later expanded to cover arrivals from all destinations. Passengers from Wuhan

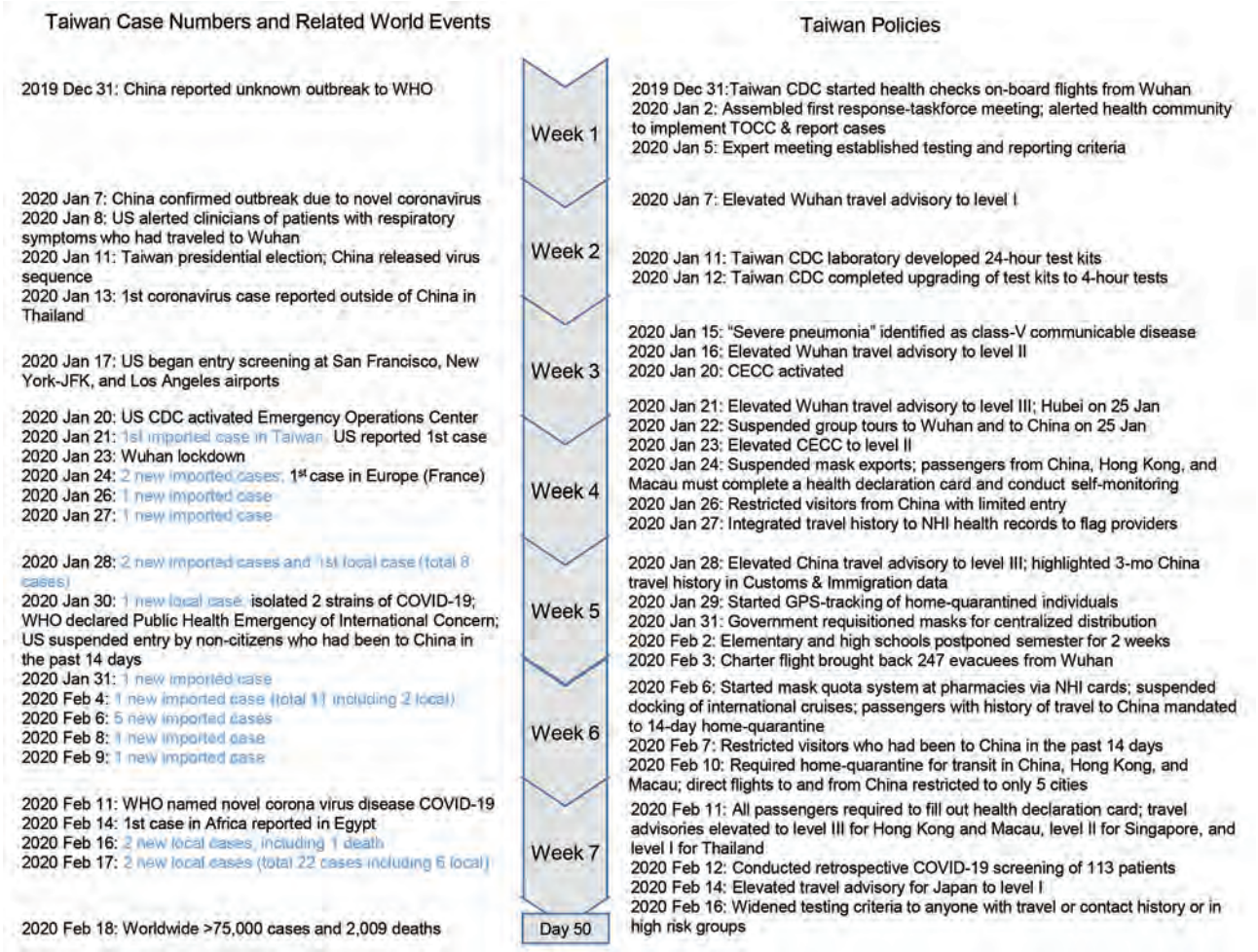


**Figure.** Timeline of policy decisions during the first 50 days of COVID-19, Taiwan. Blue text indicates cases in Taiwan. Information collected from Taiwan CDC, CDC, and WHO. Because of differences in global time zones, some events might be recorded or announced with 1-day discrepancy in different reports, news, and publications. CDC, US Centers for Disease Control and Prevention; CECC, Central Epidemic Command Center; COVID-19, coronavirus disease; NHI, National Health Insurance; Taiwan CDC, Taiwan Centers for Disease Control and Prevention; TOCC, travel, occupation, contact, and cluster; WHO, World Health Organization.

and Hubei Province and persons who had close contact with confirmed cases were mandated to a 14-day home quarantine. Quarantine involved self-isolation without going out or having visitors, recording temperature and symptoms twice daily, and if living with others, wearing a mask at all times and taking precautions with household members.

To support Taiwan CDC's surveillance, local civil offices were given the contact information of all home-quarantined persons in their jurisdiction. Local health department personnel or district administrators familiar with the communities conducted daily telephone checks on these home-quarantined persons in their areas. Persons who were not compliant with home quarantine orders were turned over to law enforcement and tracked by police officers. Repeat offenders could be fined or confined to designated facilities.

As the number of persons on home isolation in Taiwan grew to tens of thousands, GPS functionality and cameras on personal or government-dispatched smartphones were used for monitoring and case identification. Recognizing the challenges of the need for seemingly healthy persons to stay home for 2 weeks, miss work and school, and avoid outside contacts, local governments set up quarantine-care centers to provide support and counseling, which strengthened the barrier against potential community transmission. Staff in PPE could conduct home visits, arrange meal deliveries, and bring essential supplies to persons living alone to help them comply with the quarantine order. A 24-hour public epidemic hot line was opened for questions or reporting. Taiwan CDC upgraded its interactive mobile phone application, Disease-Prevention Butler, and supplemented it with an artificial

intelligence chatbot to provide accurate, timely information and gather concerns for analysis and response.

Group tours from Taiwan to China were suspended, and tours from China and residents of Hubei were banned. All citizens from China were later banned from entry into Taiwan, with few exceptions (Appendix Table). For groups already in Taiwan at the time of border quarantine, tour leaders were required to conduct and report daily health checks of their members. Students enrolled in Taiwan colleges or universities who had gone home to China for the winter break and holiday were asked to postpone their return to Taiwan for 2 weeks; those who arrived early were self-quarantined in separate dormitories.

On January 30, WHO declared a public health emergency of international concern and urged international coordination to investigate and control the spread of COVID-19 (*7*). Confirmed cases climbed to >7,800 globally; Taiwan had 9, including 1 case of local transmission in a man infected by his wife who returned from Wuhan (*8*).

### Information Technology and Cross-Departmental Cooperation

Other government agencies in Taiwan also contributed expertise and increased capacity during the crisis. Taiwan CECC partnered with civil and law enforcement departments for quarantine monitoring, as described. In addition, the CECC asked the NHI to integrate recent history of travel to China from the database of Customs and Immigration to supplement the NHI's centralized cloud-based health records. After Customs and Immigration data were integrated, the NHI system flagged records so medical providers would be aware of patients' travel history when they made an appointment or came in. Later, all confirmed and suspected case contacts reported to Taiwan CDC also were added to the NHI database.

Because all providers are required to submit claims to the single-payer platform within 24 hours, the comprehensive NHI database had near–real-time information that let clinicians and Taiwan CDC track or trace back all doctor visits. The NHI patient records included complete health history, underlying health conditions, and recent progression of symptoms, treatments, and hospitalization related to respiratory syndrome. These data helped pinpoint high-risk patients and persons likely to have had contact with infected cases. In addition, the NHI database gave Taiwan CDC the ability to quickly identify new patterns of symptoms or clustered cases and the source or path of infection. The high security and privacy policy of the NHI information technology system permitted data sharing only for purposes of combatting the epidemic and was restricted to 1-way transmission of specific information from other departments to the NHI database. No health records or other personal information were available to anyone outside of the health system.

The Customs and Immigration database also displayed warnings about travel history to Wuhan and China within the previous 3 months so border control staff could identify persons who had been to the COVID-19 epicenter for additional health screening. The Ministry of Foreign Affairs negotiated and coordinated the evacuation of Taiwan citizens stranded in Wuhan after the city went into lockdown on January 23 (*9*) and, later, those who were passengers onboard the Diamond Princess cruise ship docked in quarantine off the coast of Japan (*10*). The Ministry of Transportation managed charter flight arrangements, and the special biohazard cadets from the Ministry of Defense were called to help disinfect the planes and affected airport areas afterwards. Repatriated citizens and cruise ship passengers went through health screenings before boarding airplanes and were immediately tested for COVID-19 upon arrival in Taiwan. One person evacuated from Wuhan tested positive for the coronavirus and was directly transported to a hospital. All others passed a double-negative criterion, having 2 negative test results 24 hours apart, and went to a government-managed quarantine facility for 14 days, where they received check-ups 3 times a day. No subsequent cases manifested.

### Social Norms and Mask Shortages

After the 2003 SARS outbreak, persons in Taiwan, Japan, and several other countries in Asia began wearing medical face masks during influenza season or in crowded public spaces, such as on subways (*11*). Wearing a mask also is considered good practice for persons with a cold, and persons with allergies or a weakened immune system are expected to wear a mask (*12*). Therefore, many citizens had supplies at home or rushed to acquire masks once the epidemic was announced, despite Taiwan CDC advising that healthy persons did not need a mask, except when visiting hospitals or crowded, enclosed places.

Anticipating a surge in demand, Taiwan's prime minister suspended mask exportation at the end of January. News of shortages soon emerged in different parts of the world, partially attributed to the delayed and reduced exports from China, the largest mask-producing country in the world, because dozens of cities in China were on lockdown and demand increased in the country (*13*,*14*). The Taiwan government requisitioned domestically made medical and

surgical masks and invested to quickly expand production. To accomplish better distribution across the population, Taiwan introduced a temporary rationing system. Every resident's NHI card, which is already linked to thousands of pharmacies and hundreds of local health centers nationwide, became their identification to obtain masks in their neighborhood. In addition, a government-funded, mobile phone application (Mask Finder, https://mask.pdis.nat.gov.tw), developed through a public-private partnership, helped citizens locate supply distribution points and showed updates on availability. Health promotion messages on indications for wearing a mask and handwashing routine were widely disseminated in all media.

### Clinical and Pharmaceutical Research Capacity and Case Investigation

Starting in early January 2020, the Taiwan CDC laboratory began developing real-time reverse transcription PCR (RT-PCR) diagnostic protocols by leveraging previous experience sequencing SARS and Middle East respiratory syndrome coronaviruses. China released the full genomic sequence of the novel coronavirus on January 11, and by January 12, the Taiwan laboratory team introduced an upgraded, 4-hour test kit, shortened from the initial 24-hour test. The upgraded test had a high sensitivity of 10–100 copies/reaction, which is comparable to the standard assays recommended by WHO. The laboratory staff continued to accelerate testing speed and capacity, developing the ability to test >1,100 samples/day. By the end of February, Taiwan was able to test 2,450 samples/day by using public and select contracted private laboratories.

In late January, 2 strains of the coronavirus were successfully isolated by a university and a government-funded research institute in Taiwan. Research and development of drugs, vaccines, and a rapid testing kit continued, some through public-private or international partnerships.

As it became known that persons could have COVID-19 and have mild or no symptoms, no travel history, or no definitive case contact (*15*), Taiwan CDC further widened its testing and reporting criteria to minimize local transmission. At the time, only 3 cases of local transmission had been identified, all contracted from family members with recent travel history. To improve case detection, on February 12, Taiwan CDC conceived a retrospective COVID-19 screening scheme. The screening encompassed persons who had tested negative for influenza in the previous 14 days but who reported having severe influenza complications, were under surveillance for upper respiratory symptoms, were part of a cluster of influenza cases, or received a diagnosis of pneumonia but did not respond well to treatment. Using the NHI database, the team pinpointed 113 suspected patients, 1 of whom, case 19 in Taiwan, tested positive for COVID-19 on February 15 and died that evening. This discovery triggered the required confirmed-case contact investigation, which located and tested dozens of the patient's family members and close contacts. The patient's asymptomatic brother tested positive on the same day, and 2 more family members with minor symptoms tested positive in the next 2 days. Other close contacts tested negative but were stipulated to a 14-day home quarantine, and hundreds more possible contacts were put on self-monitoring for 2 weeks. The source of infection for case 19 later was identified by using collaborative triangulation of multiple departments' databases and disease investigation and traced to a passenger who returned from China. Without retrospective screening and access to the comprehensive NHI database, such cases would have gone undetected.

On day 50 of the global epidemic, February 18, WHO reported >75,000 cases and >2,000 deaths worldwide (*16*). Among the 22 cases confirmed in Taiwan, local transmissions were limited to 5, primarily between family members. Despite a credible international report that modeled outbreak dynamics and predicted Taiwan would have the second highest case importation outside of China (*17*), early prevention measures, stringent border control, and aggressive efforts to combat community spread have continued to be effective as of March 2020.

## Policy Implications

With the outlook of COVID-19 still unclear, health authorities around the world continue to be on high alert. Since February 2020, the Taiwan government and CECC have focused more on detecting and isolating local cases to contain potential local spread, while maintaining and updating travel restrictions to limit foreign entry from highly affected areas. The experience of SARS generated instrumental lessons in disease control measures and policy planning for government agencies and hospitals in Taiwan. It also improved the public's health behavior and hygiene practices, such as increased uptake of influenza and other vaccinations, frequent handwashing, and use of hand sanitizers and masks (*12*,*18*–*20*). In addition, the 2003 SARS outbreak had heightened infection transmission awareness and provided better mental preparedness for the new pandemic. Timely, clear communication with the public also has fostered trust and built community capacity for the public to partner with the government in containment and mitigation.

During any health crisis, a robust health system is crucial to support the surge of medical care and testing needed (*21*). Taiwan has a solid public health, medical, and insurance infrastructure distributed throughout the country. This infrastructure consists of local health departments and centers staffed by healthcare professionals trusted by local residents, particularly in the rural areas where private practices are scarce; hospitals, medical centers, and clinics that strongly support a well-coordinated infectious disease network for preparedness and response; and a comprehensive NHI that covers >99% of the population with high-quality providers and low out-of-pocket cost. The interconnected health system reduces barriers to doctor appointments and follow-up visits, which helped capture suspected cases with minor symptoms. Furthermore, the single-payer NHI model affords centralized health records of population-level longitudinal data and the capability of merging information from other government databases. This connectivity proved a valuable tool for analysis and case investigation during disease outbreaks, including dengue, influenza, SARS, and the current COVID-19 pandemic.

Interagency collaboration, data sharing, and timely mobilization of human capital and resources are equally vital to a response (*22*). Taiwan followed WHO standards on testing and case definition and shared updated disease information and virus sequences on International Health Regulations (https://www.who.int/ihr/en) and other global health platforms. With CECC's authority to coordinate works across departments and enlist additional personnel during an emergency, Taiwan CDC has been capable of handling the growing volume of regular and new tasks.

In addition, the legislature approved emergency funding to ensure disease control efforts did not fall short and to mitigate the economic effects of the outbreak. The funding included compensating lost wages for persons working part-time or without paid sick leave during the quarantine. Compensation also permitted time off for persons with children or elderly family members who were sick or had contact with confirmed cases. These incentives, modeled after actions taken during the 2003 SARS outbreak, aided in isolation compliance.

Unlike SARS, in which patients were only infectious when febrile (*23*), persons with COVID-19 could have no or minimal symptoms, remain undiagnosed but contagious, and pose a greater threat of local transmissions (*24*). As the pandemic evolves, global cases likely will increase because of community spread, expanded laboratory capacity, and wider testing criteria. The timing, locations, and policies of travel advisories and entry restrictions, in addition to testing and reporting criteria, are critical to epidemic control but vary across countries. From a public health perspective, recognizing the ideal time to institute or terminate these policies and measuring their effectiveness can be challenging.

## Conclusions

Taiwan's robust public health and healthcare systems, combined with public acceptance of protective policies influenced by the 2003 SARS outbreak, likely bolstered efficient implementation of policies in the first 50 days of the COVID-19 outbreak. At the same time, Taiwan's response to COVID-19 might have overshadowed other health threats, such as seasonal influenza and chronic diseases. Strategic prioritization of other public health functions and resources and broader government operations will be necessary. As the outbreak continues, Taiwan will need to evaluate associated policy decisions to sustain the system.

Taiwan built on lessons learned from SARS, and some of the successful strategies during the current pandemic could inform policy approaches by other governments. In countries that rely heavily on state and local actions, intergovernmental and interjurisdictional coordination and adequate funding are needed to assure emergency preparedness and response capacity. An integrated approach that incorporates public health, human services, and healthcare systems can increase resilience and better prepare nations for future events.

### Acknowledgments

We thank the members of Taiwan CDC, Central Epidemic Command Center expert team, and partnering departments who have worked tirelessly since the beginning of the COVID-19 pandemic. We especially recognize Chin-Hui Yang, Christine Ding-Ping Liu, Shu-Ying Li, Li-Li Ho, Shu-Mei Chou, Yu-Min Chou, Kai-Ling Tsao, Shu-Hui Tseng, Yi-Chun Lo, Jen-Hsiang Chuang, the border infectious disease control staff at Taiwan CDC, and all the frontline public health and healthcare professionals around the world.

## About the Author

Dr. Lin is a faculty member and codirector of the Policy and Organizational Management Program at Duke University, Durham, North Carolina, USA. Her teaching and research primarily focus on health behavior and policy, social psychology, medication adherence, and marketing management strategies.

## References


1. World Health Organization. Novel coronavirus (2019-nCoV). Situation report—1. 2020 Jan 21 [cited 2020 Feb 20]. https://www.who.int/docs/default-source/coronaviruse/situation-reports/20200121-sitrep-1-2019-ncov.pdf
2. World Health Organization. Severe acute respiratory syndrome (SARS) [cited 2020 Feb 27]. https://www.who.int/csr/sars/en
3. Nielson Holdings PLC. 2019 Outbound Chinese tourism and consumption trends [cited 2020 Feb 20]. https://www.nielsen.com/wp-content/uploads/sites/3/2019/05/outbound-chinese-tourism-and-consumption-trends.pdf
4. Centers for Disease Control and Prevention. Press release: first travel-related case of 2019 novel coronavirus detected in United States, January 21, 2020 [cited 2020 Feb 27]. https://www.cdc.gov/media/releases/2020/p0121-novel-coronavirus-travel-case.html
5. Holshue ML, DeBolt C, Lindquist S, Lofy KH, Wiesman J, Bruce H, et al.; Washington State 2019-nCoV Case Investigation Team. First case of 2019 novel coronavirus in the United States. N Engl J Med. 2020;382:929–36. https://doi.org/10.1056/NEJMoa2001191
6. News NBC. Map: The COVID-19 virus is spreading across the world. Here's where coronavirus cases have been confirmed. 2020 Jan 22 [cited 2020 Feb 27]. https://www.nbcnews.com/health/health-news/coronavirus-map-confirmed-cases-2020-n1120686
7. World Health Organization. 2019-nCoV outbreak is an emergency of international concern. 2020 Jan 31 [cited 2020 Feb 27]. http://www.euro.who.int/en/health-topics/health-emergencies/coronavirus-covid-19/news/news/2020/01/2019-ncov-outbreak-is-an-emergency-of-international-concern
8. Regan H, George S, Dewan A, Kottasová I. January 30 coronavirus news: this map tracks the coronavirus in real time. CNN World. 2020 Jan 30 [cited 2020 Feb 27]. https://edition.cnn.com/asia/live-news/coronavirus-outbreak-01-30-20-intl-hnk/h_e89dabe8ed1d4b2e-3f03048a18d98ec3
9. Feng E, Cheng A, Kennedy M. Chinese authorities begin quarantine of Wuhan City as coronavirus cases multiply. National Public Radio. 2020 Jan 23 [cited 2020 Mar 26]. https://www.npr.org/2020/01/23/798789671/chinese-authorities-begin-quarantine-of-wuhan-city-as-coronavirus-cases-multiply
10. Chappell B. Coronavirus update: Diamond Princess passengers leave ship as expert slams quarantine. National Public Radio. 2020 Feb 19 [cited 2020 Mar 26]. https://www.npr.org/sections/goatsandsoda/2020/02/19/807418497/coronavirus-update-diamond-princess-passengers-leave-ship-as-expert-slams-quaran
11. Syed Q, Sopwith W, Regan M, Bellis MA. Behind the mask. Journey through an epidemic: some observations of contrasting public health responses to SARS. J Epidemiol Community Health. 2003;57:855–6. https://doi.org/10.1136/jech.57.11.855
12. Yang J. A quick history of why Asians wear surgical masks in public. Quartz. 2014 Nov 19 [cited 2020 Feb 27]. https://qz.com/299003/a-quick-history-of-why-asians-wear-surgical-masks-in-public
13. Yang S, Kubota Y. Spreading coronavirus prompts lockdown of more Chinese cities. Wall Street Journal. 2020 Jan 24 [cited 2020 Feb 27]. https://www.wsj.com/articles/spreading-coronavirus-forces-lockdown-of-another-chinese-city-11579774393
14. Gunia A. There aren't enough medical masks to fight coronavirus. Here's why it's not going to get better anytime soon. Hong Kong: Time Magazine. 2020 Feb 27 [cited 2020 Feb 27]. https://time.com/5785223/medical-masks-coronavirus-covid-19
15. Hoehl S, Rabenau H, Berger A, Kortenbusch M, Cinatl J, Bojkova D, et al. Evidence of SARS-CoV-2 infection in returning travelers from Wuhan, China. N Engl J Med. 2020 Feb 18 [Epub ahead of print]. https://doi.org/10.1056/NEJMc2001899
16. World Health Organization. Coronavirus disease. 2019 (COVID-19) situation report—30. 2020 Feb 19 [cited 2020 Feb 27]. https://www.who.int/docs/default-source/coronaviruse/situation-reports/20200219-sitrep-30-covid-19.pdf
17. Gardner L. Update January 31: modeling the spreading risk of 2019-nCoV. Johns Hopkins University Center for Systems Science and Engineering. 2020 Jan 31 [cited 2020 Feb 20]. https://systems.jhu.edu/research/public-health/ncov-model-2
18. Meyer D, Shearer MP, Chih YC, Hsu YC, Lin YC, Nuzzo JB. Taiwan's annual seasonal influenza mass vaccination program—lessons for pandemic planning. Am J Public Health. 2018;108(S3):S188–93. https://doi.org/10.2105/AJPH.2018.304527
19. Weston M. Taiwan's measles outbreak and herd immunity. The News Lens. 2018 Apr 27 [cited 2020 Mar 1]. https://international.thenewslens.com/article/94479
20. Chung CW. Why Taiwanese love to wear face masks? China Times. 2019 Jun 3 [cited 2020 Mar 1]. https://www.chinatimes.com/realtimenews/20190603002646- 260405?chdtv
21. Neighmond P. Would the U.S. health system be ready for a surge in coronavirus cases? National Public Radio. 2020 Feb 13. [cited 2020 Feb 27]. https://www.npr.org/sections/health-shots/2020/02/13/799534865/would-the-u-s-health-system-be-ready-for-a-surge-in-coronavirus-cases
22. Testimony before the Senate Homeland Security and Governmental Affairs Committee; Robert Kadlec, M.D., Assistant Secretary for Preparedness and Response testifying for the Department Health and Human Services. The federal interagency response to the coronavirus and preparing for future global pandemics. Department of Health and Human Services. 2020 Mar 5 [cited 2020 Mar 10]. https://www.hsgac.senate.gov/imo/media/doc/Testimony-Kadlec-2020-03-05-REVISED.pdf
23. World Health Organization; Severe Acute Respiratory Syndrome (SARS) Epidemiology Working Group. Consensus document on the epidemiology of severe acute respiratory syndrome (SARS). Geneva: The Organization; 2003. [cited 2020 Feb 27] https://www.who.int/csr/sars/en/WHOconsensus.pdf
24. Harvard Health Publishing. As coronavirus spreads, many questions and some answers. Cambridge (MA, USA): Harvard University; 2020 Feb 27 [cited 2020 Mar 1]. https://www.health.harvard.edu/blog/as-coronavirus-spreads-many-questions-and-some-answers-2020022719004


Address for correspondence: Pikuei Tu, Duke University, 2204 Erwin Rd, Durham, NC 27708, USA; email: Pikuei.tu@duke.edu

# Serologic Evidence of Severe Fever with Thrombocytopenia Syndrome Virus and Related Viruses in Pakistan

Ali Zohaib,[1] Jingyuan Zhang,[1] Muhammad Saqib,[1] Muhammad Ammar Athar, Muhammad Hammad Hussain, Jing Chen, Awais-ur-Rahman Sial, M. Haleem Tayyab, Murrafa Batool, Saeed Khan, Yun Luo, Cecilia Waruhiu, Zeeshan Taj, Zulfiqar Hayder, Riaz Ahmed, Abu Bakr Siddique, Xinglou Yang, Muhammad Asif Qureshi, Ikram Uddin Ujjan, Amanullah Lail, Iahtasham Khan, Sajjad-Ur-Rahman, Tao Zhang, Fei Deng, Zhengli Shi, Shu Shen

We describe the seroprevalence of severe fever with thrombocytopenia syndrome virus (SFTSV) and the association of antibody occurrence with location, sex, and age among the human population in Pakistan. Our results indicate substantial activity of SFTSV and SFTSV-related viruses in this country.

Severe fever with thrombocytopenia syndrome (SFTS) is an emerging tickborne disease caused by the SFTS virus (SFTSV; genus *Banyangvirus*, family *Phenuiviridae*, order *Bunyavirales*). The disease is prevalent in East Asia countries. It was first detected in China in 2009 and later in Japan and South Korea (*1*) and is suspected to be widely spread across other parts of the world (*2*). The recent identification of SFTSV in Xinjiang, China (*3*), expanded our awareness of epidemic areas of SFTS and suggested the possibility of SFTSV spreading to bordering countries like Pakistan. However, the presence of SFTSV in Pakistan has been unclear. We investigated the seroprevalence of SFTSV in humans in Pakistan.

Author affiliations: Atta-ur-Rahman School of Applied Biosciences, National University of Sciences and Technology H-12 Campus, Islamabad, Pakistan (A. Zohaib); Wuhan Institute of Virology, Chinese Academy of Sciences, Wuhan, China (A. Zohaib, J.Y. Zhang, J. Chen, Y. Luo, C. Waruhiu, X.-L. Yang, T. Zhang, F. Deng, Z.-L. Shi, S. Shen); University of Agriculture Faisalabad, Faisalabad, Pakistan (M. Saqib, M. Batool, M.H. Tayyab, Sajjad-Ur-Rahman); National Institute of Virology, Dr. Panjwani Center for Molecular Medicine and Drug Research, International Center for Chemical and Biological Sciences (ICCBS) University of Karachi, Karachi, Pakistan (M.A. Athar); Animal Health Research Center, Ministry of Agriculture and Fisheries, Muscat, Oman (M.H. Hussain); PMAS Aird Agriculture University, Rawalpindi, Pakistan (A. Sial); Dow University of Health Science, Karachi, Pakistan (S. Khan, M.A. Qureshi, A. Lail); Government College University, Faisalabad, Pakistan (Z. Taj); Quaid e Azam Medical College Bahawalpur, Bahawalpur, Pakistan (Z. Hayder); Shifa Khana Sahib Zaman Hospital, Quetta, Pakistan (R. Ahmed); Pakistan Lab Diagnostic and Research Center, Rahim Yar Khan, Pakistan (A. Siddique); Liaqat University of Medical and Health Science, Jamshoro, Pakistan (I.D. Ujjan); College of Veterinary and Animal Sciences Jhang, University of Veterinary and Animal Sciences, Lahore, Pakistan (I. Khan); National Virus Resource Center, Wuhan (F. Deng, S. Shen)

DOI: https://doi.org/10.3201/eid2607.190611

## The Study

For this study, we randomly collected human serum samples (n = 1,657) from 4 provinces in Pakistan during 2016–2017 (Figure). All participants were farmers of livestock (sheep, goats, cattle, buffaloes, and camels). We recorded and summarized testing results by sex, age, and geographic location (Table). The collection of human serum samples and subsequent tests were reviewed and approved by the Ethics Committees of Government College University, Faisalabad, Pakistan (approval number: GCUF/MICRO/18/1598). Adult participants and parents of participants <18 years of age provided written informed consent.

We used a 2-step approach to detect antibodies against SFTSV. First, we screened the samples for SFTSV IgG by using a SFTSV human commercial ELISA kit (NZK Bio-tech, https://hbnzk.com), which employs SFTSV nucleocapsid protein (NP) as the viral antigen. To set up negative and positive controls, we used serum samples from 3 healthy persons from Wuhan, China (*4*), and serum samples from 2 convalescent SFTS patients from Wuhan archived in the

[1]These authors contributed equally to this article.

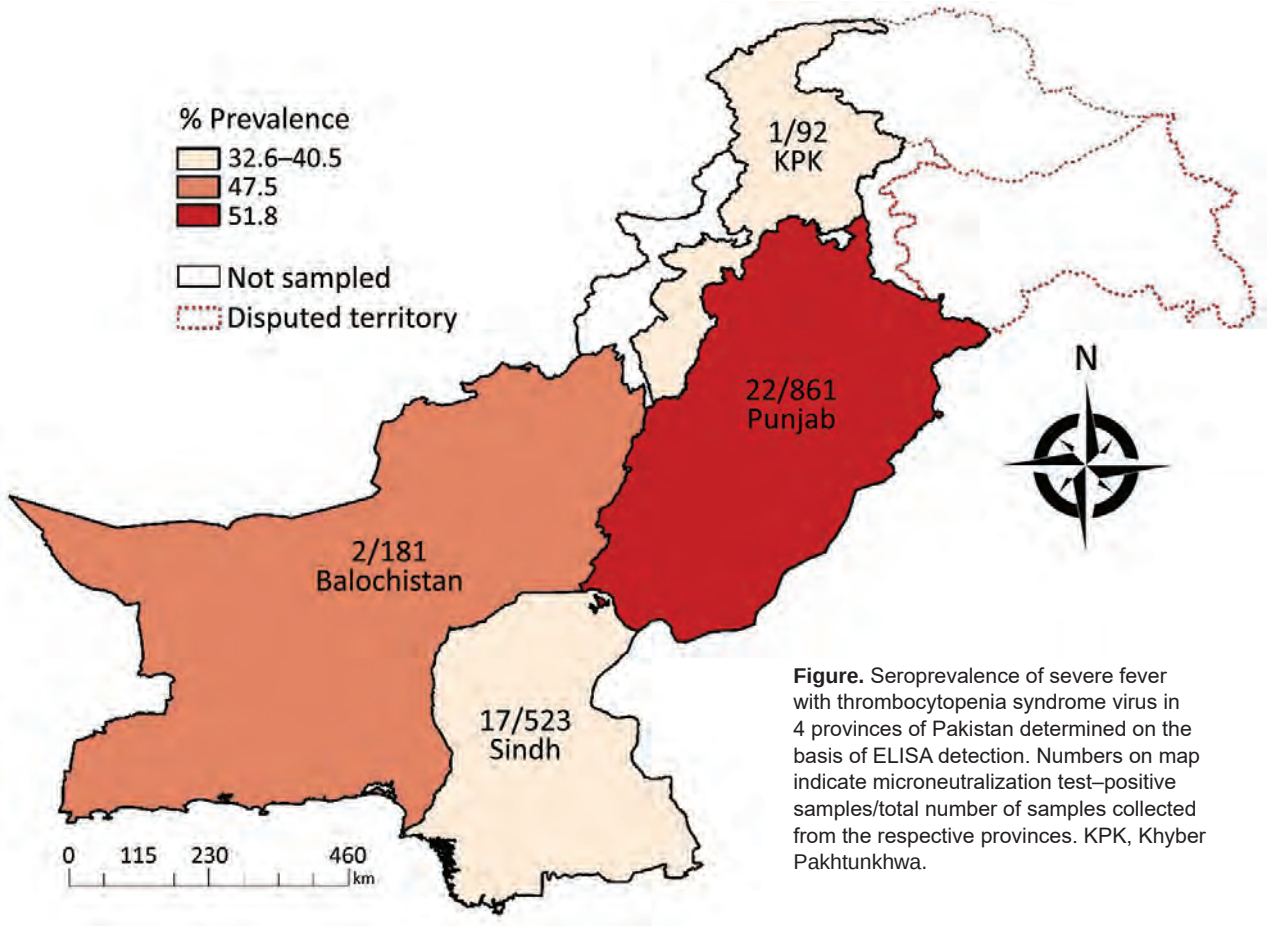


**Figure.** Seroprevalence of severe fever with thrombocytopenia syndrome virus in 4 provinces of Pakistan determined on the basis of ELISA detection. Numbers on map indicate microneutralization test–positive samples/total number of samples collected from the respective provinces. KPK, Khyber Pakhtunkhwa.

National Virus Resource Center (accession nos. YB-17WIVS286, YB17WIVS294). Following manufacturer instructions (Appendix, https://wwwnc.cdc.gov/EID/article/26/7/19-0611-App1.pdf), we tested serum samples at 1:20 dilution; we considered samples IgG-positive when the absorbance was ≥2.1 times the mean absorbance of the negative control. Samples with optical density values ≥0.41 were considered SFTSV IgG–positive (Appendix Figure 1). We used an immunofluorescence assay modified from a previous study (*5*) to verify the validity of the commercial ELISA.

In the second step, we used a microneutralization test (MNT) assay to distinguish SFTSV-specific neutralizing antibodies from SFTSV-related viruses, as described elsewhere (*6*); we estimated SFTSV prevalence from ELISA and MNT results within 95% CIs. We performed statistical analysis of the data using the $\chi^2$ test or Fisher exact test to explore the association of SFTSV with age, sex, and location. We performed the analysis in R version 3.5.1 with the Epicalc package version 2.15.1.0 (http://www.r-project.org).

The ELISA revealed a high seroprevalence (46.7%, 95% CI 44.3%–49.1%) of SFTSV in Pakistan (Table; Figure). Spatial distribution analysis indicated the highest prevalence (51.8%, 95% CI 48.4%–55.2%) in the Punjab province, followed by Balochistan (47.5%, 95% CI 40.1%–55.1%), Sindh (40.5%, 95% CI 36.3%–44.9%), and Khyber Pakhtunkhwa (32.6%, 95% CI 23.2%–43.2%). The prevalence was significantly higher (p = 0.004) in women (49. 9%, 95% CI 46.6%–53.2%) than in men (42.7%, 95% CI 39.1%–46.4%). The seroprevalence increased with age, but not uniformly; the highest seroprevalence (57.1%, 95% CI 28.9%–82.3%) was recorded in samples from persons ≥65 years of age. A technician unaware of the ELISA results and research details performed a single-blind test with 90 ELISA-negative and 252 ELISA-positive samples, randomly selected. This test confirmed results for 100% of the ELISA-negative samples and 212 (84.1%) of 252 of the ELISA-positive samples (Appendix Figure 2).

We confirmed SFTSV infection using MNT, which revealed a low prevalence (2.5%, 95% CI 1.9%–3.4%) in Pakistan (Table; Appendix Figure 3). Women had a higher occurrence of anti-SFTSV neutralizing antibodies (2.7%, 95% CI 1.8%–4.0%) than men (2.3%, 95% CI 1.4%–3.7%), however, this difference was not

Table. Seroprevalence of severe fever with thrombocytopenia syndrome virus in Pakistan based on ELISA and MNT results

| | ELISA | | | MNT | | |
|---|---|---|---|---|---|---|
| Category | No. positive/no. tested | Prevalence, % (95% CI) | p value | No. positive/no. tested | Prevalence, % (95% CI) | p value |
| Province | | | | | | |
| Punjab | 446/861 | 51.8 (48.4–55.2) | <0.001 | 22/861 | 2.6 (1.6–3.8) | 0.339 |
| Balochistan | 86/181 | 47.5 (40.1–55.1) | | 2/181 | 1.1 (0.1–3.9) | |
| Sindh | 212/523 | 40.5 (36.3–44.9) | | 17/523 | 3.3 (1.9–5.2) | |
| KPK | 30/92 | 32.6 (23.2–43.2) | | 1/92 | 1.1 (0–5.9) | |
| Sex | | | | | | |
| M | 313/733 | 42.7 (39.1–46.4) | 0.004 | 17/733 | 2.3 (1.4–3.7) | 0.619 |
| F | 461/924 | 49.9 (46.6–53.2) | | 25/924 | 2.7 (1.8–4) | |
| Age group, y | | | | | | |
| 15–24 | 196/413 | 47.5 (42.6–52.4) | 0.919 | 8/413 | 1.9 (0.8–3.8) | 0.120 |
| 25–34 | 310/669 | 46.3 (42.5–50.2) | | 21/669 | 3.1 (2–4.8) | |
| 35–44 | 149/325 | 45.9 (40.3–51.4) | | 3/325 | 0.9 (0.2–2.7) | |
| 45–54 | 89/184 | 48.4 (41–55.8) | | 8/184 | 4.4 (1.9–8.4) | |
| 55–64 | 22/52 | 42.3 (28.7–56.8) | | 1/52 | 1.9 (0–10.3) | |
| ≥65 | 8/14 | 57.1 (28.9–82.3) | | 1/14 | 7.1 (0.2–33.9) | |
| Total | 774/1657 | 46.7 (44.3–49.1) | | 42/1657 | 2.5 (1.9–3.4) | |

*KPK, Khyber Pakhtunkhwa; MNT, microneutralization test.

significant (p = 0.619). Neutralizing antibodies were detected in all age groups. Furthermore, we performed MNT for a novel virus, Guertu virus (GTV) (*4*), which is closely related to SFTSV, on 10 randomly selected serum samples that tested positive for SFTSV neutralization and 10 SFTSV IgG–positive samples that were negative for neutralization (Appendix Figure 3). All 10 samples that tested negative on the SFTSV MNT also tested negative on the GTV MNT. However, 3 of the 10 samples that tested positive on the SFTSV MNT also exhibited neutralization to GTV; the other 7 samples tested negative for neutralizing GTV.

## Conclusions

This study highlights the activity of SFTSV and its substantial risks to the population in Pakistan. The observed high ELISA-based prevalence could be ascribed to the study population in this survey being livestock farmers, who could be more frequently exposed to tick vectors and livestock reservoirs. Higher estimates of SFTS prevalence in the Punjab province of Pakistan could be attributed to the high proximity of human and livestock populations in this region. Higher prevalence among women than among men was expected because livestock is mostly tended by female farmers.

In ELISA-based estimates of SFTSV in the human population reported from different areas of East Asian countries, seroprevalence has ranged from 0.23% to 9.17% in China (*7*), from 1.9% to 7.7% in Korea (*8*,*9*), and from 0.14% to 0.3% in Japan (*10*, *11*). In contrast to the findings from these reports (*7*–*11*), our study found a markedly high ELISA-based prevalence of SFTSV (46.7%) in Pakistan. The use of different SFTSV antibody detection methods may have led to the observed differences in results (*11*); nevertheless, results of the blind test using an immunofluorescence assay still suggested a high prevalence, such that 84.12% of the randomly selected ELISA-positive serum samples could react with the SFTSV antigen. Therefore, the low prevalence of neutralizing antibodies (2.5%) against SFTSV suggests the possibility of cocirculating antigenicity-related viruses that were not discernable in the indirect ELISA tests.

The genus *Banyangvirus* currently includes the Bhanja and SFTS/Heartland groups. The 5 viruses of the SFTS/Heartland group have a wide geographic distribution. SFTSV is found mostly in China, Japan, and South Korea (*1*); GTV in northwestern China (XJUAR) (*4*), Heartland virus in the United States (*12*); Hunter Island group virus in Australia (*13*); and Malsoor virus in India (*14*).

Similar to findings in our study, a high seroprevalence (19.8%) of GTV was detected among the local residents of Guertu County in Xinjiang, China; however, only 3 (0.65%) of the 465 serum samples had neutralizing antibodies against GTV (*4*). Antigenic cross-reactivity between SFTSV and GTV was suspected because cross-neutralization was observed in mouse serum (*4*). However, serologic investigation of other bunyaviruses is limited, and serotypes of the 2 viruses, as well as other related viruses in the SFTS/Heartland group, remain unclear.

Our subsequent study found that a few serum samples exhibiting neutralization to SFTSV also exhibited cross-neutralization to GTV. All of these results indicate the presence in Pakistan of SFTSV and SFTSV-related viruses that might share antigenic similarity and could induce antibodies exhibiting cross-reactivity with each other. In addition, a recent study reported suspected

clinical SFTS cases in Pakistan; however, they were not confirmed using serologic or molecular tests (*15*).

Our findings suggest the potential risk for infection from SFTSV and SFTSV-related viruses in Pakistan. Further work on the discovery, identification, and ecology of these viruses in ticks, animal hosts, and human patients is needed because the viruses pose potential threats to public health.

This study was supported by the International Cooperation on Key Technologies of Biosafety along the China-Pakistan Economic Corridor (153B42KYSB20170004), the National Science and Technology major project (2018ZX0101004), the Intergovernmental Special Program of State Key Research and Development Plan from the Ministry of Science and Technology of China (2016YFE0113500), and the Science and Technology Basic Work Program (2013FY113500) from the Ministry of Science and Technology of China.

## About the Author

Mr. Zohaib is a doctoral student at the Wuhan Institute of Virology, Chinese Academy of Sciences, Wuhan, China. His major research interests include detection and characterization of zoonotic viruses.

## References

1. Liu Q, He B, Huang SY, Wei F, Zhu XQ. Severe fever with thrombocytopenia syndrome, an emerging tick-borne zoonosis. Lancet Infect Dis. 2014;14:763–72. https://doi.org/10.1016/S1473-3099(14)70718-2
2. Denic S, Janbeih J, Nair S, Conca W, Tariq WU, Al-Salam S. Acute thrombocytopenia, leucopenia, and multiorgan dysfunction: the first case of SFTS bunyavirus outside China? Case Rep Infect Dis. 2011;2011:204056. https://doi.org/10.1155/2011/204056
3. Zhu L, Yin F, Moming A, Zhang J, Wang B, Gao L, et al. First case of laboratory-confirmed severe fever with thrombocytopenia syndrome disease revealed the risk of SFTSV infection in Xinjiang, China. Emerg Microbes Infect. 2019; 8:1122–5. https://doi.org/10.1080/22221751.2019.1645573
4. Shen S, Duan X, Wang B, Zhu L, Zhang Y, Zhang J, et al. A novel tick-borne phlebovirus, closely related to severe fever with thrombocytopenia syndrome virus and Heartland virus, is a potential pathogen. Emerg Microbes Infect. 2018;7:95. https://doi.org/10.1038/s41426-018-0093-2
5. Zhang Y, Shen S, Shi J, Su Z, Li M, Zhang W, et al. Isolation, characterization, and phylogenic analysis of three new severe fever with thrombocytopenia syndrome bunyavirus strains derived from Hubei Province, China. Virol Sin. 2017;32:89–96. https://doi.org/10.1007/s12250-017-3953-3
6. Yu XJ, Liang MF, Zhang SY, Liu Y, Li JD, Sun YL, et al. Fever with thrombocytopenia associated with a novel bunyavirus in China. N Engl J Med. 2011;364:1523–32. https://doi.org/10.1056/NEJMoa1010095
7. Li P, Tong ZD, Li KF, Tang A, Dai YX, Yan JB. Seroprevalence of severe fever with thrombocytopenia syndrome virus in China: a systematic review and meta-analysis. PLoS One. 2017;12:e0175592. https://doi.org/10.1371/journal.pone.0175592
8. Han MA, Kim CM, Kim DM, Yun NR, Park SW, Han MG, et al. Seroprevalence of severe fever with thrombocytopenia syndrome virus antibodies in rural areas, South Korea. Emerg Infect Dis. 2018;24. https://doi.org/10.3201/eid2405.152104
9. Kim KH, Ko MK, Kim N, Kim HH, Yi J. Seroprevalence of severe fever with thrombocytopenia syndrome in southeastern Korea, 2015. J Korean Med Sci. 2017;32:29–32. https://doi.org/10.3346/jkms.2017.32.1.29
10. Kimura T, Fukuma A, Shimojima M, Yamashita Y, Mizota F, Yamashita M, et al. Seroprevalence of severe fever with thrombocytopenia syndrome (SFTS) virus antibodies in humans and animals in Ehime prefecture, Japan, an endemic region of SFTS. J Infect Chemother. 2018;24:802–6. https://doi.org/10.1016/j.jiac.2018.06.007
11. Gokuden M, Fukushi S, Saijo M, Nakadouzono F, Iwamoto Y, Yamamoto M, et al. Low seroprevalence of severe fever with thrombocytopenia syndrome virus antibodies in individuals living in an endemic area in Japan. Jpn J Infect Dis. 2018;71:225–8. https://doi.org/10.7883/yoken.JJID.2017.497
12. McMullan LK, Folk SM, Kelly AJ, MacNeil A, Goldsmith CS, Metcalfe MG, et al. A new phlebovirus associated with severe febrile illness in Missouri. N Engl J Med. 2012;367:834–41. https://doi.org/10.1056/NEJMoa1203378
13. Wang J, Selleck P, Yu M, Ha W, Rootes C, Gales R, et al. Novel phlebovirus with zoonotic potential isolated from ticks, Australia. Emerg Infect Dis. 2014;20:1040–3. https://doi.org/10.3201/eid2006.140003
14. Mourya DT, Yadav PD, Basu A, Shete A, Patil DY, Zawar D, et al. Malsoor virus, a novel bat phlebovirus, is closely related to severe fever with thrombocytopenia syndrome virus and Heartland virus. J Virol. 2014;88:3605–9. https://doi.org/10.1128/JVI.02617-13
15. Mahmood N, Khurram M, Khan MM, Umar M, Jalil A, Sharif S, et al. Characteristics of probable severe fever with thrombocytopenia syndrome patients: a perspective study from Pakistan. Int J Med Dev Coun. 2019;3:272–8. https://doi.org/10.24911/IJMDC.51-1544507442

Address for correspondence: Shu Shen, Wuhan Institute of Virology, Chinese Academy of Sciences, Xiaohongshan 44, Wuchang District, Wuhan, Hubei Province 430071, China; email: shenshu@wh.iov.cn

# Survey of Parental Use of Antimicrobial Drugs for Common Childhood Infections, China

Leesa Lin, Stephan Harbarth, Xiaomin Wang, Xudong Zhou

In a large-scale survey of 9,526 parents in China, we investigated antimicrobial drug use for common childhood infections. Of children with self-limiting conditions, formal care was sought for 69.2%; of those, 53.4% received drug prescriptions, including 11.2% from parental demands. Where drugs were taken without prescriptions, 70% were from community pharmacies.

China accounts for half of global consumption of antimicrobial drugs (*1*,*2*) and reports high rates of antimicrobial resistance, especially among children (*3*,*4*). Despite current regulations requiring a prescription to obtain antibiotics, unsupervised use in China is pervasive (*3*,*4*). To date, the few studies available on inappropriate administration to children beyond clinical settings have been limited in scope to small-scale data in one geographic area (*3*,*5*–*7*). To inform control strategies, we investigated the prevalence of inappropriate antibiotic use for common childhood infections by parents across different geographic areas and economic development stages, overall parental knowledge about antimicrobial drug use and resistance, the impact of parental pressure for antibiotics on prescribing behaviors, and parental contribution to the overall use of antibiotics in children.

## The Study

Study methods, including sampling strategy and data collection, were previously reported (*8*). Our data came from a cross-sectional survey conducted during June 2017–April 2018, which recruited 9,526 parents with children 0–13 years of age across 3 provinces (Zhejiang, Shaanxi, and Guangxi) representing different geographic areas and economic development stages in China (*9*). We conducted multistage stratified random cluster sampling in provinces, prefecture-level cities, urban and rural areas, and local sampling sites that included primary schools (children 6–13 years of age), kindergartens (3–5 years), and community-based health centers (0–2 years). The Institutional Review Board at the Zhejiang University School of Medicine (approval no. ZGL201706-2) and London School of Hygiene and Tropical Medicine (approval no. 14678) reviewed and exempted the study protocol and survey.

We recruited parents through their children, and all participants gave informed consent. We distributed a questionnaire to parents who self-identified as the primary caregiver and healthcare decision maker for the children; parents completed the questionnaire electronically. We collected data on parental sociodemographics, knowledge about antibiotic use and resistance, and last episode of illnesses and treatments experienced by the child within a month (Figure 1).

We calculated an 89% response rate by dividing the number of parents who completed the survey by the number of parents who were invited to take the survey (13,680/15,424 ). For data quality control, we used measures (including trap questions and IP address control) to detect random responses or duplications, resulting in 70% (9,526/13,680) of the completed surveys verified as valid. We classified missing data (<11%) as missing-completely-at-random and excluded from the final analysis.

We conducted descriptive analysis on the data, followed by unadjusted univariable analysis to examine the association between antibiotic prescriptions and parental demand and employed multivariable logistic regression and likelihood ratio tests for adjusted analyses, controlling for relevant sociodemographic variables. We observed profound regional differences in parental socioeconomic composition, antibiotic-use practices, and medical facilities used when children (age 5.8 years, SD $\pm$ 3.6 years) were ill

Author affiliations: London School of Hygiene and Tropical Medicine, London, UK (L. Lin); University of Geneva Hospitals and Faculty of Medicine, Geneva, Switzerland (S. Harbarth); Zhejiang University, Hangzhou, China (X. Wang, X. Zhou)

DOI: https://doi.org/10.3201/eid2607.190631

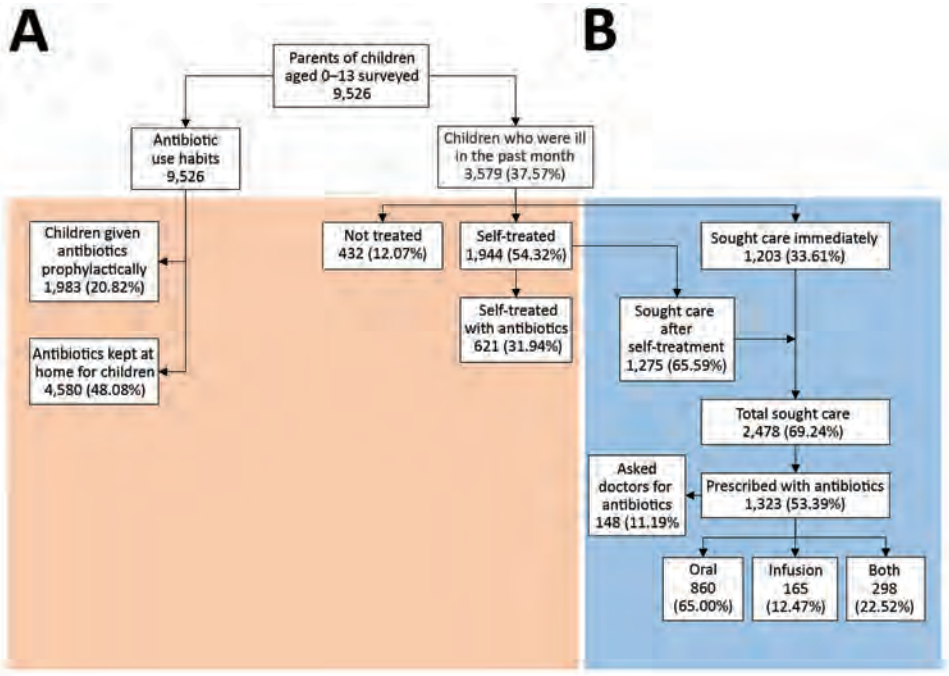


**Figure 1.** Use of antimicrobial drugs (antibiotics) for children by their parents (N = 9,526), China. Section A (left of dashed line) represents chronic antibiotic use in the previous year; section B (right of dashed line) indicates antibiotic use for common childhood illnesses in the previous month. Orange shading indicates treatment within community or household, outside of a clinical setting. Blue shading indicates use within a clinical setting.

(Table). Most parents (55.2%–78.5%) were aware of the danger that overuse of antibiotics poses, yet confused antibiotics with inflammatory drugs or drugs effective for treating colds or alleviating symptoms (Figure 2). Among the respondents, 37.6% (3,579/9,526) self-reported that their children experienced a minor illness within the previous month, with some overlap between symptoms; 82.1% (2,938/3,579) reported that it was a common cold with rhinitis, nasal congestion, or cough; 47.7% (1,707/3,579) sore throat; 31.0% (1,108/3,579) fever; 12.5% (446/3,579) diarrhea; and 3.3% (119/3,579) otitis media. Among parents who reported to have self-treated sick children, 31.9% (621/1,944) reported medicating them with antibiotics from either a local pharmacy (57.0%, 354/621) or personal stock (33.3%, 207/621). Almost all household stock of antibiotics was reported to have come from leftover prescriptions (63.1%, 2,891/4,580) or over-the-counter purchases (35.3%, 1,619/4,580); community pharmacies accounted for 70% of antibiotics for self-medication of children.

Of 3,579 parents whose children were ill in the previous month, 69.2% (2,478/3,579) sought care for the child. Before seeing a doctor, 16.5% (410/2,478) of children had already been medicated with antibiotics at home; moreover, among them, 15.4% (63/410) of parents admitted to having then asked for more antibiotics at the facility. Among those for whom care was sought after parents medicated with antibiotics, 83.9% (344/410) were prescribed antibiotics, 17.2% (59/344) of them because of parental demand. Data showed the success rate of obtaining antibiotic prescriptions for children was 79.6% (148/186); parental demand for antibiotics was more likely to occur in lower-level hospitals than tertiary hospitals and was associated with ≈4-fold increase in prescribed

**Table.** Characteristics of antibiotic prescriptions for children with common childhood illnesses in the previous month, China*

| Study question | Children brought to medical facility, N = 2,478, no. (%) | Children prescribed antibiotics, n = 1,323 [53.39%] No. (%) | OR | aOR (95% CI)† | p value‡ |
|---|---|---|---|---|---|
| What was the medical facility used when seeking care for your child? (urban/rural) | | | | | **0.04** |
| Tertiary hospital | 367 (14.8) | 174 (47.41) | Referent | Referent | |
| Secondary/county hospital | 1,057 (42.7) | 592 (56.01) | 1.41 (1.11–1.79) | 1.43 (1.11–1.84) | |
| Community health centers/township hospital | 719 (29.0) | 373 (51.88) | 1.20 (0.93–1.54) | 1.17 (0.90–1.53) | |
| Private clinics/ village clinics | 335 (13.5) | 184 (54.93) | 1.35 (1.00–1.82) | 1.21 (0.89–1.65) | |
| When seeking care at the medical facility, did you ask the doctor for antibiotics? | | | | | **<0.0001** |
| No | 2,292 (92.5) | 1,175 (88.81) | Referent | Referent | |
| Yes | 186 (7.5) | 148 (11.19) | 3.70 (2.57–5.34) | 3.71 (2.56–5.38) | |

*Bold text indicates a statistically significant difference (p<0.05). aOR, adjusted odds ratio; OR, odds ratio.
†Adjusted for children's sex and age, urban/rural residence, and province.
‡Determined by likelihood ratio test.

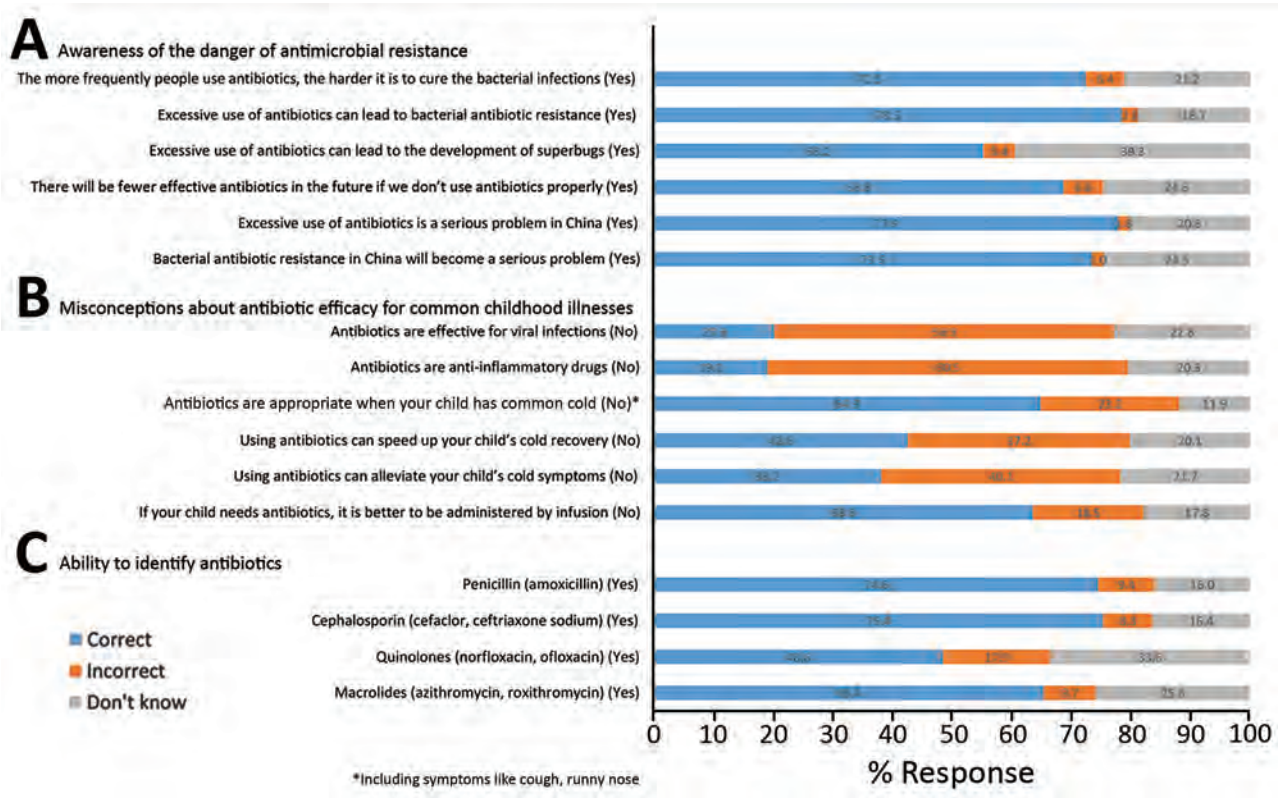


**Figure 2.** Answers to questions about antibiotics-related knowledge among parents in 3 representative provinces in China (N = 9,526). A) Knowledge of risks for antimicrobial resistance; B) understanding of drug efficacy for common illnesses; C) drug recognition. Correct answers are shown in parentheses.

antibiotics (Appendix Table, https://wwwnc.cdc.gov/EID/article/26/8/19-0631-App1.pdf).

Overall, 53.4% (1,323/2,478) of children for whom care was sought were prescribed antibiotics. The most commonly prescribed antibiotic classes were penicillins, macrolides, and cephalosporins, either alone or in combination. Differences emerged in prescription rates by type of healthcare facility, ranging from 47.4% (174/367) in tertiary hospitals to 56.0% (592/1,057) in county hospitals. More than 33% of children were administered intravenous antibiotics; about half of those infusions were combined with oral antibiotics.

Our data showed that, among the 3,579 children who had common minor childhood illnesses (mostly self-limiting) in the previous month, 621 were administered nonprescription antibiotics by their parents and 1,323 obtained a prescription, with 148 of those deemed inappropriate due to parental demand. We estimated that demand from parents contributed to 40% of antibiotic use on children for self-limiting illnesses. Although some doctors' prescriptions (supply-side) might be considered appropriate, all antibiotic demands and nonprescription uses from parents were inappropriate.

## Conclusions

Overuse of medical care for self-limiting illnesses combined with a high prescription rate and a large population size drive high antibiotic consumption in China. We found that, of children for whom care was sought, 53.4% (1,323/2,478) received prescriptions for antibiotics; this proportion is at least twice as high as the official cap of outpatient prescriptions enforced in 2012 (*10*,*11*). Unsupervised administration of antibiotics in children in the household, 3–10 times higher in China than in some countries in Europe (*12*), is a serious problem that has persisted for 15 years (*13*). Despite a 2004 ban on nonprescription sales of antimicrobial drugs (*10*,*11*), participants in all sampled sites have been able to obtain them over the counter.

Enforcing existing stewardship policies is an important step to reduce inappropriate antibiotic use in the community (*11*), as is a multifaceted program that addresses drivers of inappropriate use from both sides of healthcare system. Such a program should provide parents with education about antibiotic efficacy and care for childhood illnesses (*14*), corresponding to children's developmental stages: prenatal care, vaccination, and kindergarten and

primary school–age concerns. The program should also support healthcare providers by removing financial incentives to overprescribe medications and outpatient pediatric infusion services, enhancing clinical diagnostic capacity, and providing training on rational prescribing (*14*,*15*). Finally, interventions to improve effective patient–physician interaction and communication should consider both sides of the healthcare system (*14*).

This study is limited by its cross-sectional design; it cannot be used to establish causal conclusions and is subject to recall bias. We limited questions about healthcare-seeking behaviors to the month before the survey and recruited a large sample to reduce the risk for bias. Because we estimated antibiotic consumption by a snapshot survey and not by prescriptions or use, the true magnitude of misuse in children may be underestimated. Common childhood illness cases reported in this study were diagnosed by parents; such diagnoses may or may not reflect true prevalence of the diseases, yet were a key determinant of parents' childcare behaviors that dictated healthcare decisions parents made for their children.

### Acknowledgments

We thank the administrators and officials at the schools and health centers involved in disseminating this survey and coordinating the study for their assistance and support.

The study was funded by Zhejiang University Zijin Talent Program.

### About the Author

Dr. Lin earned her PhD at the London School of Hygiene and Tropical Medicine, specializing in implementation science and evaluation, social epidemiology, and communication and behavior sciences. Her primary research interest includes the determinants of antibiotic use, epidemic preparedness, and development of multifaceted complex interventions to reduce inappropriate antibiotic use and resistance using cross-sectional, experimental, and longitudinal studies.

### References

1. Tang Q, Song P, Li J, Kong F, Sun L, Xu L. Control of antibiotic resistance in China must not be delayed: the current state of resistance and policy suggestions for the government, medical facilities, and patients. Biosci Trends. 2016;10:1–6. https://doi.org/10.5582/bst.2016.01034
2. Heddini A, Cars O, Qiang S, Tomson G. Antibiotic resistance in China—a major future challenge. Lancet. 2009;373:30. https://doi.org/10.1016/S0140-6736(08)61956-X
3. Quan-Cheng K, Jian-Guo W, Xiang-Hua L, Zhen-Zhen L. Inappropriate use of antibiotics in children in China. Lancet. 2016;387:1273–4. https://doi.org/10.1016/S0140-6736(16)30019-8
4. Wang CQ, Wang AM, Yu H, Xu HM, Jing CM, Deng JK, et al. Report of antimicrobial resistance surveillance program in Chinese children in 2016 [in Chinese]. Zhonghua Er Ke Za Zhi. 2018;56:29–33.
5. Chang J, Lv B, Zhu S, Yu J, Zhang Y, Ye D, et al. Non-prescription use of antibiotics among children in urban China: a cross-sectional survey of knowledge, attitudes, and practices. Expert Rev Anti Infect Ther. 2018;16:163–72. https://doi.org/10.1080/14787210.2018.1425616
6. Yu M, Zhao G, Stålsby Lundborg C, Zhu Y, Zhao Q, Xu B. Knowledge, attitudes, and practices of parents in rural China on the use of antibiotics in children: a cross-sectional study. BMC Infect Dis. 2014;14:112. https://doi.org/10.1186/1471-2334-14-112
7. Cheng J, Chai J, Sun Y, Wang D. Antibiotics use for upper respiratory tract infections among children in rural Anhui: children's presentations, caregivers' management, and implications for public health policy. J Public Health Policy. 2019;40:236–52. https://doi.org/10.1057/s41271-019-00161-w
8. Sun C, Hu YJ, Wang X, Lu J, Lin L, Zhou X. Influence of leftover antibiotics on self-medication with antibiotics for children: a cross-sectional study from three Chinese provinces. BMJ Open. 2019;9:e033679. https://doi.org/10.1136/bmjopen-2019-033679
9. National Bureau of Statistics of China. National data. 2017 [cited 2018 Sep]. http://data.stats.gov.cn
10. Xiao Y, Li L. Legislation of clinical antibiotic use in China. Lancet Infect Dis. 2013;13:189–91. https://doi.org/10.1016/S1473-3099(13)70011-2
11. Wang L, Zhang X, Liang X, Bloom G. Addressing antimicrobial resistance in China: policy implementation in a complex context. Global Health. 2016;12:30. https://doi.org/10.1186/s12992-016-0167-7
12. Morgan DJ, Okeke IN, Laxminarayan R, Perencevich EN, Weisenberg S. Non-prescription antimicrobial use worldwide: a systematic review. Lancet Infect Dis. 2011;11:692–701. https://doi.org/10.1016/S1473-3099(11)70054-8
13. Bi P, Tong S, Parton KA. Family self-medication and antibiotics abuse for children and juveniles in a Chinese city. Soc Sci Med. 2000;50:1445–50. https://doi.org/10.1016/S0277-9536(99)00304-4
14. Wei X, Zhang Z, Hicks JP, Walley JD, King R, Newell JN, et al. Long-term outcomes of an educational intervention to reduce antibiotic prescribing for childhood upper respiratory tract infections in rural China: follow-up of a cluster-randomised controlled trial. PLoS Med. 2019;16:e1002733. https://doi.org/10.1371/journal.pmed.1002733
15. Ding G, Vinturache A, Lu M. Addressing inappropriate antibiotic prescribing in China. CMAJ. 2019;191:E149–50. https://doi.org/10.1503/cmaj.181417

Address for correspondence: Xudong Zhou, Institute of Social and Family Medicine, School of Medicine, Zhejiang University, 866 Yuhangtang Rd, Hangzhou, Zhejiang, 310058, China; email: zhouxudong@zju.edu.cn

# Shuni Virus in Wildlife and Nonequine Domestic Animals, South Africa

Jumari Steyn, Pebetsi Motlou, Charmaine van Eeden, Marthi Pretorius, Voula I. Stivaktas, June Williams, Louwtjie P. Snyman, Peter E. Buss, Brianna Beechler, Anna Jolles, Eva Perez-Martin, Jan G. Myburgh, Johan Steyl, Marietjie Venter

We screened nonequine animals with unexplained neurologic signs or death in South Africa during 2010–2018 for Shuni virus (SHUV). SHUV was detected in 3.3% of wildlife, 1.1% of domestic, and 2.0% of avian species. Seropositivity was also demonstrated in wildlife. These results suggest a range of possible SHUV hosts in Africa.

Shuni virus (SHUV) (*Peribunyaviridae*: *Orthobunyavirus*) was isolated in the 1960s from livestock, *Culicoides* midges, and a febrile child in Nigeria (*1*,*2*). In South Africa, SHUV was identified as the causative agent of neurologic disease in horses (*3*); seropositivity was also demonstrated in 3.0% of veterinarians, suggesting human exposures (*4*). SHUV was subsequently identified in aborted livestock and cattle with neurologic disease in Israel, suggesting an extended range beyond Africa (*5*,*6*). We investigated other potential susceptible species in South Africa.

## The Study

During February 2010–September 2018, a total of 101 whole blood, 71 serum, and 476 tissue specimens from 608 nonequine domestic animals, wildlife, and birds (19 fetuses, 118 juvenile and 471 adults) with unexplained neurologic or febrile disease or sudden unexplained death from across South Africa were submitted to the Zoonotic Arbo and Respiratory Virus Program, Centre for Viral Zoonoses, University of Pretoria (Pretoria, South Africa) as part of a passive zoonotic arbovirus surveillance program. We extracted RNA under Biosafety Level (BSL) 3 conditions using the QIAamp viral RNA mini kit (blood) or the RNeasy mini kit (tissue) (QIAGEN, https://www.qiagen.com), according to the manufacturer's recommendations. We screened all samples by a SHUV real-time reverse transcription PCR (rRT-PCR) (*7*) and a newly designed rRT-PCR targeting a conserved area of the S segment of the Simbu serogroup (Appendix, https://wwwnc.cdc.gov/EID/article/26/7/19-0770-App1.pdf). We confirmed PCR-positive samples by Sanger sequencing (Inqaba Biotech, https://www.inqababiotec.co.za) and phylogenetic analyses (Appendix). We also screened all specimens for West Nile (WNV), Wesselsbron (*8*), Middelburg (MIDV), Sindbis (*9*), and equine encephalosis viruses (*10*).

In addition, serum samples from African buffalo (*Syncerus caffer*) (n = 45) and white rhinoceros (*Ceratotherium simum*) (n = 48) from Kruger National Park were collected in March 2014 and June 2016, respectively, by South African National Parks and from wild Nile crocodiles (*Crocodylus niloticus*) (n = 34) from northern KwaZulu-Natal collected during 2009–2012 by the Faculty of Veterinary Sciences, University of Pretoria, as part of surveillance studies. We examined tissue samples from a SHUV PCR-confirmed positive buffalo (MVA43/10) microscopically under a light microscope using routinely prepared hematoxylin and eosin stained (*11*) histological sections at the Section of Pathology, Department of Paraclinical Sciences, Faculty of Veterinary Science, University of Pretoria. We subjected serum samples to an epitope-blocking ELISA (eb-ELISA) (*12*,*13*) with modifications to detect antibodies to SHUV (Appendix).

Author affiliations: University of Pretoria Faculty of Health, Pretoria, South Africa (J. Steyn, P. Motlou, C. van Eeden, M. Pretorius, V.I. Stivaktas, M. Venter); University of Pretoria Faculty of Veterinary Science, Pretoria (J. Williams, J.G. Myburgh, J. Steyl); Durban Natural Science Museum, Durban, South Africa (L.P. Snyman); South African National Parks, Kruger National Park, South Africa (P.E. Buss); Oregon State University, Corvallis, Oregon, USA (B. Beechler, A. Jolles); The Pirbright Institute, Woking, UK (E. Perez-Martin)

DOI: https://doi.org/10.3201/eid2607.190770

We calculated odds ratios (OR) and 95% CI in EpiInfo version 7.2.0.1 (https://www.cdc.gov/epiinfo/index.html). We excluded animals that were found dead, aborted, or stillborn from OR analysis.

We detected SHUV RNA in 15/608 (2.5%) animals tested from 10 different animal species: 12/361 (3.3%) wildlife, 2/196 (1.0%) nonequine domestic animals, and 1/51 avian species (2.0%) (Table 1). We detected SHUV in samples submitted from 2/62 (3.2%) white rhinoceroses, 2/50 (4.0%) sables, 1/15 (6.7%) warthog, 4/54 (7.4%) buffalo, 1/12 (8.3%) crocodiles, 1/5 (20.0%) giraffes, 1/4 (25.0%) springboks, 1/93 (1.1%) domestic bovids, and 1/10 (10.0%) alpacas (Table 1). We also detected SHUV in an exotic monal pheasant (1/13, 7.7%). Differential screening revealed co-infections with MIDV and WNV, suggesting that these arboviruses could co-circulate. A sable was also co-infected with *Theileria* sp. *sable* and *Theileria separate* (Table 1).

In 9/15 (60.0%, 95% CI 35.2%–84.8%) positive infections, we detected SHUV in the central nervous system (CNS) (Table 1), indicating passage across the blood–brain barrier, which suggests SHUV as the likely causal agent of the observed neurologic signs. This finding suggests that SHUV is not just an agent of subclinical infections or reproductive problems, such as abortion, as previously reported (*5*,*14*), but is also the likely etiology for neurologic disease in these species, as previously described for horses (*3*) and cattle (*6*). We did not detect SHUV RNA in aborted (n = 24) or stillborn (n = 16) animals. Eleven SHUV-positive animals showed neurologic signs (OR 1.8, 95% CI 0.2–14.4), with 2 animals also reported to be pyrexic (OR 2.0, 95% CI 0.4–9.4) or showing respiratory signs (OR 1.0, 95% CI 0.2–4.8) (Table 2). Three SHUV-positive animals were found dead (OR 1.8, 95% CI 0.5–6.4) (Table 2). Specific neurologic signs associated with SHUV infection included hind limb paresis progressing to quadriparesis with normal mentation (OR 6.7, 95% CI 2.0–22.5) (Table 2).

Positivity of infection was highest in the North West (4/47, 8.5% of samples submitted from North West), followed by Limpopo Province (8/132, 6.1%) (Table 1; Appendix Figure 1). SHUV was detected only in 2010 (4/15, 26.7%), 2017 (2/15, 13.3%), and 2018 (9/15, 60.0%) despite continuous surveillance throughout the years, suggesting that outbreaks may be sporadic rather than annual. SHUV PCR positives were detected during April–September in each of the 3 years (Appendix Figure 2).

Necropsy examination on the buffalo showed no specific macroscopic lesions on histopathology examination of brain tissue (Figure 1). Pathological changes that could be detected in regions of the brain

**Table 1.** Animals that tested positive for Shuni virus by real-time reverse transcription PCR, South Africa, 2010–2018*

| Animal type | ID | No. positive/ no. tested | % Positive (95% CI) | Province where submitted | Positive specimen | Clinical signs | Co-infection |
|---|---|---|---|---|---|---|---|
| Domestic bovid | ZRU116/18 | 1/93 | 1.1 (0.0–3.1) | North West | Spleen | SUD | |
| White rhinoceros (*Ceratotherium simum*) | MVA11/10<br>ZRU137/18 | 2/62 | 3.2 (0.0–7.6) | Limpopo<br>Free State | CNS | Neurologic | MIDV |
| Sable (*Hippotragus niger*) | ZRU419/17<br>ZRU121/18 | 2/50 | 4.0 (0.0–9.4) | North West<br>Limpopo | Spleen | Hemorrhagic | Theileriosis |
| Warthog *(Phaecocherus africanus)* | MVA35/10 | 1/15 | 6.7 (0.0–19.3) | Limpopo | CNS | Neurologic, respiratory | |
| Buffalo (*Syncerus caffra*) | MVA43/10<br>ZRU77/18<br>ZRU97/18<br>ZRU166/18 | 4/54 | 7.4 (0.4–14.4) | Limpopo<br>Limpopo<br>Limpopo<br>Limpopo | CNS, whole blood | Neurologic, respiratory | |
| Monal (*Lophophorus impejanus*) | ZRU119/18 | 1/13 | 7.8 (0.0–22.2) | North West | CNS | SUD | |
| Crocodile (*Crocodylus niloticus*) | MVA08/10 | 1/12 | 8.3 (0.0–24.0) | Limpopo | CNS | Neurologic | |
| Alpaca (*Vicugna pacos*) | ZRU172/18 | 1/10 | 10.0 (0.0–28–6) | Western Cape | CNS | Neurologic, respiratory | |
| Giraffe (*Giraffa camelopardalis*) | ZRU87/18 | 1/5 | 20 (0.0–55.0) | North West | Whole blood | SUD | WNV |
| Springbok (*Antidorcus marsupialis*)† | ZRU261/17/3 | 1/4 | 25.0 (0.0–67.4) | Gauteng | Spleen | Neurologic | |
| Wildlife | | 12/361 | 3.3 (1.5–5.1) | | | | |
| Domestic animals | | 2/196 | 1.1 (0.0–2.5) | | | | |
| Avian | | 1/51 | 2.0 (0.0–5.8) | | | | |
| Total | | 15/608 | 2.5 (1.2–3.7) | | | | |

*CNS, central nervous system; MIDV, Middelburg virus; SUD, sudden unexpected death; WNV, West Nile virus.
†Cluster with Sango virus.

**Table 2.** Clinical signs reported in wildlife, nonequine domestic animals, and birds upon submission to the Centre for Viral Zoonoses, South Africa, 2010–2018*

| Sign | SHUV positive (%), n = 12 | SHUV negative (%), n = 496 | Odds ratio (95% CI) | p value† |
|---|---|---|---|---|
| Neurologic signs | 11 (91.7) | 415 (83.7) | 1.8 (0.2–14.4) | 0.9 |
| Ataxia | 2 (16.7) | 102 (20.6) | 0.8 (0.2–3.5) | 1 |
| Paralysis | 3 (25.0) | 61 (12.3) | 2.3 (0.6–8.8) | 0.4 |
| Quadriparesis | 8 (66.7) | 112 (22.6) | 6.7 (2.0–22.5) | <0.05 |
| Recumbence | 2 (16.7) | 103 (20.8) | 0.7 (0.2–3.4) | 1 |
| Pyrexia | 2 (16.7) | 44 (8.9) | 2.0 (0.4–9.4) | 0.7 |
| Respiratory/dyspnea | 2 (16.7) | 79 (15.9) | 1.0 (0.2–4.8) | 1 |
| Hemorrhage | 1 (8.3) | 10 (2.0) | 4.3 (0.5–36.7) | 0.6 |
| Congenital deformities | 0 | 7 (1.4) | Undefined | 1 |

included mild white matter cerebro–cerebellar gliosis, especially microglial, associated with considerable glial apoptotic activity and occasional perivascular hemorrhage. In the spinal cord, occasional single neuronal necrosis (chromatolysis) and perineuronal hypereosinophilic bodies affecting the dorsal horns of the gray matter were distinctive. This finding seemed to be most severe in the lumbar spinal region. No evidence of demyelination or major immunological reaction was observed, apart from occasional perivascular lymphocytes. Development of appropriate antibodies for immunohistochemistry or probes for in situ hybridization may further describe the pathology of SHUV in animal tissue.

We used phylogenetic analyses on the small segment of the Simbu serogroup to verify the molecular results. All novel sequences from this study, with 1 exception, were closely related to SHUV strains identified in horses in South Africa (*3*) in clade 1a of lineage I within the Simbu serogroup (bootstopping:

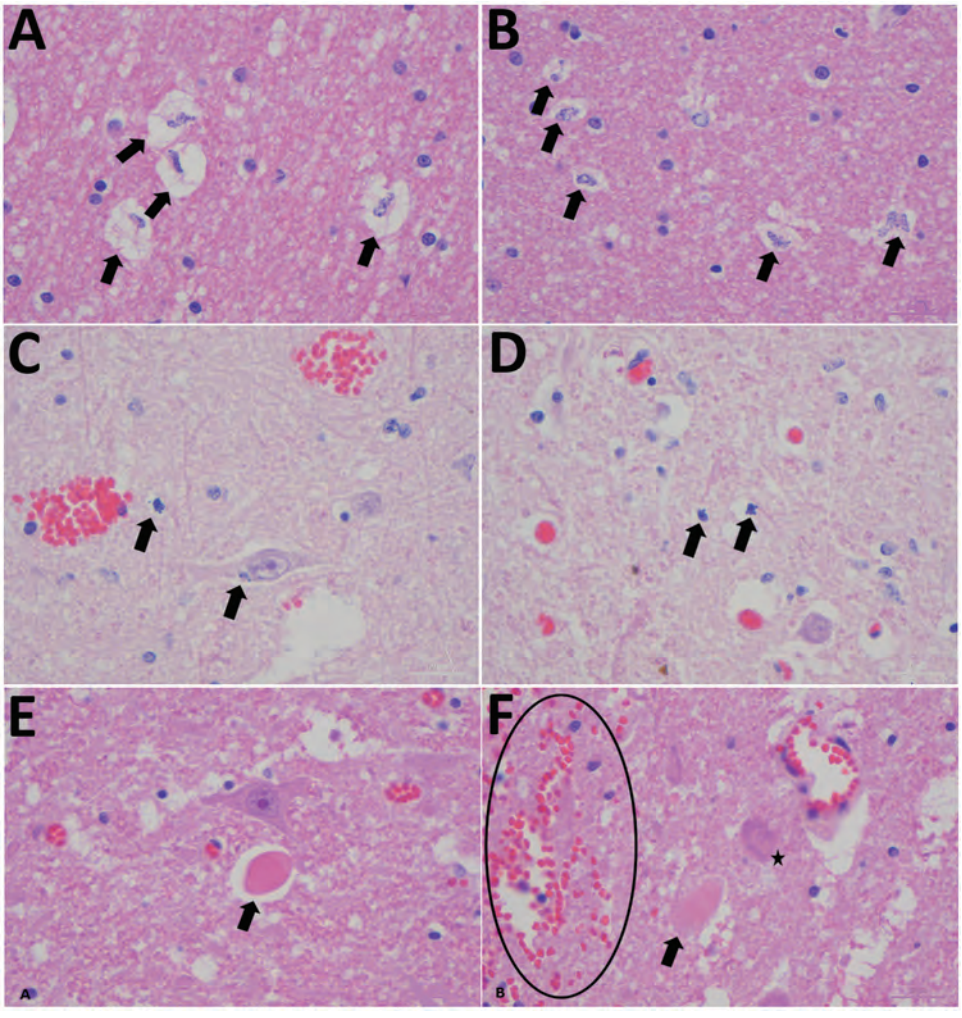


**Figure 1.** Histopathological changes in formalin-fixed brain tissue of a Shuni virus PCR-positive buffalo (MVA73/10) in South Africa that showed neurologic signs (original magnification 1000×). A, B) Cerebral white matter micro/astrogliosis and cytogenic edema (arrows). C, D) Glial (suspected oligodendroglia) apoptosis (arrows). E, F) Perineural hypereosinophilic bodies (arrows); perivascular and neuropil hemorrhage (circle); single-cell neuronal degeneration (chromatolysis) (star).

posterior probabilities = 89:0.99) (Figure 2). An isolate from a springbok (ZRU261_17_3) clustered with Sango virus (bootstopping: posterior probabilities = 67:0.94). P-distance analysis based on the partial small segment demonstrated few nucleotide differences between novel SHUV strains and reference strains (98.0%–100.0% identity). Wildlife specimens were submitted mostly from dead animals that were already undergoing postmortem cytolysis, inhibiting further genetic analysis and isolation of the virus. The use of a PCR designed to detect Simbu group/orthobunyavirus genus PCR rather than SHUV-specific PCR facilitated detection of these infections.

We detected antibodies to SHUV by an eb-ELISA in 3/44 (6.8%) African buffalo and 2/48 (4.2%) white rhinoceroses but none in crocodiles. SHUV-specific IgG was confirmed, using microtiter virus neutralization assay, in 1 buffalo and 1 rhinoceros. Two of 3 buffalo and 1 rhinoceros positive for SHUV epitope antibodies were negative by microtiter virus neutralization assay, suggesting that these antibodies may have been elicited in response to closely related orthobunyavirus. Confirmation for the third buffalo was not possible because of depleted serum.

## Conclusion

Our findings suggest that SHUV may have a wide host range, including several wildlife and domestic species, and should be included in the differential diagnosis of neurologic disease in animals. This

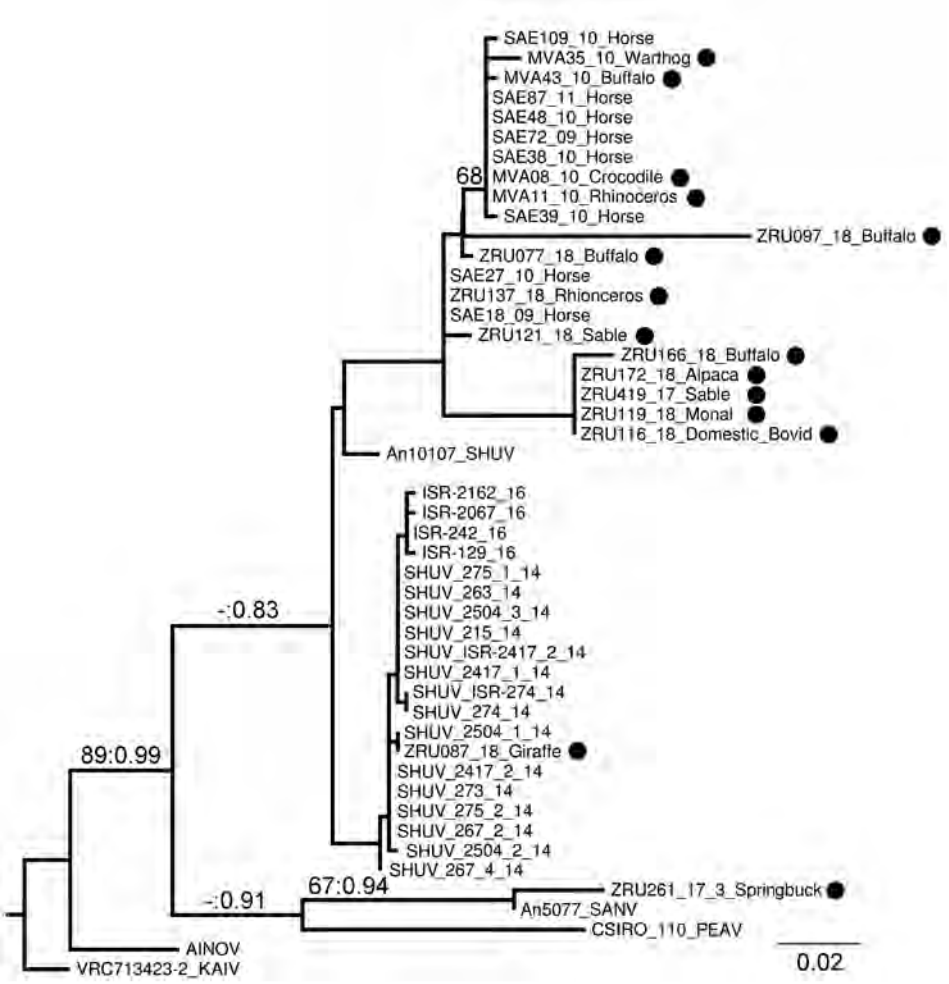


**Figure 2.** Phylogram of clade 1a, lineage I, of the Simbu serogroup (*15*) recovered from maximum-likelihood and Bayesian analyses of the small segment for SHUV isolates from wildlife and nonequine domestic animals, South Africa and reference sequences. Bootstrap values (maximum likelihood >60) and posterior probabilities (>0.8) are displayed on branches as support values. GenBank accession numbers for sequences from this study (black circles): MVA11_10_Rhinoceros, JQ726395; MVA08_10_Crocodile, JQ726396; MVA43_10_Buffalo, JQ726397; MVA35_10_Warthog, JQ726398; ZRU077_18_Buffalo, MK114084; ZRU121_18_Sable, MK114085; ZRU137_18_Rhinoceros, MK114086. GenBank accession numbers, virus types, and locations for reference sequences: An10107, AF362405, SHUV Nigeria; AINOV, M22011, Japan; VRC713423–2 KAIV, AF362394, India; SAE72_09_ Horse, HQ610138, South Africa; SAE27_10_Horse, HQ610139, South Africa; SAE38_10_Horse, HQ610140, South Africa; SAE39_10_Horse, HQ610141, South Africa; SAE48_10_Horse, HQ610142, South Africa; SAE109_10_Horse, HQ610143, South Africa; SAE18_09_Horse, KC510272, South Africa; SAE87_11_ Horse, KC525997, South Africa; Shuni_215_14, KP900859, Israel; Shuni_263_14, KP900860, Israel; Shuni_267_2_14, KP900861, Israel; Shuni_267_4_14, KP900862, Israel; Shuni_273_14, KP900865, Israel; Shuni_274_14, KP900867, Israel; Shuni_275_1_14, KP900869, Israel; Shuni_275_2_14, KP900871, Israel; Shuni_2417_1_14, KP900872, Israel; Shuni_2417_2_14, KP900875, Israel; Shuni_2504_1_14, KP900877, Israel; Shuni_2504_2_14, KP900878, Israel; Shuni_2504_3_14, KP900882, Israel; 2504_3_14, KU937313, Israel; SHUV_ISR-274_14, KT946779, Israel; SHUV_ISR-2417_2_14, KT946780, Israel; ISR-129_16, MF361846, Israel; ISR-242_16, MF361849, Israel; ISR-2067_16, MF361852, Israel; ISR-2162_16, MF361855, Israel; CSIRO 110, MH484320, Australia; An5077, AF362402, Nigeria. AINOV, ainovirus; KAIV, kaikalurvirus; PEAV, Peaton virus; SANV, Sango virus; SHUV, Shuni virus.

study highlights the role of this virus as a potential emerging zoonotic pathogen in Africa that warrants increased surveillance and further investigation. Future epidemiologic studies would benefit from an increased sample size and more extensive serosurveys. Investigation of human infections may define SHUV's importance as a zoonosis. The causative link between clinical manifestations in the various species and the evidence of SHUV infection must be regarded with caution because other possible infectious and noninfectious etiologies were not excluded by comprehensive investigations in all cases.

### Acknowledgments

We thank participating veterinarians and veterinary pathologists from South Africa, as well as L.P. Snyman, for the help with the phylogenetic analyses.

This research was funded through the US CDC Global Disease Detection grant for Zoonotic arboviruses under grant no. 1U19GH000571-01-GDD Non-Research CoAg with the NHLS project 23 and UP Zoonotic Arbo and Respiratory virus program, 2012–2015, and by cooperative agreement no. 5 NU2GGH001874-02-00 with the University of Pretoria, 2015–2016. Buffalo samples were financed through BBSRC-USDA funding (grant no. BB/L011085/1) and transported under a Red Cross permit (LDK2016/9/1) to the BSL3 lab at CVZ. J. Steyn received doctoral scholarship form the NRF (grant no. 95175), the Meat Industry Trust (grant no. IT8114/98), the Poliomyelitis Research Foundation (grant no. 15/112).

This study was cleared by section 20 (12/11/1/1) approval through the Department of Agriculture Forestry and Fisheries (DAFF) (2014-October 2018) (M.V.) as well as by the animal ethics (H12-16) and section 20 (V057-15) (2017) of the University of Pretoria and the PhD research committee.

## About the Author

Dr. Steyn is a virologist and PhD candidate at the Centre for Viral Zoonoses at the University of Pretoria, South Africa. Her primary research focuses on investigating arboviruses with zoonotic potential at human–animal interface areas.

### References

1. Causey OR, Kemp GE, Causey CE, Lee VH. Isolations of Simbu-group viruses in Ibadan, Nigeria, 1964–69, including the new types Sango, Shamonda, Sabo and Shuni. Ann Trop Med Parasitol. 1972;66:357–62. https://doi.org/10.1080/00034983.1972.11686835
2. Lee VH. Isolation of viruses from field populations of *Culicoides* (Diptera: Ceratopogonidae) in Nigeria. J Med Entomol. 1979;16:76–9. https://doi.org/10.1093/jmedent/16.1.76
3. van Eeden C, Williams JH, Gerdes TGH, van Wilpe E, Viljoen A, Swanepoel R, et al. Shuni virus as cause of neurologic disease in horses. Emerg Infect Dis. 2012;18:318–21. https://doi.org/10.3201/eid1802.111403
4. van Eeden C, Swanepoel R, Venter M. Antibodies against West Nile and Shuni viruses in veterinarians, South Africa. Emerg Infect Dis. 2014;20:1409–11. https://doi.org/10.3201/eid2008.131724
5. Golender N, Brenner J, Valdman M, Khinich Y, Bumbarov V, Panshin A, et al. Malformations caused by Shuni virus in ruminants, Israel, 2014–2015. Emerg Infect Dis. 2015;21:2267–8. https://doi.org/10.3201/eid2112.150804
6. Golender N, Bumbarov V, Assis I, Beer M, Khinich Y, Koren O, Edery N, Eldar A, et al. Shuni virus in Israel: neurological disease and fatalities in cattle. Transbound Emerg Dis. 2019;66:1126–31. https://doi.org/10.1111/tbed.13167
7. Van Eeden C, Zaayman D, Venter M. A sensitive nested real-time RT-PCR for the detection of Shuni virus. J Virol Methods. 2014;195:100–5. https://doi.org/10.1016/j.jviromet.2013.10.008
8. Zaayman D, Human S, Venter M. A highly sensitive method for the detection and genotyping of West Nile virus by real-time PCR. J Virol Methods. 2009;157:155–60. https://doi.org/10.1016/j.jviromet.2008.12.014
9. van Niekerk S, Human S, Williams J, van Wilpe E, Pretorius M, Swanepoel R, et al. Sindbis and Middelburg old world alphaviruses associated with neurologic disease in horses, South Africa. Emerg Infect Dis. 2015;21:2225–9. https://doi.org/10.3201/eid2112.150132
10. van Niekerk M, Freeman M, Paweska JT, Howell PG, Guthrie AJ, Potgieter AC, et al. Variation in the NS3 gene and protein in South African isolates of bluetongue and equine encephalosis viruses. J Gen Virol. 2003;84:581–90. https://doi.org/10.1099/vir.0.18749-0
11. Bancroft JD, Gamble M, editors. Theory and practice of histological techniques. Edinburgh: Churchill Livingstone; 2002.
12. Blitvich BJ, Marlenee NL, Hall RA, Calisher CH, Bowen RA, Roehrig JT, et al. Epitope-blocking enzyme-linked immunosorbent assays for the detection of serum antibodies to West Nile virus in multiple avian species. J Clin Microbiol. 2003a;41:1041–7. https://doi.org/10.1128/JCM.41.3.1041-1047.2003
13. Blitvich BJ, Bowen RA, Marlenee NL, Hall RA, Bunning ML, Beaty BJ. Epitope-blocking enzyme-linked immunosorbent assays for detection of West Nile virus antibodies in domestic mammals. J Clin Microbiol. 2003b;41:2676–9. https://doi.org/10.1128/JCM.41.6.2676-2679.2003
14. Mathew C, Klevar S, Elbers ARW, van der Poel WHM, Kirkland PD, Godfroid J, et al. Detection of serum neutralizing antibodies to Simbu sero-group viruses in cattle in Tanzania. BMC Vet Res. 2015;11:208. https://doi.org/10.1186/s12917-015-0526-2
15. Saeed MF, Li L, Wang H, Weaver SC, Barrett ADT. Phylogeny of the Simbu serogroup of the genus *Bunyavirus*. J Gen Virol. 2001;82:2173–81. https://doi.org/10.1099/0022-1317-82-9-2173.

Address for correspondence: Marietjie Venter, Zoonotic Arbo and Respiratory Virus Program, Centre for Viral Zoonoses, Department of Medical Virology, University of Pretoria, Pretoria, South Africa; email: marietjie.venter@up.ac.za

# Transmission of Legionnaires' Disease through Toilet Flushing

Jeanne Couturier, Christophe Ginevra, Didier Nesa, Marine Adam, Cyril Gouot, Ghislaine Descours, Christine Campèse, Giorgia Battipaglia, Eolia Brissot, Laetitia Beraud, Anne-Gaëlle Ranc, Sophie Jarraud, Frédéric Barbut

We describe 2 cases of healthcare-associated Legionnaires' disease in patients in France hospitalized 5 months apart in the same room. Whole-genome sequencing analyses showed that clinical isolates from the patients and isolates from the room's toilet clustered together. Toilet contamination by *Legionella pneumophila* could lead to a risk for exposure through flushing.

*Legionella pneumophila* is a gram-negative bacterium usually found in small amounts in water in both nature and built environments. In larger amounts, it can be responsible for a severe pneumonia known as Legionnaires' disease (LD). Transmission usually occurs when someone inhales contaminated aerosols from showers, cooling towers, faucets, or fountains. Person-to-person transmission is extremely rare (*1*). Researchers have shown evidence of a variety of other uncommon sources of contamination, such as windshield washer fluid (*2*) or dental unit waterlines (*3*). LD transmission through flushing toilets has also been suspected (*4*) but not demonstrated. We report 2 cases of LD in immunocompromised patients in France, potentially caused by *L. pneumophila* transmission through flushing toilets.

## The Study

In the first case, an 18-year-old woman who had undergone an allogeneic bone marrow transplant for acute myeloid leukemia in February 2014 in a hospital hematology unit in France was hospitalized in December 2015 in the same unit for 9 days. At that time, she received immunosuppressive agents (steroids, cyclosporine A, and ruxolitinib) for a chronic graft-versus-host disease. She was readmitted to the hematology unit with fever (38.5°C), shivering, and dyspnea 6 days after discharge. Six days later, she was transferred to the medical intensive care unit (MICU) of the same hospital with fever (40°C), bilateral pneumonia, and respiratory and renal failure. The result from a *L. pneumophila* urinary antigen test (BinaxNOW Legionella Urinary Antigen EIA kit; Abbott, https://www.abbott.com) was positive at the time of MICU admission, leading clinicians to consider this LD case to be probably healthcare associated. Physicians successfully treated the patient with spiramycin and levofloxacin, and she was discharged from the MICU after 8 days.

In the second case, a 51-year-old man was admitted to the same hematology unit in May 2016 for an autologous transplant for a recurrent Hodgkin lymphoma. A persistent fever (38.8°C) appeared on the 12th day after admission and a computed tomography scan of the chest showed a multifocal consolidation. The result from a *L. pneumophila* urinary antigen test (BinaxNOW) on day 22 was positive; therefore, this LD case was considered to be definitely healthcare associated. The patient's condition suddenly worsened, and he was transferred to the MICU, where he rapidly recovered after doctors treated him with spiramycin and levofloxacin.

For both patients, a bronchoalveolar lavage procedure found *L. pneumophila* bacteria from serogroup 1 (LP1), pulsed-field gel electrophoresis pulsotype Paris, sequence type (ST) 1, monoclonal antibody subgroup Philadelphia. Both patients had been hospitalized in the same room (room 1) of the hematology unit, 5 months apart. Air filtration systems with HEPA filters were used to control the environment of the unit. Water from the sink in each room and from the shower, shared by all of the unit's patients, was filtered through 0.1-μm pore filters. Both patients were provided only bottled water and did not take

Author affiliations: Hôpital Saint-Antoine, Paris, France (J. Couturier, D. Nesa, M. Adam, C. Gouot, G. Battipaglia, E. Brissot, F. Barbut); Faculté de Pharmacie de Paris, Université de Paris, France (J. Couturier, F. Barbut); Centre National de Référence des Légionelles, Lyon, France (C. Ginevra, G. Descours, L. Beraud, A.-G. Ranc, S. Jarraud); Université Claude Bernard Lyon 1, Villeurbanne, France (C. Ginevra, G. Descours, L. Beraud, A.-G. Ranc, S. Jarraud); Santé Publique France, Saint-Maurice, France (C. Campèse); Sorbonne Université, Paris, France (E. Brissot)

DOI: https://doi.org/10.3201/eid2607.190941

showers during their hospital stay. In addition, there was no cooling tower within the hospital.

We sampled and analyzed the potential sources of exposure in accordance with the NF T 90-431 standard (Association Française de Normalisation, https://www.afnor.org) for counting *Legionella* spp., after the second LD case. In brief, we sampled 500 mL of water in sterile vials containing 20 mg sodium thiosulfate. First, we inoculated 0.2 mL of water on GVPC (glycine, vancomycin, polymyxin, cycloheximide) plates (Oxoid France, http://www.oxoid.com/fr/blue/). Then, we filtered 10 mL and 100 mL of water through 0.2-µm pore polycarbonate membranes placed on GVPC media. We incubated plates at 36°C (± 2°C) for 8–11 days. We subcultured suspicious colonies on buffered charcoal yeast extract media with and without cystein and identified them by latex agglutination (Oxoid France).

We found no *L. pneumophila* in the hot water from the shared shower (temperature 26.0°C, chlorine 1.12 mg/L), nor in the hot or cold water from the sink in room 1 (temperatures 24°C and 25°C, chlorine 1.11 mg/L and 0 mg/L, respectively). However, sampling of the water from the toilet bowl in room 1 showed contamination (1,100 CFU/L LP1, with a temperature of 22.0°C and no chlorine). LP1 was also in the toilet bowl of the adjacent room (room 2) (100 CFU/L, temperature 24.4°C), the hot water from the sink in the nurses' office (10 CFU/L, temperature 49.8°C, chlorine 0.77 mg/L), and the cold-water inlet of the building (20 CFU/L, temperature 15.0°C). Contamination in the cold-water inlet (20 CFU/L, temperature 9.0°C) had also been detected in March 2016. Tests of samples of toilet water from tanks in nearby rooms did not show any contamination.

The room was closed, and the toilet was disinfected daily with bleach. The toilet water in the room was

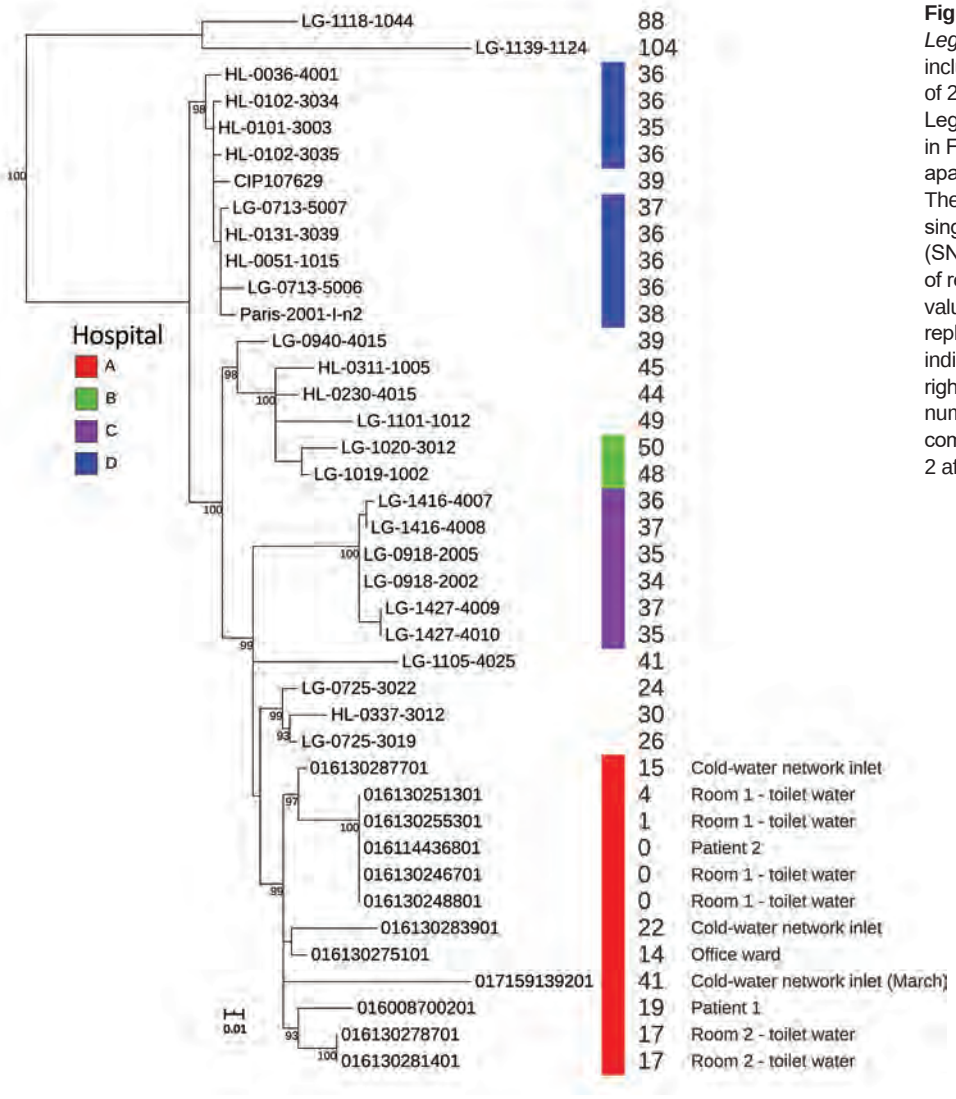


**Figure.** Maximum-likelihood tree of 39 *Legionella pneumophila* ST1 isolates, including isolates from investigation of 2 cases of healthcare-associated Legionnaires' disease in patients in France hospitalized 5 months apart in the same room (red bar). The tree was constructed using 258 single-nucleotide polymorphisms (SNPs) identified after the removal of recombination events. Bootstrap values were calculated from 500 replicates; only values >90 were indicated on the tree. Values at the right side of the tree represent the number of SNPs between the genome compared with the genome of patient 2 after recombination removal.

monitored through iterative testing; results were negative from 10 successive samples tested between June 2016 and November 2017. To determine the extent of such contamination, 29 toilets in 5 different hospital buildings were analyzed. All samples were negative, suggesting that *L. pneumophila* contamination of toilet water was not common.

We used Nextera XT technology (Illumina, https://www.illumina.com) for whole-genome sequencing of 2 clinical and 10 environmental LP1 strains and deposited raw reads into the European Nucleotide Archive (study accession no. PRJEB32615). We used SPAdes to assemble genomes (*5*) and mompS tool to extract STs from the WGS data (*6*). All 12 strains belonged to ST1. We analyzed these 12 strains in more depth by comparing their genomes to 27 other epidemiologically unrelated LP1 ST1 genomes from France available in the Sequence Read Archive database (Figure; Appendix, https://wwwnc.cdc.gov/EID/article/26/7/19-0941-App1.pdf). We also performed phylogenetic analyses on this genome's dataset, as described by David et al. (*7*).

The 2 clinical isolates were nested within and thus derived from the clade of isolates sampled from the hospital water network. All 12 strains, including the strains isolated in the cold-water inlet, were part of a cluster sharing the same most recent common ancestor (Figure). We observed no difference in single-nucleotide polymorphisms (SNPs) between the 2 isolates from the toilet water from the patients' room and the isolate of the second patient (Figure). The strains present in the toilet water were identical or closely related to the strains infecting the patients, and no other potential contamination source was identified, strongly suggesting that the toilet water was the contamination source. The few differences in SNPs between the first clinical isolate and the isolates found in the environment (0–23 SNPs; see Appendix Table) could be explained by diversity of the ST1 population in the water network or the micro-evolution of the environmental LP1 population during the 5 months between the 2 LD cases (*7*).

## Conclusions

We describe 2 cases in which LD was probably caused by *L. pneumophila* transmitted through contaminated toilet water that became aerosolized during flushing. We reached this conclusion because we found little to no detectable difference between whole genomes in isolates obtained from 2 patients hospitalized 5 months apart in the same room and those from the toilet in that room. The other commonly suspected sources, in this case the shower and the sink, tested negative for *L. pneumophila*.

This investigation suggests that transmission of *L. pneumophila* through toilet flushing should be considered when investigating a LD case. However, as previously suggested, there remains a need for a laboratory-based study to explore whether flushing toilets can generate and spread contaminated aerosols (*8*,*9*).

## About the Author

Dr. Couturier is a medical biologist at the Saint-Antoine Hospital, and a teaching assistant at the René Descartes Faculty of Pharmacy, Paris, France. Her research interests include microbiology and hospital hygiene.

## References

1. Correia AM, Ferreira JS, Borges V, Nunes A, Gomes B, Capucho R, et al. Probable person-to-person transmission of Legionnaires' disease. N Engl J Med. 2016;374:497–8. https://doi.org/10.1056/NEJMc1505356
2. Prussin AJ II, Schwake DO, Marr LC. Ten questions concerning the aerosolization and transmission of *Legionella* in the built environment. Build Environ. 2017;123:684–95. https://doi.org/10.1016/j.buildenv.2017.06.024
3. Lauritano D, Nardone M, Gaudio RM, Candotto V, Carinci F. Risk assessment of colonization of *Legionella* spp. in dental unit waterlines. Oral Implantol (Rome). 2017;10:283–8. https://doi.org/10.11138/orl/2017.10.3.283
4. Hamilton KA, Hamilton MT, Johnson W, Jjemba P, Bukhari Z, LeChevallier M, et al. Health risks from exposure to *Legionella* in reclaimed water aerosols: toilet flushing, spray irrigation, and cooling towers. Water Res. 2018;134:261–79. https://doi.org/10.1016/j.watres.2017.12.022
5. Bankevich A, Nurk S, Antipov D, Gurevich AA, Dvorkin M, Kulikov AS, et al. SPAdes: a new genome assembly algorithm. J Comput Biol. 2012;19:455–77. https://doi.org/10.1089/cmb.2012.0021
6. Gordon M, Yakunin E, Valinsky L, Chalifa-Caspi V, Moran-Gilad J; ESCMID Study Group for Legionella Infections. A bioinformatics tool for ensuring the backwards compatibility of *Legionella pneumophila* typing in the genomic era. Clin Microbiol Infect. 2017;23:306–10. https://doi.org/10.1016/j.cmi.2017.01.002
7. David S, Afshar B, Mentasti M, Ginevra C, Podglajen I, Harris SR, et al. Seeding and establishment of *Legionella pneumophila* in hospitals: implications for genomic investigations of nosocomial Legionnaires' disease. Clin Infect Dis. 2017;64:1251–9. PubMed https://doi.org/10.1093/cid/cix153
8. Hines SA, Chappie DJ, Lordo RA, Miller BD, Janke RJ, Lindquist HA, et al. Assessment of relative potential for *Legionella* species or surrogates inhalation exposure from common water uses. Water Res. 2014;56:203–13. https://doi.org/10.1016/j.watres.2014.02.013
9. Johnson D, Lynch R, Marshall C, Mead K, Hirst D. Aerosol generation by modern flush toilets. Aerosol Sci Technol. 2013;47:1047–57. https://doi.org/10.1080/02786826.2013.814911

Address for correspondence: Jeanne Couturier, Laboratoire de Microbiologie de l'Environnement, Hôpital Saint-Antoine, 184 rue du Faubourg Saint-Antoine, 75012, Paris, France; email: jeanne.couturier@aphp.fr

# Carbapenem Resistance Conferred by OXA-48 in K2-ST86 Hypervirulent *Klebsiella pneumoniae*, France

Racha Beyrouthy, Guillaume Dalmasso, Aurélien Birer, Frédéric Robin, Richard Bonnet

We recovered 2 carbapenem-resistant K2-ST86 hypermucoviscous *Klebsiella pneumoniae* isolates from patients in France. The isolates had genetic attributes of hypervirulent *K. pneumoniae* but differed in ability to cause mouse lethality. Convergence of hypervirulent *K. pneumoniae* toward resistance could cause a health crisis because such strains could be responsible for severe and untreatable infections.

*Klebsiella pneumoniae* is a threat to human health because of the emergence of hypervirulent *K. pneumoniae*, which has caused severe community-acquired infections, and classical multidrug-resistant *K. pneumoniae* involved in hospital outbreaks (*1*). Classical *K. pneumoniae* generally lacks the virulence genes associated with invasive diseases (*1*) and belongs to successful clonal groups, such as sequence type (ST) 11 and ST258 (*2*). Most hypervirulent *K. pneumoniae* isolates, which are mainly found in Asia (*3*,*4*), belong to the K1 and K2 capsular serotypes and are restricted to clonal complexes different from classical multidrug-resistant *K. pneumoniae* groups, such as K1-ST23, the most prevalent group (*2*). They rarely harbor acquired antimicrobial resistance genes but have virulence loci and a hypermucoviscous phenotype (*5*). We describe 2 hypermucoviscous K2-ST86 *K. pneumoniae* (positive string test) resistant to carbapenems isolated in northern and southern France.

Author affiliations: Institut National de la Santé et de la Recherche Médicale, Clermont-Ferrand, France (R. Beyrouthy, G. Dalmasso, F. Robin, R. Bonnet); Centre National de Référence de la Résistance aux Antibiotiques, Clermont-Ferrand (R. Beyrouthy, A. Birer, F. Robin, R. Bonnet); Centre Hospitalier Universitaire, Clermont-Ferrand (R. Beyrouthy, F. Robin, R. Bonnet); Institut National de la Recherche Agronomique (USC-2018), Clermont-Ferrand (R. Beyrouthy, F. Robin, G. Dalmasso, R. Bonnet) ; Université Clermont Auvergne, Clermont-Ferrand (G. Dalmasso, F. Robin, R. Bonnet)

DOI: https://doi.org/10.3201/eid2607.191490

## The Study

In 2017, we recovered the Kpn154 strain from the urine of a 35-year-old man with community-acquired urinary tract infection. He had fever (39°C) before local symptoms suggesting urinary tract infection caused by bacteremic spread, which was successfully treated with intravenous ceftriaxone. A second strain, Kpn2166, was hospital-acquired and recovered from the feces of a 70-year-old man in the intensive care unit of the hospital at which the 35-year-old patient was seem. Neither patient reported travel during the past 4 years. Both strains were resistant to all penicillins and their combinations with β-lactamase inhibitors, and to carbapenems according to EUCAST (European Committee on Antimicrobial Susceptibility Testing) guidelines (https://www.eucast.org) (Table). In addition, Kpn2166 was resistant to the third-generation cephalosporins, quinolones and tigecycline.

We obtained the isolates' whole-genome sequence by hybrid de novo assembly of short and long reads generated with technologies from Illumina (https://www.illumina.com) and Oxford Nanopore (https://nanoporetech.com; European Nucleotide Archive at EMBL-EBI under accession no. PRJEB34867). We typed the isolates as K2-ST86 from whole-genome sequencing using the Institut Pasteur multilocus sequence typing scheme (https://bigsdb.pasteur.fr) and Kleborate (*6*). Kpn154 harbored carbapenemase-encoding gene $bla_{\text{oxa-48}}$ and Kpn2166 the extended-spectrum β-lactamase–encoding gene $bla_{\text{CTX-M-15}}$ as the only acquired β-lactamase–encoding genes. CTX-M-15 associated with the truncation of the outer membrane protein OmpK36 caused by 11-bp deletion

**Table.** Characteristics of carbapenem and hypervirulent *Klebsiella pneumoniae* isolates from 2 patients, France, 2017*

| Characteristic | Kpn154 strain | Kpn2166 strain |
|---|---|---|
| Patient age, y/sex | 35/M | 70/M |
| Sample, context | Urine, community-acquired UTI | Feces, hospital-acquired intestinal carriage |
| MIC, μg/mL | | |
| Ertapenem | 2 | 32 |
| Imipenem | 10 | 10 |
| Meropenem | 2 | 4 |
| Ceftazidime | 0.125 | >256 |
| Ceftriaxone | 0.5 | >256 |
| Cefotaxime | 0.5 | >256 |
| Cefepime | 0.25 | >256 |
| Aztreonam | 0.06 | >256 |
| Temocillin | 256 | 32 |
| Tigecyclin | 1 | 4 |
| Colistin | 0.5 | 0.5 |
| Genome size, sequencing depth | 5,555,907 bp, 120× | 5,649,836 bp, 145× |
| Genotype | K2-ST86 | K2-ST86 |
| Resistance replicon, bp | IncL, 100,326 | IncN, 61,761 |
| Resistance marker | $bla_{OXA-48}$ | $bla_{CTX-M-15}$, Δ*ompK36*, Δ*ramR* |
| Virulence replicon | IncHI1B/IncFIB, 215,306 | IncHI1B/IncFIB, 226,677 |
| Capsule regulator | *rmpA.2*, *rmpA2*† | rmpA.2, Δ*rmpA2*‡ |
| Aerobactin-ST§ | AbST1: *iucA1B1C1D1iutA1* | AbST1: *iucA1B1C1D1iutA1* |
| Salmochelin-ST§ | SmST1: iroB1C1D1N1 | SmST1: iroB1C1D1N1 |
| Yersiniabactin-ST§ | *ICEKp3*-YbST202LV | *ICEKp12*like- YbST13LV |

*K, capsular genotype; ST, sequence type; UTI, urinary tract infection.
†New *rmpA2* allele.
‡Truncated allele harboring a frameshift mutation at base 222.
§Genotyped based on Kleborate schemes.

was probably responsible for carbapenem resistance in Kpn2166. In the absence of *rpsJ* variants previously associated with tigecycline resistance, Kpn2166 resistance to tigecycline and quinolones probably resulted from a frameshift mutation in *ramR* (C→T at position 364) (*7*).

We identified IncL replicon in Kpn154 and IncN replicon in Kpn2166. The IncL replicon of Kpn154 was a canonical pOXA-48–like plasmid encoding $bla_{OXA-48}$ (GenBank accession no. JN626286). In the Kpn2166 isolate, $bla_{CTX-M-15}$ was encoded by a new ST9-IncN plasmid, included in an IS*26*-based composite transposon and downstream a truncated IS*Ecp1* insertion sequence.

Each isolate harbored an IncHI1B/IncFIB replicon, designated pVIR-Kpn154 and pVIR-Kpn2166 (Table), typified by the reference hvKP virulence plasmid pLVPK (*8*). They shared with pLVPK 97% pairwise identity overall and all virulence genes, including the *rmpA* and *rmpA2* genes involved in the hypermucoid phenotype (*8*). We typed the *rmpA* genes as allele 2 according to the Institut Pasteur scheme. However, Kpn2166 *rmpA2* harbored in addition a frameshift mutation (coding sequence [CDS] position 196) and 2 other mutations in virulence genes encoding the siderophores (Appendix Figure 1, https://wwwnc.cdc.gov/EID/article/26/7/19-1490-App1.pdf).

We compared the pVIR-Kpn154 and pVIR-Kpn2166 plasmids with 16 complete hypervirulent *K. pneumoniae* plasmid sequences (Appendix Table) from the PATRIC database (http://www.patricbrc.org). A single-nucleotide polymorphism–based phylogenic tree showed a link between the major tree branches and the sequence types of hypervirulent *K. pneumoniae* owners but not with their geographic origin (Figure 1, panel A). This finding suggests emergence was more likely caused by spread over distant geographic areas than by local expansion and that limited horizontal transfers between hypervirulent *K. pneumoniae* isolates probably resulted from the absence of known genes involved in conjugation. Phylogenetic tree analysis also showed 5 groups based on virulence gene synteny, with the predominant group typified by pLVPK (Figure 1, panel B). Because plasmids of ST23-like hypervirulent *K. pneumoniae* all share a similar synteny of virulence genes, ST86 hypervirulent *K. pneumoniae* contains a diversity of plasmid synteny groups (Figure 1, panel A), suggesting that rearrangements of virulence genes occurred several times along plasmid evolution at rearrangement hotspots active in non-ST23 genetic background. For example, pVIR-Kpn2166 and pVIR-Kpn154 differed from reference plasmid pLVPK by the permutations in the ≈100-kb region flanked by IS5 mobile elements (Figure 1, panel C). pVIR-Kpn154 contained an additional copy of IS5, which was associated with another ≈30-kb permutation + translation event, suggesting that IS5 is a key factor in the evolution and diversity of hypervirulent *K. pneumoniae* plasmids.

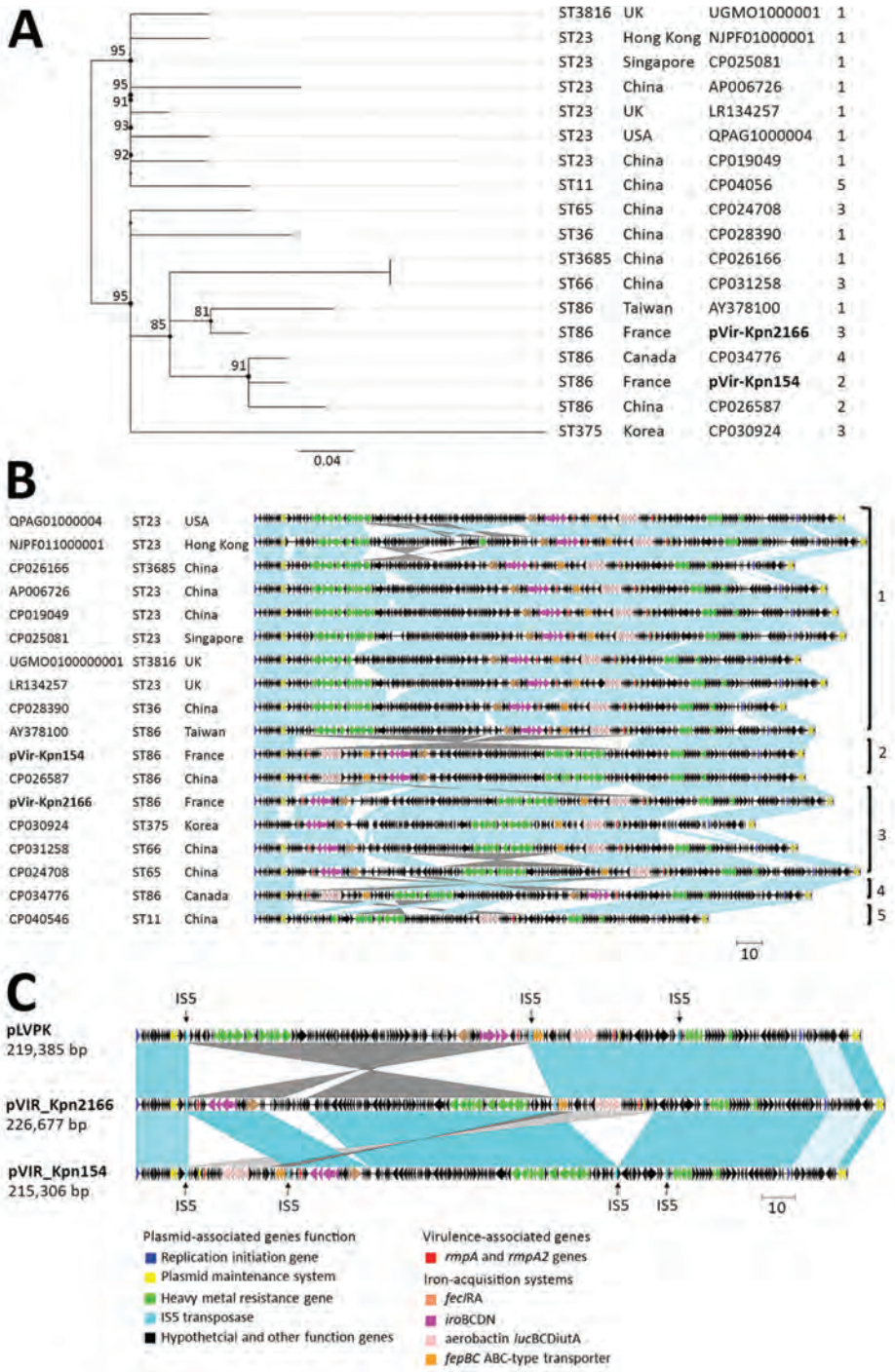


**Figure 1.** Comparison of pVIR-Kpn2166 and pVIR-Kpn154 *Klebsiella pneumoniae* isolates from 2 patients in France (bold) with 16 hypervirulent *K. pneumoniae* virulence plasmids recovered from the PATRIC database (http://www.patricbrc.org). A) Single-nucleotide polymorphism–based phylogenetic tree built by RaxML from an alignment generated by Burrows-Wheeler Aligner and filtered to remove recombination using Gubbins as previously described (*9*). The ST and the geographic origin of bacterial hosts are shown. Scale bar indicates mean number of nucleotide substitutions per site. B) Synteny analysis of hypervirulent *K. pneumoniae* virulence plasmids based on data from blastn (https://blast.ncbi.nlm.nih.gov/Blast.cgi). Virulence-based synteny groups are indicated and the operons encoding the virulence factors, virulence synteny groups of plasmids and the ST and the geographic origin of bacterial hosts. Scale bar indicates kbp. C) Comparison of the details of rearrangements observed in pVIR-Kpn2166 and pVIR-Kpn154 and in pLVPK. Scale bar indicates kbp. ST, sequence type.

The chromosome of Kpn154 and Kpn2166 exhibited similar organization but differed by 128 insertion/deletion mutations and 1,928 single-nucleotide variants (Appendix Figures 2, 3). The Kpn154 chromosome-mediated *ybt* virulence locus, which encodes the yersiniabactin, was located in the integrative conjugative element ICE*Kp3* and was typed ybST202–1LV (*6*). In Kpn2166, *ybt* was located in an original isoform of ICE*Kp12*, presenting an ≈34-kb deletion compared to the canonical 97,771-bp ICE*Kp12*, and was typed ybST13–1LV (*6*).

Although Kpn154 and Kpn2166 have the same genetic background and share the same virulence score (*6*), they also have allelic and synteny differences in virulence genes. We therefore compared the virulence of these isolates in a sepsis model based on outbred

mice challenged intraperitoneally, as described (Figure 2) (*10*). Mice injected with $10^3$ CFUs of Kpn154 or hypervirulent *K. pneumoniae* reference strain *K. pneumoniae* NTUH-2044 died in <72 h, in contrast to mice inoculated with Kpn2166 or American Type Culture Collection (ATCC) 13883, showing that only isolate Kpn154 is hypervirulent. Higher bacterial doses ($10^6$ and $10^8$ CFUs) of ATCC13883 and Kpn2166 did not lead to mouse lethality, confirming that Kpn2166 is not hypervirulent in this model, despite harboring all genetic attributes of hypervirulent *K. pneumoniae* except a functional *rmpA2* gene and allelic variants of siderophore-encoding genes.

We assessed the production of siderophores in Kpn154, Kpn2166 and the control strains as described (*11*). Although the siderophore production of the nonvirulent strain ATCC13883 (mean 30.2 ± SD 1.8 μg/mL) was at the previously reported rate predicting hypervirulent *K. pneumoniae* phenotype (≥30 μg/mL), the other strains produced significantly higher siderophore levels (107.2 ± 4.5 μg/mL to 306.7 ± 20.2 μg/mL; Bonferroni-adjusted p = 0.0035 by Mann-Whitney test), with Kpn154 producing at the lower level (Appendix Figure 4).

## Conclusions

Our results show that a hypermucoviscous K2-ST86 strain can be avirulent in a sepsis mouse model and that hypervirulence cannot be clearly explained by siderophore production alone. Gene *rmpA2*, not required for the hypermucoviscosity phenotype as previously observed (*12*), might be required for hypervirulent phenotype because it is a main, but not the only, difference we observed between the ST86-K2 strains. Finally, these results highlight the importance of in vivo virulence investigation to identify hypervirulent *K. pneumoniae*, especially in the absence of an appropriate clinical scenario.

The threat of hypervirulent *K. pneumoniae* acquiring carbapenem resistance is becoming a reality in Asia, especially in China, where hypervirulence prevalence among carbapenem-resistant *K. pneumoniae* is 7.4%–15% (*5*). Most resistant isolates are non-K1/K2-ST11 and produce carbapenemase KPC-2;. they result from the transfer of the pLVPK-like plasmid into ST11 classical multidrug-resistant *K. pneumoniae* isolates, as observed in the 2 cases reported outside China (*5*). Inversely, the carbapenemase-producing isolate Kpn154 results from the transformation of K2-ST86 hypervirulent *K. pneumoniae* by plasmid encoding carbapenemase OXA-48, the most prevalent carbapenemase in France. Similar events occurred with the KPC-2 K2-ST86 isolate recently reported in Canada (*13*) and a few KPC-2 and NDM K1-ST23 cases documented in China and recently in the United States and United Kingdom (*5*,*14*,*15*). The combination of multidrug resistance and enhanced virulence has the potential to trigger the next clinical crisis and cause severe and untreatable infections in previously healthy persons.

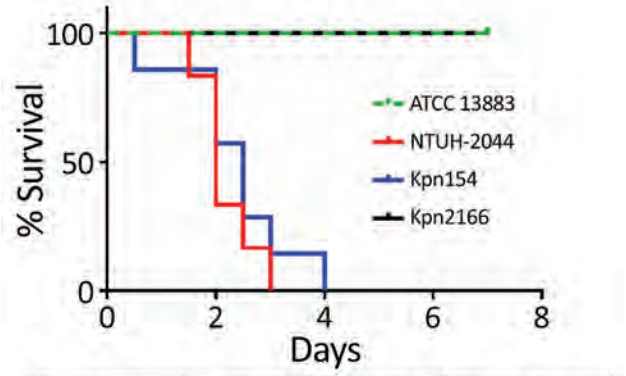


| p values | Kpn154 | Kpn2166 | NTUH-K2044 |
|---|---|---|---|
| Kpn2166 | 0.0004 | | |
| NTUH-K2044 | 0.4209 | 0.0005 | |
| ATCC 13883 | 0.0004 | 0.9999 | 0.0005 |

**Figure 2.** Kaplan–Meier survival curves of mice intraperitoneally challenged with *Klebsiella pneumoniae* strains Kpn154 and Kpn2166 from 2 patients in France, virulent strain NTUH-K2044, and nonvirulent ATCC 13883 strain, as previously described (*10*). Mice were injected with $10^3$ CFUs and monitored for 96 h. p values were calculated from the Mantel-Cox log rank test for survival curve comparison. Gray shading indicates significant values. ATCC, American Type Culture Collection.

### Acknowledgments

We thank Alexis Pontvianne and Lucie Pourpuech for their technical assistance.

This work was supported by the Ministere de l'Education Nationale, de l'Enseignement Superieur et de la Recherche, Institut National de la Santé et de la Recherche Médicale (UMR1071), INRA (USC-2018), Santé Publique France, and the Centre Hospitalier Regional Universitaire de Clermont-Ferrand, France.

### About the Author

Dr. Beyrouthy is a microbiologist in the Associated French National Reference Center for Antibiotic Resistance, Clermont-Ferrand, Clermont-Ferrand University Hospital, and a member of the Microbe, Intestine, Inflammation and Host Susceptibility (M2ISH) research group of the Institut National de la Santé et de la Recherche Médicale. Her primary research interests are antimicrobial drug resistance and *Enterobacteriaceae* epidemiology.

## References


1. Meatherall BL, Gregson D, Ross T, Pitout JDD, Laupland KB. Incidence, risk factors, and outcomes of *Klebsiella pneumoniae* bacteremia. Am J Med. 2009;122:866–73. https://doi.org/10.1016/j.amjmed.2009.03.034
2. Wyres KL, Wick RR, Judd LM, Froumine R, Tokolyi A, Gorrie CL, et al. Distinct evolutionary dynamics of horizontal gene transfer in drug resistant and virulent clones of *Klebsiella pneumoniae*. PLoS Genet. 2019;15:e1008114. https://doi.org/10.1371/journal.pgen.1008114
3. Prokesch BC, TeKippe M, Kim J, Raj P, TeKippe EME, Greenberg DE. Primary osteomyelitis caused by hypervirulent *Klebsiella pneumoniae*. Lancet Infect Dis. 2016; 16:e190–5. https://doi.org/10.1016/S1473-3099(16)30021-4
4. Shon AS, Bajwa RPS, Russo TA. Hypervirulent (hypermucoviscous) *Klebsiella pneumoniae*: a new and dangerous breed. Virulence. 2013;4:107–18. https://doi.org/10.4161/viru.22718
5. Lee CR, Lee JH, Park KS, Jeon JH, Kim YB, Cha CJ, et al. Antimicrobial resistance of hypervirulent *Klebsiella pneumoniae*: epidemiology, hypervirulence-associated determinants, and resistance mechanisms. Front Cell Infect Microbiol. 2017;7:483. https://doi.org/10.3389/fcimb.2017.00483
6. Lam MMC, Wick RR, Wyres KL, Gorrie CL, Judd LM, Jenney AWJ, et al. Genetic diversity, mobilisation and spread of the yersiniabactin-encoding mobile element ICEKp in *Klebsiella pneumoniae* populations. Microb Genom. 2018;4(9).
7. Villa L, Feudi C, Fortini D, García-Fernández A, Carattoli A. Genomics of KPC-producing *Klebsiella pneumoniae* sequence type 512 clone highlights the role of RamR and ribosomal S10 protein mutations in conferring tigecycline resistance. Antimicrob Agents Chemother. 2014;58:1707–12. https://doi.org/10.1128/AAC.01803-13
8. Chen YT, Chang HY, Lai YC, Pan CC, Tsai SF, Peng HL. Sequencing and analysis of the large virulence plasmid pLVPK of *Klebsiella pneumoniae* CG43. Gene. 2004;337:189–98. https://doi.org/10.1016/j.gene.2004.05.008
9. Beyrouthy R, Barets M, Marion E, Dananché C, Dauwalder O, Robin F, et al. Novel enterobacter lineage as leading cause of nosocomial outbreak involving carbapenemase-producing strains. Emerg Infect Dis. 2018;24:1505–15. https://doi.org/10.3201/eid2408.180151
10. Beyrouthy R, Robin F, Cougnoux A, Dalmasso G, Darfeuille-Michaud A, Mallat H, et al. Chromosome-mediated OXA-48 carbapenemase in highly virulent *Escherichia coli*. J Antimicrob Chemother. 2013;68:1558–61. https://doi.org/10.1093/jac/dkt051
11. Russo TA, Olson R, Fang CT, Stoesser N, Miller M, MacDonald U, et al. Identification of biomarkers for differentiation of hypervirulent *Klebsiella pneumoniae* from classical *K. pneumoniae*. J Clin Microbiol. 2018;56:1–12. https://doi.org/10.1128/JCM.00776-18
12. Hsu CR, Lin TL, Chen YC, Chou HC, Wang JT. The role of *Klebsiella pneumoniae* rmpA in capsular polysaccharide synthesis and virulence revisited. Microbiology. 2011;157: 3446–57. https://doi.org/10.1099/mic.0.050336-0
13. Mataseje LF, Boyd DA, Mulvey MR, Longtin Y. Two hypervirulent *Klebsiella pneumoniae* isolates producing a blaKPC-2 carbapenemase from a Canadian patient. Antimicrob Agents Chemother. 2019;63:1–4. https://doi.org/10.1128/AAC.00517-19
14. Karlsson M, Stanton RA, Ansari U, McAllister G, Chan MY, Sula E, et al. Identification of a carbapenemase-producing hypervirulent *Klebsiella pneumoniae* isolate in the United States. Antimicrob Agents Chemother. 2019;63:1–6. https://doi.org/10.1128/AAC.00519-19
15. Roulston KJ, Bharucha T, Turton JF, Hopkins KL, Mack DJF. A case of NDM-carbapenemase-producing hypervirulent *Klebsiella pneumoniae* sequence type 23 from the UK. JMM Case Rep. 2018;5:e005130. https://doi.org/10.1099/jmmcr.0.005130


Address for correspondence: Racha Beyrouthy, Centre Hospitalier Universitaire, Centre de Biologie, Service de Bactériologie, 58 rue Montalembert, 63000 Clermont-Ferrand, France; email: rbeyrouthy@chu-clermontferrand.fr

# Laboratory-Acquired Dengue Virus Infection, United States, 2018

Tyler M. Sharp, Teresa G. Fisher, Kristin Long, Garry Coulson, Freddy A. Medina, Carolyn Herzig, Mary Beth Koza, Jorge Muñoz-Jordán, Gabriela Paz-Bailey, Zack Moore, Carl Williams

Investigation of a dengue case in a laboratory worker in North Carolina, USA, revealed that the case-patient prepared high-titer dengue virus stocks soon before illness onset. Improper doffing of gloves with an open finger wound likely resulted in cutaneous exposure. This case reinforces recommendations for enhanced precautions when working with high-titer dengue virus.

Four genetically distinct but serologically related dengue viruses (DENV-1–4) cause dengue, an acute febrile illness common throughout the tropics (*1*). DENV is transmitted by *Aedes* mosquitoes and has a median incubation period of 6 days (*2*). Other routes of DENV transmission include perinatal (*3*), blood transfusion (*4*), needle stick (*5*), and laboratory exposure (*6*–*8*).

In August 2018, the North Carolina Department of Health and Human Services (NCDHHS; Raleigh, North Carolina, USA) was notified of a dengue case in a laboratory worker. NCDHHS and CDC conducted an investigation to identify the most likely route of exposure.

## The Study

We interviewed the case-patient and reviewed medical records to collect travel history, potential exposures, clinical course, and diagnostic test results. The case-patient reported no recent travel to an area with ongoing DENV transmission. No travel-associated dengue cases were reported in 2018 from the county where the case-patient worked and resided. The case-patient reported illness onset on July 18, 2018, with retroorbital eye pain, fever, myalgia, arthralgia, lethargy, chills, and lymphadenopathy (Figure 1). By July 23, the case-patient was afebrile but had a whole-body maculopapular rash. The case-patient was evaluated by a physician that day and received a diagnosis of viral illness. After reporting the illness to the institutional occupational health clinic, the case-patient was referred to an infectious disease physician. Upon evaluation 2 days later, vital signs and laboratory values were unremarkable except for leukopenia ($3.3 \times 10^6$ cells/$mm^3$).

Four serum specimens were forwarded to CDC for diagnostic testing: a baseline specimen collected ≈1.5 years before illness onset; an acute specimen collected 7 days after illness onset; an early-convalescent specimen collected ≈1 month after illness onset; and a late-convalescent specimen collected ≈6 months after illness onset (Table). The acute specimen tested positive at a commercial laboratory for detection of nonstructural protein 1 (NS1) antigen and DENV IgM and negative for *Ehrlichia* IgG. At CDC, reverse transcription PCR (*9*) performed on the acute specimen was negative; DENV IgM and IgG were detected (*10*,*11*) in acute and convalescent specimens. In the baseline specimen, neutralizing antibodies were detected for yellow fever virus but not DENV or West Nile virus. Comparison of DENV neutralizing antibody titers in acute, early convalescent, and late convalescent serum specimens confirmed incident DENV infection; however, a ≥4-fold rise in neutralizing antibody titer against multiple DENVs precluded identification of the specific infecting DENV.

We visited the research laboratory where the case-patient worked; the principal investigator and laboratory safety officer described laboratory safety protocols. We reviewed laboratory activities performed by the case-patient in the week before illness onset and interviewed the case-patient regarding practices of donning and doffing personal protective equipment (PPE).

Author affiliations: US Public Health Service, Rockville, Maryland, USA (T.M. Sharp); Centers for Disease Control and Prevention, San Juan, Puerto Rico, USA (T.M. Sharp, F.A. Medina, J. Jorge Muñoz-Jordán, G. Paz-Bailey); North Carolina Department of Health and Human Services, Raleigh, North Carolina, USA (T.G. Fisher, K. Long, C. Herzig, Z. Moore, C. Williams); University of North Carolina at Chapel Hill, Chapel Hill, North Carolina, USA (G. Coulson, M.B. Koza); Centers for Disease Control and Prevention, Atlanta, Georgia, USA (C. Herzig)

DOI: https://doi.org/10.3201/eid2607.191598

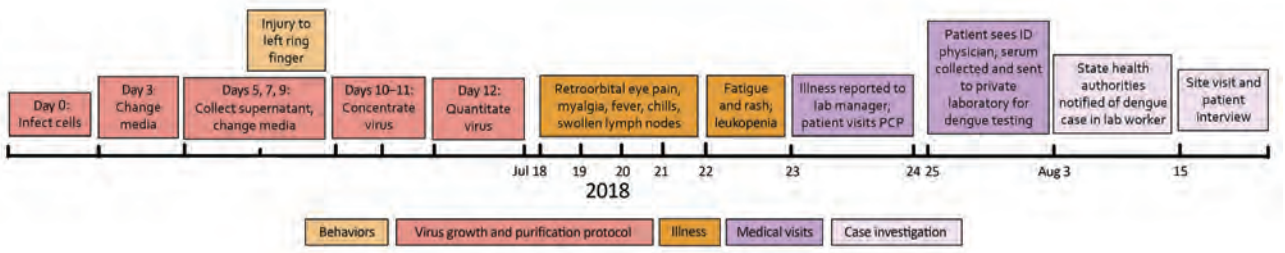


**Figure 1.** Timeline of events surrounding a case of laboratory-acquired dengue virus infection, United States, 2018. ID, infectious disease; PCP, primary care physician.

In the 2 weeks before illness onset, the case-patient reported working with a protocol to grow, purify, and concentrate DENV-4. The case-patient reported wearing a single pair of nitrile gloves, eye protection, a lab coat, and closed-toed shoes while working with infectious virus in a certified biosafety cabinet (BSC).

The protocol for virus production and concentration included inoculating ≈40 roller bottles of Vero cells with ≈$10^6$ plaque-forming units (PFU) of DENV-4 (Figure 1). Media were harvested and pooled on days 5, 7, and 9 postinoculation and concentrated by tangential flow filtration followed by sucrose gradient fractionation. Fractions were collected by piercing the centrifugation tubes and collecting fractions using a safety mechanism that prevented needle sticks. Fractions were separated by sodium dodecyl sulfate polyacrylamide gel electrophoresis and protein concentration determined using a bicinchoninic acid assay. Typical protein concentrations correlated with virus titers of $10^9$–$10^{10}$ PFU/mL. The case-patient also performed neutralization and ELISA assays for DENV-1–4 during the 2 weeks before illness onset.

The case-patient reported that small splashes often occurred during virus production and purification. The case-patient did not change gloves when splashes occurred but occasionally performed surface decontamination of gloves and the BSC with 70% ethanol. The case-patient estimated entering and exiting the BSC 6–8 times per day on most days of the protocol but not being vigilant about handwashing after removing gloves. The case-patient reported taking online Biosafety Level 2 (BSL-2) training upon joining the laboratory, receiving hands-on training for BSL-2 work, and annually reviewing laboratory safety plans and procedures.

The case-patient reported having sustained a compression wound on the ring finger of the left hand on July 9 or 10; the wound later appeared infected and oozing. The case-patient reported not bandaging or covering this wound before donning a single pair of gloves while working on the protocol for virus production and purification. The case-patient demonstrated their technique for doffing gloves (Figure 2): the base of the glove of the left hand was pinched with the thumb and forefinger of the right hand and the glove removed while turning it inside out, after which the base of the glove on the right hand was pinched with the thumb and forefinger of the now ungloved left hand. The case-patient acknowledged that the wound on the ring finger of the left hand could have contacted the potentially contaminated glove on the right hand. The case-patient also mentioned having potentially touched mucosal surfaces of the nose or mouth with the lab coat sleeve while working with infectious virus in the BSC.

## Conclusions

The presence of an open finger wound during work with high-titer DENV coupled with improper glove

**Table**. Summary of diagnostic test results of serum specimens collected from a case-patient with laboratory-acquired DENV infection, United States, 2018*

| Specimen designation | Time of specimen collection† | rRT-PCR | NS1 ELISA | IgM ELISA | DENV IgG ELISA titer | Neutralizing antibody titer | | | | | |
|---|---|---|---|---|---|---|---|---|---|---|---|
| | | | | | | DENV-1 | DENV-2 | DENV-3 | DENV-4 | WNV | YFV |
| Baseline‡ | −1.5 y | NT | NT | NT | 1:40 | <20 | <20 | <20 | <20 | <20 | 40 |
| Acute‡ | 7 d | Neg | Pos | Pos | 1:163,840 | <80 | 160 | 640 | 640 | <80 | 160 |
| Early convalescent‡ | 28 d | NT | NT | Pos | 1:163,840 | 80 | 640 | 1280 | 320 | 40 | 80 |
| Late convalescent§ | 190 d | NT | NT | Pos | 1:40,960 | 40 | <20 | 160 | 160 | NT | NT |

*DENV, dengue virus; IgM ELISA, anti-DENV IgM antibody capture enzyme linked immunosorbent assay; NS1 ELISA, nonstructural protein 1 ELISA; NT, not tested; rRT-PCR, real-time reverse transcription PCR; WNV, West Nile virus; YFV, yellow fever virus.
†Relative to illness onset.
‡Neutralizing antibody titers obtained by 90% plaque reduction neutralization test.
§Neutralizing antibody titers obtained by recombinant microfluorescence reduction neutralization test.

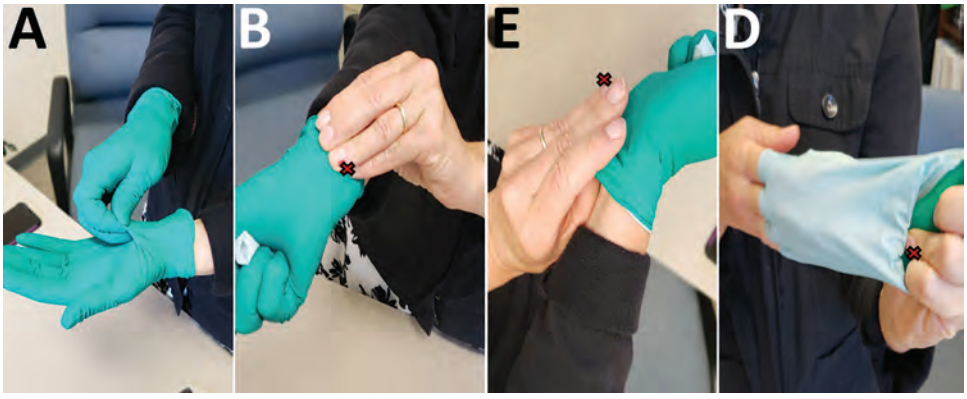


**Figure 2.** Depiction of improper protocol for doffing gloves the case-patient reported using while conducting a protocol for growth and purification of high-titer dengue virus, United States, 2018. The red X indicates the location of an open wound on the ring finger of the case-patient's left hand.

doffing suggests that laboratory-acquired infection by cutaneous exposure was the most likely route of DENV infection in this case. However, other routes of exposure, including mucosal, could not be ruled out.

Three previous cases of laboratory-associated DENV infection have been reported. In Nigeria, a laboratorian responsible for cleaning cages and disposing of mice infected with DENV-1 became infected, although mosquito-borne transmission could not be ruled out (*6*). A laboratorian in Australia was infected while working with DENV-2 (*7*), although it could not be determined if infection occurred from a bite from an infected mosquito in the laboratory or potential mucocutaneous exposure while working with infectious virus. In South Korea, a laboratorian was infected with DENV-2 following a needle stick injury while filtering cell cultures of DENV-2 (*8*).

In this case, detection of NS1 antigen independently confirmed acute DENV infection, supported by detection of DENV IgM and >4-fold rise in DENV IgG and DENV neutralizing antibody. However, historic exposure to ≥1 flavivirus complicated interpretation of neutralizing antibody titers and precluded identification of the infecting DENV. Moreover, we could not rule out infection with DENV between collection of the baseline and acute specimens. The difficulty interpreting flavivirus neutralizing antibody patterns during secondary infections is well described (*12*).

A study in Belgium conducted during 2007–2012 found that only 40% of laboratory-associated infections occurred following a known exposure event; a definitive cause of exposure could not be identified in nearly one third of cases associated with bloodborne pathogens (*13*). Thus, laboratory-acquired infections, including those with DENV, likely occur more frequently than have been documented.

Titers of infectious DENV in human blood resulting from mosquito-borne transmission are typically $10^3$–$10^7$ PFU/mL (*14*). At $10^9$–$10^{10}$ PFU/mL, the concentration of DENV the case-patient handled would have been 100 to 10 million times higher than the concentration found in the average blood specimen of a patient with DENV infection. Although BSL-2 containment is recommended for laboratory work with DENV, enhanced safety precautions including double-gloving are recommended when handling large-scale or high-titer virus (*15*). This investigation highlights the importance of developing and maintaining risk assessment and management programs to mitigate exposures to infectious agents and emphasizing good microbiological practices and procedures training for laboratorians, including proper PPE donning and doffing techniques.

## Acknowledgments

We thank the case-patient, laboratory director, and laboratory safety manager for their support of this investigation. We also thank North Carolina State Laboratory of Public Health Special Serology staff for assistance with transport of specimens to CDC for diagnostic testing.

Financial support for this investigation was provided by NCDHHS and CDC.

## About the Author

Dr. Sharp is a health scientist in the National Center for Emerging and Zoonotic Infectious Diseases, the Centers for Disease Control and Prevention, San Juan, Puerto Rico, USA. His public health and research interests are the epidemiology and pathophysiology of emerging tropical infectious diseases.

## References

1. Simmons CP, Farrar JJ, van Vinh Chau N, Wills B. Dengue. N Engl J Med. 2012;366:1423–32. https://doi.org/10.1056/NEJMra1110265
2. Chan M, Johansson MA. The incubation periods of dengue viruses. PLoS One. 2012;7:e50972. https://doi.org/10.1371/journal.pone.0050972

# Laboratory-Acquired Dengue Virus Infection, United States, 2018

Tyler M. Sharp, Teresa G. Fisher, Kristin Long, Garry Coulson, Freddy A. Medina, Carolyn Herzig, Mary Beth Koza, Jorge Muñoz-Jordán, Gabriela Paz-Bailey, Zack Moore, Carl Williams

Investigation of a dengue case in a laboratory worker in North Carolina, USA, revealed that the case-patient prepared high-titer dengue virus stocks soon before illness onset. Improper doffing of gloves with an open finger wound likely resulted in cutaneous exposure. This case reinforces recommendations for enhanced precautions when working with high-titer dengue virus.

Four genetically distinct but serologically related dengue viruses (DENV-1–4) cause dengue, an acute febrile illness common throughout the tropics (*1*). DENV is transmitted by *Aedes* mosquitoes and has a median incubation period of 6 days (*2*). Other routes of DENV transmission include perinatal (*3*), blood transfusion (*4*), needle stick (*5*), and laboratory exposure (*6*–*8*).

In August 2018, the North Carolina Department of Health and Human Services (NCDHHS; Raleigh, North Carolina, USA) was notified of a dengue case in a laboratory worker. NCDHHS and CDC conducted an investigation to identify the most likely route of exposure.

## The Study

We interviewed the case-patient and reviewed medical records to collect travel history, potential exposures, clinical course, and diagnostic test results. The case-patient reported no recent travel to an area with ongoing DENV transmission. No travel-associated dengue cases were reported in 2018 from the county where the case-patient worked and resided. The case-patient reported illness onset on July 18, 2018, with retroorbital eye pain, fever, myalgia, arthralgia, lethargy, chills, and lymphadenopathy (Figure 1). By July 23, the case-patient was afebrile but had a whole-body maculopapular rash. The case-patient was evaluated by a physician that day and received a diagnosis of viral illness. After reporting the illness to the institutional occupational health clinic, the case-patient was referred to an infectious disease physician. Upon evaluation 2 days later, vital signs and laboratory values were unremarkable except for leukopenia ($3.3 \times 10^6$ cells/$mm^3$).

Four serum specimens were forwarded to CDC for diagnostic testing: a baseline specimen collected ≈1.5 years before illness onset; an acute specimen collected 7 days after illness onset; an early-convalescent specimen collected ≈1 month after illness onset; and a late-convalescent specimen collected ≈6 months after illness onset (Table). The acute specimen tested positive at a commercial laboratory for detection of nonstructural protein 1 (NS1) antigen and DENV IgM and negative for *Ehrlichia* IgG. At CDC, reverse transcription PCR (*9*) performed on the acute specimen was negative; DENV IgM and IgG were detected (*10*,*11*) in acute and convalescent specimens. In the baseline specimen, neutralizing antibodies were detected for yellow fever virus but not DENV or West Nile virus. Comparison of DENV neutralizing antibody titers in acute, early convalescent, and late convalescent serum specimens confirmed incident DENV infection; however, a ≥4-fold rise in neutralizing antibody titer against multiple DENVs precluded identification of the specific infecting DENV.

We visited the research laboratory where the case-patient worked; the principal investigator and laboratory safety officer described laboratory safety protocols. We reviewed laboratory activities performed by the case-patient in the week before illness onset and interviewed the case-patient regarding practices of donning and doffing personal protective equipment (PPE).

Author affiliations: US Public Health Service, Rockville, Maryland, USA (T.M. Sharp); Centers for Disease Control and Prevention, San Juan, Puerto Rico, USA (T.M. Sharp, F.A. Medina, J. Jorge Muñoz-Jordán, G. Paz-Bailey); North Carolina Department of Health and Human Services, Raleigh, North Carolina, USA (T.G. Fisher, K. Long, C. Herzig, Z. Moore, C. Williams); University of North Carolina at Chapel Hill, Chapel Hill, North Carolina, USA (G. Coulson, M.B. Koza); Centers for Disease Control and Prevention, Atlanta, Georgia, USA (C. Herzig)

DOI: https://doi.org/10.3201/eid2607.191598

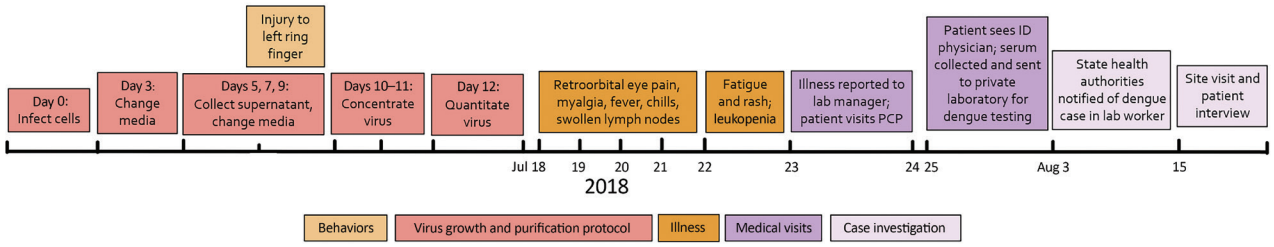


**Figure 1.** Timeline of events surrounding a case of laboratory-acquired dengue virus infection, United States, 2018. ID, infectious disease; PCP, primary care physician.

In the 2 weeks before illness onset, the case-patient reported working with a protocol to grow, purify, and concentrate DENV-4. The case-patient reported wearing a single pair of nitrile gloves, eye protection, a lab coat, and closed-toed shoes while working with infectious virus in a certified biosafety cabinet (BSC).

The protocol for virus production and concentration included inoculating ≈40 roller bottles of Vero cells with ≈$10^6$ plaque-forming units (PFU) of DENV-4 (Figure 1). Media were harvested and pooled on days 5, 7, and 9 postinoculation and concentrated by tangential flow filtration followed by sucrose gradient fractionation. Fractions were collected by piercing the centrifugation tubes and collecting fractions using a safety mechanism that prevented needle sticks. Fractions were separated by sodium dodecyl sulfate polyacrylamide gel electrophoresis and protein concentration determined using a bicinchoninic acid assay. Typical protein concentrations correlated with virus titers of $10^9$–$10^{10}$ PFU/mL. The case-patient also performed neutralization and ELISA assays for DENV-1–4 during the 2 weeks before illness onset.

The case-patient reported that small splashes often occurred during virus production and purification. The case-patient did not change gloves when splashes occurred but occasionally performed surface decontamination of gloves and the BSC with 70% ethanol. The case-patient estimated entering and exiting the BSC 6–8 times per day on most days of the protocol but not being vigilant about handwashing after removing gloves. The case-patient reported taking online Biosafety Level 2 (BSL-2) training upon joining the laboratory, receiving hands-on training for BSL-2 work, and annually reviewing laboratory safety plans and procedures.

The case-patient reported having sustained a compression wound on the ring finger of the left hand on July 9 or 10; the wound later appeared infected and oozing. The case-patient reported not bandaging or covering this wound before donning a single pair of gloves while working on the protocol for virus production and purification. The case-patient demonstrated their technique for doffing gloves (Figure 2): the base of the glove of the left hand was pinched with the thumb and forefinger of the right hand and the glove removed while turning it inside out, after which the base of the glove on the right hand was pinched with the thumb and forefinger of the now ungloved left hand. The case-patient acknowledged that the wound on the ring finger of the left hand could have contacted the potentially contaminated glove on the right hand. The case-patient also mentioned having potentially touched mucosal surfaces of the nose or mouth with the lab coat sleeve while working with infectious virus in the BSC.

## Conclusions

The presence of an open finger wound during work with high-titer DENV coupled with improper glove

**Table**. Summary of diagnostic test results of serum specimens collected from a case-patient with laboratory-acquired DENV infection, United States, 2018*

| Specimen designation | Time of specimen collection† | rRT-PCR | NS1 ELISA | IgM ELISA | DENV IgG ELISA titer | Neutralizing antibody titer | | | | | |
|---|---|---|---|---|---|---|---|---|---|---|---|
| | | | | | | DENV-1 | DENV-2 | DENV-3 | DENV-4 | WNV | YFV |
| Baseline‡ | −1.5 y | NT | NT | NT | 1:40 | <20 | <20 | <20 | <20 | <20 | 40 |
| Acute‡ | 7 d | Neg | Pos | Pos | 1:163,840 | <80 | 160 | 640 | 640 | <80 | 160 |
| Early convalescent‡ | 28 d | NT | NT | Pos | 1:163,840 | 80 | 640 | 1280 | 320 | 40 | 80 |
| Late convalescent§ | 190 d | NT | NT | Pos | 1:40,960 | 40 | <20 | 160 | 160 | NT | NT |

*DENV, dengue virus; IgM ELISA, anti-DENV IgM antibody capture enzyme linked immunosorbent assay; NS1 ELISA, nonstructural protein 1 ELISA; NT, not tested; rRT-PCR, real-time reverse transcription PCR; WNV, West Nile virus; YFV, yellow fever virus.
†Relative to illness onset.
‡Neutralizing antibody titers obtained by 90% plaque reduction neutralization test.
§Neutralizing antibody titers obtained by recombinant microfluorescence reduction neutralization test.

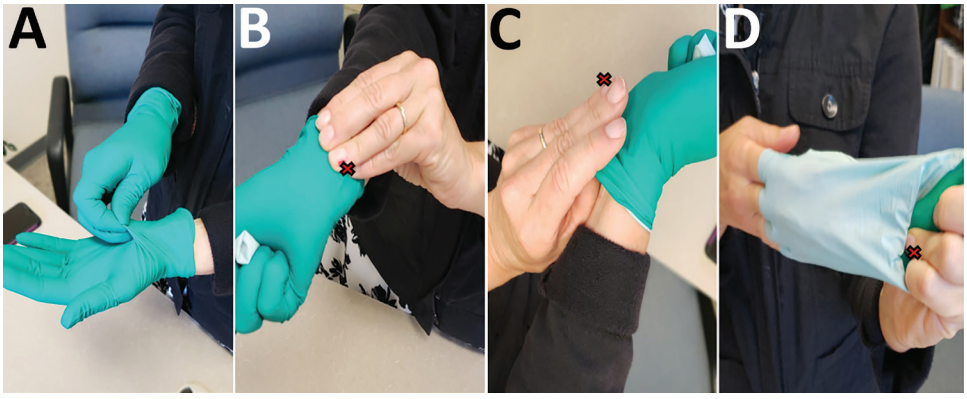


**Figure 2.** Depiction of improper protocol for doffing gloves the case-patient reported using while conducting a protocol for growth and purification of high-titer dengue virus, United States, 2018. The red X indicates the location of an open wound on the ring finger of the case-patient's left hand.

doffing suggests that laboratory-acquired infection by cutaneous exposure was the most likely route of DENV infection in this case. However, other routes of exposure, including mucosal, could not be ruled out.

Three previous cases of laboratory-associated DENV infection have been reported. In Nigeria, a laboratorian responsible for cleaning cages and disposing of mice infected with DENV-1 became infected, although mosquito-borne transmission could not be ruled out (*6*). A laboratorian in Australia was infected while working with DENV-2 (*7*), although it could not be determined if infection occurred from a bite from an infected mosquito in the laboratory or potential mucocutaneous exposure while working with infectious virus. In South Korea, a laboratorian was infected with DENV-2 following a needle stick injury while filtering cell cultures of DENV-2 (*8*).

In this case, detection of NS1 antigen independently confirmed acute DENV infection, supported by detection of DENV IgM and >4-fold rise in DENV IgG and DENV neutralizing antibody. However, historic exposure to ≥1 flavivirus complicated interpretation of neutralizing antibody titers and precluded identification of the infecting DENV. Moreover, we could not rule out infection with DENV between collection of the baseline and acute specimens. The difficulty interpreting flavivirus neutralizing antibody patterns during secondary infections is well described (*12*).

A study in Belgium conducted during 2007–2012 found that only 40% of laboratory-associated infections occurred following a known exposure event; a definitive cause of exposure could not be identified in nearly one third of cases associated with bloodborne pathogens (*13*). Thus, laboratory-acquired infections, including those with DENV, likely occur more frequently than have been documented.

Titers of infectious DENV in human blood resulting from mosquito-borne transmission are typically $10^3$–$10^7$ PFU/mL (*14*). At $10^9$–$10^{10}$ PFU/mL, the concentration of DENV the case-patient handled would have been 100 to 10 million times higher than the concentration found in the average blood specimen of a patient with DENV infection. Although BSL-2 containment is recommended for laboratory work with DENV, enhanced safety precautions including double-gloving are recommended when handling large-scale or high-titer virus (*15*). This investigation highlights the importance of developing and maintaining risk assessment and management programs to mitigate exposures to infectious agents and emphasizing good microbiological practices and procedures training for laboratorians, including proper PPE donning and doffing techniques.

## Acknowledgments

We thank the case-patient, laboratory director, and laboratory safety manager for their support of this investigation. We also thank North Carolina State Laboratory of Public Health Special Serology staff for assistance with transport of specimens to CDC for diagnostic testing.

Financial support for this investigation was provided by NCDHHS and CDC.

## About the Author

Dr. Sharp is a health scientist in the National Center for Emerging and Zoonotic Infectious Diseases, the Centers for Disease Control and Prevention, San Juan, Puerto Rico, USA. His public health and research interests are the epidemiology and pathophysiology of emerging tropical infectious diseases.

## References

1. Simmons CP, Farrar JJ, van Vinh Chau N, Wills B. Dengue. N Engl J Med. 2012;366:1423–32. https://doi.org/10.1056/NEJMra1110265
2. Chan M, Johansson MA. The incubation periods of dengue viruses. PLoS One. 2012;7:e50972. https://doi.org/10.1371/journal.pone.0050972

3. Sirinavin S, Nuntnarumit P, Supapannachart S, Boonkasidecha S, Techasaensiri C, Yoksarn S. Vertical dengue infection: case reports and review. Pediatr Infect Dis J. 2004;23:1042–7. https://doi.org/10.1097/01.inf.0000143644.95692.0e
4. Tomashek KM, Margolis HS. Dengue: a potential transfusion-transmitted disease. Transfusion. 2011;51:1654–60. https://doi.org/10.1111/j.1537-2995.2011.03269.x
5. Ohnishi K. Needle-stick dengue virus infection in a health-care worker at a Japanese hospital. J Occup Health. 2015;57:482–3. https://doi.org/10.1539/joh.14-0224-CS
6. Tomori O, Monath TP, O'Connor EH, Lee VH, Cropp CB. Arbovirus infections among laboratory personnel in Ibadan, Nigeria. Am J Trop Med Hyg. 1981;30:855–61. https://doi.org/10.4269/ajtmh.1981.30.855
7. Britton S, van den Hurk AF, Simmons RJ, Pyke AT, Northill JA, McCarthy J, et al. Laboratory-acquired dengue virus infection—a case report. PLoS Negl Trop Dis. 2011;5:e1324. https://doi.org/10.1371/journal.pntd.0001324.
8. Lee C, Jang EJ, Kwon D, Choi H, Park JW, Bae GR. Laboratory-acquired dengue virus infection by needlestick injury: a case report, South Korea, 2014. Ann Occup Environ Med. 2016;28:16. https://doi.org/10.1186/s40557-016-0104-5
9. Santiago GA, Vazquez J, Courtney S, Matias KY, Andersen LE, Colon C, et al. Performance of the Trioplex real-time RT-PCR assay for detection of Zika, dengue, and chikungunya viruses. Nat Comm. 2018;9:1391. https://doi.org/10.1038/s41467-018-03772-1
10. Johnson AJ, Martin DA, Karabatsos N, Roehrig JT. Detection of anti-arboviral immunoglobulin G by using a monoclonal antibody-based capture enzyme-linked immunosorbent assay. J Clin Microbiol. 2000;38:1827–31.
11. Martin DA, Muth DA, Brown T, Johnson AJ, Karabatsos N, Roehrig JT. Standardization of immunoglobulin M capture enzyme-linked immunosorbent assays for routine diagnosis of arboviral infections. J Clin Microbiol. 2000;38:1823–6.
12. Calisher CH, Karabatsos N, Dalrymple JM, Shope RE, Porterfield JS, Westaway EG, et al. Antigenic relationships between flaviviruses as determined by cross-neutralization tests with polyclonal antisera. J Gen Virol. 1989;70:37–43. http://dx.doi.org/10.1099/0022-1317-70-1-37
13. Willemarck NAJ, Van Vaerenbergh B, Descamps E, Brosius B, Dai Do Thi C, Amaya L, et al. Laboratory-acquired infections in Belgium (2007–2012). Brussels: Institut Scientifique de Sante Publique; 2015.
14. Moi ML, Lim CK, Kotaki A, Takasaki T, Kurane I. Detection of higher levels of dengue viremia using FcγR-expressing BHK-21 cells than FcγR-negative cells in secondary infection but not in primary infection. J Infect Dis. 2011;203:1405–14. https://doi.org/10.1093/infdis/jir053
15. US Department of Health and Human Services. Biosafety in microbiological and biomedical laboratories, 5th ed. Washington (DC): The Department; 2009.


Address for correspondence: Carl Williams, North Carolina Department of Health and Human Services, 1902 Mail Service Center, Raleigh, NC 27699-1902; email: carl.williams@dhhs.nc.gov

3. Sirinavin S, Nuntnarumit P, Supapannachart S, Boonkasidecha S, Techasaensiri C, Yoksarn S. Vertical dengue infection: case reports and review. Pediatr Infect Dis J. 2004;23:1042–7. https://doi.org/10.1097/01.inf.0000143644.95692.0e
4. Tomashek KM, Margolis HS. Dengue: a potential transfusion-transmitted disease. Transfusion. 2011;51:1654–60. https://doi.org/10.1111/j.1537-2995.2011.03269.x
5. Ohnishi K. Needle-stick dengue virus infection in a health-care worker at a Japanese hospital. J Occup Health. 2015;57:482–3. https://doi.org/10.1539/joh.14-0224-CS
6. Tomori O, Monath TP, O'Connor EH, Lee VH, Cropp CB. Arbovirus infections among laboratory personnel in Ibadan, Nigeria. Am J Trop Med Hyg. 1981;30:855–61. https://doi.org/10.4269/ajtmh.1981.30.855
7. Britton S, van den Hurk AF, Simmons RJ, Pyke AT, Northill JA, McCarthy J, et al. Laboratory-acquired dengue virus infection—a case report. PLoS Negl Trop Dis. 2011;5:e1324. https://doi.org/10.1371/journal.pntd.0001324.
8. Lee C, Jang EJ, Kwon D, Choi H, Park JW, Bae GR. Laboratory-acquired dengue virus infection by needlestick injury: a case report, South Korea, 2014. Ann Occup Environ Med. 2016;28:16. https://doi.org/10.1186/s40557-016-0104-5
9. Santiago GA, Vazquez J, Courtney S, Matias KY, Andersen LE, Colon C, et al. Performance of the Trioplex real-time RT-PCR assay for detection of Zika, dengue, and chikungunya viruses. Nat Comm. 2018;9:1391. https://doi.org/10.1038/s41467-018-03772-1
10. Johnson AJ, Martin DA, Karabatsos N, Roehrig JT. Detection of anti-arboviral immunoglobulin G by using a monoclonal antibody-based capture enzyme-linked immunosorbent assay. J Clin Microbiol. 2000;38:1827–31.
11. Martin DA, Muth DA, Brown T, Johnson AJ, Karabatsos N, Roehrig JT. Standardization of immunoglobulin M capture enzyme-linked immunosorbent assays for routine diagnosis of arboviral infections. J Clin Microbiol. 2000;38:1823–6.
12. Calisher CH, Karabatsos N, Dalrymple JM, Shope RE, Porterfield JS, Westaway EG, et al. Antigenic relationships between flaviviruses as determined by cross-neutralization tests with polyclonal antisera. J Gen Virol. 1989;70:37–43. http://dx.doi.org/10.1099/0022-1317-70-1-37
13. Willemarck NAJ, Van Vaerenbergh B, Descamps E, Brosius B, Dai Do Thi C, Amaya L, et al. Laboratory-acquired infections in Belgium (2007–2012). Brussels: Institut Scientifique de Sante Publique; 2015.
14. Moi ML, Lim CK, Kotaki A, Takasaki T, Kurane I. Detection of higher levels of dengue viremia using FcγR-expressing BHK-21 cells than FcγR-negative cells in secondary infection but not in primary infection. J Infect Dis. 2011;203:1405–14. https://doi.org/10.1093/infdis/jir053
15. US Department of Health and Human Services. Biosafety in microbiological and biomedical laboratories, 5th ed. Washington (DC): The Department; 2009.


Address for correspondence: Carl Williams, North Carolina Department of Health and Human Services, 1902 Mail Service Center, Raleigh, NC 27699-1902; email: carl.williams@dhhs.nc.gov

# Linking Epidemiology and Whole-Genome Sequencing to Investigate *Salmonella* Outbreak, Massachusetts, USA, 2018

Eric L. Vaughn,[1] Quynh T. Vo,[1] Johanna Vostok, Tracy Stiles, Andrew Lang, Catherine M. Brown, R. Monina Klevens, Lawrence Madoff

Cross-discipline collaboration among state and local health departments improved foodborne illness surveillance for a 2018 *Salmonella enterica* serovar Enteritidis outbreak in Massachusetts, USA. Prompt linking of epidemiologic and laboratory data and implementation of in-state whole-genome sequencing and analysis improved public health surveillance capacity for outbreak detection and control.

Nontyphoidal salmonellae are among the most ubiquitous pathogens associated with foodborne illness worldwide (*1*). Salmonellosis detection is of public health value because of the ease with which the pathogen is transmitted (*2*), increased pathogen antimicrobial drug resistance (*3*), and high morbidity rates (*4*). Detection of *Salmonella* in a Massachusetts resident is reportable to the Massachusetts Department of Public Health (MDPH), and submission of isolates to the MDPH State Public Health Laboratory (SPHL) is mandatory. From 2014 through 2018, an average of 1,200 confirmed cases of *Salmonella* infection in Massachusetts residents were reported each year. Since 1996, MDPH has used pulsed-field gel electrophoresis (PFGE) to identify local clusters and report isolate patterns to the Centers for Disease Control and Prevention (CDC) PulseNet network (https://www.cdc.gov/pulsenet/index.html). Increasingly, public health laboratories are using whole-genome sequencing (WGS) to identify unique strains and outbreaks. MDPH began using WGS in 2015 and fully transitioned to use of this technique in 2019.

After sequencing is complete, isolates are further analyzed by using a reference-free bioinformatics pipeline, a system first developed in Utah (*5*) and optimized by an MDPH bioinformatician for the Massachusetts SPHL. This pipeline enables creation of a phylogenetic tree, which shows relatedness between isolates. Concurrent with the analysis and development of the tree at the SPHL, the raw sequencing data (FastQ files) are uploaded to PulseNet for core genome multilocus sequence typing analysis to determine allele differences between the isolates. In 2018, a total of 583 of 803 *Salmonella* isolates underwent sequencing in Massachusetts and results were sent to CDC for confirmatory analysis.

Massachusetts uses an integrated web-based surveillance and case-management system for >90 reportable infectious diseases, including *Salmonella* (*6*). After a case is received through electronic laboratory reporting, local boards of health are notified about the need for case investigation. Clusters identified through laboratory or epidemiologic methods receive additional follow-up. The SPHL and Division of Epidemiology are part of the Bureau of Infectious Disease and Laboratory Sciences at MDPH, and these programs meet regularly to review clusters of infectious disease.

## The Study

In mid-October 2018, the SPHL notified epidemiologists about an increased number of isolates that were indistinguishable from *Salmonella enterica* serovar Enteritidis pattern JEGX01.0004, according to by PFGE testing over a 60-day period. The average baseline for this pattern is 12.5 isolates/year from August 15 through October 15; by October 15, 2018, a total of 34 isolates had been identified. Pattern JEGX01.0004 is the most common *Salmonella* Enteritidis pattern

Author affiliation: Massachusetts Department of Public Health, Boston, Massachusetts, USA

DOI: https://doi.org/10.3201/eid2607.200048

[1]These first authors contributed equally to this article.

found in Massachusetts, making cluster detection difficult. All JEGX01.0004 isolates received priority status for WGS.

Before WGS data were available, epidemiologists identified 3 persons with laboratory-confirmed *Salmonella* infection who had been interviewed by the local board of health and reported having dined at the same restaurant on November 2, 2018. All 3 case-patients lived in adjacent towns in Middlesex County and had not dined together. Two had eaten chicken Caesar salads and 1 had eaten a Greek salad with chicken. All 3 were female and 50–70 years of age. Epidemiologists notified the SPHL of the epidemiologic link on November 15. On November 16, the laboratory confirmed that isolates from all 3 case-patients were indistinguishable from *Salmonella* Enteriditis pattern JEGX01.0004.

Subsequently, the MDPH Food Protection Program notified the local board of health for the implicated restaurant, which led to a same-day inspection of the establishment. The inspection noted several food safety issues, including lack of an employee illness plan and absence of a separate sink for handwashing. The restaurant closed for cleaning on November 17 and again on November 19 while fecal samples from the food handlers were screened for *Salmonella*. Of the 11 employees who submitted fecal samples to the SPHL for *Salmonella* testing, results were positive for 1 food handler on November 23. This person had been working at the restaurant on the weekend of November 2–4, the reported exposure dates for the first case-patients. During November 19–26, WGS added an additional 6 cases to the cluster.

While the initial investigation of the restaurant was under way, the laboratory used in-house sequencing analysis to generate a phylogenetic tree; CDC performed confirmatory analyses on the accompanying FastQ files. The information resulted in identification of 7 individual clusters within isolates with the PFGE pattern JEGX01.0004. Further epidemiologic investigations linked 1 cluster to the restaurant cluster; the other 6 clusters could not be linked to a common exposure (Figure).

By mid-December 2018, a total of 10 isolates had been confirmed as being related to this cluster: 3 isolates were initially identified through epidemiologic data and later linked by sequencing, and the other 7 were initially identified through sequencing and later confirmed to be associated with the restaurant through case-patient interview. By December 20, a total of 18 isolates had been genetically linked to this cluster through WGS. The additional 8 case-patients were either not available for additional follow-up (n = 5) or did not report having dined at this restaurant (n = 3). Case-patients associated with the restaurant had ordered food during November 2–4; of those, 10 had consumed raw lettuce and tomatoes in either a salad or sandwich, and 8 had consumed grilled chicken.

## Conclusion

Our study report illustrates that classic epidemiologic case follow-up integrated with molecular approaches to cluster detection expanded the scope of a restaurant-associated outbreak. Using PFGE data only, a total of 84 isolates were included in this cluster of *Salmonella* Enteriditis pattern JEGX01.0004, making it difficult to identify which case-patients were likely to have common exposures. Open communication between epidemiologists and laboratory personnel about epidemiologic and WGS data narrowed the scope of the investigation to a clade within the larger PFGE cluster's phylogenetic tree, focusing investigative activities and improving the timeliness of control measure implementation. The real-time sequencing and analysis of all JEGX01.0004 isolates contributed to the identification of additional patients and helped identify the source for a foodborne outbreak.

We followed stringent next-generation sequencing data processing and filtering thresholds implemented by PulseNet. In brief, we trimmed reads at Q30 and included genomes only if the average coverage was >20×. This method generates high-confidence results and has been adopted by PulseNet since early 2018 (*7*).

The infected food handler was probably shedding *Salmonella* and, if hygiene practices were inadequate, could have contaminated ready-to-eat foods such as lettuce and tomatoes. Alternatively, a ready-to-eat food could have been the common source for all 18 cases in this cluster.

CDC has called for ongoing strengthening and support of state and local health departments to investigate and report outbreaks associated with foodborne disease as a necessary mechanism to reduce the burden of foodborne illness in the United States (*8*). In Massachusetts, cross-discipline collaboration among state and local health departments improved foodborne illness surveillance and response to a *Salmonella* Enteritidis outbreak associated with a restaurant. The cluster was epidemiologically identified within 2 weeks of exposure for the first 3 case-patients, inspection services were deployed to the restaurant the same day, and the probable source of contamination was confirmed by PFGE and WGS in <2 weeks. The prompt linking of epidemiologic and laboratory data and the implementation of in-state

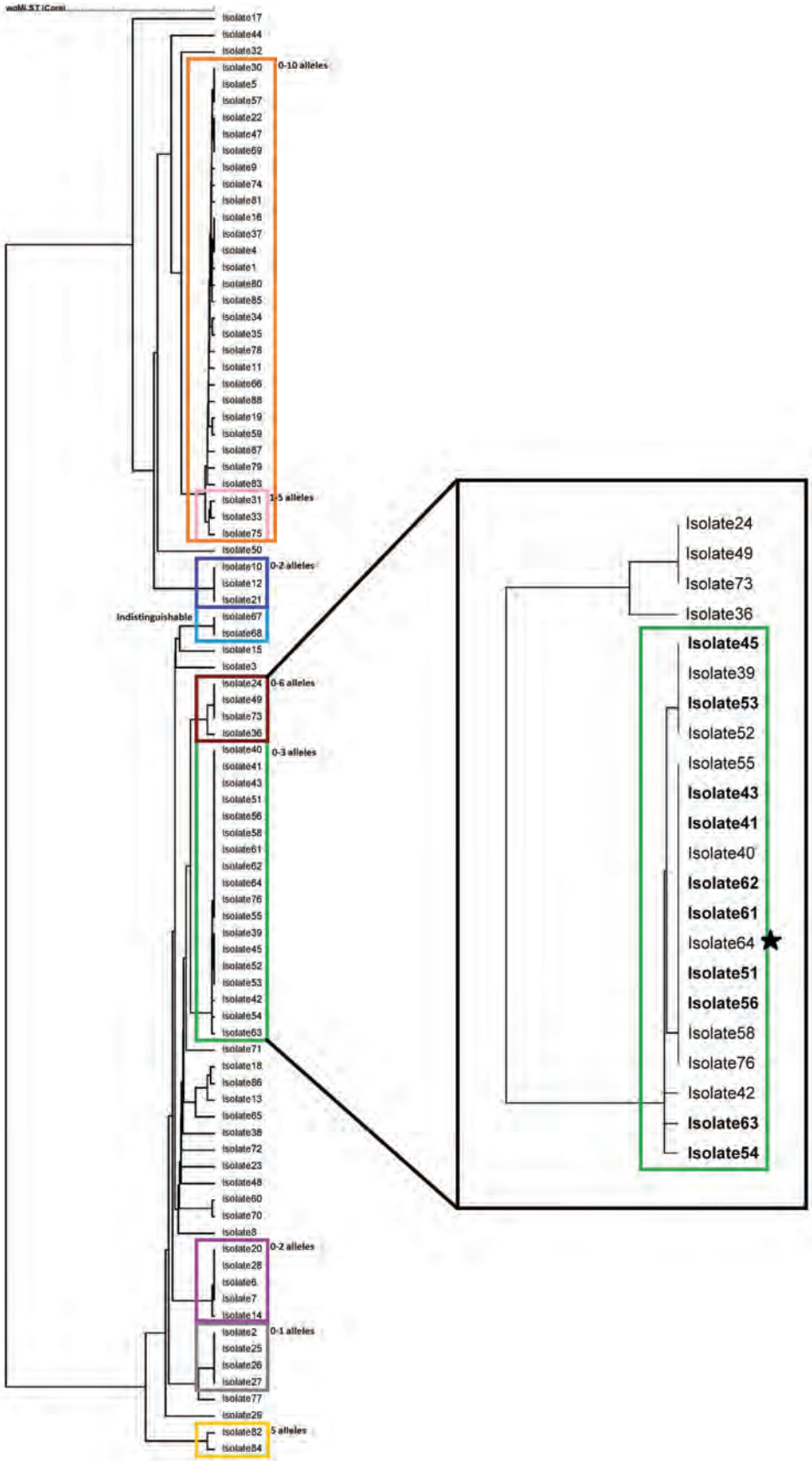


**Figure.** Phylogenetic tree for *Salmonella enterica* serotype Enteritidis isolates from outbreak in Massachusetts, USA, 2018. The colored boxes on the left indicate 9 separate subclusters for the entire 84-isolate cluster, with confirmation of allele differences coming from PulseNet (https://www.cdc.gov/pulsenet/index.html). Eight subclusters yielded no epidemiologic data, resulting in the closure of those clusters. The ninth subcluster, in the green box (right), contains the isolates associated with the restaurant cluster. Boldface indicates isolates from persons who ate at the restaurant; the star indicates the isolate from the food handler implicated in the outbreak.

WGS and analysis improved public health surveillance capacity and timeliness of outbreak detection and control.

### Acknowledgments

We thank Emily Harvey, Esther Fortes, Brandi Hopkins, Matthew Doucette, and Brandon Sabina for their assistance with the investigation.

### About the Author

Mr. Vaughn is a microbiologist for the MDPH at the State Laboratory Institute. His primary research interests include next-generation sequencing testing, validation, and data analysis of foodborne organisms.

### References

1. Kirk MD, Pires SM, Black RE, Caipo M, Crump JA, Devleesschauwer B, et al. World Health Organization estimates of the global and regional disease burden of 22 foodborne bacterial, protozoal, and viral diseases, 2010: a data synthesis. PLoS Med. 2015;12:e1001921. https://doi.org/10.1371/journal.pmed.1001921
2. Newell DG, Koopmans M, Verhoef L, Duizer E, Aidara-Kane A, Sprong H, et al. Food-borne diseases–the challenges of 20 years ago still persist while new ones continue to emerge. Int J Food Microbiol. 2010;139(Suppl 1):S3–15. https://doi.org/10.1016/j.ijfoodmicro.2010.01.021
3. Brown AC, Grass JE, Richardson LC, Nisler AL, Bicknese AS, Gould LH. Antimicrobial resistance in *Salmonella* that caused foodborne disease outbreaks: United States, 2003–2012. Epidemiol Infect. 2017;145:766–74. https://doi.org/10.1017/S0950268816002867
4. Majowicz SE, Musto J, Scallan E, Angulo FJ, Kirk M, O'Brien SJ, et al.; International Collaboration on Enteric Disease 'Burden of Illness' Studies. The global burden of nontyphoidal *Salmonella* gastroenteritis. Clin Infect Dis. 2010;50:882–9. https://doi.org/10.1086/650733
5. Oakeson KF, Wagner JM, Mendenhall M, Rohrwasser A, Atkinson-Dunn R. Bioinformatic analyses of whole-genome sequence data in a public health laboratory. Emerg Infect Dis. 2017;23:1441–5. https://doi.org/10.3201/eid2309.170416
6. Troppy S, Haney G, Cocoros N, Cranston K, DeMaria A Jr. Infectious disease surveillance in the 21st century: an integrated web-based surveillance and case management system. Public Health Rep. 2014;129:132–8. https://doi.org/10.1177/003335491412900206
7. Lüth S, Kleta S, Al Dahouk S. Whole genome sequencing as a typing tool for foodborne pathogens like *Listeria monocytogenes*–the way towards global harmonisation and data exchange. Trends Food Sci Technol. 2018;73:67–75. https://doi.org/10.1016/j.tifs.2018.01.008
8. Dewey-Mattia D, Manikonda K, Hall AJ, Wise ME, Crowe SJ. Surveillance for foodborne disease outbreaks–United States, 2009–2015. MMWR Surveill Summ. 2018;67:1–11. https://doi.org/10.15585/mmwr.ss6710a1

Address for correspondence: Quynh T. Vo, Bureau of Infectious Disease and Laboratory Sciences, Massachusetts Department of Public Health, 305 South St, Boston, MA 02130, USA; email: quynh.vo@state.ma.us

# Possible Bat Origin of Severe Acute Respiratory Syndrome Coronavirus 2

Susanna K.P. Lau,[1] Hayes K.H. Luk,[1] Antonio C.P. Wong,[1] Kenneth S.M. Li, Longchao Zhu, Zirong He, Joshua Fung, Tony T.Y. Chan, Kitty S.C. Fung, Patrick C.Y. Woo

We showed that severe acute respiratory syndrome coronavirus 2 is probably a novel recombinant virus. Its genome is closest to that of severe acute respiratory syndrome–related coronaviruses from horseshoe bats, and its receptor-binding domain is closest to that of pangolin viruses. Its origin and direct ancestral viruses have not been identified.

Seventeen years after the severe acute respiratory syndrome (SARS) epidemic, an outbreak of pneumonia, now called coronavirus disease (COVID-19), was reported in Wuhan, China. Some of the early case-patients had a history of visiting the Huanan Seafood Wholesale Market, where wildlife mammals are sold, suggesting a zoonotic origin. The causative agent was rapidly isolated from patients and identified to be a coronavirus, now designated as severe acute respiratory syndrome coronavirus 2 (SARS-CoV-2) by the International Committee on Taxonomy of Viruses (*1*). SARS-CoV-2 has spread rapidly to other places; 113,702 cases and 4,012 deaths had been reported in 110 countries/areas as of March 10, 2020 (*2*). In Hong Kong, 130 cases and 3 deaths had been reported.

SARS-CoV-2 is a member of subgenus *Sarbecovirus* (previously lineage b) in the family *Coronaviridae*, genus *Betacoronavirus*, and is closely related to SARS-CoV, which caused the SARS epidemic during 2003, and to SARS-related-CoVs (SARSr-CoVs) in horseshoe bats discovered in Hong Kong and mainland China (*3*–*5*). Whereas SARS-CoV and Middle East respiratory syndrome coronavirus were rapidly traced to their immediate animal sources (civet and dromedaries, respectively), the origin of SARS-CoV-2 remains obscure.

Author affiliations: The University of Hong Kong, Hong Kong, China (S.K.P. Lau, H.K.H. Luk, A.C.P. Wong, K.S.M. Li, L. Zhu, Z. He, J. Fung, T.T.Y. Chan, P.C.Y. Woo); United Christian Hospital, Hong Kong (K.S.C. Fung)

DOI: https://doi.org/10.3201/eid2607.200092

SARS-CoV-2 showed high genome sequence identities (87.6%–87.8%) to SARSr-Rp-BatCoV-ZXC21/ZC45, detected in *Rhinolophus pusillus* bats from Zhoushan, China, during 2015 (*6*). A closer-related strain, SARSr-Ra-BatCoV-RaTG13 (96.1% genome identity with SARS-CoV-2), was recently reported in *Rhinolophus affinis* bats captured in Pu'er, China, during 2013 (*7*). Subsequently, Pangolin-SARSr-CoV/P4L/Guangxi/2017 (85.3% genome identity to SARS-CoV-2) and related viruses were also detected in smuggled pangolins captured in Nanning, China, during 2017 (*8*) and Guangzhou, China, during 2019 (*9*). To elucidate the evolutionary origin and pathway of SARS-CoV-2, we performed an in-depth genomic, phylogenetic, and recombination analysis in relation to SARSr-CoVs from humans, civets, bats, and pangolins (*10*).

## The Study

We downloaded 4 SARS-CoV-2, 16 human/civet-SARSr-CoV, 63 bat-SARSr-CoV and 2 pangolin-SARSr-CoV genomes from GenBank and GISAID (https://www.gisaid.org). We also sequenced the complete genome of SARS-CoV-2 strain HK20 (GenBank accession no. MT186683) from a patient with COVID-19 in Hong Kong. We performed genome, phylogenetic, and recombination analysis as described (*11*).

The 5 SARS-CoV-2 genomes had overall 99.8%–100% nt identities with each other. These genomes showed 96.1% genome identities with SARSr-Ra-BatCoV-RaTG13, 87.8% with SARSr-Rp-BatCoV-ZC45, 87.6% with SARSr-Rp-BatCoV-ZXC21, 85.3% with pangolin-SARSr-CoV/P4L/Guangxi/2017, and 73.8%–78.6% with other SARSr-CoVs, including human/civet-SARSr-CoVs (Table 1, https://wwwnc.cdc.gov/EID/article/26/7/20-0092-T1.htm).

Most predicted proteins of SARS-CoV-2 showed high amino acid sequence identities with that of SARSr-Ra-BatCoV RaTG13, except the receptor-binding

[1]These authors contributed equally to this article.

domain (RBD) region. SARS-CoV-2 possessed an intact open reading frame 8 without the 29-nt deletion found in most human SARS-CoVs. The concatenated conserved replicase domains for coronavirus species demarcation by the International Committee on Taxonomy of Viruses showed ≥92.9% aa identities (threshold >90% for same species) between SARS-CoV-2 and other SARSr-CoVs, supporting their classification under the same coronavirus species (Table 2) (*1*).

Unlike other members of the subgenus *Sarbecovirus*, SARS-CoV-2 has a spike protein that contains a unique insertion that results in a potential cleavage site at the S1/S2 junction, which might enable proteolytic processing that enhances cell–cell fusion. SARS-CoV-2 was demonstrated to use the same receptor, human angiotensin-converting enzyme 2 (hACE2), as does SARS-CoV (*7*). The predicted RBD region of SARS-CoV-2 spike protein, corresponding to aa residues 318–513 of SARS-CoV (*12*), showed the highest (97% aa) identities with pangolin-SARSr-CoV/MP789/Guangdong and 74.1%–77.7% identities with human/civet/bat-SARSr-CoVs known to use hACE2 (Table 1). Moreover, similar to the human/civet/bat-SARSr-CoV hACE2-using viruses, the 2 deletions (5 aa and 12 aa) found in all other SARSr-BatCoVs (*10*) were absent in SARS-CoV-2 RBD (Appendix Figure 1, https://wwwnc.cdc.gov/EID/article/26/7/20-0092-App1.pdf). Of the 5 critical residues needed for RBD-hACE2 interaction in SARSr-CoVs (*13*), 3 (F472, N487, and Y491) were present in SARS-CoV-2 RBD and pangolin SARSr-CoV/MP789/2019-RBD.

Phylogenetic analysis showed that the RNA-dependent RNA polymerase gene of SARS-CoV-2 is most closely related to that of SARSr-Ra-BatCoV RaTG13, whereas its predicted RBD is closest to that of pangolin-SARSr-CoVs (Figure 1). This finding suggests a distinct evolutionary origin for SARS-CoV-2 RBD, possibly as a result of recombination. Moreover, the SARS-CoV-2 RBD was also closely related to SARSr-Ra-BatCoV RaTG13 and the hACE2-using cluster containing human/civet-SARSr-CoVs and Yunnan SARSr-BatCoVs previously successfully cultured in VeroE6 cells (*4*,*5*).

To identify putative recombination events, we performed sliding window analysis using SARS-CoV-2-HK20 as query and SARSr-Ra-BatCoV RaTG13, pangolin-SARSr-CoV/P4L/Guangxi/2017, SARSr-Rp-BatCoV ZC45, SARSr-Rs-BatCoV Rs3367, and SARSr-Rs-BatCoV Longquan-140 as potential parents

**Table 2.** Percentage amino acid identity between 7 conserved domains of the replicase polyprotein for species demarcation in SARS-CoV-2 and selected members of the subgenus *Sarbecovirus**

| | % Amino acid identity compared with that for SARS-CoV-2 | | | | | | | |
|---|---|---|---|---|---|---|---|---|
| Virus | ADRP | nsp5 | nsp12 | nsp13 | nsp14 | nsp15 | nsp16 | Seven concatenated domains |
| Human SARS-CoV TOR2/Toronto/Mar2003 | 79.3 | 96.1 | 96.4 | 99.8 | 95.1 | 88.7 | 93.3 | 95.0 |
| Civet SARS-CoV SZ3/Shenzhen/2013 | 79.3 | 96.1 | 96.4 | 99.7 | 95.1 | 88.7 | 93.6 | 95.0 |
| Civet SARS-CoV PC4–136/Guangdong/2004 | 78.4 | 96.1 | 96.4 | 99.3 | 94.7 | 88.7 | 93.3 | 94.8 |
| Human SARS-CoV GZ0402 | 78.4 | 95.8 | 96.2 | 99.5 | 94.9 | 51.7 | 93.3 | 94.8 |
| SARSr-Rs-BatCoV HKU3–1/R.sinicus/Hong Kong/2005 | 79.3 | 95.4 | 95.6 | 98.8 | 94.7 | 88.2 | 93.3 | 94.5 |
| SARSr-Rp-BatCoV Rp/Shaanxi2011/R.pusillus/Shaanxi/2011 | 78.4 | 96.1 | 96.1 | 99.3 | 96.0 | 88.4 | 93.6 | 95.0 |
| SARSr-Rs-BatCoV Rs672/2006/R.sinicus/Guizhou/2006 | 80.2 | 95.4 | 96.5 | 99.0 | 95.6 | 88.2 | 94.3 | 95.0 |
| SARSr-Rs-BatCoV WIV1 | 80.2 | 95.8 | 96.2 | 99.5 | 95.4 | 89.0 | 93.0 | 95.0 |
| SARSr-Rf-BatCoV YNLF_31C/R.ferrumequinum/Yunnan/2013 | 80.2 | 95.8 | 96.2 | 99.3 | 95.6 | 88.7 | 93.0 | 95.0 |
| SARSr-Rf-BatCoV 16BO133/R.ferrumequinum/Korea/2016 | 79.3 | 95.1 | 96.1 | 98.7 | 94.9 | 88.2 | 92.6 | 94.6 |
| SARSr-Rf-BatCoV JTMC15/R.ferrumequinum/Jilin/2013 | 79.3 | 94.8 | 96.2 | 98.5 | 94.9 | 88.2 | 92.6 | 94.5 |
| SARSr-Rs-BatCoV BtKY72/Rhinolophus sp./Kenya/2007 | 74.8 | 95.4 | 95.0 | 96.8 | 92.8 | 87.3 | 90.6 | 92.9 |
| SARSr-Rm-BatCoV Longquan-140/R.monoceros/Zhejiang/2012 | 79.3 | 95.8 | 95.7 | 99.2 | 94.9 | 89.0 | 94.3 | 94.8 |
| SARSr-Rb-BatCoV BM48–31/BGR/2008/R.blasii/Bulgaria/2008 | 78.4 | 94.1 | 95.2 | 97.8 | 93.5 | 89.9 | 88.6 | 93.5 |
| SARSr-Rp-BatCoV ZXC21/R.pusillus/Zhejiang/2015 | 88.3 | 99.0 | 95.6 | 98.8 | 94.7 | 88.2 | 98.0 | 95.4 |
| SARSr-Rp-BatCoV ZC45/R.pusillus/Zhejiang/2017 | 92.8 | 99.0 | 95.9 | 99.3 | 94.5 | 89.0 | 98.0 | 95.8 |
| Pangolin-SARSr-CoV Guangxi/P4L/2017 | 85.5 | 97.1 | 97.9 | 98.2 | 97.0 | 94.5 | 97.7 | 96.9 |
| SARSr-Ra-BatCoV RaTG13/R.affinis/Yunnan/2013 | 96.7 | 99.3 | 99.6 | 99.7 | 99.2 | 97.7 | 100 | 99.2 |

*ADRP, ADP-ribose-1″ phosphatase; nsp, nonstuctural protein; SARS-CoV-2, severe acute respiratory syndrome coronavirus 2; SARSr-CoV, severe acute respiratory syndrome–related coronavirus.

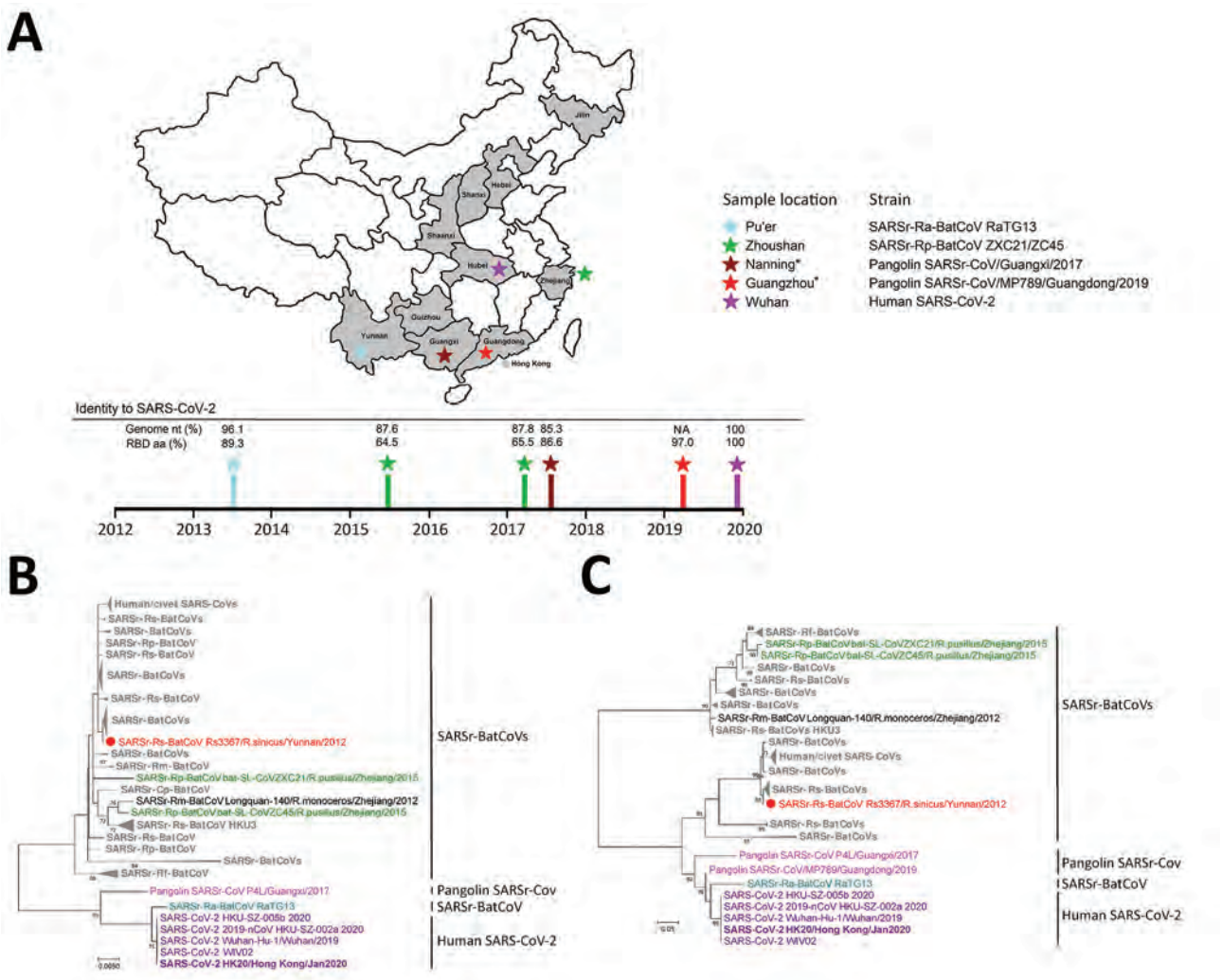


**Figure 1.** Geographic and phylogenetic comparisons of SARS-CoV-2 isolates with closely related viruses. A) Locations in China where SARS-CoV-2 first emerged (Wuhan), and where closely related viruses were found, including SARSr-Ra-BatCoV RaTG13 (Pu'er), Pangolin-SARSr-CoVs (Guangzhou and Nanning), and SARSr-Rp-BatCoV ZC45 (Zhoushan). Time of sampling and percentage genome identities to SARS-CoV-2 are shown. *Guangzhou and Nanning. The geographic origin of smuggled pangolins remains unknown. B, C) Phylogenetic analyses of RdRp (B) and RBD (C) domains of SARSr-CoVs. Trees were constructed by using maximum-likelihood methods with Jones-Taylor-Thornton plus gamma plus invariant sites (RdRp) and Whelan and Goldman plus gamma (RBD) substitution models. A total of 745 aa residues for RdRp and 177 aa residues for RBD were included in the analyses. Numbers at nodes represent bootstrap values, which were calculated from 1,000 trees. Only bootstrap values >70% are shown. Purple indicates SARS-CoV-2 (strain HK20 in bold); teal indicates SARSr-Ra-BatCoV RaTG13; pink indicates pangolin SARSr-CoVs; green indicates SARSr-Rp-BatCoVs ZXC21 and ZC45; red indicates SARSr-Rs-BatCoV Rs3367; black indicates SARSr-Rs-BatCoV Longquan-140; gray indicates remaining SARSr-BatCoVs. Dots indicate SARSr-BatCoVs reported to use angiotensin-converting enzyme 2 as receptor. Scale bars indicate estimated number of amino acid substitutions per 200 aa residues for RdRp and per 20 aa residues for RBD. SARS-CoV-2, severe acute respiratory syndrome coronavirus 2; SARSr-CoV, severe acute respiratory syndrome–related coronavirus; NA, not available; RBD, receptor-binding domain; RdRp, RNA-dependent RNA polymerase.

(Figure 2; Appendix Figure 2). A similarity plot showed that SARS-CoV-2 is most closely related to SARSr-Ra-BatCoV RaTG13 in the entire genome, except for its RBD, which is closest to pangolin-SARSr-CoV/MP789/Guangdong, and shows potential recombination breakpoints. Moreover, different regions of SARS-CoV-2 genome showed different similarities to pangolin-SARSr-CoV/P4L/Guangxi/2017, SARSr-Rp-BatCoV ZC45, SARSr-Rs-BatCoV Rs3367, and SARSr-Rs-BatCoV Longquan-140, as supported by phylogenetic analysis (Appendix Figures 2, 3).

Sequence alignment around the RBD supported potential recombination between SARSr-Ra-BatCoV RaTG13 and pangolin-SARSr-CoV/MP789/

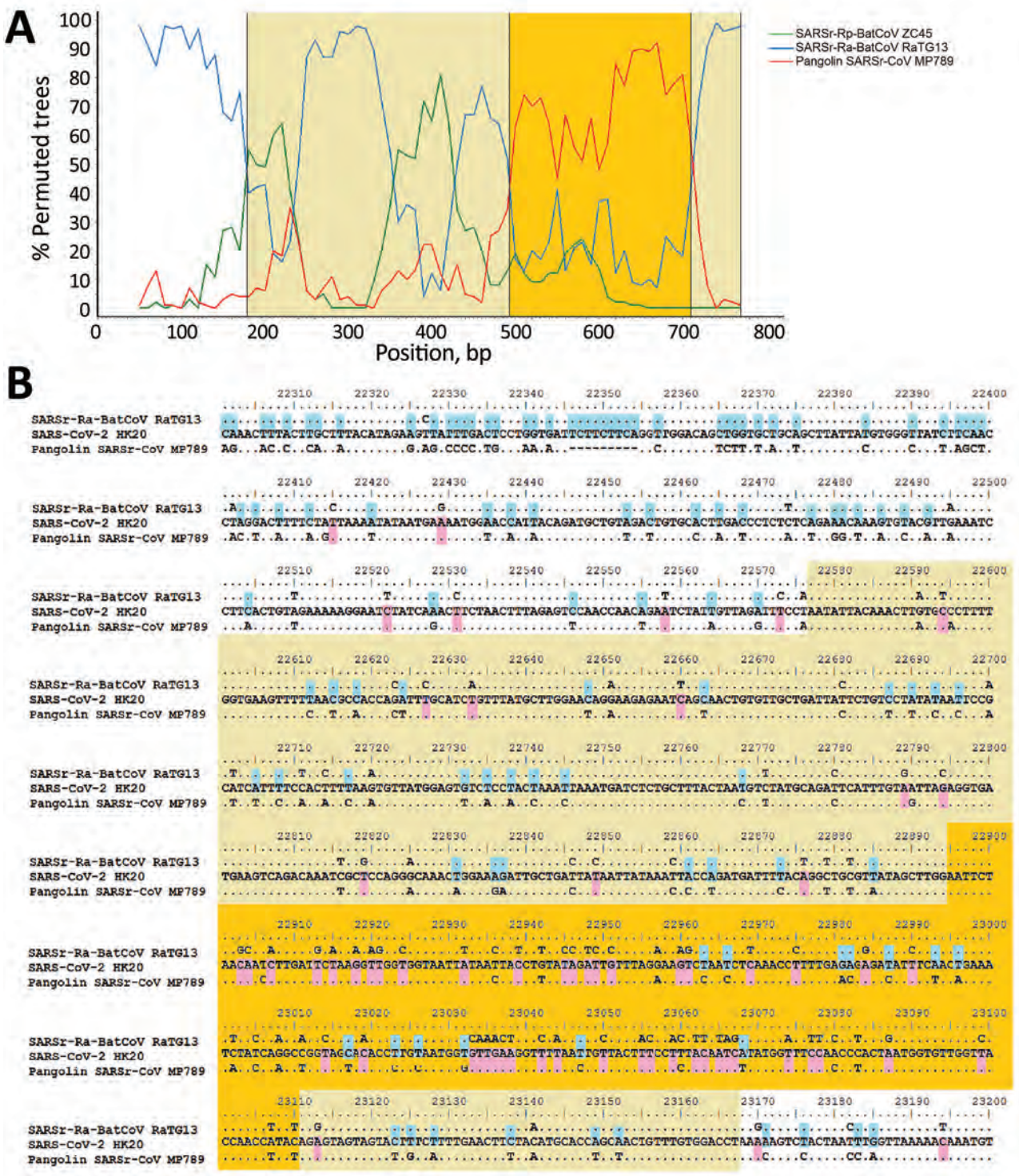


**Figure 2.** Bootscan analysis and nucleotide sequence alignment for SARS-CoV-2 isolates and closely related viruses. A) Bootscan analysis using the partial spike gene (positions 22397–23167) of SARS-CoV-2 strain HK20 as query sequence. Bootscanning was conducted with Simplot version 3.5.1 (https://sray.med.som) (F84 model; window size, 100 bp; step, 10 bp) on nucleotide alignment, generated with ClustalX (http://www.clustal.org). B) Multiple alignment of nucleotide sequences from genome positions 22300 to 23700. Yellow indicates receptor binding domain; orange indicates receptor binding motif; pink indicates bases conserved between SARS-CoV-2 HK20 and Pangolin-SARSr-CoV/MP789/Guangdong/2019; and blue indicates bases conserved between SARS-CoV-2 HK20 and SARSr-Ra-BatCoVs RaTG13.

Guangdong/2019 and the receptor-binding motif region showing exceptionally high sequence similarity to that of pangolin-SARSr-CoV/MP789/Guangdong/2019. This finding suggested that SARS-CoV-2 might be a recombinant virus between viruses closely related to SARSr-Ra-BatCoV RaTG13 and pangolin-SARSr-CoV/MP789/Guangdong/2019.

## Conclusions

Despite the close relatedness of SARS-CoV-2 to bat and pangolin viruses, none of the existing SARSr-CoVs represents its immediate ancestor. Most of the genome region of SARS-CoV-2 is closest to SARSr-Ra-BatCoV-RaTG13 from an intermediate horseshoe bat in Yunnan, whereas its RBD is closest to that of pangolin-SARSr-CoV/MP789/Guangdong/2019 from smuggled pangolins in Guangzhou. Potential recombination sites were identified around the RBD region, suggesting that SARS-CoV-2 might be a recombinant virus, with its genome backbone evolved from Yunnan bat virus–like SARSr-CoVs and its RBD region acquired from pangolin virus–like SARSr-CoVs.

Because bats are the major reservoir of SARSr-CoVs and the pangolins harboring SARSr-CoVs were captured from the smuggling center, it is possible that pangolin SARSr-CoVs originated from bat viruses as a result of animal mixing, and there might be an unidentified bat virus containing an RBD nearly identical to that of SARS-CoV-2 and pangolin SARSr-CoV. Similar to SARS-CoV, SARS-CoV-2 is most likely a recombinant virus originated from bats.

The ability of SARS-CoV-2 to emerge and infect humans is likely explained by its hACE2-using RBD region, which is genetically similar to that of culturable Yunnan SARSr-BatCoVs and human/civet-SARSr-CoVs. Most SARSr-BatCoVs have not been successfully cultured in vitro, except for some Yunnan strains that had human/civet SARS-like RBDs and were shown to use hACE2 (*4*,*5*). For example, SARSr-Rp-BatCoV ZC45, which has an RBD that is more divergent from that of human/civet-SARSr-CoVs, did not propagate in VeroE6 cells (*6*). Factors that determine hACE2 use among SARSr-CoVs remain to be elucidated.

Although the Wuhan market was initially suspected to be the epicenter of the epidemic, the immediate source remains elusive. The close relatedness among SARS-CoV-2 strains suggested that the Wuhan outbreak probably originated from a point source with subsequent human-to-human transmission, in contrast to the polyphyletic origin of Middle East respiratory syndrome coronavirus (*14*). If the Wuhan market was the source, a possibility is that bats carrying the parental SARSr-BatCoVs were mixed in the market, enabling virus recombination. However, no animal samples from the market were reported to be positive. Moreover, the first identified case-patient and other early case-patients had not visited the market (*15*), suggesting the possibility of an alternative source.

Because the RBD is considered a hot spot for construction of recombinant CoVs for receptor and viral replication studies, the evolutionarily distinct SARS-CoV-2 RBD and the unique insertion of S1/S2 cleavage site among *Sarbecovirus* species have raised the suspicion of an artificial recombinant virus. However, there is currently no evidence showing that SARS-CoV-2 is an artificial recombinant, which theoretically might not carry signature sequences. Further surveillance studies in bats are needed to identify the possible source and evolutionary path of SARS-CoV-2.

This study was partly supported by the theme-based research scheme (project no. T11-707/15-R) of the University Grant Committee; Health and Medical Research Fund of the Food and Health Bureau of HKSAR; Consultancy Service for Enhancing Laboratory Surveillance of Emerging Infectious Disease for the HKSAR Department of Health and the University Development Fund of the University of Hong Kong.

## About the Author

Dr. Lau is a professor and head of the Department of Microbiology at The University of Hong Kong, Hong Kong, China. Her primary research interest is using microbial genomics for studying emerging infectious diseases, including coronaviruses.

## References

1. Coronaviridae Study Group of the International Committee on Taxonomy of Viruses. The species severe acute respiratory syndrome-related coronavirus: classifying 2019-nCoV and naming it SARS-CoV-2. Nat Microbiol. 2020;5:536–44. https://doi.org/10.1038/s41564-020-0695-z
2. World Health Organization. Coronavirus disease 2019 (COVID-19) situation report 50, March 10, 2020 [cited 2020 Apr 11]. https://www.who.int/docs/default-source/coronaviruse/situation-reports/20200310-sitrep-50-covid-19.pdf
3. Lau SK, Woo PC, Li KS, Huang Y, Tsoi HW, Wong BH, et al. Severe acute respiratory syndrome coronavirus-like virus in Chinese horseshoe bats. Proc Natl Acad Sci U S A. 2005;102:14040–5. https://doi.org/10.1073/pnas.0506735102
4. Ge XY, Li JL, Yang XL, Chmura AA, Zhu G, Epstein JH, et al. Isolation and characterization of a bat SARS-like coronavirus that uses the ACE2 receptor. Nature. 2013;503:535–8. https://doi.org/10.1038/nature12711
5. Hu B, Zeng LP, Yang XL, Ge XY, Zhang W, Li B, et al. Discovery of a rich gene pool of bat SARS-related

coronaviruses provides new insights into the origin of SARS coronavirus. PLoS Pathog. 2017;13:e1006698. https://doi.org/10.1371/journal.ppat.1006698
6. Hu D, Zhu C, Ai L, He T, Wang Y, Ye F, et al. Genomic characterization and infectivity of a novel SARS-like coronavirus in Chinese bats. Emerg Microbes Infect. 2018;7:154. https://doi.org/10.1038/s41426-018-0155-5
7. Zhou P, Yang XL, Wang XG, Hu B, Zhang L, Zhang W, et al. A pneumonia outbreak associated with a new coronavirus of probable bat origin. Nature. 2020;579:270–3. https://doi.org/10.1038/s41586-020-2012-7
8. Liu P, Chen W, Chen JP. Viral metagenomics revealed sendai virus and coronavirus infection of Malayan pangolins (*Manis javanica*). Viruses. 2019;11:E979. https://doi.org/10.3390/v11110979
9. Lam TT, Shum MH, Zhu HC, Tong YG, Ni XB, Liao YS, et al. Identifying SARS-CoV-2 related coronaviruses in Malayan pangolins. Nature. 2020;March 26: Epub ahead of print. https://doi.org/10.1038/s41586-020-2169-0
10. Luk HK, Li X, Fung J, Lau SK, Woo PC. Molecular epidemiology, evolution and phylogeny of SARS coronavirus. Infect Genet Evol. 2019;71:21–30. https://doi.org/10.1016/j.meegid.2019.03.001
11. Lau SKP, Li KS, Huang Y, Shek CT, Tse H, Wang M, et al. Ecoepidemiology and complete genome comparison of different strains of severe acute respiratory syndrome-related *Rhinolophus* bat coronavirus in China reveal bats as a reservoir for acute, self-limiting infection that allows recombination events. J Virol. 2010;84:2808–19. https://doi.org/10.1128/JVI.02219-09
12. Wong SK, Li W, Moore MJ, Choe H, Farzan M. A 193-amino acid fragment of the SARS coronavirus S protein efficiently binds angiotensin-converting enzyme 2. J Biol Chem. 2004;279:3197–201. https://doi.org/10.1074/jbc.C300520200
13. Li W, Zhang C, Sui J, Kuhn JH, Moore MJ, Luo S, et al. Receptor and viral determinants of SARS-coronavirus adaptation to human ACE2. EMBO J. 2005;24:1634–43. https://doi.org/10.1038/sj.emboj.7600640
14. Lau SK, Wernery R, Wong EY, Joseph S, Tsang AK, Patteril NA, et al. Polyphyletic origin of MERS coronaviruses and isolation of a novel clade A strain from dromedary camels in the United Arab Emirates. Emerg Microbes Infect. 2016;5:e128. https://doi.org/10.1038/emi.2016.129
15. Huang C, Wang Y, Li X, Ren L, Zhao J, Hu Y, et al. Clinical features of patients infected with 2019 novel coronavirus in Wuhan, China. Lancet. 2020;395:497–506. https://doi.org/10.1016/S0140-6736(20)30183-5

Address for correspondence: Susanna K.P. Lau or Patrick C.Y. Woo, Department of Microbiology, Li Ka Shing Faculty of Medicine, The University of Hong Kong, Rm 26, 19/F, Block T, Queen Mary Hospital, 102 Pokfulam Rd, Hong Kong, China; email: skplau@hku.hk or pcywoo@hku.hk

# Heartland Virus in Humans and Ticks, Illinois, USA, 2018–2019

Holly C. Tuten,[1] Kristen L. Burkhalter,[1] Kylee R. Noel, Erica J. Hernandez, Seth Yates, Keith Wojnowski, John Hartleb, Samantha Debosik, April Holmes, Christopher M. Stone

In 2018, Heartland disease virus infected 2 persons in Illinois, USA. In 2019, ticks were collected at potential tick bite exposure locations and tested for Heartland and Bourbon viruses. A Heartland virus–positive pool of adult male *Amblyomma americanum* ticks was found at 2 locations, 439 km apart, suggesting widespread distribution in Illinois.

Heartland virus (HRTV), a phlebovirus in the order Bunyavirales, is an emerging zoonotic pathogen. In 2009, after 2 cases were identified in persons in Missouri, additional cases were subsequently reported from Kansas, Oklahoma, Arkansas, Missouri, Tennessee, Kentucky, Indiana, Georgia, and South Carolina. Disease onset was most often during April–September (*1*). HRTV symptoms can initially resemble those of ehrlichiosis (*2*) and include fatigue, fever, leukopenia, and thrombocytopenia (*3*). Human illness caused by HRTV infection often requires hospitalization and has resulted in death (*1*).

After 2 persons infected with HRTV in northwestern Missouri reported having noticed attached ticks before symptom onset (*4*), subsequent entomologic studies detected HRTV in nymphal *Amblyomma americanum* ticks. Laboratory studies confirmed the competence of *A. americanum* ticks for transmitting HRTV transstadially and horizontally (*5*). This body of evidence led to the implication of *A. americanum* ticks as the putative vector of HRTV (*2*,*6*). Serologic surveys of mammals and birds subsequently detected HRTV-specific neutralizing antibodies in a variety of mammals, including raccoons and white-tailed deer, suggesting that various medium- and large-sized mammals may serve as hosts (*3*,*7*).

*A. americanum* ticks are vectors of public health concern because of their aggressive biting behavior, willingness to feed on humans, and abundance. Over the past century, their distribution range has expanded northward (*8*), and population establishment continues to increase because of climate change (*9*). Habitat suitability models have suggested that this species' fundamental niche should reach the center of Illinois (*10*) or eventually encompass the state entirely (*9*).

In July 2018, a Kankakee County, Illinois, resident (case-patient 1) reported having incurred multiple tick bites while camping on private residential property. The patient was hospitalized with fever, headache, myalgia, nausea, diarrhea, and a diffuse maculopapular rash. In September 2018, a Williamson County, Illinois, resident (case-patient 2) noticed tick bites while staying at a campground near home. The patient was hospitalized with fever, headache, myalgia, fatigue, decreased appetite, nausea, and diarrhea. The Centers for Disease Control and Prevention (CDC) confirmed that clinical samples from both patients were positive for HRTV. We subsequently performed entomologic investigations to determine tick density and HRTV prevalence among tick populations at the likely sites of exposure.

## The Study

The suspected sites of human exposure were determined according to case-patient interviews conducted by local county health departments (Figure). Two of the 3 sites were in an area considered endemic for *A. americanum* ticks, and the other site was near the putative current northern distribution range limit for this tick vector.

Author affiliations: University of Illinois at Urbana-Champaign, Champaign, Illinois, USA (H.C. Tuten, K.R. Noel, E.J. Hernandez, S. Yates, C.M. Stone); Centers for Disease Control and Prevention, Fort Collins, Colorado, USA (K.L. Burkhalter); Kankakee County Health Department, Kankakee, Illinois, USA (K. Wojnowski); US Fish & Wildlife Service, Marion, Illinois, USA (J. Hartleb); Illinois Department of Public Health, Springfield, Illinois, USA (S. Debosik, A. Holmes)

DOI: https://doi.org/10.3201/eid2607.200110

[1]These authors contributed equally to this article.

For case-patient 1, the potential exposure site was an ≈40-acre rural homestead in Kankakee County, which had an assemblage of barnyard animals, including chickens, goats, horses, and turkeys (site 1) and a small amount of forest surrounded by extensive cropland. For case-patient 2, in Williamson County, a potential exposure site consisted of 2 adjacent lakeshore campgrounds located within a heavily wooded wildlife refuge (site 2) and another was a suburban home with sparse tree cover (site 3). We observed deer at site 1 during collection visits on June 21 and 25, 2019, and deer, coyotes, and racoons at site 2 during visits on July 11 and 12, 2019. A pet dog lived at the residence at site 3, which we visited on July 11, 2019.

We collected ticks by dragging along 150-m transects (sites 1 and 2) and with carbon dioxide traps consisting of a 1 $m^2$ white cloth laid on the ground with 0.5 kg of dry ice left in the center to sublimate for 2 hours before returning to collect ticks (sites 1–3). We collected live ticks into 14-mL plastic centrifuge tubes (TPP, https://www.tpp.ch) that had been

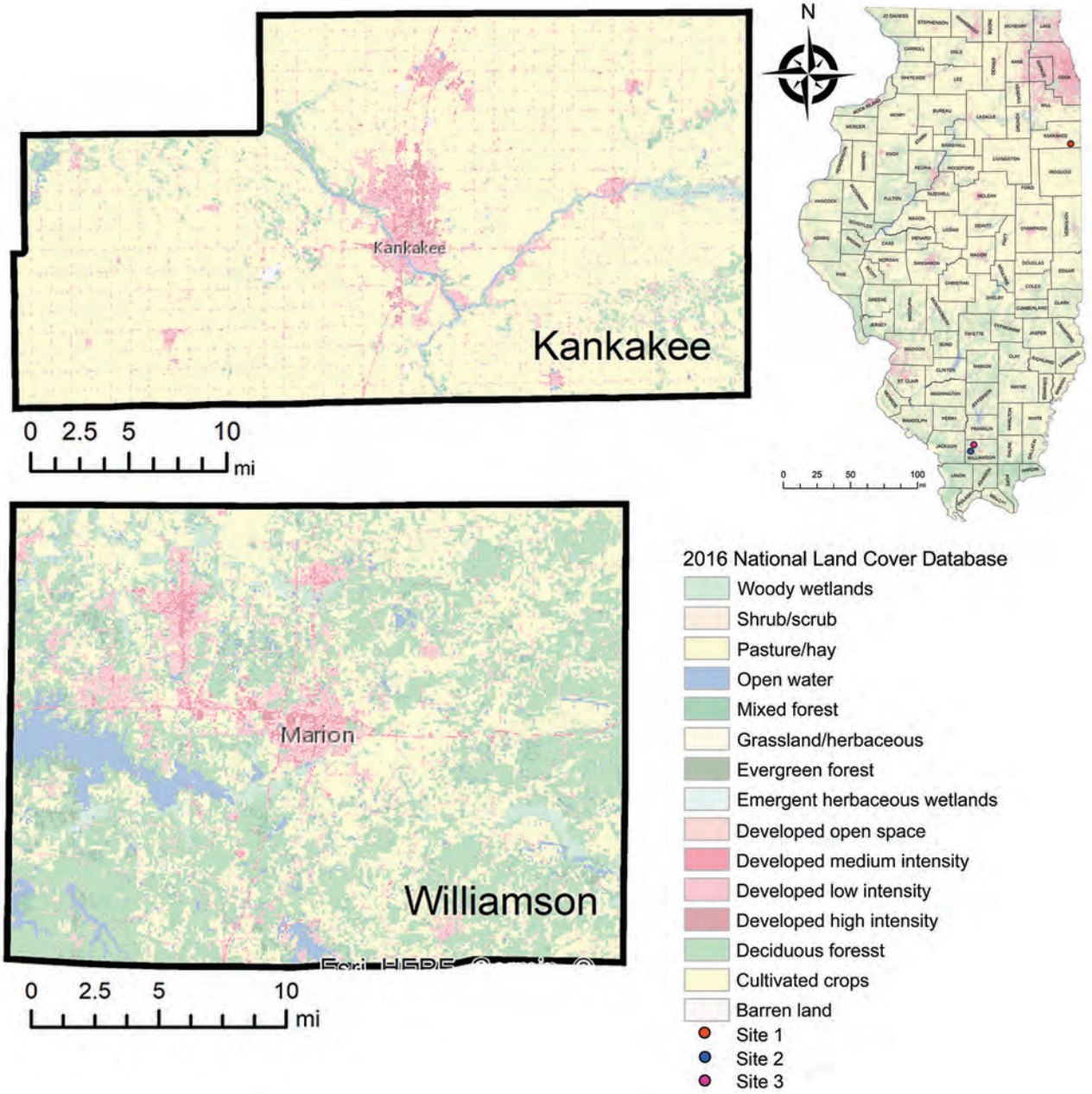


**Figure.** Tick collection sites associated with 2 cases of Heartland virus infection in humans, Kankakee and Williamson Counties, Illinois, USA, 2019. Locations of the counties are indicated by red dots on the Illinois map.

modified by applying carpet tape between the lid and tube mouth. We added ticks through a tape-covered hole punched in the center of the paper-backed side of the tape; the sticky side of the tape facing the tube interior immobilized the ticks before they could exit, enabling their secure transport while alive (Video, https://wwwnc.cdc.gov/EID/article/26/7/20-0110-V1.htm**).** Ticks were either kept alive (site 1) or killed in the field at the end of the day and kept on dry ice (sites 2 and 3) during transport to the Illinois Natural History Survey Medical Entomology Laboratory (Champaign, IL, USA), where they were identified and sorted by species, life stage, and sex (*11*,*12*) on a chill table and maintained at -80°C. Ticks were then shipped on dry ice to the CDC Arboviral Diseases Branch (Fort Collins, CO, USA) for Heartland and Bourbon virus testing, where tick pool homogenization, RNA extraction, and virus screening were performed by real-time PCR as previously described (*2*,*13*). The prevalence of virus infection from pooled samples was calculated by using PooledInfRate, which implements a bias-corrected maximum-likelihood estimation method (*14*).

A total of 70 pools of adult ticks and 23 pools of nymphs were tested (Table 1). The median pool size for adult ticks was 10 (range 1–10) and for nymphs was 30 (range 3–33). A single pool of male *A. americanum* ticks from each county was positive for HRTV (cycle threshold values of 21.7 for site 1 and 24.1 for site 2 by first PCR, 23.2 and 25.3 after confirmation by second PCR); Bourbon virus was not detected. The estimated prevalence of HRTV in adult male *A. americanum* ticks was 9.46/1,000 ticks at site 1 and 7.60/1,000 ticks at site 2 (Table 2).

## Conclusions

One year after 2 cases in humans were detected, HRTV was detected in *A. americanum* ticks collected from the suspected exposure locations in Illinois. Because of abundant suitable habitat and established *A. americanum* tick populations (*10*), it is notable but predictable that this pathogen emerged in southern Illinois. The density of and HRTV detection in *A. americanum* ticks at the northern edge of their distribution range in Kankakee County was unexpected. Our findings suggest that *A. americanum*

**Table 1.** Collection methods and number of ticks of each species and life stage collected in 2 counties, Illinois, USA, 2019

| Site, method, tick species | Stage | Sex | No. collected | Density/1,000 m$^2$ |
|---|---|---|---|---|
| Site 1* | | | 659 | |
| Dragging | | | | |
| *Amblyomma americanum* | Adult | F | 93 | 26 |
| | Adult | M | 90 | 25 |
| | Nymph | Not applicable | 338 | 93 |
| *Dermacentor variabilis* | Adult | F | 15 | 4 |
| | Adult | M | 10 | 3 |
| Carbon-dioxide trap | | | | |
| *A. americanum* | Adult | F | 18 | Not applicable |
| | Adult | M | 17 | Not applicable |
| | Nymph | Not applicable | 75 | Not applicable |
| *D. variabilis* | Adult | F | 1 | Not applicable |
| | Adult | M | 1 | Not applicable |
| *Ixodes scapularis* | Nymph | Not applicable | 1 | Not applicable |
| Site 2† | | | 498 | |
| Dragging | | | | |
| *A. americanum* | Adult | F | 32 | 15 |
| | Adult | M | 44 | 21 |
| | Nymph | Not applicable | 159 | 76 |
| *D. variabilis* | Adult | F | 1 | 0.5 |
| | Adult | M | 2 | 1 |
| Carbon-dioxide trap | | | | |
| *A. americanum* | Adult | F | 118 | Not applicable |
| | Adult | M | 88 | Not applicable |
| | Nymph | Not applicable | 48 | Not applicable |
| *D. variabilis* | Adult | F | 3 | Not applicable |
| | Adult | M | 3 | Not applicable |
| Site 3‡ | | | 9 | |
| Carbon-dioxide trap | | | | |
| *A. americanum* | Adult | F | 4 | Not applicable |
| | Nymph | Not applicable | 4 | Not applicable |
| *D. variabilis* | Adult | F | 1 | Not applicable |

*Site 1, Kankakee County, visited June 21 and 25, 2019; dragging, n = 24 × 150 m transects; carbon dioxide traps, n = 3.
†Site 2, Williamson County, visited July 11–12, 2019; dragging, n = 14 × 150 m transects; carbon dioxide traps, n = 9.
‡Site 3, Williamson County, visited July 11–12, 2019; no dragging performed because of site size; carbon dioxide trap, n = 2.

**Table 2.** Prevalence of Heartland virus in ticks, by location, species, and sex in 2 counties in Illinois, USA, 2019*

| Species | Stage | Sex | County | No. ticks collected | No. pools | No. positive pools | Infection rate/1,00 ticks, MLE (95% CI) |
|---|---|---|---|---|---|---|---|
| *Amblyomma americanum* | Adult | M | Kankakee | 107 | 16 | 1 | 9.46 (0.55–46.1) |
| *A. americanum* | Adult | F | Kankakee | 111 | 12 | 0 | 0 (0–29.5) |
| *A. americanum* | Nymph | NA | Kankakee | 413 | 15 | 0 | 0 (0–8.2) |
| *A. americanum* | Adult | M | Williamson | 132 | 15 | 1 | 7.6 (0.44–36.9) |
| *A. americanum* | Adult | F | Williamson | 154 | 17 | 0 | 0 (0–22.16) |
| *A. americanum* | Nymph | NA | Williamson | 211 | 8 | 0 | 0 (0–14.5) |
| *Dermacentor variabilis* | Adult | Both | Kankakee | 27 (16 F, 11 M) | 4 | 0 | 0 (0–92.8) |
| *D. variabilis* | Adult | Both | Williamson | 10 (5 F, 5 M) | 6 | 0 | 0 (0–248.8) |

*MLE, maximum-likelihood estimation; NA, not applicable.

ticks are established along their northern distribution range at high densities. Consequently, diseases associated with *A. americanum* ticks must be on the radar of physicians and public health officials throughout Illinois.

Detection of HRTV in adult *A. americanum* ticks suggests that infected ticks may have overwintered in the area and maintained HRTV infection transstadially. The presence of HRTV in adult male, but not female or nymph, ticks was also reported in a study in Kansas, where the infection rate varied from 3.29 to 8.62/1,000 ticks (*15*), similar to our findings. Additional tick collection efforts and wildlife serosurveys will help assess whether transmission cycles are active in Illinois and enhance our knowledge of the transmission ecology of this rare pathogen.

### Acknowledgments

We are grateful to the Heartland case-patients, who allowed us to conduct tick collections. We thank Bethany McGregor, who assisted with tick homogenization; and Kayla Valcheva, Ashley Ray, and Alan Hatia, who helped with tick dragging. We also thank Roxanne Connelly and anonymous reviewers for comments on this manuscript.

This work was supported through an agreement with the Illinois Department of Public Health. Points of view or opinions expressed in this document are those of the authors and do not necessarily represent the official position or policies of the Illinois Department of Public Health or the Centers for Disease Control and Prevention. The INHS Medical Entomology Lab is additionally supported through the State of Illinois Used Tire Management and Emergency Public Health Funds.

### About the Author

Dr. Tuten is a vector ecologist at the Illinois Natural History Survey at the University of Illinois at Urbana–Champaign, in Champaign, Illinois. Her research interests are vector behavior, control, ecology, demography, pathogens, and population genetics. Dr. Burkhalter is a microbiologist in the Division of Vector-Borne Diseases, National Center for Emerging and Zoonotic Infectious Diseases, CDC, Fort Collins, CO. Her research interests include the development and optimization of methods to improve detection of arboviruses in environmental samples and providing support for CDC's public health partners.

### References

1. Brault AC, Savage HM, Duggal NK, Eisen RJ, Staples JE. Heartland virus epidemiology, vector association, and disease potential. Viruses. 2018;10:498. https://doi.org/10.3390/v10090498
2. Savage HM, Godsey MS, Lambert A, Panella NA, Burkhalter KL, Harmon JR, et al. First detection of Heartland virus (Bunyaviridae: Phlebovirus) from field collected arthropods. Am J Trop Med Hyg. 2013;89:445–52. https://doi.org/10.4269/ajtmh.13-0209
3. Bosco-Lauth AM, Panella NA, Root JJ, Gidlewski T, Lash RR, Harmon JR, et al. Serological investigation of Heartland virus (Bunyaviridae: Phlebovirus) exposure in wild and domestic animals adjacent to human case sites in Missouri 2012-2013. Am J Trop Med Hyg. 2015;92:1163–7. https://doi.org/10.4269/ajtmh.14-0702
4. McMullan LK, Folk SM, Kelly AJ, MacNeil A, Goldsmith CS, Metcalfe MG, et al. A new phlebovirus associated with severe febrile illness in Missouri. N Engl J Med. 2012;367:834–41. https://doi.org/10.1056/NEJMoa1203378
5. Godsey MS Jr, Savage HM, Burkhalter KL, Bosco-Lauth AM, Delorey MJ. Transmission of Heartland Virus (Bunyaviridae: Phlebovirus) by experimentally infected *Amblyomma americanum* (Acari: Ixodidae). J Med Entomol. 2016;53:1226–33. https://doi.org/10.1093/jme/tjw080
6. Savage HM, Godsey MS Jr, Panella NA, Burkhalter KL, Ashley DC, Lash RR, et al. Surveillance for Heartland virus (Bunyaviridae: Phlebovirus) in Missouri during 2013: first detection of virus in adults of *Amblyomma americanum* (Acari: Ixodidae). J Med Entomol. 2016;53:607–12. https://doi.org/10.1093/jme/tjw028
7. Riemersma KK, Komar N. Heartland virus neutralizing antibodies in vertebrate wildlife, United States, 2009–2014. Emerg Infect Dis. 2015;21:1830–3. https://doi.org/10.3201/eid2110.150380
8. Sonenshine DE. Range expansion of tick disease vectors in North America: implications for spread of tick-borne disease. Int J Environ Res Public Health. 2018;15:478. https://doi.org/10.3390/ijerph15030478
9. Raghavan RK, Peterson AT, Cobos ME, Ganta R, Foley D. Current and future distribution of the lone star tick, *Amblyomma americanum* (L.) (Acari: Ixodidae) in North

America. PLoS One. 2019;14:e0209082. https://doi.org/10.1371/journal.pone.0209082
10. Springer YP, Jarnevich CS, Barnett DT, Monaghan AJ, Eisen RJ. Modeling the present and future geographic distribution of the lone star tick, *Amblyomma americanum* (Ixodida: Ixodidae), in the continental United States. Am J Trop Med Hyg. 2015;93:875–90. https://doi.org/10.4269/ajtmh.15-0330
11. Keirans JE, Durden LA. Illustrated key to nymphs of the tick genus *Amblyomma* (Acari: Ixodidae) found in the United States. J Med Entomol. 1998;35:489–95. https://doi.org/10.1093/jmedent/35.4.489
12. Keirans JE, Litwak TR. Pictorial key to the adults of hard ticks, family *Ixodidae* (Ixodida: Ixodoidea), east of the Mississippi River. J Med Entomol. 1989;26:435–48. https://doi.org/10.1093/jmedent/26.5.435
13. Savage HM, Burkhalter KL, Godsey MS Jr, Panella NA, Ashley DC, Nicholson WL, et al. Bourbon virus in field-collected ticks, Missouri, USA. Emerg Infect Dis. 2017;23:2017–22. https://doi.org/10.3201/eid2312.170532
14. Biggerstaff BJ. PooledInfRate, version 4.0: a Microsoft® Office Excel© add-in to compute prevalence estimates from pooled samples. Fort Collins (CO): Centers for Disease Control and Prevention; 2009.
15. Savage HM, Godsey MS Jr, Panella NA, Burkhalter KL, Manford J, Trevino-Garrison IC, et al. Surveillance for tick-borne viruses near the location of a fatal human case of bourbon virus (Family *Orthomyxoviridae*: Genus *Thogotovirus*) in eastern Kansas, 2015. J Med Entomol. 2018;55:701–5. https://doi.org/10.1093/jme/tjx251

Address for correspondence: Holly. C. Tuten, Biocontrol Laboratory, 1902 Griffith Dr, Champaign, IL 61820, USA; email: htuten@illinois.edu

# Approach to Cataract Surgery in an Ebola Virus Disease Survivor with Prior Ocular Viral Persistence

Jill R. Wells, Ian Crozier, Colleen S. Kraft, Mary Elizabeth Sexton, Charles E. Hill, Bruce S. Ribner, Sina Bavari, Gustavo Palacios, William A. Pearce, Russell Van Gelder, Hans Grossniklaus, Lisa Cazares, Xiankun Zeng, Jessica G. Shantha, Steven Yeh

A 46-year-old patient with previously documented Ebola virus persistence in his ocular fluid, associated with severe panuveitis, developed a visually significant cataract. A multidisciplinary approach was taken to prevent and control infection. Ebola virus persistence was assessed before and during the operation to provide safe, vision-restorative phacoemulsification surgery.

The 2013–2016 Ebola virus disease (EVD) outbreak in western Africa was unprecedented in magnitude, leading to the largest cohort of EVD survivors in history (*1*). Thousands of survivors were at risk for ophthalmic, mental health, and other EVD-associated health conditions, as well as for Ebola virus (EBOV) persistence in immune-privileged organs, including the eyes, central nervous system, and reproductive organs (*1*–*6*). Three outbreaks have also occurred in the Democratic Republic of Congo from 2016 through 2020 (*7*,*8*), underscoring the potential public health impact of medical care for EVD survivors.

Elsewhere we reported the finding of EBOV persistence in the aqueous humor, associated with sight-threatening panuveitis in a healthcare worker who is an EVD survivor (*2*). Subsequent follow-up visits showed multiple recurrences of anterior and intermediate uveitis, which required treatment with topical corticosteroids (*9*). The patient subsequently developed a visually significant cataract. Because of uncertainty about whether EBOV could persist in the eye, doctors had to consider this when developing an approach to treatment. The resulting treatment plan included revised workflow for phacoemulsification, including laboratory specimen analysis.

Author affiliations: Emory University School of Medicine, Atlanta, Georgia, USA (J.R. Wells, W.A. Pearce, H. Grossniklaus, J.G. Shantha, S. Yeh); National Cancer Institute, Frederick, Maryland, USA (I. Crozier); Emory University Hospital, Atlanta (C.S. Kraft, M.E. Sexton, C.E. Hill, B.S. Ribner); United States Army Medical Research Institute of Infectious Disease, Frederick (S. Bavari, G. Palacios, L. Cazares, X. Zeng); University of Washington, Seattle, Washington, USA (R. Van Gelder)

DOI: https://doi.org/10.3201/eid2607.191559

## Studies

The patient, a 46-year-old healthcare worker from the United States with a history of acute, severe panuveitis associated with iris heterochromia (Figure, panel A), hypotony, and persistence of ocular EBOV, had been treated with oral corticosteroids, favipiravir, periocular triamcinolone acetonide (40 mg/mL), and intensive topical difluprednate for 2 years prior to seeking treatment for the cataract (*2*,*9*). During 2015–2016, the patient experienced 2 episodes of recurrent anterior uveitis. During these episodes, we used reverse transcription PCR (RT-PCR) to test for EBOV RNA in the aqueous humor; results were negative.

Over the following 3 months, the patient experienced progressive vision loss without pain. On follow-up examination, the iris heterochromia had resolved. Visual acuities were 20/20 in the right eye and 20/125 in the left eye. Slit lamp examination results were unremarkable for the right eye but showed a 4+ posterior subcapsular cataract in the left eye. While the patient awaited surgical treatment, recurrent anterior uveitis prompted doctors to prescribe a tapering course of topical corticosteroids. Results from RT-PCR for EBOV RNA of an aqueous humor aspirate were negative. We documented 3 months of disease inactivity prior to cataract surgery. During this time, his visual acuity in the left eye declined to the hand motions level, and he developed an intumescent uveitic cataract (Figure, panels B and C).

After evaluating the risk of exposure during the operation, the surgical team chose to use personal protective equipment (PPE) including a surgical hat,

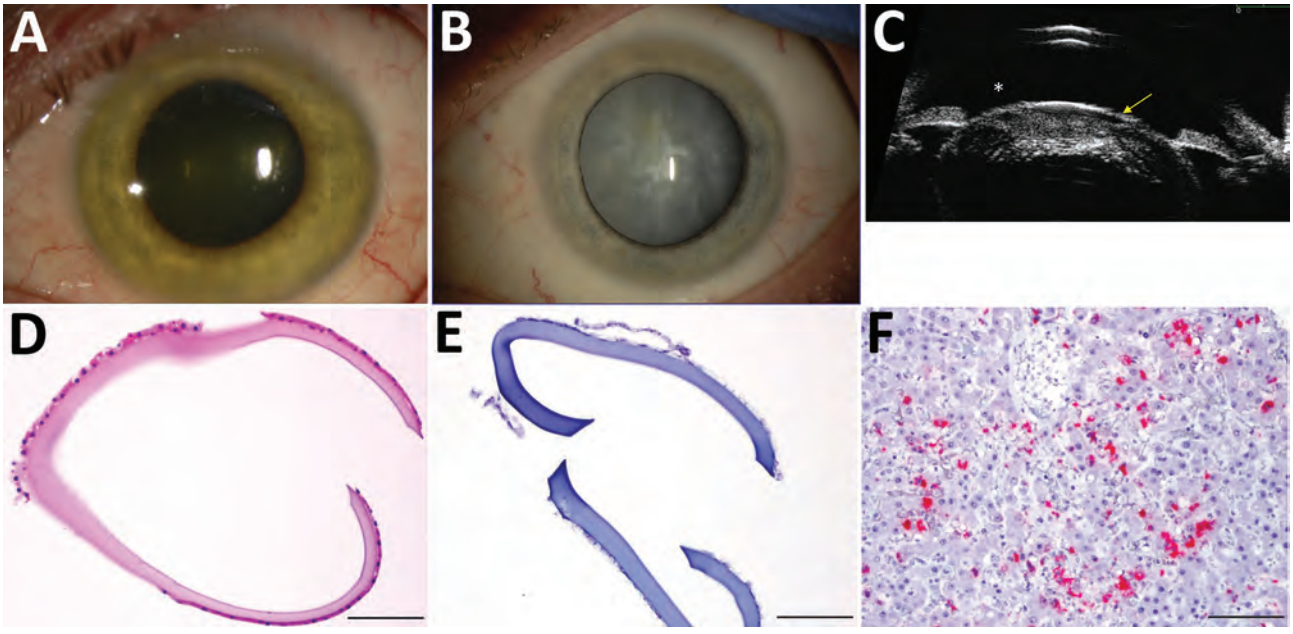


**Figure.** Cataract surgery in an Ebola virus disease survivor with prior ocular viral persistence. A) Slit lamp image shows green iris hue when patient developed panuveitis with heterochromia. B) The greenish coloration resolved but a dense intumescent cataract developed as shown in the second slit lamp image. C) Ultrasound biomicroscopic examination demonstrates the bulging of the anterior lens capsule (yellow arrow) and shallowing of the anterior chamber (*), which presents an increased risk for anterior and posterior capsular tears during surgery. D) Hematoxylin and eosin staining shows thickening of the removed anterior capsule. E) Results were negative for Ebola virus RNA by in situ hybridization. F) Positive control tissue.

mask, and fluid-impervious scrub booties. Additional PPE was not used because they considered the amount of fluid in the surgical field too small to present a significant splash risk (Appendix, https://wwwnc.cdc.gov/EID/article/26/7/19-1559-App1.pdf). The surgery was scheduled as the final procedure in the day, recognizing the possibility of the ocular fluids testing positive for EBOV RNA. In this way, the room could be terminally cleaned after surgery without disrupting subsequent patient care.

The surgical plan was modified to include taking specimens of aqueous humor and tissue at multiple points during surgery to be analyzed in the laboratory. These specimens included aqueous humor taken prior to entry through the lens capsule, liquefied lens cortex aspirate taken from the cataractous lens in situ, and aqueous humor taken after the cataract was removed but before wound closure. In addition, the anterior capsule was removed in its entirety for in situ hybridization with probe pairs targeting EBOV nucleoprotein genomes. After the cataract was extracted and the intraocular lens implanted, a 10-0 nylon suture was placed as a precautionary measure (Appendix; Video, https://wwwnc.cdc.gov/EID/article/26/7/19-1559-V1.htm). A conjunctival swab specimen taken after the procedure was sent for EBOV RNA testing in the Emory Serious Communicable Disease Program laboratory onsite using a BioFire FilmArray BioThreat E test (BioFire Defense, https://www.biofiredefense.com). Before machine and tubing breakdown and waste management, RT-PCR was performed on the collected specimens; all results were negative for EBOV.

The extracted lens capsule was formalin-fixed and paraffin-embedded for histopathology. We performed in situ hybridization, with probe pairs targeting genomic EBOV nucleoprotein genes. Anterior capsular thickening was observed, but EBOV RNA was not detected in the anterior capsule tissue (Figure, panels D–F). Transmission electron microscopy of the lens cortex showed vacuolations and examination of thick sections stained with toluidine blue showed fragments of lens cortex; no EBOV particles were observed. Mass spectrometry showed 215 peptides of human origin, with the greatest numbers of peptide spectrum matches observed for beta-crystallin, alpha-crystallin, phakinin, and gamma-crystallin proteins. We observed no EBOV-specific peptide sequences.

By 1 month after cataract surgery, visual acuity in the patient's left eye had improved to 20/20, which was maintained at 24-month follow-up. Postoperative retinal examination showed multifocal chorioretinal scars and mild vitreous opacity in the left eye.

## Conclusions

We report an approach to safe, vision-restoring phacoemulsification surgery for a visually significant cataract in an EVD survivor with previously documented ocular EBOV persistence. This stepwise approach could be used as a model for treatment of EVD survivors from affected areas after an outbreak. Negative results from RT-PCR testing of aqueous humor and liquefied lens cortex specimens provided assurance that no EBOV exposure had occurred during surgery.

Tropism of ocular tissue and cells of EBOV remains ill-defined in humans. In nonhuman primate survivors of EVD, EBOV RNA has been detected in macrophage reservoirs within the vitreous cavity (*10*). Smith et al. demonstrated, in vitro, that retinal pigment epithelial cells are a potential reservoir for EBOV infection and support viral replication with the release of virus in high titer (*11*); however, they express immunomodulatory molecules linked to ocular immune privilege.

Because of concerns about viral persistence raised in these studies, our practice had been to ensure that EBOV RNA was not detected before proceeding with ocular surgery. RT-PCR testing conducted 3 months before surgery did not detect EBOV RNA in the patient's aqueous humor. The Ebola Virus Persistence in Ocular Tissues and Fluids Study in Sierra Leone likewise used a stepwise approach to cataract surgery, requiring a negative result from an aqueous humor aspirate test for EBOV RNA prior to manual small-incision cataract surgery (*12*). This surgery has now been performed successfully for >50 EVD survivors in Sierra Leone and Liberia (*13*), but this approach, in which multiple laboratories were needed for analyses, would not be feasible in many areas affected by EBOV outbreaks.

Questions remain about the optimal length of time to wait after EBOV infection before performing cataract surgery and about the safety of other types of ophthalmic surgery. Whereas phacoemulsification was performed safely and effectively in this case, it was not done until approximately 27 months after EBOV RNA had been identified in the patient's aqueous humor. In 2 phases of a previous study, we documented that the aqueous humor tested negative for EBOV RNA at a median of 19 months in one phase and 34 months in the other (*12*). Whether cataract surgery may be performed safely prior to these time points requires better understanding of the kinetics of EBOV entry and clearance from the eye.

Our team used ultrastructural, genomic, and proteomic assessment on tissues and fluids in a multidisciplinary, multilaboratory approach to mitigate surgical risk. Given the thousands of global EVD survivors with a potential need for eye surgery, a comprehensive understanding of safety precautions for both EVD survivors and their health care providers, as well as of surgical and laboratory approaches for effective eye surgery, will be needed.

This project was supported by an unrestricted departmental grant from Research to Prevent Blindness, Inc., to the Department of Ophthalmology at the University of Washington and the Emory Eye Center, Emory University School of Medicine; National Eye Institute/National Institutes of Health core grant P30-EY06360 (Department of Ophthalmology, Emory University School of Medicine); Building Interdisciplinary Research Careers in Women's Health (BIRCWH) of the National Institutes of Health K12HD085850 (J.G. Shantha); National Eye Institute of the National Institutes of Health under award number K23 EY030158 (J.G. Shantha); RO1 EY029594 (S. Yeh); and Center for AIDS Research at the National Institutes of Health P30 AI050409 (C.S. Kraft). Funding sources also include the Mark J. Daily MD Research Fund (R. Van Gelder).

## About the Author

Dr. Wells is an assistant professor of ophthalmology, specializing in comprehensive ophthalmology and ocular oncology at the Emory Eye Center, Emory University School of Medicine, in Atlanta. Her clinical and surgical research interests include management of complex cataract surgery, conjunctival tumors, choroidal melanoma, and retinoblastoma.

## References

1. Vetter P, Kaiser L, Schibler M, Ciglenecki I, Bausch DG. Sequelae of Ebola virus disease: the emergency within the emergency. Lancet Infect Dis. 2016;16:e82–91. https://doi.org/10.1016/S1473-3099(16)00077-3
2. Varkey JB, Shantha JG, Crozier I, Kraft CS, Lyon GM, Mehta AK, et al. Persistence of Ebola virus in ocular fluid during convalescence. N Engl J Med. 2015;372:2423–7. https://doi.org/10.1056/NEJMoa1500306
3. Jacobs M, Rodger A, Bell DJ, Bhagani S, Cropley I, Filipe A, et al. Late Ebola virus relapse causing meningoencephalitis: a case report. Lancet. 2016;388:498–503. https://doi.org/10.1016/S0140-6736(16)30386-5
4. Deen GF, Broutet N, Xu W, Knust B, Sesay FR, McDonald SLR, et al. Ebola RNA persistence in semen of Ebola virus disease survivors—final report. N Engl J Med. 2017;377:1428–37. https://doi.org/10.1056/NEJMoa1511410
5. PREVAIL III Study Group. Sneller MC, Reilly C, Badio M, Bishop RJ, Eghrari AO, Moses SJ, et al. A longitudinal study of Ebola sequelae in Liberia. N Engl J Med. 2019;380:924–34. https://doi.org/10.1056/NEJMoa1805435
6. Shantha JG, Crozier I, Hayek BR, Bruce BB, Gargu C, Brown J, et al. Ophthalmic manifestations and causes of

vision impairment in Ebola virus disease survivors in Monrovia, Liberia. Ophthalmology. 2017;124:170–7. https://doi.org/10.1016/j.ophtha.2016.10.011
7. Mbala-Kingebeni P, Pratt CB, Wiley MR, Diagne MM, Makiala-Mandanda S, Aziza A, et al. 2018 Ebola virus disease outbreak in Équateur Province, Democratic Republic of the Congo: a retrospective genomic characterisation. Lancet Infect Dis. 2019;19:641–7. https://doi.org/10.1016/S1473-3099(19)30124-0
8. Nsio J, Kapetshi J, Makiala S, Raymond F, Tshapenda G, Boucher N, et al. Outbreak of Ebola virus disease in northern Democratic Republic of Congo. J Infect Dis. 2020;221:701–6. https://doi.org/10.1093/infdis/jiz107
9. Shantha JG, Crozier I, Varkey JB, Kraft CS, Lyon GM III, Mehta AK, et al. Long-term management of panuveitis and iris heterochromia in an Ebola survivor. Ophthalmology. 2016;123:2626–2628.e2. https://doi.org/10.1016/j.ophtha.2016.07.013
10. Zeng X, Blancett CD, Koistinen KA, Schellhase CW, Bearss JJ, Radoshitzky SR, et al. Identification and pathological characterization of persistent asymptomatic Ebola virus infection in rhesus monkeys. Nat Microbiol. 2017;2:17113. https://doi.org/10.1038/nmicrobiol.2017.113
11. Smith JR, Todd S, Ashander LM, Charitou T, Ma Y, Yeh S, et al. Retinal pigment epithelial cells are a potential reservoir for Ebola virus in the human eye. Transl Vis Sci Technol. 2017;6:12. https://doi.org/10.1167/tvst.6.4.12
12. Shantha JG, Mattia JG, Goba A, Barnes KG, Ebrahim FK, Kraft CS, et al. Ebola Virus Persistence in Ocular Tissues and Fluids (EVICT) study: reverse transcription-polymerase chain reaction and cataract surgery outcomes of Ebola survivors in Sierra Leone. EBioMedicine. 2018;30:217–24. https://doi.org/10.1016/j.ebiom.2018.03.020
13. Bishop R, Ross R, Shantha JG, Hayek B, Gradin D, Roberts B, et al. Ebola virus persistence in aqueous humor and 12-month outcomes of cataract surgery in survivors of Ebola virus disease [abstract 1012]. Investigative Ophthalmology and Visual Science 2019; 60: 1012. https://iovs.arvojournals.org/article.aspx?articleid=2741574

Address for correspondence: Steven Yeh, MD, Emory Eye Center, 1365B Clifton Rd. NE, Atlanta, GA 30322, USA; email: syeh3@emory.edu

# Sub-Saharan Africa and Eurasia Ancestry of Reassortant Highly Pathogenic Avian Influenza A(H5N8) Virus, Europe, December 2019

Edyta Świętoń, Alice Fusaro, Ismaila Shittu, Krzysztof Niemczuk, Bianca Zecchin, Tony Joannis, Francesco Bonfante, Krzysztof Śmietanka, Calogero Terregino

We report detection of a highly pathogenic avian influenza A(H5N8) clade 2.3.4.4b virus in Europe. This virus was generated by reassortment between H5N8 subtype virus from sub-Saharan Africa and low pathogenicity avian influenza viruses from Eurasia.

Highly pathogenic avian influenza (HPAI) H5 viruses belonging to clade 2.3.4.4 of the Goose/Guangdong/96 (GS/Gd) lineage continue to pose a threat to poultry and wild birds worldwide (*1*–*6*). Reassortment events between HPAI H5 and low pathogenicity avian influenza (LPAI) viruses of wild-bird origin have led to generation of novel variants that might be periodically spread by wild birds across continents (*6*).

After detection of the unofficially defined clade 2.3.4.4b (*7*) in May 2016 in Lake Uvs-Nur, Russia (*8*), and Qinghai Lake, China (*9*), the virus spread to Europe and Africa, causing one of the largest epizootics reported (*1*). This virus reached several countries in northern, western, eastern, central, and southern areas of Africa (*10*). Nigeria, Namibia, South Africa (*11*), and Egypt reported H5N8 cases throughout 2019, suggesting ongoing circulation of the virus in Africa.

No HPAI H5N8 viruses were detected in Europe during June–November 2019 (*12*). We report detection of a reassortant HPAI A(H5N8) clade 2.3.4.4b virus in Europe during December 2019.

Author affiliations: National Veterinary Research Institute, Puławy, Poland (E. Świętoń, K. Niemczuk, K. Śmietanka); Istituto Zooprofilattico Sperimentale delle Venezie, Legnaro, Italy (A. Fusaro, B. Zecchin, F. Bonfante, C. Terregino); National Veterinary Research Institute, Vom, Nigeria (I. Shittu, T. Joannis)

DOI: https://doi.org/10.3201/eid2607.200165

## The Study

In July 2019, in the framework of active surveillance measures implemented in live bird markets in 18 of the 36 states in Nigeria, the National Veterinary Research Institute in Vom, Nigeria, identified a HPAI H5N8 virus in a guinea fowl in the southwestern state of Ogun. Months later, at the end of December 2019, a suspicion of an HPAI virus was raised in a holding of 14-week-old meat turkeys in Poland, located near water bodies (fish ponds and lakes of the Łęczna-Włodawa Lakeland). A sudden increase in deaths was observed, accompanied by neurologic signs such as trembling, inability to walk, paralysis of the wings, and pedaling movements of the legs. A total of 3,000–5,000 birds died during the first 3 days after the onset of clinical signs. Organ samples submitted to the National Reference Laboratory for Avian influenza at the National Veterinary Research Institute, Pulawy, Poland, were positive for avian influenza virus and were characterized as HPAI H5N8.

We conducted antigenic characterization of the virus isolate by using the hemagglutination inhibition (HI) assay, which showed that the H5N8 virus in Poland had higher antigenic reactivity with European Union Reference Laboratory reference HPAI H5N8 A/turkey/Italy/7898/2014 (IT-7898) chicken antiserum (clade 2.3.4.4, GS/Gd lineage) compared with reactivity determined for European Union Reference Laboratory HPAI H5N1 A/chicken/Scotland/1/59 (SCOT-59) and LPAI H5N3 A/teal/England/7394–2805/06 (ENG-7394) antiserum.

A comparison of HI titers obtained with the IT-7898, SCOT-59 and ENG-7394 homologous antigens and those recorded against the strain from Poland showed differences of 2 log2, 4 log2, and 5 log2, respectively. The H5N1 and H5N3 strains belong to the H5 Eurasian

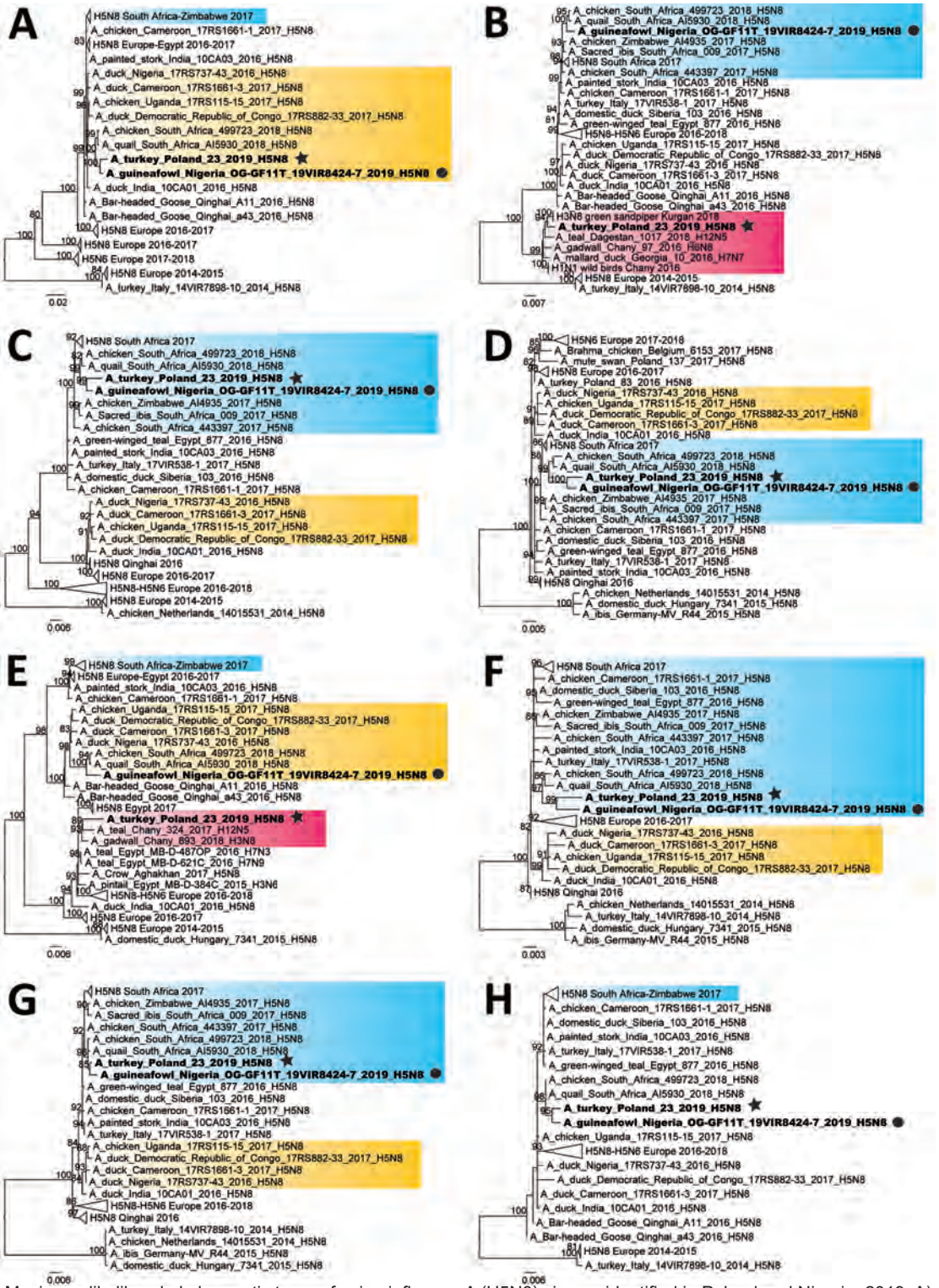


**Figure 1.** Maximum-likelihood phylogenetic trees of avian influenza A (H5N8) viruses identified in Poland and Nigeria, 2019. A) Polymerase basic protein 2, C) polymerase basic protein 1, C) polymerase acidic protein, D) hemagglutinin, E) nucleoprotein, F) neuraminidase, G) matrix protein, H) nonstructural protein. H5N8 viruses detected in Poland and Nigeria in 2019 are indicated in bold, A/turkey/Poland/23/2019(H5N8) is indicated by a black star, and A/guinea_fowl/Nigeria/OG-GF11T_19VIR8424–7/2019(H5N8) is indicated by a black circle. Blue box indicates the South Africa 2017 H5N8 cluster, yellow boxes indicate the West-Central Africa 2016–2017 cluster, and purple box indicates Eurasian LPAI viruses. Numbers next to each node represent ultrafast bootstrap supports (>80). Scale bars indicate nucleotide substitutions per site. LPAI, low pathogenicity avian influenza virus.

lineage and are unrelated to the GS/Gd lineage, which supports the marked difference in reactivity. Pathotyping of the virus from Poland by using the intravenous pathogenicity index recorded a value of 3.0, confirming the highly pathogenic phenotype in chickens.

As of January 31, 2020, a total of 20 outbreaks in poultry (commercial and backyard holdings) and 1 case in a wild bird (a dead goshawk found near the index farm) had been detected in different regions from eastern to western Poland. Since the reassortant virus was detected in Poland, the World Organisation for Animal Health has been notified about similar outbreaks in Slovakia, Hungary, Romania, Germany, and the Czech Republic. A greater white-fronted goose (*Anser albifrons*) in Germany, near the border with Poland, was also found to be infected (*13*).

The genomes of HPAI H5N8 strains from index cases from Nigeria (A/guinea fowl/Nigeria/OG-GF11T_19VIR8424–7/2019) and Poland (A/turkey/Poland/23/2019) have been sequenced (Appendix, https://wwwnc.cdc.gov/EID/article/26/7/20-0165-App1.pdf) and submitted to the GISAID EpiFlu database (https://www.gisaid.org) under isolate nos. EPI_ISL_405278 and EPI_ISL_402134, respectively. Phylogenetic analysis (Appendix) of the hemagglutinin (HA) gene showed that both viruses belonged to clade 2.3.4.4b (Figure 1).

Topology of the polymerase basic protein 2, polymerase acidic protein, HA, neuraminidase, matrix, and nonstructural protein gene phylogenies showed that the viruses from Poland and Nigeria clustered together (nucleotide identity 98.9%–99.5%) (Table) and also with two 2018 H5N8 viruses from South Africa (*3*), which have been demonstrated to be a novel genotype that originated from reassortment events between clade 2.3.4.4b H5N8 viruses from South Africa and West-Central Africa (Figure 1). In contrast, the 2 strains clustered separately for the polymerase basic protein 1 and nucleoprotein gene phylogenies (Figure 1).

For the polymerase basic protein 1 and nucleoprotein genes, the virus from Nigeria grouped with the 2018 viruses from South Africa as for the other gene segments, whereas the virus from Poland clustered with LPAI viruses identified in recent years in the Chany and Kurgan regions of Russia. This finding indicates that the strain from Poland is a reassortant virus derived from LPAI viruses identified in wild birds in those areas of Asia (Figure 2), which represent staging areas for wild birds migrating to Europe. However, where this reassortment event occurred cannot be assessed from the available data. Analysis of molecular markers associated with zoonotic potential demonstrated the absence in the HA and polymerase basic protein 2 genes of major signatures associated with increased replication in humans.

## Conclusions

Our data describe a novel HPAI H5N8 genotype of clade 2.3.4.4b in Europe, in which 6 gene segments originated from sub-Saharan Africa HPAI H5N8 clade 2.3.4.4b viruses and 2 gene segments from Eurasia LPAI viruses. It has been shown that Africa might serve as a

**Table.** Nucleotide identity of A/turkey/Poland/23/2019(H5N8) and A/guinea_fowl/Nigeria/OG-GF11T_19VIR8424–7/2019 influenza virus gene segments with the most similar sequences available in GenBank and EpiFlu*

| Gene segment | Virus 1 | Virus 2 | Nucleotide identity, % |
|---|---|---|---|
| PB2 | H5N8 Poland 2019† | H5N8 Nigeria 2019‡ | 98.9 |
| | H5N8 Nigeria 2019 | H5N8 South Africa 2018§ | 98.7 |
| PB1 | H5N8 Poland 2019 | H3N8 Kurgan 2018¶ | 99.1 |
| | H5N8 Poland 2019 | H5N8 Nigeria 2019 | 94.7 |
| | H5N8 Nigeria 2019 | H5N8 South Africa 2018 | 99.2 |
| PA | H5N8 Poland 2019 | H5N8 Nigeria 2019 | 98.9 |
| | H5N8 Nigeria 2019 | H5N8 South Africa 2018 | 99.2 |
| HA | H5N8 Poland 2019 | H5N8 Nigeria 2019 | 99.1 |
| | H5N8 Nigeria 2019 | H5N8 South Africa 2018 | 98.7 |
| NP | H5N8 Poland 2019 | H3N8 Chany 2018# | 98.5 |
| | H5N8 Poland 2019 | H5N8 Nigeria 2019 | 92.8 |
| | H5N8 Nigeria 2019 | H5N8 South Africa 2018 | 98.9 |
| NA | H5N8 Poland 2019 | H5N8 Nigeria 2019 | 98.8 |
| | H5N8 Nigeria 2019 | H5N8 South Africa 2018 | 98.9 |
| M | H5N8 Poland 2019 | H5N8 Nigeria 2019 | 99.5 |
| | H5N8 Nigeria 2019 | H5N8 South Africa 2018 | 99.4 |
| NS | H5N8 Poland 2019 | H5N8 Nigeria 2019 | 99.0 |
| | H5N8 Nigeria 2019 | H5N8 South Africa 2018 | 99.2 |

*HA, hemagglutinin; M, matrix protein; NA, neuraminidase; NP, nucleoprotein; NS, nonstructural protein; PA, polymerase acidic protein; PB1, polymerase basic protein 1; PB2, polymerase basic protein 2.
†A/turkey/Poland/23/2019(H5N8).
‡A/guinea_fowl/Nigeria/OG-GF11T_19VIR8424–7/2019(H5N8).
§A/chicken/South Africa/499723/2018(H5N8).
¶A/green sandpiper/Kurgan/1043/2018(H3N8).
#A/gadwall/Chany/893/2018(H3N8).

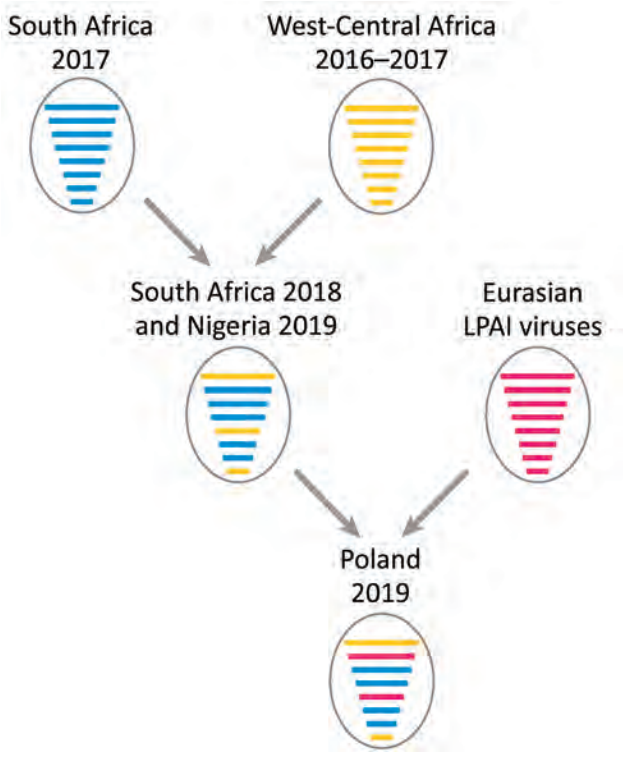


**Figure 2.** Reassortment events between highly pathogenic avian influenza virus H5N8 viruses from South Africa (2017), HPAI H5N8 viruses from West-Central Africa (2017); and LPAI viruses from Eurasia giving rise to A/guinea_fowl/Nigeria/OG-GF11T_19VIR8424–7/2019(H5N8) (Nigeria 2019) and A/turkey/Poland/23/2019(H5N8) (Poland 2019). Each gene segment is represented by a bar of different length, from top to bottom: polymerase basic protein 2 (PB2), polymerase basic protein 1 (PB1), polymerase acidic protein (PA), hemagglutinin (HA), nucleoprotein (NP), neuraminidase (NA), matrix protein (M), and nonstructural protein (NS). Each color represents a different viral origin: blue, H5N8 South Africa (2017); yellow, H5N8 West-Central Africa (2017); purple, Eurasian LPAI viruses. LPAI, low pathogenicity avian influenza virus.

strong epidemiologic area of circulation for Gs/GD H5 (*10*). However, despite extensive circulation in poultry in several countries in Africa, virus spread by wild birds from Africa to Europe has not been documented.

Possible introduction of an influenza A virus from Africa into Eurasia might be caused by widespread virus circulation in previously unaffected areas, high prevalence of the virus in wild birds in Africa, or alterations of the migratory bird exposure risks after changes in migratory routes caused by unusual weather patterns. Identification of highly related virus strains 1 year apart in 2 countries in Africa >5,000 km apart confirms the high mobility of the HPAI H5N8 virus and suggests a gap in surveillance efforts in these areas. The lack of such surveillance data makes it impossible to determine where this virus originated and whether it spread from South Africa to Nigeria or to both countries from unsampled locations, and to assess its prevalence in Africa.

Our results suggest that H5N8 virus might have been spread from Africa to Asia or Europe by wild bird migratory movements, likely in 2019, although other routes of virus spread cannot be ruled out. Until its detection in Poland in December 2019, the virus might have circulated in an unknown region of Europe or Asia where it reassorted with local LPAI strains of the Eurasian lineage, although we cannot completely exclude that this reassortment event might have occurred in Africa. Late detection in Europe (end of December 2019), compared with the epidemic wave during 2016–17 (October 2016), might be explained by unusually mild temperatures in molting areas in Russia during November and December 2019 (*14*,*15*) and the late westward movement of infected wintering wild birds.

Subclinical infections or insufficient active surveillance efforts in clinically healthy wild population might be the cause of the few detections of the H5N8 virus in wild birds in Eurasia and along the Africa–Eurasia flyways. A better understanding of factors regulating wild bird migrations, as well as increasing wild and domestic bird surveillance in Africa and Eurasia, is needed to improve our ability to early detect and monitor virus spread.

### Acknowledgments

We thank Mauro Delogu for critically reading the manuscript, Francesca Ellero for providing technical assistance, and the originating and submitting laboratories of the sequences from the GISAID EpiFlu Database on which this research is partially based. All submitters of data may be contacted directly through the GISAID website (http://www.gisaid.org).

### About the Author

Dr. Świętoń is a research associate in the Department of Poultry Diseases, National Veterinary Research Institute, Puławy, Poland. Her primary research interests are avian influenza epidemiology and pathogenesis.

### References

1. Alarcon P, Brouwer A, Venkatesh D, Duncan D, Dovas CI, Georgiades G, et al. Comparison of 2016–17 and previous epizootics of highly pathogenic avian influenza H5 Guangdong lineage in Europe. Emerg Infect Dis. 2018;24:2270–83. https://doi.org/10.3201/eid2412.171860
2. Poen MJ, Venkatesh D, Bestebroer TM, Vuong O, Scheuer RD, Oude Munnink BB, et al. Co-circulation of genetically distinct highly pathogenic avian influenza A clade 2.3.4.4 (H5N6) viruses in wild waterfowl and poultry in Europe and East Asia, 2017–18. Virus Evol. 2019;5:vez004. https://doi.org/10.1093/ve/vez004

3. Abolnik C. Outbreaks of clade 2.3.4.4 H5N8 highly pathogenic avian influenza in 2018 in the northern regions of South Africa were unrelated to those of 2017. Transbound Emerg Dis. 2019 Dec 23 [Epub ahead of print]. https://doi.org/10.1111/tbed.13448
4. Salaheldin AH, El-Hamid HS, Elbestawy AR, Veits J, Hafez HM, Mettenleiter TC, et al. of Influenza A(H5N8) virus into poultry, Egypt, 2017. Emerg Infect Dis. 2018;24:943–6. https://doi.org/10.3201/eid2405.171935
5. Baek YG, Lee YN, Lee DH, Cheon SH, Kye SJ, Park YR, et al. A novel reassortant clade 2.3.4.4 highly pathogenic avian influenza H5N6 virus identified in South Korea in 2018. Infect Genet Evol. 2020;78:104056. https://doi.org/10.1016/j.meegid.2019.104056
6. Tsunekuni R, Sudo K, Nguyen PT, Luu BD, Phuong TD, Tan TM, et al. Isolation of highly pathogenic H5N6 avian influenza virus in Southern Vietnam with genetic similarity to those infecting humans in China. Transbound Emerg Dis. 2019;66:2209–17. https://doi.org/10.1111/tbed.13294
7. Lee D, Bertran K, Kwon J, Swayne DE. Emergence and evolution of HPAI H5Nx clade 2.3.4.4. J Vet Sci. 2017;18:269–80. https://doi.org/10.4142/jvs.2017.18.S1.269
8. Lee D-H, Sharshov K, Swayne DE, Kurskaya O, Sobolev I, Kabilov M, et al. Novel reassortant clade 2.3.4.4 avian influenza A(H5N8) virus in wild aquatic birds, Russia, 2016. Emerg Infect Dis. 2017;23:359–60. https://doi.org/10.3201/eid2302.161252
9. Li M, Liu H, Bi Y, Sun J, Wong G, Liu D, et al. Highly pathogenic avian influenza A(H5N8) virus in wild migratory birds, Qinghai Lake, China. Emerg Infect Dis. 2017;23:637–41. https://doi.org/10.3201/eid2304.161866
10. Fusaro A, Zecchin B, Vrancken B, Abolnik C, Ademun R, Alassane A, et al. Disentangling the role of Africa in the global spread of H5 highly pathogenic avian influenza. Nat Commun. 2019;10:5310. https://doi.org/10.1038/s41467-019-13287-y
11. World Organisation for Animal Health. Update on avian influenza in animals (types H5 and H7), 2019 [cited 2020 Jan 23]. https://www.oie.int/en/animal-health-in-the-world/update-on-avian-influenza/2019
12. Adlhoch C, Fusaro A, Kuiken T, Monne I, Smietanka K, Staubach C, et al. Avian influenza overview February–August 2019. European Food Safety Authority Journal. 2019. [cited 2020 Apr 6]. https://www.ecdc.europa.eu/sites/default/files/documents/avian-influenza-overview-february-august-2019.pdf
13. World Organisation for Animal Health. Update on avian influenza in animals (types H5 and H7), 2020 [cited 2020 Jan 23]. https://www.oie.int/en/animal-health-in-the-world/update-on-avian-influenza/2020
14. Veen J, Yurlov AK, Delany SN, Mihantiev AI, Selivanova MA, Boere GC. An atlas of movements of southwest Siberian waterbirds. Wageningen (The Netherlands): Wetlands International; 2005 [cited 2020 Jan 22]. https://www.researchgate.net/publication/270215317_An_Atlas_of_Movements_of_Southwest_Siberian_Waterbirds
15. Copernicus. Surface air temperature maps [cited 2020 Jan 23]. https://climate.copernicus.eu/surface-air-temperature-maps


Address for correspondence: Alice Fusaro, European Union Reference Laboratory for Avian Influenza and Newcastle Disease, Istituto Zooprofilattico Sperimentale delle Venezie, Viale dell'Università 10, 35020 Legnaro, Italy; email: afusaro@izsvenezie.it

# Clinical Management of Argentine Hemorrhagic Fever using Ribavirin and Favipiravir, Belgium, 2020

Ioannis Veliziotis, Alain Roman, Delphine Martiny, Gerlind Schuldt, Marc Claus, Nicolas Dauby, Sigi Van den Wijngaert, Charlotte Martin, Rakan Nasreddine, Claudia Perandones, Romain Mahieu, Corien Swaan, Serge Van Praet, Deborah Konopnicki, Maria A. Morales, Denis Malvy, Etienne Stevens, Philippe Dechamps, Erika Vlieghe, Olivier Vandenberg, Stephan Günther,[1] Michèle Gérard[1]

We report a case of Argentine hemorrhagic fever diagnosed in a woman in Belgium who traveled from a disease-endemic area. Patient management included supportive care and combination therapy with ribavirin and favipiravir. Of 137 potential contacts, including friends, relatives, and healthcare and laboratory workers, none showed development of clinical symptoms of this disease.

Argentine hemorrhagic fever (AHF) is a severe hemorrhagic fever caused by a New World arenavirus, Junin virus (JUNV), which was discovered in 1958 (*1*). The virus reservoir consists of rodents found in humid pampas in South America. The endemic area covers 150,000 km$^2$ distributed over 4 provinces in Argentina; ≈5.6 million persons are at risk (*2*).

Until 1992, the year when a prophylactic vaccine was introduced, annual outbreaks affected mainly male agricultural workers (*2*). The number of confirmed cases reported annually has decreased from 400–500 before 1992 to 13 cases in 2018 (*3*).

In January 2020, AHF was diagnosed in a woman in Brussels, Belgium, who had traveled from Argentina to Europe. We report clinical manifestations, management, and public health response for this case.

## The Study

In early January 2020, a 41-year old woman was admitted to the hospital in Brussels because of lethargy, confusion, and fever. She had been in Argentina and arrived in Amsterdam, the Netherlands, by a connecting flight from Madrid. After 4 days in Amsterdam, she traveled by bus to Brussels.

At admission, her travel partner reported that she had an influenza-like illness (including headache, myalgia, anorexia, and sore throat) since 1 week before admission. The patient had consulted a physician before departure from Argentina. The physician performed a blood sample analysis that showed the following results: hemoglobin 16 g/dL, leukocyte count 3,200 cells/mm$^3$, and platelet count 144,000 cells/mm$^3$. Episodes of vomiting at home were reported during her stay in Amsterdam.

In the emergency department, the patient had a seizure. Physical examination showed no petechia or purpura, but vaginal bleeding was observed. Emergency department laboratory results indicated thrombocytopenia, leukopenia, and severe rhabdomyolysis (Table 1). Results of whole-body computed tomography scan were unremarkable. A lumbar puncture was performed, and results of cerebrospinal fluid analysis were within reference ranges. The patient was admitted to the intensive care unit (ICU), and empirical antimicrobial drug therapy with ceftriaxone was started.

Author affiliations: Université de Bruxelles, Brussels, Belgium (I. Veliziotis, A. Roman, D. Martiny, M. Claus, N. Dauby, S. Van den Wijngaert, C. Martin, R. Nasreddine, D. Konopnicki, E. Stevens, P. Dechamps, O. Vandenberg, M. Gérard); Saint-Pierre University Hospital, Brussels (I. Veliziotis, A, Roman, M. Claus, N. Dauby, C. Martin, R. Nasreddine, S. Van Praet, D. Konopnicki, E. Stevens, P. Deschamps, M. Gérard); Bernhard Nocht Institute for Tropical Medicine, Hamburg, Germany. (G. Schuldt, S. Günther); National Administration of Laboratories and Institutes of Health, Buenos Aires, Argentina (C. Perandones); Common Community Commission, Brussels (R. Mahieu); National Institute for Public Health and the Environment, Bilthoven, the Netherlands (C. Swaan); Instituto Nacional de Enfermedades Virales Humanas, Pergamino, Argentina (M.A. Morales); World Health Organization Collaborating Centre for Reference and Research of Arbovirus and Hemorrhagic Fever Virosis, Pergamino (M.A. Morales); University Hospital Center of Bordeaux, Bordeaux, France (D. Malvy); University Hospital Antwerp, Belgium (E. Vlieghe); University College London, London, UK (O. Vandenberg)

DOI: https://doi.org/10.3201/eid2607.200275

[1]These senior authors contributed equally to this article.

**Table 1.** Laboratory findings for a patient with Argentine hemorrhagic fever, Belgium, 2020*

| Parameter | Reference ranges/values | Day 1 (ED) | Day 2 (ICU) | Day 9 | Day 21 | Day 43 |
|---|---|---|---|---|---|---|
| Hemoglobin, g/dL | 12.0–16.0 | 15.1 | 12.3 | 6.1 | 7.2 | 9.3 |
| Erythrocytes, x $10^6$/μL | 3.80–5.00 | 5.2 | 4.3 | 2.12 | 2.6 | 3.2 |
| Hematocrit, % | 35.0–47.0 | 43.1 | 35.2 | NA | 22.8 | 30.8 |
| Platelets, x $10^3$/μL | 150–440 | 66 | 48 | 76 | 268 | 350 |
| Leukocytes, x $10^3$/μL | 3.50–11.00 | 1.48 | 0,81 | 4 | 0.9 | 5.8 |
| Neutrophils, % | 40.0–75.0 | 72.5 | 61,7 | 80.5 | NA | 40.4 |
| Lymphocytes, % | 2.0–10.0 | 12.4 | NA | 11 | NA | 41.9 |
| CRP, mg/L | <5.0 | 3.1 | 2,4 | 60.9 | 137 | 5 |
| Schistocytes/1,000 RBC | <10 | 3 | 4 | NA | NA | NA |
| Haptoglobin, mg/dL | 30–200 | NA | <10 | NA | NA | NA |
| Serum iron, μg/dL | 50–170 | NA | 163 | NA | NA | NA |
| Serum ferritin, μg/L | 30–200 | NA | 36,209 | NA | NA | NA |
| aPTT, s | 18.7–32.1 | 38.8 | 38,3 | NA | NA | NA |
| INR, s | 0.95–1.31 | 1.19 | 1.34 | NA | NA | NA |
| Fibrinogen, mg/dL | 150–400 | 138 | 100 | NA | NA | NA |
| D-dimer, ng/mL | 0–500 | NA | >4,500 | NA | NA | NA |
| AST, U/L | <32 | 1416 | 1,502 | 518 | 72 | NA |
| ALT, U/L | <33 | 238 | 245 | 94 | 48 | NA |
| ALP, U/L | 35–104 | 165 | 187 | NA | NA | NA |
| γ-GT, U/L | 6–42 | 115 | 193 | NA | NA | NA |
| LDH, U/L | 135–214 | NA | 2,359 | NA | NA | NA |
| Total bilirubin, mg/dL | <1.2 | NA | 0,6 | 3.9 | 2.4 | 1.1 |
| Creatinine kinase, U/L | 26–192 | NA | 7,341 | 2,363 | 15 | 28 |
| Triglycerides, mg/dL | <150 | NA | 135 | NA | NA | NA |
| C3, g/L | 0.80–1.64 | NA | 0.3 | NA | NA | NA |
| C4, g/L | 0.10–0.40 | NA | 0.24 | NA | NA | NA |
| HIV | NA | NA | Negative | NA | NA | NA |
| Yellow fever IgG/IgM | NA | NA | Negative | NA | NA | NA |
| Dengue virus IgG/IgM | NA | NA | Negative | NA | NA | NA |
| *Leptospira* sp. | NA | NA | Negative | NA | NA | NA |
| Chikungunya IgG/IgM | NA | NA | Negative | NA | NA | NA |
| Hantavirus IgG/IgM | NA | NA | Negative | NA | NA | NA |
| Malaria | NA | Negative | Negative | NA | NA | NA |

*ALP, alkaline phosphatase; ALT, alanine aminotransferase; aPTT, activated partial thromboplastin time; AST, aspartate aminotransferase; CRP, C-reactive protein; ED, emergency department; γ-GT, γ-glutamyltransferase; ICU, intensive care unit; INR, international normalized ratio; LDH, lactate dehydrogenase; NA, not available; RBC, red blood cells.

We obtained blood culture, and results became positive the next day for *Escherichia coli*. Bone marrow aspiration examination was compatible with hemophagocytic lymphohisticytosis. The early stage of the patient's hospital course was marked by fluctuating fever, ginigival bleeding, and bleeding at the site of the central venous catheter. We managed the seizure by using levetiracetam. At this stage, a diagnosis of AHF was being considered as a possible explanation for the patient's illness.

On day 3 of hospitalization, we identified the city of origin for the patient as Perez, Argentina, which is located in Santa Fe Province. After consultation with experts from Argentina (C.P. and M.A.M.), AHF was considered as highly possible. Consequently, a confirmatory blood sample was sent to the World Health Organization Collaborating Center for Arbovirus and Hemorrhagic Fever Reference and Research at the Bernhard Nocht Institute for Tropical Medicine in Hamburg, Germany. Treatment with oral ribavirin was initiated because the intravenous form of this drug was not available.

On day 5 of hospitalization, the patient was confirmed to be positive for JUNV by real-time PCR and conventional reverse transcription PCR (RT-PCR) (*4*). The cycle threshold in the real-time RT-PCR was 18, indicating a high viral load. JUNV infection was confirmed by Sanger sequencing of the amplicons. Intravenous ribavirin was not available immediately but was available the next day. This drug was given orally and then intravenously the next day. The patient had to be intubated because of airway obstruction secondary to tongue hematoma and epistaxis.

The next day, because of its antiviral activity in JUNV infection animal models (*5*,*6*) and previous experience with Lassa fever (*7*), oral favipiravir was given through a nasogastric tube (2,000 mg loading dose, followed by 1,200 mg 2×/d) (Figure, panel A). Hemolytic anemia secondary to ribavirin therapy resulted in its discontinuation on day 9. Because of persistently high viral load, the dose of favipiravir was progressively increased (to 1,800 mg 2×/d) and finally stopped after 14 days.

Throughout her time in the ICU, the patient received broad-spectrum antimicrobial drugs for ventilator-associated pneumonia, voriconazole for probable invasive pulmonary aspergillosis, and filgrastim for persistent neutropenia (Figure, panel B). The patient was successfully extubated on day 23 of hospitalization and discharged from the hospital after 50 days without sequelae.

All residual samples for the patient stored in the laboratory were traced and destroyed. Starting from when the patient first came to our hospital, all healthcare workers who came in contact with the patient used gloves, gowns, and filtering facepiece 2 respiratory masks. Needlestick or sharp injuries were not reported. Starting from day 7 because of signs of bleeding, enhanced personal protective equipment was used in the ICU, including full-body suits and powered air-purifying respirators. Donning and doffing procedures were followed and included observation by another staff member. Body fluids from the patient were gelified and inactivated with peracetic acid. Standard biosecurity measures were applied for laboratory workers until day 4. Afterward, all laboratory investigations were conducted in a Biosafety Level 3 laboratory with enhanced personal protective equipment.

We conducted contact tracing for all healthcare workers who had come in contact with the patient or her samples before the diagnosis of AHF. Public health authorities from the 3 countries in Europe involved conducted contract tracing activities among all potential contacts, including family and friends. In Amsterdam, 2 low-risk contacts were identified among those who had cleaned the apartment in

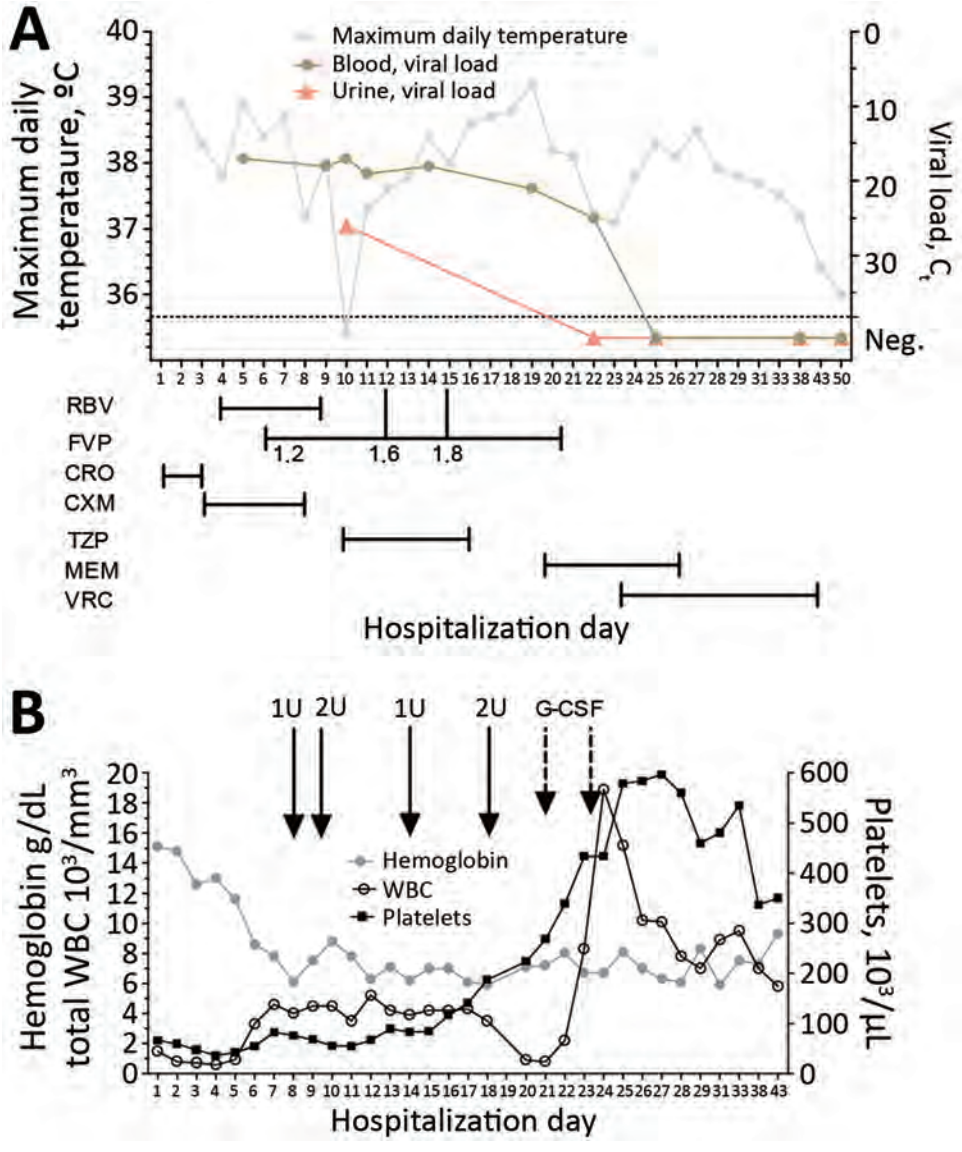


**Figure.** Biologic and virologic evolution in relation to treatment and supportive care for a patient with Argentine hemorrhagic fever, Belgium, 2020. A) Evolution of maximum daily temperature and blood and urine viral load during hospitalization. Antiviral and antimicrobial drug treatment scheme are shown. Dosages of FVP are indicated in grams. B) Evolution of hemoglobin, total leukocytes, and platelets during hospitalization. Solid arrows indicate administration of red blood cell units, and dashed arrows indicate administration of G-CSF. $C_t$ values <40 indicate undetectable viral load. CRO, ceftriaxone; $C_t$, cycle threshold; CXM, cefuroxime; FVP, favipiravir; G-CSF, granulocyte colony-stimulating factor; MEM, meropenem; Neg., negative; RBV, ribavirin; TZP, piperacillin/tazobactam; VRC, voriconazole; WBC, white blood cells.

which the patient stayed. According to the European Centre for Disease Prevention and Control Risk Assessment Guidelines for Infectious Diseases Transmitted on Aircraft for viral hemorrhagic fever (*7*), fellow airline and bus passengers were not considered to be at risk because the patient had not begun to show symptoms of bleeding, vomiting, diarrhea, or urine loss at that time.

We classified contacts as high risk (n = 77) or low risk (n = 60) according to the extent of exposure to body fluids of the patient (Table 2). All contacts were notified by telephone or mail and asked to monitor themselves for fever for 21 days from the day of most recent exposure (upper limit of incubation period). During the surveillance period, 1 high-risk contact became symptomatic (fever) but was ultimately given a diagnosis of infection with influenza A virus. Testing for AHF was not performed. We identified no clinically apparent secondary cases of AHF among the 137 contacts.

## Conclusions

This case illustrates the possibility of imported New World arenavirus hemorrhagic fever outside South America. Interruption of vaccine production has been reported in Argentina and if persistent, this interruption could increase the number of persons at risk for contracting the disease (*3*). This patient was not vaccinated and did not engage in any agricultural activities. The only identifiable at-risk activity was jogging on a dirt road next to her house.

Immune plasma obtained from convalescent-phase patients and containing neutralizing antibody has been shown to decrease the mortality rate from 30% to 1% if initiated within the first 8 days of disease (*8*). The delay between initial symptomatology and AHF diagnosis (13 days) was considered too long to administer immune plasma to the patient. The National Institute of Human Viral Diseases of Argentina provided us with immune plasma matched to blood groups of 3 high-risk contacts identified among the relatives of the patient. Because none of them showed development of illness, immune plasma was ultimately not administered.

Nosocomial transmission of New World arenavirus causing hemorrhagic fever has been reported (*9*). For this patient, we identified no secondary case among healthcare workers and laboratory personnel, confirming the low infectious risk for infection with JUNV when appropriate biosafety and personal protection measures are taken.

**Table 2.** Contact with Junin virus for laboratory personnel, healthcare workers, and relatives for a patient with Argentine hemorrhagic fever, Belgium, 2020*

| Contact, generic description | High risk | Low risk | No risk |
|---|---|---|---|
| Laboratory | | | |
| Present in laboratory where patient's blood was processed | | | X |
| Touching, moving closed blood tube | | | X |
| Opening blood tube without touching sample | | X | |
| Pipetting or other sample handling in biosafety cabinet with gloves | | X | |
| Pipetting or other sample handling without gloves or not in biosafety cabinet | X | | |
| Microscopy of wet sample or preparing thick smear outside biosafety cabinet | X | | |
| Microscopy of dried or fixated sample outside biosafety cabinet | | X | |
| Preparing smears, including thick smear in biosafety cabinet, with gloves | | X | |
| Serologic test outside biosafety cabinet | X | | |
| Discarding samples in waste bucket on floor | X | | |
| Rinsing cell counting chambers and other reused materials | X | | |
| Care giver | | | |
| Brief presence in patient room, without touching anything | | | X |
| Examining the patient and using gloves, mask, or glasses | | X | |
| Examining the patient and not using gloves, mask, or glasses | X | | |
| Drawing blood or handling other body fluids with gloves, mask, glasses | | X | |
| Drawing blood or handling other body fluids without gloves, mask, or glasses | X | | |
| Resuscitating patient and using gloves, mask, glasses | | X | |
| Invasive procedure (catheter placement, puncture, lumbar puncture) with gloves, mask, glasses | | X | |
| General | | | |
| Sexual contact | X | | |
| Household contact with patient's body fluids | X (Brussels, Belgium) | X (Amsterdam, the Netherlands) | |
| Having been near patient without contact with body fluids | | | X |

*High risk indicates unprotected contact (skin, mucosa) with body fluids or aerosols, not wearing intact PPE; low risk indicates protected contact with patient or body fluids, wearing intact and correct PPE; no risk indicates no contact with patient of body fluid. X indicates to which group the contact in the first column belongs. PPE, personal protective equipment.

### Acknowledgments

We thank the National Administration of Laboratories and Institutes of Health–Dr. Carlos Malbrán Institute for providing immune plasma; nurses at the intensive care unit of Saint-Pierre University Hospital and members of the infection control team (Stéphanie Francenne, Françoise Antoine, and Salma Flis for providing continuous effort and dedication; laboratory staff at the Laboratoire Hospitalier Universitaire de Bruxelles, Universitair Laboratorium Brussels, and the Bernhard Nocht Institute for Tropical Medicine, particularly Stefanie Ruben, Alexander Schlaphof, Birgit Muntau, and Petra Emmerich for providing contributions to laboratory management of the patient; Andres Mangiarotti, Micaela Paz, Paul Pardon, and the Vaccine Provision and Prevention Service at the National Institute for Public Health and the Environment (Bilthoven, the Netherlands) for providing favipiravir; and all experts consulted worldwide for providing assistance during the study.

## About the Author

Dr. Veliziotis is a specialist in anesthesiology and resident in critical care medicine at Saint-Pierre University Hospital Brussels, Université Libre de Bruxelles, Brussels, Belgium. His primary research interests include sepsis hemodynamics and echocardiography.

### References

1. Blumberg L, Enria D, Bausch DG. Viral haemorrhagic fevers. In: Farrar J, Hotez P, Junghanss T, Kang G, Lalloo D, White N, editors. Manson's tropical infectious diseases. New York: Elsevier; 2014. p. 171–94.
2. Romanowski V, Pidre M, Ferrelli ML, Bender C, Gomez R. Argentine hemorrhagic fever. In: Singh SK, Ruzek D, editors. Viral hemorrhagic fevers. Boca Raton (FL): CRC Press; 2013. p. 317–38.
3. SAVE. Argentine Society of Virology and Argentine Association of Microbiology. Argentine Hemorrhagic Fever. Position paper, 2019 [in Spanish] [cited 2020 Jan 25]. https://save.org.ar/noticias-de-interes/posicion-sobre-fha
4. Vieth S, Drosten C, Charrel R, Feldmann H, Günther S. Establishment of conventional and fluorescence resonance energy transfer-based real-time PCR assays for detection of pathogenic New World arenaviruses. J Clin Virol. 2005;32:229–35. https://doi.org/10.1016/j.jcv.2004.07.011
5. Gowen BB, Juelich TL, Sefing EJ, Brasel T, Smith JK, Zhang L, et al. Favipiravir (T-705) inhibits Junín virus infection and reduces mortality in a guinea pig model of Argentine hemorrhagic fever. PLoS Negl Trop Dis. 2013;7:e2614. https://doi.org/10.1371/journal.pntd.0002614
6. Westover JB, Sefing EJ, Bailey KW, Van Wettere AJ, Jung K-H, Dagley A, et al. Low-dose ribavirin potentiates the antiviral activity of favipiravir against hemorrhagic fever viruses. Antiviral Res. 2016;126:62–8. https://doi.org/10.1016/j.antiviral.2015.12.006
7. Raabe VN, Kann G, Ribner BS, Morales A, Varkey JB, Mehta AK, et al.; Emory Serious Communicable Diseases Unit. Favipiravir and ribavirin treatment of epidemiologically linked cases of Lassa fever. Clin Infect Dis. 2017;65:855–9. https://doi.org/10.1093/cid/cix406
8. Enria DA, Briggiler AM, Sánchez Z. Treatment of Argentine hemorrhagic fever. Antiviral Res. 2008;78:132–9. https://doi.org/10.1016/j.antiviral.2007.10.010
9. Peters CJ, Kuehne RW, Mercado RR, Le Bow RH, Spertzel RO, Webb PA. Hemorrhagic fever in Cochabamba, Bolivia, 1971. Am J Epidemiol. 1974;99:425–33. https://doi.org/10.1093/oxfordjournals.aje.a121631

Address for correspondence: Nicolas Dauby, Department of Infectious Diseases, Centre Hospitalier Universitaire, Saint-Pierre, Rue Haute 322, 1000 Brussels, Belgium; email: nicolas_dauby@stpierre-bru.be

# Early Introduction of Severe Acute Respiratory Syndrome Coronavirus 2 into Europe

Sonja J. Olsen, Meng-Yu Chen, Yu-Lun Liu, Mark Witschi, Alexis Ardoin, Clémentine Calba, Pauline Mathieu, Virginie Masserey, Francesco Maraglino, Stefano Marro, Pasi Penttinen, Emmanuel Robesyn, Jukka Pukkila; and the European COVID-19 Work Group[1]

Early infections with severe acute respiratory syndrome coronavirus 2 in Europe were detected in travelers from Wuhan, China, in January 2020. In 1 tour group, 5 of 30 members were ill; 3 cases were laboratory confirmed. In addition, a healthcare worker was infected. This event documents early importation and subsequent spread of the virus in Europe.

A novel coronavirus, severe acute respiratory syndrome coronavirus 2 (SARS-CoV-2), associated with severe respiratory illness emerged in Wuhan, China, in late 2019 (*1*). Epidemiologic data indicate that the virus can cause a wide spectrum of clinical disease (mild-to-severe illness), including death (*2*–*4*), and spreads through direct contact and droplets.

Estimates are 5–6 days (range 2–14 days) for the incubation period and 2.2–3.6 for the reproduction rate; this rate is higher than those for seasonal and pandemic influenza (*5*,*6*). Extensive control efforts are now in place as part of a global containment strategy to minimize exportation from China and rapidly identify and stop international spread.

In the World Health Organization European Region, Rome, Paris, London, Istanbul, and Moscow have direct flights to Wuhan, China, and the risk for importation was considered high (*7*). SARS-CoV-2 was reported to have been introduced into Europe by a person from France who had traveled to Wuhan, China, for work, became ill on January 16, and returned ill to France on January 22 (*8*). We report a cluster of illness in a tour group from Wuhan that predates this case detection and led to subsequent transmission in Europe.

Author affiliations: World Health Organization Regional Office for Europe, Copenhagen, Denmark (S.J. Olsen, J. Pukkila); Taiwanese Centers for Disease Control, Taipei (M.-Y. Chen, Y.-L. Liu); Swiss Federal Office of Public Health, Bern, Switzerland (M. Witschi, V. Masserey); Agence Régionale de Santé Ile-de-France, Paris, France (A. Ardoin); Santé Publique France, Paris (C. Calba); Direction Générale de la Santé, Paris (P. Mathieu); Ministry of Health, Rome, Italy (F. Maraglino, S. Marro); European Centre for Disease Prevention and Control, Stockholm, Sweden (P. Penttinen, E. Robesyn)

DOI: https://doi.org/10.3201/eid2607.200359

## The Study

A 55-year-old woman (Taiwanese tour guide) who resided in Wuhan came to airport health authorities in Taipei on January 25, 2020, complaining of a cough since January 22. She was transported to a designated hospital and showed a PCR-positive result for SARS-CoV-2 on January 26. She indicated that she had led a group of tourists from Wuhan to Europe on January 16–24. Further interviews with her and discussions with the rest of the group through social media yielded detailed information.

A group of 30 persons departed Wuhan on January 16, 2020, for a 9-day tour in Italy, Switzerland, and France (Table; Figure). During the flight on January 16 from Wuhan to Rome, 1 tour member was mildly ill and coughing. Her daughter became ill during the tour on January 21.

On January 23, while in Paris, the mother and daughter decided to seek medical care. They called the Chinese embassy, who told them to call the emergency hotline (at SAMU Centre 15 Hospital, Paris, France) dedicated to evaluation of suspected 2019 novel coronavirus disease (COVID-19) cases in France (*8*). The emergency hotline routed the call to the 24-hour ambulatory service, but no information about suspicion of COVID-19 was given. A physician came to their hotel room and gave them a diagnosis of the common cold. The interaction lasted »20 min, including a 15-minute face-to-face examination, without protective masks for

[1]Group members are listed at the end of this article.

**Table.** Characteristics of 6 persons with suspected or confirmed cases of infection with severe acute respiratory syndrome coronavirus 2 associated with transmission in a tour group from Wuhan, China, to Europe, January–February, 2020*

| Person | Age, y/sex | Onset of symptoms | Symptoms | Date of test result (specimen type) | Days between onset and test | Date of test result | Hospitalization date |
|---|---|---|---|---|---|---|---|
| Mother | 53/F | Before Jan 16 | Cough, no fever, odynophagia (cough still noted on return flight to China) | Not tested | NA | NA | None |
| Daughter | 29/F | Jan 21 | Cough, no fever, odynophagia (cough still noted on return flight to China) | Not tested | NA | NA | None |
| Tour guide | 55/F | Jan 22 | Dry cough, fever (Jan 26–Feb 2, Feb 10) | Jan 25 (throat and sputum) | 3 | Jan 26 | Jan 25 |
| Tour member | 31/F | Jan 24 | Diarrhea (Jan 24), cough (Jan 25), fever (Jan 31–Feb 3), facial palsy (Feb 3) | Jan 31 (throat swab) | 7 | Feb 1 | Jan 31 |
| Tour leader | 27/F | Jan 25 | Febrile sensation (low-grade fever of 37.4°C) | Feb 1 (throat swab) | 7 | Feb 3 | Feb 5 |
| Physician | 53/M | Jan 28 | Fever, headache, general weakness | Jan 29, first positive; Feb 2–4, daily positive; Feb 5–9, daily positive (low); Feb 11–14, daily negative | 1 | Jan 29 | Jan 29 |

*NA, not applicable.

the patients or any personal protective equipment for the physician. Also present was another member of the group who translated. While in Paris, the 3 ill persons bought surgical face masks and began wearing them on January 21 (mother and daughter) and on January 22 (tour guide).

The tour group departed on January 24 from Paris to Guangzhou, China (arrival on January 25), because Wuhan ceased air traffic on January 23. The tour guide subsequently continued from Guangzhou to Taipei on January 25, where she arrived on January 25 and was hospitalized. After returning to China, 2 additional tour members, including the tour leader, reported illness and were hospitalized in Hubei and Jiangsu Provinces, where they showed positive test results for SARS-CoV-2. Five (17%) of the 30 tour members were ill; 3 had laboratory-confirmed infection, and 2 were never tested. Because of prolonged and overlapping exposure of the group, it is impossible to determine the exact source of all infections. The source for the physician could have been the ill suspected case-patients, whose infections were never confirmed, or the then-presymptomatic person who translated (contact was 2 days before illness onset).

The tour group was a fairly contained group that did not have much prolonged contact with others. Other than the 3 ill persons, the group members did not wear masks during the tour.

As part of the investigation, the countries the tour visited identified low-risk (<15 min, ≥1–2 m) and high-risk (≥15 min, <1–2 m) contacts (*8*). Most transport was made by using 1 bus, except for 1 section of travel by train in Switzerland. The bus driver, from Slovakia, was a high-risk contact; he returned to Slovakia after the tour and denied having any symptoms in the 14 days after last contact with the tour group.

In Italy, because seat numbers on the flight from Wuhan to Rome, during which 1 tour group member had a cough, were not reported in the passengers list, authorities contacted and informed all passengers (n = 176) and crew members (n = 17). The information provided was to watch for development of symptoms and call if any developed. No other high-risk contacts of the symptomatic group member in Italy were identified.

In Switzerland, health authorities identified 0 high-risk and 3 low-risk contacts, (1 restaurant owner and 2 shop clerks). These 3 persons were told to watch for development of symptoms and call if any developed. None were reported.

In France, the group visited several tourist attractions and used public transportation; contacts in the shops and hotel were interviewed and defined as low-risk contacts. Only 1 high-risk contact was identified. This person was the physician.

The physician was not wearing a mask during the consultation because he had not been informed of the risk of COVID-19. He became ill on January 28 and stopped seeing patients. He went to a designated referral hospital on January 29 and showed a positive PCR result for SARS-CoV-2 for 12 days; he has since

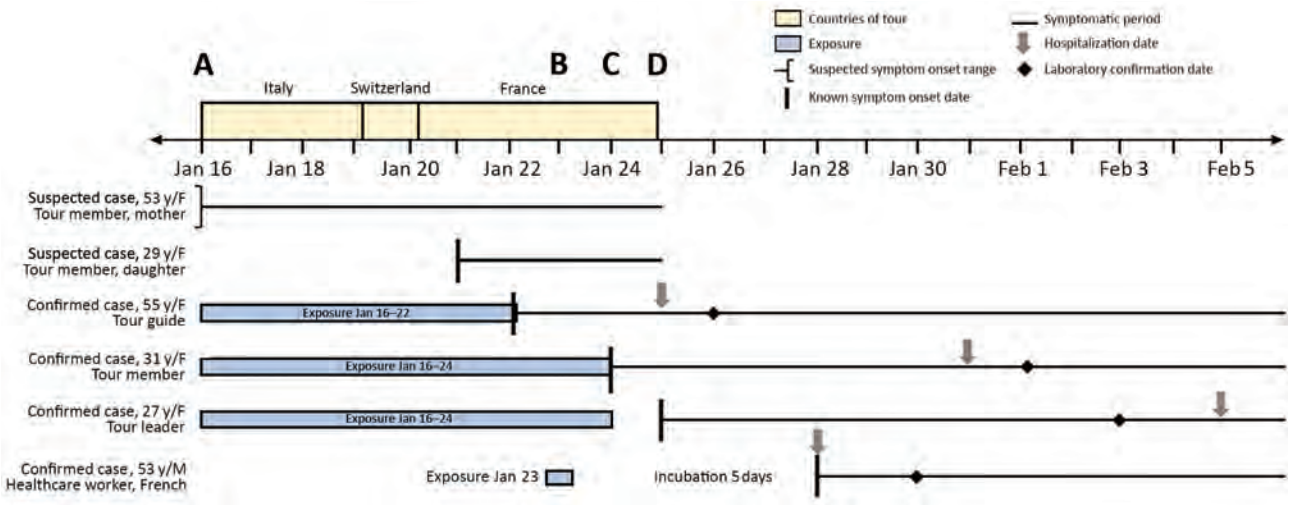


**Figure.** Timeline showing illness onsets and exposures for 6 persons with suspected or confirmed cases of infection with severe acute respiratory syndrome coronavirus 2 associated with transmission in a tour group flying from Wuhan, China, to Europe, January–February, 2020. A) Flight from Wuhan to Rome; B) 2 case-patients visited by healthcare worker; C) return flight from Paris to Guangdong; D) tour guide flight to Taipei.

recovered. A total of 58 contacts (20 low risk and 38 high risk) of the physician were identified, including patients and their family members he saw during home visits the day before onset of symptoms. All involved persons have been investigated and followed-up for 14 days; none showed development of illness.

Authorities in China were notified of symptomatic persons on the flight from Paris to Guangzhou. However, we were unable to confirm whether any contact tracing was performed.

As of February 10, the tour guide remained hospitalized, but had a normal chest radiograph and was clinically well. She remains in isolation because of a virus-positive sputum test result 19 days after illness onset. The other 3 tour members who were ill reportedly experienced mild illness, and all are now well. Because the first 2 symptomatic persons were never tested, we cannot conclude that they were the source of infection. However, given that the virus was not circulating in France, the source was most likely in the tour group. It is also possible that additional transmission resulting in mild illness occurred, particularly in the tour group, but was not identified.

## Conclusions

This event represents early introduction of SARS-CoV-2 into Europe, before implementation of extensive travel restrictions in Wuhan on January 23, and could explain additional chains of transmission in France, where the disease has now spread widely. The event was characterized by clinically mild illness in 6 persons; 2 showed documented prolonged virus shedding. Excluding members of the tour group, 1 of 40 high-risk and 0 of 216 low-risk contacts became ill. The 1 high-risk exposure event was short but entailed close contact during a clinical examination. Assuming this was the sole exposure, the incubation time was 5 days, which is consistent with reported data.

This event represented a coordinated international effort and highlights the effectiveness of working through the established mechanisms of the European Union Early Warning and Response System and the International Health Regulations. This effort will be key to the effective implementation of the current global containment strategy.

Members of the European COVID-19 Work Group: Lauren E. MacDonald, Richard Pebody (World Health Organization Regional Office for Europe, Copenhagen, Denmark); Anne Simondon, Agnès Lepoutre, Pascal Beaudeau (Santé Publique France, Paris, France); Guillaume Martin, Coralie Giese, Marin Cottin, Clément Lazarus, Elise Klément (Direction Générale de la Santé, Ministère des Solidarités et de la Santé, Paris, France); Anna Caraglia, Patrizia Parodi, Alessia Rapiti (Swiss Federal Office of Public Health, Bern, Switzerland); Elise Klément (Hôpitaux de Paris and Sorbonne Université, Paris, France).

### Acknowledgments

We thank the Taiwanese tour guide and the French physician for providing extensive details for this study and Catherine Smallwood, Dorit Nitzan, and the European Centre for Disease Prevention Technical Group for COVID-19 for providing assistance.

## About the Author

Dr. Olsen is a technical officer at the World Health Organization Regional Office for Europe, Copenhagen, Denmark. Her primary research interest is the epidemiology of influenza and other respiratory diseases.

## References

1. Zhu N, Zhang D, Wang W, Li X, Yang B, Song J, et al.; China Novel Coronavirus Investigating and Research Team. A novel coronavirus from patients with pneumonia in China, 2019. N Engl J Med. 2020;382:727–33. https://doi.org/10.1056/NEJMoa2001017
2. Chen N, Zhou M, Dong X, Qu J, Gong F, Han Y, et al. Epidemiological and clinical characteristics of 99 cases of 2019 novel coronavirus pneumonia in Wuhan, China: a descriptive study. Lancet. 2020;395:507–13. https://doi.org/10.1016/S0140-6736(20)30211-7
3. Team TNCPERE. The epidemiological characteristics of an outbreak of 2019 novel coronavirus diseases (COVID-19) in China. China CDC Weekly. 2020;2 [cited 2020 Mar 16]. https://www.ncbi.nlm.nih.gov/pubmed/32064853
4. Wu P, Hao X, Lau EH, Wong JY, Leung KS, Wu JT, et al. Real-time tentative assessment of the epidemiological characteristics of novel coronavirus infections in Wuhan, China, as at 22 January 2020. Euro Surveill. 2020;25. https://doi.org/10.2807/1560-7917.ES.2020.25.3.2000044
5. Biggerstaff M, Cauchemez S, Reed C, Gambhir M, Finelli L. Estimates of the reproduction number for seasonal, pandemic, and zoonotic influenza: a systematic review of the literature. BMC Infect Dis. 2014;14:480. https://doi.org/10.1186/1471-2334-14-480
6. Zhao S, Lin Q, Ran J, Musa SS, Yang G, Wang W, et al. Preliminary estimation of the basic reproduction number of novel coronavirus (2019-nCoV) in China, from 2019 to 2020: a data-driven analysis in the early phase of the outbreak. Int J Infect Dis. 2020;92:214–7. https://doi.org/10.1016/j.ijid.2020.01.050
7. Pullano G, Pinotti F, Valdano E, Boëlle PY, Poletto C, Colizza V. Novel coronavirus (2019-nCoV) early-stage importation risk to Europe, January 2020. Euro Surveill. 2020;25. https://doi.org/10.2807/1560-7917.ES.2020.25.4.2000057
8. Bernard Stoecklin S, Rolland P, Silue Y, Mailles A, Campese C, Simondon A, et al.; Investigation Team. First cases of coronavirus disease 2019 (COVID-19) in France: surveillance, investigations and control measures, January 2020. Euro Surveill. 2020;25. https://doi.org/10.2807/1560-7917.ES.2020.25.6.2000094

Address for correspondence: Sonja J. Olsen, World Health Organization Regional Office for Europe, Marmormolen 51, 2100 Copenhagen, Denmark; email: olsens@who.int

# Surveillance and Testing for Middle East Respiratory Syndrome Coronavirus, Saudi Arabia, March 2016–March 2019

Abdullah Alzahrani, Stephanie A. Kujawski, Glen R. Abedi, Safaa Tunkar, Holly M. Biggs, Nada Alghawi, Hani Jokhdar, Abdullah M. Assiri, John T. Watson

During March 2016–March 2019, a total of 200,936 suspected cases of Middle East respiratory syndrome coronavirus infection were identified in Saudi Arabia; infections were confirmed in 698 cases (0.3% [0.7/100,000 population per year]). Continued surveillance is necessary for early case detection and timely infection control response.

Middle East respiratory syndrome coronavirus (MERS-CoV) can cause severe respiratory illness and has a reported case-fatality rate of ≈35% (*1*). Transmission typically occurs through close contact with MERS-CoV–infected patients, particularly in healthcare settings (*2*,*3*), or through contact with dromedaries (*4*). Most cases worldwide have been reported by Saudi Arabia (*1*).

By using the Health Electronic Surveillance Network (HESN), a national electronic surveillance platform, the Saudi Arabia Ministry of Health (MoH) monitors MERS-CoV testing and cases throughout the country. Since 2015, clinicians and health authorities have been mandated to report all suspected MERS-CoV cases to HESN. In April 2018, the MoH revised the case definition for suspected MERS-CoV (*5*). This change provided an opportunity to assess testing practices under 2 different case definitions. We describe trends in MERS-CoV surveillance and laboratory testing in Saudi Arabia during March 1, 2016–March 20, 2019.

## The Study

In Saudi Arabia, persons meeting the MoH case definition for suspected MERS-CoV infection are tested for the virus (Table 1, https://wwwnc.cdc.gov/EID/article/267/20-0437-T1.htm) (*5*,*6*). Persons may also be tested if recommended by an infectious disease consultant or if they had exposure to a MERS-CoV patient (*5*,*6*). In April 2018, the MoH published a 4-category revision to the 2015 case definition, with the goal of making the definition more specific (Table 1) (*5*,*6*). This revision was implemented in HESN in July 2018.

Information on suspected and confirmed cases is submitted electronically to HESN. For each suspected MERS-CoV case, the treating hospital creates an electronic record in HESN and submits a clinical sample to a designated laboratory for confirmatory testing. After testing is complete, the laboratory updates the electronic record in HESN with the results. Upon report of a confirmed case, additional clinical and epidemiologic data are entered into the HESN system by the hospital, local health authorities, or both.

We analyzed demographic and laboratory data for suspected and confirmed MERS-CoV cases reported to HESN during March 1, 2016–March 20, 2019 by using Microsoft Excel (https://www.microsoft.com) and SAS 9.4 (https://www.sas.com). For this analysis, we defined a suspected case as suspected MERS-CoV infection in a person with compatible symptoms during the study period, with >14 days separating illness episodes for persons in whom MERS-CoV infection is suspected more than once. We defined a confirmed case as laboratory confirmation of MERS-CoV infection in a person during the study period. By using MoH population estimates (*7*), we calculated rates of testing and positivity for the country, by local Health Affairs Directorate (HAD), and for Hajj pilgrims.

During the study period, 200,936 suspected MERS-CoV case-patients were tested and their cases

Author affiliations: Ministry of Health, Riyadh, Saudi Arabia (A. Alzahrani, S. Tunkar, N. Alghawi, H. Jokhdar, A.M. Assiri); Centers for Disease Control and Prevention, Atlanta, GA, USA (S.A. Kujawski, G.R. Abedi, H.M. Biggs, J.T. Watson)

DOI: https://doi.org/10.3201/eid2607.200437

**Table 2.** Demographic characteristics of persons with suspected and confirmed MERS-CoV infection, Health Electronic Surveillance Network, Saudi Arabia, March 1, 2016–March 20, 2019*

| Characteristic | Total | Confirmed | Not confirmed | % Positive (confirmed) |
|---|---|---|---|---|
| Overall | 200,936 | 698 (0.3) | 200,238 (99.7) | 0.3 |
| Age, y, median (IQR) | 47 (28–67) | 54 (40–65) | 47 (28–67) | |
| Age group, y | | | | |
| 0–14 | 17,455 (8.7) | 3 (0.4) | 17,452 (8.8) | 0.02 |
| 15–34 | 54,483 (27.3) | 121 (18.0) | 54,362 (27.3) | 0.2 |
| 35–49 | 33,993 (17.0) | 164 (24.3) | 33,829 (17.0) | 0.5 |
| 50–65 | 41,283 (20.7) | 228 (33.8) | 41,055 (20.6) | 0.6 |
| >65 | 52,400 (26.3) | 158 (23.4) | 52,242 (26.3) | 0.3 |
| Total | 199,614 | 674 | 198,940 | |
| Missing | 1,322 (0.7) | 24 (3.4) | 1,298 (0.6) | |
| Sex | | | | |
| M | 108,940 (54.3) | 517 (74.1) | 108,423 (54.2) | 0.5 |
| F | 91,822 (45.7) | 181 (25.9) | 91,641 (45.8) | 0.2 |
| Total | 200,762 | 698 | 200,064 | |
| Missing | 174 (0.09) | 0 | 174 (0.09) | |
| Nationality | | | | |
| Saudi | 146,254 (72.8) | 501 (71.8) | 145,753 (72.8) | 0.3 |
| Non-Saudi | 54,682 (27.2) | 197 (28.2) | 54,485 (27.2) | 0.4 |
| Total | 200,936 | 698 | 200,238 | |
| Missing | 0 | 0 | 0 | |
| Healthcare personnel | | | | |
| Yes | 9,289 (5.6) | 67 (11.2) | 9,222 (5.6) | 0.7 |
| No | 155,825 (94.4) | 531 (88.8) | 155,294 (94.4) | 0.3 |
| Total | 165,114 | 598 | 164,516 | |
| Missing | 35,822 (17.8) | 100 (14.3) | 35,722 (17.8) | |

*Values are no. (%) unless indicated. IQR, interquartile range; MERS-CoV, Middle East respiratory syndrome coronavirus.

reported to HESN; MERS-CoV was confirmed in 698 case-patients (0.3%) (Table 2). Overall, 54.3% of suspected case-patients were male, 72.8% were Saudi nationals, and the median age was 47 years (interquartile range 28–67 years). Among suspected case-patients for whom healthcare personnel status was available, 5.6% (n = 9,222) were healthcare personnel. Among confirmed case-patients, 517 (74.1%) were male, 501 (71.8%) were Saudi nationals, and the median age was 54 years (interquartile range 40–65 years). The age group with the highest proportion of confirmed case-patients was 50–65 years (0.6%), and the group with the lowest proportion was 0–14 years (0.02%). Healthcare personnel status was reported for 598 (85.7%) confirmed case-patients; among these, 11.2% (n = 67) were healthcare personnel. Outcome information was available for 84.0% (n = 586) of the confirmed case-patients, 164 (28.0%) of whom died.

Each surveillance year, an average of 66,979 (range 60,659–77,886) suspected case-patients were tested for MERS-CoV. On average, 5,431 (range 2,836–9,154) suspected case-patients were tested monthly during the study period (Figure). The average monthly number of suspected case-patients tested did not change

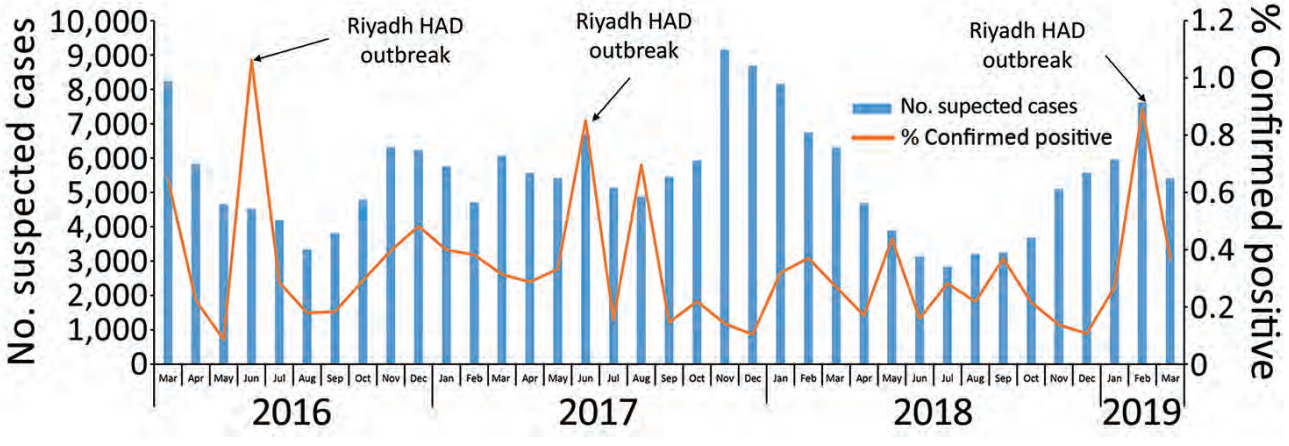


**Figure.** Number of suspected cases and percentage of confirmed positive cases of Middle East respiratory syndrome, Health Electronic Surveillance Network, Saudi Arabia, March 1, 2016–March 20, 2019. HAD, Health Affairs Directorate.

significantly from before (5,654 tests during March 2016–June 2018) to after (4,914 tests during August 2018–February 2019) the case definition change (p = 0.31). Overall, and both before and after the definition change, the average monthly percentage of suspected case-patients testing positive was 0.3%. Peaks in positivity occurred in June 2016 (1.1%), June 2017 (0.9%), and February 2019 (0.9%).

Annually, 203.0 suspected case-patients/100,000 population were tested for MERS-CoV, and 0.7/100,000 population were positive (Table 3). Testing and positivity rates did not vary substantially from year to year (Appendix Table 1, https://wwwnc.cdc.gov/EID/article/26/7/20-0437-App1.xlsx). Riyadh HAD had the highest annual testing rate (328.0 suspected cases/100,000 per year). The highest positivity rate per population was in Jouf HAD (2.5 confirmed cases/100,000 population per year) and was largely attributable to an August 2017 outbreak. The study period encompassed 3 Hajj pilgrimage seasons; during these periods, 2,738 pilgrims were tested for MERS-CoV, none of whom tested positive.

For 82.2% of persons with suspected MERS-CoV infection, a reason for testing was reported (Appendix Table 2). Most were tested because they had signs of pneumonia or acute respiratory distress syndrome (69.9%). Testing because of an epidemiologic link accounted for the highest proportion of positive results overall (0.8%). A higher proportion were tested because of an epidemiologic link after the definition change (19.5%) than before (7.5%).

## Conclusions

Saudi Arabia continues to perform extensive surveillance and testing for MERS-CoV. During the 3-year study period, the MoH tested >65,000 suspected MERS-CoV case-patients per year on average. Of these, 0.3% were positive for MERS-CoV, representing 0.7 confirmed cases/100,000 population per year. As a robust, national surveillance system, HESN enables the geographic and temporal monitoring of trends in testing and surveillance. Compared with HESN MERS-CoV surveillance data from 2015–2016, the percentage of suspected case-patients testing positive (0.7%) and the rate of confirmed cases (1.2/100,000 population) decreased (*8*). Peaks in percentage positivity corresponded to documented MERS-CoV outbreaks (*9*–*11*). The few large recent outbreaks and the reduction in cases might be indicative of robust testing and contact-tracing efforts and early intervention for healthcare infection control.

During the study period, the case definition for suspected cases was revised with the goal of maintaining the sensitivity of the case definition while increasing specificity. Based on limited data (7 complete months of data postrevision), the average number of monthly tests remained constant before and after this change. The change in the case definition

**Table 3.** Suspected and confirmed cases of MERS-CoV infection, by local Health Affairs Directorate and among Hajj pilgrims, Health Electronic Surveillance Network, Saudi Arabia, March 1, 2016-March 20, 2019

| Local Health Affairs Directorate | Population* | No. confirmed cases/no. suspected cases | % Confirmed positive | No. suspected cases/100,000 population per year | No. confirmed cases/100,000 population per year |
|---|---|---|---|---|---|
| Riyadh | 8,216,284 | 340/80,852 | 0.4 | 328.0 | 1.4 |
| Jeddah | 4,626,109 | 37/18,929 | 0.2 | 136.4 | 0.3 |
| Eastern | 3,228,261 | 16/15,856 | 0.1 | 163.7 | 0.2 |
| Makkah | 2,319,426 | 8/13,843 | 0.06 | 198.9 | 0.1 |
| Madinah | 2,132,679 | 25/13,334 | 0.2 | 208.4 | 0.4 |
| Aseer | 1,822,189 | 24/5,560 | 0.4 | 101.7 | 0.4 |
| Jazan | 1,567,547 | 0/1,082 | 0.0 | 23.0 | 0.0 |
| Qaseem | 1,423,935 | 85/9,873 | 0.9 | 231.1 | 2.0 |
| Taif | 1,301,778 | 25/6,342 | 0.4 | 162.4 | 0.6 |
| Ahsa | 1,224,600 | 32/13,009 | 0.2 | 354.1 | 0.9 |
| Tabouk | 910,030 | 9/2,848 | 0.3 | 104.3 | 0.3 |
| Hail | 699,774 | 11/4,946 | 0.2 | 235.6 | 0.5 |
| Najran | 582,243 | 32/2,951 | 1.1 | 168.9 | 1.8 |
| Bahah | 476,172 | 4/2,163 | 0.2 | 151.4 | 0.3 |
| Hafr Al-Baten | 447,464 | 8/681 | 1.2 | 50.7 | 0.6 |
| Bishah | 389,686 | 5/1,131 | 0.4 | 112.1 | 0.4 |
| Nothern | 365,231 | 8/855 | 0.9 | 78.0 | 0.7 |
| Jouf | 339,198 | 25/2,885 | 0.9 | 283.5 | 2.5 |
| Qunfudah | 310,453 | 1/412 | 0.2 | 44.2 | 0.1 |
| Quarayyat | 169,277 | 3/466 | 0.6 | 91.8 | 0.6 |
| Total | 32,552,336 | 698/198,198 | 0.4 | 203.0 | 0.7 |
| Hajj pilgrims | 2,352,122 | 0/2,738 | 0.0 | 38.8 | 0.0 |

*Health Affairs Directorate and Hajj pilgrim population estimates are from 2017 Saudi Arabia Ministry of Health Annual Statistics Book (*7*). MERS-CoV, Middle East respiratory syndrome coronavirus.

is reflected in the reasons for testing persons with suspected MERS-CoV infection. A comparison of the reasons for testing before and after the change found that most persons were tested because they had signs of pneumonia or acute respiratory distress syndrome. Unsurprisingly, in both periods, the highest percentage positive was among those with an epidemiologic link to a MERS-CoV patient or exposure to dromedaries.

Comparing data from before and after the case definition change, however, was limited by the relatively short period examined after the definition change and a high percentage of missing data, particularly during implementation of the revised case definition. Although the case definition change took effect in April 2018, HESN was not updated to reflect the change until July 2018. This lag might have affected reporting, and actual implementation of the case definition change likely varied by site. In addition, completeness of the data varied and was likely influenced by differential reporting practices, which affected the availability of data for analysis. Targeted efforts continue to improve the accuracy and completeness of reporting. Additional analysis using more complete data over a longer period would be informative to determine whether the revised case definition might result in changes in testing practices.

Surveillance for MERS-CoV in Saudi Arabia captures and provides important information on suspected and confirmed cases and trends in testing. Continued robust MERS-CoV surveillance is pivotal for the early ascertainment of cases and the effective implementation of control measures.

## About the Author

Dr. Abdullah Alzahrani is the general supervisor of the Health Electronic Surveillance Network, Ministry of Health, Saudi Arabia. His primary research interests include public health surveillance for infectious diseases.

## References

1. World Health Organization. MERS situation update 2019 Sep [cited 2019 Oct 18]. http://applications.emro.who.int/docs/EMROPub-MERS-SEP-2019-EN.pdf
2. Assiri A, McGeer A, Perl TM, Price CS, Al Rabeeah AA, Cummings DA, et al.; KSA MERS-CoV Investigation Team. Hospital outbreak of Middle East respiratory syndrome coronavirus. N Engl J Med. 2013;369:407–16. https://doi.org/10.1056/NEJMoa1306742
3. Oboho IK, Tomczyk SM, Al-Asmari AM, Banjar AA, Al-Mugti H, Aloraini MS, et al. 2014 MERS-CoV outbreak in Jeddah—a link to health care facilities. N Engl J Med. 2015;372:846–54. https://doi.org/10.1056/NEJMoa1408636
4. Hui DS, Azhar EI, Kim YJ, Memish ZA, Oh MD, Zumla A. Middle East respiratory syndrome coronavirus: risk factors and determinants of primary, household, and nosocomial transmission. Lancet Infect Dis. 2018;18:e217–27. https://doi.org/10.1016/S1473-3099(18)30127-0
5. Ministry of Health of the Kingdom of Saudi Arabia. Middle East respiratory syndrome coronavirus: guidelines for healthcare professionals 2018 [cited 2019 Oct 18]. https://www.moh.gov.sa/ccc/healthp/regulations/documents/ mers-cov%20guidelines%20for%20healthcare%20professionals%20-%20may%202018%20-%20v5.1%20%281%29.pdf
6. Ministry of Health of the Kingdom of Saudi Arabia. Infection prevention and control guidelines for Middle East respiratory syndrome coronavirus (MERS-CoV) infection 2015. 3rd edition [cited 2019 Oct 18]. https://www.moh.gov.sa/Documents/2015%20update.pdf
7. Ministry of Health of the Kingdom of Saudi Arabia. Annual statistical book 2017 [cited 2019 Oct 18]. https://www.moh.gov.sa/en/ministry/statistics/book/documents/annual-statistical-book-1438h.pdf
8. Saeed AA, Abedi GR, Alzahrani AG, Salameh I, Abdirizak F, Alhakeem R, et al. Surveillance and testing for Middle East respiratory syndrome coronavirus, Saudi Arabia, April 2015–February 2016. Emerg Infect Dis. 2017;23:682–5. https://doi.org/10.3201/eid2304.161793
9. Alanazi KH, Killerby ME, Biggs HM, Abedi GR, Jokhdar H, Alsharef AA, et al. Scope and extent of healthcare-associated Middle East respiratory syndrome coronavirus transmission during two contemporaneous outbreaks in Riyadh, Saudi Arabia, 2017. Infect Control Hosp Epidemiol. 2019;40:79–88. https://doi.org/10.1017/ice.2018.290
10. World Health Organization. Middle East respiratory syndrome coronavirus (MERS-CoV)—Saudi Arabia: disease outbreak news, 21 Jun 2016 [cited 2019 Oct 18]. https://www.who.int/csr/don/21-june-2016-mers-saudi-arabia
11. World Health Organization. Middle East respiratory syndrome coronavirus (MERS-CoV)—the Kingdom of Saudi Arabia: disease outbreak news update, 24 April 2019 [cited 2019 Oct 18]. https://www.who.int/csr/don/24-April-2019-mers-saudi-arabia

Address for correspondence: Glen R. Abedi, Centers for Disease Control and Prevention, 1600 Clifton Rd NE, Mailstop H24-5, Atlanta, GA 30329-4027, USA; email: huv3@cdc.gov

# Community Responses during Early Phase of COVID-19 Epidemic, Hong Kong

Kin On Kwok, Kin Kit Li, Henry Ho Hin Chan, Yuan Yuan Yi, Arthur Tang, Wan In Wei, Samuel Yeung Shan Wong

During the early phase of the coronavirus disease epidemic in Hong Kong, 1,715 survey respondents reported high levels of perceived risk, mild anxiety, and adoption of personal-hygiene, travel-avoidance, and social-distancing measures. Widely adopted individual precautionary measures, coupled with early government actions, might slow transmission early in the outbreak.

Hong Kong was relatively successful in mitigating transmission early in the outbreak of coronavirus disease (COVID-19). Confirmed cases were first reported in the city of Wuhan, China, in December 2019 (*1*). Situated at the southern tip of China, Hong Kong was at risk for importing COVID-19, given its shared border and high infrastructural and social connectivity with China. In 2019, >236 million passengers crossed the border between China and Hong Kong by land (*2*). Hong Kong is also vulnerable to virus transmission owing to its high population density and heavy reliance on public transportation. Despite these risks, as of March 20, 2020, transmission control efforts in Hong Kong, as reflected in the numbers of confirmed cases and deaths (256 cases, 4 deaths) (*3*), had been relatively successful compared with nearby countries and regions, including mainland China (80,967 cases, 3,248 deaths), South Korea (8,652 cases, 94 deaths), and Japan (950 cases, 33 deaths, in addition to the 712 cases from a cruise ship) (*4*).

JC School of Public Health and Primary Care, The Chinese University of Hong Kong, Hong Kong, China (K.O. Kwok, H.H.H. Chan, Y.Y. Yi, W.I. Wei, S.Y.S. Wong); Stanley Ho Centre for Emerging Infectious Diseases, The Chinese University of Hong Kong, Hong Kong (K.O. Kwok); Shenzhen Research Institute of The Chinese University of Hong Kong, Shenzhen, China (K.O. Kwok); City University of Hong Kong College of Liberal Arts and Social Sciences, Hong Kong (K.K. Li); Sungkyunkwan University College of Software, Seoul, South Korea (A. Tang)

DOI: https://doi.org/10.3201/eid2607.200500

Health officials in Hong Kong have enacted multipronged interventions to slow disease spread (*5*). Adopted strategies include border screening (measuring body temperature, imposing a health declaration form system, imposing a 14-day mandatory quarantine period on persons entering Hong Kong from mainland China; parts of Korea, Japan, France, Germany, and Spain; and all of Italy and Iran), social distancing (shutting down the border, reducing cross-border commuting services, delaying the resumption of classes in schools, arranging telework for civil servants, and suspending of public services), and extending the Enhanced Laboratory Surveillance Program to adult patients with fever and mild respiratory symptoms at emergency departments or general outpatient clinics in the public sector.

The behaviors of the public are important for outbreak management, particularly during the early phase when no treatment or vaccination is available and nonpharmaceutical interventions are the only options. The efficacy of nonpharmaceutical interventions depends on persons' degree of engagement and compliance in precautionary behaviors, such as facemask wearing, hand hygiene, and self-isolation. Willingness to engage in precautionary behaviors voluntarily depends on risk perception toward the current health threat. In fact, risk perception is a main theme in common health behavior theories (*6*,*7*). In addition, with advanced information technology in recent years comes the uncertainty of how risk perception is shaped by various information sources. Hong Kong's experience with outbreaks of novel pathogens (e.g., 2003 severe acute respiratory syndrome [SARS] and 2009 pandemic influenza) also provides a reference point to evaluate the risk perceptions of COVID-19. In comparison, Hong Kong was more affected by SARS than COVID-19 thus far. In 2003, a total of 1,755 persons in Hong Kong contracted SARS, resulting in 299 deaths (*8*).

In light of the importance of persons' behavior in mitigating transmission and the goal of informing policy formation in a timely manner, we examined risk perceptions and behavioral responses of the general community during the early phase of the COVID-19 epidemic in Hong Kong. Considering the rapid development of the epidemic during the survey period and the potential variability in the adoption of preventive measures among persons, we also examined the temporal changes in anxiety levels, the factors associated with adoption of preventive measures, and sources of information about the epidemic.

## The Study

District councilors distributed an online survey including measures of preventive behaviors, general anxiety, risk perceptions, and information exposure to the residents of Hong Kong within 36 hours after detection of the first confirmed case of COVID-19 in Hong Kong (Appendix, https://wwwnc.cdc.gov/EID/article/26/7/20-0500-App1.pdf). The survey was conducted for 3 weeks. We compiled a chronology of major events related to COVID-19 both inside and outside Hong Kong and the number of confirmed cases in Hong Kong before and during the period covered by the survey (Figure 1).

Analysis of 1,715 respondents' data indicated high levels of perceived susceptibility to (89%) and severity of (97%) COVID-19 (Table 1). However, the general anxiety level, measured by the Hospital Anxiety and Depression Scale (*9*), was mild (9.01 out of 21). Most respondents (≥98%) had their daily routines disrupted and were alert to COVID-19. The most trusted information sources were doctors (84%) and radio broadcasts (57%), but they were not the sources by which respondents typically received their information (doctors 5%, broadcast 34%).

Among preventive measures and their perceived efficacy, enhanced personal hygiene (from 78% of respondents disinfecting their homes to 99% wearing

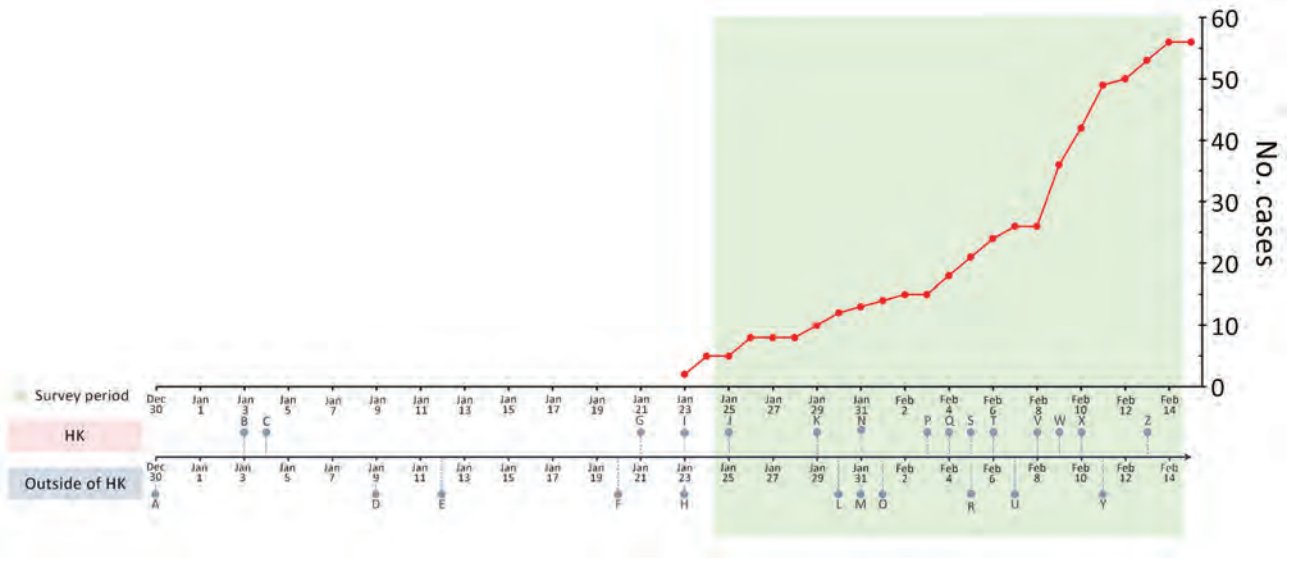


**Figure 1.** Chronology of major events during the early phase of the coronavirus disease epidemic and laboratory-confirmed cases in Hong Kong, December 30, 2019–February 14, 2020. A, unexplained pneumonia reported in Wuhan, China; B, HK begins temperature screenings at border checkpoints for travelers from Wuhan; C, HK launches preparedness and response plan for novel infectious disease of public health significance, serious response level; D, first death reported in Wuhan; E, World Health Organization (WHO) names disease 2019-nCoV acute respiratory disease and the virus 2019-nCoV (refer to Y for subsequent renaming); F, China confirms human-to-human transmission; G, HK introduces health declaration form system on inbound travelers by air from Wuhan; H, WHO declines to declare COVID-19 a public health emergency of international concern; I, first first confirmed COVID-19 case in HK, halt of sale of high-speed rail tickets to and from Wuhan; J, HK activates emergency response level; K, HK closes public leisure and cultural facilities until further notice; L, WHO declares COVID-19 a public health emergency of international concern; M, United States declares COVID-19 a public health emergency, imposes entry restriction; N, HK imposes 4-week school suspension, 1-week extension for home-office arrangement for civil servants; O, first COVID-19 death outside China in the Philippines; P, HK medical workers strike to call for border shutdown; Q, first COVID-19 death in HK, closure of 4 more border control points; R, 46 foreign airlines cancelled flights to mainland China; S, HK implements further port hygiene measures; T, HK offers home-office arrangement for civil servants until February 16; U, first death of a doctor in China (Wuhan); V, HK begins mandatory 14-day quarantine on persons entering from China; W, HK reports COVID-19 cluster involving 9 people in a gathering on January 26; X, HK reports COVID-19 cluster involving 5 residents (2 families) in the same building; Y, WHO and ICTV rename disease COVID-19 and virus SARS-CoV-2; Z, HK extends home-office arrangement for civil servants until February 23, school suspension until March 16. HK, Hong Kong.

**Table 1.** Risk perception of the community toward COVID-19 during the early phase of the COVID-19 epidemic in Hong Kong*

| Characteristic | No. (%) respondents | | | | |
|---|---|---|---|---|---|
| | Level 1 | Level 2 | Level 3 | Level 4 | Level 5 |
| Perceived susceptibility (assuming no preventive measure) | | | | | |
| How likely you will be infected† | 776 (45) | 751 (44) | 160 (9) | 23 (1) | 5 (0) |
| How likely your families will be infected† | 924 (54) | 660 (38) | 113 (7) | 14 (1) | 4 (0) |
| Perceived severity | | | | | |
| Seriousness of symptoms caused by SARS-CoV-2‡ | 1102 (64) | 569 (33) | 33 (2) | 7 (0) | 4 (0) |
| Chance of having COVID-19 cured§ | 190 (11) | 552 (32) | 708 (41) | 239 (14) | 26 (2) |
| Chance of survival if infected with COVID-19§ | 136 (8) | 476 (28) | 788 (46) | 290 (17) | 25 (1) |

*COVID-19, coronavirus disease; SARS-CoV-2, severe acute respiratory syndrome coronavirus 2.
†Level 1, very likely; level 2, likely; level 3, neutral; level 4, unlikely; level 5, very unlikely.
‡Level 1, very serious; level 2, serious; level 3, neutral; level 4, not serious; level 5, not serious at all.
§Level 1, very low; level 2, low; level 3, neutral; level 4, high; level 5, very high.

facemasks) and travel avoidance (from 90% avoiding Hubei Province, China, to 92% avoiding mainland China altogether) were frequently adopted and were considered effective (>90%) (Figure 2). The adoption of social-distancing measures was moderate to high (from 39% respondents avoiding public transportation to 93% avoiding contact with persons with respiratory disease symptoms). Higher levels of adoption of social-distancing measures were associated with being female, living in the New Territories (1 of the 3 geographic regions in Hong Kong that shares the border with mainland China), perceiving oneself as having a good understanding of COVID-19, and being more anxious (Table 2).

## Conclusions

The relative success in transmission control in Hong Kong could be attributed to the widely adopted precautionary behaviors of the public, together with early government interventions (e.g., border control and compulsory quarantine for those from affected regions). Unlike in many other countries, visitors from mainland China have never been fully banned from entering Hong Kong. The citizens of Hong Kong assumed responsibility for infection control on their own and became very attentive to personal preventive measures. Our findings showed that nearly all respondents adopted enhanced personal hygiene (e.g., wearing facemasks) and travel avoidance. The experience in outbreak management during the 2003 SARS epidemic might also have contributed to these swift and strong psychological and behavioral responses. Metaphorically, these responses resembled a secondary immune response, which is fast and strong during re-exposure to the same pathogen.

The case of Hong Kong demonstrates the extent to which voluntary preventive measures by persons might be required for slowing transmission (e.g., ≥78% adoption of enhanced personal-hygiene measures, ≥90% adoption of travel-avoidance, and

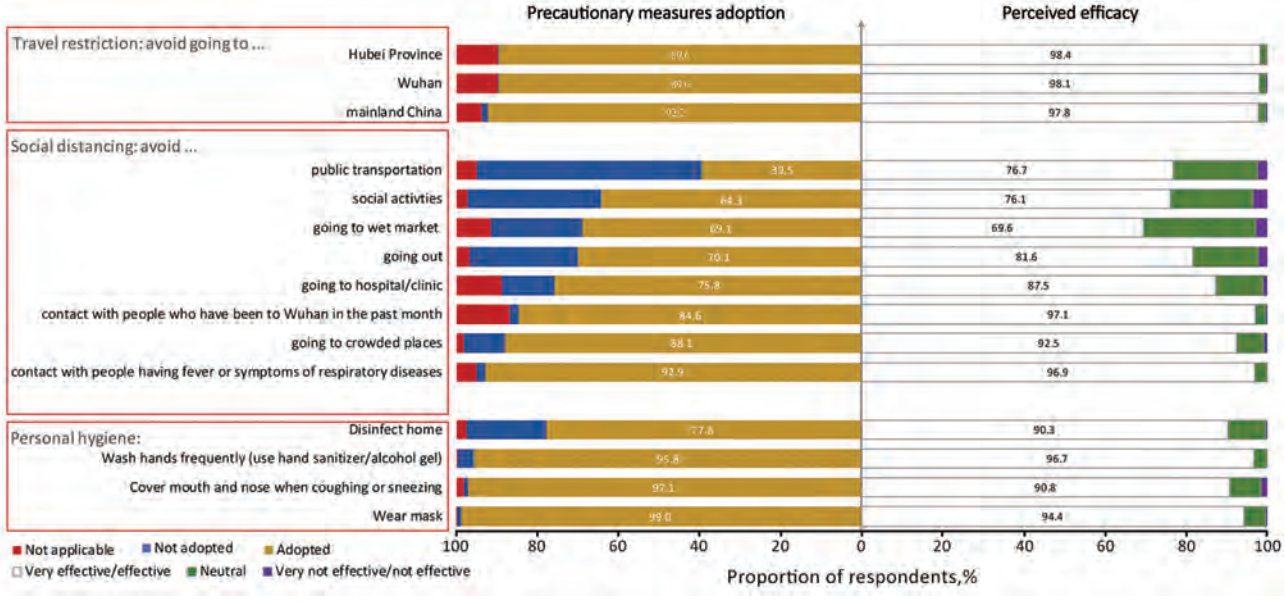


**Figure 2.** Perceived efficacy and actual adoption of precautionary measures to prevent transmission of severe acute respiratory syndrome coronavirus 2 and avoid contracting coronavirus disease, Hong Kong.

**Table 2.** Factors associated with greater adoption of social-distancing interventions during the early phase of the COVID-19 epidemic in Hong Kong*

| Characteristic | aOR (95% CI) | p value† |
|---|---|---|
| Sex | | |
| M | Referent | |
| F | 1.31 (1.06–1.63) | 0.01 |
| Age group, y | | |
| 18–24 | Referent | |
| 25–34 | 1.26 (0.97–1.63) | 0.08 |
| 35–44 | 1.17 (0.88–1.56) | 0.28 |
| 45–54 | 1.34 (0.94–1.92) | 0.11 |
| ≥55 | 0.93 (0.61–1.41) | 0.74 |
| District of residence | | |
| Hong Kong Island | Referent | |
| Kowloon East | 0.96 (0.68–1.36) | 0.83 |
| Kowloon West | 0.95 (0.62–1.46) | 0.82 |
| New Territories East | 1.57 (1.18–2.11) | 0.00 |
| New Territories West | 1.37 (1.02–1.85) | 0.04 |
| Left Hong Kong in the previous month | | |
| No | Referent | |
| Yes | 0.72 (0.57–0.91) | 0.01 |
| Made regular visits to mainland China | | |
| No | Referent | |
| Yes | 0.48 (0.24–0.91) | 0.03 |
| Perceived understanding about COVID-19 | | |
| Not well or not well at all | Referent | |
| Neutral | 1.07 (0.76–1.51) | 0.70 |
| Well or very well | 1.80 (1.27–2.56) | 0.00 |
| Presence of chronic diseases | | |
| No | Referent | |
| Yes | 0.77 (0.55–1.06) | 0.11 |
| Anxiety level | | |
| Normal | Referent | |
| Mild | 1.38 (1.08–1.76) | 0.01 |
| Moderate or severe | 1.71 (1.34–2.17) | 0.00 |

*aOR, adjusted odds ratio; COVID-19, coronavirus disease.
†By 2-tailed *t*-test.

39%–93% adoption of social-distancing). Being in agreement with the findings of Anderson et al. (*10*), we hope that these behavioral standards are useful in promoting person-level preventive measures for countries in the early phase of the COVID-19 outbreak, especially when border-control measures are not viable. This high level of civil engagement toward disease control also enables most businesses to continue as usual, which reduces the economic toll from strict quarantine measures.

In addition, we consider the increased anxiety levels reported as a double-edged sword. On one hand, anxiety can motivate precautionary measures. On the other hand, it might adversely affect school, work, or family life. Besides providing accurate information about the epidemic, public health institutions (e.g., Hong Kong Department of Health) also should promote a healthy lifestyle and psychological well-being. Further discussion of the interpretation of some specific findings, including assessing the sustainability of the preventive measures, the general anxiety level of the public in different outbreaks, the effective communication channels for COVID-19 information, and the drivers of social-distancing behaviors are provided (Appendix).

In conclusion, we identified high levels of risk perception regarding COVID-19 in the community in Hong Kong. Most respondents were alert to the disease progression of COVID-19 and adopted self-protective measures. Our findings contribute to the body of research examining the psychobehavioral responses of the public, in addition to the already widely studied biological and mechanistic aspects of COVID-19, during the early phase of the current COVID-19 epidemic. The timely psychological and behavioral assessment of the community can inform subsequent intervention and risk-communication strategies as the epidemic progresses.

### Acknowledgments

We thank Edelweiss Chui, Ivy Huang, and Margaret Tsoi for technical support.

K.O.K. acknowledges support from the Research Fund for the Control of Infectious Diseases, Hong Kong (grant no. INF-CUHK-1), the General Research Fund (reference no. 14112818), the Wellcome Trust Fund (reference no. 200861/Z/16/Z), and internal funding from the Chinese University of Hong Kong.

K.O.K., K.K.L., A.T., W.I.W., and S.Y.S.W. conceptualized the study; K.O.K. and W.I.W. performed data curation; K.O.K., H.H.H.C., Y.Y.Y., and W.I.W. analyzed the data; K.O.K., W.I.W., and S.Y.S.W. wrote the first draft of the manuscript; K.K.L., H.H.H.C., Y.Y.Y., and A.T. edited the manuscript.

### About the Author

Dr. Kwok is an assistant professor affiliated with the JC School of Public Health and Primary Care at The Chinese University of Hong Kong. His primary research interests include infectious disease epidemiology and infection control, with a current focus on mitigating emerging infectious disease outbreaks from the mathematic, epidemiologic, and behavioral perspectives.

### References

1. Wuhan Municipal Health Commission. Briefing on the current pneumonia epidemic situation. 2019 [cited 21 Mar 2020]. http://wjw.wuhan.gov.cn/front/web/showDetail/2019123108989
2. Immigration Department (Hong Kong). Immigration clearance. 2020 [cited 21 Mar 2020]. https://www.immd.gov.hk/eng/facts/control.html
3. Hong Kong Centre for Health Protection. Latest situation of cases of COVID-19. 2020 [cited 21 Mar 2020]. https://www.chp.gov.hk/files/pdf/local_situation_covid19_en.pdf

4. Hong Kong Centre for Health Protection. Countries/areas with reported cases of coronavirus disease-2019 (COVID-19). 2020 [cited 21 Mar 2020]. https://www.chp.gov.hk/files/pdf/statistics_of_the_cases_novel_coronavirus_infection_en.pdf
5. Government of the Hong Kong Special Administrative Region. Hong Kong's multi-pronged response to COVID-19. 2020 [cited 21 Mar 2020]. https://www.hketojakarta.gov.hk/doc/pdf/Factsheet_coronavirus_Mar_17_E.pdf
6. Skinner CS, Tiro J, Champion VL. The health belief model. In: Glanz K, Rimer BK, Viswanath K, editors. Health behavior: theory, research, and practice. 5th edition. San Francisco: Jossey-Bass; 2015. p. 75–94.
7. Rogers RW, Prentice-Dunn S. Protection motivation theory. In: Gochman DS, editor. Handbook of health behavior research I: personal and social determinants. New York: Springer; 1997. p. 113–32.
8. Leung GM, Ho LM, Lam TH, Hedley AJ. Epidemiology of SARS in the 2003 Hong Kong epidemic. Hong Kong Med J. 2009;15(Suppl 9):12–6.
9. Leung CM, Wing YK, Kwong PK, Lo A, Shum K. Validation of the Chinese-Cantonese version of the hospital anxiety and depression scale and comparison with the Hamilton Rating Scale of Depression. Acta Psychiatr Scand. 1999;100:456–61. https://doi.org/10.1111/j.1600-0447.1999.tb10897.x
10. Anderson RM, Heesterbeek H, Klinkenberg D, Hollingsworth TD. How will country-based mitigation measures influence the course of the COVID-19 epidemic? Lancet. 2020;395:931–4. https://doi.org/10.1016/S0140-6736(20)30567-5

Address for correspondence: Kin On Kwok, Room 419, 4/F, JC School of Public Health and Primary Care Building, Prince of Wales Hospital, Shatin, N.T., Hong Kong; email: kkokwok@cuhk.edu.hk; or Wan In Wei, Room 427, 4/F, JC School of Public Health and Primary Care Building, Prince of Wales Hospital, Shatin, N.T., Hong Kong; email: vivian1628@cuhk.edu.hk

# Clinical Characteristics of Patients Hospitalized with Coronavirus Disease, Thailand

Wannarat A. Pongpirul, Joshua A. Mott, Joseph V. Woodring, Timothy M. Uyeki, John R. MacArthur, Apichart Vachiraphan, Pawita Suwanvattana, Sumonmal Uttayamakul, Supamit Chunsuttiwat, Tawee Chotpitayasunondh, Krit Pongpirul, Wisit Prasithsirikul

Among 11 patients in Thailand infected with severe acute respiratory syndrome coronavirus 2, we detected viral RNA in upper respiratory specimens a median of 14 days after illness onset and 9 days after fever resolution. We identified viral co-infections and an asymptomatic person with detectable virus RNA in serial tests. We describe implications for surveillance.

During January 2020, persons in Thailand were tested for the presence of severe acute respiratory syndrome coronavirus 2 (SARS-CoV-2) infection if they had a combination of fever or respiratory illness and a history of travel to Wuhan, China. Persons determined to be close contacts of a laboratory-confirmed coronavirus disease (COVID-19) case-patient also were tested during enrollment into contact tracing. Clinicians were able to request testing if they had a concern regarding persons who were exposed to travelers. During January 8–31, 2020, Bamrasnaradura Infectious Diseases Institute, the national infectious disease referral hospital in Bangkok, admitted 11 patients with laboratory-confirmed COVID-19. We describe clinical features, clinical management, and results of serial reverse transcription PCR (RT-PCR) testing for SARS-CoV-2 RNA for these patients.

Author affiliations: Bamrasnaradura Infectious Diseases Institute, Bangkok, Thailand (W.A. Pongpirul, A. Vachiraphan, P. Suwanvattana, S. Uttayamakul, W. Prasithsirikul); US Centers for Disease Control and Prevention–Thailand Ministry of Public Health Collaboration, Bangkok (J.A. Mott, J.V. Woodring, J.R. MacArthur); US Centers for Disease Control and Prevention, Atlanta, Georgia, USA (T.M. Uyeki); Thailand Ministry of Public Health, Bangkok (S. Chunsuttiwat); Queen Sirikit National Institute for Child Health, Bangkok (T. Chotpitayasunondh); Chulalongkorn University, Bangkok (K. Pongpirul)

DOI: https://doi.org/10.3201/eid2607.200598

## The Study

The 11 hospitalized patients had daily nasopharyngeal and oropharyngeal sampling for SARS-CoV-2 RNA testing. Specimens were collected by using synthetic fiber swabs, which were combined and placed into a single sterile tube containing »3 mL of viral transport medium. RNA was extracted and tested with conventional RT-PCR and real-time RT-PCR (rRT-PCR). We developed SARS-CoV-2–specific primers and probes by using a protocol from the World Health Organization (*1*) and validated results by using clinical specimens. Nasopharyngeal and oropharyngeal swabs and sputum specimens also were tested for 33 respiratory pathogens by using the Fast-Track Diagnostic rRT-PCR Respiratory Panel (Fast Track Diagnostics, http://www.fast-trackdiagnostics.com), according to the manufacturer's instructions. During the study period, Thailand's discharge criteria for hospitalized COVID-19 patients required resolution of clinical signs and symptoms and 2 respiratory specimens without detectable SARS-CoV-2 RNA collected ≥24 hours apart.

The median age of the patients was 61 years (range 28–74 years; Table 1). Cough, malaise, and sore throat were the most common signs and symptoms among the 11 patients (Figure 1). In patients with fever (temperature >38°C; 10/11), defervescence took a median of 6 days (4–11.5 days). Some patients had signs and symptoms that lasted ≥10 days (Figure 1; Table 2). Most patients received supportive care; none required mechanical or noninvasive ventilation during their hospitalization.

Patient 4 remained asymptomatic throughout hospitalization despite daily monitoring. However, her chest radiograph at admission revealed unilateral pneumonia (Appendix Figure, http://wwwnc.cdc.gov/EID/article/26/7/20-0598-App1.pdf). Patient 4's nasopharyngeal and oropharyngeal specimens had detectable SARS-CoV-2 RNA on 4 consecutive

days. She finally had 2 negative specimens separated by ≥24 hours and was discharged on day 7 after symptom onset (Figure 2).

Patient 10, a taxi driver with no history of air travel, had the most severe clinical presentation among these cases (2). He reported close contact

**Table 1.** Demographics, baseline characteristics, illness histories, laboratory values and treatment therapies of confirmed COVID-19 patients in Bamrasnaradura Infectious Diseases Institute, Bangkok, Thailand, 2020*

| | Patient no. | | | | | | | | | | | |
|---|---|---|---|---|---|---|---|---|---|---|---|---|
| Demographics | 1 | 2 | 3 | 4 | 5 | 6 | 7 | 8 | 9 | 10† | 11 | Total, % |
| Age, y/sex | 61/F | 74/F | 68/M | 66/F | 57/F | 34/M | 61/M | 63/M | 28/F | 51/M | 49/M | 55 M/45 F |
| Ethnicity | CH | CH | CH | CH | CH | CH | CH | CH | CH | TH | TH | 82 CH/18 TH |
| Occupation | Ret | Ret | Ret | Ret | Ret | EE | Ret | Ret | Tour guide | Taxi driver | Officer | 54 Ret/46 other |
| Detected through airport screening | Y | Y | Y | N | N | N | N | N | N | N | N | 27 Y/73 N |
| Detected through contact tracing | N | N | N | Y | N | N | N | N | N | N | N | 9 Y/91 N |
| Detected after patient voluntarily sought medical care | N | N | N | N | Y | Y | Y | Y | Y | Y | Y | 64 Y/36 N |
| Visited Hunan Seafood Market | N | N | N | N | N | N | N | N | N | N | N | 0 |
| Underlying conditions | | | | | | | | | | | | |
| Diabetes | N | N | N | N | N | Y | N | N | N | Y | N | 18 Y/82 N |
| Hypertension | Y | Y | N | Y | N | N | N | N | N | Y | N | 36 Y/64 N |
| COPD | N | N | N | N | N | N | N | N | N | N | N | 0 |
| Asthma | N | N | N | N | N | N | N | N | N | N | N | 0 |
| Cancer | N | N | N | N | N | N | N | N | N | N | N | 0 |
| Cardiovascular disease | N | Y | N | Y | N | N | N | Y | N | N | N | 27 Y/73 N |
| Cerebrovascular disease | N | N | N | N | N | N | N | Y | N | N | N | 9 Y/91 N |
| Chronic liver disease | N | N | N | N | N | N | N | N | N | N | Y | 9 Y/91 N |
| Any chronic condition | Y | Y | N | Y | N | Y | N | Y | N | Y | Y | 64 Y/36 N |
| Current smoker | N | N | N | N | N | N | N | N | N | N | N | 0 |
| Pregnant | NA | NA | NA | NA | NA | NA | NA | NA | N | NA | NA | 0 |
| Laboratory values at time of admission (reference range) | | | | | | | | | | | | |
| Leukocytes ×$10^9$/L (4.5–8) | 1.9↓ | 3.3↓ | 4 | 3.6 | 3.9 | 3.4↓ | 5.8 | 4.1 | 4.9 | 5.8 | 2.5↓ | |
| Neutrophils, % (36–70) | 48 | 64 | 66 | 63 | 56 | 80↑ | 63 | 83 | 73↑ | 58 | 54 | |
| Lymphocytes, % (23–57) | 40 | 19↓ | 25 | 25 | 33 | 1↓ | 30 | 16↓ | 23 | 31 | 30 | |
| Platelets ×$10^6$/μL (140–400) | 127↓ | 16.4↓ | 12.6↓ | 177 | 167 | 169 | 168 | 18.4↓ | 153 | 368 | 167 | |
| Hemoglobin, g/dL (11–14) | 13.3 | 12.8 | 11.5 | 13.1 | 13.2 | 13.3 | 15.3↑ | 13.8 | 11.4 | 14 | 14.8↑ | |
| Hematocrit, % (35–41) | 38 | 38 | 33↓ | 37 | 37.9 | 38 | 45↑ | 39 | 34 | 41 | 43↑ | |
| ALT, U/L (0–31) | 18 | 27 | 18 | 83↑ | 23 | 16 | 22 | 22 | 24 | 24 | 26 | |
| AST, U/L (0–31) | 14 | 12 | 15 | 47↑ | 16 | 19 | 20 | 14 | 25 | 16 | 22 | |
| Other diagnostics | | | | | | | | | | | | |
| Oxygen saturation on room air at admission | 98 | 97 | 95 | 98 | 99 | 99 | 98 | 99 | 96 | 91↓ | 97 | |
| Results from Biofire-33 multiplex PCR‡ | | | | | | | | | | | | |
| *Haemophilus influenzae* | + | + | – | – | + | + | – | – | – | – | – | |
| Adenovirus | – | + | – | – | – | – | – | – | – | – | – | |
| Influenza A | – | – | – | – | – | – | + | – | – | – | – | |
| *Klebsiella pneumoniae* | – | – | – | – | – | – | – | – | – | – | + | |
| Treatments | | | | | | | | | | | | |
| Antimicrobial drugs, dose | | | | | | | | | | | | |
| Ceftriaxone, 2 g 4×/d IV | 1 | 0 | 7 | 0 | 0 | 0 | 7 | 0 | 0 | 7 | 0 | |
| Ceftriaxone, 2 g/d orally | 0 | 7 | 0 | 0 | 0 | 0 | 0 | 0 | 0 | 0 | 0 | |
| AMOX/CLAV, 2 g 4×/d orally | 6 | 0 | 0 | 0 | 0 | 0 | 0 | 0 | 0 | 0 | 7 | |
| Oseltamivir, 150 mg 4×/d orally | 5 | 0 | 0 | 0 | 0 | 0 | 5 | 0 | 0 | 0 | 5 | |
| Nasal cannula, 5 L, no. days | 0 | 0 | 0 | 0 | 0 | 0 | 0 | 0 | 0 | 3 | 0 | |
| Duration of signs and symptoms reported at admission, d | | | | | | | | | | | | Median (IQR)/ mean (SD) |
| Cough | 1 | 1 | 1 | 0 | 2 | 1 | 4 | 2 | 3 | 8 | 5 | 2 (1–4)/2.5 (2.3) |
| Malaise or fatigue | 4 | 2 | 4 | 0 | 2 | 4 | 13 | 2 | 3 | 5 | 5 | 4 (2–5)/4.0 (3.3) |
| Fever | 2 | 2 | 4 | 0 | 3 | 4 | 4 | 2 | 2 | 8 | 5 | 3 (2–4)/3.3 (2.1) |
| Sore throat | 4 | 0 | 3 | 0 | 3 | 2 | 4 | 2 | 3 | 7 | 5 | 3 (2–4)/3.0 (2.0) |
| Rhinorrhea | 2 | 2 | 4 | 0 | 2 | 1 | 3 | 2 | 2 | 2 | 4 | 2 (2–3)/2.2 (1.2) |
| Headache | 1 | 0 | 2 | 0 | 0 | 0 | 0 | 2 | 1 | 5 | 3 | 1 (0–2)/1.3 (1.6) |
| Vomiting | 0 | 1 | 1 | 0 | 0 | 0 | 0 | 1 | 0 | 0 | 0 | 0 (0–1)/0.3 (0.5) |
| Diarrhea | 0 | 0 | 1 | 0 | 0 | 0 | 0 | 1 | 0 | 0 | 0 | 0/0.2 (0.4) |

*ALT, alanine aminotransferase; AMOX/CLAV, amoxicillin/clavulanate; AST, aspartate aminotransferase; COVID-19, coronavirus disease; CH, Chinese; EE, electrical engineer; IV, intravenous; NA, not applicable; Ret, retired; TH, Thai; ↓, low; ↑, high; +, positive; –, negative.
†(*2*)
‡BioFire Diagnostics (https://www.biofiredx.com)

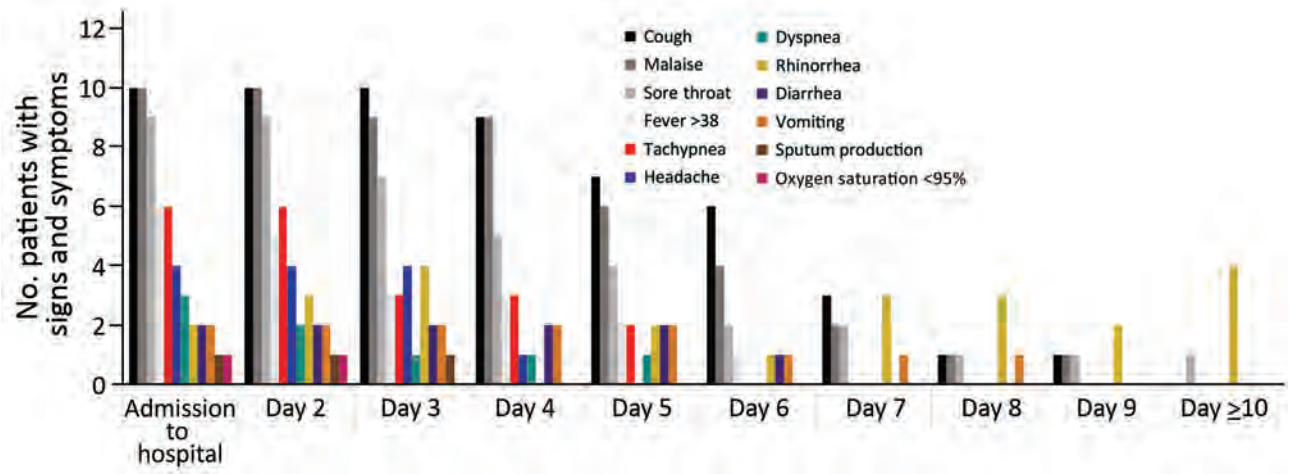


**Figure 1.** Number of patients with signs and symptoms by days following admission based on 11 patients with confirmed coronavirus disease, Bamrasnaradura Infectious Diseases Institute, Bangkok, Thailand, January 8–31, 2020

while transporting symptomatic travelers from China, a mechanism of exposure that has been described elsewhere (*3*–*5*). Patient 10 did not seek care for 10 days after his reported onset of fever. In Thailand, workers in the tourist industry, including those who transport tourists, are among the risk groups monitored for occupational exposures under updated clinical practice guidelines (*6*).

**Table 2.** Clinical illness history and calculated intervals of confirmed COVID-19 patients in Bamrasnaradura Infectious Diseases Institute, Bangkok, Thailand, 2020*

| | Patient no. | | | | | | | | | | | Median no. days since symptom onset (IQR) | Mean no. days since symptom onset (SD) | T-test comparison between means |
|---|---|---|---|---|---|---|---|---|---|---|---|---|---|---|
| Duration of signs and symptoms, d | 1 | 2 | 3 | 4† | 5 | 6 | 7 | 8 | 9 | 10 | 11 | | | |
| Onset of symptoms | 0 | 0 | 0 | NA | 0 | 0 | 0 | 0 | 0 | 0 | 0 | NA | NA | NA |
| Onset of fever | 2 | 0 | 0 | NA | 0 | 0 | 9 | 0 | 1 | 0 | 0 | 0 (0–1.25) | 1.2 (2.8) | – |
| First medical visit | 4 | 2 | 4 | 0 | 3 | 4 | 13 | 2 | 3 | 3 | 2 | 3 (2–4) | 3.6 (3.3) | – |
| Admitted to BIDI | 4 | 2 | 4 | 0 | 3 | 4 | 13 | 2 | 3 | 8 | 5 | 4 (2–5) | 4.4 (3.5) | – |
| SARS-CoV-2 RNA detected | 4 | 2 | 4 | 0 | 3 | 4 | 13 | 2 | 3 | 8 | 5 | 4 (2–5) | 4.4 (3.5) | – |
| Fever resolution | 4 | 3 | 6 | NA | 6 | 4 | 13 | 4 | 6 | 13 | 11 | 6 (4–11.5) | 7.0 (3.9) | – |
| Clinical resolution | 13 | 10 | 11 | NA | 9 | 9 | 17 | 15 | 9 | 13 | 13 | 12 (9–13.5) | 11.9 (2.8) | – |
| SARS-CoV-2 RNA undetectable | 14 | 10 | 13 | 4 | 9 | 26 | 24 | 29 | 9 | 14 | 30 | 14 (9–26) | 16.5 (9.1) | – |
| Discharge | 15 | 11 | 14 | 6 | 15 | 29 | 26 | 32 | 11 | 16 | 33 | 15 (11–29) | 18.9 (9.4) | – |
| Calculated intervals | | | | | | | | | | | | | | |
| Admission to discharge | 11 | 9 | 10 | 6 | 12 | 25 | 13 | 30 | 8 | 8 | 28 | 11 (8–25) | 14.5 (8.7) | – |
| Fever resolution to SARS-COV-2 RNA undetectable | 10 | 7 | 7 | NA | 3 | 22 | 11 | 25 | 3 | 1 | 19 | 9 (3–19.75) | 10.8 (8.4) | – |
| Admission to fever resolution | 0 | 1 | 2 | NA | 3 | 0 | 0 | 2 | 3 | 5 | 6 | 2 (0–3.5) | 2.2 (2.1) | – |
| Fever resolution to clinical resolution | 9 | 7 | 5 | NA | 3 | 5 | 4 | 11 | 3 | 0 | 2 | 5 (3–7.5) | 4.9 (3.3) | – |
| Admission to clinical resolution | 9 | 8 | 7 | NA | 6 | 5 | 4 | 13 | 6 | 5 | 8 | 7 (5–8.25) | 7.1 (2.6) | – |
| Fever onset to fever resolution | 2 | 3 | 6 | NA | 6 | 4 | 4 | 4 | 5 | 13 | 11 | 5 (4–7.25) | 5.8 (3.5) | – |
| Admission to SARS-COV-2 RNA undetectable | 10 | 8 | 9 | 4 | 6 | 22 | 11 | 27 | 6 | 6 | 25 | 10 (6–22.75) | 12.2 (8.3) | – |
| Fever resolution to discharge | 11 | 8 | 8 | NA | 9 | 25 | 13 | 28 | 5 | 3 | 22 | 10 (7–22.75) | 13.2 (8.7) | – |
| Fever duration by stratified condition | | | | | | | | | | | | | | |
| Patients detected through airport screening | 2 | 3 | 6 | – | – | – | – | – | – | – | – | 3 (2–6) | 3.7 (2.1) | 0.14 |
| Patients seeking medical care | – | – | – | – | 6 | 4 | 4 | 4 | 5 | 13 | 11 | 5 (4–11) | 6.7 (3.7) | – |
| Detectable SARS-COV-2 RNA duration by stratified condition | | | | | | | | | | | | | | |
| Patients detected through airport screening | 10 | 9 | 8 | – | – | – | – | – | – | – | – | 9 (8–10) | 9.0 (1.0) | 0.17 |
| Patients seeking medical care | – | – | – | – | 6 | 22 | 11 | 27 | 6 | 6 | 25 | 11 (6–25) | 14.7 (9.6) | – |

*COVID-19, coronavirus disease; NA, not applicable
†Patient 4 was asymptomatic throughout hospitalization and PCR results reflects days with detectable SARS-CoV-2 RNA following admission.

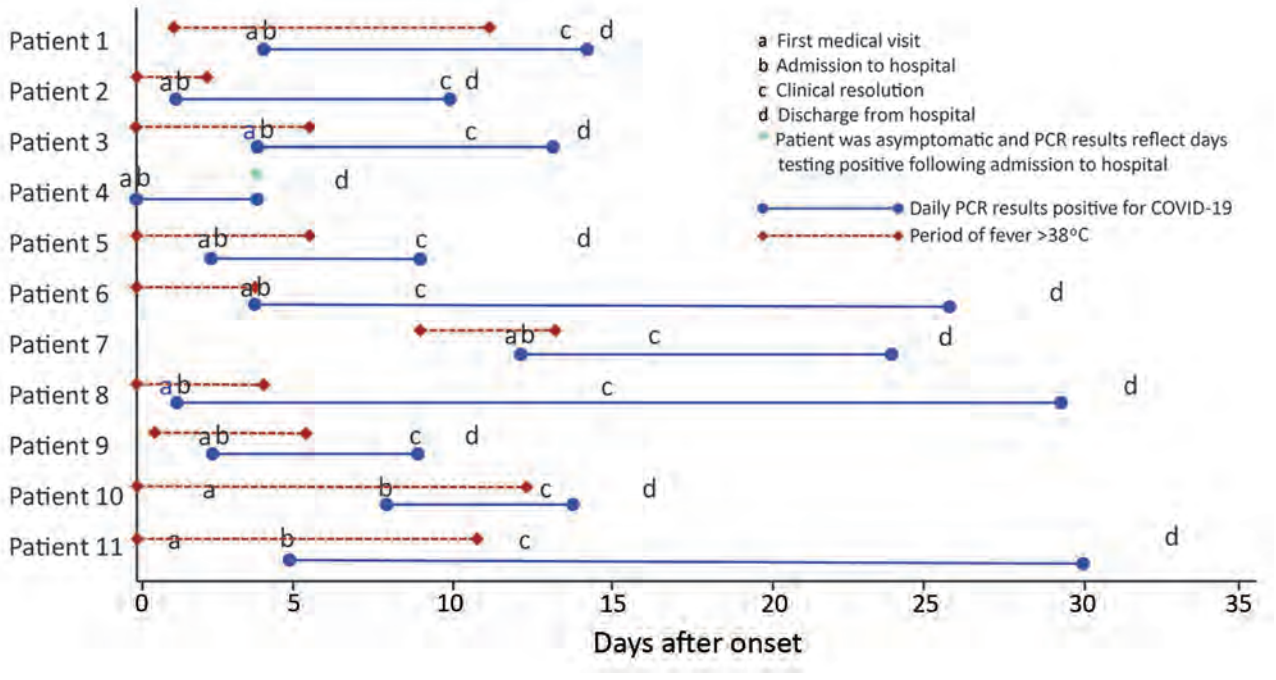


**Figure 2.** Clinical course for 11 patients with laboratory-confirmed COVID-19 by days since onset of their first symptom, Bamrasnaradura Infectious Diseases Institute, Bangkok, Thailand, January 2020. Blue solid bars indicate number of days each patient had detectable severe acute respiratory syndrome coronavirus 2 RNA. Red dashed bars indicate the number of days each patient had a fever ≥38°C. Asterisk denotes that patient 4 remained asymptomatic during hospitalization with detectable viral RNA for 4 consecutive days. COVID-19, coronavirus disease.

We detected viral co-infections in 2 patients during their hospitalization. Patient 2 had an adenovirus co-infection, and patient 7 had an influenza A virus co-infection (Table 1). Patient 7 was hospitalized for 13 days and influenza might have contributed to his clinical course. In Thailand, influenza A infection occurs most frequently during the rainy season, July–November (*7*).

## Conclusions

We describe the clinical characteristics, clinical management, and laboratory findings from 11 COVID-19 patients hospitalized at Bamrasnaradura Infectious Diseases Institute. Most were febrile, but the onset of fever occurred early in the course of illness and fever resolution occurred 5 days before full clinical recovery and 10 days before discharge. Although no patient required mechanical ventilation or intubation, all had radiographic evidence of pneumonia, even those without respiratory symptoms. Together, these findings suggest that whereas fever and lower respiratory illness are commonly observed, case definitions requiring both fever and lower respiratory illness as signs and symptoms might not have detected several of these cases, especially later in the clinical course of illness.

Clinical resolution occurred a median of 12 (9–13.5) days after illness onset, and these patients had detectable SARS-CoV-2 RNA in upper respiratory tract specimens for a median of 14 (9–26) days after illness onset (Table 2). However, patients became afebrile 6 days after illness onset, with a median of 9 (3–19.75) additional days of detectable SARS-CoV-2 RNA in respiratory specimens after resolution of fever (Table 2). The required duration of hospitalization and observed period of viral RNA positivity for these patients underscore the potential burden of COVID-19 patients on hospital, diagnostic, treatment, and isolation capacities. Despite mild-to-moderate illness, the protracted period of SARS-CoV-2 RNA positivity in these patients' specimens might indicate a lengthy period of infectiousness and highlights risks to providers caring for COVID-19 patients.

Among persons of Chinese ethnicity in our study, only 3/9 who traveled from China were detected through airport screening. During the study period, <7% of all persons under investigation for COVID-19 in Thailand were detected through airport screening (*8*). Given the proportion of cases identified through community surveillance, countries should not focus exclusively on point of entry

screening or travel histories to detect cases of COVID-19, and maintaining healthcare providers' awareness remains critical.

Patient 4 had detectable SARS-CoV-2 RNA for 4 consecutive days, but we were only able to follow her for 7 days before she returned to China. Her case is an example of a person without reported symptoms but radiologic evidence of disease and detectable virus over several days. Other studies have described asymptomatic patients with upper respiratory specimens positive for SARS-CoV-2 (*9*), and evidence suggests such cases pose a risk for transmission (*10*–*12*).

Our case series has some limitations. Patients could have recall bias regarding symptom onset before hospitalization. We were unable to complete a 14-day observation for some patients because they returned to China after discharge, including patient 4, who had no reported respiratory symptoms.

The relatively long duration of hospitalizations in our study highlights the effects that current surveillance and isolation procedures can have on clinical care surge capacity. Duration of hospitalization was extended by Ministry of Public Health requirements for patients to remain in the hospital until symptom resolution and clearing of SARS-CoV-2 RNA in clinical samples. We observed that it took a median of 9 days to clear SARS-CoV-2 after fever resolution. In addition, we noted serial detection of SARS-CoV-2 RNA in respiratory specimens of an asymptomatic patient.

Our observations of possible viral co-infections in COVID-19 patients and the resolution of fever relatively early during clinical course also have implications for surveillance strategies. Specifically, case definitions requiring fever could miss COVID-19 cases, especially later in the clinical course, and surveillance strategies that test only for SARS-CoV-2 could miss co-infections. Clinicians should consider the possibility of co-infection because the presence of other respiratory pathogens does not exclude the possibility of SARS-CoV-2 virus infection. Clinicians also need to better understand the relationship of RT-PCR detection of SARS-Cov-2 via multiple shedding routes (*13*) compared with the presence of culturable virus, especially in patients with few or no symptoms, because this might affect screening and isolation criteria. Whereas the current outbreak will undoubtedly change in character and magnitude, the information in this report could be combined with additional data sources to refine public health response and clinical management.

Data collection and analyses were approved by the institutional review board at Bamrasnaradura Infectious Diseases Institute, Bangkok, Thailand (IRB no. S004h/63_ExPD). The findings and conclusions in this report are those of the authors and do not necessarily represent the official position of the Centers for Disease Control and Prevention.

## About the Author

Dr. Pongpirul is a nephrologist at Bamrasnaradura Infectious Diseases Institute, Bangkok, Thailand. She has led the management of the patients with COVID-19 admitted to the primary public COVID-19 referral center in Bangkok, Thailand. Her primary research interests, beyond COVID-19, include chronic kidney disease and histoplasmosis in patients infected with HIV, biomarkers of kidney diseases, and studies of kidney transplantation.

## References

1. Department of Medical Sciences, Ministry of Public Health, Thailand. Diagnostic detection of novel coronavirus 2019 by real time RT-PCR. Version 0. 23 January 2020. [cited 2020 Feb 16] https://www.who.int/docs/default-source/coronaviruse/conventional-rt-pcr-followed-by-sequencing-for-detection-of-ncov-rirl-nat-inst-health-t.pdf?sfvrsn=42271c6d_4
2. Pongpirul WA, Pongpirul K, Ratnarathon AC, Prasithsirikul W. Journey of a Thai taxi driver and novel coronavirus. N Engl J Med. 2020;382:1067–8. https://doi.org/10.1056/NEJMc2001621
3. Phan LT, Nguyen TV, Luong QC, Nguyen TV, Nguyen HT, Le HQ, et al. Importation and human-to-human transmission of a novel coronavirus in Vietnam. N Engl J Med. 2020;382:872–4. 10.1056/NEJMc2001272 https://doi.org/10.1056/NEJMc2001272
4. Chan JF, Yuan S, Kok KH, To KK, Chu H, Yang J, et al. A familial cluster of pneumonia associated with the 2019 novel coronavirus indicating person-to-person transmission: a study of a family cluster. Lancet. 2020;395:514–23. https://doi.org/10.1016/S0140-6736(20)30154-9
5. Wang D, Hu B, Hu C, Zhu F, Liu X, Zhang J, et al. Clinical characteristics of 138 hospitalized patients with 2019 novel coronavirus-infected pneumonia in Wuhan, China. JAMA. 2020;323:1061. PubMed https://doi.org/10.1001/jama.2020.1585
6. Department of Disease Control, Thailand. Guidelines for medical practice, diagnosis, treatment and prevention of healthcare-associated infection in response to patients with COVID-19 infection, revised version dated 16 February 2020 [cited 2020 Feb 21]. https://ddc.moph.go.th/viralpneumonia/eng/file/guidelines/G_CPG_en.pdf
7. Prachayangprecha S, Vichaiwattana P, Korkong S, Felber JA, Poovorawan Y. Influenza activity in Thailand and occurrence in different climates. Springerplus. 2015;4:356. https://doi.org/10.1186/s40064-015-1149-6
8. Department of Disease Control, Ministry of Public Health, Thailand. Novel coronavirus 2019 pneumonia situation: Thailand situation update on 15 February 2020 [cited 2020 Feb 16] https://ddc.moph.go.th/viralpneumonia/eng/file/situation/situation-no43-150263.pdf

9. Zou L, Ruan F, Huang M, Liang L, Huang H, Hong Z, et al. SARS-Cov-2 viral load in upper respiratory specimens of infected patients. N Eng J Med. 2020;389:1177–9. https://doi.org/10.1056/NEJMc2001737
10. Bai Y, Yao L, Wei T, Tian F, Jin DY, Chen L, et al. Presumed asymptomatic carrier transmission of COVID-19. JAMA. 2020 Feb 20 [Epub ahead of print]. https://doi.org/10.1001/jama.2020.2565
11. Zhang W, Du R, Li B, Zheng X-S, Yang X-L, Hu B, et al. Molecular and serological investigation of 2019-nCoV infected patients: implication of multiple shedding routes. Emerg Microbes Infect. 2020;9:386–9. https://doi.org/10.1080/22221751.2020.1729071
12. Yu P, Zhu J, Zhang Z, Han Y, Huang L. A familial cluster of infection associated with the 2019 novel coronavirus indicating potential person-to-person transmission during the incubation period. J Infect Dis. 2020 Feb 18 [Epub ahead of print] https://doi.org/10.1093/infdis/jiaa077
13. Chen N, Zhou M, Dong X, Qu J, Gong F, Han Y, et al. Epidemiological and clinical characteristics of 99 cases of 2019 novel coronavirus pneumonia in Wuhan, China: a descriptive study. Lancet. 2020;395:507–13. https://doi.org/10.1016/S0140-6736(20)30211-7

Address for correspondence: Joseph Woodring, US Centers for Disease Control and Prevention–Thailand Ministry of Public Health Collaboration, DDC7 Building, Soi 4 Ministry of Public Health, Bangkok 10300, Thailand; email: wjd9@cdc.gov

# Aerosol and Surface Distribution of Severe Acute Respiratory Syndrome Coronavirus 2 in Hospital Wards, Wuhan, China, 2020

Zhen-Dong Guo,[1] Zhong-Yi Wang,[1] Shou-Feng Zhang,[1] Xiao Li, Lin Li, Chao Li, Yan Cui, Rui-Bin Fu, Yun-Zhu Dong, Xiang-Yang Chi, Meng-Yao Zhang, Kun Liu, Cheng Cao, Bin Liu, Ke Zhang, Yu-Wei Gao, Bing Lu, Wei Chen

To determine distribution of severe acute respiratory syndrome coronavirus 2 in hospital wards in Wuhan, China, we tested air and surface samples. Contamination was greater in intensive care units than general wards. Virus was widely distributed on floors, computer mice, trash cans, and sickbed handrails and was detected in air ≈4 m from patients.

As of March 30, 2020, approximately 750,000 cases of coronavirus disease (COVID-19) had been reported globally since December 2019 (*1*), severely burdening the healthcare system (*2*). The extremely fast transmission capability of severe acute respiratory syndrome coronavirus 2 (SARS-CoV-2) has aroused concern about its various transmission routes.

The main transmission routes for SARS-CoV-2 are respiratory droplets and close contact (*3*). Knowing the extent of environmental contamination of SARS-CoV-2 in COVID-19 wards is critical for improving safety practices for medical staff and answering questions about SARS-CoV-2 transmission among the public. However, whether SARS-CoV-2 can be transmitted by aerosols remains controversial, and the exposure risk for close contacts has not been systematically evaluated. Researchers have detected SARS-CoV-2 on surfaces of objects in a symptomatic patient's room and toilet area (*4*). However, that study was performed in a small sample from regions with few confirmed cases, which might not reflect real conditions in outbreak regions where hospitals are operating at full capacity. In this study, we tested surface and air samples from an intensive care unit (ICU) and a general COVID-19 ward (GW) at Huoshenshan Hospital in Wuhan, China (Figure 1).

## The Study

From February 19 through March 2, 2020, we collected swab samples from potentially contaminated objects in the ICU and GW as described previously (*5*). The ICU housed 15 patients with severe disease and the GW housed 24 patients with milder disease. We also sampled indoor air and the air outlets to detect aerosol exposure. Air samples were collected by using a SASS 2300 Wetted Wall Cyclone Sampler (Research International, Inc., https://www.rsrchintl.com) at 300 L/min for of 30 min. We used sterile premoistened swabs to sample the floors, computer mice, trash cans, sickbed handrails, patient masks, personal protective equipment, and air outlets. We tested air and surface samples for the open reading frame (ORF) *1ab* and nucleoprotein (N) genes of SARS-CoV-2 by quantitative real-time PCR. (Appendix, https://wwwnc.cdc.gov/EID/article/26/7/20-0885-App1.pdf).

Almost all positive results were concentrated in the contaminated areas (ICU 54/57, 94.7%; GW 9/9, 100%); the rate of positivity was much higher for the ICU (54/124, 43.5%) than for the GW (9/114, 7.9%) (Tables 1, 2). The rate of positivity was

Author affiliations: Academy of Military Medical Sciences, Beijing, China (Z.-D. Guo, Z.-Y. Wang, S.-F. Zhang, X. Li, L. Li, Y.-Z. Dong, X.-Y. Chi, M.-Y. Zhang, C. Cao, K. Zhang, Y.-W. Gao, B. Lu, W. Chen); Institute of Medical Support Technology, Institute of Systems Engineering, Academy of Military Sciences, Tianjin, China (C. Li); Wuhan Huoshenshan Hospital, Wuhan, China (Y. Cui, R.-B. Fu, B. Liu); Central Theater General Hospital, Wuhan (K. Liu)

DOI: https://doi.org/10.3201/eid2607.200885

[1]These authors contributed equally to this article.

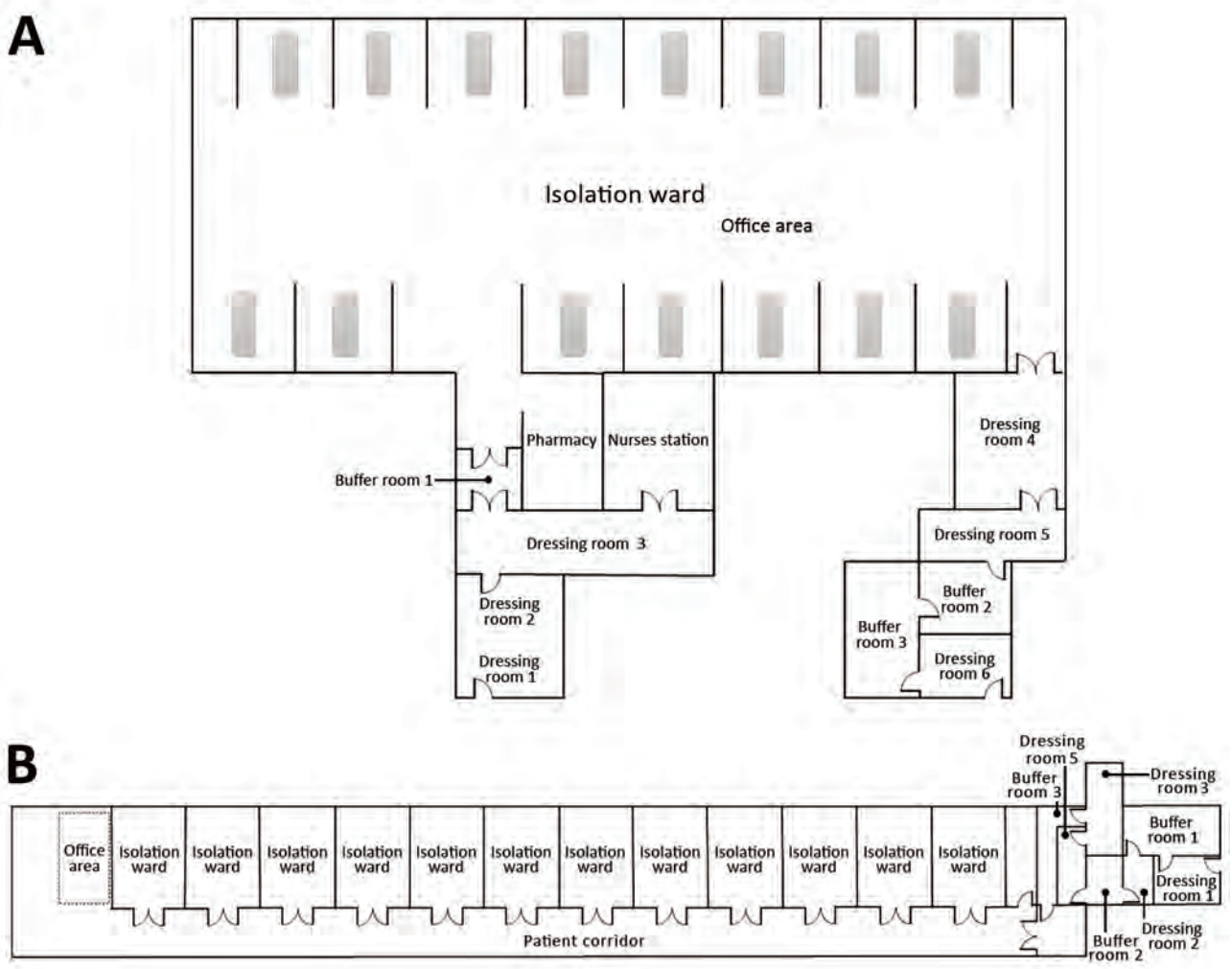


**Figure 1.** Layout of the intensive care unit (ICU) (A) and general ward (B) at Huoshenshan Hospital, Wuhan, China. For the ICU, the order of dressing is dressing room 1, dressing room 2, and dressing room 3; the order of undressing is dressing room 4, dressing room 5, and dressing room 6. The isolation ward of ICU is a large floor space with 15 cubicles (each with a patient bed) along the 2 opposite perimeters. Each cubicle is open to the central open area without any partition. For the general ward, the order of dressing is dressing room 1, dressing room 2, and dressing room 3; the order of undressing is dressing room 4, dressing room 5, and buffer room 1. The contaminated area of the general ward contains a patient corridor, and the 1-sided cubicles are all enclosed with door access to the corridor.

relatively high for floor swab samples (ICU 7/10, 70%; GW 2/13, 15.4%), perhaps because of gravity and air flow causing most virus droplets to float to the ground. In addition, as medical staff walk around the ward, the virus can be tracked all over the floor, as indicated by the 100% rate of positivity from the floor in the pharmacy, where there were no patients. Furthermore, half of the samples from the soles of the ICU medical staff shoes tested positive. Therefore, the soles of medical staff shoes might function as carriers. The 3 weak positive results from the floor of dressing room 4 might also arise from these carriers. We highly recommend that persons disinfect shoe soles before walking out of wards containing COVID-19 patients.

The rate of positivity was also relatively high for the surface of the objects that were frequently touched by medical staff or patients (Tables 1, 2). The highest rates were for computer mice (ICU 6/8, 75%; GW 1/5, 20%), followed by trash cans (ICU 3/5, 60%; GW 0/8), sickbed handrails (ICU 6/14, 42.9%; GW 0/12), and doorknobs (GW 1/12, 8.3%). Sporadic positive results were obtained from sleeve cuffs and gloves of medical staff. These results suggest that medical staff should perform hand hygiene practices immediately after patient contact.

Because patient masks contained exhaled droplets and oral secretions, the rate of positivity for those masks was also high (Tables 1, 2). We recommend adequately disinfecting masks before discarding them.

**Table 1.** Results of testing for SARS-CoV-2 in intensive care unit, Huoshenshan Hospital, Wuhan, China, 2020*

| Area, sample | Intense positive/weak positive/negative† | Rate of positivity, % | Average virus concentration‡ |
|---|---|---|---|
| Contaminated area | | | |
| Isolation wards | | | |
| Floor | 6/1/3 | 70 | $6.6 \times 10^4$ |
| Computer mouse | 4/2/2 | 75 | $2.8 \times 10^4$ |
| Trash can | 0/3/2 | 60 | $3.4 \times 10^4$ |
| Sickbed handrail | 2/4/8 | 42.9 | $4.3 \times 10^4$ |
| Patient mask | 1/1/3 | 40 | $3.3 \times 10^3$ |
| Air outlet filter | 4/4/4 | 66.7 | $1.5 \times 10^5$ |
| Indoor air near the air outlet (sampling site 1 in Figure 2, panel A) | 2/3/9 | 35.7 | 3.8 |
| Indoor air near the patients (sampling site 2 in Figure 2, panel A) | 2/6/10 | 44.4 | 1.4 |
| Indoor air near the doctors' office area (sampling site 3 in Figure 2, panel A) | 0/1/7 | 12.5 | 0.52 |
| Pharmacy | | | |
| Floor | 3/0/0 | 100 | $7.45 \times 10^4$ |
| Indoor air | 0/0/5 | 0 | ND |
| PPE | | | |
| Face shield of medical staff | 0/0/6 | 0 | ND |
| Sleeve cuff of medical staff | 0/1/5 | 16.7 | $7.1 \times 10^3$ |
| Glove of medical staff | 0/1/3 | 25 | $2.9 \times 10^3$ |
| Shoe sole of medical staff | 3/0/3 | 50 | $3.2 \times 10^4$ |
| Subtotal | 27/27/70 | 43.5 | NA |
| Semicontaminated area | | | |
| Buffer room 1 | | | |
| Floor | 0/0/5 | 0 | ND |
| Air outlet filter | 0/0/3 | 0 | ND |
| Indoor air | 0/0/5 | 0 | ND |
| Doorknob | 0/0/3 | 0 | ND |
| Dressing room 4 | | | |
| Floor | 0/3/5 | 37.5 | $3.8 \times 10^3$ |
| Air outlet filter | 0/0/3 | 0 | ND |
| Indoor air | 0/0/5 | 0 | ND |
| Doorknob | 0/0/4 | 0 | ND |
| Subtotal | 0/3/33 | 8.3 | NA |
| Clean area | | | |
| Dressing rooms 1, 2, and 3 | | | |
| Doorknob | 0/0/10 | 0 | ND |
| Floor | 0/0/12 | 0 | ND |
| Indoor air | 0/0/8 | 0 | ND |
| Nurse station | | | |
| Doorknob | 0/0/5 | 0 | ND |
| Floor | 0/0/5 | 0 | ND |
| Indoor air | 0/0/5 | 0 | ND |
| Dressing rooms 5 and 6, buffer rooms 2 and 3 | | | |
| Doorknob | 0/0/12 | 0 | ND |
| Floor | 0/0/12 | 0 | ND |
| Indoor air | 0/0/12 | 0 | ND |
| Subtotal | | | |
| Total | 27/30/184 | 23.7 | NA |

*NA, not applicable; ND, not determined; PPE, personal protective equipment; SARS-CoV-2, severe acute respiratory syndrome coronavirus 2.
†Intense positive indicates a positive result for both open reading frame *1ab* gene and nucleoprotein gene of SARS-CoV-2; weak positive indicates a positive result for only 1 of the genes.
‡The average virus concentration of indoor air expressed as copies/L and of swab samples, as copies/sample.

We further assessed the risk for aerosol transmission of SARS-CoV-2. First, we collected air in the isolation ward of the ICU (12 air supplies and 16 air discharges per hour) and GW (8 air supplies and 12 air discharges per hour) and obtained positive test results for 35% (14 samples positive/40 samples tested) of ICU samples and 12.5% (2/16) of GW samples. Air outlet swab samples also yielded positive test results, with positive rates of 66.7% (8/12) for ICUs and 8.3% (1/12) for GWs. These results confirm that SARS-CoV-2 aerosol exposure poses risks.

Furthermore, we found that rates of positivity differed by air sampling site, which reflects the distribution of virus-laden aerosols in the wards (Figure 2, panel A). Sampling sites were located near the air outlets (site 1), in patients' rooms (site 2), and (site 3). SARS-CoV-2 aerosol was detected at all 3 sampling sites; rates of positivity were 35.7% (5/14) near air outlets, 44.4% (8/18) in patients' rooms, and 12.5%

(1/8) in the doctors' office area. These findings indicate that virus-laden aerosols were mainly concentrated near and downstream from the patients. However, exposure risk was also present in the upstream area; on the basis of the positive detection result from site 3, the maximum transmission distance of SARS-CoV-2 aerosol might be 4 m. According to the aerosol monitoring results, we divided ICU workplaces into high-risk and low-risk areas (Figure 2, panel B). The high-risk area was the patient care and treatment area, where rate of positivity was 40.6% (13/32). The low-risk area was the doctors' office area, where rate of positivity was 12.5% (1/8).

In the GW, site 1 was located near the patients (Figure 2, panel C). Site 2 was located ≈2.5 m upstream of the air flow relative to the heads of patients. We also sampled the indoor air of the patient corridor. Only air samples from site 1 tested positive (18.2%, 2/11). The workplaces in the GW were also divided into 2 areas: a high-risk area inside the patient wards (rate of positivity 12.5, 2/16) and a low-risk area outside the wards (rate of positivity 0) (Figure 2, panel D).

## Conclusions

This study led to 3 conclusions. First, SARS-CoV-2 was widely distributed in the air and on object surfaces in both the ICU and GW, implying a potentially high infection risk for medical staff and other close contacts. Second, the environmental

**Table 2.** Results of testing for SARS-CoV-2 in general ward, Huoshenshan Hospital, Wuhan, China, 2020*

| Area, sample | Intense positive/weak positive/negative† | Rate of positivity, % | Average virus concentration‡ |
|---|---|---|---|
| Contaminated area | | | |
| Isolation ward | | | |
| Floor | 1/1/11 | 15.4 | $1.6 \times 10^4$ |
| Doorknob | 0/1/11 | 8.3 | $6.5 \times 10^2$ |
| Air outlet | 0/1/11 | 8.3 | $3.4 \times 10^3$ |
| Sickbed handrail | 0/0/12 | 0 | ND |
| Patient mask | 1/1/8 | 20 | $9.2 \times 10^3$ |
| Indoor air (sampling site 1 in Figure 2, panel C) | 0/2/9 | 18.2 | 0.68 |
| Indoor air (sampling site 2 in Figure 2, panel C) | 0/0/5 | 0 | ND |
| Patient corridor | | | |
| Floor | 0/0/10 | 0 | ND |
| Computer mouse or keyboard | 0/1/4 | 20 | $3.9 \times 10^3$ |
| Trash can | 0/0/8 | 0 | ND |
| Indoor air | 0/0/4 | 0 | ND |
| PPE | | | |
| Face shield of medical staff | 0/0/3 | 0 | ND |
| Sleeve cuff of medical staff | 0/0/3 | 0 | ND |
| Glove of medical staff | 0/0/3 | 0 | ND |
| Shoe sole of medical staff | 0/0/3 | 0 | ND |
| Subtotal | 2/7/105 | 7.9 | NA |
| Semicontaminated area | | | |
| Dressing Room 4 | | | |
| Floor | 0/0/5 | 0 | ND |
| Indoor air | 0/0/5 | 0 | ND |
| Doorknob | 0/0/3 | 0 | ND |
| Buffer Room 3 | | | |
| Floor | 0/0/5 | 0 | ND |
| Indoor air | 0/0/3 | 0 | ND |
| Doorknob | 0/0/3 | 0 | ND |
| Subtotal | 0/0/24 | 0 | NA |
| Clean area | | | |
| Dressing Rooms 1, 2, 3, and 5 | | | |
| Doorknob | 0/0/12 | 0 | ND |
| Floor | 0/0/12 | 0 | ND |
| Indoor air | 0/0/6 | 0 | ND |
| Buffer rooms 1 and 2 | | | |
| Doorknob | 0/0/6 | 0 | ND |
| Floor | 0/0/6 | 0 | ND |
| Indoor air | 0/0/4 | 0 | ND |
| Subtotal | 0/0/46 | 0 | NA |
| Total | 2/7/175 | 4.9 | NA |

*NA, not applicable; ND, not determined; PPE, personal protective equipment; SARS-CoV-2, severe acute respiratory syndrome coronavirus 2.
†Intense positive indicates a positive result for both open reading frame *1ab* gene and nucleoprotein gene of SARS-CoV-2; weak positive indicates a positive result for only 1 of the genes.
‡The average virus concentration of indoor air expressed as copies/L and of swab samples, as copies/sample.

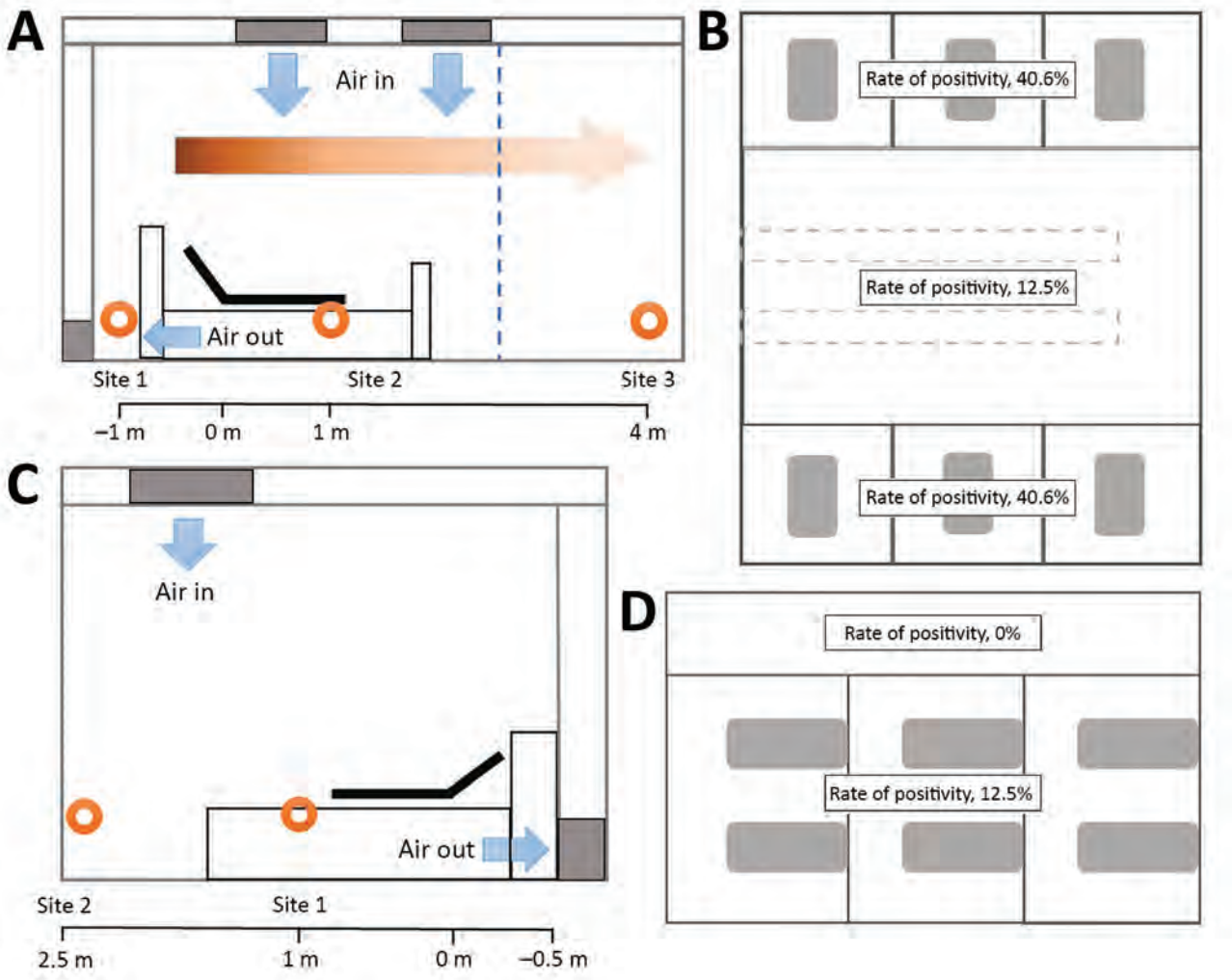


**Figure 2.** Spatial distribution of severe acute respiratory syndrome coronavirus 2 aerosols in isolation wards of the intensive care unit (ICU) and the general ward at Huoshenshan Hospital, Wuhan, China. A) The air sampling sites in the ICU were distributed in different regions: near the air outlet (site 1), near the patients (site 2), and around the doctors' office area (site 3). Orange circles represent sampling sites; blue arrows represent direction of the fresh air flow; and the graded orange arrow and scale bar indicate the horizontal distance from the patient's head. B) In terms of viral aerosol distribution, the space in the ICU was divided into 2 parts: a high-risk area with a 40.6% rate of virus positivity and a low-risk area with a 12.5% rate of virus positivity. C) The air sampling sites in the general ward were distributed in different regions around the patient (site 1), under the air inlet (site 2), and in the patient corridor. D) In terms of the viral aerosol distribution, the space in the general ward was divided into 2 parts: a high-risk area with a 12.5% rate of virus positivity and a low-risk area with a 0% rate of virus positivity.

contamination was greater in the ICU than in the GW; thus, stricter protective measures should be taken by medical staff working in the ICU. Third, the SARS-CoV-2 aerosol distribution characteristics in the ICU indicate that the transmission distance of SARS-CoV-2 might be 4 m.

As of March 30, no staff members at Huoshenshan Hospital had been infected with SARS-CoV-2, indicating that appropriate precautions could effectively prevent infection. In addition, our findings suggest that home isolation of persons with suspected COVID-19 might not be a good control strategy. Family members usually do not have personal protective equipment and lack professional training, which easily leads to familial cluster infections (*6*). During the outbreak, the government of China strove to the fullest extent possible to isolate all patients with suspected COVID-19 by actions such as constructing mobile cabin hospitals in Wuhan (*7*), which ensured that all patients with suspected disease were cared for by professional medical staff and that virus transmission was effectively cut off. As of the end of March, the SARS-COV-2 epidemic in China had been well controlled.

Our study has 2 limitations. First, the results of the nucleic acid test do not indicate the amount of viable virus. Second, for the unknown minimal infectious dose, the aerosol transmission distance cannot be strictly determined.

Overall, we found that the air and object surfaces in COVID-19 wards were widely contaminated by SARS-CoV-2. These findings can be used to improve safety practices.

This work was financially supported by the National Major Research & Development Program of China (2020YFC0840800).

## About the Author

Drs. Guo, Z.Y. Wang, and S.F. Zhang are researchers at the Academy of Military Medical Sciences, Academy of Military Sciences in Beijing, China. Their research interests are the detection, monitoring, and risk assessment of aerosolized pathogens.

## References

1. World Health Organization. Coronavirus disease 2019 (COVID-19) situation report-71 [cited 2020 Mar 30]. https://www.who.int/emergencies/diseases/novel-coronavirus-2019/situation-reports
2. Remuzzi A, Remuzzi G. COVID-19 and Italy: what next? Lancet. 2020 March 13 [Epub ahead of print]. https://doi.org/10.1016/S0140–6736(20):30627–9
3. Peng X, Xu X, Li Y, Cheng L, Zhou X, Ren B. Transmission routes of 2019-nCoV and controls in dental practice. Int J Oral Sci. 2020;12:9. https://doi.org/10.1038/s41368-020-0075-9
4. Ong SWX, Tan YK, Chia PY, Lee TH, Ng OT, Wong MSY, et al. Air, surface environmental, and personal protective equipment contamination by severe acute respiratory syndrome coronavirus 2 (SARS-CoV-2) from a symptomatic patient. JAMA. 2020 Mar 4 [Epub ahead of print]. https://doi.org/10.1001/jama.2020.3227
5. Zhang Y, Gong Y, Wang C, Liu W, Wang Z, Xia Z, et al. Rapid deployment of a mobile biosafety level-3 laboratory in Sierra Leone during the 2014 Ebola virus epidemic. PLoS Negl Trop Dis. 2017;11:e0005622. https://doi.org/10.1371/journal.pntd.0005622
6. Huang R, Xia J, Chen Y, Shan C, Wu C. A family cluster of SARS-CoV-2 infection involving 11 patients in Nanjing, China. Lancet Infect Dis. 2020 Feb 28 [Epub ahead of print]. https://doi.org/10.1016/S1473–3099(20)30147-X.
7. Health protection guideline of mobile cabin hospitals during novel coronavirus pneumonia (NPC) outbreak [in Chinese]. Zhonghua Yu Fang Yi Xue Za Zhi. 2020; 54:E006.

Address for correspondence: Wei Chen, Bing Lu, and Yu-Wei Gao, Academy of Military Medical Sciences, Academy of Military Sciences, 27 Taiping Rd, Haidian District, Beijing, China; email: cw0226@foxmail.com, lubing@nic.bmi.ac.cn, and gaoyuwei@gmail.com

# Inactivation of Severe Acute Respiratory Syndrome Coronavirus 2 by WHO-Recommended Hand Rub Formulations and Alcohols

Annika Kratzel, Daniel Todt, Philip V'kovski, Silvio Steiner, Mitra Gultom, Tran Thi Nhu Thao, Nadine Ebert, Melle Holwerda, Jörg Steinmann, Daniela Niemeyer, Ronald Dijkman, Günter Kampf, Christian Drosten, Eike Steinmann, Volker Thiel, Stephanie Pfaender

Infection control instructions call for use of alcohol-based hand rub solutions to inactivate severe acute respiratory syndrome coronavirus 2. We determined the virucidal activity of World Health Organization–recommended hand rub formulations, at full strength and multiple dilutions, and of the active ingredients. All disinfectants demonstrated efficient virus inactivation.

Severe acute respiratory syndrome coronavirus 2 (SARS-CoV-2) is the third highly pathogenic human coronavirus to cross the species barrier into the human population during the past 20 years (*1*–*3*). SARS-CoV-2 infection is associated with coronavirus disease (COVID-19), which is characterized by severe respiratory distress, fever, and cough and high rates of mortality, especially in older persons and those with underlying health conditions (*3*). The World Health Organization (WHO) declared SARS-CoV-2 a pandemic on March 11, 2020 (*4*), and by April 8, a total of 1,447,466 confirmed cases and 83,471 deaths from SARS-CoV-2 had been reported worldwide (*5*).

Human-to-human transmission of SARS-CoV-2 is efficient, and infected persons can transmit the virus even when they have no, or only mild, symptoms (*3*). Because no antiviral drugs or vaccines are available, virus containment and prevention of infection are the current highest priorities. To limit virus spread, effective hand hygiene is crucial. Therefore, easily available but efficient disinfectants are needed. WHO's guidelines for hand hygiene in healthcare suggest 2 alcohol-based formulations for hand sanitization to reduce the infectivity and spread of pathogens (*6*). WHO's recommendations are based on fast-acting, broad-spectrum microbicidal activity, along with accessibility and safety. The original WHO formulations failed to meet the efficacy requirements of European Norm 1500 in previous tests (*7*). However, Suchomel et al. (*8*) suggested modified versions with increased concentrations of ethanol: 80% (wt/wt) (85.5% [vol/vol]; formulation I), or isopropanol, 75% (wt/wt) (81.3% [vol/vol]; formulations II). Later, they complemented these by reducing the glycerol concentrations (*9*).

We previously showed that these modified WHO formulations were able to inactivate severe acute respiratory syndrome coronavirus (SARS-CoV) and Middle East respiratory syndrome coronavirus (MERS-CoV; *10*), which are related to SARS-CoV-2. Current recommendations to inactivate SARS-CoV-2 were translated from findings of other coronaviruses (*11*). To evaluate whether these alcohol-based disinfectants also effectively inactivate SARS-CoV-2, we tested different concentrations of the original and modified WHO formulations I and II (*6*,*9*), ethanol, and 2-propanol for virucidal activity.

Institute of Virology and Immunology, Bern and Mittelhäusern, Switzerland (A. Kratzel, P. V'kovski, S. Steiner, M. Gultom, T.T.N. Thao, N. Ebert, M. Holwerda, R. Dijkman, V. Thiel); University of Bern, Bern (A. Kratzel, P. V'kovski, S. Steiner, M. Gultom, T.T.N. Thao, N. Ebert, M. Holwerda, R. Dijkman, V. Thiel); Ruhr University Bochum, Germany (D. Todt, E. Steinmann, S. Pfaender); Institute of Medical Microbiology, University Hospital of Essen, Essen, Germany (J. Steinmann); Institute of Clinical Hygiene, Medical Microbiology and Infectiology General Hospital Nürnberg, Paracelsus Medical University, Nürnberg, Germany (J. Steinmann); Institute of Virology, Charité Berlin, Berlin, Germany (D. Niemeyer, C. Drosten); Institute for Hygiene and Environmental Medicine, University Medicine Greifswald, Greifswald, Germany (G. Kampf)

DOI: https://doi.org/10.3201/eid2607.200915

## The Study

We propagated SARS-CoV-2 (SARS-CoV-2/München-1.1/2020/929) on VeroE6 cells (kindly provided by M. Müller and C. Drosten; Charité, Berlin, Germany). We cultured VeroE6 cells in Dulbecco's modified minimal essential medium supplemented with 10% heat inactivated fetal bovine serum, 1% nonessential amino acids, 100 µg/mL of streptomycin and 100 IU/mL of penicillin, and 15 mMol of HEPES (Gibco; ThermoFisher, https://www.thermofisher.com).

Original WHO formulation I consists of 80% (vol/vol) ethanol, 1.45% (vol/vol) glycerol, and 0.125% (vol/vol) hydrogen peroxide. Original WHO formulation II consists of 75% (vol/vol) 2-propanol, 1.45% (vol/vol) glycerol, and 0.125% (vol/vol) hydrogen peroxide. The modified WHO formulation I used in our study consists of 80% (wt/wt) ethanol, 0.725% (vol/vol) glycerol, and 0.125% (vol/vol) hydrogen peroxide. The modified isopropyl-based WHO formulation II contains 75% (wt/wt) 2-propanol, 0.725% (vol/vol) glycerol, and 0.125% (vol/vol) hydrogen peroxide (*9*). We also prepared ethanol (CAS 64–17–5) and 2-propanol (CAS 67–63–0) in vol/vol dilutions for investigation.

We performed virucidal activity studies by using a quantitative suspension test with 30 s exposure time (*6*). In brief, we mixed 1 part virus suspension with 1 part organic load (0.3% bovine serum albumin as an interfering substance) and 8 parts disinfectant solution of different concentrations. After a 30 s exposure, we serially diluted samples and determined the 50% tissue culture infectious dose ($TCID_{50}$) per milliliter by using crystal violet staining and subsequently scoring the number of wells displaying cytopathic effects. We calculated $TCID_{50}$ by the Spearman-Kärber algorithm, as described (*12*). We monitored the cytotoxic effects of disinfectants by using crystal violet staining and optical analysis for altered density and morphology of the cellular monolayer in the absence of virus. We quantified cytotoxic effects analogous to the $TCID_{50}$/mL of the virus infectivity.

We determined dose-response curves as percent normalized virus inactivation versus percent log disinfectant concentration by nonlinear

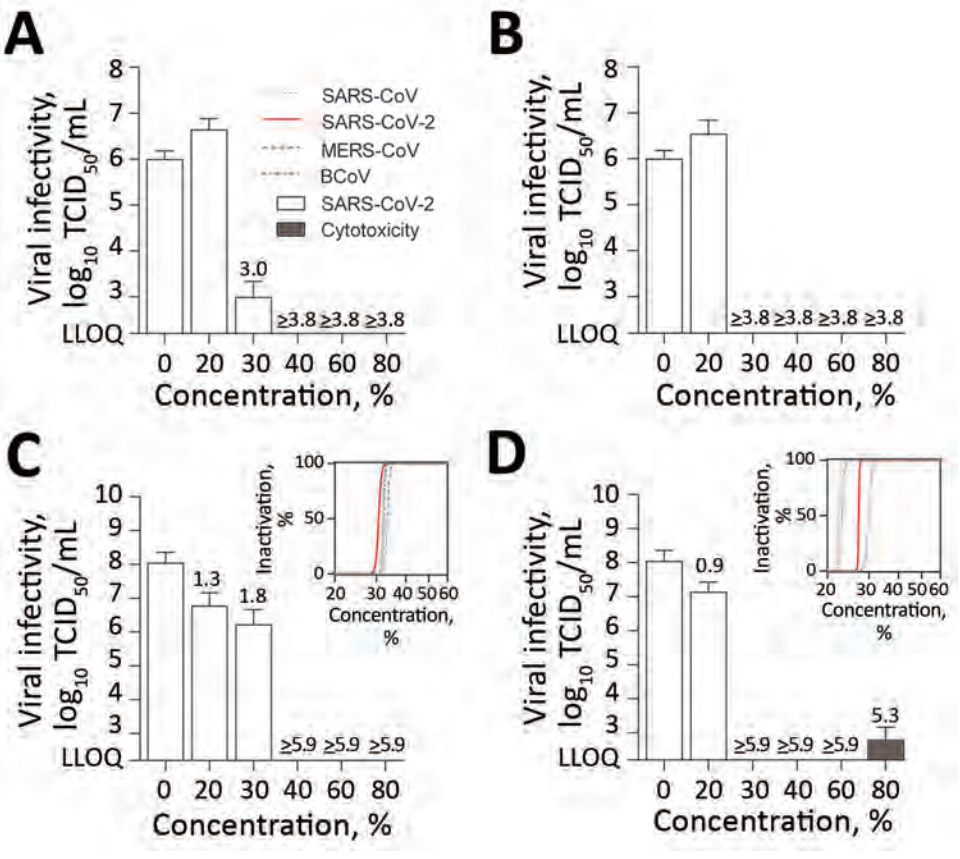


**Figure 1.** Virucidal activity of original and modified World Health Organization (WHO)–recommended hand rub formulations I and II for inactivating severe acute respiratory syndrome coronavirus 2 (SARS-CoV-2). The means of 3 independent experiments with SDs (error bars) and percentage of inactivation at different concentrations are shown. A) WHO original formulation I; B) WHO original formulation II; C) WHO modified formulation I; D) WHO modified formulation II. Insets in panels C and D show regression analyses of the inactivation of coronaviruses. Dark gray bar shows cytotoxic effects, calculated analogous to virus infectivity. Reduction factors are included above the bar. Dilutions of the WHO formulations ranged from 0–80% with an exposure time of 30 s. Viral titers are displayed as $TCID_{50}$/mL values. BCoV, bovine coronavirus; LLOQ, lower limit of quantification; MERS-CoV, Middle East respiratory syndrome coronavirus; SARS-CoV, severe acute respiratory syndrome coronavirus; SARS-CoV-2, severe acute respiratory syndrome coronavirus 2; $TCID_{50}$/mL, 50% tissue culture infectious dose.

regression using the robust fitting method on the normalized $TCID_{50}$ data implemented in Prism version 8.0.3 (GraphPad, https://www.graphpad.com). We plotted reference curves for SARS-CoV, MERS-CoV, and bovine CoV (BCoV) by using previously published data (*9*). BCoV is often used as surrogate for highly pathogenic human CoVs. We assessed the mean $TCID_{50}$ and standard deviations of means from 3 individual experiments. We identified outliers by using Grubb's test in Prism. We calculated reduction factors (RFs) for each treatment condition as follows:

$$RF = treatment - control = log_{10}\left(\frac{\sum_{i=1}^{n} x_i}{n}\right) - log_{10}\left(\frac{\sum_{j=1}^{m} x_j}{m}\right)$$

Our results showed that SARS-CoV-2 was highly susceptible to the original and the modified WHO formulations (Figure 1). The original and modified versions of formulation I efficiently inactivated the virus. The original formulation I of 80% (vol/vol) ethanol had an RF of ≥3.8 (Figure 1, panel A) and the modified formulation I of 80% (wt/wt) ethanol had an RF of ≥5.9 (Figure 1, panel C). Dilutions ≥40% were still effective (Figure 1, panels A and C). Subsequent regression analysis of modified formulation I revealed similar inactivation profiles compared with SARS-CoV, MERS-CoV, and BCoV. (Figure 1, panel C). The original and modified versions of formulation II also were effective. The original formulation II of 75% (vol/vol) 2-propanol had a $log_{10}$-reduction of ≥3.8 (Figure 1, panel B) and the modified formulation II of 75% (wt/wt) 2-propanol had a $log_{10}$-reduction of ≥5.9. Dilution ≥30% (vol/vol) also resulted in complete viral inactivation (Figure 1, panel D). Regression analysis of modified WHO formulation II showed the inactivation profile of SARS-CoV-2 was comparable to those of SARS-CoV, BCoV, and MERS-CoV (Figure 1, panel D).

We also investigated the susceptibility of SARS-CoV-2 against the active components of the WHO-recommended formulations, which are also the active ingredients of commercially available hand disinfectants. Ethanol (Figure 2, panel A) and 2-propanol (Figure 2, panel B) were able to reduce viral titers to background levels in 30 s with RFs of between 4.8 and ≥5.9. Furthermore, we noted that a concentration of ≥30% (vol/vol) ethanol or 2-propanol is sufficient for complete viral inactivation (Figure 2).

## Conclusions

We found that SARS-CoV-2 was efficiently inactivated by WHO-recommended formulations, supporting their use in healthcare systems and viral outbreaks. Of note, both the original and modified formulations were able to reduce viral titers to background level within 30 s. In addition, ethanol and 2-propanol were efficient in inactivating the virus in 30 s at a concentration of ≥30% (vol/vol). Alcohol constitutes the basis for many hand rubs routinely used in healthcare settings. One caveat of this study is the defined inactivation time of exactly 30 s, which is the time recommended but not routinely performed in practice. Our findings are crucial to minimize viral transmission and maximize virus inactivation in the current SARS-CoV-2 outbreak.

This article was preprinted at https://www.biorxiv.org/content/10.1101/2020.03.10.986711v1.

### Acknowledgments

We thank the members of Institute of Virology and Immunology, Bern, Switzerland and the Department for Molecular and Medical Virology, Ruhr University Bochum, Bochum, Germany for helpful suggestions and discussions.

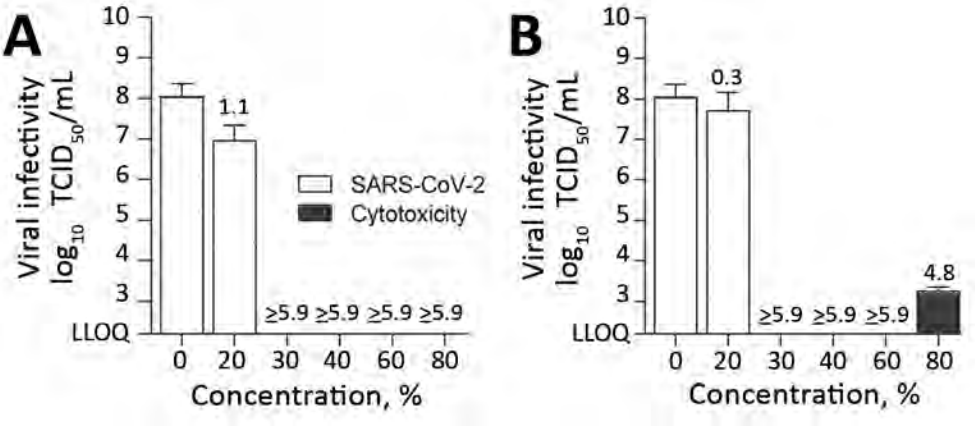


**Figure 2.** Effect of commercially available alcohols in inactivating SARS-CoV-2. The means of 3 independent experiments with SDs (error bars) are shown. A) Results for ethanol. B) Results for 2-propanol. Dark gray bar indicates cytotoxic effects, calculated analogous to virus infectivity. Reduction factors are included above the bar. The biocide concentrations ranged from 0–80% with an exposure time of 30 s. Viral titers are displayed as $TCID_{50}$/mL values. LLOQ, lower limit of quantification; SARS-CoV-2, severe acute respiratory syndrome coronavirus 2; $TCID_{50}$/mL, 50% tissue culture infectious dose.

This study was supported by the European Commission Marie Sklodowska-Curie Innovative Training Network Honours (grant agreement no. 721367), and by the Federal Ministry of Education and Research, Germany (grant no. 01KI1723A).

Ms. Kratzel is a PhD candidate affiliated with the Institute of Virology and Immunology, Bern and Mittelhäusern, Switzerland, the Department of Infectious Diseases and Pathobiology, Vetsuisse Faculty, University of Bern, Bern, Switzerland and the Graduate School for Cellular and Biomedical Sciences, University of Bern. Her research interests include coronaviruses.

## References

1. Drosten C, Günther S, Preiser W, van der Werf S, Brodt HR, Becker S, et al. Identification of a novel coronavirus in patients with severe acute respiratory syndrome. N Engl J Med. 2003;348:1967–76. https://doi.org/10.1056/NEJMoa030747
2. Zaki AM, van Boheemen S, Bestebroer TM, Osterhaus ADME, Fouchier RAM. Isolation of a novel coronavirus from a man with pneumonia in Saudi Arabia. N Engl J Med. 2012;367:1814–20. https://doi.org/10.1056/NEJMoa1211721
3. Lai C-C, Shih T-P, Ko W-C, Tang H-J, Hsueh P-R. Severe acute respiratory syndrome coronavirus 2 (SARS-CoV-2) and coronavirus disease-2019 (COVID-19): the epidemic and the challenges. Int J Antimicrob Agents. 2020;55:105924. https://doi.org/10.1016/j.ijantimicag.2020.105924
4. World Health Organization. WHO Director-General's opening remarks at the media briefing on COVID-19: 11 March 2020 [cited 2020 Apr 8] https://www.who.int/dg/speeches/detail/who-director-general-s-opening-remarks-at-the-media-briefing-on-covid-19---11-march-2020
5. Gardner L. Update January 31: modeling the spreading risk of 2019-nCoV. Johns Hopkins University Center for Systems Science and Engineering; 2020 Jan 31 [cited 2020 Mar 31] https://systems.jhu.edu/research/public-health/ncov-model-2
6. World Health Organization. WHO guidelines on hand hygiene in health care: first global patient safety challenge clean care is safer care. Geneva: the Organization; 2009 [cited 2020 Apr 08] https://apps.who.int/iris/bitstream/handle/10665/44102/9789241597906_eng.pdf
7. European Committee for Standardization. Chemical disinfectants and antiseptics. Hygienic hand disinfection. Test method and requirement. Brussels: the Committee; 2013 [cited 2020 Apr 8] https://standards.globalspec.com/std/1597777/EN%201500
8. Suchomel M, Kundi M, Allegranzi B, Pittet D, Rotter ML. Testing of the World Health Organization-recommended formulations for surgical hand preparation and proposals for increased efficacy. J Hosp Infect. 2011;79:115–8. https://doi.org/10.1016/j.jhin.2011.05.005
9. Suchomel M, Kundi M, Pittet D, Rotter ML. Modified World Health Organization hand rub formulations comply with European efficacy requirements for preoperative surgical hand preparations. Infect Control Hosp Epidemiol. 2013;34:245–50. https://doi.org/10.1086/669528
10. Siddharta A, Pfaender S, Vielle NJ, Dijkman R, Friesland M, Becker B, et al. Virucidal activity of World Health Organization-recommended formulations against enveloped viruses, including Zika, Ebola, and emerging coronaviruses. J Infect Dis. 2017;215:902–6. https://doi.org/10.1093/infdis/jix046
11. Kampf G, Todt D, Pfaender S, Steinmann E. Persistence of coronaviruses on inanimate surfaces and their inactivation with biocidal agents. J Hosp Infect. 2020;104:246–51. https://doi.org/10.1016/j.jhin.2020.01.022
12. George VG, Hierholzer JC, Ades EW. Cell culture. In: Virology methods manual. Mahy BWJ, Kangro HO, editors. Academic Press: London; 1996. p. 3–24.

Address for correspondence: Stephanie Pfaender, Department for Molecular and Medical Virology, Ruhr-Universität Bochum, Universitätsstrasse 150, 44801 Bochum, Germany; email: stephanie.pfaender@ruhr-uni-bochum.de

# Severe Acute Respiratory Syndrome Coronavirus 2 Infection among Returnees to Japan from Wuhan, China, 2020

Yuzo Arima,[1] Satoshi Kutsuna,[1] Tomoe Shimada, Motoi Suzuki, Tadaki Suzuki, Yusuke Kobayashi, Yuuki Tsuchihashi, Haruna Nakamura, Kaoru Matsumoto, Asuka Takeda, Keisuke Kadokura, Tetsuro Sato, Yuichiro Yahata, Noriko Nakajima, Minoru Tobiume, Ikuyo Takayama, Tsutomu Kageyama, Shinji Saito, Naganori Nao, Tamano Matsui, Tomimasa Sunagawa, Hideki Hasegawa, Kayoko Hayakawa, Shinya Tsuzuki, Yusuke Asai, Tetsuya Suzuki, Satoshi Ide, Keiji Nakamura, Yuki Moriyama, Noriko Kinoshita, Yutaro Akiyama, Yusuke Miyazato, Hidetoshi Nomoto, Takato Nakamoto, Masayuki Ota, Sho Saito, Masahiro Ishikane, Shinichiro Morioka, Kei Yamamoto, Mugen Ujiie, Mari Terada, Haruhito Sugiyama, Norihiro Kokudo, Norio Ohmagari, Makoto Ohnishi, Takaji Wakita, the COVID-19 Response Team

In early 2020, Japan repatriated 566 nationals from China. Universal laboratory testing and 14-day monitoring of returnees detected 12 cases of severe acute respiratory syndrome coronavirus 2 infection; initial screening results were negative for 5. Common outcomes were remaining asymptomatic (n = 4) and pneumonia (n = 6). Overall, screening performed poorly.

With the emergence of severe acute respiratory syndrome coronavirus 2 (SARS-CoV-2) in Wuhan, China, several countries, including Japan, repatriated their nationals (*1*–*3*). During January 29–31, 2020, a total of 566 Japanese nationals were repatriated via 3 chartered flights from Wuhan (206, 210, and 150 passengers). After passengers disembarked in Tokyo, Japan, quarantine officials assessed them for signs/symptoms (e.g., fever, respiratory illness) of coronavirus disease (COVID-19) (*4*). A total of 28 symptomatic passengers were transferred to select hospitals for isolation. The remaining 538 were transported to a designated hospital, where another 35 were found to be symptomatic and were hospitalized there or transferred to other hospitals, leaving 503 asymptomatic persons for observation in quarantine (Figure).

Author affiliations: National Institute of Infectious Diseases, Tokyo, Japan (Y. Arima, T. Shimada, M. Suzuki, T. Suzuki, Y. Kobayashi, Y. Tsuchihashi, H. Nakamura, K. Matsumoto, A. Takeda, K. Kadokura, T. Sato, Y. Yahata, N. Nakajima, M. Tobiume, I. Takayama, T. Kageyama, S. Saito, N. Nao, T. Matsui, T. Sunagawa, H. Hasegawa, M. Ohnishi, T. Wakita); National Center for Global Health and Medicine, Tokyo (S. Kutsuna, K. Hayakawa, S. Tsuzuki, Y. Asai, T. Suzuki, S. Ide, K. Nakamura, Y. Moriyama, N. Kinoshita, Y. Akiyama, Y. Miyazato, H. Nomoto, T. Nakamoto, M. Ota, S. Saito, M. Ishikane, S. Morioka, K. Yamamoto, M. Ujiie, M. Terada, H. Sugiyama, N. Kokudo, N. Ohmagari)

DOI: https://doi.org/10.3201/eid2607.200994

## The Study

We conducted day 1 entry screening by testing oropharyngeal swab samples collected from all 566 returnees at the hospitals to which they were initially transported for SARS-CoV-2 (*4*); all tests were based on the real-time reverse transcription PCR developed by the National Institute of Infectious Diseases (*5*). Hospitalized patients in isolation and asymptomatic returnees in quarantine were monitored daily for 14 days. If any signs/symptoms developed in a quarantined person, that person was transported to a designated hospital and oropharyngeal swab samples were collected for testing. We conducted exit screening for quarantined persons who remained illness-free by collecting oropharyngeal swab samples on day 14. The National Institute of Infectious Diseases Ethics Committee approved the study (registration no. 1096), and all 566 returnees who provided specimens gave written informed consent.

Among the 63 passengers who were symptomatic at entry screening, 2 (3.2%) were positive by PCR

[1]These authors contributed equally to this article.

(Figure); test results were subsequently positive for 2 more. For 1 of these patients, pneumonia was diagnosed on day 1 and a sputum sample was positive on day 3; the other patient had fever and cough on day 1, pneumonia diagnosed on day 2, and a positive oropharyngeal swab sample on day 6. Excluding 1 patient who remained hospitalized for stroke, the remaining 58 patients were transferred to designated quarantine facilities after confirmation of good health and negative PCR results; all 58 remained asymptomatic after discharge, and PCR results were negative at exit screening.

For the 503 asymptomatic/subclinical passengers, entry-screening PCR results were positive for 5 (1.0%) (Figure); 3 remained asymptomatic, but mild signs/symptoms (fever, headache, sore throat) developed for 2 persons (1 on day 2, 1 on day 4). Of the remaining 498 persons with negative PCR results, 484 were quarantined at designated facilities and 14 at home. During quarantine, fever developed in 1 facility-quarantined and 1 home-quarantined person on day 10; both were confirmed positive by PCR, and pneumonia subsequently developed in both. The facility-quarantined case-patient was in a single room; no other person from this facility acquired COVID-19 or had a positive test result at exit screening. One person who remained asymptomatic had a positive test result at exit screening. Exit-screening results are pending for the patient hospitalized for stroke and the remaining 13 home-quarantined persons.

Among the 566 returnees, 12 cases of SARS-CoV-2 infection were detected; 540/541 facility-quarantined persons were confirmed negative by PCR performed on days 1 and 14 (197/197, 199/199, and 144/145 for the 3 flights). Entry screening detected 7 infections, for an infection point prevalence of 1.2%; infection period prevalence was 2.2% (12/552 returnees with complete follow-up). Despite universal testing, entry screening captured only 7/12 cases (58.3% sensitivity).

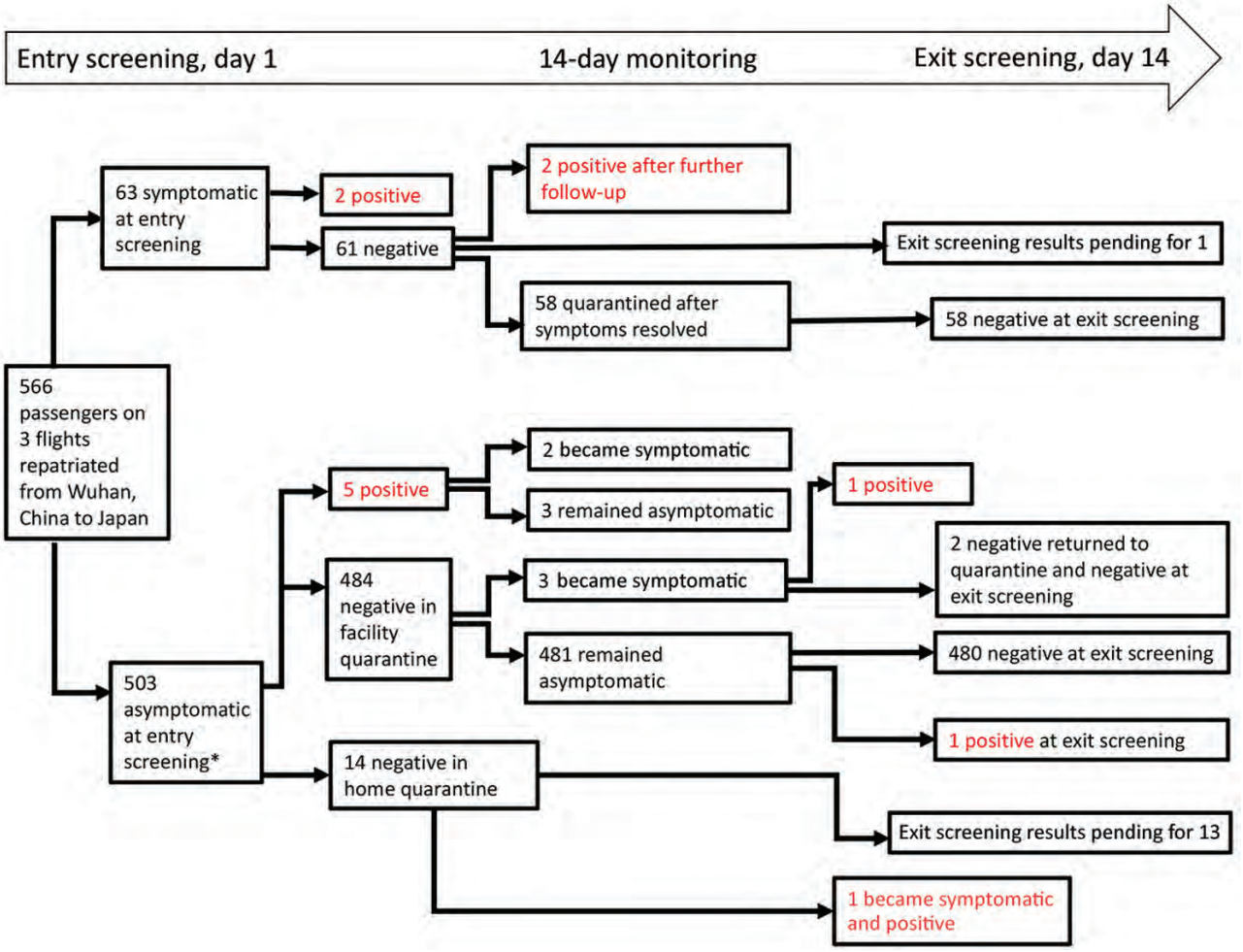


**Figure.** Results of testing 566 Japanese returnees from Wuhan, China, for severe acute respiratory syndrome coronavirus 2 by real-time reverse transcription PCR, January–February 2020. *Two persons were sampled on day 3, when they provided informed consent.

**Table.** Distribution of severe acute respiratory syndrome coronoavirus 2 infections and clinical outcomes, by age group, among 566 Japanese returnees from Wuhan, China, January–February 2020

| Age group, y | No. returnees* | No. (%) infected† | Outcome | | | |
|---|---|---|---|---|---|---|
| | | | No. asymptomatic | No. with mild illness | No. with pneumonia | No. deaths |
| <10 | 6 | 0 | 0 | 0 | 0 | 0 |
| 10–19 | 4 | 0 | 0 | 0 | 0 | 0 |
| 20–29 | 90 | 0 | 0 | 0 | 0 | 0 |
| 30–39 | 138 | 2 (1.4) | 2 | 0 | 0 | 0 |
| 40–49 | 168 | 4 (2.4) | 0 | 1 | 3 | 0 |
| 50–59 | 119 | 5 (4.2) | 1 | 1 | 3 | 0 |
| 60–69 | 26 | 1 (3.8) | 1 | 0 | 0 | 0 |
| 70–79 | 1 | 0 | 0 | 0 | 0 | 0 |

*Day-14 exit-screening test results pending for 14 persons.
†Testing by reverse transcription PCR.

Although screening symptomatic passengers (3.2%) was more efficient than screening all passengers (1.2%), screening only symptomatic passengers missed 5/7 prevalent infections at entry. Among symptomatic passengers, with 2 initially negative persons subsequently testing positive, entry-screening sensitivity was 2/4 (50%). Among asymptomatic passengers, with 3 initially negative persons subsequently testing positive, entry-screening sensitivity was 5/8 (62.5%).

## Conclusions

Testing all returnees—with follow-up for disease onset and course—enabled us to evaluate the spectrum of severity for SARS-CoV-2 infections (Table). From least to most severe, 4 patients experienced asymptomatic infection, 2 mild illness, and 6 pneumonia. Prospective monitoring proved essential because of the 7 prevalent infections at entry, 5 were asymptomatic, 1 mild, and 1 pneumonia. Even with potential underascertainment of asymptomatic cases because of a lack of serologic assessment (*6*,*7*) (i.e., interval-censoring during screening tests), it is noteworthy that 4/12 persons with infections were asymptomatic. Although numbers are small, severity seemed to be age dependent (Table). No infections were detected among the 100 persons <30 years of age; of the 2 infections detected among the 138 persons 30–39 years of age, both persons were asymptomatic. Although no person in this study died, only 1 was >69 years of age. Regarding sex, excluding 1 returnee for whom sex was unknown and 14 for whom exit-screening results are pending, of the remaining 551 returnees, 9 (1.8%) of the 506 male passengers (2 asymptomatic, 2 mild, 5 pneumonia) and 3 (6.7%) of the 45 female passengers (2 asymptomatic, 1 pneumonia) were infected.

Our findings have public health implications. As recently reported (*1*), we found that symptom-based screening performed poorly, missing asymptomatic and presymptomatic cases. Even with universal screening, nearly half of cases were missed. Because an asymptomatic case was detected at exit screening, limiting testing of quarantined persons to those with signs/symptoms would have missed such a case; with exit-screening results pending for 14 returnees, sensitivity could be lower. The poor sensitivity of single-point testing highlights the challenges of detecting SARS-CoV-2 infections.

The potentially long incubation period of COVID-19 was consistent with that recently reported (*8*,*9*) and contributed to the large proportion of missed cases. Active daily monitoring ensured that specific illness-onset times were captured, protected from the limitations associated with patient recall of symptom onset (*10*). Although exposure to SARS-CoV-2 occurred at some time before quarantine (i.e., left-censore d), our setting enabled us to estimate the minimum incubation period for each incident symptomatic case by taking the return date as the exposure time. Determining the specific exposure time can be difficult and is conditional according to the definition of contact. Given such qualifications, a conservative minimum incubation period of 10 days obtained prospectively in a clean quarantine setting, without recall or assumptions regarding transmission modes, is noteworthy.

Testing and follow-up of all returnees provided valuable information about the spectrum of SARS-CoV-2 infection. Most reported data have been from medically attended patients, skewed toward symptomatic patients and more severe cases, limiting our knowledge of the clinical spectrum of infection (*6*,*11*). In our setting, we could remove the influence of patients' health-seeking behaviors and clinicians' diagnostic practices and found that 4/12 case-patients were asymptomatic. At the same time, of the 8 case-patients who experienced symptoms, pneumonia developed in 6. Our findings were also consistent with the reported age-dependent nature

of COVID-19 (*2*,*12*–*14*); infection and clinical attack rates were lower among younger persons. Shedding light on the severity pyramid among those infected—not only among those who sought care—provides an evidence base for risk communication, healthcare planning, and public health response. Combined with reports suggesting transmissibility of SARS-CoV-2 from asymptomatic/subclinical case-patients (*1*,*10*,*15*,*16*), our findings suggest that controlling COVID-19 through the usual tools of syndrome-based surveillance and contact tracing alone may be difficult.

When confronted with an emerging pathogen, researchers can generate critical epidemiologic information by studying quarantined populations. As with the First Few X study (*7*), our design is protected from the usual biases of passively reported surveillance data. Aggregating high-quality data from these types of investigations can build a larger severity pyramid, enabling reliable estimation of various severity measures (e.g., symptomatic proportion of infected case-patients, case severity proportion among those who are symptomatic). We recommend using similar assessments to help elucidate the epidemiology of SARS-CoV-2 and inform public health response.

Members of the COVID-19 response team: Akira Ainai, Minetaro Arita, Tomoko Arita, Hideki Asanuma, Seiichiro Fujisaki, Itsuki Hamamoto, Yuichi Harada, Shinichiro Hirai, Shun Iida, Yoshiyuki Ishii, Shigeyuki Itamura, Naoko Iwata-Yoshikawa, Takayuki Kanno, Harutaka Katano, Fumihiro Kato, Hirofumi Kato, Hiroshi Katoh, Minoru Kidokoro, Noriko Kishida, Osamu Kotani, Toru Kubota, Iwao Kukimoto, Madoka Kuramitsu, Tomoko Kuwahara, Shutoku Matsuyama, Seiichiro Mori, Yoshio Mori, Koichi Murakami, Tsutomu Murakami, Noriyo Nagata, Seishiro Naito, Kazuya Nakamura, Yuichiro Nakatsu, Mina Nakauchi, Eri Nobusawa, Kiyoko Okamoto, Kazu Okuma, Noriyuki Otsuki, Masumichi Saito, Koji Sakai, Kouji Sakai, Masafumi Sakata, Kaori Sano, Kayoko Sato, Yuko Sato, Fumio Seki, Noriko Shimasaki, Hiroyuki Shimizu, Masayuki Shirakura, Kazuya Shirato, Kenji Someya, Ryosuke Suzuki, Yasushi Suzuki, Maino Tahara, Hitoshi Takahashi, Kenta Takahashi, Emi Takashita, Makoto Takeda, Takamasa Takeuchi, Michiko Tanaka, Kenta Tezuka, Kenzo Tokunaga, Yuji Wada, Kana Watanabe, Shinji Watanabe, Aya Zamoto-Niikura, (National Institute of Infectious Diseases); Tomoko Date (National Center for Global Health and Medicine); Takashi Chiba, Mami Nagashima, Kenji Sadamasu, Kazuhisa Yoshimura (Tokyo Metropolitan Institute of Public Health); Manami Yanagawa (Ministry of Health, Labour and Welfare).

## Acknowledgments

We acknowledge the dedicated work of the frontline clinicians and the staff at the quarantine facilities, the workers at the local public health centers and prefectural and municipal public health institutes, and the Japan Ministry of Health, Labour and Welfare.

We also thank the quarantined returnees for their patience and participation.

This study was supported in part by a grant-in-aid from the Japan Agency for Medical Research and Development (grant nos. JP19fk0108104 and JP19fk0108110).

Dr. Arima is an affiliate researcher at the Infectious Disease Surveillance Center, National Institute of Infectious Diseases in Tokyo, Japan. His research interests include infectious disease epidemiology and surveillance in the context of public health practice.

## References

1. Hoehl S, Rabenau H, Berger A, Kortenbusch M, Cinatl J, Bojkova D, et al. Evidence of SARS-CoV-2 infection in returning travelers from Wuhan, China. N Engl J Med. 2020;382:1278–80. https://doi.org/10.1056/NEJMc2001899
2. Jernigan DB; CDC COVID-19 Response Team. Update: public health response to the coronavirus disease 2019 outbreak—United States, February 24, 2020. MMWR Morb Mortal Wkly Rep. 2020;69:216–9. https://doi.org/10.15585/mmwr.mm6908e1
3. Ng OT, Marimuthu K, Chia PY, Koh V, Chiew CJ, De Wang L, et al. SARS-CoV-2 infection among travelers returning from Wuhan, China. N Engl J Med. 2020;382:1476–8. https://doi.org/10.1056/NEJMc2003100
4. Kutsuna S, Suzuki T, Hayakawa K, Tsuzuki S, Asai Y, Suzuki T, et al. SARS-CoV-2 screening test for Japanese returnees 1 from Wuhan, China. 2 January 2020. Open Forum Infectious Diseases. In press 2020.
5. Shirato K, Nao N, Katano H, Takayama I, Saito S, Kato F, et al. Development of genetic diagnostic methods for novel coronavirus 2019 (nCoV-2019) in Japan. Jpn J Infect Dis. 2020 Feb 18 [Epub ahead of print]. https://doi.org/10.7883/yoken.JJID.2020.061
6. Lipsitch M, Swerdlow DL, Finelli L. Defining the epidemiology of COVID-19–studies needed. N Engl J Med. 2020;382:1194–6. https://doi.org/10.1056/NEJMp2002125
7. World Health Organization. The First Few X (FFX) cases and contact investigation protocol for 2019-novel coronavirus (2019-nCoV) infection [cited 2020 Mar 23]. https://www.who.int/publications-detail/the-first-few-x-(ffx)-cases-and-contact-investigation-protocol-for-2019-novel-coronavirus-(2019-ncov)-infection
8. Morens DM, Daszak P, Taubenberger JK. Escaping Pandora's box—another novel coronavirus. N Engl J Med. 2020;382:1293–5. https://doi.org/10.1056/NEJMp2002106
9. Backer JA, Klinkenberg D, Wallinga J. Incubation period of 2019 novel coronavirus (2019-nCoV) infections among travellers from Wuhan, China, 20–28 January 2020. Euro Surveill. 2020;25. https://doi.org/10.2807/1560-7917.ES.2020.25.5.2000062
10. Tong ZD, Tang A, Li KF, Li P, Wang HL, Yi JP, et al. Potential presymptomatic transmission of SARS-CoV-2, Zhejiang Province, China, 2020. Emerg Infect Dis. 2020;26:1050–2. https://doi.org/10.3201/eid2605.200198

11. Munster VJ, Koopmans M, van Doremalen N, van Riel D, de Wit E. A novel coronavirus emerging in China—key questions for impact assessment. N Engl J Med. 2020;382:692–4. https://doi.org/10.1056/NEJMp2000929
12. World Health Organization. Report of the WHO-China Joint Mission on Coronavirus Disease 2019 (COVID-19) [cited 2020 Mar 23]. https://www.who.int/docs/default-source/coronaviruse/who-china-joint-mission-on-covid-19-final-report.pdf
13. Li Q, Guan X, Wu P, Wang X, Zhou L, Tong Y, et al. Early transmission dynamics in Wuhan, China, of novel coronavirus-infected pneumonia. N Engl J Med. 2020;382:1199–207. https://doi.org/10.1056/NEJMoa2001316
14. Guan WJ, Ni ZY, Hu Y, Liang WH, Ou CQ, He JX, et al.; China Medical Treatment Expert Group for COVID-19. Clinical characteristics of coronavirus disease 2019 in China. N Engl J Med. 2020 Feb 28 [Epub ahead of print]. https://doi.org/10.1056/NEJMoa2002032
15. Zou L, Ruan F, Huang M, Liang L, Huang H, Hong Z, et al. SARS-CoV-2 viral load in upper respiratory specimens of infected patients. N Engl J Med. 2020;382:1177–9.
16. Rothe C, Schunk M, Sothmann P, Bretzel G, Froeschl G, Wallrauch C, et al. Transmission of 2019-nCoV infection from an asymptomatic contact in Germany. N Engl J Med. 2020;382:970–1.

Address for correspondence: Yuzo Arima, Infectious Disease Surveillance Center, National Institute of Infectious Diseases, 1-23-1 Toyama, Shinjuku-ku, Tokyo 162-8640, Japan; email arima@niid.go.jp

# A Critique of Coronavirus

Elana R. Osen

Why did the quiet descend?
Does this plague not know
that apocalypses come with fanfare,
wails of lamentation,
howls of wayward dogs,
explosive blasts?
Or, maybe, silence.
Just shop-window glass crunching underfoot
puncturing the eerie nothing.
Not quiet.
Never quiet.

Why does the sun still shine?
Can it not see what transpires
from its lofty throne
above the Earth?
Read the room, sun.
Now's the time for greyscale filter.
Or, maybe, an eclipse.
One last blinding ray of blazing flare
to scorch the land,
to boil the sea,
to serve up *des hommes brûlés*
to whichever vengeful deity
dines with us tonight.
Not sunshine.
Never sunshine.

Why can I smell the tulips?
I thought the virus
wiped olfaction from our
paltry list of powers?
Or, maybe, smoke.
You know, from voracious flames
feasting on our foliage and flesh,
the smog of industry,
of mushroom clouds.
Why does that not sting my nostrils?
Not flowers.
Never flowers.

Why does life go on inexorably?
Is Ragnarök not supposed to happen
around now?
Where are the horsemen?
Where are the double gates of Paradise?
What a lame apocalypse:
we've been sold a lemon.
Or, maybe, pop culture eschatology
isn't all it is cracked up to be.
I thought the zombies would be roaming
all my haunts
by now.
Not life.
Never life.

## About the Author

Miss Osen is a Specialty Registrar in the ENT Department at St George's University Hospitals NHS Foundation Trust, London. Her professional interests include ENT and history of medicine; extracurricular interests include composing bleak poetry and flash/sudden fiction.

Address for correspondence: Elana R. Osen, ENT Department, St George's University Hospitals NHS Foundation Trust, Blackshaw Rd, Tooting, London, SW17 0QT, UK; email: elana.osen@doctors.org.uk

Author affiliation: St George's University Hospitals National Health Service Foundation Trust, London, UK

DOI: https://doi.org/10.3201/eid2607.201426

# Zika Virus Detection with 2013 Serosurvey, Mombasa, Kenya

Elizabeth Hunsperger, Dennis Odhiambo, Albina Makio, Moshe Alando, Melvin Ochieng, Victor Omballa, Peninah Munyua, Godfrey Bigogo, M. Kariuki Njenga, Marc-Alain Widdowson

Author affiliations: US Centers for Disease Control and Prevention, Nairobi, Kenya (E. Hunsperger, P. Munyua, M.-A. Widdowson); Kenya Medical Research Institute, Nairobi, Kenya (D. Odhiambo, A. Makio, M. Alando, M. Ochieng, V. Omballa, G. Bigogo); Washington State University, Pullman, Washington, USA (M.K. Njenga); Institute of Tropical Medicine, Antwerp, Belgium (M.-A. Widdowson)

DOI: https://doi.org/10.3201/eid2607.191363

Acute Zika virus (ZIKV) infection has not been confirmed in Kenya. In 2018, we used specimens collected in a 2013 dengue serosurvey study in Mombasa to test for ZIKV IgM. We confirmed specific ZIKV IgM positivity in 5 persons. These results suggest recent ZIKV transmission in the coastal region of Kenya.

Zika virus (ZIKV), an arbovirus belonging to the family *Flaviviridae*, was initially isolated in 1947 from the serum of a pyrexic sentinel rhesus macaque in the canopy of the Zika Forest in Uganda (*1*). In 1970, ZIKV antibodies were reported in humans in Kenya, using immunoassays with limited sensitivity and specificity (*2*); since then, only past infections have been reported (*3*,*4*).

In 2015, the emergence of ZIKV in the Americas (*5*) raised the possibility that ZIKV infections were also occurring in Kenya but were undetected due to mild or asymptomatic infections and rudimentary birth defect surveillance. In 2016, Cape Verde and, in 2017, Angola reported ZIKV outbreaks associated with microcephaly. Genome sequencing from Angola identified the similarity of the Asian lineage of ZIKV to the American strain (*6*); this evidence implies that the African lineage may be less likely to cause microcephaly, thus explaining the few reported number of ZIKV-associated microcephaly cases in Africa (*7*).

To understand prior transmission of ZIKV in Kenya, in 2018, we used specimens collected in 2013 for a dengue serosurvey from Mombasa amidst a dengue outbreak. During May 3–11, 2013, serum specimens were collected from 1,500 consenting household members in 986 randomly selected households (*8*). Specimens were tested for dengue virus (DENV) by real-time reverse transcription PCR (rRT-PCR) and DENV IgM ELISA (InBios International, Inc., https://inbios.com). Concurrent with this serosurvey, hospital surveillance of suspected dengue patients was established (*8*).

For our study, we used only the DENV-negative serum specimens and tested them for ZIKV by Centers for Disease Control and Prevention rRT-PCR and ZIKV IgM antibody capture ELISA (MAC ELISA). A ZIKV MAC ELISA specimen with a positive-to-negative ratio ≥3.00 was positive and a ratio of 2–2.99 was equivocal. We confirmed all positive specimens with 90% plaque reduction neutralization test ($PRNT_{90}$) against ZIKV strain MR766 (African lineage) and DENV (ChimeraVax; Sanofi Pasteur, https://www.sanofi.com) (*9*). We defined recent ZIKV infection by a positive result in the ZIKV MAC ELISA and a $PRNT_{90}$ titer of ZIKV that was 4-fold higher than the titer of DENV. The institutional review board at US Centers for Disease Control and Prevention and Kenya Medical Research Institute Scientific Ethics Review Unit approved the study.

We identified a total of 745 DENV-negative persons from the dengue serosurvey (n = 704) and hospital surveillance (n = 41); median age was 28 (range 0–94) years. None were positive by ZIKV rRT-PCR. Thirty-four (4.6%) were positive by ZIKV MAC ELISA, 7 captured in hospital surveillance; 24 (3.2%) were equivocal and 687 (92.2%) negative. Of the 34 ZIKV MAC ELISA positives, the ZIKV $PRNT_{90}$ assay confirmed 5 (15.1%, 4 from serosurvey and 1 hospital) as ZIKV, 7 (21.2%) as DENV, 3 (9.1%) as cross-reactive to both viruses, and 18 (54.5%) as negative for ZIKV and DENV; 1 (2.9%) could not be confirmed due to insufficient sample (Table). Of the 5 ZIKV MAC ELISA–positive patients confirmed by ZIKV $PRNT_{90}$, median age was 57 (range 50–70) years.

We identified 5 persons sampled in 2013 who were positive for ZIKV IgM and confirmed by $PRNT_{90}$. Of note, the positive participants (median age 57 years) were older than the sample group tested (median age 29 years). The level of transmission of ZIKV in Kenya is unknown, although Kenya has the competent vector (*Aedes aegypti* mosquitoes), and parts of Kenya are ecologically similar to the Zika forest (*1*). ZIKV has not been detected in Kenya despite recent intensive follow-up of pregnant women in coastal Kenya (*10*). Our study suggests that ZIKV may circulate in Mombasa and cause asymptomatic disease not captured in hospital surveillance systems. In addition, severely ill ZIKV patients might not have been identified from the original dengue study because it only captured clinical endpoints related to severe dengue.

**Table.** Test results for 16 participants in a 2013 serosurvey in Kenya whose samples were positive for ZIKV by testing conducted in 2018*

| Participant no. | Age, y | CDC ZIKV MAC ELISA P/N ratio (IgM) | ZIKV $PRNT_{90}$ titer | DENV $PRNT_{90}$ titer | Participant type | Final interpretation of case |
|---|---|---|---|---|---|---|
| 2 | 63 | 3.56 | 1:20 | <1:20 | Serosurvey | ZIKV |
| 3 | 50 | 10.00 | >1:320 | <1:20 | Serosurvey | ZIKV |
| 5 | 70 | 3.17 | 1:20 | <1:20 | Serosurvey | ZIKV |
| 10 | NA | 3.51 | 1:20 | <1:20 | Hospital | ZIKV |
| 31 | 51 | 5.50 | >1:320 | 1:20 | Serosurvey | ZIKV |
| 4 | 45 | 3.26 | <1:20 | 1:20 | Serosurvey | DENV |
| 7 | 36 | 8.65 | 1:20 | 1:320 | Serosurvey | DENV |
| 20 | 58 | 13.18 | 1:20 | 1:320 | Serosurvey | DENV |
| 25 | 45 | 3.70 | 1:20 | >1:320 | Serosurvey | DENV |
| 26 | 27 | 5.00 | 1:80 | >1:320 | Serosurvey | DENV |
| 27 | 42 | 3.20 | 1:80 | 1:320 | Serosurvey | DENV |
| 33 | 30 | 10.70 | 1:20 | 1:80 | Serosurvey | DENV |
| 1 | 32 | 4.49 | 1:20 | 1:20 | Serosurvey | Cross-reactive |
| 9 | 27 | 3.82 | 1:20 | 1:20 | Serosurvey | Cross-reactive |
| 30 | 58 | 3.20 | >1:320 | >1:320 | Serosurvey | Cross-reactive |
| 6 | 41 | 16.35 | 1:20 | ND | Serosurvey | Inconclusive |

*CDC, Centers for Disease Control and Prevention; DENV, dengue virus; MAC, IgM antibody capture; NA, not available; ND, not done due to insufficient specimen; $PRNT_{90}$, plaque reduction neutralization test 90%; ZIKV, Zika virus.

We found 1 participant positive by ZIKV MAC ELISA but negative by ZIKV and DENV $PRNT_{90}$, suggesting the presence of another co-circulating cross-reactive flavivirus in this region of Kenya (e.g., West Nile virus). This finding merits further investigation to determine all circulating flaviviruses in Mombasa. ZIKV transmission season in Kenya most likely coincides with other arboviruses that share the same vector. Of interest, titers of neutralizing antibodies against ZIKV were low for 3 of the 5 positive participants (1:20 $PRNT_{90}$ titer), typically observed in acute infections (<10 days after onset of illness). Two participants had high neutralization titers (>1:320), suggesting recent infection (within the previous 90 days).

Our study had some limitations. It was conducted in 2018, so specimens had been archived for 5 years. We also had incomplete demographic and clinical data and could not discount concurrent DENV infections. Finally, we might have underestimated ZIKV positives because of weak neutralization by IgM.

In conclusion, ZIKV may have circulated at low levels in Kenya in 2013. More research is needed to evaluate current ZIKV circulation and characterize other co-circulating flaviviruses. Enhanced surveillance systems, including for microcephaly and other birth defects, could capture ZIKV patients and determine the epidemiology of ZIKV African lineage in this country.

This research was made possible through support provided by the Office of Infectious Disease, Bureau for Global Health, US Agency for International Development, under the terms of an Interagency Agreement with CDC.

## About the Author

Dr. Hunsperger is a researcher with the US Centers for Disease Control and Prevention, Nairobi, Kenya. Her research interest is vectorborne diseases.

## References

1. Dick GW, Kitchen SF, Haddow AJ. Zika virus. I. Isolations and serological specificity. Trans R Soc Trop Med Hyg. 1952;46:509–20. http://dx.doi.org/10.1016/0035-9203(52)90042-4
2. Geser A, Henderson BE, Christensen S. A multipurpose serological survey in Kenya. 2. Results of arbovirus serological tests. Bull World Health Organ. 1970;43:539–52.
3. Chepkorir E, Tchouassi DP, Konongoi SL, Lutomiah J, Tigoi C, Irura Z, et al. Serological evidence of flavivirus circulation in human populations in northern Kenya: an assessment of disease risk 2016–2017. Virol J. 2019;16:65. http://dx.doi.org/10.1186/s12985-019-1176-y
4. Kisuya B, Masika MM, Bahizire E, Oyugi JO. Seroprevalence of Zika virus in selected regions in Kenya. Trans R Soc Trop Med Hyg. 2019;113:735–9. http://dx.doi.org/10.1093/trstmh/trz077
5. de Oliveira WK, de França GVA, Carmo EH, Duncan BB, de Souza Kuchenbecker R, Schmidt MI. Infection-related microcephaly after the 2015 and 2016 Zika virus outbreaks in Brazil: a surveillance-based analysis. Lancet. 2017;390:861–70. http://dx.doi.org/10.1016/S0140-6736(17)31368-5
6. Hill SC, Vasconcelos J, Neto Z, Jandondo D, Zé-Zé L, Aguiar RS, et al. Emergence of the Asian lineage of Zika virus in Angola: an outbreak investigation. Lancet Infect Dis. 2019;19:1138–47. http://dx.doi.org/10.1016/S1473-3099(19)30293-2
7. Sheridan MA, Yunusov D, Balaraman V, Alexenko AP, Yabe S, Verjovski-Almeida S, et al. Vulnerability of primitive human placental trophoblast to Zika virus. Proc Natl Acad Sci U S A. 2017;114:E1587–96. http://dx.doi.org/10.1073/pnas.1616097114
8. Ellis EM, Neatherlin JC, Delorey M, Ochieng M, Mohamed AH, Mogeni DO, et al. A household serosurvey to estimate the magnitude of a dengue outbreak in Mombasa, Kenya, 2013. PLoS Negl Trop Dis. 2015;9:e0003733. http://dx.doi.org/10.1371/journal.pntd.0003733

9. Johnson BW, Kosoy O, Hunsperger E, Beltran M, Delorey M, Guirakhoo F, et al. Evaluation of chimeric Japanese encephalitis and dengue viruses for use in diagnostic plaque reduction neutralization tests. Clin Vaccine Immunol. 2009;16:1052–9. http://dx.doi.org/10.1128/CVI.00095-09
10. Inwani I, Osoro E, Mugo C, Hunsperger E, Omballa V, Wamalwa D, et al. Zika infection among pregnant women in Mombasa, Coastal Kenya, 2017–2018: preliminary results of a cohort study. Poster presented at: American Society for Tropical Medicine and Hygiene 67th annual meeting; 2018 Oct 30; New Orleans, LA, USA.

Address for correspondence: Marc-Alain Widdowson, Institute of Tropical Medicine, Kronenburgstraat 43, 2000 Antwerp, Belgium; email: mawiddowson@itg.be; Elizabeth Hunsperger, Centers for Disease Control and Prevention, Unit 8900 Box 3600, DPO, AE 09831, USA; email: enh4@cdc.gov

# *Mycobacterium bovis* Pulmonary Tuberculosis after Ritual Sheep Sacrifice in Tunisia

Jamal Saad, Sophie Baron, Jean-Christophe Lagier, Michel Drancourt, Phillipe Gautret

Author affiliations: IHU Méditerranée Infection, Marseille, France (J. Saad); Aix-Marseille-Université, Marseille (J. Saad, S. Baron, J.-C. Lagier, M. Drancourt, P. Gautret)

DOI: https://doi.org/10.3201/eid2607.191597

A woman in France was diagnosed with pulmonary tuberculosis caused by *Mycobacterium bovis* after a ritual sheep sacrifice in her home country of Tunisia. This investigation sheds light on ritual sacrifice of sheep as a circumstance in which religious tradition and practices can expose millions of Muslims worldwide to this disease.

*Mycobacterium bovis* is historically responsible for zoonotic, deadly tuberculosis and has seemingly reemerged in countries where it had previously vanished following eradication programs in cattle and the pasteurization of dairy products (*1*–*3*). In most cases, *M. bovis* tuberculosis results from consuming unpasteurized milk; extrapulmonary disease is thus the most frequent clinical manifestation (*4*–*6*). Also, *M. bovis* could be an airborne zoonotic pathogen causing pulmonary tuberculosis (*7*). In western Europe countries, most of *M. bovis* human tuberculosis cases are seen in migrants and are associated with travel to the country of origin (*4*,*5*,*8*,*9*). *M. bovis* tuberculosis is traced to animal sources, yet reporting of clinical signs and symptoms is often delayed (*3*). The observation of a woman affected by *M. bovis* tuberculosis who participated in a precisely dated religious practice involving sheep slaughtering provided an opportunity to shed light on these medical aspects.

A 43-year-old unemployed woman born in Tunisia emigrated to France in 2000, married, and had 2 children. The patient had no underlying chronic condition, no medical history, no treatment, no history of smoking, and no toxic habits. She had received the bacillus Calmette-Guérin vaccine during childhood. Her last trip to Tunis and surrounding areas was during July 10–August 28, 2018. The patient denied any contacts with ill persons during her stay. She participated in the Aid-el-Kebir (the Great Festival) Muslim festivities on August 22–23, 2018. After the ritual, her husband slaughtered a veterinary-uncontrolled sheep outside the house by cutting through its neck in an open place and then insufflating air beneath the skin of the dead animal using bellows before butchering the viscera, including lungs, heart, liver, and kidneys, which were put into a container while the digestive tract was put separately into another container. His wife then washed the lungs and the other viscera for ≈2 hours in a confined kitchen, cooked them, and consumed them with her family; she did not experience any injury while butchering the animal.

After her return to France, the patient was apyretic with productive cough, fatigue, and anorexia, which started exactly 22 days after the Aid-el-Kebir festivities ended. The patient attributed symptoms to allergy and did not consult with a healthcare professional. In December 2018, her respiratory tract symptoms persisted; she also developed fatigue, fever, and night sweats and consulted a general practitioner. In January 2019, a computerized tomodensitometry scan confirmed an abscess in the inferior lobe of the patient's left lung with thick walls and an infiltrate in the lower lobe of the right lung. The patient reported fever, cough, expectoration, and anorexia, and lost 5 kg within 1 month (body mass index 15); we found crackles in both the left inferior and right superior lobes. She did not report hemoptysis, and her physical examination was otherwise unremarkable. Blood examination showed an iron deficiency in microcytic anemia, and her leukocyte count was normal.


**Figure.** Pangenome tree of *Mycobacterium bovis* from a patient in France (bold; GenBank accession no. CSURQ0209) with 11 reference *Mycobacterium bovis* strains isolated from different regions and hosts. The patient had visited her home country, Tunisia, where she participated in the ritual slaughter of a sheep. Scale bar represents 5% sequence divergence.

We performed a GenExpert assay (Cepheid, https://www.cepheid.com) and detected *M. tuberculosis* complex DNA in 1 sputum sample; we cultured the *M. tuberculosis* complex CSURQ0209 strain. None of the patient's other family members had any pulmonary symptoms at any time, and their chest radiographs results were normal. Before the precise *M. bovis* identification was known, we administered to the patient a daily oral regimen of rifampin (480 mg), isoniazid (200 mg), pyrazinamide (1,200 mg), and ethambutol (1,000 mg) for 2 months, followed by rifampin (600 mg/d) and isoniazid (300 mg/d) for 4 additional months, with favorable clinical and radiological outcomes and excellent tolerance. Whole-genome sequence analysis of strain CSURQ0209 (GenBank accession no. PRJEB39431) showed that it grouped more proximately with 1 *M. bovis* strain isolated from a patient from Algeria (Figure).

In this case, slaughtering a sheep during the annual ritual Aid-el-Kebir festivities was a probable source of infection, although no animal remains were available to confirm this hypothesis. Genome sequence analysis confirmed the identification of *M. bovis*, clustering with isolates from Algeria, in the absence of any other sequence from Tunisia. These results reinforced that this patient had been infected in her native country. During previous years, the festivities took place at the time the family was in France, and no animal sacrifice was performed on these occasions.

Transmission of *M. bovis* may occur during slaughtering through the inhalation of aerosols exhaled by infected animals (*9*). In this case, the patient was most likely infected by aerosols after prolonged manipulation of the crude viscera. This case potentially concerns millions of Muslim persons worldwide. Our findings indicate that, in countries where ritual animal sacrifices take place, health authorities may want to work with religious authorities to advocate veterinary inspection of slaughtered animals to discard viscera from animals with suspected tuberculosis, in phase with the current World Health Organization roadmap against zoonotic tuberculosis (*10*).

## About the Author

Mr. Saad is a PhD student at Aix-Marseille Université, Marseille, France, with interest in developing appropriate methods for the real-time genomics diagnosis of mycobacterial infections, including tuberculosis.

## References

1. Good M, Bakker D, Duignan A, Collins DM. The history of in vivo tuberculin testing in bovines: tuberculosis, a "One Health" issue. Front Vet Sci. 2018;5:59. https://doi.org/10.3389/fvets.2018.00059
2. Cousins DV. *Mycobacterium bovis* infection and control in domestic livestock. Rev Sci Tech. 2001;20:71–85. https://doi.org/10.20506/rst.20.1.1263

3. Good M, Duignan A. Perspectives on the history of bovine TB and the role of tuberculin in bovine TB eradication. Vet Med Int. 2011;2011:410470. https://doi.org/10.4061/2011/410470
4. Majoor CJ, Magis-Escurra C, van Ingen J, Boeree MJ, van Soolingen D. Epidemiology of *Mycobacterium bovis* disease in humans, the Netherlands, 1993–2007. Emerg Infect Dis. 2011;17:457–63. https://doi.org/10.3201/eid1703.101111
5. Scott C, Cavanaugh JS, Pratt R, Silk BJ, LoBue P, Moonan PK. Human tuberculosis caused by *Mycobacterium bovis* in the United States, 2006–2013. Clin Infect Dis. 2016;63:594–601. https://doi.org/10.1093/cid/ciw371
6. Torres-Gonzalez P, Cervera-Hernandez ME, Martinez-Gamboa A, Garcia-Garcia L, Cruz-Hervert LP, Bobadilla-Del Valle M, et al. Human tuberculosis caused by *Mycobacterium bovis*: a retrospective comparison with *Mycobacterium tuberculosis* in a Mexican tertiary care centre, 2000–2015. BMC Infect Dis. 2016;16:657. https://doi.org/10.1186/s12879-016-2001-5
7. Vayr F, Martin-Blondel G, Savall F, Soulat JM, Deffontaines G, Herin F. Occupational exposure to human *Mycobacterium bovis* infection: a systematic review. PLoS Negl Trop Dis. 2018;12:e0006208. https://doi.org/10.1371/journal.pntd.0006208
8. Nebreda-Mayoral T, Brezmes-Valdivieso MF, Gutiérrez-Zufiaurre N, García-de Cruz S, Labayru-Echeverría C, López-Medrano R, et al. Human *Mycobacterium bovis* infection in Castile and León (Spain), 2006–2015 [in Spanish]. Enferm Infecc Microbiol Clin. 2019;37:19–24. https://doi.org/10.1016/j.eimc.2017.11.018
9. Lepesqueux G, Mailles A, Aubry A, Veziris N, Jaffré J, Jarlier V, et al. Epidémiologie des cas de tuberculose à *Mycobacterium bovis* diagnostiqués en France. Med Mal Infect. 2018;48:S115–6. https://doi.org/10.1016/j.medmal.2018.04.291
10. World Health Organization. Roadmap for zoonotic tuberculosis. 2017 [cited 2019 Nov 29]. https://www.who.int/tb/publications/2017/Roadmap_for_zoonotic_tuberculosis_med_red.pdf

Address for correspondence: Michel Drancourt, Aix-Marseille Université IHU Méditerranée Infection, Unité de Recherche sur les Maladies Infectieuses et Tropicales Emergentes, UMR CNRS 6236 IRD 3R198, IFR 48 27 Bd., Jean Moulin, Marseille 13385 CEDEX 05, France; email: michel.drancourt@univ-amu.fr

# Urogenital Schistosomiasis in Fisherman, Nepal, 2019

Ranjit Sah, Jürg Utzinger, Andreas Neumayr

Author affiliations: Tribhuvan University Teaching Hospital, Kathmandu, Nepal (R. Sah); Swiss Tropical and Public Health Institute, Basel, Switzerland (J. Utzinger, A. Neumayr); University of Basel, Basel (J. Utzinger, A. Neumayr)

DOI: https://doi.org/10.3201/eid2607.191828

We report a case of urogenital schistosomiasis in a 34-year-old male patient in Nepal and summarize additional case reports. These cases provide putative evidence for the potential existence of human-pathogenic (most likely zoonotic) schistosome species on the Indian subcontinent.

We report the case of a 34-year-old male patient from Siraha District, Nepal, in the outer Terai Region bordering India. The patient was referred to us in October 2019 by his regional hospital because of a diagnosed microhematuria and reported intermittently observed episodes of macrohematuria. The patient reported no relevant medical history and had never traveled abroad other than to visit neighboring districts in Nepal and across the border to India. He earned his living as a fisherman.

Results of the physical examination were unremarkable. Laboratory test results showed a white cell count within reference ranges with mild eosinophilia (14%; 728 cells/μL) and unremarkable results for renal and liver function tests. Urine analysis confirmed microhematuria, and microscopic examination of the urine sediment showed very few but typical trematode eggs, resembling those of *Schistosoma haematobium*, the causative agent of urogenital schistosomiasis (*1*) (Figure, panel A). An abdominal ultrasound examination revealed diffuse bladder wall thickening, which was confirmed by computed tomography (Figure, panel B).

After praziquantel treatment (40 mg/kg for 3 d), hematuria resolved, and no more eggs were detectable at follow-up 2 weeks later.

Although several zoonotic schistosome species have been reported from the Indian subcontinent, human-pathogenic schistosome species are considered absent from the region (*2*) because none of the known intermediate host snails involved in the lifecycle of human-pathogenic schistosome species are present. Nevertheless, some reports of parasitologic confirmed autochthonously acquired infections

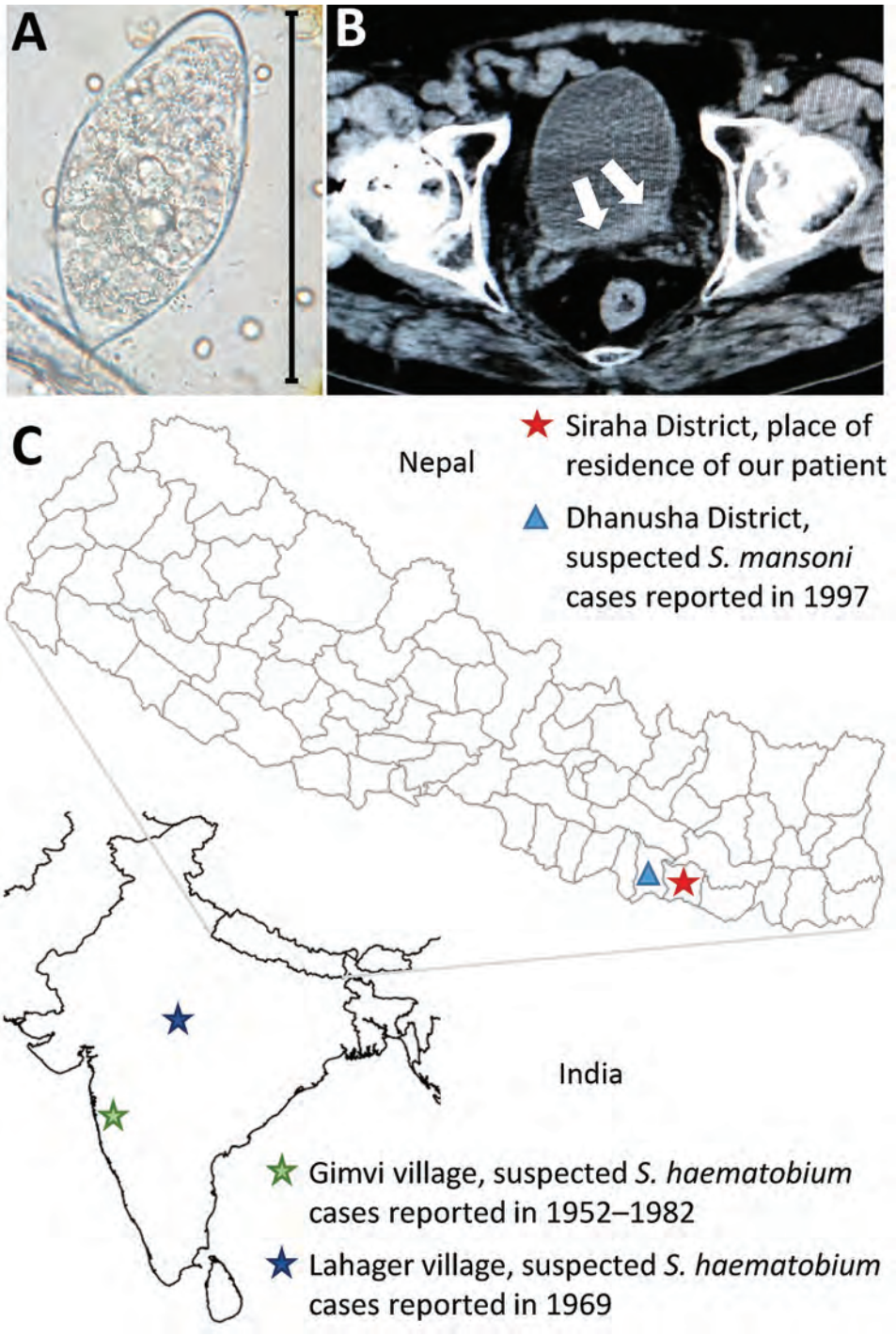


**Figure.** Investigation of urogenital schistosomiasis in a 34-year-old male patient in Nepal. A) Trematode egg, resembling the typical *Schistosoma haematobium* morphology, detected upon microscopic investigation of patient's urine sediment. Original magnification ×40. B) Computed tomography image showing bladder wall thickening (white arrows). C) Geographic location of patient's place of residence and of cases of human schistosomiasis reported previously in India and Nepal.

question the assumption that human schistosomiasis is nonexistent on the subcontinent.

In 1952, Gadgil and Shah (*3*) reported the detection of terminal-spined trematode eggs resembling those of *S. haematobium* in human urine samples from Gimvi, a village 250 km south of Bombay in India. In Gimvi village, terminal-spined trematode eggs were detected in 250 of 1,200 villagers; hematuria was the most common clinical manifestation. At the time of this discovery, available information suggested that the infectious focus area had existed for at least 60 years (*3*). Malacologic investigations in the river running through the village and infection experiments identified the *Ferrissia tenuis* snail as a competent intermediate host that, to date, has been reported nowhere else as intermediate host of *S. haematobium* (*4*).

After the river was treated with copper sulfate and the patients with antimontartrate, a follow-up survey in 1957 showed that 11.1% of the male and 8.7% of the female villagers were still infected; the highest infection rate (36.8%) was observed in boys 10–15 years of age (*5*). After the introduction of praziquantel in the 1980s, the Gimvi focus was successfully eliminated (*6*).

The parasite identified at Gimvi village was named and reported as *S. haematobium* on the basis of its egg morphology and the clinical manifestation in infected patients. However, the lifecycle of the Gimvi schistosome does not include the classical snail intermediate host genus *Bulinus,* raising questions about on its identification as *S. haematobium* in the 1950s. Unfortunately, parasitologic samples from that time are no longer available for in-depth molecular testing.

In 1969, seventeen years after the first description of the Gimvi cases, Shrivastava and Arora (*7*) reported the finding of *Schistosoma* typical egg granuloma in the bladder biopsy of a 26-year-old woman from Lahager village, situated in Raipur District of Madhya Pradesh, India. A village survey revealed a high prevalence of hematuria among the villagers. Upon urine microscopy, eggs "highly suspicious of *S. haematobium*" were found in some of the samples and "in one deposit features of *S. haematobium* eggs were seen." No further cases were reported from this region thereafter.

In 1997, Sherchand and Ohara reported the finding of lateral-spined trematode eggs, resembling those of *S. mansoni*, in a fecal sample from an inhabitant of Dhanusha District in the Terai Region, Nepal, during a coprologic survey conducted in 1995 (*8*). In 1997, similarly shaped eggs were detected in fecal samples of another 2 inhabitants in Dhanusha District (*9*). No clinical data are available for these 3 cases. In 1999, a serologic survey conducted among 508 inhabitants of the same district, reported an overall seroprevalence of 18.1% (range 1%–42.7%, depending on the surveyed village) (*9*). Of interest, Dhanusha is the neighboring district to that of the patient we report.

In summary, it appears that *Schistosoma* species capable of infecting humans are present on the Indian subcontinent. However, although the reported morphology of microscopically detected eggs in fecal samples resemble those of human-pathogenic species, the local absence of any classical intermediate host snails and the apparently low number of cases questions the assumption that endemic foci may simply have been overlooked in the past. We suspect that our case, as well as the previously reported cases, most likely depicts zoonotic infections. Unfortunately, we were unable to continue follow-up on the patient we describe, and no diagnostic samples were stored that would allow us to clarify the species by molecular-genetic investigations. We hope this shortfall can be rectified in future cases.

### Acknowledgment

We thank Sanjit Sah, Ranjana Sah, Shyam Sundar Sah, and Suzanne Donovan for their help and support.

### About the Author

Dr. Sah is a clinical infectious disease expert at Tribhuvan University Teaching Hospital and research coordinator at the National Public Health Laboratory, Kathmandu, Nepal. His research interests include infectious diseases with an emphasis on neglected tropical diseases.

### References

1. McManus DP, Dunne DW, Sacko M, Utzinger J, Vennervald BJ, Zhou XN. Schistosomiasis. Nat Rev Dis Primers. 2018;4:13. https://doi.org/10.1038/s41572-018-0013-8
2. Agrawal MC, Rao VG. Indian schistosomes: a need for further investigations. J Parasitol Res. 2011;2011:250868. https://doi.org/10.1155/2011/250868
3. Gadgil RK, Shah SN. Human schistosomiasis in India: discovery of an endemic focus in the Bombay state. Indian J Med Sci. 1952;6:760.
4. Gadgil RK, Shah SN. Human schistosomiasis in India. Part II. Infection of snails with *Schistosoma hematobium.* Indian J Med Res. 1995;43:695–701.
5. Dave PJ, Dhage KR. Re-survey and present status of the endemic focus of schistosomiasis. Indian J Med Res. 1958;46:546–56.
6. Agrawal MC, Rao VG. Some facts on South Asian schistosomiasis and need for international collaboration. Acta Trop. 2018;180:76–80. https://doi.org/10.1016/j.actatropica.2017.12.022
7. Shrivastava KK, Arora MM. *Schistosoma haematobium* infection in Lahager, a village in Raipur district of Madhya Pradesh. Indian J Med Res. 1969;57:2016–7.
8. Sherchand JB, Ohara H. *Schistosoma mansoni*-like eggs detected in stool of inhabitants in southern Nepal. J Nepal Med Assoc. 1997;37:386–7.
9. Sherchand JB, Ohara H, Sherchand S, Matsuda H. The suspected existence of *Schistosoma mansoni* in Dhanusha district, southern Nepal. Ann Trop Med Parasitol. 1999;93:273–8. 37 https://doi.org/10.1080/00034983.1999.11813423

Address for correspondence: Ranjit Sah, Department of Microbiology, Tribhuvan University Teaching Hospital, Institute of Medicine, Kathmandu, Nepal; email: ranjitsah@iom.edu.np

# Detection and Characterization of New Coronavirus in Bottlenose Dolphin, United States, 2019

Leyi Wang, Carol Maddox, Karen Terio, Saraswathi Lanka, Richard Fredrickson, Brittany Novick, Celeste Parry, Abby McClain, Kyle Ross

Author affiliations: University of Illinois, Urbana, Illinois, USA (L. Wang, S. Lanka, R. Fredrickson); University of Illinois College of Veterinary Medicine, Urbana (C. Maddox); University of Illinois College of Veterinary Medicine, Brookfield, Illinois, USA (K. Terio); National Marine Mammal Foundation, San Diego, California, USA (B. Novick, C. Parry, A. McClain); Naval Information Warfare Center Pacific, San Diego (K. Ross)

DOI: https://doi.org/10.320/eid2607.200093

We characterized novel coronaviruses detected in US bottlenose dolphins (BdCoVs) with diarrhea. These viruses are closely related to the other 2 known cetacean coronaviruses, Hong Kong BdCoV and beluga whale CoV. A deletion in the spike gene and insertions in the membrane gene and untranslated regions were found in US BdCoVs (unrelated to severe acture respiratory syndrome coronavirus 2).

The coronavirus family consists of single-stranded, positive-sense RNA viruses that cause respiratory, gastrointestinal, hepatic, and neurologic diseases of different host species. On the basis of genetic characterization, coronaviruses have been classified into 4 genera: *Alphacoronavirus*, *Betacoronavirus*, *Gammacoronavirus*, and *Deltacoronavirus*. *Cetacean coronavirus* is a recently proposed new species in the genus *Gammacoronavirus*, in addition to a common species (*Avian coronavirus*) (*1*). *Cetacean coronavirus* species contains bottlenose dolphin coronavirus (BdCoV) HKU22, identified in 2014, and beluga whale coronavirus (BWCoV) SW1, identified in 2008 (*1*,*2*). We report detection and genetic characterization of BdCoV in bottlenose dolphins in the United States; all dolphins had clinical signs consistent with gastrointestinal discomfort.

Four Atlantic bottlenose dolphins cared for by the US Navy Marine Mammal Program (San Diego, CA) showed development of an acute onset of clinical illness with clinical signs consisting of inappetence (n = 4), diarrhea (n = 3), and lethargy (n = 2) during April and May 2019. We collected fecal samples as part of the minimum workup for acute illness. Among all viruses we tested by using conventional PCRs, only coronavirus showed a positive result for all 4 dolphins.

We further evaluated samples by using next-generation sequencing as described (*3*). De novo assembly analysis of raw FASTQ data showed that 4 near complete genomes of BdCoV were assembled. Gaps were closed by Sanger sequencing at ACGT, Inc. (https://www.acgtinc.com). The genomes of all 4 US BdCoVs (37112–1, -2, -3, and -4) comprised 31,728 nt (GenBank accession nos. MN690608–11), which were shorter than those of 3 Hong Kong BdCoVs (HK-BdCoVs) (31,750–31,758 nt).

Further analysis of all individual genes showed that the 4 US BdCoV strains showed similar identities to both HK-BdCoVs and BWCoV in open reading frame (ORF) 1a, ORF1b, nonstructural (NS) 7, NS8, NS9, and NS10. However, US BdCoV strains showed higher identities to HK-BdCoVs than to BWCoV only in spike (S), envelope (E), membrane (M), and NS5a instead of all remaining genes (Appendix Table, Figure 1, https://wwwnc.cdc.gov/EID/article/26/7/20-0093-App1.pdf).

The 4 US BdCoV strains showed relatively higher identities to BWCoV than to HK-BdCoVs in NS5b (95.9% vs. 93.8%–94.0%), NS5c (98.4% vs. 97.7%–97.9%), NS6 (94.9% vs. 88.6%–88.9%), and nucleocapsid protein (97.9% vs. 96.1%–96.5%) genes. Analysis of amino acid identities of different ORFs also showed similar patterns (Appendix Table).

Phylogenetic analysis of complete genomes showed that the 4 US BdCoVs were clustered with 3 HK-BdCoVs strains and distantly related to BdCoV SW1 but were distinct from avian coronaviruses (Figure). Phylogenetic trees for individual genes showed that US BdCoV strains have a greater correlation with HK-BdCoVs than BWCoV in the S, E, M, NS5a, and NS7 genes and to BWCoV than HK-BdCoVs in remaining genes (Figure; Appendix Figures 2, 3).

Compared with the Hong Kong CF090331 strain, all US BdCoV strains have a 42-nt deletion in the S1 region at positions 21366–21407 encoding an S protein that is 14-aa shorter (Appendix Figure 4). Compared with 3 HK-BdCoVs strains, a 3-nt insertion (ACA) at positions 25417–25419 was found in the M gene of the 4 US BdCoVs, leading to a frameshift mutation in the M protein that was 1 amino acid longer (Appendix Figure 5).

In addition, a 4-nt insertion (TATA) was found in the 5′ untranslated region (UTR) of US BdCoV strains, and a 1-nt insertion (T) was found in the 3′ UTR of US BdCoV strains (Appendix Figure 6). Similar to findings of a previous report (*1*), because of 1 nt mutation (G→T at position 28268) of the US BdCoV strains, a premature stop codon in the NS7 gene resulted in

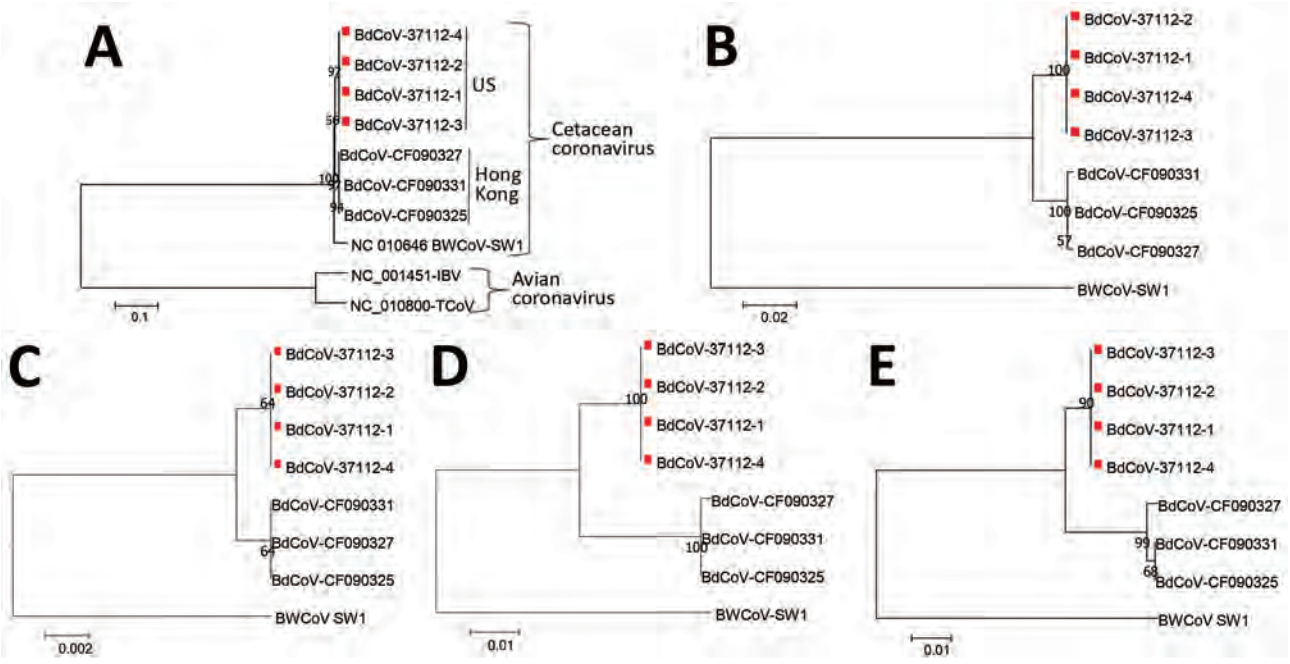


**Figure.** Phylogenetic analysis of A) complete genome, B) spike, C) envelope, D) matrix, and E) nonstructural protein 5a genes of gammacoronaviruses, including 4 US BdCoVs, 37112-1 to -4 (GenBank accession nos. MN690608–MN690611, indicated with red squares); 3 Hong Kong BdCoVs (accession nos.: CF090327, KF793825; CF090331, KF793826; CF090325, KF793824); and 1 BWCoV (SW1, accession no. NC_010646). Numbers along branches are bootstrap values. Scale bars indicate nucleotide substitutions per site. BdCoV, bottlenose dolphin coronavirus; BWCoV, beluga whale coronavirus.

an NS7a (42 aa) and an NS7b (117 aa). The position of the premature stop codon in the US BdCoVs was different from that for 2 HK-BdCoVs (CF090325 and CF090331), which encode different sizes of NS7a (63 aa) and NS7b (34 aa) proteins.

S deletion variants are commonly observed in coronaviruses. Porcine respiratory coronavirus is an S gene deletion mutant of transmissible gastroenteritis virus and causes a respiratory disease instead of gastroenteritis in pigs because of a large deletion (>600 nt) in the N terminal of the S gene (*4*). In addition, a large deletion (591 nt) in S1 resulted in a change in virulence of porcine epidemic diarrhea virus (*5*). In our study, we observed that 4 US BdCoVs had a 42-nt deletion in the S1 gene. It is unclear whether this deletion region is related to the viral tropism and virulence, and warrants further studies.

During a surveillance study in Hong Kong, China, BdCoV was identified only in fecal samples from dolphins that had no notable clinical signs (*1*). In our study, genetically related BdCoVs were detected in dolphins that had diarrhea, lethargy, and inappetence in the United States. It is possible that unique genetic features of US BdCoVs, including a sequence deletion in the S gene and an insertion in the M gene and 5′ and 3′ UTRs, and mutations in different genes might have contributed to the observed clinical diarrhea signs in US dolphins. Additional surveillance is needed to monitor the evolution of this virus worldwide.

## About the Author

Dr. Wang is a clinical assistant professor at the College of Veterinary Medicine, University of Illinois, Urbana. His research interests are diagnosis of viral infectious diseases and novel pathogen discovery.

## References

1. Woo PC, Lau SK, Lam CS, Tsang AK, Hui SW, Fan RY, et al. Discovery of a novel bottlenose dolphin coronavirus reveals a distinct species of marine mammal coronavirus in Gammacoronavirus. J Virol. 2014;88:1318–31. https://doi.org/10.1128/JVI.02351-13
2. Mihindukulasuriya KA, Wu G, St Leger J, Nordhausen RW, Wang D. Identification of a novel coronavirus from a beluga whale by using a panviral microarray. J Virol. 2008;82:5084–8. https://doi.org/10.1128/JVI.02722-07
3. Wang L, Stuber T, Camp P, Robbe-Austerman S, Zhang Y. Whole-genome sequencing of porcine epidemic diarrhea virus by Illumina MiSeq platform. In: Wang L, editor. Animal coronaviruses. Springer protocols handbooks. Totowa (NJ): Humana Press; 2016. p. 201–8.
4. Wang L, Zhang Y. Genomic characterization of a new PRCV variant, United States, 2014. Transbound Emerg Dis. 2017;64:672–4. https://doi.org/10.1111/tbed.12400
5. Hou Y, Lin CM, Yokoyama M, Yount BL, Marthaler D,

Douglas AL, et al. Deletion of a 197-amino-acid region in the N-terminal domain of spike protein attenuates porcine epidemic diarrhea virus in piglets. J Virol. 2017;91:e00227-17. https://doi.org/10.1128/JVI.00227-17

Address for correspondence: Leyi Wang, Department of Veterinary Clinical Medicine and the Veterinary Diagnostic Laboratory, College of Veterinary Medicine, University of Illinois, Urbana, IL, 61802, USA; email: leyiwang@illinois.edu

# Human Case of Severe Fever with Thrombocytopenia Syndrome Virus Infection, Taiwan, 2019

Shih-Huan Peng,[1] Su-Lin Yang,[1] Shih-En Tang, Tzy-Chen Wang, Tung-Chien Hsu, Chien-Ling Su, Meng-Yu Chen, Masayuki Shimojima, Tomoki Yoshikawa, Pei-Yun Shu

Author affiliations: Centers for Disease Control, Ministry of Health and Welfare, Taipei, Taiwan (S.-H. Peng, S.-L. Yang, T.-C. Wang, T.-C. Hsu, C.-L. Su, M.-Y. Chen, P.-Y. Shu); Tri-Service General Hospital, Taipei (S.-E. Tang); National Defense Medical Center, Taipei (S.-E. Tang); Institute of Aerospace and Undersea Medicine, National Defense Medical Center, Taipei (S.-E. Tang); National Institute of Infectious Diseases, Tokyo, Japan (M. Shimojima, T. Yoshikawa)

DOI: https://doi.org/10.3201/eid2607.200104

We report on a 70-year-old man with fever, leukopenia, thrombocytopenia, vomiting, malaise, dyspnea, and consciousness disturbance who was infected with severe fever with thrombocytopenia syndrome virus in northern Taiwan, 2019. This autochthonous case was confirmed by reverse transcription PCR, virus isolation, and genomic sequencing.

Severe fever with thrombocytopenia syndrome (SFTS) is a tickborne infection caused by the SFTS virus (SFTSV, also known as *Huaiyangshan banyangvirus*), which was identified in China in 2009 (*1*) and afterward in South Korea (*2*), Japan (*3*), and Vietnam (*4*). Since then, the number of SFTS cases in East Asia has risen rapidly. Therefore, laboratory-based surveillance of SFTS has been conducted in the routine molecular diagnosis of arboviral infections in the Taiwan Centers for Disease Control (Taiwan CDC) since 2013. We identified a patient in Taiwan with laboratory-confirmed SFTS who was originally suspected of having dengue or rickettsial infections.

In November 2019, a 70-year-old man who lived in northern Taiwan and had no travel history was admitted to the hospital with a 9-day history of fever (38.8°C–39.2°C), chills, nausea, vomiting, and malaise. The patient had underlying hypertension and type 2 diabetes mellitus that was controlled without medication. At hospital admission, we noted a generalized rash over the trunk and both feet. Laboratory examinations showed that the patient had leukopenia; thrombocytopenia; abnormal prothrombin time; elevated levels of aspartate transaminase, alanine transaminase, creatinine kinase, and C-reactive protein; and diagnostic disseminated intravascular coagulation (Table). Chest radiography and chest computed tomography showed patchy consolidations and ground-glass opacities of both lungs. A few hours after admission, the patient experienced a general tonic–clonic seizure, with worsening consciousness and dyspnea. He was transferred to the intensive care unit, where intubation and ventilator support began. He also received massive blood transfusions for severe thrombocytopenia, active mucosal (oral, nasal, and gastrointestinal tract) bleeding, and disseminated intravascular coagulation. Blood and sputum cultures revealed that the patient was infected with *Pseudomonas aeruginosa*; he received piperacillin/tazobactam, doxycycline, and clarithromycin as empirical therapy. Results of laboratory tests for hepatitis A and B viruses, cytomegalovirus, herpes simplex virus, adenovirus, and influenza were all negative. After the patient received a diagnosis of SFTSV infection, he received treatment with intravenous immunoglobulin for 5 days. However, his condition continued to deteriorate progressively. The patient died on day 40 after illness onset as a result of multiorgan failure. Delayed diagnosis and the presence of underlying conditions in this patient, including hypertension and diabetes mellitus, may be associated with his severe disease and death (*5*).

The patient often spent time on a vegetable farm in a mountainous area without wearing shoes, raising suspicions for arboviral and rickettsial infections. The hospital sent blood samples, collected from the patient before the blood transfusions on day 12 after illness onset, to the Taiwan CDC for

[1]These first authors contributed equally to this article.

**Table.** Laboratory findings of patient with severe fever with thrombocytopenia syndrome virus infection, Taiwan, 2019.

| Laboratory finding | Patient value | Reference range |
|---|---|---|
| Leukocytes, cells/μL | $1.550 \times 10^3$ | $3.9–10.6 \times 10^3$ |
| Erythrocytes, cells/μL | $5.550 \times 10^6$ | $3.9–5.4 \times 10^6$ |
| Hemoglobin, g/dL | 16.0 | 12–16 |
| Platelets/μL | $41 \times 10^3$ | $150–400 \times 10^3$ |
| % Neutrophils | 68.4 | 42–74 |
| % Lymphocytes | 29.7 | 25–56 |
| Aspartate transaminase, U/L | 1,326 | 0–37 |
| Alanine transaminase, U/L | 569 | 0–40 |
| Creatinine kinase, U/L | 1,310 | 56–224 |
| Creatinine, mg/dL | 1.7 | 0.44–1.03 |
| C-reactive protein, mg/L | 7.8 | <5 |
| Total bilirubin, mg/dL | 1.7 | 0.2–1.2 |
| Glucose, mg/dL | 250 | 70–100 |
| Prothrombin time, s | 14.4 | 6.6–11.6 |
| Activated partial thromboplastin time, s | 63.4 | 23.9–34.9 |

laboratory diagnosis of arboviral and rickettsial diseases. Arboviral infections were detected using primer sets (Appendix Table 1, https://wwwnc.cdc.gov/EID/article/26/7/20-0104-App1.pdf) by SYBR-Green I-based real-time reverse transcription PCR (RT-PCR). In addition, we detected the SFTSV genome using SFTSV-specific primer sets targeting nonstructural protein and nucleocapsid protein genes. Results of RT-PCR and PCR for flavivirus and chikungunya virus infections, scrub typhus, murine typhus, spotted fever rickettsiae, and leptospirosis were all negative.

SFTSV was isolated from patient serum with the Vero cell line and confirmed by RT-PCR and immunofluorescence assays. SFTSV RNA remained undetected in the urine sample. The viral loads in serum continuously decreased from day 12 after disease onset and became undetectable on day 29 after disease onset (Appendix Figure 1). SuperScript III 1-step RT-PCR (http://www.thermofisher.com) identified partial small (S), medium (M), and large (L) segments of SFTSV in the serum collected on day 12 after disease onset using a different set of primers (Appendix Table 2). SFTSV has been classified into 6 different genotypes according to its genome sequence (*6*). Phylogenetic analyses of the partial S (1,704 bp; GenBank accession no. MN830173), M (3,340 bp; GenBank accession no. MN830174), and L (6,332 bp; GenBank accession no. MN910270) segment sequences using MEGA7 (*7*) using the maximum-likelihood method (Appendix Figures 2, 3) showed that the partial S, M, and L segments of SFTSV from this patient belong to genotype B and are closely related to Japanese strains. SFTSV identified in *Rhipicephalus microplus* ticks in central Taiwan belongs to genotype A/C (*8*).

All of the patient's close contacts, including 8 family members, a friend, and 60 medical personnel, were healthy and without symptoms during the monitoring period. Six mites from 2 brown rats (*Rattus norvegicus*) and 2 Asian house shrews (*Suncus murinus*) were captured in the area surrounding the residence of the patient. All the RNA samples from animals and mites showed SFTSV negative results by RT-PCR.

Although the main SFTSV tick vector, *Haemaphysalis longicornis*, has not been documented in Taiwan, other tick vectors, such as *R. microplus* and *Amblyomma testudinarium*, have been found in wild and domestic animals (*8*–*10*). Further studies on the identification of natural vectors and routes of transmission are needed. The presence of an emerging SFTS case highlights the need for further studies of the prevalence, geographic distribution, and surveillance of SFTSV in Taiwan.

This work was supported by grant no. MOHW108-CDC-C-315-133121 from the Centers for Disease Control, Ministry of Health and Welfare, Taiwan.

### About the Authors

Dr. Peng is a postdoctoral research fellow at the Center for Diagnostics and Vaccine Development, Taiwan Centers for Disease Control. His research interests include the epidemiology of rickettsial diseases and development of molecular detection methods for vectorborne infectious diseases. Dr. Yang is a senior technical specialist at the Center for Diagnostics and Vaccine Development, Taiwan Centers for Disease Control. Her research interests include the epidemiology of rickettsial diseases and development of serological detection methods for vectorborne infectious diseases.

### References

1. Yu XJ, Liang MF, Zhang SY, Liu Y, Li JD, Sun YL, et al. Fever with thrombocytopenia associated with a novel bunyavirus in China. N Engl J Med. 2011;364:1523–32. http://dx.doi.org/10.1056/NEJMoa1010095
2. Kim KH, Yi J, Kim G, Choi SJ, Jun KI, Kim NH, et al. Severe fever with thrombocytopenia syndrome, South Korea, 2012. Emerg Infect Dis. 2013;19:1892–4. http://dx.doi.org/10.3201/eid1911.130792
3. Takahashi T, Maeda K, Suzuki T, Ishido A, Shigeoka T, Tominaga T, et al. The first identification and retrospective study of severe fever with thrombocytopenia syndrome in Japan. J Infect Dis. 2014;209:816–27. http://dx.doi.org/10.1093/infdis/jit603
4. Tran XC, Yun Y, Van An L, Kim SH, Thao NTP, Man PKC, et al. Endemic severe fever with thrombocytopenia syndrome, Vietnam. Emerg Infect Dis. 2019;25:1029–31. http://dx.doi.org/10.3201/eid2505.181463
5. Zhang SF, Yang ZD, Huang ML, Wang ZB, Hu YY, Miao D, et al. Preexisting chronic conditions for fatal outcome among SFTS patients: an observational cohort study. PLoS Negl Trop Dis. 2019;13:e0007434. http://dx.doi.org/10.1371/journal.pntd.0007434
6. Yun SM, Park SJ, Park SW, Choi W, Jeong HW, Choi YK, et al. Molecular genomic characterization of tick- and

human-derived severe fever with thrombocytopenia syndrome virus isolates from South Korea. PLoS Negl Trop Dis. 2017;11:e0005893. http://dx.doi.org/10.1371/journal.pntd.0005893
7. Kumar S, Stecher G, Tamura K. MEGA7: Molecular evolutionary genetics analysis version 7.0 for bigger datasets. Mol Biol Evol. 2016;33:1870–4. http://dx.doi.org/10.1093/molbev/msw054
8. Lin TL, Ou SC, Maeda K, Shimoda H, Chan JPW, Tu WC, et al. The first discovery of severe fever with thrombocytopenia syndrome virus in Taiwan. Emerg Microbes Infect. 2020;9:148–51. http://dx.doi.org/10.1080/22221751.2019.1710436
9. Tsai YL, Shyu CL, Yao CT, Lin JA. The ixodid ticks collected from dogs and other animals in Taiwan and Kinmen Island. Int J Acarol. 2012;38:110–5. http://dx.doi.org/10.1080/01647954.2011.594812
10. Chao LL, Lu CW, Lin YF, Shih CM. Molecular and morphological identification of a human biting tick, *Amblyomma testudinarium* (Acari: Ixodidae), in Taiwan. Exp Appl Acarol. 2017;71:401–14. http://dx.doi.org/10.1007/s10493-017-0119-9

Address for correspondence: Pei-Yun Shu, Vector-Borne Viral and Rickettsial Diseases Laboratory, Center for Diagnostics and Vaccine Development, Centers for Disease Control, Ministry of Health and Welfare, Taipei 11561, Taiwan; email: pyshu@cdc.gov.tw

# Lesions of *Mycobacterium avium* spp. *hominissuis* Infection Resembling *M. bovis* Lesions in a Wild Mule Deer, Canada[1]

Kirsten M.F. Frayne, Brock R. Chappell, Jennifer L. Davies, Bryan J. Macbeth, Musangu Ngeleka, Jamie L. Rothenburger

Author affiliations: University of Calgary Faculty of Veterinary Medicine, Calgary, Alberta, Canada (K.M.F. Frayne, B.R. Chappell, J.L. Davies, J.L. Rothenburger); Banff National Park, Parks Canada Agency, Banff, Alberta, Canada (B.J. Macbeth); Prairie Diagnostic Services, Saskatoon, Saskatchewan, Canada (M. Ngeleka); Canadian Wildlife Health Cooperative Alberta Region, Calgary (J.L. Rothenburger)

[1]Preliminary results from this study were presented at the American College of Veterinary Pathologists Annual Meeting, November 9-13, 2019, San Antonio, Texas, USA

We used molecular analyses to confirm *Mycobacterium avium* spp. *hominissuis* infection in lung granulomas and pyogranulomas in the tracheobronchial lymph node in a wild mule deer in Banff, Canada. These lesions are similar to those found in *M. bovis*–infected animals, emphasizing the critical need for disease surveillance in wildlife populations.

DOI: https://doi.org/10.3201/eid2607.200187

In November 2018, a wild yearling male mule deer (*Odocoileus hemionus*) was found dead in Banff National Park, Alberta, Canada. The carcass was submitted to the Canadian Wildlife Health Cooperative Alberta Region at the University of Calgary (Calgary, Alberta, Canada) for diagnostic investigation. The University of Calgary Veterinary Sciences Animal Care Committee approved this research (AC17-0010).

Necropsy revealed that the deer had died of blunt-force trauma, presumably having been struck by a vehicle. During the necropsy, we found mineralized granulomas in the right caudal lung lobe and multifocal pyogranulomatous lymphadenitis in the tracheobronchial lymph node (Figure). We fixed lesion samples in 10% neutral buffered formalin for 48 h, then processed the samples by routine methods; we stained 4-μm-thick sections of paraffin-embedded tissues with hematoxylin and eosin before examination with light microscopy by an anatomic veterinary pathologist (J.L.R.), certified by the American College of Veterinary Pathologists.

Histopathology of the lung confirmed granulomatous pneumonia. Affected multifocal areas were characterized by central necrotic debris that was variably mineralized, surrounded by macrophage aggregates, multinucleated giant cells, lymphocytes, plasma cells, and variably thick fibrous capsules. Histopathology of the lymph node revealed similar multifocal areas of necrosis, variable mineralization, and infiltration of macrophages in the edges of some affected areas. Because of autolysis and freeze-thaw artifact, further characterization of the inflammatory cell population was not possible.

We designated the lymph node lesions as pyogranulomatous lymphadenitis because of the suppurative gross appearance of the lymph node combined with the microscopic presence of macrophages and mineralization revealed during histologic examination. We identified acid-fast organisms in multifocal macrophages at the margin of necrotic areas in both the lung and lymph node lesions. We submitted frozen samples to the Prairie Diagnostic Services laboratory

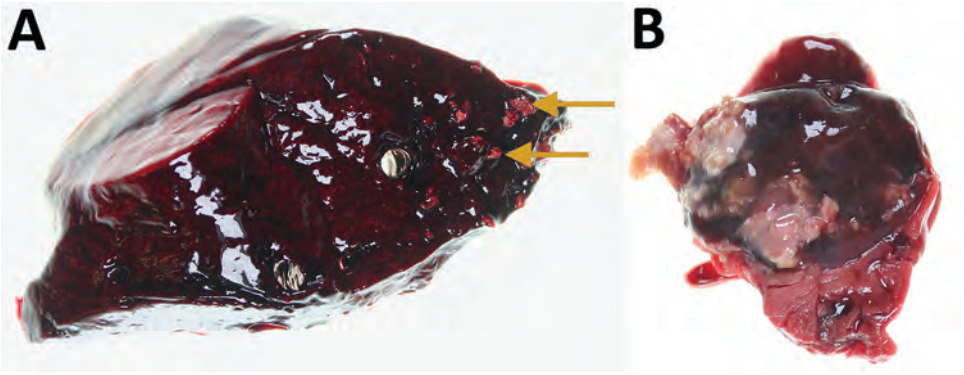


**Figure.** Lung and tracheobronchial lymph nodes from a wild mule deer (*Odocoileus hemionus*) infected with *Mycobacterium avium* spp. *hominissuis*, Banff National Park, Alberta, Canada. A) Mineralized granulomas in the right caudal lung lobe (arrows). B) Pyogranulomatous lymphadenitis of a tracheobronchial lymph node. The lesions resemble those caused by infection with *M. bovis*.

(Saskatoon, Saskatchewan, Canada), for further analyses. Results of routine bacterial culture and PCR for *Mycobacterium bovis* were both negative. Subsequently, results were positive from a generic *Mycobacterium* spp. PCR of the lung and lymph node using nested internal primers of 439bp, as described elsewhere (*1*). Genomic sequencing analysis identified *M. avium* spp. *hominissuis* (GenBank accession no. MT012364).

*M. avium* complex disease, caused by 4 species of *M. avium*, including *M. avium* spp. *hominissuis*, is considered a potentially zoonotic disease of global importance (*4*). *M. avium* spp. *hominissuis* is a rare nontuberculosis mycobacterium that infects a wide range of species, most commonly humans and pigs (*2*,*3*). An opportunistic environmental pathogen that persists in soil and water, *M. avium* spp. *hominissuis* typically infects the lungs and intestinal tract, presumably by inhalation and ingestion, respectively (*4*,*5*).

In humans, *M. avium* spp. *hominissuis* typically results in chronic granulomatous infections in the lungs and cervical lymph nodes (*6*), most commonly in immunocompromised persons (*3*). In children, infection causes lymphadenitis of the head and neck region (*3*). In pigs and other animals, however, *M. avium* spp. *hominissuis* infection primarily manifests as gastrointestinal disease, with granulomatous lesions in mesenteric lymph nodes and abdominal organs, such as the liver, spleen, and small intestines (*6*). Yoshida et al. described lung granulomas as an incidental finding in a slaughtered steer that were similar to the ones identified in the mule deer in this study (*7*). However, these lesions are an unusual manifestation for this bacterium in animals. More typically, respiratory *Mycobacterium* infections in cattle are caused by *M. bovis,* the causative agent of bovine tuberculosis and a zoonotic pathogen of global importance with extensive regulatory and trade implications (*8*).

The lesions in this case were morphologically similar to those described in animals infected with *M. bovis*. Pyogranulomas and granulomas in the lungs and cervical lymph nodes are found in wildlife reservoirs of *M. bovis,* including cervids (*8*). The similarity of these lesions emphasizes the importance of continuing surveillance and thorough investigation of suspected *M. bovis* cases. Cattle in Canada are regarded as free of *M. bovis*; however, 3 separate cattle herds in western Canada have tested positive from 2011 through March 2020 (*9*).

*M. bovis* is endemic in wild wood bison (*Bison bison athabascae*) and elk (*Cervus canadensis*) in 2 other national parks in Canada geographically separated from Banff by hundreds of kilometers (*10*). The presence of wildlife reservoirs elsewhere, combined with the sporadic identification of *M. bovis*–infected cattle herds in Canada, has led to concerns over surveillance in wildlife (*8*,*9*). This case demonstrates that routine disease surveillance activities in wildlife populations, including molecular investigations, are crucial to providing ongoing assurance to agricultural and public health sectors of the absence of *M. bovis* in wild cervid populations outside of known endemic areas.

### Acknowledgments

We thanks Susan Calder-Lodge, Jennifer Larios, Melencio Nicolas, Chris Bergeron, Jim Carlsen, and Betty Pollock for invaluable technical support.

Funding and logistical support for this case was provided by the Faculty of Veterinary Medicine, University of Calgary.

### About the Author

Ms. Frayne is a final-year veterinary medicine student at the University of Calgary. She is interested in ecosystem and public health and has a background in both wildlife and laboratory animal medicine.

## References

1. Telenti A, Marchesi F, Balz M, Bally F, Böttger EC, Bodmer T. Rapid identification of mycobacteria to the species level by polymerase chain reaction and restriction enzyme analysis. J Clin Microbiol. 1993;31:175–8. https://doi.org/10.1128/JCM.31.2.175-178.1993
2. Klotz D, Barth SA, Baumgärtner W, Hewicker-Trautwein M. *Mycobacterium avium* subsp. *hominissuis* infection in a domestic rabbit, Germany. Emerg Infect Dis. 2018;24:596–8. https://doi.org/10.3201/eid2403.171692
3. Agdestein A, Olsen I, Jørgensen A, Djønne B, Johansen TB. Novel insights into transmission routes of *Mycobacterium avium* in pigs and possible implications for human health. Vet Res (Faisalabad). 2014;45:46. https://doi.org/10.1186/1297-9716-45-46
4. Ignatov D, Kondratieva E, Azhikina T, Apt A. *Mycobacterium avium*-triggered diseases: pathogenomics. Cell Microbiol. 2012;14:808–18. https://doi.org/10.1111/j.1462-5822.2012.01776.x
5. Nishiuchi Y, Iwamoto T, Maruyama F. Infection sources of a common non-tuberculous mycobacterial pathogen, *Mycobacterium avium* complex. Front Med (Lausanne). 2017;4:27. https://doi.org/10.3389/fmed.2017.00027
6. Komatsu T, Inaba N, Kondo K, Nagata R, Kawaji S, Shibahara T. Systemic mycobacteriosis caused by '*Mycobacterium avium* subspecies *hominissuis*' in a 14-month-old Japanese black beef steer. J Vet Med Sci. 2017;79:1384–8. https://doi.org/10.1292/jvms.17-0204
7. Yoshida S, Araki T, Asai T, Tsuyuguchi K, Arikawa K, Iwamoto T, et al. Phylogenetic uniqueness of *Mycobacterium avium* subspecies *hominissuis* isolated from an abnormal pulmonary bovine case. Infect Genet Evol. 2018;62:122–9. https://doi.org/10.1016/j.meegid.2018.04.013
8. Fitzgerald SD, Kaneene JB. Wildlife reservoirs of bovine tuberculosis worldwide: hosts, pathology, surveillance, and control. Vet Pathol. 2013;50:488–99. https://doi.org/10.1177/0300985812467472
9. Canada Food Inspection Agency, Government of Canada. Bovine tuberculosis. 2019 [cited 2020 Jan 13]. https://inspection.gc.ca/animal-health/terrestrial-animals/diseases/reportable/bovine-tuberculosis/eng/1330205978967/1330206128556
10. Wobeser G. Bovine tuberculosis in Canadian wildlife: an updated history. Can Vet J. 2009;50:1169–76.


Address for correspondence: Jamie L. Rothenburger, Faculty of Veterinary Medicine, University of Calgary, 3280 Hospital Dr NW, Calgary, Alberta T2N 4Z6, Canada; email: jamie.rothenburger@ucalgary.ca.

# Public Mental Health Crisis during COVID-19 Pandemic, China

Lu Dong, Jennifer Bouey

Author affiliations: RAND Corporation, Santa Monica, California, USA (L. Dong); RAND Corporation, Arlington, Virginia, USA (J. Bouey); Georgetown University, Washington, DC, USA (J. Bouey)

DOI: https://doi.org/10.3201/eid2607.200407

The 2019 novel coronavirus disease emerged in China in late 2019–early 2020 and spread rapidly. China has been implementing emergency psychological crisis interventions to reduce the negative psychosocial impact on public mental health, but challenges exist. Public mental health interventions should be formally integrated into public health preparedness and emergency response plans.

China was the first country affected by the pandemic of 2019 novel coronavirus disease (COVID-19), caused by severe acute respiratory syndrome coronavirus 2. Several unique characteristics of China's COVID-19 epidemic patterns and its management policy prompted a heightened public mental health crisis. First, many Chinese residents still remember the 2003 outbreak of severe acute respiratory syndrome (SARS) and its effect on China's social life and economy (*1*). COVID-19 is more transmissible than SARS, and the case-fatality rate (2.3%) is substantially higher than that for seasonal influenza (*2*). The uncertain incubation period of the virus and its possible asymptomatic transmission cause additional fear and anxiety. Second, the government's initial downplaying of the epidemic's severity eroded public trust in the government's decision-making transparency and competency. Third, unprecedented large-scale quarantine measures in all major cities, which essentially confine residents to their homes, are likely to have a negative psychosocial effect on residents (*3*). Fourth, reports of shortages of medical protective supplies, medical staff, and hospital beds in Wuhan and the surrounding areas soon followed the citywide quarantine and caused enormous concern throughout the nation. Last, a unique "infodemic"—an overabundance of (mis)information on social media (*4*) and elsewhere—poses a major risk to public mental health during this health crisis.

As during the 2003 SARS and 2014 Ebola virus disease outbreaks, generalized fear and fear-induced overreactive behavior were common among the public; both can impede infection control (*5*,*6*). In addition, psychiatric disorders, such as depression,

anxiety, and posttraumatic stress disorder, developed in high-risk persons, especially survivors and frontline healthcare workers (*7*).

On the basis of these recent experiences, the National Health Commission of China released a notification on January 26, 2020, providing guiding principles of the emergency psychological crisis interventions to reduce the psychosocial effects of the COVID-19 outbreak (*8*). This notification specified that psychological crisis intervention should be part of the public health response to the COVID-19 outbreak, organized by the joint prevention and control mechanism at the city, municipal, and provincial levels, and that the interventions should be differentiated by group. The intervention workforce comprises psychological outreach teams led by psychiatrists and mental health professionals and psychological support hotline teams. An attachment to this notification further outlined the key intervention targets for 6 groups: confirmed patients, persons under investigation for COVID-19, healthcare workers, persons in immediate contact with patients, ill persons who refuse to seek care, and susceptible persons/the general public (Appendix, https://wwwnc.cdc.gov/EID/article/26/7/20-0407-App1.pdf).

The release of such policy guidance acknowledges China's recognition of public mental health needs during the outbreak. However, the notification does not specify how different resources should be mobilized and coordinated or, more important, who should deliver which type of interventions, for which group in need, and by which delivery mode(s). The policy guidance also does not indicate operationalization of how various groups should be screened or assessed to determine the type and level of interventions to provide to each. This level of detail is needed because China lacks a well-established mental healthcare system and has no existing national-level emergency response system and designated workforce to provide the psychological crisis interventions during a national emergency or disaster (X. Chen, X. Fu, unpub. data, https://doi.org/10.16418/j.issn.1000-3045.20200213001) (*9*). Other major challenges to successfully implementing the emergency psychological crisis interventions include China's severe shortage of mental healthcare providers (1.49 psychiatrists/100,000 population, and only half of these psychiatrists have attained a bachelor's degree in medicine), unevenly distributed healthcare resources, and the limitations posed by the mass quarantine (*9*). For example, hospitals, universities, and a variety of organizations have set up numerous hotlines staffed by volunteers with varying degrees of qualification and experience (*8*). These well-meaning efforts can be uncoordinated and inadequately supervised and thus are likely to cause confusion to service consumers and inefficient use of resources.

The challenges reported in China indicate that, for many developing countries, telemedicine should be considered, given the widespread adoption of smartphones, to help remove barriers to accessing quality care for mental health. Task-shifting or -sharing (i.e., shifting service delivery of specific tasks from professionals to persons with fewer qualifications or creating a new cadre of providers with specific training) might help, especially in low-resource areas (*10*). Countries should also consider requesting support and guidance from global mental healthcare authorities and research communities through international collaborations.

Given lessons learned from past outbreaks in China and other parts of the world, public mental health interventions should be formally integrated into public health preparedness and emergency response plans to effectively curb all outbreaks. The World Health Organization's strategic preparedness and response plan for COVID-19, however, has not yet specified any strategies to address mental health needs of any kind (*4*). As the virus spreads globally, governments must address public mental health needs by developing and implementing well-coordinated strategic plans to meet these needs during the COVID-19 pandemic.

## About the Authors

Dr. Dong is an associate behavioral scientist and a licensed clinical psychologist at RAND Corporation. Her primary research interests are development and improvement of evidence-based psychosocial interventions for youth and adults.

Dr. Bouey is a senior policy researcher and the Tang Chair in China Policy Studies at RAND Corporation and an associate professor of Global Health at Georgetown University. Her primary research interests include the social determinants of health among underserved populations.

## References

1. Bouey J. From SARS to 2019-coronavirus (nCoV): U.S.–China collaborations on pandemic response: addendum. Santa Monica (CA): RAND Corporation; 2020 [cited 2020 Mar 23]. https://www.rand.org/pubs/testimonies/CT523z2.html
2. The Novel Coronavirus Pneumonia Emergency Response Epidemiology Team. The epidemiological characteristics of an outbreak of 2019 novel coronavirus diseases (COVID-19)—China, 2020. China CDC Weekly. 2020;2:113–22.
3. Brooks SK, Webster RK, Smith LE, Woodland L, Wessely S, Greenberg N, et al. The psychological impact of quarantine and how to reduce it: rapid review of the

evidence. Lancet. 2020;395:912–20. https://doi.org/10.1016/S0140-6736(20)30460-8
4. World Health Organization. 2019 Novel coronavirus (2019-nCoV): strategic preparedness and response plan Feb 3, 2020 [cited 2020 Feb 7]. https://www.who.int/docs/default-source/coronaviruse/srp-04022020.pdf
5. Shultz JM, Cooper JL, Baingana F, Oquendo MA, Espinel Z, Althouse BM, et al. The role of fear-related behaviors in the 2013–2016 West Africa Ebola virus disease outbreak. Curr Psychiatry Rep. 2016;18:104. https://doi.org/10.1007/s11920-016-0741-y
6. Person B, Sy F, Holton K, Govert B, Liang A, Garza B, et al.; National Center for Infectious Diseases/SARS Community Outreach Team. Fear and stigma: the epidemic within the SARS outbreak. Emerg Infect Dis. 2004;10:358–63. https://doi.org/10.3201/eid1002.030750
7. Mak IW, Chu CM, Pan PC, Yiu MG, Chan VL. Long-term psychiatric morbidities among SARS survivors. Gen Hosp Psychiatry. 2009;31:318–26. https://doi.org/10.1016/j.genhosppsych.2009.03.001
8. National Health Commission of China. Principles of the emergency psychological crisis interventions for the new coronavirus pneumonia [in Chinese] [cited 2020 Feb 7]. http://www.nhc.gov.cn/jkj/s3577/202001/6adc08b966594253b2b791be5c3b9467
9. Liang D, Mays VM, Hwang WC. Integrated mental health services in China: challenges and planning for the future. Health Policy Plan. 2018;33:107–22. https://doi.org/10.1093/heapol/czx137
10. World Health Organization. Joint WHO/OGAC technical consultation on task shifting: key elements of a regulatory framework in support of in-country implementation of task shifting. Geneva: The Organization; 2007.

Address for correspondence: Lu Dong, RAND Corporation, 1776 Main St, Santa Monica, CA 90401, USA; email: ldong@rand.org

# Rhabdomyolysis as Potential Late Complication Associated with COVID-19

Min Jin, Qiaoxia Tong

Author affiliations: Cancer Center, Union Hospital, Tongji Medical College, Huazhong University of Science and Technology, Wuhan, China (M. Jin); Department of Infectious Diseases, Union Hospital, Tongji Medical College, Huazhong University of Science and Technology, Wuhan (Q. Tong)

DOI: https://doi.org/10.3201/eid2607.200445

We describe a patient in Wuhan, China, with severe acute respiratory syndrome coronavirus 2 infection who had progressive pulmonary lesions and rhabdomyolysis with manifestations of lower limb pain and fatigue. Rapid clinical recognition of rhabdomyolysis symptoms in patients with severe acute respiratory syndrome coronavirus 2 infection can be lifesaving.

Recently, the outbreak of severe acute respiratory syndrome coronavirus 2 (SARS-CoV-2) infection in Wuhan, China, has attracted great attention worldwide (*1*). SARS-CoV-2, the cause of 2019 novel coronavirus disease (COVID-19), belongs to the β-coronavirus family, which also includes 2 other highly pathogenic human coronaviruses (*2*): severe acute respiratory syndrome coronavirus and Middle East respiratory syndrome coronavirus. Fever, cough, myalgia, and fatigue are the common symptoms of COVID-19, whereas expectoration, headache, hemoptysis, and diarrhea are relatively rare (*3*).

Rhabdomyolysis is a life-threatening disorder that manifests with myalgia, fatigue, and pigmenturia; it can also manifest as acute renal failure (*4*). The inducing factors of rhabdomyolysis include autoimmune myopathies, septicemia, electrolyte abnormalities, substance abuse, alcohol use, or infection (*5*). Viral infection, especially influenza virus infection, can lead to rhabdomyolysis (*6*). We report rhabdomyolysis related to COVID-19 in Wuhan, China.

A 60-year-old man in Wuhan sought care in February 2020 for a 6-day history of fever up to 38.3°C and cough. Chest computed tomography performed 3 days before in another hospital showed that the texture of both lungs was thickened and scattered with ground glass shadows (Appendix Figure, https://wwwnc.cdc.gov/EID/article/26/7/20-0445-App1.pdf). When the patient arrived, he was alert; heart rate was 89 bpm, blood pressure was 135/91 mm Hg, respiratory rate was 18 breaths/min, temperature was 38.5°C, and saturation of peripheral oxygen was 93%. Physical examination revealed a rough breath sound in the lungs. Laboratory findings included mild leukopenia (3.31 × 109 neutrophils/L [reference 3.5–9.5 × 109 neutrophils/L]), increased lactate dehydrogenase (280 U/L [reference 109–245 U/L]), and increased C-reactive protein (111 mg/L [reference 0–8 mg/L]) (Table). Results were in the normal range for creatine kinase (CK) and indicators of hepatic and kidney function. Screenings for common infectious diseases were negative. Real-time reverse-transcription PCR analysis of the patient's throat swab specimen indicated SARS-CoV-2 infection.

**Table.** Biochemistry and blood gas parameters of a 60-year-old man with severe acute respiratory syndrome coronavirus 2 infection and rhabdomyolysis, by day of hospitalization, Wuhan, China, 2020*

| Parameter (reference range) | Day 1 | Day 3 | Day 6 | Day 9† | Day 10 | Day 11 | Day 12‡ | Day 15 | Day 17 | Day 20 |
|---|---|---|---|---|---|---|---|---|---|---|
| Myoglobin (0–140 μg/L) | ND | ND | ND | >12,000 | 12,550 | 7,905 | 3,280 | 928 | 152 | 86 |
| Creatine kinase (38–174 U/L) | 47 | ND | ND | 11,842 | 17,434 | 14,318 | 11,067 | 2,954 | 1,447 | 251 |
| LDH (109–245 U/L) | 280 | ND | ND | 2,347 | 2,137 | 1,979 | 1,754 | 1,265 | 923 | 597 |
| α-hbdh (72–182 U/L) | 277 | ND | ND | 1,612 | 1,436 | 1,171 | 1,143 | 1,037 | 911 | 189 |
| Amyloid A (0–10 mg/L) | 746 | ND | ND | 429 | 192 | 105 | 126 | 93 | 84 | 25 |
| CRP (0–8 mg/L) | 111 | 123 | 206 | 58 | 45 | 23.4 | 23.4 | 21.4 | 6.1 | 15 |
| ALT (5–40 U/L) | 37 | 82 | 61 | 111 | 162 | 171 | 172 | 142 | 133 | 56 |
| AST (8–40 U/L) | 48 | 88 | 35 | 213 | 373 | 348 | 320 | 183 | 135 | 38 |
| Albumin (35–55 g/L) | 33.7 | 31.8 | 27.6 | 32.3 | 28.5 | 30.3 | 30 | 30.7 | 29.3 | 30.3 |
| Creatine (44–133 μmol/L) | 72.5 | 74.4 | 72.6 | 65.2 | 68.9 | 68.8 | 59.2 | 68 | 65.7 | 67.3 |
| PH (7.35–7.45) | ND | ND | ND | ND | 7.51 | 7.4 | 7.48 | 7.45 | ND | 7.40 |
| $PCO_2$ (35–45 mm Hg) | ND | ND | ND | ND | 29.2 | 34.8 | 34.6 | 36 | ND | 38 |
| $PO_2$ (83–103 mm Hg) | ND | ND | ND | ND | 49 | 147 | 142 | 120 | ND | 102 |

*α-hbdh, α-hydroxybutyrate dehydrogenase; ALT, alanine aminotransferase; AST, aspartate aminotransferase; LDH, lactate dehydrogenase; ND, not done.
†Rhabdomyolysis symptoms appeared on hospital day 9.
‡Real-time reverse transcription PCR conducted on hospital day 12 was negative for severe acute respiratory syndrome coronavirus 2.

We treated the patient with oxygen inhalation, opinavir, moxifloxacin, interferon nebulization, an antitussive, and nutritional support. On day 6 after admission, the patient still had an intermittent fever up to 38°C. We broadened the antibiotic treatment to include meropenem and added methylprednisolone. His fever abated on hospital day 7. However, serologic examination showed that C-reactive protein had increased to 206 mg/L.

On hospital day 9, the patient felt pain and weakness in his lower limbs. He denied medication exposure, illicit drug use, or alcohol use. Physical examination indicated tenderness in the lower limbs. Urgent laboratory examination indicated that myoglobin was >12,000.0 μg/L (reference 0–140 μg/L), CK was 11,842 U/L (reference 38–174 U/L), lactate dehydrogenase was 2,347 U/L (reference 109–245 U/L), alanine aminotransferase was 111 U/L (reference 5–40 U/L), and aspartate aminotransferase was 213 U/L (reference 8–40 U/L) (Table). The patient's kidney function and electrolytes were normal. Urine analysis revealed light yellow color of urine, occult blood was positive, and urine protein was suspiciously positive. These results indicated the onset of rhabdomyolysis.

In addition to the ongoing treatments, the patient was immediately treated with hydration, alkalization, plasma transfusion, gamma globulin, and symptomatic supportive therapy. On hospital day 10, the laboratory index continuously increased (Table). Blood gas analysis showed that PCO2 was 29.2 mm Hg (reference 35–45 mm Hg), PO2 was 49 mm Hg (reference 83–103 mm Hg), and pH was 7.51 (reference 7.35–7.45). A computed tomography reexamination of the lungs showed that the pulmonary lesions had substantially deteriorated (Appendix Figure). We continued the aggressive fluid therapy and maintained the acid–base balance while also continuing treatment with opinavir and moxifloxacin. The patient reported less pain and fatigue in his lower limbs in the following days. Biochemistry and blood gas indicators gradually returned to normal levels (Table). Moreover, a second real-time reverse transcription PCR test conducted on hospital day 12 was negative for SARS-CoV-2. The patient's symptoms improved daily, and he was again able to move his lower limbs freely.

The initial manifestations of SARS-CoV-2 infection in this patient were fever and cough. After a short period of antimicrobial drug treatment, his fever abated, but the condition of both lungs was deteriorating. Meanwhile, symptoms of rhabdomyolysis began.

General muscle pain and fatigue are common symptoms of COVID-19, but clinicians should consider the diagnosis of rhabdomyolysis when patients have focal muscle pain and fatigue (*7*). CK and myoglobin levels are important indexes for rhabdomyolysis (*5*); however, they are not tested routinely, so rhabdomyolysis is easily misdiagnosed. The key to avoid acute renal failure from rhabdomyolysis is early detection and treatment with aggressive hydration (*7*).

We generally know very little of the multifaceted biologic characteristics of COVID-19. Moreover, to our knowledge, COVID-19–associated rhabdomyolysis has not been previously reported; therefore, clinicians might have low clinical suspicion for rhabdomyolysis.

The case we describe lacks a final etiology for rhabdomyolysis. Also, our findings are limited by the absence of virus sequencing and confirmation of rhabdomyolysis pathology analysis. However, our findings indicate that rapid clinical recognition and positive hydration treatment of COVID-19–associated rhabdomyolysis can reduce the risk for serious outcomes.

### Acknowledgment

We thank Dean G. Tang and Jia Liu for linguistic assistance during the preparation of this manuscript.

This work was supported by grants from the National Natural Science Foundation of China (grant no. 81602255).

### About the Authors

Dr. Jin and Dr. Tong graduated from Tongji Medical College, Huazhong University of Science and Technology in China. While completing this work, they are working in the COVID-19 isolation ward of Tongji Medical College's Union Hospital. Their primary research interests are infectious diseases.

### References

1. Cowling BJ, Leung GM. Epidemiological research priorities for public health control of the ongoing global novel coronavirus (2019-nCoV) outbreak. Euro Surveill. 2020;25. https://doi.org/10.2807/1560-7917.ES.2020.25.6.2000110
2. Jin YH, Cai L, Cheng ZS, Cheng H, Deng T, Fan YP, et al. A rapid advice guideline for the diagnosis and treatment of 2019 novel coronavirus (2019-nCoV) infected pneumonia (standard version). Mil Med Res. 2020;7:4. https://doi.org/10.1186/s40779-020-0233-6
3. Huang C, Wang Y, Li X, Ren L, Zhao J, Hu Y, et al. Clinical features of patients infected with 2019 novel coronavirus in Wuhan, China. Lancet. 2020;395:497–506. https://doi.org/10.1016/S0140-6736(20)30183-5
4. Zutt R, van der Kooi AJ, Linthorst GE, Wanders RJ, de Visser M. Rhabdomyolysis: review of the literature. Neuromuscul Disord. 2014;24:651–9. https://doi.org/10.1016/j.nmd.2014.05.005
5. Nance JR, Mammen AL. Diagnostic evaluation of rhabdomyolysis. Muscle Nerve. 2015;51:793–810. https://doi.org/10.1002/mus.24606
6. Ayala E, Kagawa FT, Wehner JH, Tam J, Upadhyay D. Rhabdomyolysis associated with 2009 influenza A(H1N1). JAMA. 2009;302:1863–4. https://doi.org/10.1001/jama.2009.1582
7. Parekh R, Care DA, Tainter CR. Rhabdomyolysis: advances in diagnosis and treatment. Emerg Med Pract. 2012; 14:1–15, quiz 15.

Address for correspondence to: Qiaoxia Tong, Union Hospital, Tongji Medical College, Huazhong University of Science and Technology, 1277 JieFang Ave, Wuhan 430022, China; email: 2639985873@qq.com

# etymologia

## Rhabdomyolysis [rab"do-mi-ol'ə-sis]

Ronnie Henry[1]

From the Greek rhabdos ("rod") + mus ("muscle") + lusis ("loosening"), rhabdomyolysis refers to the rapid breakdown of skeletal (striated) muscle, releasing myoglobin into the blood, which can lead to kidney failure. In the Book of Numbers in the Bible, the Israelites grew tired of eating manna. They demanded that God send them meat. God, angry at their insolence, sent them quail but then strikes those who ate the meat with a plague (Numbers 11:31–35). This may have been an early account of rhabdomyolysis, since migrating quail eat large amounts of hemlock, a known cause of rhabdomyolysis.

Brown quail (*Coturnix ypsilophora*) by Duncan Wright, own work, CC BY-SA 3.0, https://commons.wikimedia.org/w/index.php?curid=2998176

[1]Deceased.

### Sources

1. Huerta-Alardín AL, Varon J, Marik PE. Bench-to-bedside review: rhabdomyolysis—an overview for clinicians. Crit Care. 2005;9:158–69. https://doi.org/10.1186/cc2978
2. Rosner F. Biblical quail incident. JAMA. 1970;211: 1544. https://doi.org/10.1001/jama.1970.03170090060017
3. Warren JD, Blumbergs PC, Thompson PD. Rhabdomyolysis: a review. Muscle Nerve. 2002;25:332–47. https://doi.org/10.1002/mus.10053

DOI: https://doi.org/10.3201/eid2607.ET2607

# Detection of Influenza A(H3N2) Virus RNA in Donated Blood

Rafael dos Santos Bezerra, Daniel Macedo de Melo Jorge, Ítalo Araújo Castro, Edson Lara Moretto, Leonardo Scalon de Oliveira, Eugênia Maria Amorim Ubiali, Dimas Tadeu Covas, Eurico Arruda, Simone Kashima, Svetoslav Nanev Slavov

Author affiliations: Blood Center of Ribeirao Preto, Ribeirao Preto, Brazil (R.S. Bezerra, E.L. Moretto, L.S. Oliveira, E.M.A. Ubiali, D.T. Covas, S. Kashima, S.N. Slavov); Faculty of Medicine of Ribeirao Preto–University of São Paulo, Ribeirao Preto (D.M.M. Jorge, I.A. Castro, E. Arruda)

DOI: https://doi.org/10.3201/eid2607.200549

Influenza A virus infection has rarely been documented to cause viremia. In 28 blood donations in Brazil that were deferred because of postdonation information, we identified influenza A(H3N2) virus RNA in 1 donation using metagenomic analysis. Our finding implies theoretical risk for viremia and transfusion transmission.

Influenza A virus is easily transmitted by respiratory aerosols and droplets and has high epidemic and pandemic potential (*1*). Influenza viremia may be established within 2–3 days before onset of clinical symptoms (*2*), implying that this virus is hypothetically transmissible by blood transfusion. However, transmission has never been confirmed, and efforts to detect influenza virus RNA among blood donors have been unsuccessful (*3*–*5*).

We performed next-generation sequencing and viral metagenomic survey in plasma samples aiming to identify viruses potentially associated with adverse effects reported by blood donors up to 14 days after donation (fever, exanthema, headache, myalgia, diarrhea, jaundice, sore throat, cough, conjunctivitis), which is defined as postdonation information. Such information generally results in disposal of the donated blood to prevent transfusion transmission of not routinely tested infectious agents.

During 2019, we performed Illumina sequencing (https://www.illumina.com) on blood donations identified through postdonation information in the Ribeirao Preto Blood Center (Ribeirao Preto, Brazil). We manually extracted viral nucleic acids from plasma using the High Pure Viral Nucleic Acids kit (Roche, https://www.roche.com) and performed reverse transcription using the SuperScript First Strand Synthesis System (ThermoFisher Scientific, https://www.thermofisher.com) following the manufacturer's guidelines. We generated cDNA libraries using Nextera DNA Flex Library preparation kit (Illumina) and sequenced them in Illumina NextSeq 550 equipment. We conducted viral metagenomic analysis using a bioinformatic pipeline focused on viral discovery comprising FastQC version 0.11.8 (https://www.bioinformatics.babraham.ac.uk/projects/fastqc), Trimmomatic version 0.3.9 (http://www.usadellab.org/cms/?page=trimmomatic), AfterQC version 0.9.7 (https://github.com/OpenGene/AfterQC), Kraken2 2.0.8 (https://ccb.jhu.edu/software/kraken2), SPAdes version 3.13.0 (http://cab.spbu.ru/software/spades), and Diamond 0.9.29 (https://github.com/bbuchfink/diamond) software.

In 1 (4%) of 28 blood donations, we identified RNA fragments of influenza A. The donor, a 25-year-old woman, donated blood on January 28, 2019, after an interview in which she was approved as eligible for blood donation. Three days later (January 30) she reported low-grade fever, cough, and coryza to the blood center. The blood donation positive for influenza A was processed into packed red cells, plasma, and platelets, but because of the timely postdonation information report, all hemoderivatives were discarded. Because of the low severity of the reported symptoms, which were not directly related to the blood donation procedure, the donor was not followed up.

The viral metagenomic pipeline identified a 756-bp fragment of polymerase base (PB) 2 gene of influenza A, but targeted assembly using Burrow-Wheeler Aligner version 0.6 (http://bio-bwa.sourceforge.net) detected other genomic regions like matrix 1 and 2 (252 bp), nucleoprotein (257 bp), and polymerase acidic frameshift protein (707 bp). We directly confirmed influenza A using multisegment reverse transcription PCR (RT-PCR) as described previously (*6*). We then amplified the hemagglutinin and neuraminidase segments individually by conventional PCR (*7*) using the multisegment RT-PCR product as input volume and sequenced. Consensus sequences of hemagglutinin (477 bp) and neuraminidase (647 bp) were aligned with MAFFT 7.0 software (ThermoFisher Scientific) using a dataset obtained from GISAID (https://www.gisaid.org), selecting strains from Brazil that circulated during 2011–2019. The phylogenetic analysis with IQ-TREE 2.0 software (http://www.iqtree.org) using hemagglutinin (264 sequences) and neuraminidase (419 sequences) applying the K3Pu+F+G4 and TVMe+G4 substitution models demonstrated that the strain clustered with isolates circulating during the 2019 epidemic season. The influenza A in the donated blood was phylogenetically determined


**Figure.** Maximum-likelihood phylogenetic tree of hemagglutinin (A) and neuraminidase (B) of influenza A(H3N2) virus detected in blood donation, Brazil. A total of 264 hemagglutinin and 419 neuraminidase sequences from seasonal strains circulating during 2011–2019 and available in GISAID (https://www.gisaid.org) were used to estimate the phylogenetic relationships with the influenza A virus detected in Ribeirao Preto, Brazil. Green indicates the H3N2 strain obtained from blood donor from Ribeirao Preto; diamonds at each node indicate statistical support along branches defined as ultrafast bootstrapping >90% (of 10,000 replicates). The cluster where the donor strain obtained from Ribeirao Preto is located is shown in detail at bottom. Scale bars indicate nucleotide substitutions per site.

to belong to H3N2 type (Figure). We deposited the magglutinin sequence in GenBank under accession no. MT126243 and the neuraminidase sequence under accession no. MT126244.

Influenza A viremia has been reported during acute-phase illness, mainly in patients infected with more pathogenic influenza viruses, such as H5N1 (*8*). Our study demonstrates the asymptomatic presence of influenza A virus RNA in blood donors preceding symptom onset, which provides theoretical grounds for the possibility of influenza transmission by blood transfusion. A study performed by the American Red Cross on 1,004 samples from blood donors reporting postdonation influenza symptoms detected no influenza-positive samples by RT-PCR during the first H1N1 outbreak in 2009 in the United States (*5*). Other studies conducted during the 2009 H1N1 pandemic also detected no viral RNA in persons who donated blood during the incubation period and in whom influenza symptoms developed 2-7 days after donation (*3*,*4*).

Although our report is based on a single blood donation, the finding raises the theoretical possibility of transmission of influenza by blood transfusion, which may be of great concern for transfusion services during seasonal influenza outbreaks or pandemics. Unfortunately, we could not confirm whether the detected influenza virus H3N2 remained infectious in the donated plasma. Nevertheless, identification of influenza RNA is especially important because a substantial proportion of persons who receive blood transfusions may have permanent or transient immune dysfunction, which might lead to unfavorable clinical outcome if transfusion-acquired influenza infection occurs. The transmission of influenza by transfusion remains understudied, and more detailed surveys are needed, including assessment of influenza viremia in blood donors during seasonal outbreaks and confirmation of cell-associated peripheral blood circulation of influenza subtypes.

### Acknowledgments

We thank Wilson Araujo da Silva, Jr., for providing the bioinformatic structure of the Blood Center of Ribeirao Preto and Sandra Navarro Bresciani for the figure.

The São Paulo Research Foundation (grant nos. 17/23205-8, 18/15826-5, 19/08528-0, and 19/07861-8) provided financial support for this study.

### About the Author

Mr. Bezerra is an MSc student in bioinformatics at Clinical Oncology, Stem Cells and Cell Therapy of the Faculty of Medicine of Ribeirao Preto, University of São Paulo. His research interests include emerging viruses in transfusion medicine and omics data analysis for their identification.

### References

1. Paules C, Subbarao K. Influenza. Lancet. 2017;390:697–708. https://doi.org/10.1016/S0140-6736(17)30129-0
2. Stanley ED, Jackson GG. Viremia in Asian influenza. Trans Assoc Am Physicians. 1966;79:376–87.
3. Sobata R, Matsumoto C, Igarashi M, Uchida S, Momose S, Hino S, et al. No viremia of pandemic (H1N1) 2009 was demonstrated in blood donors who had donated blood during the probable incubation period. Transfusion. 2011;51:1949–56. https://doi.org/10.1111/j.1537-2995.2011.03109.x
4. Matsumoto C, Sobata R, Uchida S, Hidaka T, Momose S, Hino S, et al. Risk for transmission of pandemic (H1N1) 2009 virus by blood transfusion. Emerg Infect Dis. 2010;16:722–3. https://doi.org/10.3201/eid1604.091795
5. Stramer SL, Collins C, Nugent T, Wang X, Fuschino M, Heitman JW, et al.; NHLBI Retrovirus Epidemiology Donor Study-II (REDS-II). Sensitive detection assays for influenza RNA do not reveal viremia in US blood donors. J Infect Dis. 2012;205:886–94. https://doi.org/10.1093/infdis/jir863
6. Venkatesh D, Poen MJ, Bestebroer TM, Scheuer RD, Vuong O, Chkhaidze M, et al. Avian influenza viruses in wild birds: virus evolution in a multihost ecosystem. J Virol. 2018;92:e00433–18. https://doi.org/10.1128/JVI.00433-18
7. Hoffmann E, Stech J, Guan Y, Webster RG, Perez DR. Universal primer set for the full-length amplification of all influenza A viruses. Arch Virol. 2001;146:2275–89. https://doi.org/10.1007/s007050170002
8. Likos AM, Kelvin DJ, Cameron CM, Rowe T, Kuehnert MJ, Norris PJ; National Heart, Lung, Blood Institute Retrovirus Epidemiology Donor Study-II (REDS-II). Influenza viremia and the potential for blood-borne transmission. Transfusion. 2007;47:1080–8. https://doi.org/10.1111/j.1537-2995.2007.01264.x

Address for correspondence: Svetoslav Nanev Slavov, Laboratory of Molecular Biology, Blood Center of Ribeirao Preto, Faculty of Medicine of Ribeirao Preto, University of São Paulo, 14051-060, Ribeirao Preto, São Paulo, Brazil; email: svetoslav.slavov@hemocentro.fmrp.usp.br

# Severe Acute Respiratory Syndrome Coronavirus 2 Shedding by Travelers, Vietnam, 2020

Thi Quynh Mai Le,[1] Taichiro Takemura,[1] Meng Ling Moi, Takeshi Nabeshima, Le Khanh Hang Nguyen, Vu Mai Phuong Hoang, Thi Hong Trang Ung, Thi Thanh Le, Vu Son Nguyen, Hong Quynh Anh Pham, Tran Nhu Duong, Hai Tuan Nguyen, Duy Nghia Ngu, Cong Khanh Nguyen, Kouichi Morita, Futoshi Hasebe, Duc Anh Dang

Author affiliations: National Institute of Hygiene and Epidemiology, Hanoi, Vietnam (T.Q.M. Le, L.K.H. Nguyen, V.M.P. Hoang, T.H.T. Ung, T.T. Le, V.S. Nguyen, H.Q.A. Pham, T.N. Duong, H.T. Nguyen, D.N. Ngu, C.K. Nguyen, D.A. Dang); World Health Organization Collaborating Center for Reference and Research on Tropical and Emerging Virus Diseases, Institute of Tropical Medicine, Nagasaki University, Nagasaki, Japan (T. Takemura, M.L. Moi, T. Nabeshima, K. Morita, F. Hasebe)

DOI: https://doi.org/10.3201/eid2607.200591

We analyzed 2 clusters of 12 patients in Vietnam with severe acute respiratory syndrome coronavirus 2 infection during January–February 2020. Analysis indicated virus transmission from a traveler from China. One asymptomatic patient demonstrated virus shedding, indicating potential virus transmission in the absence of clinical signs and symptoms.

During the past 2 months, emergence of 2019 novel coronavirus disease (COVID-19) has caused global public health concern (*1*,*2*). In light of the rapid global expansion of the disease, we performed a detailed epidemiologic and clinical assessment to determine the transmission patterns of the severe acute respiratory syndrome coronavirus 2 (SARS-CoV-2) outside China. As of March 6, 2020, imported SARS-CoV-2 infections have been identified in Vietnam; 17 cases (none severe) have been confirmed. Patients were 3 months to 65 years of age. Although transmission of SARS-CoV-2 may occur within days after illness onset, data on the early viremia kinetics in travelers are limited. We describe the virus shedding patterns in a cluster of travelers and in a cluster of patients who had close contact with the travelers.

On November 15, 2019, eight employees from a company in northern Vietnam (7 from Vinh Phuc Province, 1 from Thanh Hoa Province) were sent to Wuhan, China, for technical training for ≈2 months. On January 17, 2020, they returned to Vietnam via a flight from Wuhan to Guangzhou, China, followed by a flight from Guangzhou to Hanoi, Vietnam. During January 21–27, 2020, fever and cough developed in 6 of those travelers. Real-time PCR confirmed SARS-CoV-2 infection in all 6 travelers. Virus isolation and next-generation sequencing were performed for samples that were positive for viral RNA. The remaining 2 employees that had been on the same flight were quarantined, but real-time PCR indicated that they were negative for viral RNA. Patients were hospitalized at the National Hospital of Tropical Diseases, Thanh Hoa Provincial Hospital, and Tam Dao District Hospitals in Vinh Phuc Province, where they were closely monitored in isolated wards and followed up. Patient throat swab samples were sent to the Institute of Hygiene and Epidemiology, Hanoi, Vietnam, for laboratory diagnosis. The patients provided consent to have their details shared.

Among those tested for viral RNA by SARS-CoV–specific reverse transcription PCR, results were negative for 155 persons who had been in close contact with the 6 SARS-CoV–positive travelers and 1,092 persons exhibiting clinical signs, including cough and fever (*3*). Those with positive results were 6 of the persons sent to Wuhan for training (cluster 1), another 5 (cluster 2) who had been in close contact with a patient from cluster 1, and 1 patient in cluster 2 (patient 12) who had been in close contact with 2 other patients from cluster 2 (Table). We monitored SARS-CoV-2 viremia in 30 throat swab specimens obtained from the 12 patients in hospitals throughout Vietnam (3 male and 9 female; average age 31.2 years [range 3 months–55 years]).

Clinical signs, including fever and cough, were demonstrated by 11 patients an average of 9.9 (± 5.4) days after travel or close contact with patients, indicating that the incubation period was 1–2 weeks after exposure (*4*) (Appendix, https://wwwnc.cdc.gov/EID/article/26/7/20-0591-App1.pdf). In these patients, virus shedding was detected from day 1 after illness onset through day 19 (4.6 days) after potential initial exposure (Table). Of note, 1 patient in cluster 2 (patient 9, a 55-year-old man) was asymptomatic, but virus shedding was detected for up to 9 days (Table). This finding confirms virus shedding in asymptomatic patients and indicates possible transmission during the asymptomatic period. In this context, virus was isolated from 3 patients by inoculation of throat swab samples onto Vero cells.

[1]These authors contributed equally to this article.

**Table.** Characteristics of patients within 2 clusters of severe acute respiratory syndrome coronavirus 2 infection in Hanoi, Vietnam, December 2019–February 2020*

| Cluster, contact period, patient no. (relationship) | Age/sex | Possible incubation period, d† | Disease onset | Symptom onset to sample collection, d | Virus genome levels, Ct | | | Virus shedding period, d‡ |
|---|---|---|---|---|---|---|---|---|
| | | | | | E gene | *RdRp* gene | N gene | |
| Cluster 1: Travelers returning from Wuhan | | | | | | | | |
| 2019 Nov 15–2020 Jan 17 | | | | | | | | |
| 1 | 25 y/F | 7 | Jan 24 | 0 | 25.1 | 28.0 | 28.3 | 7 |
| 2 | 29 y/M | 4 | Jan 21 | 5 | 35.3 | 38.6 | 38.0 | 6 |
| 3 | 23 y/F | 8 | Jan 25 | 2 | 32.0 | 34.7 | 34.6 | 6 |
| 4 | 29 y/F | 12 | Jan 29 | 4 | 30.2 | 37.1 | 27.7 | 7 |
| 5 | 30 y/M | 9 | Jan 26 | 6 | 28.4 | >40.0 | 30.0 | 1 |
| 6 | 30 y/F | 14 | Jan 31 | 0 | 33.2 | >40.0 | 35.1 | 7 |
| Cluster 2: Contact with patient 3 | | | | | | | | |
| 2020 Jan 17–24, 28 | | | | | | | | |
| 7 (mother) | 49 y/F | 6 | Feb 3 | 1 | 28.1 | >40.0 | 32.5 | 9 |
| 8 (sister) | 16 y/F | 7 | Feb 4 | 0 | 28.8 | >40.0 | 23.3 | 9 |
| 9 (father)§ | 50 y/M | NA | Feb 4¶ | NA | >40.0 | >40.0 | >40.0 | 9 |
| | | NA | Feb 11 | NA | 30.0 | 34.0 | 33.0 | |
| | | NA | Feb 18 | NA | 26.0 | 28.0 | 30.0 | |
| 2020 Jan 22, 28 | | | | | | | | |
| 10 (cousin) | 42 y/F | 4 | Feb 1 | 2 | 29.4 | 36.0 | 31.4 | 4 |
| 2020 Jan 28 | | | | | | | | |
| 11 (neighbor) | 55 y/F | 3 | Jan 31 | 6 | 23.0 | 30.0 | 28.0 | 6 |
| 2020 Jan 28–Feb 3, contact with patients 10 and 11 | | | | | | | | |
| 12 (grandchild of patient 10)# | 3 mo/M | 3 | Feb 6 | 0 | 30.0 | 30.9 | 30.8 | 8 |

*Ct, cycle threshold; NA, not applicable because patient was asymptomatic; *RdRp*, RNA-dependent RNA polymerase.
†Possible incubation period calculation was based on last day of possible contact with patients and onset of disease. Cluster 1 travelers had returned from Wuhan, China, on January 17, 2020, on the same flight from Guangzhou, China, to Hanoi, Vietnam. All cluster 2 patients had contact with patient 3 of cluster 1. Although patient 3 returned from the epicenter of the outbreak and is the only patient with a link to cluster 2, the possibility of virus transmission between patients within the same cluster cannot be ruled out.
‡Virus shedding period was the interval from the day on which a sample was positive by real-time PCR to the day on which virus RNA was negative by real-time PCR. Real-time PCR was performed to detect 3 genes of the severe acute respiratory syndrome coronavirus 2 virus; namely, the E, N, and *RdRp* genes. Ct values ≥40.0 were considered negative.
§Patient was virus positive by real-time PCR on 2 consecutively collected samples.
¶Denotes sampling date because this patient was asymptomatic
#Patient had no direct contact with persons in cluster 1 but had close contact with persons in cluster 2.

Phylogenetic analyses of an isolate from patient 3 showed that the full-length genome had high sequence homology (99.96%) to a SARS-CoV-2 isolate identified in Wuhan, China (*5*).

Although close-contact transmission of SARS-CoV-2 between family members has been identified (*6*), evidence of virus circulation within the community in Vietnam is limited. We describe 6 cases of close-contact transmission between family members and those living in close proximity and determined virus shedding patterns of 12 patients in Vietnam. Because the virus was not circulating locally, our data provide insight into viral RNA shedding patterns from a potential point of exposure. Although patients were discharged after 2 consecutive negative PCR results, further assessment of the correlation of virus shedding with infectivity will be key for determining the risk for transmission during the viral RNA–positive phase. Given that the possibility of virus transmission between patients within the same cluster could not be ruled out and that the incubation period varies among individuals, uncertainties remain surrounding the estimated incubation period based on contact with patients. Further epidemiologic data are expected to improve the estimates of incubation period. We found limited community transmission of SARS-CoV-2 in Vietnam, and our data indicate that viremic travelers may pose a risk for introduction of virus strains that could potentially lead to outbreaks within a local community.

**Acknowledgment**

We thank healthcare practitioners of the clinics and hospitals in Vietnam who supported the study.

This research was supported by Vingroup Innovation Foundation, Vietnam (VINIF.2020.COVID-19.DA01), the Japan Agency for Medical Research and Development Japan Initiative for Global Research Network on Infectious Diseases (JP19fm010800), the Japan Agency for Medical Research and Development Research on Emerging and Re-emerging Infectious Diseases (19fk0108035j0003 and 19fk0108109h0001), and the Japan Society for the Promotion of Science KAKENHI (JP19K24679).

## About the Authors

Dr. Le is deputy director at the National Institute of Hygiene and Epidemiology, Hanoi, Vietnam. Her research interest is the epidemiology of tropical and emerging infectious diseases. Dr. Takemura is assistant professor at the Institute of Tropical Medicine, Nagasaki University, Japan. His research interests include molecular epidemiologic studies on viral and bacterial diseases.

## References


1. World Health Organization. Statement on the second meeting of the International Health Regulations (2005) Emergency Committee regarding the outbreak of novel coronavirus (2019-nCoV) [cited 2020 Feb 18]. https://www.who.int/news-room/detail/30-01-2020-statement-on-the-second-meeting-of-the-international-health-regulations-(2005)-emergency-committee-regarding-the-outbreak-of-novel-coronavirus-(2019-ncov)
2. Zhu N, Zhang D, Wang W, Li X, Yang B, Song J, et al.; China Novel Coronavirus Investigating and Research Team. A novel coronavirus from patients with pneumonia in China, 2019. N Engl J Med. 2020;382:727–33. https://doi.org/10.1056/NEJMoa2001017
3. Corman VM, Landt O, Kaiser M, Molenkamp R, Meijer A, Chu DKW, et al. Detection of 2019 novel coronavirus (2019-nCoV) by real-time RT-PCR. Euro Surveill. 2020;25:25. https://doi.org/10.2807/1560-7917.ES.2020.25.3.2000045
4. Rothe C, Schunk M, Sothmann P, Bretzel G, Froeschl G, Wallrauch C, et al. Transmission of 2019-nCoV infection from an asymptomatic contact in Germany. N Engl J Med. 2020;382:970–1. https://doi.org/10.1056/NEJMc2001468
5. Chen N, Zhou M, Dong X, Qu J, Gong F, Han Y, et al. Epidemiological and clinical characteristics of 99 cases of 2019 novel coronavirus pneumonia in Wuhan, China: a descriptive study. Lancet. 2020;395:507–13. https://doi.org/10.1016/S0140-6736(20)30211-7
6. Phan LT, Nguyen TV, Luong QC, Nguyen TV, Nguyen HT, Le HQ, et al. Importation and human-to-human transmission of a novel coronavirus in Vietnam. N Engl J Med. 2020;382:872–4. https://doi.org/10.1056/NEJMc2001272


Address for correspondence: Futoshi Hasebe, WHO Collaborating Center for Reference and Research on Tropical and Emerging Virus Diseases, Institute of Tropical Medicine, Nagasaki University, 1-12-4 Sakamoto, Nagasaki 852-8523, Japan; email: rainbow@nagasaki-u.ac.jp; Duc Anh Dang, National Institute of Hygiene and Epidemiology, 1 Yersin St, Hanoi 10000, Vietnam; email: dda@nihe.org.vn

# Asymptomatic and Human-to-Human Transmission of SARS-CoV-2 in a 2-Family Cluster, Xuzhou, China

Chunyang Li,[1] Fang Ji,[1] Liang Wang,[1] Liping Wang, Jungui Hao, Mingjia Dai, Yan Liu, Xiucheng Pan, Juanjuan Fu, Li Li, Guangde Yang, Jianye Yang, Xuebing Yan, Bing Gu

Author affiliations: Department of Infectious Disease, Affiliated Hospital of Xuzhou Medical University, Xuzhou, China (C. Li, F. Ji, L. Wang, J. Hao, M. Dai, Y. Liu, X. Pan, J. Fu, L. Li, G. Yang, X Yan); Department of Bioinformatics, School of Medical Informatics, Xuzhou Medical University, Xuzhou (L. Wang); Jiangsu Key Laboratory of New Drug Research and Clinical Pharmacy, School of Pharmacy, Xuzhou Medical University, Xuzhou (L. Wang); Medical Technology School of Xuzhou Medical University, Xuzhou Key Laboratory of Laboratory Diagnostics, Xuzhou (B. Gu); Department of Laboratory Medicine, Affiliated Hospital of Xuzhou Medical University, Xuzhou (B. Gu)

DOI: https://doi.org/10.3201/eid2607.200718

We report epidemiologic, laboratory, and clinical findings for 7 patients with 2019 novel coronavirus disease in a 2-family cluster. Our study confirms asymptomatic and human-to-human transmission through close contacts in familial and hospital settings. These findings might also serve as a practical reference for clinical diagnosis and medical treatment.

The ongoing outbreak of 2019 novel coronavirus disease (COVID-19) originating from Wuhan, China, has spread rapidly across the world (*1*). Both human-to-human and asymptomatic transmission have been reported (*2*,*3*). Phylogenetic study reveals that severe acute respiratory syndrome (SARS) coronavirus 2 (SARS-CoV-2), the causative agent of COVID-19, is closely related to 2 SARS-CoV–like bat coronaviruses, bat-SL-CoVZC45 and bat-SL-CoVZXC2 (*4*). Although case-fatality rate for COVID-19 is not finalized yet (*5*), it is largely accepted that the infection is less fatal than that for SARS-CoV infection, which had an ≈10% case-fatality rate (*6*).

Typical symptoms of COVID-19 include fever, cough, and fatigue, whereas sputum, headache, hemoptysis, and diarrhea are less common (*7*). No vaccine to prevent the infection exists. In this study, we describe a cluster of 7 COVID-19 case-patients among whom interfamilial and intrafamilial transmission

[1]These authors contribute equally to the study.

occurred. Our findings are consistent with previous confirmation of asymptomatic and human-to-human transmission of SARS-CoV-2 in family and hospital settings and also provide practical reference for clinical diagnosis and treatment of COVID-19.

On January 14, 2020, a 56-year-old man (index patient) departed from Guangzhou, China, transferred at Hankou Station in Wuhan, China, for 6 hours, and arrived at Xuzhou, China, showing no symptoms on the same day in the evening. During January 14–22, he had close contact with his 2 daughters, a 32-year-old pregnant teacher (patient 1) and a 21-year-old undergraduate student (patient 2). On January 15, he began caring for his 42-year-old son-in-law (patient 3, husband of patient 1), who had been hospitalized at the Affiliated Hospital of Xuzhou Medical University in Xuzhou until January 23. Meanwhile, a 62-year-old man (patient 4) stayed in the hospital during January 2–19 because of pancreatic surgery; he shared the same ward with patient 3 and was cared for by his 34-year-old son (patient 5). During January 15–January 18, patients 4 and 5 had close contact with the index patient, who was asymptomatic during that time. On January 19, patient 4 was discharged to home and had close contact with his 56-year-old wife (patient 6). We compiled a comprehensive illustration of the contact history of the clustered cases (Figure).

On January 25, the index patient was confirmed to have COVID-19 and was admitted to the Affiliated Hospital of Xuzhou Medical University with symptoms of fever, cough, and sore throat. His illness rapidly became severe; he had a high respiratory rate (38 breaths/min) and low oximetry saturation (≤93%). Subsequently, during January 26–31, another 6 members of the 2 families all tested positive for SARS-CoV-2 by real-time fluorescent reverse transcription PCR of their throat swab samples. The clinical features of these patients varied (Appendix Table 1, https://wwwnc.cdc.gov/EID/article/26/7/20-0718-App1.pdf).

We used imaging features of pneumonia (detected using chest computed tomography) as clinical confirmation for all patients except patient 1. We performed laboratory diagnostic tests, including routine blood tests, comprehensive metabolic panels, coagulation tests, and screening for infection for all patients (Appendix Tables 2–4). We provided all patients with medical therapy (Appendix Table 5, Figure 1) except patient 1, who was pregnant. Because the index patient was in severe condition during his hospitalization, we have included a more detailed description of his medical treatment.

During January 26–February 3, we administered to the index patient the antiviral drugs lopinavir/ritonavir (400 mg/100 mg 2×/d by mouth), umifenovir (200 mg 3×/d by mouth), and interferon α-2b (5 MIU 2×/d by aerosolized inhalation). We administered the antibacterial drug moxifloxacin hydrochloride (400 mg 1×/d by intravenous drip)

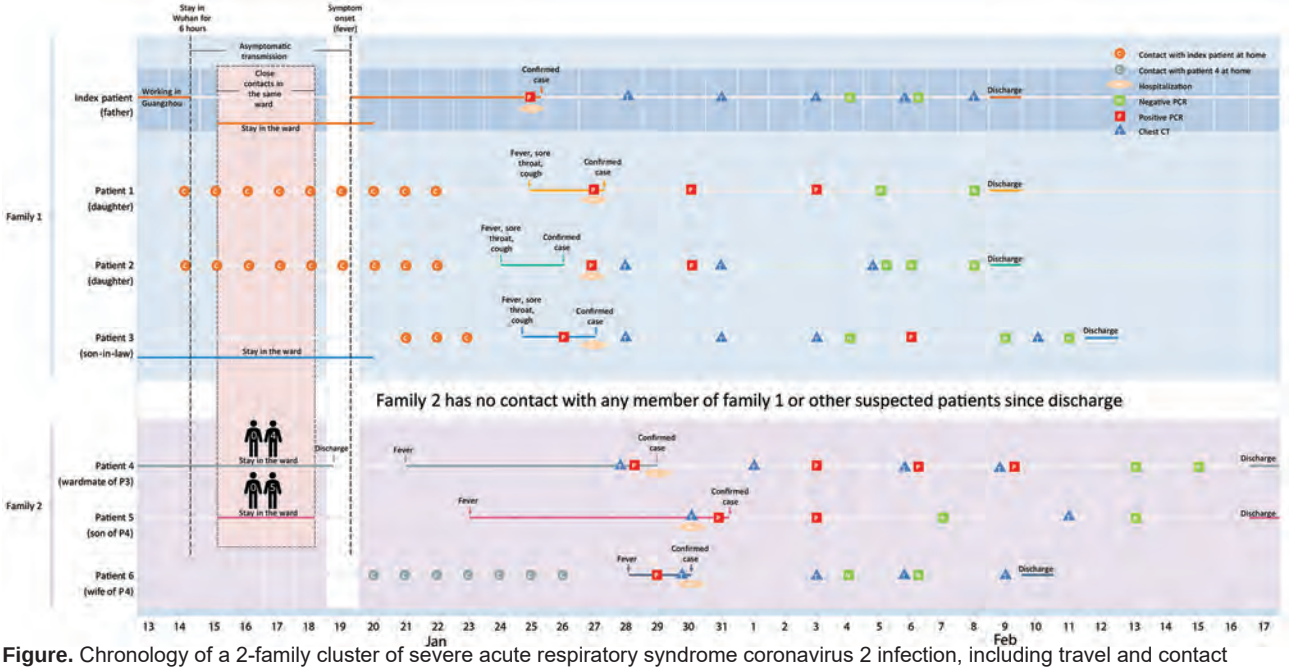


**Figure.** Chronology of a 2-family cluster of severe acute respiratory syndrome coronavirus 2 infection, including travel and contact history, in familial and hospital settings, Xuzhou, China, January 13–February 17, 2020. Dates of case confirmation, hospitalization, and discharge are labeled. Real-time fluorescent reverse transcription PCR for severe acute respiratory syndrome coronavirus 2 infection and corresponding results are indicated, together with the dates of chest CT. CT, computed tomography.

during January 28–February 6, 2020, and intravenous immunoglobulin therapy (20 g/d) during January 28–February 1. In addition, we administered glucocorticoid therapy with methylprednisolon (20–60 mg 2×/d by intravenous drip) during January 29–February 1. The patient's fever abated on January 29. He tested negative for SARS-CoV-2 on February 4 and again on February 6. During the progression of his recovery, we observed gradual reduction of the white patches in the lung caused by SARS-CoV-2 infection (Appendix Figure 2). On January 28 and January 31, we observed multiple ground-glass–like high-density shadows on both lungs with blurred edges and interstitial changes. On February 3, high-density shadows were slightly absorbed in the upper lobe of the bilateral lungs. On February 6, some lesions in the lower lobe of both lungs were slightly absorbed, and we observed the same situation on February 8. The index patient was discharged to home on February 9.

In summary, our epidemiologic study demonstrates asymptomatic and human-to-human transmission of SARS-CoV-2 infection through close contacts in both familial and hospital settings. In addition, the laboratory test results, together with course of medical therapies described, can provide a practical reference for COVID-19 diagnosis and treatment.

### About the Author

Dr. Li specializes in infectious diseases and works as a clinical doctor at the Department of Infectious Disease at the Affiliated Hospital of Xuzhou Medical University, Xuzhou, Jiangsu Province, China. His primary research interests included clinical microbiologic detection and emerging infectious diseases.

### References


1. To KK-W, Tsang OT-Y, Chik-Yan Yip C, Chan K-H, Wu T-C, Chan JMC, et al. Consistent detection of 2019 novel coronavirus in saliva. Clin Infect Dis. 2020 Feb 12 [Epub ahead of print]. https://doi.org/10.1093/cid/ciaa149
2. Chan JF-W, Yuan S, Kok K-H, To KK-W, Chu H, Yang J, et al. A familial cluster of pneumonia associated with the 2019 novel coronavirus indicating person-to-person transmission: a study of a family cluster. Lancet. 2020;395:514–23. https://doi.org/10.1016/S0140-6736(20)30154-9
3. Rothe C, Schunk M, Sothmann P, Bretzel G, Froeschl G, Wallrauch C, et al. Transmission of 2019-nCoV infection from an asymptomatic contact in Germany. N Engl J Med. 2020;382:970–1. https://doi.org/10.1056/NEJMc2001468
4. Lu R, Zhao X, Li J, Niu P, Yang B, Wu H, et al. Genomic characterisation and epidemiology of 2019 novel coronavirus: implications for virus origins and receptor binding. Lancet. 2020;395:565–74. https://doi.org/10.1016/S0140-6736(20)30251-8
5. Baud D, Qi X, Nielsen-Saines K, Musso D, Pomar L, Favre G. Real estimates of mortality following COVID-19 infection. Lancet Infect Dis. 2020 Mar 12 [Epub ahead of print]. http://doi.org/10.1016/S1473-3099(20)30195-X
6. Jiang S, Xia S, Ying T, Lu L. A novel coronavirus (2019-nCoV) causing pneumonia-associated respiratory syndrome. Cell Mol Immunol. 2020 Feb 5 [Epub ahead of print]. https://doi.org/10.1038/s41423-020-0372-4
7. Huang C, Wang Y, Li X, Ren L, Zhao J, Hu Y, et al. Clinical features of patients infected with 2019 novel coronavirus in Wuhan, China. Lancet. 2020;395:497–506. https://doi.org/10.1016/S0140-6736(20)30183-5


Addresses for correspondence: Dr. Bing Gu, Department of Laboratory Medicine, Affiliated Hospital of Xuzhou Medical University, No. 99 West Huai'hai Rd, Xuzhou, Jiangsu, 221006, China; email: binggu2015@xzhmu.edu.cn; or Dr. Xuebing Yan, Department of Infectious Disease, Affiliated Hospital of Xuzhou Medical University, No. 99 West Huai'hai Rd, Xuzhou, Jiangsu, 221006, China; email: yxbxuzhou@126.com

# COVID-19 Outbreak Associated with Air Conditioning in Restaurant, Guangzhou, China, 2020

Jianyun Lu,[1] Jieni Gu,[1] Kuibiao Li,[1] Conghui Xu,[1] Wenzhe Su, Zhisheng Lai, Deqian Zhou, Chao Yu, Bin Xu, Zhicong Yang

Author affiliations: Guangzhou Center for Disease Control and Prevention, Guangzhou, China (J. Lu, K. Li, C. Xu, W. Su, C. Yu, Z. Yang); Guangzhou Yuexiu District Center for Disease Control and Prevention, Guangzhou, China (J. Gu, Z. Lai, D. Zhou, B. Xu)

DOI: https://doi.org/10.3201/eid2607.200764

During January 26–February 10, 2020, an outbreak of 2019 novel coronavirus disease in an air-conditioned restaurant in Guangzhou, China, involved 3 family clusters. The airflow direction was consistent with droplet transmission. To prevent the spread of the virus in restaurants, we recommend increasing the distance between tables and improving ventilation.

From January 26 through February 10, 2020, an outbreak of 2019 novel coronavirus disease (COVD-19) affected 10 persons from 3 families (families A–C)

[1]These authors contributed equally to this article.

who had eaten at the same air-conditioned restaurant in Guangzhou, China. One of the families had just traveled from Wuhan, Hubei Province, China. We performed a detailed investigation that linked these 10 cases together. Our study was approved by the Ethics Committee of the Guangzhou Center for Disease Control and Prevention.

On January 23, 2020, family A traveled from Wuhan and arrived in Guangzhou. On January 24, the index case-patient (patient A1) ate lunch with 3 other family members (A2–A4) at restaurant X. Two other families, B and C, sat at neighboring tables at the same restaurant. Later that day, patient A1 experienced onset of fever and cough and went to the hospital. By February 5, a total of 9 others (4 members of family A, 3 members of family B, and 2 members of family C) had become ill with COVID-19.

The only known source of exposure for the affected persons in families B and C was patient A1 at the restaurant. We determined that virus had been transmitted to ≥1 member of family B and ≥1 member of family C at the restaurant and that further infections in families B and C resulted from within-family transmission.

Restaurant X is an air-conditioned, 5-floor building without windows. The third floor dining area occupies 145 $m^2$; each floor has its own air conditioner (Figure). The distance between each table is about 1 m. Families A and B were each seated for an overlapping period of 53 minutes and families A and C for an overlapping period of 73 minutes. The air outlet and the return air inlet for the central air conditioner were located above table C (Figure, panel B).

On January 24, a total of 91 persons (83 customers, 8 staff members) were in the restaurant. Of these, a total of 83 had eaten lunch at 15 tables on the third floor. Among the 83 customers, 10 became ill with COVID-19; the other 73 were identified as close contacts and quarantined for 14 days. During that period, no symptoms developed, and throat swab samples from the contacts and 6 smear samples from the air conditioner (3 from the air outlet and 3 from the air inlet) were negative for severe acute respiratory syndrome coronavirus 2 by reverse transcription PCR.

From our examination of the potential routes of transmission, we concluded that the most likely cause of this outbreak was droplet transmission. Although the index patient (patient A1) was asymptomatic during the lunch, presymptomatic transmission has been reported (*1*). Given the incubation periods for family B (Appendix Figure, https://wwwnc.cdc.gov/EID/article/26/7/20-0764-App1.pdf), the most likely scenario is that all 3 family B members were directly infected by patient A1. However, we cannot not exclude the possibility that patients B2 and B3 were infected by patient B1, the first family B member to become ill. For family C, a possible scenario is that both patients C1 and C2 were infected by patient A1; another scenario is that the patient C1 acquired the infection while caring for patient C2, beginning on January 27.

Virus transmission in this outbreak cannot be explained by droplet transmission alone. Larger respiratory droplets (>5 μm) remain in the air for only a short time and travel only short distances, generally <1 m (*2*,*3*). The distances between patient A1 and persons at other tables, especially those at table C, were all >1 m. However, strong airflow from the air conditioner could have propagated droplets from table C to table A, then to table B, and then back to table C (Figure).

Virus-laden small (<5 μm) aerosolized droplets can remain in the air and travel long distances, >1 m (*4*). Potential aerosol transmission of severe acute respiratory syndrome and Middle East respiratory syndrome viruses has been reported (*5*,*6*). However, none of the staff or other diners in restaurant X were infected. Moreover, the smear samples from the air conditioner were all nucleotide negative. This finding is less consistent with aerosol transmission. However, aerosols would tend to follow the airflow, and the lower concentrations of aerosols at greater distances might have been insufficient to cause infection in other parts of the restaurant.

Our study has limitations. We did not conduct an experimental study simulating the airborne transmission route. We also did not perform serologic studies of swab sample–negative asymptomatic family members and other diners to estimate risk for infection.

We conclude that in this outbreak, droplet transmission was prompted by air-conditioned ventilation. The key factor for infection was the direction of the airflow. Of note, patient B3 was afebrile and 1% of the patients in this outbreak were asymptomatic, providing a potential source of outbreaks among the public (*7*,*8*). To prevent spread of COVID-19 in restaurants, we recommend strengthening temperature-monitoring surveillance, increasing the distance between tables, and improving ventilation.

This study was supported by the Medical Health Technology Project for Guangzhou (20181A011051), the Science and Technology Project of Guangzhou (201804010093, 201707010451), and the Project for Key Medicine Discipline Construction of Guangzhou Municipality (2017-2019-07).

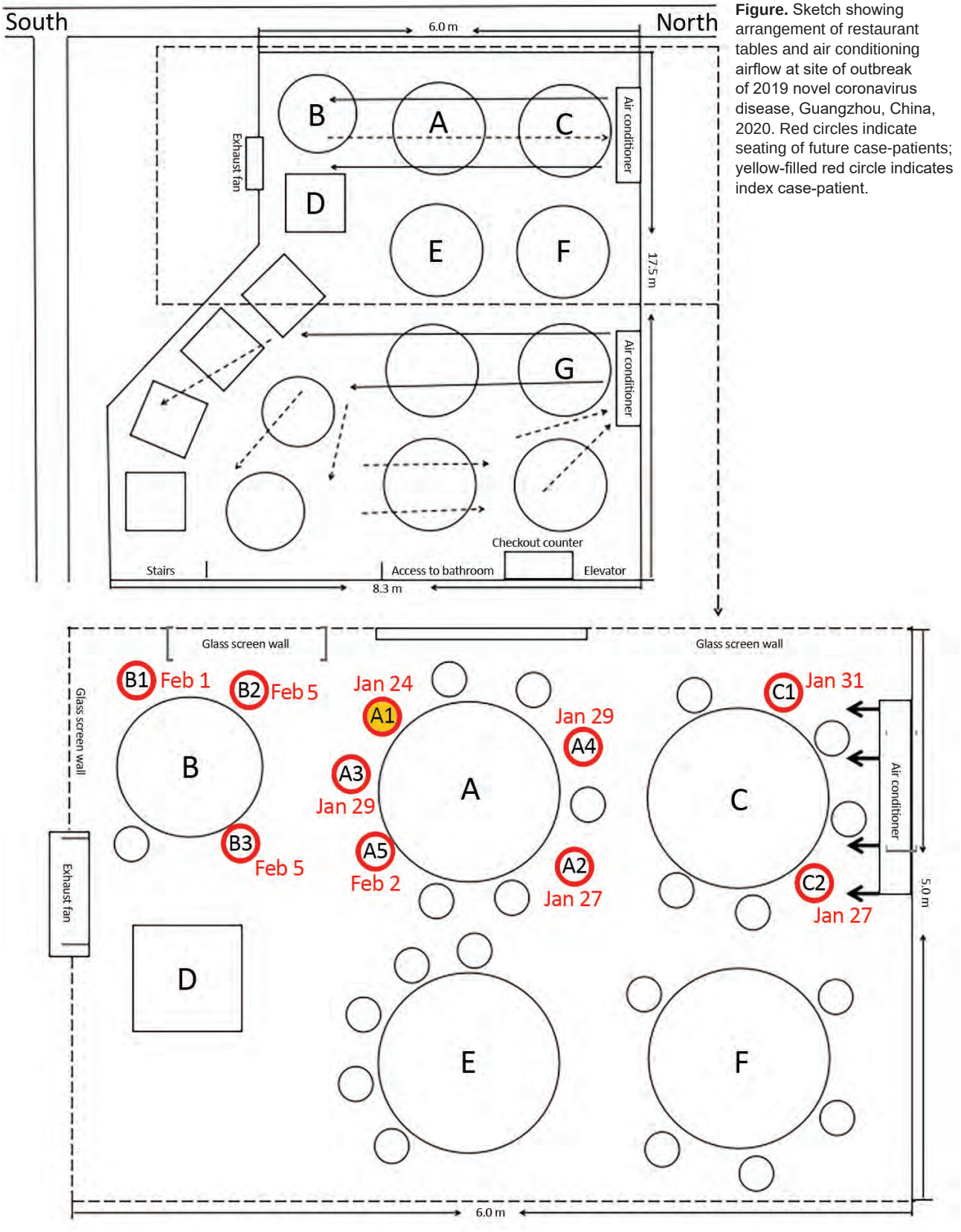


**Figure.** Sketch showing arrangement of restaurant tables and air conditioning airflow at site of outbreak of 2019 novel coronavirus disease, Guangzhou, China, 2020. Red circles indicate seating of future case-patients; yellow-filled red circle indicates index case-patient.

## About the Author

Mr. Lu is deputy chief of the Department of Control and Prevention for Infectious Disease at the Guangzhou Center for Disease Control and Prevention. His research interests are the surveillance, control, and prevention of respiratory infectious diseases, including influenza, avian influenza, and scarlet fever.

## References


1. Han Y, Zhang Z, Zhu J, Yu P. A familial cluster of infection associated with the 2019 novel coronavirus indicating possible person-to-person transmission during the incubation period. J Infect Dis. 2020;395:514–23.
2. Pica N, Bouvier NM. Environmental factors affecting the transmission of respiratory viruses. Current Opin Virol. 2012;2:90–5.
3. Kutter JS, Spronken MI, Fraaij PL, Fouchier RA, Herfst S. Transmission routes of respiratory viruses among humans. Curr Opin Virol. 2018;28:142–51. https://doi.org/10.1016/j.coviro.2018.01.001
4. Fernstrom A, Goldblatt M. Aerobiology and its role in the transmission of infectious diseases. J Pathogens. 2013;2013:493960. https://doi.org/10.1155/2013/493960
5. Lee N, Hui D, Wu A, Chan P, Cameron P, Joynt GM, et al. A major outbreak of severe acute respiratory syndrome in Hong Kong. N Engl J Med. 2003;348:1986–94. https://doi.org/10.1056/NEJMoa030685
6. Kim SH, Chang SY, Sung M, Park JH, Bin Kim H, Lee H, et al. Extensive viable Middle East respiratory syndrome (MERS) coronavirus contamination in air and surrounding environment in MERS isolation wards. Clin Infect Dis. 2016;63:363–9. https://doi.org/10.1093/cid/ciw239
7. Tong ZD, Tang A, Li KF, Li P, Wang HL, Yi JP, et al. Potential presymptomatic transmission of SARS-CoV-2, Zhejiang Province, China, 2020. Emerg Infect Dis. 2020 Mar 9 [Epub ahead of print]. https://doi.org/10.3201/eid2605.200198
8. Chan JF-W, Yuan S, Kok K-H, To KK-W, Chu H, Yang J, et al. A familial cluster of pneumonia associated with the 2019 novel coronavirus indicating person-to-person transmission: a study of a family cluster. Lancet. 2020;395:514–23. https://doi.org/10.1016/S0140-6736(20)30154-9


Address for correspondence: Zhicong Yang, Guangzhou Center for Disease Control and Prevention, Guangzhou, Guangdong Province 510440, China; email: yangzc@gzcdc.org.cn; Bin Xu, Guangzhou Yuexiu District Center for Disease Control and Prevention, Guangzhou, Guangdong Province 510100, China; email: xubin6710@163.com

# Severe Acute Respiratory Syndrome Coronavirus 2 RNA Detected in Blood Donations

Le Chang,[1] Lei Zhao,[1] Huafei Gong, Lunan Wang, Lan Wang

Author affiliations: National Center for Clinical Laboratories, Beijing Hospital, National Center of Gerontology; Institute of Geriatric Medicine, Chinese Academy of Medical Sciences, Beijing, China (L. Chang, Lunan Wang); Wuhan Blood Center, Wuhan, China (L. Zhao, Lan Wang); Shanghai Haoyuan Biotech Co., Ltd, Shanghai, China (H. Gong); Peking Union Medical College Graduate School, Chinese Academy of Medical Sciences, Beijing (Lunan Wang)

DOI: https://doi.org/10.3201/eid2607.200839

Because of high rates of 2019 novel coronavirus disease in Wuhan, China, Wuhan Blood Center began screening for severe acute respiratory syndrome coronavirus 2 RNA on January 25, 2020. We screened donations in real-time and retrospectively and found plasma samples positive for viral RNA from 4 asymptomatic donors.

Because of the rapid increase of cases of 2019 novel coronavirus disease (COVID-19; *1*) and detection of severe acute respiratory syndrome coronavirus 2 (SARS-CoV-2) RNA in plasma (*2*,*3*), the safety of China's blood supply became a major concern (*4*). Most blood centers and blood banks in China began taking measures to ensure blood safety (*5*); on January 25, 2020, we began screening all donations collected at the Wuhan Blood Center.

We performed real-time reverse transcription PCR (RT-PCR) for SARS-CoV-2 RNA by using MultiScreen Pro RT-PCR assay (SYM-BIO LifeScience, https://www.sym-bio.com.cn). We performed pool testing by mixing plasma from 6–8 samples or individual testing by using 1.6 mL of plasma. We eluted 100 μL of nucleic acid template and added 40 μL of it to the RT-PCR mix.

By March 4, we had screened 2,430 donations in real-time, including 1,656 platelet and 774 whole blood donations. We identified the first positive donor in our center in a positive pool with a weak amplification of the open reading frame 1ab gene. The donor gave 2 units of platelets on January 28, which were included in the pool. However, the donor's prior donations collected on December 12 and 26 and January 13 were negative for viral RNA. Hubei Province Center for Disease Control and Prevention performed follow-up

[1]These authors contributed equally to this article.

tests on plasma on February 2, which showed a weak positive result near the limit of detection; a throat swab specimen collected from the donor on February 10 also was positive, indicating an extremely low viral load in plasma. The donor reported no symptoms and was quarantined in a cabin hospital in Wuhan until 2 consecutive negative throat swab results on February 23 and February 25 (Figure).

We also performed retrospective testing of 4,995 donations collected during December 21, 2019–January 22, 2020, by using retained nucleic acid template after routine pool testing. On February 10, we found a positive result in a nucleic acid template derived from donations collected on January 19. We individually tested samples that were in storage at 2°C–8°C for 23 days because no plasma samples stored at -20°C were available. We identified another positive donor of whole blood. We tested plasma products from his donation twice and noted similar results, which suggests that viral RNA is relatively stable in plasma (Appendix Table, https://wwwnc.cdc.gov/EID/article/26/7/20-0839-App1.pdf). We immediately traced all blood products produced from donor 2's whole blood, and they had not been used. Telephone follow-ups on February 15 and 25 showed donor 2 remained asymptomatic and quarantined at home.

In telephone follow-ups with donors who gave blood during January and February, we identified 33 donors who developed a fever after donation; all of their donations were removed from circulation. We performed retrospective individual screening on frozen plasma products from 17 donors and tested the retained nucleic acid templates after routine pool testing of the other 16 donors. We found 2 more positive donors who donated whole blood on January 20. Both had weak positive results, and donors reported fever onset on January 21 (Figure; Appendix Table). Donor 3 treated patients infected with SARS-CoV-2 in a Wuhan hospital. His temperature returned to normal 8 days after donation. Donor 4's temperature also returned to normal 7 days after taking self-prescribed antipyretic medications.

By March 4, we identified 4 blood donors in Wuhan whose plasma samples tested positive for SARS-CoV-2 RNA (Figure; Appendix Table). Samples from these donors were further tested for specific IgG and IgM against SARS-CoV-2 by ELISA; results were negative, indicating the possibility of infection in the early stage and the need to follow-up with these donors.

We found SARS-CoV-2 RNA in plasma during routine screening of blood donors, considered a healthy population. We tested the 4 donors multiple times, using different sample sources, including sample tubes, retained nucleic acid templates, or blood products, indicating the accuracy and validity of our results (Appendix Table). One limitation of our study is that we did not have more detailed information on donors 2, 3, and 4. Although we could not confirm virions in blood or whether the virus could be transmitted in blood products, the potential risk should not be neglected. However, detectable RNA might not signify infectivity. Further studies, such as virus culture, should be done to explore the possibility of viremia and follow-up of donors also is essential.

Of note, the donors all donated in late January, and we did not detect SARS-CoV-2 in plasma samples after then, indicating the strict containment measures taken by the government of China were effective. In China, donors are screened for related symptoms and asked if they feel healthy when they donate blood. Having donors call the blood donation center if they have any symptoms after donating is essential to avoid the risk of donation during the COVID-19 incubation period. Moreover, as more asymptomatic cases occur, screening donors

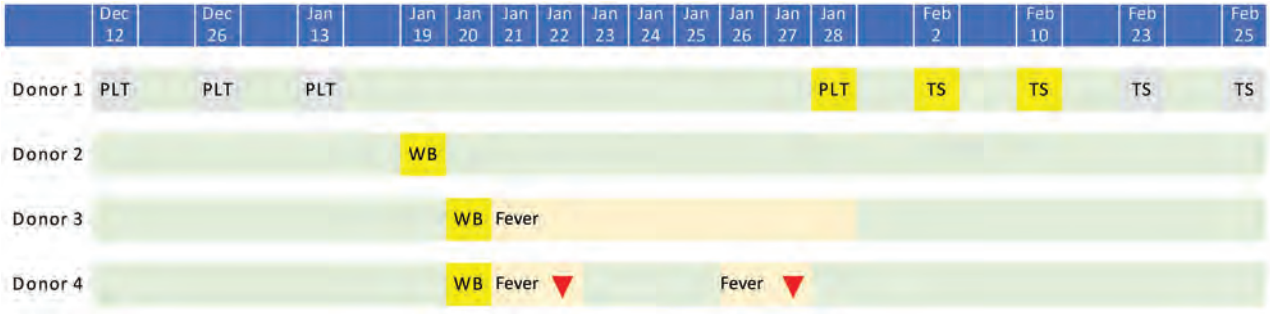


**Figure.** Timeline of donations and symptom onset of 2019 novel coronavirus disease from 4 blood donors, China. Gray indicates a negative result for severe acute respiratory syndrome coronavirus 2 (SARS-CoV-2) RNA; yellow indicates a positive result. Green indicates the donor was asymptomatic or their temperature returned to normal; orange indicates fever; red triangle indicates the donor's fever subsided after taking self-prescribed antipyretic medications. PLT, platelet; TS, throat swab; WB, whole blood.

for viral RNA with high-sensitivity assays, as we are doing in Hubei Province, will be critical to ensure blood safety.

H.G. is employed by Shanghai Haoyuan Biotech Co., Ltd. No other authors have disclosures to declare.

### About the Author

Dr. Chang works as research assistant professor in National Center for Clinical Laboratories, Beijing Hospital, focusing on the detection of transfusion-transmitted infectious pathogens. Dr. Zhao is chief of the laboratory department of Wuhan Blood Center. His primary focus is detection of transfusion-transmitted infectious pathogens.

### References

1. Chinese Center for Disease Control and Prevention; The Novel Coronavirus Pneumonia Emergency Response Epidemiology Team. Vital surveillances: the epidemiological characteristics of an outbreak of 2019 novel coronavirus diseases (COVID-19)—China, 2020. China CDC weekly 2020;2:113–122 [cited 2020 Mar 18]. http://www.ne.jp/asahi/kishimoto/clinic/cash/COVID-19.pdf
2. Huang C, Wang Y, Li X, Ren L, Zhao J, Hu Y, et al. Clinical features of patients infected with 2019 novel coronavirus in Wuhan, China. Lancet. 2020;395:497–506. https://doi.org/10.1016/S0140-6736(20)30183-5
3. Zhang W, Du RH, Li B, Zheng XS, Yang XL, Hu B, et al. Molecular and serological investigation of 2019-nCoV infected patients: implication of multiple shedding routes. Emerg Microbes Infect. 2020;9:386–9. https://doi.org/10.1080/22221751.2020.1729071
4. Chang L, Yan Y, Wang L. Coronavirus disease 2019: coronaviruses and blood safety. Transfus Med Rev. 2020 Feb 21 [Epub ahead of print]. https://doi.org/10.1016/j.tmrv.2020.02.003
5. Chinese Society of Blood Transfusion. Recommendations on blood collection and supply during the epidemic of novel coronavirus pneumonia in China, 1st edition [in Chinese]. 2020 Feb 5 [cited 2020 Mar 18] https://www.csbt.org.cn/plus/view.php?aid=16530

Addresses for correspondence: Lunan Wang, National Center for Clinical Laboratories, Beijing Hospital, No. 1 Dahua Rd, Beijing 100730, China; email: lunan99@163.com; Lan Wang, Wuhan Blood Center, No. 8 Baofengyi Rd, Wuhan 430030, China; email: wlan66@126.com

# Triplex Real-Time RT-PCR for Severe Acute Respiratory Syndrome Coronavirus 2

Jesse J. Waggoner, Victoria Stittleburg, Renee Pond, Youssef Saklawi, Malaya K. Sahoo, Ahmed Babiker, Laila Hussaini, Colleen S. Kraft, Benjamin A. Pinsky, Evan J. Anderson, Nadine Rouphael

Author affiliations: Emory University, Atlanta, Georgia, USA (J.J. Waggoner, V. Stittleburg, R. Pond, Y. Saklawi, A. Babiker, L. Hussaini, C.S. Kraft, E.J. Anderson, N. Rouphael); Stanford University, Stanford, California, USA (M.K. Sahoo, B.A. Pinsky)

DOI: https://doi.org/10.3201/eid2607.201285

Most reverse transcription PCR protocols for severe acute respiratory syndrome coronavirus 2 (SARS-CoV-2) include 2–3 targets for detection. We developed a triplex, real-time reverse transcription PCR for SARS-CoV-2 that maintained clinical performance compared with singleplex assays. This protocol could streamline detection and decrease reagent use during current high SARS-CoV-2 testing demands.

Detection of severe acute respiratory syndrome coronavirus 2 (SARS-CoV-2) typically relies on molecular testing of respiratory tract specimens, although viral RNA can be detected in other specimens (*1*). Real-time reverse transcription PCR (rRT-PCR) protocols have been described for SARS-CoV-2, but most involve testing with multiple, singleplex reactions (*2*–*6*). Such algorithms use large volumes of reagents and limit laboratory testing capacity, both of which have become crucial during the ongoing coronavirus disease pandemic (*7*). Multiplex assays are commercially available (*8*,*9*) but require specific platforms and are more expensive than laboratory-developed methods.

Our objective was to develop an internally controlled, triplex assay to detect SARS-CoV-2 RNA in clinical samples. We initially evaluated 6 individual rRT-PCRs, 3 published by the US Centers for Disease Control and Prevention (*2*) that target the nucleocapsid (N) gene, N1, N2, and N3; and 3 published by Corman, et al. (*4*) that target RNA-dependent RNA polymerase (RdRp), envelope (E), and N genes. We performed assays in 20 μL reactions of the Luna Universal Probe One-Step RT-qPCR Kit (New England Biolabs, https://www.neb.com) on a Rotor-Gene Q (QIAGEN, https://www.qiagen.com) by using 5 μL of eluate and our standard cycling protocol (*10*). We extracted total nucleic acids from samples on an

EMAG (bioMérieux, https://www.biomerieux.com). We compared analytical sensitivity of the assays by using dilutions of 2 SARS-CoV-2 strains, BetaCoV/Germany/BavPat1/2020p.1 and USA-WA1/2020. The N2 and E-gene assays were the most sensitive singleplex reactions and we noted no substantial change in cycle threshold ($C_t$) when the assays were combined. We then optimized a triplex assay to include the following targets: N2, which is SARS-CoV-2 specific; E, which also detects SARS-related coronaviruses; and RNase P, which serves as a heterologous, intrinsic specimen control (Appendix Table). We considered samples positive when they produced exponential amplification curves that crossed the threshold for both N2 and E targets.

The dynamic range of both SARS-CoV-2 targets in the triplex assay extended from 8.0 to 2.0 $\log_{10}$ copies/μL of eluate. We evaluated the lower limit of detection by performing serial dilutions of viral transport media (VTM) from a confirmed case by using VTM from confirmed negative cases. We tested eluates in quadruplicate and calculated RNA concentrations from a 4-point standard curve of quantified ssDNA (Integrated DNA Technologies, https://www.idtdna.com). The lowest concentration at which all replicates were detected by both targets was 45 copies/μL. When performed in singleplex, the N2 assay detected RNA down to 5 copies/μL, but all replicates had $C_t \geq 40$, and the sensitivity of the E-gene assay did not change.

To evaluate specificity, we extracted total nucleic acids from 42 archived nasopharyngeal swab samples in VTM from patients who had laboratory-confirmed infections with the following viruses: other circulating coronaviruses in the United States (n = 20), influenza (n = 7), parainfluenza (n = 7), human rhinovirus (n = 6), respiratory syncytial virus (n = 3), human metapneumovirus (n = 3), and adenovirus (n = 2). Among the 42 swab samples, 6 had laboratory-confirmed co-infections with 2 viruses. All samples tested negative for both SARS-CoV-2 targets and positive for RNase P.

Finally, we tested nasopharyngeal or oropharyngeal swab samples from 27 patients with a suspected symptomatic SARS-CoV-2 infection (Table). Ten patients tested positive in the triplex assay. Results demonstrated 100% agreement with either the US Centers for Disease Control and Prevention or Corman et al. (2,4) protocols performed at CLIA-certified laboratories (Clinical Laboratory Improvement Amendments,

**Table.** Comparison of cycle threshold results for 27 clinical samples tested in triplex real-time reverse transcription PCR and singleplex PCR for severe acute respiratory syndrome coronavirus 2

| | Triplex real-time reverse transcription PCR | | | Singleplex reactions | |
|---|---|---|---|---|---|
| Sample | N2 target | E target | RNase P | N2 target | E target |
| No template control | ND | ND | ND | ND | ND |
| Positive control, RNA† | 29.9 | 32.0 | ND | 30.7 | 33.0 |
| CoV 01 | 19.0 | 23.1 | 21.0 | 19.2 | 23.1 |
| CoV 02 | ND | ND | 22.1 | ND | ND |
| CoV 03 | ND | ND | 22.0 | ND | ND |
| CoV 04 | ND | ND | 21.9 | ND | ND |
| CoV 05 | ND | ND | 22.4 | ND | ND |
| CoV 06 | ND | ND | 21.4 | ND | ND |
| CoV 07 | ND | ND | 21.6 | ND | ND |
| CoV 08 | 26.1 | 28.0 | 25.5 | 26.1 | 27.7 |
| CoV 09 | 20.1 | 22.0 | 22.5 | 20.3 | 22.2 |
| CoV 10 | ND | ND | 21.1 | ND | ND |
| CoV 11 | ND | ND | 22.0 | ND | ND |
| CoV 12 | ND | ND | 20.5 | ND | ND |
| CoV 13 | ND | ND | 20.9 | ND | ND |
| CoV 14 | ND | ND | 24.6 | ND | ND |
| CoV 15 | ND | ND | 28.7 | ND | ND |
| CoV 16 | 14.6 | 16.3 | 22.0 | 14.9 | 16.5 |
| CoV 17 | ND | ND | 27.6 | 44.8 | ND |
| CoV 18 | 33.1 | 35.7 | 22.5 | 31.0 | 32.9 |
| CoV 19 | ND | ND | 28.2 | ND | ND |
| CoV 20 | 18.6 | 21.3 | 22.5 | 18.9 | 21.5 |
| CoV 21 | 33.4 | 34.2 | 25.1 | 30.6 | 33.2 |
| CoV 22 | ND | ND | 21.1 | ND | ND |
| CoV 23 | 28.9 | 31.3 | 21.3 | 28.2 | 30.4 |
| CoV 24 | 30.0 | 33.4 | 21.6 | 29.1 | 31.6 |
| CoV 25 | 9.8 | 13.2 | 20.6 | 9.8 | 13.1 |
| CoV 26 | ND | ND | 21.5 | ND | ND |
| CoV 27 | ND | ND | 24.6 | ND | ND |

*CoV, coronavirus; E, envelope gene; N2, nucleocapsid 2 gene; ND, not detected; RNase P, ribonuclease P.
†Strain BetaCoV/Germany/BavPat1/2020p.1.

https://www.cdc.gov/clia/about.html). Triplex results also agreed with testing in singleplex reactions except for 1 negative sample, number CoV 17, that gave a late positive signal in the N2 singleplex assay ($C_t$ 44.8). However, no signal was detected in the E-gene singleplex. Therefore, had singleplex testing been performed, the final interpretation would not have differed.

We describe the development of an internally controlled triplex SARS-CoV-2 rRT-PCR that targets the N and E genes. The N2 and E-gene targets have proven to be sensitive in singleplex formats and assay performance remained robust to protocol changes we made during optimization in our laboratory. Of note, the triplex SARS-CoV-2 rRT-PCR has been validated only for the instruments and chemistries we describe here. This assay should be thoroughly validated before implementation in other laboratories.

Current molecular diagnostic workflows for SARS-CoV-2 contain 2 or 3 viral targets for confirmation (*2*–*6*). The triplex SARS-CoV-2 rRT-PCR we describe is consistent with this standard and demonstrated equivalent clinical performance to testing at CLIA-certified laboratories and to the component singleplex assays. In addition, the triplex format streamlines workflow and decreases reagent use. This triplex assay should, therefore, maintain accurate viral detection and improve laboratory capacity to meet the current high demand for testing.

### Acknowledgments

We thank Mehul Suthar for providing extracted RNA from cultured SARS-CoV-2 at Emory University; Laurel R. Bristow, Ghina Alaaeddine, and Ariel Kay for specimen collection; and Alejandra Rojas for her helpful comments throughout the course of this project.

SARS-CoV-2 RNA was provided by the European Virus Archive Global (EVA-GLOBAL) project, which has received funding from the European Union's Horizon 2020 research and innovation program under grant no. 871029. Samples with other viral pathogens also were collected as part of the RSV in Older Adults and Pregnant women Study (ROAPS) sponsored by Pfizer (https://www.pfizer.com).

E.J.A. has received personal fees from AbbVie and Pfizer for consulting, and his institution receives funds to conduct clinical research from MedImmune, Regeneron, PaxVax, Pfizer, GSK, Merck, Novavax, Sanofi-Pasteur, and Micron. No other authors have conflicts to declare.

### About the Author

Dr. Waggoner is an assistant professor in the Emory University Department of Medicine, Division of Infectious Diseases, Atlanta, Georgia, USA. His research focuses on the development and implementation of new diagnostic methods for viral infections and pathogens that cause an acute febrile illness in the tropics.

### References

1. Wang W, Xu Y, Gao R, Lu R, Han K, Wu G, et al. Detection of SARS-CoV-2 in different types of clinical specimens. JAMA. 2020. https://doi.org/10.1001/jama.2020.3786
2. US Centers for Disease Control and Prevention. Real-time RT-PCR panel for detection 2019-novel coronavirus, instructions for use. 2020 Feb 4 [cited 2020 Feb 12] https://www.cdc.gov/coronavirus/2019-ncov/downloads/rt-pcr-panel-for-detection-instructions.pdf
3. Chu DKW, Pan Y, Cheng SMS, Hui KPY, Krishnan P, Liu Y, et al. Molecular diagnosis of a novel coronavirus (2019-nCoV) causing an outbreak of pneumonia. Clin Chem. 2020;66:549–55. https://doi.org/10.1093/clinchem/hvaa029
4. Corman VM, Landt O, Kaiser M, Molenkamp R, Meijer A, Chu DKW, et al. Detection of 2019 novel coronavirus (2019-nCoV) by real-time RT-PCR. Euro Surveill. 2020;25. https://doi.org/10.2807/1560-7917.ES.2020.25.3.2000045
5. Chan JF, Yip CC, To KK, Tang TH, Wong SC, Leung KH, et al. Improved molecular diagnosis of COVID-19 by the novel, highly sensitive and specific COVID-19-RdRp/Hel real-time reverse transcription-polymerase chain reaction assay validated *in vitro* and with clinical specimens. J Clin Microbiol. 2020 Mar 4 [Epub ahead of print]. https://doi.org/10.1128/JCM.00310-20
6. Shirato K, Nao N, Katano H, Takayama I, Saito S, Kato F, et al. Development of genetic diagnostic methods for novel coronavirus 2019 (nCoV-2019) in Japan. Jpn J Infect Dis. 2020 Feb 18 [Epub ahead of print]. https://doi.org/10.7883/yoken.JJID.2020.061
7. Babiker A, Myers CW, Hill CE, Guarner J. SARS-CoV-2 testing. Am J Clin Pathol. 2020 Mar 30 [Epub ahead of print]. https://doi.org/10.1093/ajcp/aqaa052
8. cobas SARS-CoV-2. Instructions for use. Roche. 2020 [cited 2020 Mar 29]. https://diagnostics.roche.com/us/en/products/params/cobas-sars-cov-2-test.html
9. TaqPath COVID-19 Combo Kit. Instructions for use. ThermoFisher Scientific. 2020 [cited 2020 Mar 29]. https://www.thermofisher.com/content/dam/LifeTech/Documents/PDFs/clinical/taqpath-COVID-19-combo-kit-full-instructions-for-use.pdf
10. Rojas A, Diagne CT, Stittleburg VD, Mohamed-Hadley A, de Guillén YA, Balmaseda A, et al. Internally controlled, multiplex real-time reverse transcription PCR for dengue virus and yellow fever virus detection. Am J Trop Med Hyg. 2018;98:1833–6. https://doi.org/10.4269/ajtmh.18-0024

Address for correspondence: Jesse J. Waggoner, Emory University School of Medicine, Division of Infectious Diseases, 1760 Haygood Dr NE, Room E-132, Atlanta, GA 30303-3073, USA; email: jjwaggo@emory.edu

# Fatal Invasive Aspergillosis and Coronavirus Disease in an Immunocompetent Patient

Marion Blaize, Julien Mayaux, Cécile Nabet, Alexandre Lampros, Anne-Geneviève Marcelin, Marc Thellier, Renaud Piarroux, Alexandre Demoule, Arnaud Fekkar

Author affiliations: Assistance Publique–Hôpitaux de Paris, Groupe Hospitalier La Pitié-Salpêtrière, Paris, France (M. Blaize, J. Mayaux, C. Nabet, A. Lampros, A.-G. Marcelin, M. Thellier, R. Piarroux, A. Demoule, A. Fekkar); Sorbonne Université, Paris (C. Nabet, A.G. Marcelin, M. Thellier, R. Piarroux, A. Fekkar)

DOI: https://doi.org/10.3201/eid2607.201603

Invasive pulmonary aspergillosis is a complication in critically ill patients with acute respiratory distress syndrome, especially those with severe influenza pneumonia. We report a fatal case of invasive pulmonary aspergillosis in an immunocompetent patient in France who had severe coronavirus disease–associated pneumonia.

Patients infected with severe acute respiratory syndrome coronavirus 2 (SARS-CoV-2) experience major lung damage due to viral replication and the ensuing cytokine storm and complex inflammatory processes (*1*). The severe damage to lung tissue can lead to secondary infections within a median of 17 days after onset of coronavirus disease (COVID-19) (*2*). Most immunocompetent patients who develop severe forms of COVID-19 have ≥1 underlying condition, such as chronic obstructive pulmonary disease, hypertension, diabetes, or chronic kidney disease (*3*), but none of these predisposing factors generally are associated with an increased risk for developing fungal infections.

Invasive aspergillosis is a well-described complication of severe influenza pneumonia (*4*,*5*), but many intensivists seem to overlook this superinfection (*6*). A recent study reported a 19% incidence among 432 patients admitted to an intensive care unit (ICU) for influenza-related acute respiratory failure (*4*). Moreover, in a small autopsy series of patients who died in 2003 from SARS, 10% (2/20) had an invasive infection suggestive of aspergillosis (*7*). As the medical community confronts the ongoing COVID-19 pandemic, determining whether patients infected with SARS-CoV-2 develop fungal complications, especially invasive aspergillosis, is crucial.

We report the case of a 74-year-old immunocompetent man with severe COVID-19–associated pneumonia who rapidly developed invasive pulmonary aspergillosis. The patient had several underlying chronic diseases but no pulmonary disease. Among his existing conditions were asymptomatic and untreated myelodysplastic syndrome, diagnosed on the basis of hypereosinophilia, with CD8+ T-cell lymphocytosis, a normal karyotype and low-risk International Prognostic Scoring System score; Hashimoto's thyroiditis; hypertension; and benign prostatic hypertrophy.

On the morning of March 23, day 1, the patient fell out of bed, was unable to get up on his own, and called emergency services. The patient described a 1-week history of fever and cough followed by onset of dyspnea that day. Clinical examination showed signs of acute respiratory failure, tachypnea, and hypoxemia. The patient was intubated, transported to the hospital, and transferred to the ICU, where he required mechanical ventilation and vasopressor support. The same day, we took a protected distal aspiration before intravenous administration of cefotaxime. SARS-CoV-2 viral RNA was detected in this sample by using 2 distinct reverse transcription PCRs. The sample revealed $10^4$/mL of *Haemophilus influenzae*, which was not found in a second protected distal aspiration performed on day 2.

The patient's condition worsened, and he had a $PaO_2/FIO_2$ ratio <140 mm Hg with $FIO_2$ of 100%. We performed a tracheal aspirate on day 4 and sent samples to the mycology laboratory. PCR for *Aspergillus fumigatus* was positive (430 copies/mL; 2.6 log), but galactomannan in the aspirate assay was negative, and culture on Sabouraud agar remained sterile. Results of testing of a second tracheal aspiration performed on day 9 yielded branched septate hyphae suggestive of *Aspergillus* sp. under microscopic examination after silver staining (Figure). *A. fumigatus* PCR was once again positive with a higher number of copies (3,600 copies/mL; 3.55 log); the galactomannan assay was not available. The patient died that day of severe respiratory failure. Culture on Sabouraud agar later grew a mold identified as *A. fumigatus* by mass spectrometry. Of note, SARS-CoV-2 RNA still was detectable in the tracheal aspirations. Results of serum analyses, including galactomannan index determination, β-D-glucan assay, and *A. fumigatus* PCR, were negative in serum samples collected on day 4 and day 8.

This case fulfills the criteria of putative invasive aspergillosis according to the classification defined by Blot et al. for the diagnosis of invasive pulmonary aspergillosis in critically ill patients (*8*). Because the patient's illness took a rapid and fatal course, we did not have time to initiate appropriate antifungal treatment. As previously reported, respiratory samples

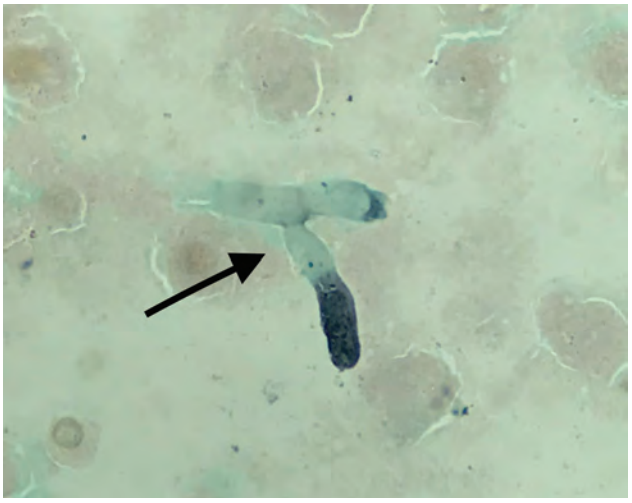

**Figure.** Microscopic image of silver-stained tracheal aspirate from an immunocompetent patient critically ill with coronavirus disease, France. Filaments suggestive of *Aspergillus* sp. are shown (black arrow). Original magnification ×1,000.

led to a diagnosis of aspergillosis, but blood samples lacked sensitivity (*4*). Moreover, *Aspergillus* PCR contributed to the diagnosis, but the galactomannan was negative, consistent with what we previously reported about the lower sensitivity of the galactomannan compared with PCR and culture in respiratory samples (*9*).

A patient with a fatal SARS-CoV-2 infection recently was reported to have *A. flavus* on tracheal aspirates culture, but other evidence was missing, and diagnosis of aspergillosis was not substantiated (*10*). Additional assessments are urgently needed to thoroughly investigate cases and promptly establish and define the cumulative incidence of invasive aspergillosis in ICU patients with severe COVID-19.

In conclusion, we report a case of invasive pulmonary aspergillosis in an immunocompetent patient during severe COVID-19–associated pneumonia. As the COVID-19 outbreak continues to spread worldwide, other reports are needed to assess the occurrence and frequency of fungal complications during severe SARS-CoV-2 infections.

## About the Author

Dr. Blaize is a microbiologist at Centre Hospitalier Universitaire La Pitié-Salpêtrière, Paris, France. Her primary research interest is medical diagnosis of fungal diseases.

## References


1. Mehta P, McAuley DF, Brown M, Sanchez E, Tattersall RS, Manson JJ; HLH Across Speciality Collaboration, UK. COVID-19: consider cytokine storm syndromes and immunosuppression. Lancet. 2020;395:1033–4. https://doi.org/10.1016/S0140-6736(20)30628-0
2. Zhou F, Yu T, Du R, Fan G, Liu Y, Liu Z, et al. Clinical course and risk factors for mortality of adult inpatients with COVID-19 in Wuhan, China: a retrospective cohort study. Lancet. 2020;395:1054–62. https://doi.org/10.1016/S0140-6736(20)30566-3
3. Onder G, Rezza G, Brusaferro S. Case-fatality rate and characteristics of patients dying in relation to COVID-19 in Italy. JAMA. 2020 Mar 23 [Epub ahead of print]. https://doi.org/10.1001/jama.2020.4683
4. Schauwvlieghe AFAD, Rijnders BJA, Philips N, Verwijs R, Vanderbeke L, Van Tienen C, et al.; Dutch-Belgian Mycosis study group. Invasive aspergillosis in patients admitted to the intensive care unit with severe influenza: a retrospective cohort study. Lancet Respir Med. 2018;6:782–92. https://doi.org/10.1016/S2213-2600(18)30274-1
5. Schwartz IS, Friedman DZP, Zapernick L, Dingle TC, Lee N, Sligl W, et al. High rates of influenza-associated invasive pulmonary aspergillosis may not be universal: a retrospective cohort study from Alberta, Canada. Clin Infect Dis. 2020 Jan 6 [Epub ahead of print]. https://doi.org/10.1093/cid/ciaa007
6. Toda M, Beekmann SE, Polgreen PM, Chiller TM, Jackson BR, Beer KD. Knowledge of infectious disease specialists regarding aspergillosis complicating influenza, United States. Emerg Infect Dis. 2020;26:809–11. https://doi.org/10.3201/eid2604.190953
7. Hwang DM, Chamberlain DW, Poutanen SM, Low DE, Asa SL, Butany J. Pulmonary pathology of severe acute respiratory syndrome in Toronto. Mod Pathol. 2005;18:1–10. https://doi.org/10.1038/modpathol.3800247
8. Blot SI, Taccone FS, Van den Abeele AM, Bulpa P, Meersseman W, Brusselaers N, et al.; AspICU Study Investigators. A clinical algorithm to diagnose invasive pulmonary aspergillosis in critically ill patients. Am J Respir Crit Care Med. 2012;186:56–64. https://doi.org/10.1164/rccm.201111-1978OC
9. Imbert S, Meyer I, Palous M, Brossas JY, Uzunov M, Touafek F, et al. *Aspergillus* PCR in bronchoalveolar lavage fluid for the diagnosis and prognosis of aspergillosis in patients with hematological and non-hematological conditions. Front Microbiol. 2018;9:1877. https://doi.org/10.3389/fmicb.2018.01877
10. Lescure FX, Bouadma L, Nguyen D, Parisey M, Wicky PH, Behillil S, et al. Clinical and virological data of the first cases of COVID-19 in Europe: a case series. Lancet Infect Dis. 2020 Mar 27 [Epub ahead of print]. https://doi.org/10.1016/S1473-3099(20)30200-0


Address for correspondence: Arnaud Fekkar, Service de Parasitologie-Mycologie, Pavillon Laveran, Hôpital de La Pitié-Salpêtrière, Boulevard de l'Hôpital, 75013 Paris, France; email: arnaud.fekkar@aphp.fr

# Enterovirus A71 Infection and Neurologic Disease, Madrid, Spain, 2016

Pascal Del Giudice

Author affiliation: Centre Hospitalier Intercommunal, Fréjus, France

DOI: https://doi.org/10.3201/eid2607.190037

**To the Editor:** Taravilla et al. (*1*) observed mucocutaneous manifestations of 6 children with enterovirus, and "the main manifestation was petechial rash on the extremities." This finding is unusual for enterovirus A71 (EV-A71) infections. Cutaneous manifestations of EV-A71 are reported as vesicular skin lesions, not purpura (*2*). It is important that physicians distinguish between petechial and vesicular rashes because petechial rashes in children are linked to other infectious agents, including parvovirus B19 and (especially within the context of encephalitis) *Neisseria meningitidis*. A precise dermatologic description is necessary for a correct clinical diagnosis. A too-rapid clinical examination might result in confusion between vesicular rash and petechial rash, especially when vesicles are very small. To avoid confusion, the authors should have provided high-quality clinical photos of the rashes, skin biopsy results, or both before considering EV-A71 as a new cause of febrile petechial rash in children.

## References

1. Taravilla CN, Pérez-Sebastián I, Salido AG, Serrano CV, Extremera VC, Rodríguez AD, et al. Enterovirus A71 infection and neurologic disease, Madrid, Spain, 2016. Emerg Infect Dis. 2019;25:25–32. https://doi.org/10.3201/eid2501.181089
2. Hubiche T, Schuffenecker I, Boralevi F, Léauté-Labrèze C, Bornebusch L, Chiaverini C, et al.; Clinical Research Group of the French Society of Pediatric Dermatology. Dermatological spectrum of hand, foot and mouth disease from classical to generalized exanthema. Pediatr Infect Dis J. 2014;33:e92–8. https://doi.org/10.1097/INF.0000000000000120

Address for correspondence: Pascal del Giudice Infectiologie-Dermatologie, Centre Hospitalier Intercommunal, CHI Fréjus-Saint-Raphaël, 240 Av de Saint Lambert, 83600 Fréjus, France; email: del-giudice-p@chi-fsr.fr

# The Poison Squad: One Chemist's Single-Minded Crusade for Food Safety at the Turn of the Twentieth Century

**Deborah Blum; Penguin, New York, NY, USA, 2018; ISBN-10: 1594205140; ISBN-13: 978-1594205149; Pages: 352; Price: $25.12**

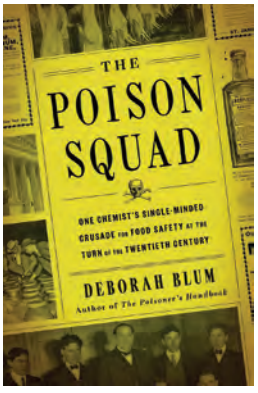


Formaldehyde made spoiled milk taste tolerable. Ground coffee was more than likely ground chicory. The yellow coating of children's candies often contained arsenic. Ketchup was a soup of "waste products from canners, like coal-tar colors or starch paste." Thus was the status of the foods the US public ate during the late 1800s. In The Poison Squad, author Deborah Blum tells the story of Harvey Washington Wiley and his dogged pursuit of government regulation for food safety and purity at the turn from the 19th to the 20th century.

She first details the food industry before his work, when dangerous chemicals were used without regulation to cut, mimic, or enhance the flavor of foods with little regard for effects on human health. She then describes the initial failed attempts of food safety advocates and their efforts to focus the attention of the general public and then the US Congress on food safety. Passage of the Pure Food and Drug Act of 1906 was only the first part of Wiley's story. Appropriately, the first section of The Poison Squad ends there.

In the second half, Blum deftly walks through the varied and complex difficulties Wiley faced in enforcing the laws mandated by the act. These difficulties included a hesitant and sometimes antagonistic boss, co-workers pitted against him, the various priorities of multiple presidents, and large and powerful food and chemical companies looking to work around the law. However, as Blum so keenly explains, Wiley was not alone in his quest. He had loyal supporters inside his own Bureau of Chemistry at the US Department of Agriculture, of course. But more important, he made allies along the way, such as Alice Lakey of the National Consumers League; colleagues at the American Medical Association; and even H.J. Heinz, founder of the food company that still bears his name. Blum does a wonderful job describing the value of these supporters to Wiley as he struggled for food purity and public health.

With intriguing anecdotes, vivid quotations, and expert attention to detail, Blum guides readers through the tedious process of moving an idea into legislation, applied regulation, and finally enforcement, and she does so with a storyteller's touch. This captivating book relates the importance and practical impacts of Wiley's endeavors to the life of an ordinary citizen of the time. It is equal parts informative and entertaining.

Blum's optimistic book demonstrates that, with hard work and determination, laws can be passed to protect public health, even when opposition is fierce. It also shows that forming and nurturing partnerships with citizen groups, academic institutions, and industry leaders is key to these endeavors. Although the book does an excellent job describing Wiley's contributions, it only briefly addresses some of the ethical issues regarding his actual "Poison Squad" studies, or the flaws in their study design. This book will educate and inspire readers who have worked in public health for decades and those who are just entering the field. It will also inform persons who work toward other public service endeavors and entertain those who simply like a good story. A Public Broadcasting Service special that closely follows this book is also available (https://www.pbs.org/wgbh/americanexperience/films/poison-squad).

Michael C. Bazaco

Author affiliation: US Food and Drug Administration, College Park, Maryland, USA; University of Maryland School of Public Health, College Park

DOI: https://doi.org/10.3201/eid2607.200184

Address for correspondence: Michael C. Bazaco, US Food and Drug Administration—Center for Food Safety and Applied Nutrition, 4300 River Rd, College Park, MD 20740, USA; email: michael.bazaco@fda.hhs.gov

**Pierre Joseph Redouté (1759–1840).** ***Iris Germanica*** **(1812)** (detail). Watercolor on vellum. 21 in x 13¾ in/53.3 cm x 35 cm. Public domain image from Biodiversity Heritage Library. Holding institution Missouri Botanical Garden, Peter H. Raven Library, St. Louis, Missouri, USA.

# Intricacy, Symmetry, Diversity

Byron Breedlove

Belgian artist Pierre-Joseph Redouté is the "most celebrated flower painter of quite possibly the entire history of botanical art" and "remembered as one of the greatest botanical illustrators in history," notes Grace Costantino, from the Biodiversity Heritage Library. Redouté, whose patrons included members of French royalty and other luminaries interested in botany, published more than 2,100 plates depicting more than 1,800 species of flowers, many of which had never been illustrated before.

Author affiliation: Centers for Disease Control and Prevention, Atlanta, Georgia, USA

DOI: https://doi.org/10.3201/eid2607.AC2607

Born in 1759 at St. Hubert in the Belgian province that is now Luxembourg, Redouté was descended from a family of Belgian painters. He trained in his father's studio, and by the time he was 13 years old, Redouté was earning his living as an artist. In 1782, he teamed with his elder brother, Antoine-Ferdinand, to design the stage scenery for the Théâtre-Italien in the rue de Louvois, Paris. There Redouté started painting flowers during his free time and studied with Dutch artist Gerard van Spaendonck, a professor of flower painting at the Muséum National d'Histoire Naturelle. Spaendonck taught the young Redouté engraving and watercolor techniques, which he continued to use and refine. Artist and author Wilfrid Blunt asserts

that Redouté owes much of his success to those discoveries and describes Redouté's technique as using "pure water colour, gradated with infinite subtlety and very occasionally touched with body-colour to suggest sheen."

The image *Iris germanica* featured on this month's cover comes from *Les liliacées*, a misleading title for a volume of prints that also features many other plants. This collection was published while the artist was under patronage from the Empress Joséphine, first wife of Napoleon, and is considered to be Redouté's masterpiece.

The plant's gentle intricacy and distinctive three-fold symmetry are apparent in the two indigo blooms, each shown from a different perspective, paired with a third stalk poised to bloom. Faintly striated sword-shaped leaves fan out around the stalks and petals, tapering into finely pointed tips. The upright petals, or standards, and the pendant petals, or falls, are the same color. Author and gardener Steve Bender notes that "Standards and falls may be the same color or radically different colors. Dream up any color combination, and you can probably find it."

Named for the Greek goddess Iris, who traveled along rainbows to deliver messages between the gods and the Underworld, the genus *Iris* comprises more than 300 species and perhaps 50,000 varieties of flowers. Flowering irises fill gardens with an assortment of eye-catching colors in the spring and summer and have been the subject of many well-known paintings by renowned artists.

The Missouri Botanical Garden notes that "the presumed father of most modern bearded iris cultivars," *Iris germanica*—which is not actually native to Germany but rather to the Mediterranean and central Asia—has become established throughout the world and naturalized throughout much of Europe and the United States. Irises are diverse in their ecology, flourish under myriad conditions, and have increased in variety and geographic range largely because of human activity.

Although generally hardy, irises are susceptible to a number of viruses, including iris mild mosaic virus, iris severe mosaic virus, iris fulva mosaic virus, bean yellow mosaic virus, narcissus latent virus, and the more recently documented cucumber mosaic virus, broad bean wilt virus, and tobacco ringspot virus. Irises can be affected by multiple viruses at the same time, and the viruses are typically spread by aphids.

During the late 19th century, about 50 years after Redouté died, Adolf Eduard Mayer showed that tobacco mosaic disease could be transferred among plants. Dmitry Iosifovich Ivanovsky discovered a microscopic infectious agent that could permeate porcelain Chamberland filters (bacteria could not). And Martinus Beijerinck replicated Ivanovsky's discovery and called this new pathogen "*contagium vivum fluidum.*"

Since that time, rapid transit, global trade, urbanization and destruction of natural habitats, and modern agricultural practices have accelerated the emergence and spread of viruses among humans, animals, and plants. As the landmark 1992 Institute of Medicine report on Emerging Infections reminds us ". . . in the context of infectious diseases, there is nowhere in the world from which we are remote and no one from whom we are disconnected." The emergence of SARS-CoV-2 underscores how connected the modern world is, and shows that, like the artist's iris, emerging viruses continue to expand their diversity and range. Spending a few quiet moments enjoying Redouté's striking botanical illustration may offer a brief respite to public health professionals, clinicians, and researchers engaged in detecting, preventing, and responding to emerging viruses.

## Bibliography


1. Bender S. Grumpy Gardener: An A to Z Guide from the Galaxy's Most Irritable Green Thumb. New York: Oxmoor House; 2017. p. 33–4.
2. Buck J, Rice C. The era of Pierre Joseph Redouté. American Society of Botanical Artists [cited 2020 May 14]. https://www.asba-art.org/article/chapter-14-era-pierre-joseph-redouté
3. Costantino G. The botanical art of Redouté [cited 2020 May 14]. https://blog.biodiversitylibrary.org/2017/06/the-botanical-art-of-redoute.html
4. Lederberg J, Shope RE, Oaks SC Jr, editors. Committee on Microbial Threats to Health, Institute of Medicine. Emerging infections: microbial threats to health in the United States (1992) [cited 2020 May 24]. http://www.nap.edu/catalog/2008/emerging-infections-microbial-threats-to-health-in-the-united-states
5. Marston HD, Folkers GK, Morens DM, Fauci AS. Emerging viral diseases: confronting threats with new technologies [cited 2020 Jun 8]. https://stm.sciencemag.org/content/6/253/253ps10
6. Pacific Bulb Society. Iris [cited 2020 May 26]. https://www.pacificbulbsociety.org/pbswiki/index.php/Iris
7. Schmidt AM, Jacoby TB. Herbs to orchids: botanical illustration in the nineteenth century [cited 2020 May 26]. https://digitalrepository.trincoll.edu/exhibitions/3
8. Wilfrid B. The art of botanical illustration. Chapter 14. The age of Redouté. London: Collins; 1967. p. 173–83.


Address for correspondence: Byron Breedlove, EID Journal, Centers for Disease Control and Prevention, 1600 Clifton Rd NE, Mailstop H16-2, Atlanta, GA 30329-4027, USA; email: wbb1@cdc.gov

# EMERGING INFECTIOUS DISEASES®

## Upcoming Issue

- Epidemiology of Legionnaires' Disease, Hong Kong, China, 2005–2015
- Coronavirus Disease Outbreak in Call Center, South Korea
- Tuberculosis in Internationally Displaced Children Resettling in Harris County, Texas, USA, 2010–2015
- Investigation and Serologic Follow-Up of Contacts of Early Confirmed Case-Patient with COVID-19, United States
- US CDC Real-Time Reverse Transcription PCR Panel for Detection of Severe Acute Respiratory Syndrome Coronavirus 2
- Characteristics and Outcomes of Coronavirus Disease Patients under Nonsurge Conditions, Northern California, USA, March–April 2020
- Analysis of MarketScan Data for Immunosuppressive Conditions and Hospitalizations for Acute Respiratory Illness, United States
- Evaluating the Effectiveness of Social Distancing Interventions to Delay or Flatten the Epidemic Curve of Coronavirus Disease
- Sporadic Creutzfeldt-Jakob Disease among Physicians, Germany, 1993–2018
- Characterizing Norovirus Transmission from Outbreak Data, United States
- CrAssphage as a Novel Tool to Detect Human Fecal Contamination on Environmental Surfaces and Hands
- Virome Analysis of Wild Rodents Reveals the Presence of Segmented Flaviviruses in North America
- Population Genomic Structure and Recent Evolution of *Plasmodium knowlesi*, Peninsular Malaysia
- Human Outbreak of Trichinellosis Caused by *Trichinella papuae*, Central Kampong Thom Province, Cambodia
- Increased Sensitivity of *Plasmodium falciparum* to Artesunate/Amodiaquine Despite 14 Years as First-Line Malaria Treatment, Zanzibar
- Genotypic Heterogeneity of *Orientia tsutsugamushi* in Scrub Typhus Patients and Co-infection with Thrombocytopenia Syndrome Virus, Myanmar
- Population-Based Estimates of Chronic Conditions Affecting Risk for Complications from Coronavirus Disease, United States
- Prolonged Persistence of SARS-CoV-2 RNA in Body Fluids
- Plasma-Derived Extracellular Vesicles as Potential Biomarkers in Heart Transplant Patient with Chronic Chagas Disease
- Imported Monkeypox, Singapore
- Moth Flies in the Hospital Distributing Multidrug-Resistant Bacteria from the Waste Water System
- Increasing Malaria Parasite Clearance Time following Chloroquine Therapy, South Korea, 2000–2016
- Prognostic Value of Leukocytosis and Lymphopenia for Coronavirus Disease Severity
- In Vivo Observation of Trombiculosis with Fluorescence–Advanced Videodermatoscopy
- Disseminated *Echinococcus multilocularis* Infection without Liver Involvement in Child, Canada, 2018
- SARS-CoV-2 Phylogenetic Analysis, Lazio Region, Italy, February–March 2020
- *Leishmania infantum* in US-Born Dog
- Canine *Dracunculus* Worm Infection, Toledo, Spain
- Autochthonous Gnathostomiasis with Severe Ocular Infection, Madagascar, 2016

**Complete list of articles in the August issue at http://www.cdc.gov/eid/upcoming.htm**

# Earning CME Credit

To obtain credit, you should first read the journal article. After reading the article, you should be able to answer the following, related, multiple-choice questions. To complete the questions (with a minimum 75% passing score) and earn continuing medical education (CME) credit, please go to http://www.medscape.org/journal/eid. Credit cannot be obtained for tests completed on paper, although you may use the worksheet below to keep a record of your answers.

You must be a registered user on http://www.medscape.org. If you are not registered on http://www.medscape.org, please click on the "Register" link on the right hand side of the website.

Only one answer is correct for each question. Once you successfully answer all post-test questions, you will be able to view and/or print your certificate. For questions regarding this activity, contact the accredited provider, CME@medscape.net. For technical assistance, contact CME@medscape.net. American Medical Association's Physician's Recognition Award (AMA PRA) credits are accepted in the US as evidence of participation in CME activities. For further information on this award, please go to https://www.ama-assn.org. The AMA has determined that physicians not licensed in the US who participate in this CME activity are eligible for AMA PRA Category 1 Credits™. Through agreements that the AMA has made with agencies in some countries, AMA PRA credit may be acceptable as evidence of participation in CME activities. If you are not licensed in the US, please complete the questions online, print the AMA PRA CME credit certificate, and present it to your national medical association for review.

## Article Title

**Rickettsioses as Major Etiologies of Unrecognized Acute Febrile Illness, Sabah, East Malaysia**

## CME Questions

**1. You are advising a hospital in Malaysia about management of acute febrile illness (AFI). On the basis of the retrospective study by Grigg and colleagues, which one of the following statements about findings of diagnostic testing for rickettsioses among patients with nonmalarial AFI in Sabah, East Malaysia, from 2013 to 2015 is correct?**

A. Past or acute rickettsial infection (indirect fluorescent antibody immunoglobulin G [IgG] titer ≥160) was identified in one fifth of patients
B. Acute rickettsioses (4-fold IgG titer rise to ≥160 with paired sera) were confirmed in 10% of patients
C. The most frequent cause of acute rickettsiosis was *Orientia tsutsugamushi* (OT)
D. Polymerase chain reaction was positive in one quarter of acute rickettsioses

**2. According to the retrospective study by Grigg and colleagues, which one of the following statements about clinical and laboratory findings among patients with nonmalarial AFI in Sabah, East Malaysia, who were diagnosed with rickettsioses from 2013 to 2015 is correct?**

A. Mortality rate was 15%
B. Eschars and vomiting were common and reported more often with acute rickettsioses than in AFI without rickettsial disease
C. Doxycycline was administered to more than half of patients and was effective in most cases
D. Common laboratory findings (eg, abnormal white blood cell count, thrombocytopenia, anemia, and raised liver transaminases) were all nonspecific

**3. According to the retrospective study by Grigg and colleagues, which one of the following statements about clinical implications of clinical and epidemiological findings among patients with nonmalarial AFI in Sabah, East Malaysia, who were diagnosed with rickettsioses from 2013 to 2015 is correct?**

A. Acute rickettsioses are common, underrecognized, and often untreated causes of nonmalarial AFI in East Malaysia, meriting consideration of empirical doxycycline
B. Risk factors for rickettsioses were female sex and slaughterhouse/animal husbandry work
C. The epidemiology of rickettsial infections in this study differs markedly from previous reports of scrub typhus and spotted fever rickettsioses in rural areas in Southeast Asia
D. Rickettsioses in Sabah appear to be decreasing

# Earning CME Credit

To obtain credit, you should first read the journal article. After reading the article, you should be able to answer the following, related, multiple-choice questions. To complete the questions (with a minimum 75% passing score) and earn continuing medical education (CME) credit, please go to http://www.medscape.org/journal/eid. Credit cannot be obtained for tests completed on paper, although you may use the worksheet below to keep a record of your answers.

You must be a registered user on http://www.medscape.org. If you are not registered on http://www.medscape.org, please click on the "Register" link on the right hand side of the website.

Only one answer is correct for each question. Once you successfully answer all post-test questions, you will be able to view and/or print your certificate. For questions regarding this activity, contact the accredited provider, CME@medscape.net. For technical assistance, contact CME@medscape.net. American Medical Association's Physician's Recognition Award (AMA PRA) credits are accepted in the US as evidence of participation in CME activities. For further information on this award, please go to https://www.ama-assn.org. The AMA has determined that physicians not licensed in the US who participate in this CME activity are eligible for AMA PRA Category 1 Credits™. Through agreements that the AMA has made with agencies in some countries, AMA PRA credit may be acceptable as evidence of participation in CME activities. If you are not licensed in the US, please complete the questions online, print the AMA PRA CME credit certificate, and present it to your national medical association for review.

.

## Article Title

**Atypical Manifestations of Cat-Scratch Disease, United States, 2005–2014**

## CME Questions

**1. Your patient is a 12-year-old girl with headache and decreased level of consciousness several weeks after being scratched by a cat. On the basis of the analysis of data from the 2005 to 2014 MarketScan national health insurance claims databases by Nawrocki and colleagues, which one of the following statements about the epidemiology of atypical cat-scratch disease (CSD) in the United States is correct?**

A. In this study, atypical CSD accounted for 15% of all cases of CSD
B. Average annual incidence was 0.7/100,000 population
C. Atypical CSD was most common among men at least 50 years of age
D. Most atypical CSD cases occurred in the Northwest and in the spring to summer months

**2. On the basis of the analysis of data from the 2005 to 2014 MarketScan national health insurance claims databases by Nawrocki and colleagues, which one of the following statements about the clinical features of atypical CSD in the United States is correct?**

A. Neurological manifestations were the most common presentation among patients with atypical CSD
B. Compared with typical CSD, atypical CSD was associated with twice the risk for hospitalization
C. Children aged 14 years or younger were at greater risk for hepatosplenic disease and osteomyelitis compared with persons aged at least 15 years
D. Patients with ocular manifestations were most likely to be hospitalized

**3. According to the analysis of data from the 2005 to 2014 MarketScan national health insurance claims databases by Nawrocki and colleagues, which one of the following statements about the clinical and public health implications of the epidemiology and clinical features of atypical CSD in the United States is correct?**

A. Better understanding of atypical CSD may improve clinician recognition of cases and inform efforts to clarify the underlying pathophysiology
B. The seasonality of atypical vs typical CSD is unlikely to result from delays in diagnosis
C. Bacteriological studies in pet cats suggest that clinicians in regions with dry climates should be especially vigilant in recognizing CSD
D. The study proves that persons at least 65 years of age are less vulnerable to developing atypical CSD